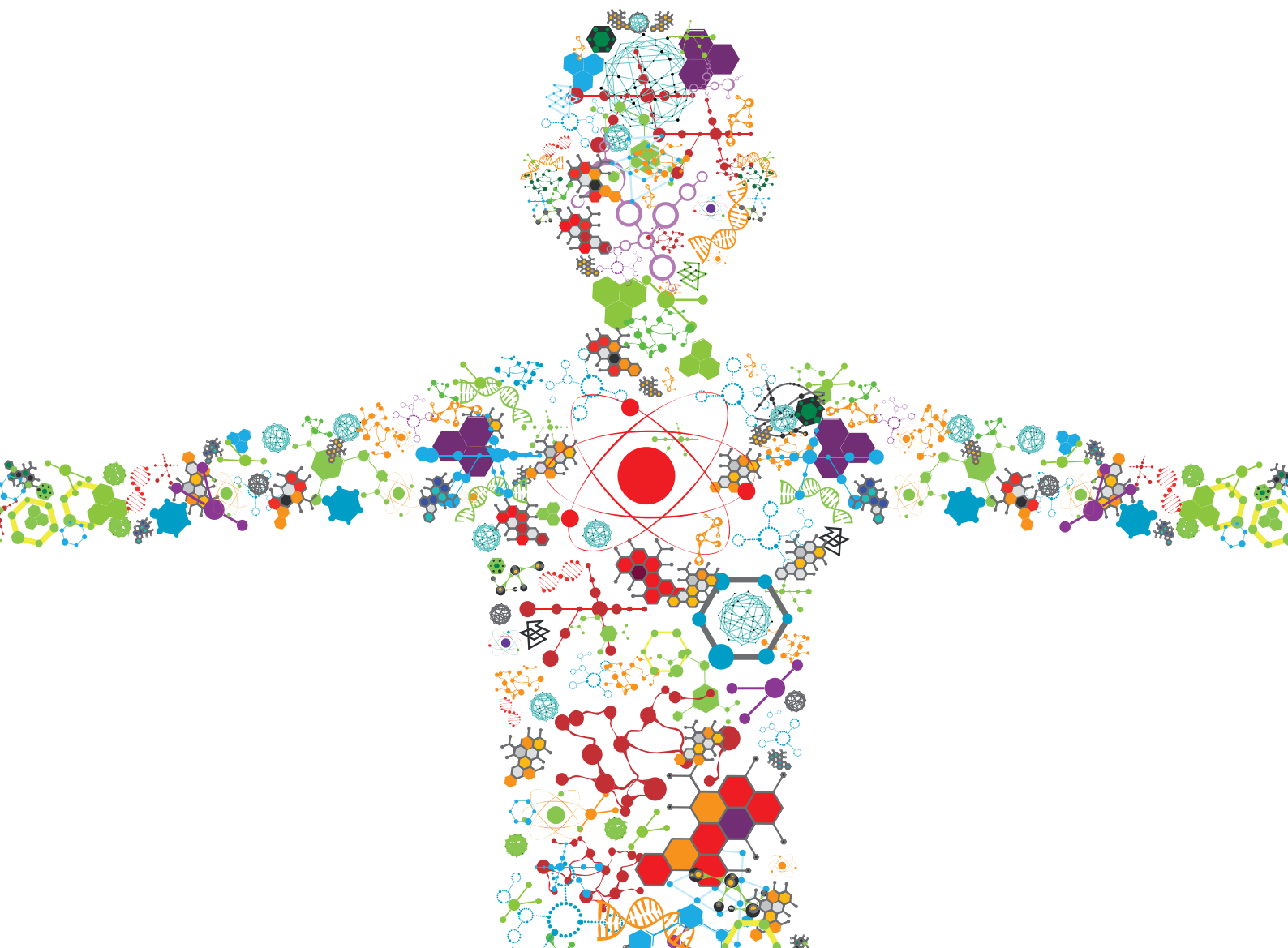


ADVANCES IN ADDITIVE MANUFACTURING TECHNOLOGIES FOR THE PRODUCTION OF TISSUE-ENGINEERED BONE SCAFFOLDS FOR DENTAL APPLICATIONS

EDITED BY: Barbara Zavan, Stefano Sivoella and Nikos Donos
PUBLISHED IN: Frontiers in Bioengineering and Biotechnology





frontiers

Frontiers eBook Copyright Statement

The copyright in the text of individual articles in this eBook is the property of their respective authors or their respective institutions or funders. The copyright in graphics and images within each article may be subject to copyright of other parties. In both cases this is subject to a license granted to Frontiers.

The compilation of articles constituting this eBook is the property of Frontiers.

Each article within this eBook, and the eBook itself, are published under the most recent version of the Creative Commons CC-BY licence.

The version current at the date of publication of this eBook is CC-BY 4.0. If the CC-BY licence is updated, the licence granted by Frontiers is automatically updated to the new version.

When exercising any right under the CC-BY licence, Frontiers must be attributed as the original publisher of the article or eBook, as applicable.

Authors have the responsibility of ensuring that any graphics or other materials which are the property of others may be included in the CC-BY licence, but this should be checked before relying on the CC-BY licence to reproduce those materials. Any copyright notices relating to those materials must be complied with.

Copyright and source acknowledgement notices may not be removed and must be displayed in any copy, derivative work or partial copy which includes the elements in question.

All copyright, and all rights therein, are protected by national and international copyright laws. The above represents a summary only. For further information please read Frontiers' Conditions for Website Use and Copyright Statement, and the applicable CC-BY licence.

ISSN 1664-8714

ISBN 978-2-83250-011-8

DOI 10.3389/978-2-83250-011-8

About Frontiers

Frontiers is more than just an open-access publisher of scholarly articles: it is a pioneering approach to the world of academia, radically improving the way scholarly research is managed. The grand vision of Frontiers is a world where all people have an equal opportunity to seek, share and generate knowledge. Frontiers provides immediate and permanent online open access to all its publications, but this alone is not enough to realize our grand goals.

Frontiers Journal Series

The Frontiers Journal Series is a multi-tier and interdisciplinary set of open-access, online journals, promising a paradigm shift from the current review, selection and dissemination processes in academic publishing. All Frontiers journals are driven by researchers for researchers; therefore, they constitute a service to the scholarly community. At the same time, the Frontiers Journal Series operates on a revolutionary invention, the tiered publishing system, initially addressing specific communities of scholars, and gradually climbing up to broader public understanding, thus serving the interests of the lay society, too.

Dedication to Quality

Each Frontiers article is a landmark of the highest quality, thanks to genuinely collaborative interactions between authors and review editors, who include some of the world's best academicians. Research must be certified by peers before entering a stream of knowledge that may eventually reach the public - and shape society; therefore, Frontiers only applies the most rigorous and unbiased reviews.

Frontiers revolutionizes research publishing by freely delivering the most outstanding research, evaluated with no bias from both the academic and social point of view. By applying the most advanced information technologies, Frontiers is catapulting scholarly publishing into a new generation.

What are Frontiers Research Topics?

Frontiers Research Topics are very popular trademarks of the Frontiers Journals Series: they are collections of at least ten articles, all centered on a particular subject. With their unique mix of varied contributions from Original Research to Review Articles, Frontiers Research Topics unify the most influential researchers, the latest key findings and historical advances in a hot research area! Find out more on how to host your own Frontiers Research Topic or contribute to one as an author by contacting the Frontiers Editorial Office: frontiersin.org/about/contact

ADVANCES IN ADDITIVE MANUFACTURING TECHNOLOGIES FOR THE PRODUCTION OF TISSUE-ENGINEERED BONE SCAFFOLDS FOR DENTAL APPLICATIONS

Topic Editors:

Barbara Zavan, University of Padua, Italy

Stefano Sivoletta, University Hospital of Padua, Italy

Nikos Donos, Queen Mary University of London, United Kingdom

Citation: Zavan, B., Sivoletta, S., Donos, N., eds. (2022). Advances in Additive Manufacturing Technologies for the Production of Tissue-Engineered Bone Scaffolds for Dental Applications. Lausanne: Frontiers Media SA.
doi: 10.3389/978-2-83250-011-8

Table of Contents

- 05 Editorial: Advances in additive manufacturing technologies for the production of tissue-engineered bone scaffolds for dental applications**
Giulia Brunello, Nikolaos Donos, Stefano Sivoletta and Barbara Zavan
- 08 Activation of Human Osteoblasts via Different Bovine Bone Substitute Materials With and Without Injectable Platelet Rich Fibrin in vitro**
Solomiya Kyyak, Sebastian Blatt, Eik Schiegnitz, Diana Heimes, Henning Staedt, Daniel G. E. Thiem, Keyvan Sagheb, Bilal Al-Nawas and Peer W. Kämmerer
- 19 Leonurine Promotes the Osteoblast Differentiation of Rat BMSCs by Activation of Autophagy via the PI3K/Akt/mTOR Pathway**
Bingkun Zhao, Qian Peng, Enoch Hin Lok Poon, Fubo Chen, Rong Zhou, Guangwei Shang, Dan Wang, Yuanzhi Xu, Raorao Wang and Shengcai Qi
- 30 Case Report: Histological and Histomorphometrical Results of a 3-D Printed Biphasic Calcium Phosphate Ceramic 7 Years After Insertion in a Human Maxillary Alveolar Ridge**
Carlo Mangano, Alessandra Giuliani, Ilaria De Tullio, Mario Raspanti, Adriano Piattelli and Giovanna Iezzi
- 39 Enlightenment of Growth Plate Regeneration Based on Cartilage Repair Theory: A Review**
Xianggang Wang, Zuhao Li, Chenyu Wang, Haotian Bai, Zhonghan Wang, Yuzhe Liu, Yirui Bao, Ming Ren, He Liu and Jincheng Wang
- 61 Positive Effects of Three-Dimensional Collagen-Based Matrices on the Behavior of Osteoprogenitors**
Zhikai Lin, Cristina Nica, Anton Sculean and Maria B. Asparuhova
- 78 Regenerative Medicine Technologies to Treat Dental, Oral, and Craniofacial Defects**
Jessica M. Latimer, Shogo Maekawa, Yao Yao, David T. Wu, Michael Chen and William V. Giannobile
- 105 Tissue Engineering in Stomatology: A Review of Potential Approaches for Oral Disease Treatments**
Lilan Cao, Huiying Su, Mengying Si, Jing Xu, Xin Chang, Jiajia Lv and Yuankun Zhai
- 121 Ectopic Bone Tissue Engineering in Mice Using Human Gingiva or Bone Marrow-Derived Stromal/Progenitor Cells in Scaffold-Hydrogel Constructs**
Siddharth Shanbhag, Carina Kamplaitner, Samih Mohamed-Ahmed, Mohammed Ahmad Yassin, Harsh Dongre, Daniela Elena Costea, Stefan Tangl, Mohamad Nageeb Hassan, Andreas Stavropoulos, Anne Isine Bolstad, Salwa Suliman and Kamal Mustafa
- 135 Corrigendum: Ectopic Bone Tissue Engineering in Mice Using Human Gingiva or Bone Marrow-Derived Stromal/Progenitor Cells in Scaffold-Hydrogel Constructs**
Siddharth Shanbhag, Carina Kamplaitner, Samih Mohamed-Ahmed, Mohammed Ahmad Yassin, Harsh Dongre, Daniela Elena Costea, Stefan Tangl, Mohamad Nageeb Hassan, Andreas Stavropoulos, Anne Isine Bolstad, Salwa Suliman and Kamal Mustafa

136 *Recent Advances in Vertical Alveolar Bone Augmentation Using Additive Manufacturing Technologies*

Cedryck Vaquette, Joshua Mitchell and Sašo Ivanovski

152 *Application of BMP in Bone Tissue Engineering*

Liwei Zhu, Yuzhe Liu, Ao Wang, Zhengqing Zhu, Youbin Li, Chenyi Zhu, Zhenjia Che, Tengyue Liu, He Liu and Lanfeng Huang

177 *Mineralizing Coating on 3D Printed Scaffolds for the Promotion of Osseointegration*

Abshar Hasan, Romain Bagnol, Robert Owen, Arsalan Latif, Hassan M. Rostam, Sherif Elsharkawy, Felicity R. A. J. Rose, José Carlos Rodríguez-Cabello, Amir M. Ghaemmaghami, David Eglin and Alvaro Mata



OPEN ACCESS

EDITED AND REVIEWED BY

Ranieri Cancedda,
Independent researcher, Genova, Italy

*CORRESPONDENCE

Barbara Zavan,
zvnbb@unife.it

[†]These authors share senior authorship

SPECIALTY SECTION

This article was submitted to Tissue Engineering and Regenerative Medicine, a section of the journal Frontiers in Bioengineering and Biotechnology

RECEIVED 28 June 2022

ACCEPTED 04 July 2022

PUBLISHED 09 August 2022

CITATION

Brunello G, Donos N, Sivoilella S and Zavan B (2022), Editorial: Advances in additive manufacturing technologies for the production of tissue-engineered bone scaffolds for dental applications. *Front. Bioeng. Biotechnol.* 10:980430. doi: 10.3389/fbioe.2022.980430

COPYRIGHT

© 2022 Brunello, Donos, Sivoilella and Zavan. This is an open-access article distributed under the terms of the Creative Commons Attribution License (CC BY). The use, distribution or reproduction in other forums is permitted, provided the original author(s) and the copyright owner(s) are credited and that the original publication in this journal is cited, in accordance with accepted academic practice. No use, distribution or reproduction is permitted which does not comply with these terms.

Editorial: Advances in additive manufacturing technologies for the production of tissue-engineered bone scaffolds for dental applications

Giulia Brunello^{1,2}, Nikolaos Donos^{3†}, Stefano Sivoilella^{2†} and Barbara Zavan^{4*†}

¹Department of Oral Surgery, University Hospital of Düsseldorf, Düsseldorf, Germany, ²Department of Neurosciences, University of Padua, Padua, Italy, ³Centre for Oral Clinical Research, Barts and the London School of Medicine and Dentistry, Institute of Dentistry, Queen Mary University of London, London, United Kingdom, ⁴Department of Medical Sciences, University of Ferrara, Ferrara, Italy

KEYWORDS

bone regeneration, 3D printing, biocompatibility, regenerative medicine, personalized therapy, additive manufacturing

Editorial on the Research Topic

Advances in Additive Manufacturing Technologies for the Production of Tissue-Engineered Bone Scaffolds for Dental Applications

In the attempt to repair bone tissue defects, a plethora of bone substitute materials of various origins have been utilized so far. Despite the fact that autogenous, allogenic and xenogeneic bone grafts still constitute valid therapeutic options in daily practice, bone tissue engineering strategies have gained popularity for the regeneration of damaged tissues (Cao et al.). Cells, scaffolds and growth factors represent the key elements of tissue engineering. Due to the ability of the bone to self-regenerate due to the migration of cells and growth factors from the adjacent tissues, the success of bone tissue engineering largely relies in the ability of the scaffold to act as a template for guiding tissue regeneration. Indeed, not only cell-laden scaffolds, but also cell-free biomimetic matrixes are considered appealing solutions in bone regeneration, as they can stimulate cell colonization and recruitment from neighbouring tissues. In this context, additive manufacturing (AM) technologies have gained considerable interest owing to their versatility and the possibility to produce personalized scaffolds with complex geometry, matching the patient's bone defects (Brunello et al.; Latimer et al.).

Although several endeavours intended to promote vertical bone augmentation have been reported, they are characterized by inconsistent long-term results and varying degrees of success (Retzepi and Donos, 2010; Donos et al., 2015; Urban et al., 2019). AM is endorsing novel alveolar ridge augmentation strategies for vertical bone gain, aiming at achieving prolonged volumetric space maintenance during extra-skeletal bone

remodelling and maturation (Vaquette et al.). Nevertheless, the routine clinical use of AM is still very limited and is based on single case reports (Mangano et al.).

Combining stem cells with 3D scaffolds may represent a step forward in the pursuit of a faster and improved bone healing. Cells can be directly seeded onto 3D scaffolds before implantation or can be incorporated within biodegradable scaffolds during the manufacturing process using bioprinting techniques (Latimer et al.). As an alternative cell delivery method, cell-encapsulated hydrogel-scaffold constructs have been developed for the controlled release of stem cells at the surgical site. When 3D cell cultures are preferred over monolayer cultures, the encapsulation of the self-assembled cell aggregates within a hydrogel has the advantage to protect the 3D assemblage from disaggregation. In an ectopic bone formation model in mice, a 3D printed polymeric scaffold was found to promote ectopic mineralization to a higher extent when combined with a hydrogel containing spheroid bone marrow-derived stem cells (BMSCs), than when combined with a hydrogel laden with dissociated BMSCs (Shanbhag et al.; Shanbhag et al.).

Other strategies to foster bone tissue ingrowth and mineralization within porous additive manufactured scaffolds rely in the chemical and topographical modification of their surfaces. An acellular organic-inorganic mineralizing construct has been successfully produced, combining a 3D printed nylon scaffold with an elastin-like recombinamer coating, that can be pre-mineralized in the lab prior to implantation (Hasan et al.).

Scaffold bio-functionalization with bioactive agents offers the great advantage of inducing stem-cell homing, while avoiding the several concerns related to stem cell implantation. Among various molecules, the incorporation of bone morphogenetic protein 2 (BMP-2) in 3D scaffolds has been widely explored, demonstrating its ability to trigger stem cell osteogenic differentiation (Zhu et al.). As such, 3D collagen-based matrices functionalized with BMP-2 or with an enamel matrix derivative were found to stimulate *in vitro* the osteogenic commitment of osteoprogenitor cell lines (Lin et al.).

Beside exogenous growth factors, autologous platelet concentrates (APCs) can be employed to enhance the biological properties of bone substitutes. Promising *in vitro* results have been reported in this Research Topic, where the addition of injectable platelet-rich fibrin to different 3D scaffolds positively affected osteoblast cell viability and metabolic activity (Kyyak et al.).

In dentistry, bone augmentation procedures are performed in the vast majority of the cases to restore adequate alveolar ridge dimensions for dental implant placement (Donos et al., 2008; Retzepi and Donos, 2010; Donos et al., 2019). Beside the treatment of alveolar bone deficiencies aiming at replacing missing teeth with implant-supported restorations, the regeneration of the periodontal tissues around compromised

teeth as well as of the pulp-dentin complex or of the whole tooth is attracting increasing attention (Latimer et al.). Up-to-date periodontal regeneration strategies include the use of stem cells and the design of multi-material and micropatterned scaffolds, favouring compartmentalized tissue healing and periodontal fiber orientation. Despite the significant advancements noticed in this field, further studies are required to improve the complex multi-tissue periodontal regeneration (Latimer et al.). Furthermore, different tissue engineering strategies, including and not limited to the use of bio-printing, have been introduced to regenerate dental tissues (Cao et al.; Latimer et al.). However, the development of fully formed functional teeth seems far from being achievable in the near future. A deeper understanding of cell-cell and cell-matrix interactions during tooth formation, together with progresses in AM, is needed so that bio-engineered teeth become a clinical reality.

This issue focused mainly in bone regeneration in the oral and maxilla-facial area. However, a broader view on recent developments in the area of orthopaedics was also maintained. Therefore, clinically challenging topics such as non-union fractures and delayed bone healing can also be addressed in the information provided in this issue (Zhu et al.).

Taking into consideration the ageing population and the fact that chronic diseases associated with bone healing and metabolism (i.e., osteoporosis) have high prevalence, novel ways addressing bone healing should be introduced. In this context, the discovery of selective drugs for targeting osteoporosis is particularly relevant. In this issue, an *in vitro* study utilizing BMSCs, leonurine, a natural herbal compound, promoted BMSC osteoblastic differentiation by activating autophagy, making it a potential candidate in the treatment of osteoporosis (Zhao et al.).

However, bone fractures are not limited only to osteoporotic conditions. Special attention has to be devoted to the treatment of pathologies occurring at the growth plate in the paediatric age. This cartilaginous region, which acts as the primary centre for endochondral bone formation in immature long bones, is particularly susceptible to fractures. Current treatments often lead to the development of an undesired bone bridge and to related growth disturbance risks. AM, in combination with cell seeding and active substance delivery, could offer alternative options to existing clinical solutions, in order to achieve cartilaginous tissue reconstruction at the growth plate, thus avoiding the formation of calcified physal scars (Wang et al.).

Overall, AM, in combination with tissue engineering strategies, offers emerging opportunities in bone regeneration, by enabling the production and the biofunctionalization of customized site-specific 3D scaffold with tunable properties. Looking at the future, remarkable efforts should be directed to the optimization of current technologies and to overcome the hurdles that are delaying the translation of additive manufactured tissue-engineered bone scaffolds into everyday clinical use.

Author contributions

All authors made substantial contributions to the conception of the work; GB drafted the manuscript; ND, SS and BZ edited and proof-read the manuscript. All authors read and approved the submitted version.

Acknowledgments

We sincerely thank the efforts and contributions of all the authors of this successful research topic. We are extremely grateful to all the reviewers for the time and expertise devoted to reviewing the articles, as well as to Frontiers for the exceptional editorial support along the whole process.

References

- Brunello, G., Sivoletta, S., Meneghello, R., Ferroni, L., Gardin, C., Piattelli, A., et al. (2016). Powder-based 3D printing for bone tissue engineering. *Biotechnol. Adv.* 34, 740–753. doi:10.1016/j.biotechadv.2016.03.009
- Donos, N., Dereka, X., and Calciolari, E. (2019). The use of bioactive factors to enhance bone regeneration: A narrative review. *J. Clin. Periodontol.* 46 (Suppl. 21), 124–161. doi:10.1111/jcpe.13048
- Donos, N., Dereka, X., and Mardas, N. (2015). Experimental models for guided bone regeneration in healthy and medically compromised conditions. *Periodontol.* 2000 68, 99–121. doi:10.1111/prd.12077

Conflict of interest

The authors declare that the research was conducted in the absence of any commercial or financial relationships that could be construed as a potential conflict of interest.

Publisher's note

All claims expressed in this article are solely those of the authors and do not necessarily represent those of their affiliated organizations, or those of the publisher, the editors and the reviewers. Any product that may be evaluated in this article, or claim that may be made by its manufacturer, is not guaranteed or endorsed by the publisher.

- Donos, N., Mardas, N., and Chadha, V. (2008). Clinical outcomes of implants following lateral bone augmentation: Systematic assessment of available options (barrier membranes, bone grafts, split osteotomy). *J. Clin. Periodontol.* 35, 173–202. doi:10.1111/j.1600-051x.2008.01269.x
- Retzepi, M., and Donos, N. (2010). Guided bone regeneration: Biological principle and therapeutic applications. *Clin. Oral Implants Res.* 21, 567–576. doi:10.1111/j.1600-0501.2010.01922.x
- Urban, I. A., Montero, E., Monje, A., and Sanz-Sánchez, I. (2019). Effectiveness of vertical ridge augmentation interventions: A systematic review and meta-analysis. *J. Clin. Periodontol.* 46 (Suppl. 21), 319–339. doi:10.1111/jcpe.13061



Activation of Human Osteoblasts via Different Bovine Bone Substitute Materials With and Without Injectable Platelet Rich Fibrin *in vitro*

Solomiya Kyyak¹, Sebastian Blatt¹, Eik Schiegnitz¹, Diana Heimes¹, Henning Staedt^{2,3}, Daniel G. E. Thiem¹, Keyvan Sagheb¹, Bilal Al-Nawas¹ and Peer W. Kämmerer^{1*}

¹ Department of Oral- and Maxillofacial Surgery, University Medical Center Mainz, Mainz, Germany, ² Private Practice, University Medical Center Rostock, Rostock, Germany, ³ Department of Prosthodontics and Materials Science, University Medical Center Rostock, Rostock, Germany

OPEN ACCESS

Edited by:

Nikos Donos,
Queen Mary University of London,
United Kingdom

Reviewed by:

Livia Visai,
University of Pavia, Italy
Carlos Fernando de Almeida
Barros Mourao,
Fluminense Federal University, Brazil

*Correspondence:

Peer W. Kämmerer
peer.kaemmerer@unimedizin-
mainz.de

Specialty section:

This article was submitted to
Tissue Engineering and Regenerative
Medicine,
a section of the journal
Frontiers in Bioengineering and
Biotechnology

Received: 26 August 2020

Accepted: 21 January 2021

Published: 17 February 2021

Citation:

Kyyak S, Blatt S, Schiegnitz E,
Heimes D, Staedt H, Thiem DGE,
Sagheb K, Al-Nawas B and
Kämmerer PW (2021) Activation
of Human Osteoblasts via Different
Bovine Bone Substitute Materials
With and Without Injectable Platelet
Rich Fibrin *in vitro*.
Front. Bioeng. Biotechnol. 9:599224.
doi: 10.3389/fbioe.2021.599224

Introduction: The aim of the *in vitro* study was to compare the effect of four bovine bone substitute materials (XBSM) with and without injectable platelet-rich fibrin for viability and metabolic activity of human osteoblasts (HOB) as well as expression of alkaline phosphatase (ALP), bone morphogenetic protein 2 (BMP-2), and osteonectin (OCN).

Materials and Methods: Cerabone® (CB), Bio-Oss® (BO), Creos Xenogain® (CX) and MinerOss® X (MO) ± i-PRF were incubated with HOB. At day 3, 7, and 10, cell viability and metabolic activity as well as expression of ALP, OCN, and BMP-2, was examined.

Results: For non-i-PRF groups, the highest values concerning viability were seen for CB at all time points. Pre-treatment with i-PRF increased viability in all groups with the highest values for CB-i-PRF after 3 and 7 and for CX-i-PRF after 10 days. For metabolic activity, the highest rate among non-i-PRF groups was seen for MO at day 3 and for CB at day 7 and 10. Here, i-PRF groups showed higher values than non-i-PRF groups (highest values: CB + i-PRF) at all time points. There was no difference in ALP-expression between groups. For OCN expression in non-i-PRF groups, CB showed the highest values after day 3, CX after day 7 and 10. Among i-PRF-groups, the highest values were seen for CX + i-PRF. At day 3, the highest BMP-2 expression was observed for CX. Here, for i-PRF groups, the highest increase was seen for CX + i-PRF at day 3. At day 7 and 10, there was no significant difference among groups.

Conclusion: XBSM sintered under high temperature showed increased HOB viability and metabolic activity through the whole period when compared to XBSM manufactured at lower temperatures. Overall, the combination of XBSM with i-PRF improved all cellular parameters, ALP and BMP-2 expression at earlier stages as well as OCN expression at later stages.

Keywords: bone substitute, bovine bone, platelet rich fibrin (PRF), *in vitro*, osteoblast, vitality, proliferation, PCR

INTRODUCTION

The composition of bovine bone substitutes is similar to human bone due to the preserved microstructure of the osseous frame (Glowacki, 2005; Yamada and Egusa, 2018). These xenografts are known for osteoconduction and a low (if any) absorbability rate (Klein et al., 2013b; Dau et al., 2016). Deproteinization potentially allows elimination of transmission risk and antigenicity (Lei et al., 2015). However, different cleaning and manufacturing methods may affect the regeneration capacity of the a bovine bone substitute material. For example, manufacturing of deproteinized bovine bone by sintering consists of high temperature treatment with stepwise heating up to >1,000°C leading to the removal of all organic components including collagen (Lei et al., 2015). On contrary, manufacturing with lower temperatures usually comprise an additional chemical treatment, i.e., with sodium hydroxide with efficiently inactivated viruses (Tadic and Epple, 2004). Cerabone® (Botiss, Zossen, Germany) is produced via three-stage temperature treatment including a final sintering at >1,200°C, hence all organic compounds are removed and potential prions, bacteria and viruses are eliminated. This preparation process might alter the microstructure (Perić Kačarević et al., 2018). However, it has been shown that Cerabone® resembles the structure of natural bone with high porosity and rough surface (Trajkovski et al., 2018). Bio-Oss® (Geistlich Pharma AG, Wolhusen, Switzerland) has a fiber-like surface with a much smaller crystal size (Barbeck et al., 2015; Perić Kačarević et al., 2018). It is manufactured at a lower temperature of 300°C followed by sodium hydroxide treatment (Kübler et al., 2004); thus, it is considered to be a hydroxyapatite ceramic with a high porosity including large interconnective pores and residual proteins (Kübler et al., 2004; Klein et al., 2009). Creos Xenogain® (Nobel Biocare GmbH, Gothenburg, Sweden) is produced by sodium hypochloride treatment followed by heating under 400°C. MinerOss® X (BioHorizons, Birmingham, United Kingdom) is also produced via low-heat processing of bovine bone, preserving the coarseness of bone with a high porosity.

In *in vitro* and *in vivo* studies, for injectable platelet-rich fibrin (i-PRF) a high share of leukocytes and platelets was proven. It promotes fibroblast migration and has a potential to release higher concentration of cytokines and selective growth factors over time when compared to PRP/L-PRF and A-PRF (Ghanaati et al., 2014; El Bagdadi et al., 2017; Miron et al., 2017; Wend et al., 2017; Choukroun and Ghanaati, 2018; Wang et al., 2018). Additionally, due to its consistency as well as composition, i-PRF can be used in combination with various biomaterials in order to increase their bioactivity in bone/soft tissue regeneration, and to improve healing in impaired wound healing cases (Wend et al., 2017; Miron and Zhang, 2018; Abd El Raouf et al., 2019). Thus, a combination of a bovine bone substitute material with i-PRF may be promising in terms of soft and hard tissue regeneration (Mourão et al., 2015). In our previous *in vitro* study (Kyyak et al., 2020), we compared an allograft and a bovine bone substitute material with and without i-PRF in regard of their effect on human osteoblasts' viability, gap closure and metabolic activity. Here, the allogenic material showed an improved performance,

possibly due to its (minimal) osteoinductive potential. The previous study was limited as there was only one commercially available bovine bone substitute material under examination. Thus, the aim of the study was to compare four different commercially available bovine bone substitutes with and without i-PRF for viability, metabolic activity, and differentiation of human osteoblasts. The null hypothesis was that pre-treatment of bovine bone substitute materials with i-PRF affects osteoblast viability, metabolic activity, and differentiation. A secondary hypothesis was that there are also differences between the different xenogenic materials.

MATERIALS AND METHODS

Bone Substitute Materials

In the study, four bone substitute materials of bovine origin and their combination with i-PRF were included: cerabone® (CB, botiss biomaterials GmbH, Zossen, Germany, granularity: 1–2 mm), Bio-Oss® (BO, Geistlich Pharma AG, Wolhusen, Switzerland, granularity: 1–2 mm), CREOS Xenogain® (CX, Nobel Biocare GmbH, Gothenburg, Sweden, granularity: 1–2 mm), MinerOss® X (MO, BioHorizons, Birmingham, United Kingdom, granularity: 0.5–1 mm).

I-PRF

In accordance with the ethical standards of the national research committee (Ärztchamber Rheinland-Pfalz, no. "2019-14705_1"), 10 ml peripheral venous blood per sample was collected from three healthy donors without severe illnesses after puncture of the cephalic or the median cubital vein. The vacutainer system and specific sterile plain vacuum tubes with additional silicone within their coating surface for solid (A-PRF+, Mectron, Carasco, Italy) and liquid PRF were used, respectively (iPRF, Mectron, Carasco, Italy). PRF was directly manufactured at a fixed angle rotor with a radius of 110 mm with 1,200 rpm and a relative centrifugal force of 177 g for 8 min (Duo centrifuge, Mectron, Carasco, Italy) after manufacturer's instructions as described (Blatt et al., 2020).

Cells

For the *in vitro* study, commercially available human osteoblasts from one donor were chosen (HOB, PromoCell, Heidelberg, Germany). A standard HOB medium was applied for cultivation including fetal calf serum (FCS, Gibco Invitrogen, Karlsruhe, Germany), Dulbecco's modified Eagle's medium (DMEM, Gibco Invitrogen), dexamethasone (100 nmol/l, Serva Bioproducts, Heidelberg, Germany), L-glutamine (Gibco Invitrogen), and streptomycin (100 mg/ml, Gibco Invitrogen). Cultivation of HOB was administered at the air temperature of 37°C, 95% humidity 95 and 5% of CO₂. The passaging of HOB was carried out when reaching 70% confluence by application of 0.25% trypsin (Seromed Biochrom KG, Berlin, Germany). Passage five HOB were seeded in a density of 5×10^4 cells per well. Afterward, 100 mg of each bone substitute material were added to the corresponding wells with HOB. Into the first half of the wells, 150 µl of i-PRF was applied, one well with each bone substitute material was left without i-PRF. Incubation of the

compositions was divided into 3, 7, and 10 days at 37°C, 95% humidity, and 5% CO₂. For negative controls, wells without bone substitute material as well as with i-PRF without bone substitute material were used.

Cell Viability

For cell viability, CellTracker staining (Life Technologies, Thermo Fisher Scientific, Darmstadt, Germany; catalog number: C34552) was applied on day 3, 7, and 10. Red dye was produced following the manufacturer's instructions. After the culture media was removed, Red dye was applied into wells and incubated for 30 min in 37°C. Serum-free medium was added, following the removal of the Red dye, and incubated for 30 min in 37°C. Red fluorescence was observed using a fluorescence BZ-9000 microscope (Keyence, Osaka, Japan). ImageJ software (ACTREC, Navi Mumbai, India) was used for cell quantification (Fuchs et al., 2009). At first, images (magnification 10×) were converted to grayscale. Through image subtraction, a correction of the background was conducted. Cell structures were extracted from the background using automatic thresholding and the area fraction (%) was calculated. Measures were conducted in triplication for each group and each time point (three time points).

Cellular Metabolic Activity

Metabolic activity was measured by 3-(4,5-Dimethylthiazol-2-yl)-2,5-diphenyltetrazolium bromide (MTT) assay on day 3, 7, and 10. Briefly, MTT (200 µl, 2 mg/ml) was added to the wells and incubated for 4 h at 37°C. Culture medium was removed, and lysis buffer (10 ml) was pipetted into each well. Plates values were acquired using a fluorescence microplate reader (570 nm; Versamax, Molecular Devices, San Jose, CA, United States). Measures were conducted in triplication for each group and each time point (three time points).

Expression of Bone Gene Markers

In accordance with Liu et al. (2003), the runx-2-dependent early osteogenic differentiation marker collagen alkaline phosphatase (ALP) as well as the late differentiation marker osteocalcin (OCN) was examined, whose expression is also highly controlled by runx-2 levels (Stein et al., 2004). ALP plays an important regulatory role during matrix mineralization (Hessle et al., 2002; Anderson et al., 2004). For osteogenic cells, the integrin subunits β_1 and α_v have been shown to trigger effects of cytokines like bone morphogenetic protein 2 (BMP-2) (Lai and Cheng, 2005). OCN, which is only synthesized by mature osteoblasts, is directly associated with bone matrix mineralization as well (Lian et al., 1998, 2004; Klein et al., 2013a).

For this purpose, total RNA was extracted after day 3, 7, and 10 (Qiagen, Hilden, Germany). Subsequently, RNA was converted to cDNA with the help of iScript cDNA synthesis kit (BioRad, Hercules, United States) in accordance to manufacturers' recommendations. For normalization, internal control Actin and GAPDH genes were used. The sequences of the primers are presented in Table 1. PCR was conducted

TABLE 1 | Primers Actin, GAPDH, ALP, OCN, and BMP-2 and their sequences.

Primers	Sequences
Actin	sense-GGAGCAATGATCTTGATCTT antisense-CTTCCTGGGCATGGAGTCCT
GAPDH	sense-AAAACCCCTGCCAATTATGAT antisense-CAGTGAGGGTCTCTCTCTTC
ALP	sense- ACTGCAGACATTCTCAAAGC antisense-GAGTGAGTGAGTGAGCAAGG
OCN	sense-GSAAAGGTGCAGCCTTTGGT antisense-GGCTCCCAGCCATTGATACAG
BMP-2	sense-(1)-CCTGAAACAGAGACCCACCC antisense-(1)-TCTGGTCACGGGAATTCG

using a CFX Connect Real-Time PCR Detection System (BioRad, Germany) and SYBR Green Supermix (BioRad, Hercules, United States). Following proportions were applied: 11 µl of SYBR, 1 µl of primer sense, 1 µl of primer antisense, and 5 µl RNA-free water. The conditions of the thermal cycler were the following: first step—95°C for 3 min; second step (repeated 39 times)—95°C for 10 s, then 58°C for 30 s and finally 72°C for 20 s; final step—65°C for 0.5 s and then 95°C for 5 s. Quantification of gene expression was conducted through Ct value. Measures were conducted in triplication for each group and each time point (three time points).

Statistical Analyses

Data was converted into mean values with the estimate of its standard error of the mean (SEM) (for parametric data) and median values (for non-parametric data). Numbers were round off to second decimal place. Normal distribution was determined by Shapiro-Wilk test (SWT). For comparison of two groups, two-sided Student's *t*-tests for paired samples (*t*-test) were applied in case of normal distributions. In case of non-normal distributions, Mann-Whitney test (MWT) was applied to compare two groups. Kruskal-Wallis rank sum test (KWT) was applied to compare all groups. A *p*-value of ≤ 0.05 was considered to be statistically descriptive significant. Data was visualized using bar charts with error bars.

RESULTS

Cell Viability

At day 3, the highest cell viability was seen in the Cerabone® (CB) group, which was significantly higher when compared to BioOss® (BO; $p \leq 0.05$, *t*-test) that showed the lowest indexes among all tested materials. Viability of Xenogain® (CX) was significantly higher when compared to controls ($p \leq 0.05$, *t*-test) (Figures 1, 2A). At day 7, controls had the highest cell viability ($p > 0.05$, MWT). Additionally, when compared to other bovine bone substitute material (XBSM) groups, CB presented the highest indexes ($p > 0.05$, *t*-test), followed by CX ($p > 0.05$, *t*-test) and MO ($p > 0.05$, *t*-test). At day 10, the highest viability value was seen for CB, followed by CX (when compared to controls

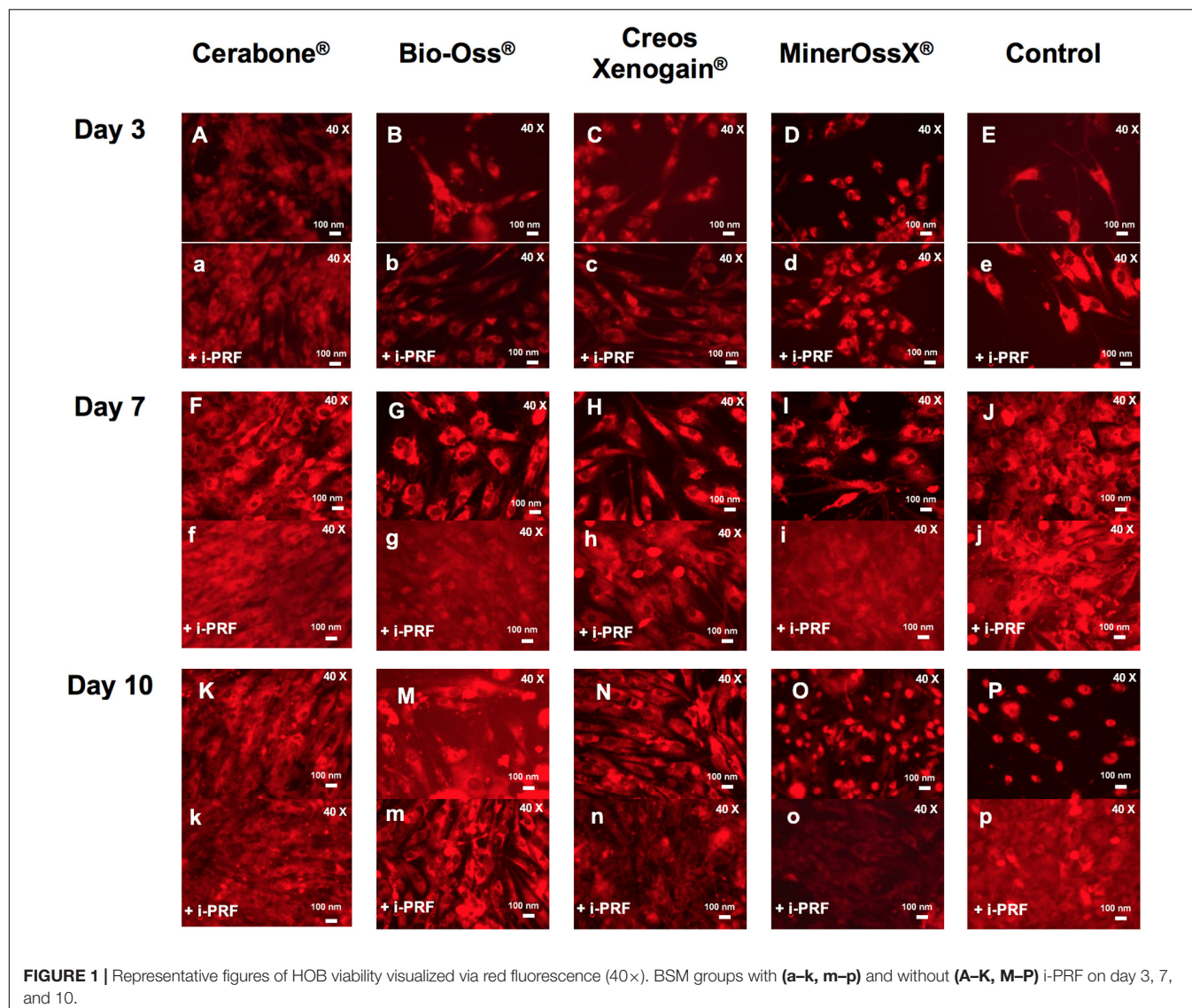


FIGURE 1 | Representative figures of HOB viability visualized via red fluorescence (40 \times). BSM groups with (a–k, m–p) and without (A–K, M–P) i-PRF on day 3, 7, and 10.

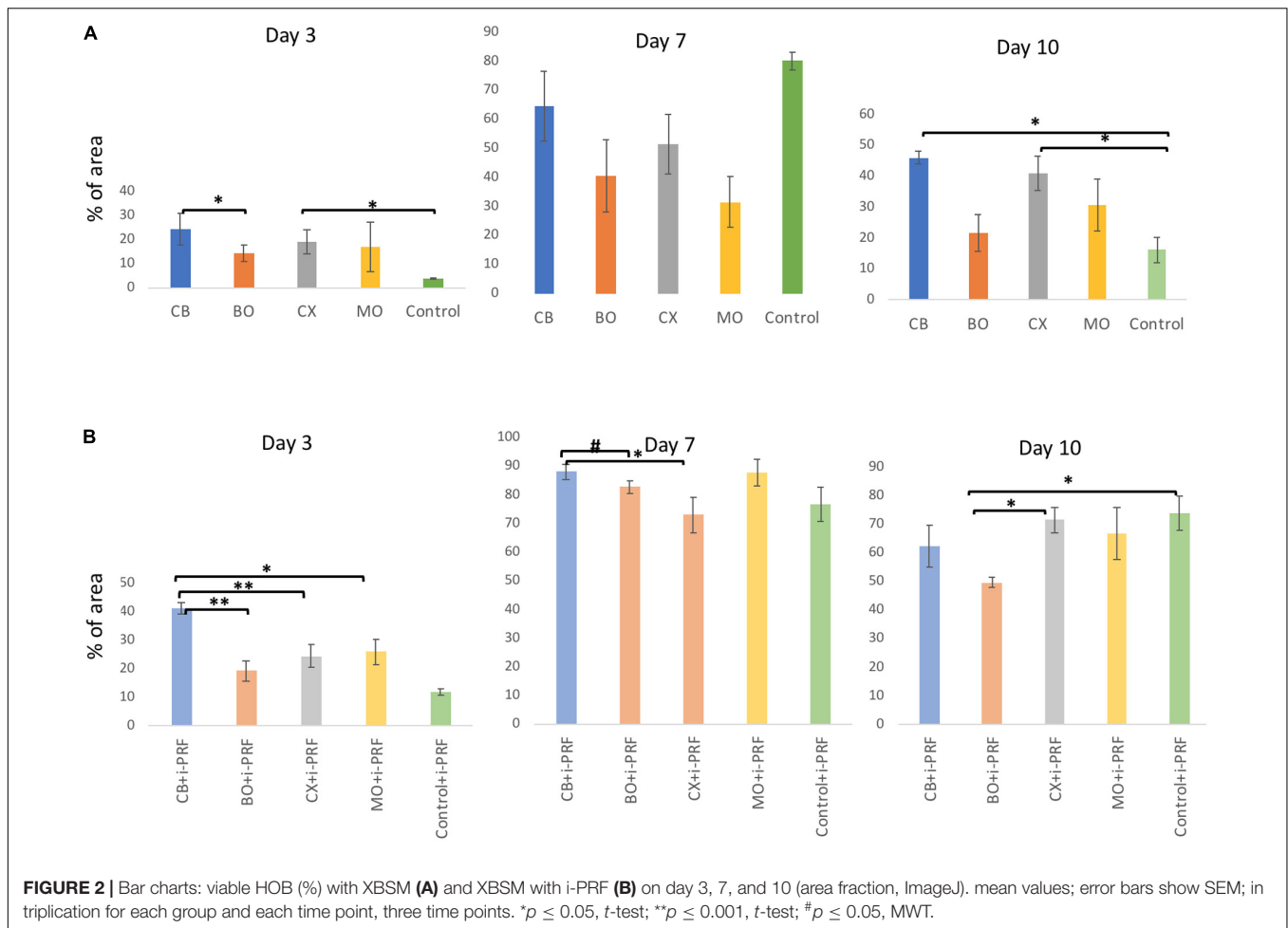
($p \leq 0.05$, t -test), BO and MO ($p > 0.05$, MWT). The lowest rate showed BO ($p > 0.05$, MWT) (Figures 1, 2A and Table 2A).

At day 3, among i-PRF containing groups, significant higher values were observed for CB + i-PRF when compared to BO + i-PRF ($p \leq 0.001$, t -test), CX + i-PRF ($p \leq 0.001$, t -test), MO + i-PRF ($p \leq 0.05$, t -test), and Control + i-PRF groups ($p > 0.05$, MWT). Control + i-PRF showed the lowest viability among i-PRF-groups (significant in comparison to all others, $p > 0.05$, MWT) and among i-PRF-XBSM groups, the lowest indexes were seen for BO + i-PRF ($p > 0.05$, t -test) (Figures 1, 2 and Table 2). At day 7, the highest increase in viability was observed in CB + i-PRF groups [when compared to BO + i-PRF ($p \leq 0.05$, MWT), CX + i-PRF ($p \leq 0.05$, t -test), controls ($p > 0.05$, t -test)] and MO + i-PRF groups ($p > 0.05$, MWT). At day 10, the highest viability was seen for controls, followed by CX + i-PRF [when compared to BO + i-PRF ($p \leq 0.05$, t -test), CB + i-PRF, and MO + i-PRF (each: $p > 0.05$, MWT)] (Figures 1, 2B and Table 2B).

All i-PRF treated groups showed higher values in comparison to their equivalent pure non-i-PRF groups through the whole period. At day 7, values of all groups doubled in comparison to day 3 and were the highest of all the periods (Figures 1, 2 and Table 2).

Cell Metabolic Activity

On the third day, MTT test showed the non-significant highest metabolic activity in MO ($p > 0.05$, t -test), followed by CX ($p > 0.05$, t -test). The least metabolic activity was observed for BO ($p > 0.05$, t -test). At day 7, the non-significant highest values were observed for CB, followed by controls ($p > 0.05$, t -test, MWT). At day 10, considerably higher values were seen in CB [when compared to BO ($p > 0.05$, MWT), CX ($p \leq 0.01$, t -test), MO ($p \leq 0.05$, t -test), and controls ($p > 0.05$, t -test)], followed by controls (in comparison to MO ($p \leq 0.05$, t -test), CX ($p > 0.05$, t -test), and BO ($p > 0.05$, MWT) (Figure 3A and Table 3A). At day 3, 7, and 10 among i-PRF-groups, the non-significant highest



metabolic activity was seen in CB + i-PRF ($p > 0.05$, t -test) and controls + i-PRF ($p > 0.05$, t -test). The lowest metabolic activity was seen for MO + i-PRF on day 3 and 7 as well as BO + i-PRF on day 10 (Figure 3B and Table 3B).

Overall, groups containing i-PRF showed a higher value than non-i-PRF groups, except for MO on day 3. Metabolic activity levels of all groups had a general tendency to decline through the whole period (Figure 3 and Table 3).

Expression of Bone Gene Markers

Alkaline Phosphatase (ALP) Expression

On day 3, 7, and 10, all groups showed almost the same ALP expression level ($p > 0.05$, t -test), except MO, which didn't show any expression at all through the whole period. On day 3 and 10, in the i-PRF-groups, the values were also almost on the same level ($p > 0.05$, t -test) with no expression in MO + i-PRF on day 10. At day 7, the highest expression was observed in BO + i-PRF [when compared to MO + i-PRF ($p \leq 0.05$, t -test)], followed by CB + i-PRF ($p > 0.05$, t -test).

Overall, on day 3, 7, and 10, i-PRF-groups had slightly increased ALP expression over non-treated bone substitute materials, with the exception of CX + i-PRF on day 7 and MO + i-PRF on day 10.

Osteonectin (OCN) Expression

On day 3, CB had the highest OCN expression [significant in comparison to BO ($p \leq 0.05$, t -test)]. On day 7, CX showed a significantly increased expression when compared to BO ($p \leq 0.05$, t -test) and (non-significant) to CB ($p > 0.05$, t -test). On day 10, CX had significant highest values when compared to BO ($p \leq 0.05$, t -test) and CB ($p \leq 0.001$, t -test). There was no expression in MO through the whole period. On day 3, among i-PRF treated groups, the non-significant highest value of all groups was observed in CX + i-PRF ($p > 0.05$, t -test), the non-significant lowest in CB + i-PRF ($p > 0.05$, t -test). MO + i-PRF showed no OCN expression. On day 7, values of CX + i-PRF were higher than of MO + i-PRF ($p \leq 0.05$, t -test) and CB + i-PRF ($p > 0.05$, t -test), followed by BO + i-PRF ($p > 0.05$, t -test). On day 10, CX + i-PRF showed the non-significant highest expression among treated groups ($p > 0.05$, t -test). Through the whole period, pre-treated groups showed increased expression rates when compared to non-treated XBSM, except for MO + i-PRF on day 3.

Bone Morphogenetic Protein 2 (BMP-2) Expression

Considering BMP-2 expression, on the day 3, the significant highest rate was observed in CX in comparison to BO ($p \leq 0.05$,

TABLE 2 | Cell viability of XBSM (A) and XBSM with i-PRF (B) by area fraction (%) on days 3, 7, and 10; experiments in triplication for each group and each time point, three time points.

XBSM	Day 3					Day 7					Day 10				
	CB	BO	CX	MO	Control	CB	BO	CX	MO	Control	CB	BO	CX	MO	Control
	Mean value with SEM**Median	Mean value with SEM**Median	Mean value with SEM**Median	Mean value with SEM**Median	Mean value with SEM**Median	Mean value with SEM**Median	Mean value with SEM**Median	Mean value with SEM**Median	Mean value with SEM**Median	Mean value with SEM**Median	Mean value with SEM**Median	Mean value with SEM**Median	Mean value with SEM**Median	Mean value with SEM**Median	Mean value with SEM**Median
A	*24.27 + 6.63	*14.37 + 3.29	*19.11 + 4.81	*17.10 + 10.27	*3.75 ± 0.28	*64.46 + 11.99	**28.50	*51.51 + 10.21	**28.00	**80.53	*46.0 + 2.14	**24.77	*40.82 + 5.6	**30.42	*16.19 + 4.18
	*Mean values for parametric data.														
	**Median values for non-parametric data.														
XBSM	CB+i-PRF	BO+i-PRF	CX+i-PRF	MO+i-PRF	Control+i-PRF	CB+i-PRF	BO+i-PRF	CX+i-PRF	MO+i-PRF	Control+i-PRF	CB+i-PRF	BO+i-PRF	CX+i-PRF	MO+i-PRF	Control+i-PRF
	Mean value with SEM**Median	Mean value with SEM**Median	Mean value with SEM**Median	Mean value with SEM**Median	Mean value with SEM**Median	Mean value with SEM**Median	Mean value with SEM**Median	Mean value with SEM**Median	Mean value with SEM**Median	Mean value with SEM**Median	Mean value with SEM**Median	Mean value with SEM**Median	Mean value with SEM**Median	Mean value with SEM**Median	Mean value with SEM**Median
	Mean value with SEM**Median	Mean value with SEM**Median	Mean value with SEM**Median	Mean value with SEM**Median	Mean value with SEM**Median	Mean value with SEM**Median	Mean value with SEM**Median	Mean value with SEM**Median	Mean value with SEM**Median	Mean value with SEM**Median	Mean value with SEM**Median	Mean value with SEM**Median	Mean value with SEM**Median	Mean value with SEM**Median	Mean value with SEM**Median
B	*41.25 + 1.92	*19.33 + 3.68	*24.49 ± 4.07	*25.95 + 4.51	**11.2	*87.98 + 2.44	**84.34	*73.08 + 6.11	**90.19	*76.7 + 5.86	**56.22	*49.71 + 1.86	*71.72 + 4.44	**64.42	*73.95 + 6.15
	*Mean values for parametric data.														
	**Median values for non-parametric data.														

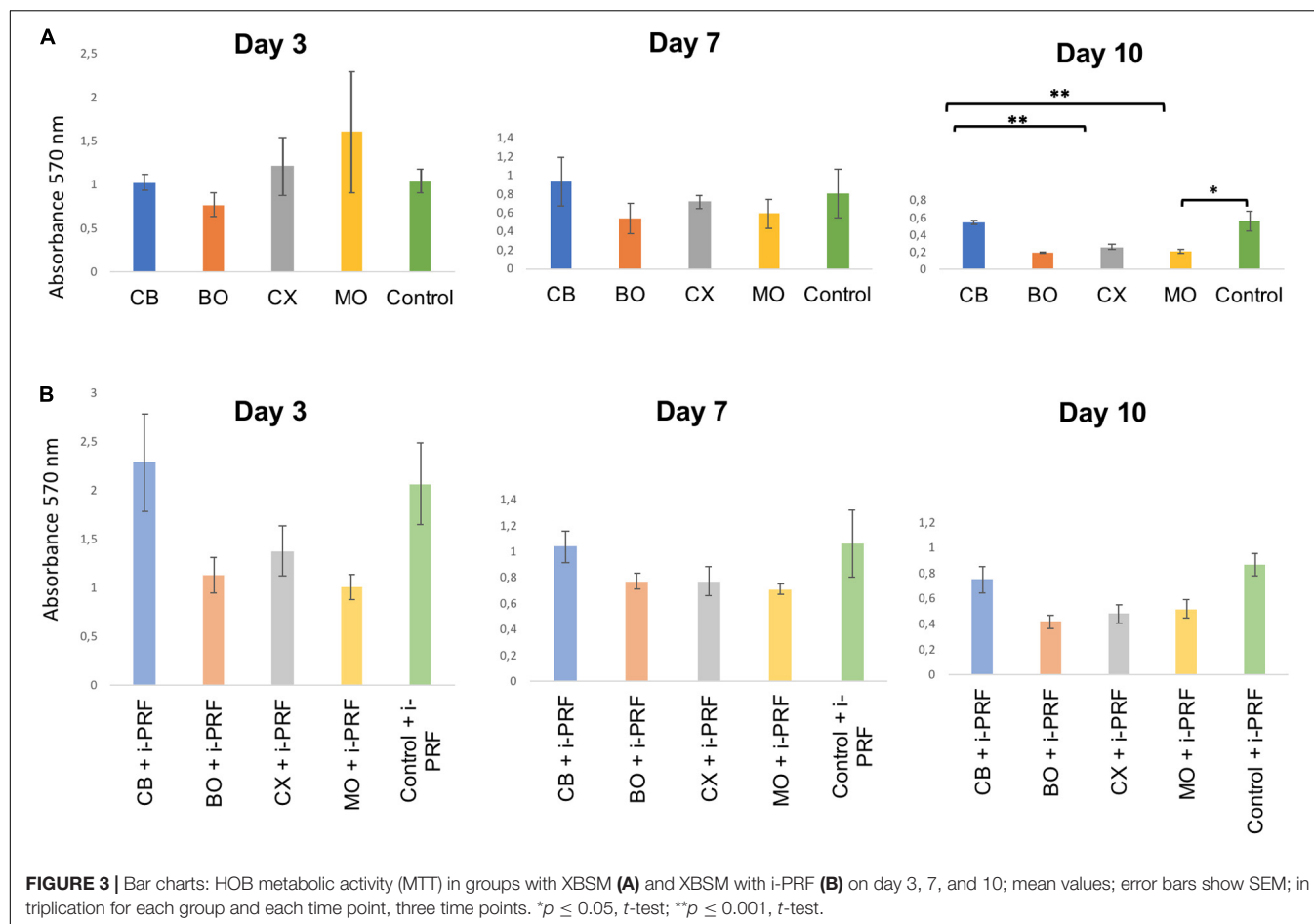
t-test), followed by CB ($p > 0.05$, *t*-test). On day 7 and 10, there was no considerable difference among the groups. Through the whole period, there was no expression in MO. On day 3, among the i-PRF-groups, CX + i-PRF demonstrated a significant increase when compared to MO + i-PRF ($p \leq 0.05$, *t*-test) as well as a non-significant increase when compared to BO + i-PRF and CB + i-PRF (both $p > 0.05$, *t*-test). On day 7 and 10, there was no considerable difference among the groups with the exception of no expression of MO + i-PRF on day 10.

To sum up, on day 3, there was increased BMP-2 expression in all i-PRF-groups when compared to non-i-PRF-XBSM. On day 7, a positive effect of adding i-PRF on BMP-2 expression was seen in BO + i-PRF and MO + i-PRF, and on day 10 in BO + i-PRF.

DISCUSSION

For this *in vitro* study, four commercially available xenogenic, bovine bone substitute materials (XBSM)—alone and in combination with injectable platelet-rich fibrin (i-PRF) were evaluated regarding their biological effect on human osteoblast cells (HOB) after 3, 7 and 10 days. Cell viability, metabolic activity as well as expression of three bone regeneration markers (alkaline phosphatase (ALP), osteonectin (OCN), and bone morphogenic protein-2 (BMP-2) were analyzed. As a result, especially the high-sintered group showed beneficial *in vitro* effects when compared to low-sintered XBSM. Besides, addition of i-PRF to XBSM resulted in a significantly increased biological activity of HOB in most of the cases.

The main difference among the four XBSM is the preparation process, namely the temperature. They have a hydroxyapatite phase (Bohner, 2000), which causes a good biocompatibility due to similarity with crystalline phase of human bone, high porosity and micro-architecture (Laschke et al., 2007). Okumura et al. gave evidence that the reason of early osteogenesis on hydroxyapatite lies in the faster initial attachment of HOB (Stephan et al., 1999; Okumura et al., 2001). It was also reported that bovine hydroxyapatite materials treated at different temperatures show significant variation in osteoblastic activity because of changed surface roughness and biological performance (osteoconductivity) (Ong et al., 1998; Perić Kačarević et al., 2018; De Carvalho et al., 2019), which may result in different healing outcomes (Barbeck et al., 2015; Perić Kačarević et al., 2018). In our study, XBSM sintered at high temperatures [cerabone® (CB)] showed a significantly increased HOB viability and metabolic activity when compared to other materials processed at lower temperatures. CB is composed of hydroxyapatite with traces of calcium oxide with a porous bone-like morphology (Tadic and Eppler, 2004). Being sintered at a high temperature ($>1,200^{\circ}\text{C}$), it loses all organic compounds. It was reported, that CB presents the highest level of hydrophilicity in comparison to Bio-Oss® (BO) (Trajkovski et al., 2018). Besides, in $1,200^{\circ}\text{C}$ sintered bovine hydroxyapatite, additional traces of NaCaPO_4 and CaO were detected, which could result from decomposition of the bone carbonate and could improve HOB reaction (Tadic and Eppler, 2004) as detected in the present study.



Additionally, when considering the carbonate component, the influence of the surface energy of the bone substitute material may also increase initial HOB attachment and proliferation. Thus, the strengthening of the polar components of the dense surface of a bone substitute material may enhance HOB attachment and osteoconduction (Redey et al., 2000). The temperature of processing effects the elimination of carbonate content in the bone, which can be only initiated at 400°C and higher (Tadic and Eppele, 2004). Besides, the high sintering temperature increases crystallinity, subsequently lowers biodegradation rates and increases volume stability (Ong et al., 1998; Bohner, 2000; Accorsi-Mendonça et al., 2008; Kusrini and Sontang, 2012; Riachi et al., 2012). On the other hand, it was stated in another study, that high-temperature sintering of a XBSM did not affect phase stability, densification behavior, fluid intrusion, and porosity when compared to non-sintered XBSM (Gehrke et al., 2019). In addition, no clinical long-term influence of osseous healing using differently processed bone substitute materials was found. Though, Kapogianni et al. (2019) analyzed samples from biopsies 6 months after sinus floor evaluation and after this considerable amount of time in a biological less demanding defect, no differences can be expected (Rickert et al., 2012; Kapogianni et al., 2019).

Despite the claim of no organic component, histological analyzes gave evidence for (xenogenic) organic remnants in XBSM treated under lower temperature, which may lead to decreased biocompatibility and osteoconductivity (Piattelli et al., 1999). BO is a carbonated hydroxyapatite, containing water, with porous granulate morphology and nanocrystallinity (Tadic and Eppele, 2004). It is manufactured at a temperature of 300°C, thus, is considered to include residual proteins (Kübler et al., 2004). In the present *in vitro* investigation, BO showed less distinct results for cell viability and metabolic activity as compared to other XBSMs. These findings are in accordance with other *in vitro* studies (Kübler et al., 2004; Liu et al., 2011). Sufficient osteogenic cell adhesion a bone substitute material is important for cellular proliferation, differentiation and matrix synthesis. Whereas initial cell attachment is based on unspecific cell-substrate interactions, later cell adhesion displays complex interactions between extracellular ligands and specific cellular receptors with high impact on further intracellular signal transduction (Keselowsky et al., 2007). Integrin receptors are transmembrane heterodimers consisting of non-covalently associated α and β sub-units. The sub-units β_1 and α_v have affinity to extracellular matrix proteins like fibronectin, collagen, and osteonectin via the RGD tri-peptide sequence (Heller et al., 2018). Integrin-mediated outside-in-signaling has

TABLE 3 | HOB metabolic activity (MTT, absorbance 570 nm) in groups with XBSM (A) and XBSM with i-PRF (B) on days 3, 7, and 10; in triplication for each group and each time point, three time points.

XBSM	Day 3						Day 7						Day 10					
	CB		BO		CX		CB		BO		CX		CB		BO		CX	
	Control	MO	Control	MO	Control	MO	Control	MO	Control	MO	Control	MO	Control	MO	Control	MO	Control	MO
*Mean value with SEM	1.02 ± 0.09	1.6 ± 0.69	0.77 ± 0.14	1.21 ± 0.33	1.04 ± 0.14	0.59 ± 0.16	1.19 ± 0.16	0.54 ± 0.16	0.72 ± 0.07	0.59 ± 0.16	0.76 ± 0.16	0.55 ± 0.02	0.26 ± 0.03	0.21 ± 0.03	0.56 ± 0.11	0.52 ± 0.07	0.48 ± 0.07	0.42 ± 0.05
**Median values for non-parametric data.																		

XBSM	Day 3						Day 7						Day 10					
	CB+i-PRF		BO+i-PRF		CX+i-PRF		CB+i-PRF		BO+i-PRF		CX+i-PRF		CB+i-PRF		BO+i-PRF		CX+i-PRF	
	Control+i-PRF	MO+i-PRF	Control+i-PRF	MO+i-PRF	Control+i-PRF	MO+i-PRF	Control+i-PRF	MO+i-PRF	Control+i-PRF	MO+i-PRF	Control+i-PRF	MO+i-PRF	Control+i-PRF	MO+i-PRF	Control+i-PRF	MO+i-PRF	Control+i-PRF	MO+i-PRF
*Mean value with SEM	2.29 ± 0.5	1.01 ± 0.14	1.13 ± 0.18	1.38 ± 0.26	2.07 ± 0.42	1.04 ± 0.12	0.77 ± 0.06	0.77 ± 0.11	0.71 ± 0.04	0.77 ± 0.11	1.06 ± 0.26	0.75 ± 0.1	0.42 ± 0.05	0.52 ± 0.07	0.87 ± 0.09	0.52 ± 0.07	0.48 ± 0.07	0.42 ± 0.05
**Median values for non-parametric data.																		

*Mean values for parametric data.

**Median values for non-parametric data.

been shown to regulate osteogenic cytoskeleton organization and gene expression (Anselme, 2000; El-Ghannam et al., 2004). Furthermore, during osteoblast/substrate interactions, the expression of these adhesion molecules is modified according to distinct surface characteristics (Anselme, 2000; Klein et al., 2013a). In the present study, ALP, OCN (early as well as late osteogenic differentiation markers), and BMP-2 expression of BO without and with i-PRF was comparably high. In combination with i-PRF, Creos Xenogain® (CX) showed a significantly elevated OCN expression through the whole period in comparison to other groups. However, the results of gene expression markers were inconsistent and it is possible that the inclusion of other gene expression markers such as type I collagen, Runt-related transcription factor 2 (Runx2) and Osteopontin would have shown different results.

Cell viability/metabolic activity of CX and MO more or less correlated to each other. MO is produced via low-heat processing of bovine bone, preserving the coarseness of bone with its high porosity. In a recent preclinical *in vivo* study, MO showed more osteogenic cells as well as more newly formed bone when compared to BO and autogenous bone (Esfahanizadeh et al., 2019). Nevertheless, the impact if cells are seeded on the well and the BSM is added afterward (Khanijou et al., 2020) or if the cells have been seeded on the BSM itself (Parisi et al., 2020) remains unclear.

Interactions of biomaterials such as BSM with the surrounding microenvironment define the respective biocompatibility and biochemical signaling pathways might play key roles in determining the materials' success after implantation (Rahmati et al., 2020). *In vitro* assessment of cell metabolic activity may allow conclusions to be drawn about biocompatibility of biomaterials, and cells that are metabolically active are a precondition for osteoconductivity and osteoinductivity. But it should be clearly understood that *in vitro* studies still display only a limited part of the general *in vivo* set-up and there might be a substantial gap between cellular biocompatibility and *in vivo* models (Reichert et al., 2009; Rahmati et al., 2020). For example, surface characteristics of hydroxyapatite changes after getting in contact with blood proteins and extracellular matrix components (Herten et al., 2009). Thus, monotonous conditions of *in vitro* studies may distort *in vivo* results.

To the best of our knowledge, there are no *in vitro* studies on combination of i-PRF with different XBSMs. In a clinical study, Zhang et al. (2012) showed improvement in parameters of bone regeneration when adding PRF to XBSM but there was no statistical significance. In our previous *in vitro* study, we revealed that allogenic bone substitute material with i-PRF has a significant higher impact on HOB viability, migration and metabolic activity when compared to BO with i-PRF. Still, i-PRF-BO showed better results when compared to non-i-PRF-BO groups (Kyyak et al., 2020). In the present *in vitro* study, combination of i-PRF with xenogenic BSM significantly affected cell viability and metabolic activity of HOB, however not equally among the different XBSMs. Noteworthy is that material processed at high temperatures (CB + i-PRF) showed two times higher values of cell viability on day 3, when compared to other

i-PRF-XBSM groups. Interestingly, all abovementioned indexes of i-PRF-CB were even higher than those of i-PRF-controls on day 3 and almost the same at most of the later time-points.

Still, it is not fully clear why the sintered XBSM showed better *in vitro* results above all studied materials—either with i-PRF or without. Therefore, further *in vitro* as well as preclinical studies for comparison between different bovine bone substitutes—for example using different amounts of bone substitute as they might have a dose-dependent effective range, using different media or using cells from different donors—are needed.

According to our *in vitro* study, it could be assumed that i-PRF addition to XBSM may have the potential to improve bone regeneration in clinical application. This might be of greatest importance, in particular, in cases with large complex defects or medically compromised patients. Additionally, XBSM sintered in a higher temperature showed an advantage over the XBSM treated in lower temperatures. The knowledge of the materials' advantages leads to a better understanding of the regenerative processes and may improve the industrial production process.

CONCLUSION

XBSM sintered under high temperature showed better HOB viability through the whole period as well metabolic activity on day 7 and 10 when compared to XBSM groups treated at lower

temperatures. The same XBSM with addition of i-PRF showed even better HOB viability on day 3 and 7 as well as metabolic activity through the whole period in comparison to other XBSMs combined with i-PRF.

Overall, combination of XBSMs with i-PRF improves HOB viability and metabolic activity (except for one XBSM on day 3), ALP and BMP-2 expression at earlier stages as well as OCN expression at later stages *in vitro*.

DATA AVAILABILITY STATEMENT

The original contributions presented in the study are included in the article/supplementary material, further inquiries can be directed to the corresponding author/s.

AUTHOR CONTRIBUTIONS

PK, SK, and SB: hypothesis, concept, and methodology. SK, ES, DH, HS, DT, KS, SB, and PK: formal analysis and investigation. SK, BA-N, and PK: writing—original draft preparation. SK, ES, DH, HS, DT, KS, BA-N, SB, and PK: writing—review and editing. PK, KS, and BA-N: supervision. All authors contributed to the article and approved the submitted version.

REFERENCES

- Abd El Raouf, M., Wang, X., Miusi, S., Chai, J., Mohamed Abdel-Aal, A. B., Nefissa Helmy, M. M., et al. (2019). Injectable-platelet rich fibrin using the low speed centrifugation concept improves cartilage regeneration when compared to platelet-rich plasma. *Platelets* 30, 213–221. doi: 10.1080/09537104.2017.1401058
- Accorsi-Mendonça, T., Conz, M. B., Barros, T. C., Sena, L. ÁD., Soares, G. D. A., and Granjeiro, J. M. (2008). Physicochemical characterization of two deproteinized bovine xenografts. *Braz. Oral Res.* 22, 5–10. doi: 10.1590/s1806-83242008000100002
- Anderson, H. C., Sipe, J. B., Hessle, L., Dhanyamraju, R., Atti, E., Camacho, N. P., et al. (2004). Impaired calcification around matrix vesicles of growth plate and bone in alkaline phosphatase-deficient mice. *Am. J. Pathol.* 164, 841–847. doi: 10.1016/s0002-9440(10)63172-0
- Anselme, K. (2000). Osteoblast adhesion on biomaterials. *Biomaterials* 21, 667–681. doi: 10.1016/s0142-9612(99)00242-2
- Barbeck, M., Udeabor, S., Lorenz, J., Schlee, M., Holthaus, M. G., Raetscho, N., et al. (2015). High-temperature sintering of xenogeneic bone substitutes leads to increased multinucleated giant cell formation: in vivo and preliminary clinical results. *J. Oral Implantol.* 41, e212–e222.
- Blatt, S., Burkhardt, V., Kämmerer, P. W., Pabst, A. M., Sagheb, K., Heller, M., et al. (2020). Biofunctionalization of porcine-derived collagen matrices with platelet rich fibrin: influence on angiogenesis in vitro and in vivo. *Clin. Oral Invest.* 24, 3425–3436. doi: 10.1007/s00784-020-03213-8
- Bohner, M. (2000). Calcium orthophosphates in medicine: from ceramics to calcium phosphate cements. *Injury* 31, D37–D47.
- Choukroun, J., and Ghanaati, S. (2018). Reduction of relative centrifugation force within injectable platelet-rich-fibrin (PRF) concentrates advances patients' own inflammatory cells, platelets and growth factors: the first introduction to the low speed centrifugation concept. *Eur. J. Trauma Emerg. Surg.* 44, 87–95. doi: 10.1007/s00068-017-0767-9
- Dau, M., Kämmerer, P. W., Henkel, K. O., Gerber, T., Frerich, B., and Gundlach, K. K. (2016). Bone formation in mono cortical mandibular critical size defects after augmentation with two synthetic nanostructured and one xenogenous hydroxyapatite bone substitute - in vivo animal study. *Clin. Oral Implants Res.* 27, 597–603. doi: 10.1111/clr.12628
- De Carvalho, B., Rompen, E., Lecloux, G., Schupbach, P., Dory, E., Art, J.-F., et al. (2019). Effect of sintering on in vivo biological performance of chemically deproteinized bovine hydroxyapatite. *Materials* 12:3946. doi: 10.3390/ma12233946
- El Bagdadi, K., Kubesch, A., Yu, X., Al-Maawi, S., Orłowska, A., Dias, A., et al. (2017). Reduction of relative centrifugal forces increases growth factor release within solid platelet-rich-fibrin (PRF)-based matrices: a proof of concept of LSCC (low speed centrifugation concept). *Eur. J. Trauma Emerg. Surg.* 45, 467–479. doi: 10.1007/s00068-017-0785-7
- El-Ghannam, A. R., Ducheyne, P., Risbud, M., Adams, C. S., Shapiro, I. M., Castner, D., et al. (2004). Model surfaces engineered with nanoscale roughness and RGD tripeptides promote osteoblast activity. *J. Biomed. Mater. Res. A* 68, 615–627. doi: 10.1002/jbm.a.20051
- Esfahanizadeh, N., Daneshparvar, P., Takzaree, N., Rezvan, M., and Daneshparvar, N. (2019). Histologic evaluation of the bone regeneration capacities of Bio-Oss and MinerOss X in rabbit calvarial defects. *Int. J. Periodontics Restorative Dent.* 39, e219–e227.
- Fuchs, S., Jiang, X., Schmidt, H., Dohle, E., Ghanaati, S., Orth, C., et al. (2009). Dynamic processes involved in the pre-vascularization of silk fibroin constructs for bone regeneration using outgrowth endothelial cells. *Biomaterials* 30, 1329–1338. doi: 10.1016/j.biomaterials.2008.11.028
- Gehrke, S. A., Mazón, P., Pérez-Díaz, L., Calvo-Guirado, J. L., Velásquez, P., Aragonese, J. M., et al. (2019). Study of two bovine bone blocks (Sintered and Non-Sintered) used for bone grafts: physico-chemical characterization and in vitro bioactivity and cellular analysis. *Materials* 12:452. doi: 10.3390/ma12030452
- Ghanaati, S., Booms, P., Orłowska, A., Kubesch, A., Lorenz, J., Rutkowski, J., et al. (2014). Advanced platelet-rich fibrin: a new concept for cell-based tissue engineering by means of inflammatory cells. *J. Oral Implantol.* 40, 679–689. doi: 10.1563/aaid-joi-d-14-00138
- Glowacki, J. (2005). A review of osteoinductive testing methods and sterilization processes for demineralized bone. *Cell Tissue Bank.* 6, 3–12. doi: 10.1007/s10561-005-4252-z

- Heller, M., Kumar, V. V., Pabst, A., Brieger, J., Al-Nawas, B., and Kämmerer, P. W. (2018). Osseous response on linear and cyclic RGD-peptides immobilized on titanium surfaces in vitro and in vivo. *J. Biomed. Mater. Res. A* 106, 419–427. doi: 10.1002/jbm.a.36255
- Herten, M., Rothamel, D., Schwarz, F., Friesen, K., Koegler, G., and Becker, J. (2009). Surface- and non-surface-dependent in vitro effects of bone substitutes on cell viability. *Clin. Oral Invest.* 13, 149–155. doi: 10.1007/s00784-008-0214-8
- Hessle, L., Johnson, K. A., Anderson, H. C., Narisawa, S., Sali, A., Goding, J. W., et al. (2002). Tissue-nonspecific alkaline phosphatase and plasma cell membrane glycoprotein-1 are central antagonistic regulators of bone mineralization. *Proc. Natl. Acad. Sci. U.S.A.* 99, 9445–9449. doi: 10.1073/pnas.142063399
- Kapogianni, E., Barbeck, M., Jung, O., Arslan, A., Kuhnel, L., Xiong, X., et al. (2019). Comparison of material-mediated bone regeneration capacities of sintered and non-sintered xenogeneic bone substitutes via 2D and 3D Data. *In Vivo* 33, 2169–2179. doi: 10.21873/in vivo.11719
- Keselowsky, B. G., Wang, L., Schwartz, Z., Garcia, A. J., and Boyan, B. D. (2007). Integrin $\alpha(5)$ controls osteoblastic proliferation and differentiation responses to titanium substrates presenting different roughness characteristics in a roughness independent manner. *J. Biomed. Mater. Res. A* 80, 700–710. doi: 10.1002/jbm.a.30898
- Khanijou, M., Zhang, R., Boonsiriset, K., Srisatjaluk, R. L., Suphangul, S., Pairuchvej, V., et al. (2020). Physicochemical and osteogenic properties of chairside processed tooth derived bone substitute and bone graft materials. *Dent. Mater. J.* 40, 173–183. doi: 10.4012/dmj.2019-341
- Klein, M., Goetz, H., Pazen, S., Al-Nawas, B., Wagner, W., and Duschner, H. (2009). Pore characteristics of bone substitute materials assessed by microcomputed tomography. *Clin. Oral Implants Res.* 20, 67–74. doi: 10.1111/j.1600-0501.2008.01605.x
- Klein, M. O., Bijelic, A., Ziebart, T., Koch, F., Kämmerer, P. W., Wieland, M., et al. (2013a). Submicron scale-structured hydrophilic titanium surfaces promote early osteogenic gene response for cell adhesion and cell differentiation. *Clin. Implant Dent. Relat. Res.* 15, 166–175. doi: 10.1111/j.1708-8208.2011.00339.x
- Klein, M. O., Kämmerer, P. W., Götz, H., Duschner, H., and Wagner, W. (2013b). Long-term bony integration and resorption kinetics of a xenogeneic bone substitute after sinus floor augmentation: histomorphometric analyses of human biopsy specimens. *Int. J. Periodontics Restorative Dent.* 33, e101–e110.
- Kübler, A., Neugebauer, J., Oh, J.-H., Scheer, M., and Zöller, J. E. (2004). Growth and proliferation of human osteoblasts on different bone graft substitutes in vitro study. *Implant Dentistry* 13, 171–179. doi: 10.1097/01.id.0000127522.14067.11
- Kusrini, E., and Sontang, M. (2012). Characterization of x-ray diffraction and electron spin resonance: effects of sintering time and temperature on bovine hydroxyapatite. *Radiat. Phys. Chem.* 81, 118–125. doi: 10.1016/j.radphyschem.2011.10.006
- Kyyak, S., Blatt, S., Pabst, A., Thiem, D., Al-Nawas, B., and Kämmerer, P. W. (2020). Combination of an allogenic and a xenogenic bone substitute material with injectable platelet-rich fibrin - A comparative in vitro study. *J. Biomater. Appl.* 35, 83–96. doi: 10.1177/0885328220914407
- Lai, C. F., and Cheng, S. L. (2005). α 5 β 1 integrins play an essential role in BMP-2 induction of osteoblast differentiation. *J. Bone Miner Res.* 20, 330–340. doi: 10.1359/jbmr.041013
- Laschke, M. W., Witt, K., Pohlemann, T., and Menger, M. D. (2007). Injectable nanocrystalline hydroxyapatite paste for bone substitution: in vivo analysis of biocompatibility and vascularization. *J. Biomed. Mater. Res. Part B Appl. Biomater.* 82, 494–505. doi: 10.1002/jbm.b.30755
- Lei, P., Sun, R., Wang, L., Zhou, J., Wan, L., Zhou, T., et al. (2015). A new method for xenogeneic bone graft deproteinization: comparative study of radius defects in a rabbit model. *PLoS One* 10:e0146005. doi: 10.1371/journal.pone.0146005
- Lian, J. B., Javed, A., Zaidi, S. K., Lengner, C., Montecino, M., Van Wijnen, A. J., et al. (2004). Regulatory controls for osteoblast growth and differentiation: role of Runx/Cbfa/AML factors. *Crit. Rev. Eukaryot Gene Exp.* 14, 1–41. doi: 10.1615/critrevukaryotgeneexpr.v14.i12.10
- Lian, J. B., Stein, G. S., Stein, J. L., and Van Wijnen, A. J. (1998). Osteocalcin gene promoter: unlocking the secrets for regulation of osteoblast growth and differentiation. *J. Cell Biochem. Suppl.* 3, 62–72. doi: 10.1002/(sici)1097-4644(1998)72:30<31%2B62::aid-jcb10>3.0.co;2-s
- Liu, F., Malaval, L., and Aubin, J. E. (2003). Global amplification polymerase chain reaction reveals novel transitional stages during osteoprogenitor differentiation. *J. Cell Sci.* 116, 1787–1796. doi: 10.1242/jcs.00376
- Liu, Q., Douglas, T., Zamponi, C., Becker, S. T., Sherry, E., Sivananthan, S., et al. (2011). Comparison of in vitro biocompatibility of NanoBone® and BioOss®S for human osteoblasts. *Clin. Oral Implants Res.* 22, 1259–1264. doi: 10.1111/j.1600-0501.2010.02100.x
- Miron, R. J., Fujioka-Kobayashi, M., Hernandez, M., Kandalam, U., Zhang, Y., Ghanaati, S., et al. (2017). Injectable platelet rich fibrin (i-PRF): opportunities in regenerative dentistry? *Clin. Oral Invest.* 21, 2619–2627. doi: 10.1007/s00784-017-2063-9
- Miron, R. J., and Zhang, Y. (2018). Autologous liquid platelet rich fibrin: a novel drug delivery system. *Acta Biomater.* 75, 35–51. doi: 10.1016/j.actbio.2018.05.021
- Mourão, C. F. D. A. B., Valiense, H., Melo, E. R., Mourão, N. B. M. F., and Maia, M. D.-C. (2015). Obtention of injectable platelets rich-fibrin (i-PRF) and its polymerization with bone graft. *Revista do Colégio Brasileiro de Cirurgiões* 42, 421–423. doi: 10.1590/0100-69912015006013
- Okumura, A., Goto, M., Goto, T., Yoshinari, M., Masuko, S., Katsuki, T., et al. (2001). Substrate affects the initial attachment and subsequent behavior of human osteoblastic cells (Saos-2). *Biomaterials* 22, 2263–2271. doi: 10.1016/s0142-9612(00)00415-4
- Ong, J., Hoppe, C., Cardenas, H., Cavin, R., Carnes, D., Sogal, A., et al. (1998). Osteoblast precursor cell activity on HA surfaces of different treatments. *J. Biomed. Mater. Res.* 39, 176–183. doi: 10.1002/(sici)1097-4636(199802)39:2<176::aid-jbm2>3.0.co;2-m
- Parisi, L., Buser, D., Chappuis, V., and Asparuhova, M. B. (2020). Cellular responses to deproteinized bovine bone mineral biofunctionalized with bone-conditioned medium. *Clin. Oral Invest.* 2020:1–15.
- Perić Kačarević, Z., Kavehei, F., Houshmand, A., Franke, J., Smeets, R., Rimashevskiy, D., et al. (2018). Purification processes of xenogeneic bone substitutes and their impact on tissue reactions and regeneration. *Int. J. Artif. Organs* 41, 789–800. doi: 10.1177/0391398818771530
- Piattelli, M., Favero, G. A., Scarano, A., Orsini, G., and Piattelli, A. (1999). Bone reactions to anorganic bovine bone (Bio-Oss) used in sinus augmentation procedures: a histologic long-term report of 20 cases in humans. *Int. J. Oral Maxillofacial Implants* 14, 835–840.
- Rahmati, M., Silva, E. A., Reseland, J. E., Heyward, C., and Haugen, H. J. (2020). Biological responses to physicochemical properties of biomaterial surface. *Chem. Soc. Rev.* 49, 5178–5224. doi: 10.1039/d0cs00103a
- Redey, S. A., Nardin, M., Bernache-Assolant, D., Rey, C., Delannoy, P., Sedel, L., et al. (2000). Behavior of human osteoblastic cells on stoichiometric hydroxyapatite and type A carbonate apatite: role of surface energy. *J. Biomed. Mater. Res.* 50, 353–364. doi: 10.1002/(sici)1097-4636(20000605)50:3<353::aid-jbm9>3.0.co;2-c
- Reichert, C., Al-Nawas, B., Smeets, R., Kasaj, A., Götz, W., and Klein, M. O. (2009). In vitro proliferation of human osteogenic cells in presence of different commercial bone substitute materials combined with enamel matrix derivatives. *Head Face Med.* 5:23.
- Riachi, F., Naaman, N., Tabarani, C., Aboelsaad, N., Aboushelib, M. N., Berberi, A., et al. (2012). Influence of material properties on rate of resorption of two bone graft materials after sinus lift using radiographic assessment. *Int. J. Dentis.* 2012:737262.
- Rickert, D., Slater, J. J., Meijer, H. J., Vissink, A., and Raghoobar, G. M. (2012). Maxillary sinus lift with solely autogenous bone compared to a combination of autogenous bone and growth factors or (solely) bone substitutes. A systematic review. *Int. J. Oral Maxillofac Surg.* 41, 160–167. doi: 10.1016/j.ijom.2011.10.001
- Stein, G. S., Lian, J. B., Van Wijnen, A. J., Stein, J. L., Montecino, M., Javed, A., et al. (2004). Runx2 control of organization, assembly and activity of the regulatory machinery for skeletal gene expression. *Oncogene* 23, 4315–4329. doi: 10.1038/sj.onc.1207676
- Stephan, E. B., Jiang, D., Lynch, S., Bush, P., and Dziak, R. (1999). Anorganic bovine bone supports osteoblastic cell attachment and proliferation. *J. Periodontol.* 70, 364–369. doi: 10.1902/jop.1999.70.4.364
- Tadic, D., and Epple, M. (2004). A thorough physicochemical characterisation of 14 calcium phosphate-based bone substitution materials in comparison to natural bone. *Biomaterials* 25, 987–994. doi: 10.1016/s0142-9612(03)00621-5

- Trajkovski, B., Jaunich, M., Müller, W.-D., Beuer, F., Zafropoulos, G.-G., and Houshmand, A. (2018). Hydrophilicity, viscoelastic, and physicochemical properties variations in dental bone grafting substitutes. *Materials* 11:215. doi: 10.3390/ma11020215
- Wang, X., Zhang, Y., Choukroun, J., Ghanaati, S., and Miron, R. J. (2018). Effects of an injectable platelet-rich fibrin on osteoblast behavior and bone tissue formation in comparison to platelet-rich plasma. *Platelets* 29, 48–55. doi: 10.1080/09537104.2017.1293807
- Wend, S., Kubesch, A., Orlowska, A., Al-Maawi, S., Zender, N., Dias, A., et al. (2017). Reduction of the relative centrifugal force influences cell number and growth factor release within injectable PRF-based matrices. *J. Mater. Sci.* 28:188.
- Yamada, M., and Egusa, H. (2018). Current bone substitutes for implant dentistry. *J. Prosthodontic Res.* 62, 152–161. doi: 10.1016/j.jpor.2017.08.010
- Zhang, Y., Tangl, S., Huber, C. D., Lin, Y., Qiu, L., and Rausch-Fan, X. (2012). Effects of Choukroun's platelet-rich fibrin on bone regeneration in combination with deproteinized bovine bone mineral in maxillary sinus augmentation: a histological and histomorphometric study. *J. Cranio Maxillofacial Surg.* 40, 321–328. doi: 10.1016/j.jcms.2011.04.020
- Conflict of Interest:** The authors declare that the research was conducted in the absence of any commercial or financial relationships that could be construed as a potential conflict of interest.

Copyright © 2021 Kyyak, Blatt, Schiegnitz, Heimes, Staedt, Thiem, Sagheb, Al-Nawas and Kämmerer. This is an open-access article distributed under the terms of the Creative Commons Attribution License (CC BY). The use, distribution or reproduction in other forums is permitted, provided the original author(s) and the copyright owner(s) are credited and that the original publication in this journal is cited, in accordance with accepted academic practice. No use, distribution or reproduction is permitted which does not comply with these terms.



Leonurine Promotes the Osteoblast Differentiation of Rat BMSCs by Activation of Autophagy via the PI3K/Akt/mTOR Pathway

Bingkun Zhao¹, Qian Peng¹, Enoch Hin Lok Poon^{2,3}, Fubo Chen¹, Rong Zhou¹, Guangwei Shang¹, Dan Wang^{2,3}, Yuanzhi Xu^{1*}, Raorao Wang^{1*} and Shengcai Qi^{1*}

OPEN ACCESS

Edited by:

Barbara Zavan,
University of Padua, Italy

Reviewed by:

Kaili Lin,
Shanghai Jiao Tong University, China
Yong-Can Huang,
Peking University Shenzhen Hospital,
China

*Correspondence:

Raorao Wang
raoraowang@hotmail.com
Yuanzhi Xu
amyxyz01@sina.com
Shengcai Qi
dentistqi@163.com

Specialty section:

This article was submitted to
Tissue Engineering and Regenerative
Medicine,
a section of the journal
Frontiers in Bioengineering and
Biotechnology

Received: 08 October 2020

Accepted: 08 January 2021

Published: 23 February 2021

Citation:

Zhao B, Peng Q, Poon EHL,
Chen F, Zhou R, Shang G, Wang D,
Xu Y, Wang R and Qi S (2021)
Leonurine Promotes the Osteoblast
Differentiation of Rat BMSCs by
Activation of Autophagy via
the PI3K/Akt/mTOR Pathway.
Front. Bioeng. Biotechnol. 9:615191.
doi: 10.3389/fbioe.2021.615191

¹ Department of Stomatology, Shanghai Tenth People's Hospital, School of Medicine, Tongji University, Shanghai, China,
² Institute for Tissue Engineering and Regenerative Medicine, The Chinese University of Hong Kong, Hong Kong, China,
³ School of Biomedical Sciences, The Chinese University of Hong Kong, Hong Kong, China

Background: Leonurine, a major bioactive component from *Herba leonuri*, has been shown to exhibit anti-inflammatory and antioxidant effects. The aim of this study was to investigate the effect of leonurine on bone marrow-derived mesenchymal stem cells (BMSCs) as a therapeutic approach for treating osteoporosis.

Materials and Methods: Rat bone marrow-derived mesenchymal stem cells (rBMSCs) were isolated from 4-weeks-old Sprague–Dawley rats. The cytocompatibility of leonurine on rBMSCs was tested via CCK-8 assays and flow cytometric analyses. The effects of leonurine on rBMSC osteogenic differentiation were analyzed via ALP staining, Alizarin red staining, quantitative real-time polymerase chain reaction (qRT-PCR), and Western blot. Additionally, autophagy-related markers were examined via qRT-PCR and Western blot analyses of rBMSCs during osteogenic differentiation with leonurine and with or without 3-methyladenine (3-MA) as an autophagic inhibitor. Finally, the PI3K/Akt/mTOR signaling pathway was evaluated during rBMSC osteogenesis.

Results: Leonurine at 2–100 μ M promoted the proliferation of rBMSCs. ALP and Alizarin red staining results showed that 10 μ M leonurine promoted rBMSC osteoblastic differentiation, which was consistent with the qRT-PCR and Western blot results. Compared with those of the control group, the mRNA and protein levels of Atg5, Atg7, and LC3 were upregulated in the rBMSCs upon leonurine treatment. Furthermore, leonurine rescued rBMSC autophagy after inhibition by 3-MA. Additionally, the PI3K/AKT/mTOR pathway was activated in rBMSCs upon leonurine treatment.

Conclusion: Leonurine promotes the osteoblast differentiation of rBMSCs by activating autophagy, which depends on the PI3K/Akt/mTOR pathway. Our results suggest that leonurine may be a potential treatment for osteoporosis.

Keywords: BMSCs, leonurine, autophagy, osteoporosis, PI3K/Akt/mTOR pathway

INTRODUCTION

Osteoporosis is the most common bone disease and is found in one-tenth of the population aged above 50 years and one-quarter of the population aged above 80 years (Wright et al., 2014). Concurrently, the rate of occurrence of osteoporosis-related bone fractures is increasing; it is estimated that one in two women and one in five men aged above 50 years are at risk of bone fracture as a direct result of osteoporosis (Das and Crockett, 2013). This condition is a major clinical and public health concern, and high morbidity, disability, and mortality rates are associated with the disease. The risks of osteoporosis include age, inadequate calcium, vitamin D deficiency, female sex, lack of activity, smoking, alcohol consumption, and some chronic inflammatory diseases (Jing et al., 2016).

Osteoporosis is characterized by the fundamental imbalance between bone formation and resorption, which is caused by the overactivation of osteoclasts, an increase in cell apoptosis, and a decrease in the osteogenesis of BMSCs. This process results in a defining feature of osteoporosis: the loss of bone mass, which increases the risk of fracture. Inadequate bone formation by osteoblasts originating from bone marrow mesenchymal stem cells (BMSCs) to compensate for bone resorption by osteoclasts is considered the major cause of osteoporosis. Several studies have revealed that osteogenic differentiation is impaired in patients with osteoporosis and that recovering osteogenic capacities could treat osteoporosis (Jing et al., 2016).

Autophagy is a cellular process wherein the primary function is to clear damaged cellular components such as long-lived proteins and organelles, thus participating in conservation across multiple cell types. In pathological situations, autophagy plays an important role in maintaining bone homeostasis (Pierrefite-Carle et al., 2015). Current evidence indicates the dysregulation of autophagy as a major contributor to the development of metabolic disorders, including insulin resistance, diabetes mellitus, obesity, atherosclerosis, and osteoporosis. Autophagy plays an integral role in maintaining bone homeostasis, with substantial evidence demonstrating its contribution to the survival of osteoblasts, regulation of osteoblast differentiation, maintenance of bone mass, and improvement of bone strength (Yao et al., 2016; Geng et al., 2019). In contrast, decreased autophagy leads to an increase in BMSC apoptosis and inhibition of osteoblast differentiation (Nollet et al., 2014). Recent literature demonstrates the relationship between autophagy and osteoblast differentiation: BMSCs contain many autophagosomes in their initial differentiation stage, illustrating a fundamental linkage between autophagy and metabolism involved in osteoblastic differentiation (Nuschke et al., 2014). This evidence provides a logical foundation for pursuing the treatment of osteoporosis via autophagic regulation in BMSCs.

Current medical treatments for osteoporosis commonly encompass diphosphonate, calcitonin, estrogen receptor modulators, and parathyroid hormone (PTH); accordingly, such treatments can cause undesired side effects, including gastrointestinal responses, renal toxicity (Xu et al., 2013), hypocalcemia (Smith et al., 2009), and an increased risk of cancer (Choi et al., 2020). For example, bisphosphonates

trigger osteoclast apoptosis with therapeutic efficiency reaching bottlenecks at 3–5 years post-treatment, along with an increased risk of atypical femoral fractures (Han et al., 2017); Denosumab was reported to be correlated with atypical femoral fracture and osteonecrosis of the jaw, reported drug withdrawal symptoms, an increase risk of bone fractures due to a rapid increase in bone remodeling, and potential cardiovascular events (Adhikary et al., 2018); PTH was reported to induce abnormal psychiatric symptoms and a restricted anabolic window within 2 years of treatment (Lee et al., 2010). Alternatively, traditional Chinese medicine has been used to prevent and treat osteoporosis with a recorded history of over a thousand years; the use of herbal medicine and its extracts, including *Epimedium*, *Salvia*, *Rehmanniae radix*, and *Ophiopogon*, has been shown to elicit fewer side effects and demonstrated higher sustainability over long-term periods than synthetic drugs (Guo et al., 2014; Xu et al., 2016; Liu et al., 2017; Xi et al., 2018). Despite a deficit in the current understanding of drug–receptor interactions and signaling pathways involved in herbal medicine, traditional Chinese medicine still holds potential and empirical evidence identifies it as a safe and effective alternative in treating osteoporosis.

Leonurine is a natural chemical compound extracted from the traditional Chinese herbal medicine *Herba leonuri*. In particular, its high anti-inflammatory and antioxidant effects have been extensively illustrated and can reduce the damage caused by excessive ROS in many diseases, such as cardiovascular diseases, ischemic stroke, and atherosclerosis (Liu et al., 2010; Loh et al., 2010; Zhang et al., 2012). In motor system-related diseases, leonurine could contribute to the reconstruction of cartilage in disease situations and alleviate osteoporotic progression in a rat model by inhibiting osteoclast differentiation (Hu et al., 2019; Chen et al., 2020). A recent study demonstrated that leonurine can regulate autophagy to ameliorate cognitive dysfunction (Liu et al., 2016). Therefore, we hypothesized that leonurine may be a selective medicine for targeting osteoporosis by regulating autophagic activity in BMSCs.

The aim of this study was to confirm the roles of leonurine in BMSCs and the underlying molecular mechanisms. The proliferation of BMSCs cocultured with leonurine was detected by CCK-8 assays and flow cytometry *in vitro*. The osteogenic differentiation of leonurine on BMSCs was evaluated by ALP staining, PCR, and Western blot (WB) analysis. The PI3K/Akt/mTOR pathway was analyzed using WBs.

MATERIALS AND METHODS

Cell Culture and Differentiation Assays

Sprague–Dawley (SD) rat primary BMSCs were isolated from the bone marrow of 4-week-old rats. In brief, bone marrow cells were first flushed with cell culture medium and cultivated in Petri dishes. After 24 h of incubation, adherent cells (BMSCs) were extracted from each dish.

Extracted BMSCs were maintained in α -MEM (α -MEM, HyClone, United States) with 10% fetal bovine serum (FBS, Gibco, United States) and 1% penicillin/streptomycin (PS, Gibco,

United States). The cells were cultured at 37°C/5% CO₂, and the medium was replaced every 3 days. With cells passaged upon reaching 80% confluency, BMSCs of passages 3–6 were used in the ensuing experiments.

For osteogenic differentiation, BMSCs were cultured with osteogenic induction medium containing 10% FBS, 1% penicillin/streptomycin, 50 µg/ml ascorbic acid (Sigma, United States), 10 mM sodium β-glycerophosphate (Sigma, United States), and 10 nM dexamethasone (Sigma, United States).

The Biocompatibility of Leonurine on BMSCs

CCK8 (Cell Counting Kit-8) Assays

Cell proliferation was measured by Cell Counting Kit-8 assays (CCK-8, Dojindo, Shanghai, China) according to the manufacturer's protocol with three replicates. The experimental group was treated with different concentrations of leonurine (0–100 µM). Briefly, the cells were cultivated in 96-well plates at a density of 3×10^3 cells per well. The seeding density was measured after an initial overnight incubation with a CCK-8 assay to test whether they were equal. Another repeat was performed after 3 days of culture, in which the medium was replaced with 10 µl of CCK 8 solution dissolved in 200 µl of cell culture medium. The plate was incubated for 2 h before absorbance at 450 nm was measured.

Flow Cytometric Analysis of Cell Cycle and Apoptosis

BMSCs were seeded in six-well plates at a density of 2×10^4 cells per well and treated with leonurine for 3 days. Subsequently, the cells were collected and fixed with 75% ethanol overnight at 4°C and washed with cold PBS twice before staining with 200 µl of PI/RNase staining buffer for 30 min at room temperature. Cell cycle distribution was detected by a BD FACSCanto II flow cytometer (BD BioScience, United States).

Apoptosis assays were further performed to ascertain the effect of leonurine on cell viability with FITC-Annexin V apoptosis detection kits (BD Bioscience, United States) according to the manufacturer's protocols. Briefly, the cells were collected, washed with cold PBS, and resuspended in $1 \times$ binding buffer. Then, they were stained with 5 µl of Annexin V-FICT and 5 µM propidium iodide (PI) in the dark for 15 min at room temperature. Cell apoptosis was detected by a BD FACSCanto II flow cytometer (BD BioScience, United States).

The Osteogenic Differentiation of BMSCs Induced by Leonurine

Alkaline Phosphatase (ALP) Staining and Alizarin Red Staining

BMSCs at a density of 2×10^4 cells/well were seeded in 24-well plates. After 24 h, the baseline medium was replaced with osteogenic induction medium containing various concentrations of leonurine (0, 2, 5, and 10 µM). The cells were cultured in osteogenic induction medium for either 6 days (ALP staining) or 14 days (Alizarin red staining).

ALP staining was conducted to ascertain the effect of leonurine on BMSC differentiation. In brief, BMSCs were harvested after 6 days of culture and fixed with 4% paraformaldehyde for 10 min. An ALP color development kit (Beyotime, Shanghai, China) was used in the study according to the manufacturer's protocols. Briefly, the cells were stained for 15 min and washed three times with PBS. The stained cells were subsequently observed under phase-contrast microscopy, with representative images captured.

Alizarin red staining was further performed to determine the degree of calcium deposition in BMSCs between the leonurine treatment groups at various concentrations. Briefly, BMSCs were harvested after 14 days of culture in osteogenic medium as outlined above. After fixation in 4% paraformaldehyde for 10 min, the cells were stained with Alizarin red staining kits (Beyotime, Shanghai) for 60 min and washed three times with ddH₂O.

The stained cells were subsequently observed under phase-contrast microscopy, with representative images captured.

RNA Isolation and Quantitative Real-Time PCR (qRT-PCR) Analysis

BMSCs were seeded in six-well plates at a density of 5×10^4 cells/well. After 24 h, osteogenic induction medium containing 10 µM leonurine was added to the experimental groups, with the control groups receiving medium without leonurine. Total RNA from the BMSCs was isolated following osteogenic induction for 6 days with the TRIzol (Invitrogen, United States) extraction method according to the manufacturer's protocol. The total RNA concentration was measured by a Nanodrop system (Thermo Fisher Scientific, United States). cDNA was reverse transcribed with a PrimeScript RT reagent Kit (TaKaRa, Japan). qPCR was conducted with HieffTM qPCR SYBR[®] Green Master Mix in an ABI 7500 Real-Time PCR System (Applied Biosystems, Foster City, CA, United States). Relative gene expression was calculated using the comparative $2^{-\Delta\Delta Ct}$ method. The primers used are listed in **Table 1**.

TABLE 1 | Nucleotide sequences of primers used for qRT-PCR.

Gene		Primer sequence(5'–3')
OCN	Forward primer	TGAGGACCOCTCTCTCTGCTC
OCN	Reverse primer	GGGCTCCAAGTCCATTGTT
OPN	Forward primer	ATCTGAGTCCTTCACTG
OPN	Reverse primer	GGGATACTGTTTCATCAGAAA
RUNX2	Forward primer	GCACCCAGCCCATAATAGA
RUNX2	Reverse primer	TTGGAGCAAGGAGAAGCCC
p62/SQSTM1	Forward primer	ACCCATCCACAGAGGCTGAT
p62/SQSTM1	Reverse primer	GCCTTCATCCGAGAAACCCA
ATG5	Forward primer	ACGTGTGGTTTGACGGATT
ATG5	Reverse primer	AAGGCCGTTCAGTTGTGGTC
ATG7	Forward primer	TGGAGCATGCCCTACGATGAC
ATG7	Reverse primer	TTTGGGGTCCATACATCCGC
GAPDH	Forward primer	CAGGGCTGCCTTCTCTTGT
GAPDH	Reverse primer	TCCCGTTGATGACGAGCTTC

Protein Extraction and WB Analysis

BMSCs at a density of 5×10^4 cells/well were seeded in six-well plates and divided into a control group or treatment group (10 μ M leonurine). Total protein from the rBMSCs was isolated following osteogenic induction for 6 days with RIPA

buffer containing protease inhibitor and phosphatase inhibitor. Equal amounts of protein were separated and transferred onto nitrocellulose membranes (Millipore Corporation, Billerica, United States). Primary antibodies (GAPDH, OPG, and Runx2) were incubated with membranes at 4°C overnight, with the

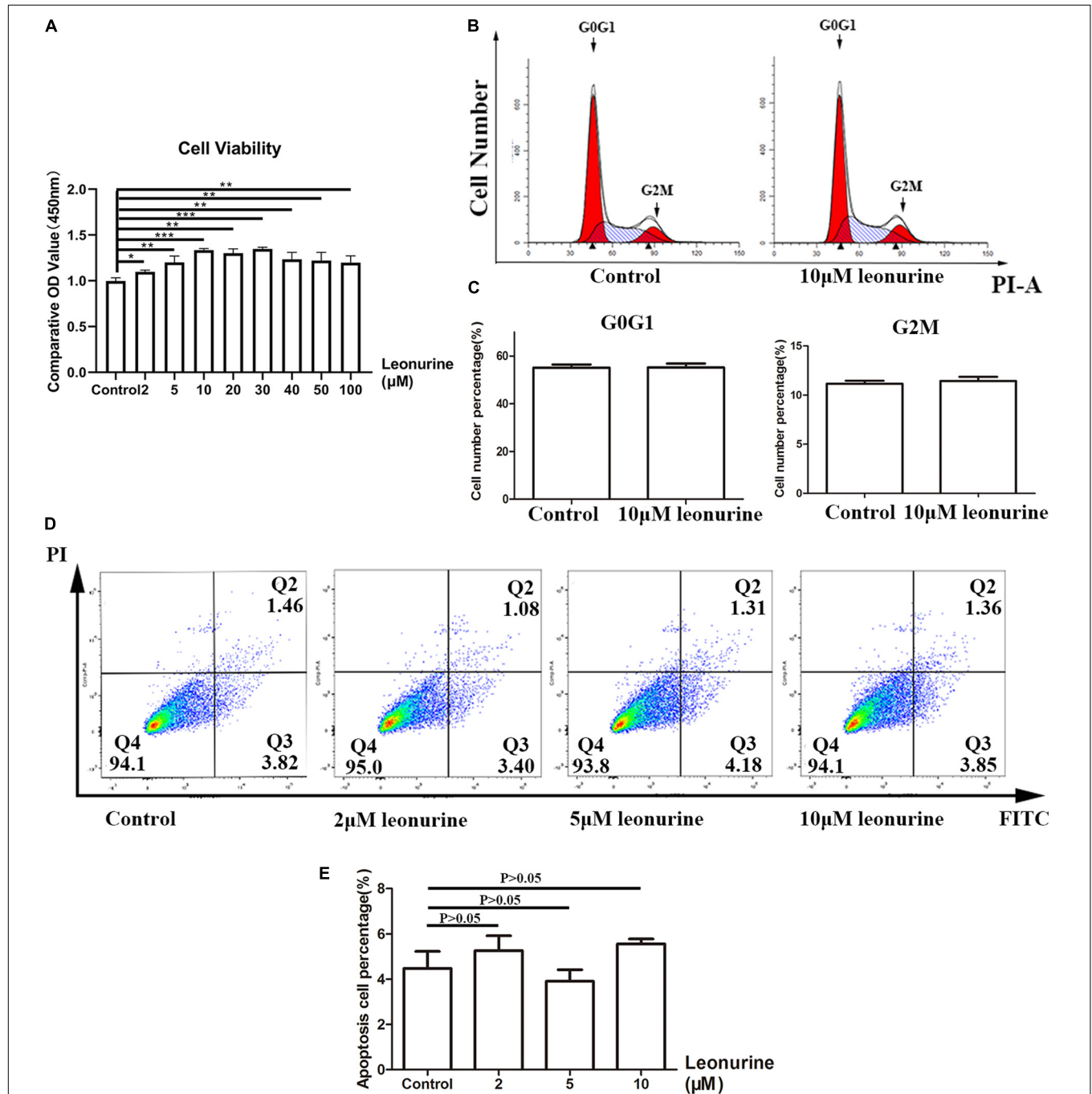


FIGURE 1 | Assessment of toxicity of leonurine and its effect on BMSC proliferation. **(A)** CCK-8 assay for BMSCs co-cultured with leonurine for 3 days illustrated increases in viability with leonurine-treated BMSCs. **(B)** Assessment of cell cycle phase distribution of leonurine-treated BMSCs. **(C)** Quantitative analysis of cell cycle phase distribution. No significant differences were measured between groups. **(D)** Distribution of apoptotic BMSCs observed under flow cytometry (FITC-Annexin V apoptotic detection assay). **(E)** Ratio of apoptotic BMSCs cultured in 0-10 μ M leonurine for 6 days. No significant differences were measured between groups (* $p < 0.05$, ** $p < 0.01$, *** $p < 0.001$).

ensuing secondary antibody incubated at room temperature for 1 h. The membranes were visualized using the Odyssey LI-CDR system. GAPDH (1:2,000) was purchased from Cell Signaling Technology (CST, Beverly, MA, United States). OPG (1:500) and Runx2 (1:500) were purchased from Abcam (Cambridge, MA, United States).

The Effect of Leonurine on Autophagy-Related Genes

BMSCs at a density of 5×10^4 cells/well were seeded in six-well plates. For autophagic inhibition, BMSCs were treated with 2 mM 3-methyladenine (3-MA, Sigma, United States) with or without leonurine (10 μ M). First, 3-MA was dissolved in dimethyl sulfoxide (DMSO) prior to addition to the culture medium, with the final concentration of DMSO below 0.1% of the medium. Alizarin red staining was performed for 14 days and ALP staining was performed for 6 days as described above.

Additionally, WB and qPCR were performed with the no treatment (control) group, leonurine treatment group, 3-MA treatment group, and 3-MA with leonurine treatment group. The antibodies LC3AB I/II (1:1,000) and ATG7 (1:500) used in WB analyses were purchased from Cell Signaling Technology (CST, Beverly, MA, United States); P62 (1:1,000) was purchased from

Abcam (Cambridge, MA, United States). The primers used in the qPCR analysis are listed in **Table 1**.

Analysis of Pathways Related to Leonurine

For PI3K activation, BMSCs were pretreated with 2 μ M of the PI3K activator 740Y-P (APEX-BIO, United States) for 2 h separately prior to coculturing with 10 μ M leonurine. Briefly, 740Y-P was dissolved in DMSO, and the final concentration of DMSO contributed to less than 0.1% of the medium, inducing no notable cytotoxic effect. WB assays were performed as stated above. The experimental groups were the control group, pretreatment with the 740Y-P group, leonurine treatment with the 740Y-P pretreatment group, and the leonurine treatment group. Antibodies against AKT (1:1,000), p-AKT (1:1,000), and p-mTOR (1:1,000) were purchased from Cell Signaling Technology (CST, Beverly, MA, United States). Antibodies against PI3K (1:1,000) and p-PI3K (1:500) were purchased from Abcam (Cambridge, MA, United States).

Statistical Analysis

Statistical analysis was performed by SPSS 20.0 (IBM, Somers, NY, United States). Each experiment was independently repeated

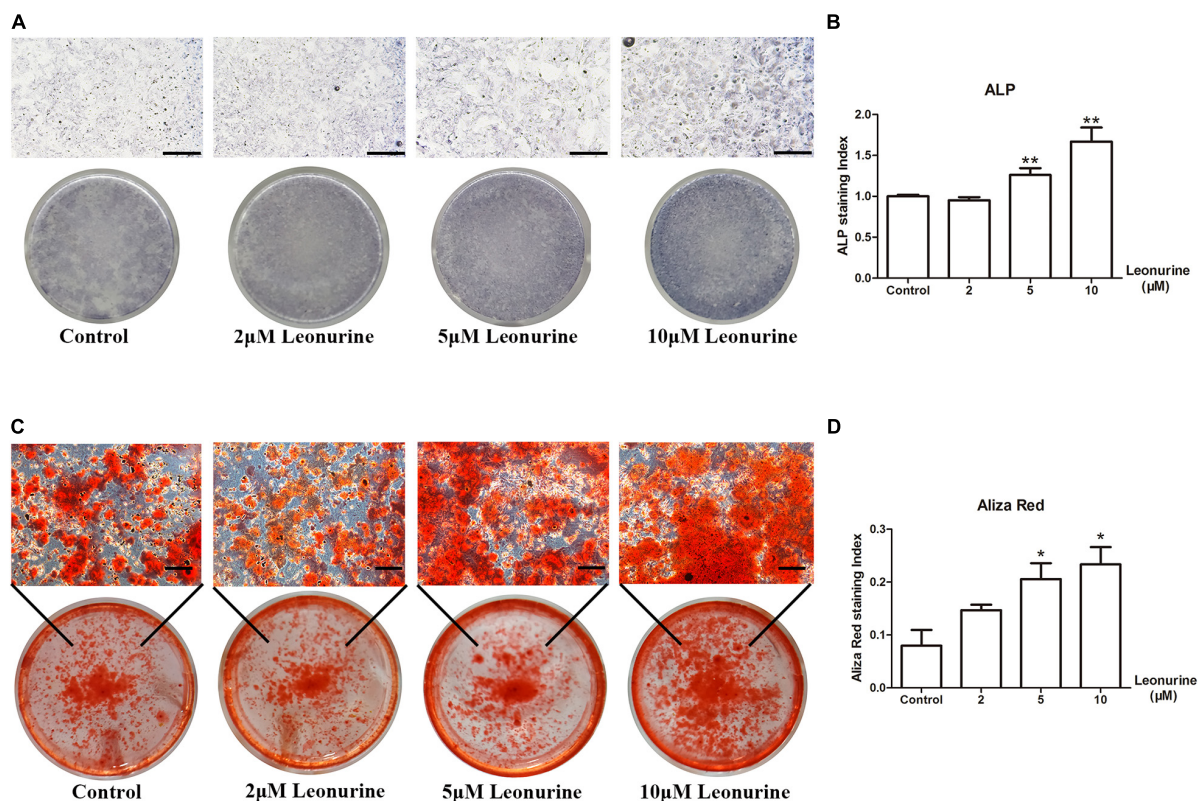


FIGURE 2 | Effects of leonurine on osteoblast differentiation and mineralization of BMSCs. **(A)** ALP staining of leonurine-treated groups (0–10 μ M) at day 6. **(B)** Quantitative analysis of ALP staining. Significant increases were recorded for 5 and 10 μ M leonurine-treated groups. **(C)** Alizarin red staining of leonurine-treated groups (0–10 μ M) at day 14. **(D)** Quantitative analysis of ALP staining. Significant increases in mineralization were recorded for 5 and 10 μ M leonurine-treated group (* p < 0.05, ** p < 0.01, *** p < 0.001 vs. Control group). Scale bar = 500 μ m.

at least three times. Differences between two groups were analyzed with unpaired Student's *t*-test, and more than three groups were analyzed with one-way analysis of variance followed by the Bonferroni post-test. Data are presented as the mean \pm standard error (SEM). $P < 0.05$ were considered to indicate significant differences.

RESULTS

Leonurine Exhibits No Notable Toxicity and Contributes to BMSC Proliferation

To assess the cytotoxicity of leonurine and its effect on the proliferation of BMSCs, we conducted a series of CCK-8 cell viability assays, cell cycle distribution analyses, and apoptosis assays with flow cytometry. As shown in **Figure 1A**, our results demonstrated that no apparent cytotoxicity was observed in the leonurine-treated group after 72 h of coculture with BMSCs. In contrast, viability was significantly increased in the BMSCs treated with leonurine at a range of 2–100 μ M, with a concentration of 10 μ M resulting in a peak increase in viability followed by a gradual decrease at higher concentrations (40–100 μ M). It reflects the fact that 10 μ M leonurine is the lowest and most proper functional concentration on BMSCs.

The flow cytometric results of BMSCs cocultured with leonurine demonstrated no notable change in the distribution of any particular cell cycle stage (**Figures 1B,C**). We observed an effect only on cell proliferation. However, whether the cell cycle period was changed was unclear. Apoptosis assays after coculture for 3 days further confirmed that leonurine did not have

apparent toxicity and did not cause cell apoptosis (including early apoptosis and late apoptosis) (**Figures 1D,E**). These data proved the security of leonurine on BMSCs, and the lowest functional concentration is 10 μ M.

Leonurine Contributes to Osteoblast Differentiation

To investigate the effect of leonurine on osteoblast differentiation, we performed ALP staining and Alizarin red staining after 6 and 14 days of culture, respectively, as an early marker for osteoblastic differentiation and a late marker for calcium deposition in osteoblasts.

As shown in **Figure 2**, leonurine contributed to osteoblastic differentiation in a dose-dependent manner, which was most apparent in the 10 μ M leonurine-treated group (**Figure 2A**), with a significant increase at day 6 (**Figure 2B**). Alizarin red staining yielded comparable results after 14 days of culture, where a significant increase in mineralization was recorded for the 10 μ M leonurine-treated BMSCs (**Figures 2C,D**). Combined, these results demonstrated the significant effect of 10 μ M leonurine (compared to lower concentrations) in improving osteogenesis; we thereafter selected 10 μ M leonurine as the concentration for subsequent analyses.

Leonurine Promotes Osteogenic Differentiation via the Activation of Autophagy

To determine the contribution of leonurine to osteogenesis, we performed qRT-PCR and WB analysis to further quantify the results obtained via ALP and Alizarin red staining. As shown

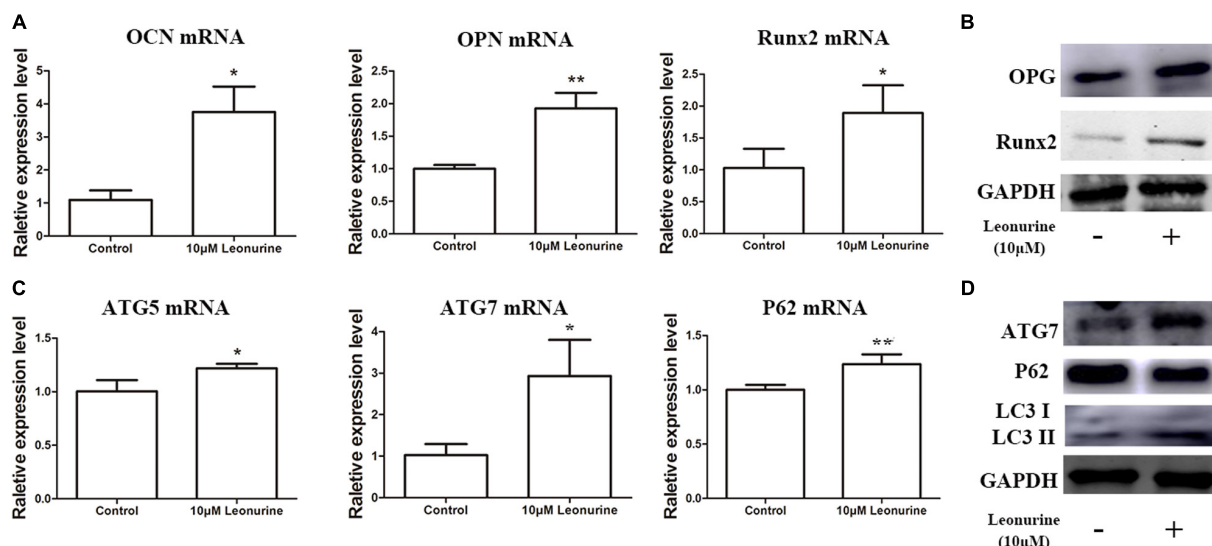


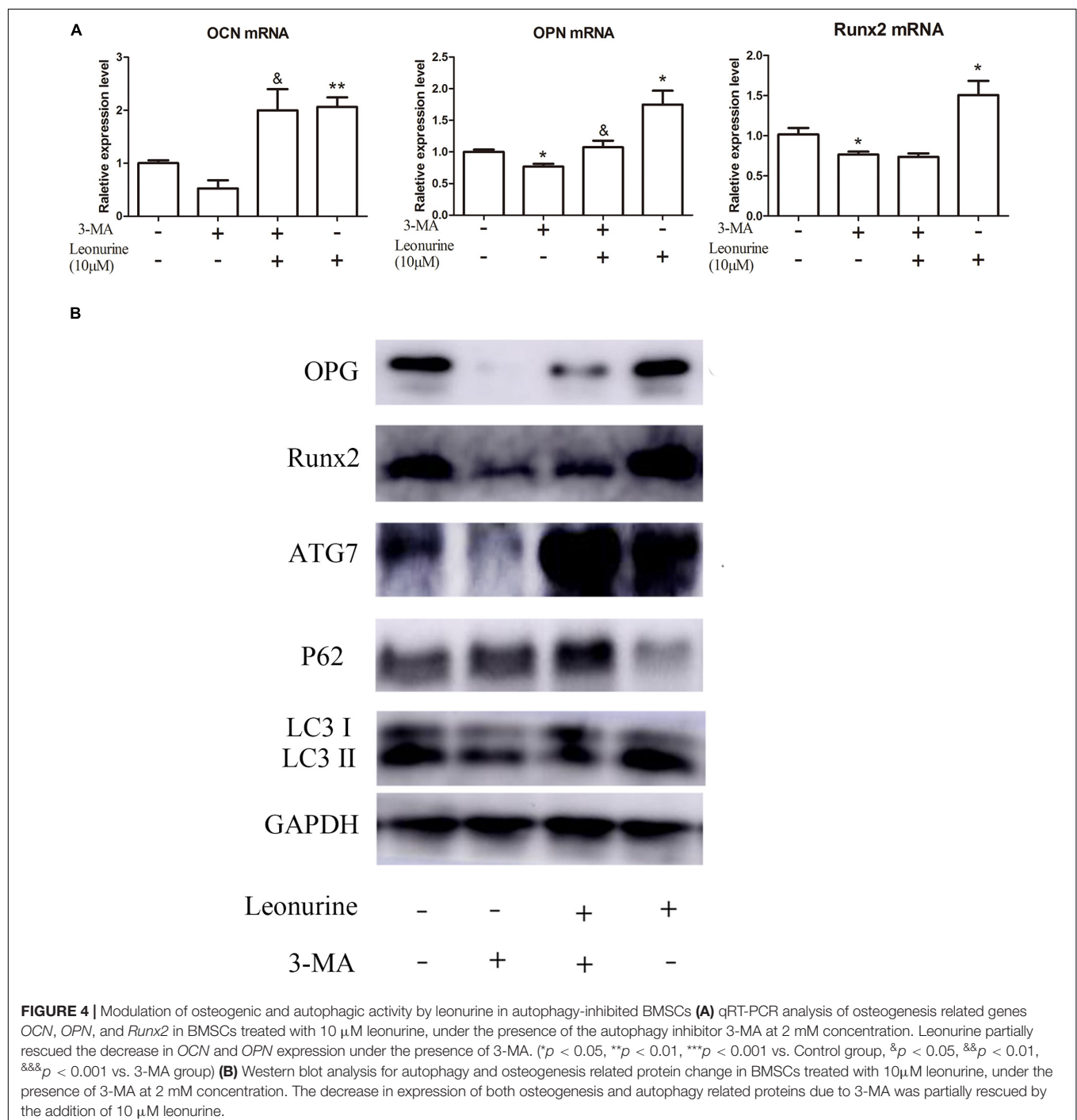
FIGURE 3 | Effects of leonurine on osteogenic and autophagic activity in BMSCs. **(A)** qRT-PCR analysis of osteogenesis related genes *OCN*, *OPN*, and *Runx2* expression in BMSCs after 6 days of 10 μ M leonurine treatment. Expression of all 3 mRNAs were significantly increased compared to control. **(B)** Western blot analysis of osteogenesis related proteins OPG and Runx2 in BMSCs after 6 days of 10 μ M leonurine treatment. Both proteins were significantly increased post-treatment. **(C)** Expression of autophagy related genes *ATG5*, *ATG7*, and *P62* in BMSCs after 6 days of 10 μ M leonurine treatment. Expression of all 3 mRNAs were significantly increased compared to control. **(D)** Expression of autophagy related proteins ATG7, P62, LC3 I, and LC3 II in BMSCs after 6 days of 10 μ M leonurine treatment. Both proteins were significantly increased post-treatment (* $p < 0.05$, ** $p < 0.01$, *** $p < 0.001$ vs. Control group).

in **Figure 3**, the addition of 10 μ M leonurine improved the expression of osteogenesis-related markers (OCN, OPN, and Runx2) at both the mRNA and protein levels (**Figures 3A,B**).

Owing to the significant correlation present between autophagic activity and osteogenesis, autophagy-related mRNA and proteins, including ATG7, P62, and LC3 I/II, were subsequently quantified to determine whether leonurine could significantly modulate autophagy in BMSCs. Both qRT-PCR and WB analyses demonstrated that autophagy was enhanced in the

leonurine-treated BMSCs compared to the untreated control cells (**Figures 3C,D**). This finding indicates that leonurine activated autophagy while accelerating the osteogenic process, demonstrating a strong relationship between them.

To further investigate the correlation between leonurine-induced activation of autophagy and its contribution to osteogenesis, we applied the autophagic inhibitor 3-MA with or without coculture treatment with leonurine. qRT-PCR and WB analyses both demonstrated significant inhibition of osteogenic



activity with 3-MA treatment (Figures 4A,B), indicating a decrease in osteogenesis via the inhibition of autophagy in BMSCs; concurrently, autophagy was partly rescued with leonurine supplemented with 3-MA (Figures 4A,B).

As additional evidence of the autophagic and osteogenic modulation of leonurine, significant inhibition of osteoblastic differentiation and mineralization by 3-MA was shown by ALP assays and Alizarin red staining after 6 and 14 days of culture, respectively, this phenomenon was reversed after the addition of 10 μ M leonurine (Figures 5A,C). The quantitative analysis is shown in Figures 5B,D.

As shown by this evidence, autophagic deficiency caused by 3-MA significantly decreased the osteogenic differentiation process, and these results support our hypothesis that leonurine can activate autophagy to contribute to osteogenesis.

Leonurine Can Activate Autophagy by Inhibiting the PI3K/Akt/mTOR Pathway

Considering the importance of the PI3K pathway involved in autophagy and leonurine previous report, we investigated the influence of leonurine on the PI3K pathway to ascertain

its possible effect in modulating autophagy. Our results indicated that the PI3K activator activates PI3K within 2 h, which is accompanied by the inhibition of autophagy (Figure 6A). Leonurine inhibited PI3K/Akt/mTOR activity with downregulation of phosphorylated PI3K/AKT/mTOR and exerted a negative effect against the PI3K activator 740-Y-P (Figure 6B). This evidence demonstrated that leonurine potentially activates autophagy via inhibition of the PI3K/Akt/mTOR pathway.

DISCUSSION

In this study, we demonstrated that leonurine, a natural compound derived from *Leonurus*, contributes to autophagy to improve BMSC differentiation without apparent cytotoxicity. Next, we further investigated its mechanism of autophagic activation by inhibiting the PI3K/Akt/mTOR pathway. Our results provide a rationale for developing leonurine as a new medicine for treatment of osteoporosis.

Many antiosteoporotic medicines result in various unavoidable side effects. In contrast, substantial evidence indicates a lowered risk of adverse events in treating osteoporosis

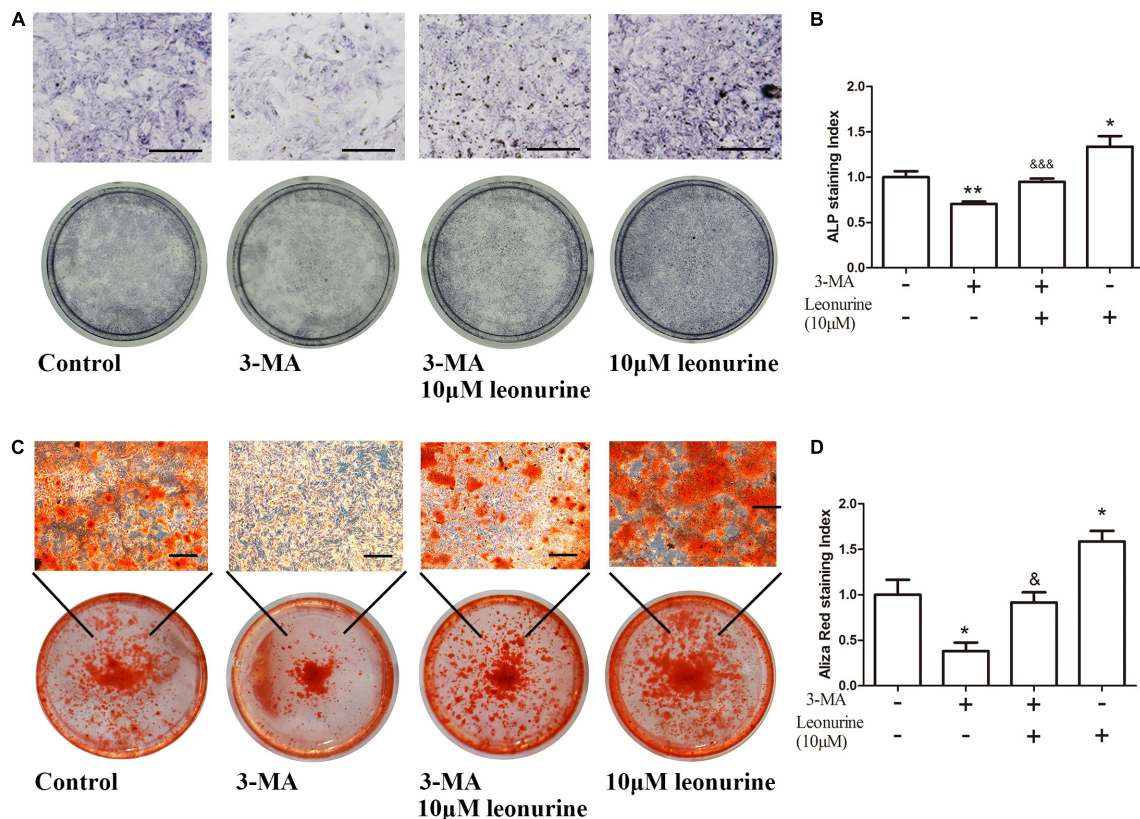


FIGURE 5 | Effects of leonurine on osteoblast differentiation and mineralization of autophagy-inhibited BMSCs. **(A)** ALP staining of 0–10 μ M leonurine treated BMSCs at day 6, with or without 2 mM 3-MA for autophagy inhibition. 10 μ M leonurine partially reversed the inhibition of osteoclastic differentiation by 3-MA. **(B)** Quantitative analysis of ALP staining. **(C)** Alizarin red staining of 0–10 μ M leonurine treated BMSCs at day 14, with or without 2 mM 3-MA for autophagy inhibition. 10 μ M leonurine partially reversed the inhibition of mineralization by 3-MA. **(D)** Quantitative analysis of Alizarin red staining (Scale bar is 200 μ M) (* p < 0.05, ** p < 0.01, *** p < 0.001 vs. Control group, & p < 0.05, && p < 0.01, &&& p < 0.001 vs. 3-MA group).

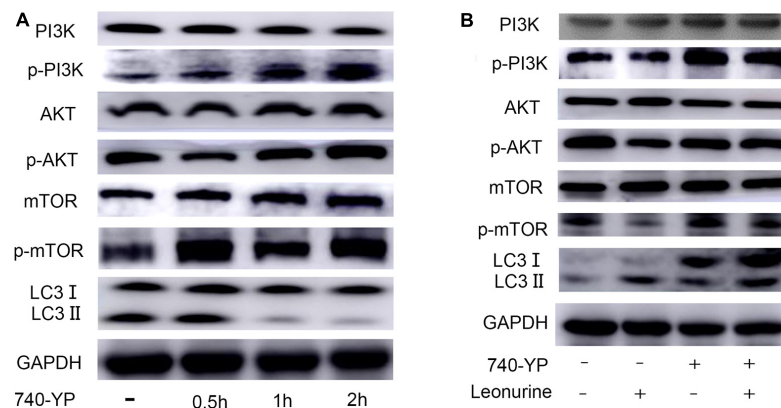


FIGURE 6 | Modulation of PI3K-AKT-mTOR pathway by leonurine. **(A)** Western blot analysis on the addition of the PI3K activator 740-YP in BMSCs. 740-YP at a concentration of 2 μ M increased expression of all downstream proteins in the PI3K-AKT-mTOR pathway. **(B)** Western blot analysis of the effect of leonurine on PI3K-AKT-mTOR pathway in BMSCs at 2 h. Expression of downstream proteins in PI3K-AKT-mTOR pathway in BMSCs treated with or without 2 μ M 740-YP was negatively regulated by the addition of 10 μ M leonurine.

with traditional Chinese medicine. Clinical studies have demonstrated that certain traditional Chinese medicines and their compounds can not only decrease bone resorption but also contribute to bone formation through estrogen-like effects, antioxidant activity, and modulation of bone metabolism (Zhang et al., 2016). For example, berberine promotes the differentiation of osteoblasts of BMSCs by stabilizing Runx2/Osterix through the increased activation of PKA signaling (Han et al., 2017). Kaempferol inhibits glucocorticoid-induced bone loss by promoting osteoblast survival through activation of the ERK pathway (Adhikary et al., 2018). Alisol-B suppresses RANKL-induced osteoclast formation to prevent bone loss through suppression of RANKL-mediated JNK pathway activation (Lee et al., 2010). Regarding the activity and effects of leonurine, it has been demonstrated that leonurine exhibits a protective function against cardiovascular disease, stroke, and nervous system disease by suppressing oxidative stress and chronic inflammation (Liu et al., 2013; Li et al., 2017). A recent study confirmed that leonurine has an antiosteoporotic effect on osteoclasts by inhibiting the PI3K-AKT and NF- κ B signaling pathways (Yuan et al., 2015). To further elucidate this topic, we investigated the antiosteoporotic effect of leonurine on BMSC functional recovery. Our results illustrated that leonurine promoted the proliferation of BMSCs at appropriate concentrations. Concurrently, leonurine promoted bone mineralization, as shown by ALP staining and Alizarin red staining, along with upregulation of both osteogenic genes and proteins at a concentration of 10 μ M. Combined, these results primarily indicated that leonurine can contribute to BMSC proliferation and differentiation, improving mineralization.

Osteoporosis associated with aging is characterized by consistent changes in bone metabolism with suppression of bone formation as well as increased bone resorption, both of which are associated with abnormal autophagic activity in osteoblasts (Bianco et al., 2011). Currently, there is substantial evidence to illustrate that autophagy can strongly contribute to

osteoblast survival, regulate osteoblast differentiation, maintain bone mass, and improve bone strength : in detail, bone marrow-derived mesenchymal stem cells have been regarded as the main contributors of osteoblasts to bone formation (Noort et al., 2002). With increasing age, bone marrow-derived mesenchymal stem cells tend to lose their self-renewal capacity and are directed toward adipogenic differentiation instead of osteogenesis; this phenomenon contributes significantly to bone loss and lipid accumulation in bone marrow (Moerman et al., 2004). Related studies have revealed that autophagy is a necessary factor for maintaining stemness and differentiation and that defective autophagy contributes to a decline in both cell count and cellular functions (Garcia-Prat et al., 2016).

The decline in autophagic activity is strongly correlated with osteoporosis, in which the inhibition of autophagy leads to increased cell apoptosis and activation of autophagy contributes to increased cell viability (Yang et al., 2014). Previous studies have demonstrated that knockout of the autophagy-related genes *BECN-1*, *ATG7*, and *LC3* results in defective bone mineralization; concurrently, enhancing autophagy helps BMSCs retain their multipotency (Sargolzaeiaval et al., 2018). Prior research has examined the contribution of leonurine to the regulation of autophagy. In this study, we demonstrated that leonurine successfully activated autophagy in BMSCs and increased the expression of autophagy-related proteins during the BMSC differentiation stage. Following leonurine administration, the impaired osteogenic differentiation in BMSCs induced by the autophagic inhibitor 3-MA was partially recovered. Combined, this evidence indicates that leonurine could regulate BMSC function by activating autophagy.

Substantial evidence has confirmed the relationship between dysregulated autophagy and osteoporosis *in vitro* and *in vivo* (Liu et al., 2018). Based on these studies, autophagic activation was shown to contribute to osteogenesis and serves as a promising target in treating osteoporosis. Many studies have investigated autophagy-related pathways. Among them,

mTOR-related pathways, including PI3K/Akt/mTOR, are highly involved in the regulation of cell autophagy (Gao et al., 2016), and evidence identifies the mTOR signaling pathway as a modulatory factor in mediating human osteoblastic differentiation. Deletion of Raptor, an essential component of the mTORC1 gene, in osteocytes did not affect bone development and growth but led to increased trabecular bone mass (Liu et al., 2018). Relevant studies have indicated that suppressing the phosphorylation of mTOR leads to the activation of autophagy, concurrently eliciting antiapoptotic effects on BMSCs and osteoblasts (Yang et al., 2019). Furthermore, the latest research indicates that suppression of the PI3K/AKT/mTOR pathway is a protective factor in glucocorticoid-induced osteoporosis (Wang et al., 2020).

Recent research has shown that leonurine can inhibit RANKL-mediated osteoclastogenesis, reducing the loss of bone volume caused by estrogen deficiency, and evidence of its antiosteoporotic function via upregulated osteogenesis in BMSCs was presented. Our overall results support the hypothesis that leonurine promotes BMSC osteoblastic differentiation via its main action of autophagic activation through PI3K/Akt/mTOR pathway inhibition. Previous literature has demonstrated the successful modulation of the PI3K/Akt/mTOR pathway by leonurine in various diseases (Loh et al., 2010; Yuan et al., 2015). In another study, leonurine inhibited PI3K/Akt/mTOR pathway activation, and the results strongly indicated direct binding to the PI3K protein in chondrocyte cells. Therefore, there is a strong relationship between PI3K/Akt/mTOR and autophagy. We first clarified that leonurine induced inhibition of the PI3K pathway, which has a direct relationship with autophagy. Comparable results were found in our research, in which PI3K phosphorylation was inhibited after leonurine treatment. Concurrently, our results suggested that leonurine induces a negative effect on the PI3K/AKT/mTOR pathway, acting as a direct antagonist of the PI3K/AKT activator (740Y-P)-dependent signaling pathway in this study. This finding contributes to our understanding of the mechanism by which leonurine harnesses autophagic activity to stimulate osteogenesis. However, a majority of other research on the leonurine-involved pathway has mainly focused on the NF- κ B pathway, which has a strong relationship with inflammation (Hoesel and Schmid, 2013). Osteoporosis-related research on leonurine reported that leonurine impedes osteoclasts differentiation by inhibition of PI3K/AKT and NF- κ B pathway (Yuan et al., 2015). We combined the evidence of direct combination to PI3K protein to further test leonurine mechanism of PI3K/Akt/mTOR pathway regulation in osteoblasts. This compensates the research on anti-osteoporosis

mechanism from another aspect. However, our research did not examine NF- κ B pathway function in autophagy, and this crosstalk with the PI3K pathway should further be taken into consideration for analysis of the mechanism of leonurine in a future study.

In conclusion, our research suggests the possible use of leonurine in activating BMSC autophagy to treat osteoporosis. Leonurine inhibits the PI3K/Akt/mTOR pathway to activate autophagy, subsequently contributing to osteoblast differentiation. These results strongly suggest that leonurine is a candidate medicine for potential studies in developing new therapies for osteoporosis.

DATA AVAILABILITY STATEMENT

The original contributions presented in the study are included in the article, further inquiries can be directed to the corresponding authors.

AUTHOR CONTRIBUTIONS

SQ designed the experiment and was responsible for the reviewers' suggestion. RW helped designed the experiments and checked uploaded data and rearranged the documents. YX and RW funded the experiments. BZ carried out the experiment and wrote the manuscript. QP, RZ, and GS were assistant of experiments. DW and EP helped the language edition. All authors contributed to the article and approved the submitted version.

FUNDING

This research was funded by the Science and Technology Commission of Shanghai Municipality, grant no. 03.02.18.003 and the Shanghai Municipal Health Commission, grant no. 20ZR1443100.

ACKNOWLEDGMENTS

We give thanks to Prof. Yizhun Zhu from the Department of Pharmacology, State Key Laboratory of Quality Research in Chinese Medicine and School of Pharmacy, Macau University of Science and Technology, for providing leonurine.

REFERENCES

- Adhikary, S., Choudhary, D., Ahmad, N., Karvande, A., Kumar, A., Banala, V. T., et al. (2018). Dietary flavonoid kaempferol inhibits glucocorticoid-induced bone loss by promoting osteoblast survival. *Nutrition* 53, 64–76. doi: 10.1016/j.nut.2017.12.003
- Bianco, P., Sacchetti, B., and Riminucci, M. (2011). Stem cells in skeletal physiology and endocrine diseases of bone. *Endocr. Dev.* 21, 91–101. doi: 10.1159/000328138
- Chen, C., Zhu, Z., Hu, N., Liang, X., and Huang, W. (2020). Leonurine hydrochloride suppresses inflammatory responses and ameliorates cartilage degradation in osteoarthritis via NF- κ B signaling pathway. *Inflammation* 43, 146–154. doi: 10.1007/s10753-019-01104-z
- Choi, D., Choi, S., Chang, J., and Park, S. M. (2020). Exposure to oral bisphosphonates and risk of gastrointestinal cancer. *Osteoporos. Int.* 31, 775–782. doi: 10.1007/s00198-020-05327-x
- Das, S., and Crockett, J. C. (2013). Osteoporosis - a current view of pharmacological prevention and treatment. *Drug Des. Devel. Ther.* 7, 435–448. doi: 10.2147/dddt.s31504

- Gao, J., Cheng, T. S., Qin, A., Pavlos, N. J., Wang, T., Song, K., et al. (2016). Glucocorticoid impairs cell-cell communication by autophagy-mediated degradation of connexin 43 in osteocytes. *Oncotarget* 7, 26966–26978. doi: 10.18632/oncotarget.9034
- García-Prat, L., Martínez-Vicente, M., Perdiguer, E., Ortet, L., Rodríguez-Ubrea, J., Rebollo, E., et al. (2016). Autophagy maintains stemness by preventing senescence. *Nature* 529, 37–42. doi: 10.1038/nature16187
- Geng, W., Shi, H., Zhang, X., Tan, W., Cao, Y., and Mei, R. (2019). Substance P enhances BMSC osteogenic differentiation via autophagic activation. *Mol. Med. Rep.* 20, 664–670.
- Guo, Y., Li, Y., Xue, L., Severino, R. P., Gao, S., Niu, J., et al. (2014). Salvia miltiorrhiza: an ancient Chinese herbal medicine as a source for anti-osteoporotic drugs. *J. Ethnopharmacol.* 155, 1401–1416. doi: 10.1016/j.jep.2014.07.058
- Han, Y., Jin, Y., Lee, S. H., Khadka, D. B., Cho, W. J., and Lee, K. Y. (2017). Berberine bioisostere Q8 compound stimulates osteoblast differentiation and function in vitro. *Pharmacol. Res.* 119, 463–475. doi: 10.1016/j.phrs.2017.03.002
- Hoessel, B., and Schmid, J. A. (2013). The complexity of NF-kappaB signaling in inflammation and cancer. *Mol. Cancer* 12:86. doi: 10.1186/1476-4598-12-86
- Hu, Z. C., Gong, L. F., Li, X. B., Fu, X., Xuan, J. W., Feng, Z. H., et al. (2019). Inhibition of PI3K/Akt/NF-kappaB signaling with leonurine for ameliorating the progression of osteoarthritis: in vitro and in vivo studies. *J. Cell Physiol.* 234, 6940–6950. doi: 10.1002/jcp.27437
- Jing, H., Liao, L., An, Y., Su, X., Liu, S., Shuai, Y., et al. (2016). Suppression of EZH2 prevents the shift of osteoporotic MSC fate to adipocyte and enhances bone formation during Osteoporosis. *Mol. Ther.* 24, 217–229. doi: 10.1038/mt.2015.152
- Lee, J. W., Kobayashi, Y., Nakamichi, Y., Udagawa, N., Takahashi, N., Im, N. K., et al. (2010). Alisol-B, a novel phyto-steroid, suppresses the RANKL-induced osteoclast formation and prevents bone loss in mice. *Biochem. Pharmacol.* 80, 352–361. doi: 10.1016/j.bcp.2010.04.014
- Li, N., Xu, Q., Liu, Q., Pan, D., Jiang, Y., Liu, M., et al. (2017). Leonurine attenuates fibroblast-like synovocyte-mediated synovial inflammation and joint destruction in rheumatoid arthritis. *Rheumatology* 56, 1417–1427. doi: 10.1093/rheumatology/kex142
- Liu, C., Ma, R., Wang, L., Zhu, R., Liu, H., Guo, Y., et al. (2017). Rehmanniae Radix in osteoporosis: a review of traditional Chinese medicinal uses, phytochemistry, pharmacokinetics and pharmacology. *J. Ethnopharmacol.* 198, 351–362. doi: 10.1016/j.jep.2017.01.021
- Liu, C., Yin, H., Gao, J., Xu, X., Zhang, T., and Yang, Z. (2016). Leonurine ameliorates cognitive dysfunction via antagonizing excitotoxic glutamate insults and inhibiting autophagy. *Phytomedicine* 23, 1638–1646. doi: 10.1016/j.phymed.2016.10.005
- Liu, Q., Liu, C., Yang, Y., Yang, H., and Chen, J. (2018). Osteocyte-intrinsic mTORC1 signaling restrains trabecular bone accrual in mice. *J. Cell Biochem.* 119, 8743–8749. doi: 10.1002/jcb.27470
- Liu, X. H., Pan, L. L., Chen, P. F., and Zhu, Y. Z. (2010). Leonurine improves ischemia-induced myocardial injury through antioxidative activity. *Phytomedicine* 17, 753–759. doi: 10.1016/j.phymed.2010.01.018
- Liu, X. H., Pan, L. L., Deng, H. Y., Xiong, Q. H., Wu, D., Huang, G. Y., et al. (2013). Leonurine (SCM-198) attenuates myocardial fibrotic response via inhibition of NADPH oxidase 4. *Free Radic. Biol. Med.* 54, 93–104. doi: 10.1016/j.freeradbiomed.2012.10.555
- Loh, K. P., Qi, J., Tan, B. K., Liu, X. H., Wei, B. G., and Zhu, Y. Z. (2010). Leonurine protects middle cerebral artery occluded rats through antioxidant effect and regulation of mitochondrial function. *Stroke* 41, 2661–2668. doi: 10.1161/strokeaha.110.589895
- Moerman, E. J., Teng, K., Lipschitz, D. A., and Lecka-Czernik, B. (2004). Aging activates adipogenic and suppresses osteogenic programs in mesenchymal marrow stroma/stem cells: the role of PPAR-gamma2 transcription factor and TGF-beta/BMP signaling pathways. *Aging Cell* 3, 379–389. doi: 10.1111/j.1474-9728.2004.00127.x
- Nollet, M., Santucci-Darmanin, S., Breuil, V., Al-Sahlane, R., Cros, C., Topi, M., et al. (2014). Autophagy in osteoblasts is involved in mineralization and bone homeostasis. *Autophagy* 10, 1965–1977. doi: 10.4161/auto.36182
- Noort, W. A., Kruisselbrink, A. B., In't A. P., Kruger, M., van Bezooijen, R. L., de Paus, R. A., et al. (2002). Mesenchymal stem cells promote engraftment of human umbilical cord blood-derived CD34(+) cells in NOD/SCID mice. *Exp. Hematol.* 30, 870–878. doi: 10.1016/s0301-472x(02)00820-2
- Nuschke, A., Rodrigues, M., Stolz, D. B., Chu, C. T., Griffith, L., and Wells, A. (2014). Human mesenchymal stem cells/multipotent stromal cells consume accumulated autophagosomes early in differentiation. *Stem Cell Res. Ther.* 5:140. doi: 10.1186/s13287-014-0140-2
- Pierrefite-Carle, V., Santucci-Darmanin, S., Breuil, V., Camuzard, O., and Carle, G. F. (2015). Autophagy in bone: self-eating to stay in balance. *Age. Res. Rev.* 24, 206–217. doi: 10.1016/j.arr.2015.08.004
- Sargolzaeiav, F., Zhang, J., Schleit, J., Lessel, D., Kubisch, C., Precioso, D. R., et al. (2018). CTC1 mutations in a Brazilian family with progeroid features and recurrent bone fractures. *Mol. Genet. Genom. Med.* 6, 1148–1156. doi: 10.1002/mgg3.495
- Smith, M. R., Egerdie, B., Hernandez, T. N., Feldman, R., Tammela, T. L., Saad, F., et al. (2009). Denosumab in men receiving androgen-deprivation therapy for prostate cancer. *N. Engl. J. Med.* 361, 745–755.
- Wang, X. Y., Gong, L. J., Huang, J. M., Jiang, C., and Yan, Z. Q. (2020). Pinocembrin alleviates glucocorticoid-induced apoptosis by activating autophagy via suppressing the PI3K/Akt/mTOR pathway in osteocytes. *Eur. J. Pharmacol.* 880:173212. doi: 10.1016/j.ejphar.2020.173212
- Wright, N. C., Looker, A. C., Saag, K. G., Curtis, J. R., Delzell, E. S., Randall, S., et al. (2014). The recent prevalence of osteoporosis and low bone mass in the United States based on bone mineral density at the femoral neck or lumbar spine. *J. Bone Miner. Res.* 29, 2520–2526. doi: 10.1002/jbmr.2269
- Xi, H. R., Ma, H. P., Yang, F. F., Gao, Y. H., Zhou, J., Wang, Y. Y., et al. (2018). Total flavonoid extract of epimedium herb increases the peak bone mass of young rats involving enhanced activation of the AC10/cAMP/PKA/CREB pathway. *J. Ethnopharmacol.* 223, 76–87. doi: 10.1016/j.jep.2018.05.023
- Xu, F., Ding, Y., Guo, Y., Liu, B., Kou, Z., Xiao, W., et al. (2016). Anti-osteoporosis effect of Epimedium via an estrogen-like mechanism based on a system-level approach. *J. Ethnopharmacol.* 177, 148–160. doi: 10.1016/j.jep.2015.11.007
- Xu, X. L., Gou, W. L., Wang, A. Y., Wang, Y., Guo, Q. Y., Lu, Q., et al. (2013). Basic research and clinical applications of bisphosphonates in bone disease: what have we learned over the last 40 years? *J. Transl. Med.* 11:303. doi: 10.1186/1479-5876-11-303
- Yang, X., Jiang, T., Wang, Y., and Guo, L. (2019). The role and mechanism of SIRT1 in resveratrol-regulated osteoblast autophagy in osteoporosis rats. *Sci. Rep.* 9:18424.
- Yang, Y. H., Li, B., Zheng, X. F., Chen, J. W., Chen, K., Jiang, S. D., et al. (2014). Oxidative damage to osteoblasts can be alleviated by early autophagy through the endoplasmic reticulum stress pathway—implications for the treatment of osteoporosis. *Free Radic. Biol. Med.* 77, 10–20. doi: 10.1016/j.freeradbiomed.2014.08.028
- Yao, W., Dai, W., Jiang, L., Lay, E. Y., Zhong, Z., Ritchie, R. O., et al. (2016). Sclerostin-antibody treatment of glucocorticoid-induced osteoporosis maintained bone mass and strength. *Osteoporos. Int.* 27, 283–294. doi: 10.1007/s00198-015-3308-6
- Yuan, F. L., Xu, R. S., Jiang, D. L., He, X. L., Su, Q., Jin, C., et al. (2015). Leonurine hydrochloride inhibits osteoclastogenesis and prevents osteoporosis associated with estrogen deficiency by inhibiting the NF-kappaB and PI3K/Akt signaling pathways. *Bone* 75, 128–137. doi: 10.1016/j.bone.2015.02.017
- Zhang, N. D., Han, T., Huang, B. K., Rahman, K., Jiang, Y. P., Xu, H. T., et al. (2016). Traditional Chinese medicine formulas for the treatment of osteoporosis: Implication for antiosteoporotic drug discovery. *J. Ethnopharmacol.* 189, 61–80. doi: 10.1016/j.jep.2016.05.025
- Zhang, Y., Guo, W., Wen, Y., Xiong, Q., Liu, H., Wu, J., et al. (2012). SCM-198 attenuates early atherosclerotic lesions in hypercholesterolemic rabbits via modulation of the inflammatory and oxidative stress pathways. *Atherosclerosis* 224, 43–50. doi: 10.1016/j.atherosclerosis.2012.06.066

Conflict of Interest: The authors declare that the research was conducted in the absence of any commercial or financial relationships that could be construed as a potential conflict of interest.

Copyright © 2021 Zhao, Peng, Poon, Chen, Zhou, Shang, Wang, Xu, Wang and Qi. This is an open-access article distributed under the terms of the Creative Commons Attribution License (CC BY). The use, distribution or reproduction in other forums is permitted, provided the original author(s) and the copyright owner(s) are credited and that the original publication in this journal is cited, in accordance with accepted academic practice. No use, distribution or reproduction is permitted which does not comply with these terms.



Case Report: Histological and Histomorphometrical Results of a 3-D Printed Biphasic Calcium Phosphate Ceramic 7 Years After Insertion in a Human Maxillary Alveolar Ridge

Carlo Mangano¹, Alessandra Giuliani², Ilaria De Tullio^{3*}, Mario Raspanti⁴, Adriano Piattelli^{3,5,6} and Giovanna Iezzi³

OPEN ACCESS

Edited by:

Barbara Zavan,
University of Padua, Italy

Reviewed by:

Antonio Scarano,
University of Studies G. d'Annunzio
Chieti and Pescara, Italy
Masoud Mozafari,
University of Toronto, Canada
Saso Ivanovski,
The University of
Queensland, Australia

*Correspondence:

Ilaria De Tullio
ilaria.detullio@gmail.com

Specialty section:

This article was submitted to
Tissue Engineering and Regenerative
Medicine,
a section of the journal
Frontiers in Bioengineering and
Biotechnology

Received: 05 October 2020

Accepted: 08 March 2021

Published: 15 April 2021

Citation:

Mangano C, Giuliani A, De Tullio I,
Raspanti M, Piattelli A and Iezzi G
(2021) Case Report: Histological and
Histomorphometrical Results of a 3-D
Printed Biphasic Calcium Phosphate
Ceramic 7 Years After Insertion in a
Human Maxillary Alveolar Ridge.
Front. Bioeng. Biotechnol. 9:614325.
doi: 10.3389/fbioe.2021.614325

¹ Independent Researcher, Gravedona, Italy, ² Department of Clinical Sciences, Polytechnic University of Marche, Ancona, Italy, ³ Department of Medical, Oral and Biotechnological Sciences, University "G. D'Annunzio" of Chieti-Pescara, Chieti, Italy, ⁴ Department of Medicine and Surgery, University of Insubria, Varese, Italy, ⁵ Chair of Biomaterials Engineering, Catholic University of San Antonio de Murcia (UCAM), Murcia, Spain, ⁶ Fondazione Villaserena per la Ricerca, Città Sant'Angelo, Italy

Introduction: Dental implant placement can be challenging when insufficient bone volume is present and bone augmentation procedures are indicated. The purpose was to assess clinically and histologically a specimen of 30%HA-60% β -TCP BCP 3D-printed scaffold, after 7-years.

Case Description: The patient underwent bone regeneration of maxillary buccal plate with 3D-printed biphasic-HA block in 2013. After 7-years, a specimen of the regenerated bone was harvested and processed to perform microCT and histomorphometrical analyses.

Results: The microarchitecture study performed by microCT in the test-biopsy showed that biomaterial volume decreased more than 23% and that newly-formed bone volume represented more than 57% of the overall mineralized tissue. Comparing with unloaded controls or peri-dental bone, Test-sample appeared much more mineralized and bulky. Histological evaluation showed complete integration of the scaffold and signs of particles degradation. The percentage of bone, biomaterials and soft tissues was, respectively, 59.2, 25.6, and 15.2%. Under polarized light microscopy, the biomaterial was surrounded by lamellar bone. These results indicate that, while unloaded jaws mimicked the typical osteoporotic microarchitecture after 1-year without loading, the BCP helped to preserve a correct microarchitecture after 7-years.

Conclusions: BCP 3D-printed scaffolds represent a suitable solution for bone regeneration: they can lead to straightforward and less time-consuming surgery, and to bone preservation.

Keywords: bone substitutes, biomaterials, bone regeneration, bone augmentation, histological analysis, micro-ct, clinical research, clinical study

INTRODUCTION

Dental implant placement can be challenging when an insufficient bone volume is present at the recipient site (Araújo and Lindhe, 2005). Autogenous bone has been described as the gold standard in bone regeneration techniques but, due to its limitations (limited intraoral sources, tendency to rapid and partial resorption and additional surgery with increased morbidity; Yamamichi et al., 2008; Scarano et al., 2011; Iezzi et al., 2012), allografts and xenografts have been developed and proposed as suitable alternatives: they are theoretically available in limitless amounts and in different dimensions and profiles, and can be customized or combined with growth factors, hormones, drugs, and stem cells (Piattelli et al., 1996a; Pettinichio et al., 2012; Mangano et al., 2015a; Paré et al., 2020).

Different bone substitute materials have been tested but it remains still unknown which graft material could be considered the best (Mazor et al., 2009; Iezzi et al., 2012; Pettinichio et al., 2012; Danesh-Sani et al., 2016). Biphasic calcium phosphate ceramics (BCPs) have been reported to have a high biocompatibility and a capability to enhance cell viability and proliferation (Castilho et al., 2014; Asa'ad et al., 2016; Zeng et al., 2020). With the improvement of computer-aided design/computer-aided manufacturing (CAD/CAM) technologies it has been feasible to analyze the bone deficiency of a patient on a 3D-CT scan and to create bone grafts that fit perfectly into the receiving site (Mangano et al., 2015b; Luongo et al., 2016; Raymond et al., 2018). Several techniques have been used to produce three dimensional scaffolds [e.g., inkjet printing, stereo lithography, fused deposition modeling, and selective laser sintering (Bose et al., 2013; Hwang et al., 2017; Liu et al., 2019; Chung et al., 2020)]. These techniques allow the creation of solid constructs with an excellent pore interconnectivity, high biocompatibility, capabilities of maintaining space and, for bone regeneration procedures, they seem to be able to provide greater osteoconductivity (Carrel et al., 2016; Hwang et al., 2017; Raymond et al., 2018; Kim et al., 2020).

The purpose of the present study was to assess clinically, histologically and under high resolution X-ray tomography a specimen of 30% hydroxyapatite (HA) and 70% tricalcium phosphate (TCP) BCP-3D-printed scaffold, harvested after 7 years of healing.

Case Description

The Ethical Committee of the Hospital of Varese, Italy approved the study protocol (N°826 del 03/10/2013). In 2013, the patient requested fixed prosthetic rehabilitation due to the lack of the second premolar and first molar of the right upper jaw. As there was lack of bone support, and the patient refused a sinus lift, it was decided to insert a dental implant in zone 1.5 with simultaneous bone regeneration of the atrophic buccal wall. The patient, who signed a written informed consent form, had undergone implant therapy with bone regeneration of the maxilla buccal plate to replace the second premolar, in 2013. Horizontal bone augmentation procedure was performed using 3D-printed biphasic HA-blocks, which were placed on the bone wall and stabilized by sutures. In CBCT 1, it is possible to see the HA 3D

printed graft characterized by its particular predefined porous structure. In X-ray and CBCT 2, 4 months after regeneration, the prosthetic rehabilitation was performed with a bridge from 1.4 to 1.7. After 7 years, during which the patient had no clinical control, the patient came back with serious periodontal problems affecting the first upper right premolar (1.4) and the second upper right molar (1.7), as shown in X-ray and CBCT 3. Therefore, the patient underwent another implant surgery, to replace the first premolar in the regenerated region, and a core of regenerated bone was obtained with a trephine.

MATERIALS AND METHODS

Scaffold Fabrication

In this study, the ceramic scaffold was made-up by the direct rapid prototyping technique dispense-plotting (Deisinger et al., 2008). The biomaterials was produced by Biomed Center (Bayrouth, Germany) following the systematic approach to the biological evaluation of the medical device, as part of the risk management process present in the ISO standard ISO 10993-1:2018 and according with ISO 14971 and ISO 13175-3: "Implants for surgery—Calcium phosphates—Part 3: Hydroxyapatite and beta-tricalcium," as shown in the flowchart. 3D printed Biphasic HA chemical composition is manufactured under highly controlled process. A computer-generated scaffold model was designed with a cylinder-shaped outer geometry by using a 3D-CAD software. In the later sintering process, the size of the scaffold prototype was customized to the shrinkage of the ceramic material. Physical rods consisting of paste-like aqueous ceramic slurry were extruded out of a container through a jet and deposited using an industrial robot (GLT, Pforzheim, Germany), to build up the green bodies. In this study HA and TCP powders (Merck, Germany) were combined to get a biphasic powder blend with a HA/TCP weight proportion of 30/70. Thermal treatment of the raw HA powder at 900°C for 1 h and the addition of a compatible binder/dispersant system of organic additives, of 10.5 wt% relative to the amount of ceramic powder, provided to the aqueous biphasic ceramic slurry its specific rheological behavior. The rod deposition was well-ordered in x, y, and z direction to build 3D scaffolds layer by layer on a deposition platform. The rotation of the direction of the rod deposition by 60° from layer to layer produced a 3D network with an interconnecting pore arrangement. The assemblies built of ceramic slurry were dehydrated at room temperature and then sintered at 1,250°C for 1 h. The double packaging and labeling process was carried out in clean rooms (classified as ISO 6). The sterilization of the product was performed by gamma irradiation. Identification and traceability of the devices was also guaranteed.

High-Resolution Tomography

MicroCT experiments were performed in two sessions: (1) at a laboratory-based microCT device (CISMIN Center, Polytechnic University of Marche, Ancona, Italy), achieving morphometric information on microarchitecture of the overall mineralized bone, of the newly formed bone and of the residual biomaterial, (2) at the SYRMEP microCT beamline of the ELETTRA Synchrotron Radiation Facility (Basovizza, Trieste, Italy),

achieving quantitative information on osteocyte lacunae size and distribution in the newly formed bone. For laboratory-based microCT, a Skyscan 1174 (SkyScan-Bruker, Antwerp, Belgium) tomographic acquisition was set with the following parameters: voltage: 50 kV; current: 800 μ A; pixel size: 6.5 μ m; rotation step over $180^\circ:0.1^\circ$; exposure time per projection: 0.1°; filter: 1 mm of Al. The absorption projection images (8 bit-TIFF) were reassembled using the NRecon software (SkyScan-Bruker, Antwerp, Belgium) to obtain a set of cross-sectional slices (8 bit-BMP), with ring artifact and beam hardening corrections. For the synchrotron-based microCT acquisition, the scans were performed using the following parameters: energy: white beam with peak energy at ~ 19 keV; voxel size: (890 nm³); rotation step over $180^\circ:0.1^\circ$; specimen-detector distance: ~ 100 mm. Due to the coherence of the synchrotron source, the recorded radiographs included phase contrast signals. The method was based on the discrimination between the absorption index β and the refractive index decrement δ of the index of refraction $n = 1 - \delta + i\beta$ in the tissues of the biopsy. The reconstruction was performed using Paganin's method (Paganin et al., 2002), together with the usual filtered back projection (FBP) algorithm. In the Paganin's method, the phase was retrieved by assuming a linear correlation between β and δ . The δ/β ratio, in the present experimental protocol, was set to 5.

The commercial software VG Studio MAX 1.2 (Volume Graphics, Heidelberg, Germany) was used to create 3D images and visualize the 3D phase distribution. X-ray contrast variations within samples turned into different peaks in the gray level scale, conforming to the several phases. The volume of each phase was acquired by multiplying the volume of a voxel by the quantity of voxels underlying the peak associated with the relevant phase. The Mixture Modeling algorithm (NIH ImageJ Plugin) was employed to threshold the histograms. Thresholded slices were used to automatically detach the new bone phase from the scaffold phase. The analyzed subvolumes were 3D portions completely embraced in the sample bulk.

The microarchitecture investigation was centered on the Parfitt structural indices (Parfitt et al., 1987): the following morphometric parameters were evaluated for the entire mineralized tissue: specific specimen volume (SV/TV—expressed as a percentage), specific specimen surface (SS/SV—per millimeter), Strut thickness (STh—expressed in micrometers), Strut number (SNr—per millimeter), and Strut spacing (SSp—expressed in micrometers). Varying bone orientation with dependency on mechanical loading, information on the eventual presence of preferential orientation(s) were extracted (Harrigan and Mann, 1984) by calculation of the anisotropy degree index (Tb.DA). Tb.DA was investigated by BoneJ Plugin (Doubé et al., 2010) of the ImageJ software (Abramoff et al., 2004; Schneider et al., 2012; Rasband, 2019): it varies between 0 (perfect isotropy) and 1 (strong anisotropy). Finally, trabecular connectivity density (Tb.Conn.D) was calculated: it supplies an overall quantitative evaluation, with greater values for better-connected organizations and lower values for poorly-connected ones. For the calculation of the regenerated bone, the same quantitative descriptors, previously related to the full mineralized tissue were applied in order to quantify: overall Bone Volume (BV—mm³),

overall Bone Surface (BS—mm²), Bone Volume to Total Volume ratio (BV/TV—expressed as a percentage), Bone Surface to Bone Volume ratio (BS/BV—per millimeter), Bone thickness (BTh—expressed in micrometers), Bone number (BNr—per millimeter), and Bone spacing (BSp—expressed in micrometers). The kinetics of the scaffold dissolution was also examined using again the same quantitative descriptors used to the entire mineralized tissue and to the regenerated bone [i.e., overall Scaffold Volume (ScV—mm³), overall Scaffold Surface (ScS—mm²), Scaffold Volume to Total Volume ratio (ScV/TV—expressed as a percentage), Scaffold Surface to Scaffold Volume ratio (ScS/ScV—per millimeter), Scaffold thickness (ScTh—expressed in micrometers), Scaffold number (ScNr—per millimeter), and Scaffold spacing (ScSp—expressed in micrometers)].

Synchrotron-based imaging allowed to achieve information on morphometric properties of the osteocyte lacunar network, with data on the mean lacunar thickness (Lc.Th), the mean lacunar volume (Lc.V), and the lacunar density (amount of lacunae per whole volume—Lc.Nr/TV).

Histology

The biopsy was fixed in 10% buffered formalin and processed (Precise 1 Automated System; Assing, Rome, Italy) to obtain thin ground sections. The specimen was dehydrated in an ascending sequence of alcohol solutions and embedded in an ascending sequence of glycol-methacrylate resin (Technovit 7200 VLC; Kulzer, Wehrheim, Germany). After polymerization, the specimen was segmented, along its longitudinal axis, with a high precision diamond disk at about 150 μ m and ground down to about 30 μ m with a specifically designed grinding machine. Each slice was stained with acid fuchsin and toluidine blue and analyzed under a light microscope (Laborlux S, Leitz, Wetzlar, Germany) associated to a high-resolution video camera (3CCD, JVC KY-F55B, JVC, Yokohama, Japan) and interfaced with a monitor and PC (Intel Pentium III 1200 MMX, Intel, Santa Clara, CA, USA). This optical system was connected with a digitizing pad (Matrix Vision GmbH, Oppenweiler, Germany) and a histomorphometry software set with image capturing means (Image-Pro Plus 4.5, Media Cybernetics Inc., Immagini & Computer Snc, Milano, Italy). One single well-trained examiner (GI), who was not involved in the surgical treatment, assessed the histological results. The following outcome measures were carried out: percentages of newly formed bone, marrow spaces and residual graft particles. Birefringence was measured as a sign of transverse collagen orientation using polarized light. Collagen fibers were observed by placing the thin bone sections under an Axiolab light microscope (Laborlux S, Leitz, Wetzlar, Germany) equipped with two linear polarizers and two quarter wave plates set to have a transferred circularly polarized light. Collagen fibers aligned perfectly transverse to the course of the light spread (parallel to the specimen slice plane) appeared bright due to a modification in the refraction of existing light, while the collagen fibers aligned along the axis of light spread (perpendicular to the specimen slice plane) looked dark because no refraction happened.

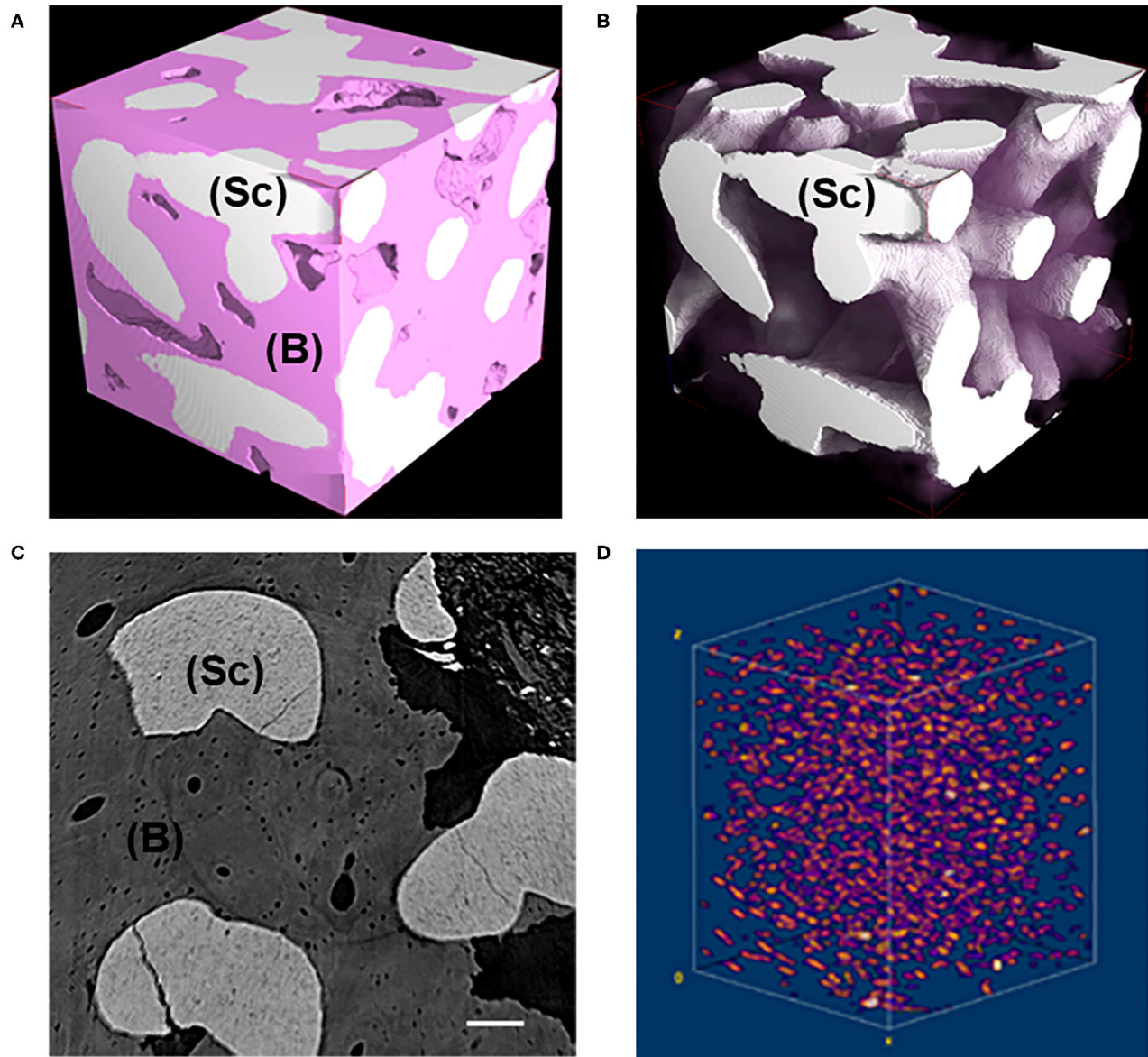


FIGURE 1 | (A,B) Representative 3D subvolumes as obtained at desktop microCT: **(A)** block-based TCP/HA scaffold as retrieved from *in vivo* test after 7 years; **(B)** same sample of **(A)** showing the residual scaffold not fully resorbed after 7 years *in-vivo*. Bone was virtually made transparent. Pink phase: bone; White phase: residual scaffold; **(C)** Representative transversal 2D section as obtained at synchrotron microCT; light gray phase: residual scaffold; dark gray phase: bone; black phase: medullar spaces; Scale bar = 100 μm . **(D)** Representative 3D distribution of the osteocyte lacunae in a 3D bone subvolume, as obtained at synchrotron microCT. Sc, scaffold; B, bone.

RESULTS

Scaffold Characterization

The sintered dispense-plotted assemblies had a typical mesh like organization with rod diameters of $300 \pm 30 \mu\text{m}$ and pore sizes between the rods of about $370 \pm 25 \mu\text{m}$. By determining the geometrical density of the sintered scaffolds, a total porosity of about 60% was estimated. Relative bulk density of the sintered specimens was assessed to 99% th.d. by pycnometry. Two main material phases of the sintered ceramic were identified by

semi-quantitative XRD measurements: 30% HA, 60% β -TCP, plus a small peak of α -TCP (70% of TCP in total).

High-Resolution X-Ray Tomography

MicroCT images of representative subvolumes of the Test-sample (i.e., of the maxilla biopsy grafted with the BCP and retrieved after 7 years, were shown in **Figure 1**). All tissues, but mineralized bone and residual scaffold, have been made virtually transparent in **Figure 1A**, while in **Figure 1B** the

TABLE 1 | Study of microarchitecture in the test-maxillary biopsy (Test) retrieved after 7 years *in-vivo*: whole Mineralized Structure (S), Newly Formed Bone (B), and Scaffold Residuals (Sc) were considered.

	Test			Ctrl-Sc
	Whole mineralized structure (S)	Newly formed bone (B)	Scaffold residuals (Sc)	BCP scaffold
Specific surface [mm^{-1}]	6	19	17	13
Specific volume [%]	93.3	53.6	39.8	51.9
Mean thickness [μm]	318	107	116	147
Mean number [mm^{-1}]	3	5	3	3
Mean spacing [μm]	23	93	176	146

Comparisons are made with the BCP scaffold before *in-vivo* tests (Ctrl-Sc).

TABLE 2A | Study of microarchitecture in the test-maxillary biopsy (Test) retrieved after 7 years *in-vivo*: comparison with peri-dental bone microarchitecture (Pd-Ctr) and with unloaded bone control (UnL-Ctr).

	Test	Peri-dental [†] Pd-Ctr	Unloaded site [†] UnL-Ctr
SS/BV [mm^{-1}]	6.0	12.0 (2.1)	21.0 (0.1)
SV/TV [%]	93.3	57.8 (0.5)	42.2 (5.4)
S.Th [μm]	318	166 (40)	104 (16)
S.Nr [mm^{-1}]	3.0	3.3 (0.7)	4.0 (0.0)
S.Sp [μm]	23	120 (22)	141 (10)
Tb.DA	0.553	0.590 (0.048)	0.752 (0.010)
Tb.Conn.D [mm^{-3}]	8	56 (10)	60 (56)

Pd-Ctr and UnL-Ctr data were extracted (Iezzi et al., 2020). Mean (std.dev.) are indicated.

[†]Iezzi et al. (2012).

same subvolume was shown with also the newly formed bone made transparent for a better visualization of the residual scaffold, not fully resorbed after 7 years *in-vivo*. A transversal section and the 3D distribution of the osteocyte lacunae in a representative subvolume were respectively reported in **Figures 1C,D**. Numerous subvolumes, collected in different areas and completely included in the biopsy, were chosen, producing the microarchitecture data described in **Tables 1, 2A**.

The study of the microarchitecture in the test-maxillary biopsy (Test-sample retrieved after 7 years *in-vivo*) was detailed in **Table 1**: the full mineralized structure (S), the newly-formed bone (B), and the scaffold residuals (Sc) were considered. A comparison was made with the BCP scaffold as produced [i.e., before the *in-vivo* test (Ctrl-Sc)]. After 7 years, against a comparable number of struts, an increase in the specific volume of almost 80% was observed and the average thickness of the struts by more than 100%, together with a decrease in the specific surface of almost 54% and average spacing between struts of over 80%. Furthermore, after 7 years *in vivo*, a reduction of the

TABLE 2B | Three-dimensional morphometric investigation of the osteocyte lacunar network in the test-maxilla (Test) retrieved after 7 years *in-vivo*: comparison with peri-dental bone (Pd-Ctr) and with unloaded bone (UnL-Ctr).

	Test	Peri-dental [†] Pd-Ctr	Unloaded [†] Ctr
Lac.Th [μm]	5.9 \pm 0.6	5.2 \pm 1.3	5.6 \pm 0.7
Lac.V [μm^3]	637 \pm 152	409 \pm 180	371 \pm 133
Lac.Nr [$\times 10^3 \text{ mm}^{-3}$]	25.0 \pm 0.5	31.4 \pm 10.6	25.6 \pm 6.9

Pd-Ctr and UnL-Ctr data were extracted (Iezzi et al., 2020). Mean \pm std.dev. are indicated.

[†]Iezzi et al. (2020).

biomaterial volume of more than 23% was observed and the newly formed bone volume was more than 57% of the overall mineralized volume. In this context, it has been widely accepted in literature that jawbones, 6 months after tooth extraction, were perfectly healed in healthy patients (Guralnick, 1968; Jahangiri et al., 1998). Basing on the previously shown data, also the Test-sample had to be considered healed. However, this Test-sample did not participate in mastication for 7 years; thus, it was particularly interesting to study possible alterations with the physiological conditions of the peri-dental bone (Pd-Ctr) and with unloaded controls (UnL-Ctr), (i.e., with bone biopsies spontaneously healed in 12 months after tooth extraction but not participating in mastication). This comparative study, shown in **Tables 2A,B**, was supported by the data of a recent study (Iezzi et al., 2020). **Table 2A** showed such comparison in terms of microarchitecture quantitative study: it was observed that the Test-sample turned out to be much more mineralized and bulky not only compared to UnL-Ctr, with an increase of the mineralized volume of 121%, but also compared to the peri-dental physiological context (Pd-Ctr), with an increase by over 61%. Interestingly, the anisotropy degree (DA) of the Test-sample resembled that of the peri-dental site and it was shown to be much less oriented than the UnL-Ctr samples. The increasing in terms of mineralized volume of the BCP-based Test-sample was correlated to the study of bone architecture at the length-scale pertaining the observation of the osteocyte lacunar network; the same subvolumes investigated for producing the microarchitecture data were also studied for the osteocyte lacunae 3D morphometric analysis (**Table 2B**): considering the standard deviations, comparable values in Test and in Control sites (both Pd-Ctr and UnL-Ctr), when evaluating Lac.V, Lac.Th, and Lac.Nr. However, the observation of the pure mean values, revealed the same values in Test-sample and the UnL-Ctr samples in terms of lacunar density (Lac.Nr), but an increased mean Lac.Nr in the physiological context of the peri-dental site (Pd-Ctr), in agreement with previous observations (Iezzi et al., 2020).

Histological Results

After microCT testing the biopsy was available for histological evaluation. At low magnification, the sample revealed a complete integration of the scaffold, and only in the most peripheral portion, a small amount of soft tissue was present. Indeed, the residual biomaterial block, constituted by interconnected

pores, was filled with bone. This portion was close to a thin layer of cortical bone with very small marrow spaces (at the bottom of the sample) (**Figure 2A**). At high magnification, the biomaterial was well-incorporated in the mature bone both in areas close to the cortical bone and in the areas far from it. At the bone-biomaterial particles interface, the particles showed a lower density compared to their central portion (**Figure 2B**). No gaps were detected at the bone-particles interface, and the bone was always in intimate contact with the particles. The porous structure of the biomaterial was partially modified, and the shape of the particles revealed signs of degradation. Moreover, in one field, close to the residual biomaterial, a multinucleated giant cell was observed, showing that the process of biomaterial resorption happened slowly over time (**Figure 2C**). In the small marrow spaces, some blood vessels were present, and in a few fields, foci of bone remodeling were observed (**Figure 2D**) with osteoblastic activity. No inflammatory cells were present. The percentage of bone, residual biomaterials and soft tissues was respectively 59.2, 25.6, and 15.2%.

Polarized Light Observations

The same fields of the samples were examined under polarized light and compared to the light microscopic images in order to study the quality of the bone and the orientation of collagen fibers. In all cases, the biomaterial block was surrounded by lamellar bone with oriented parallel collagen fibers (**Figures 2E,F**), and only in small areas they were randomly oriented.

DISCUSSION

The purpose of the present study was to assess the healing and resorption process of BCP 3D printed bone substitute and the nature and amount of regenerated bone. The newly formed tissues were evaluated by an innovative experimental approach based on histological and X-ray high-resolution tomography (microCT) analysis. MicroCT was widely shown to be a powerful tool for scaffold characterization (Landi et al., 2000; John and Wenz, 2004; Iezzi et al., 2012, 2020; Giuliani et al., 2018a,b,c), obtaining not only a 3D image of a scaffold, but also providing qualitative and quantitative information on its structure (Renghini et al., 2013; Giuliani et al., 2014, 2016).

It is possible, starting from CBCT files, to create a 3D prototype of the patient's maxilla/mandible, obtained by transferring the files to specific reconstruction software (Mangano et al., 2015b; Luongo et al., 2016). Potent CAD software can design a custom-made bone graft straightforwardly on this 3D model (Figliuzzi et al., 2013; Mangano et al., 2015b; Luongo et al., 2016; Chung et al., 2020). The file of the 3D designed scaffold is sent to a computer-numeric-control (CNC) machine, which mills the custom-made bone graft of the chosen material (Figliuzzi et al., 2013; Mangano et al., 2015b; Luongo et al., 2016). Finally, the surgeon can easily adapt the customized scaffold in the surgical site, performing a straightforward and less time consuming surgery procedure, with reduced discomfort for the patient (Figliuzzi et al., 2013; Mangano et al., 2015b; Luongo et al., 2016; Kim et al., 2020). Micro- and macro-porous biphasic

calcium phosphate (BCP) have been mainly recommended and characterized in oral surgery practices (Piattelli et al., 1996b; Mangano et al., 2013a, 2015b, 2019; Giuliani et al., 2014, 2016; Kim et al., 2020). They are produced by combining HA and beta-TCP in various compositions rates (HA/beta-TCP ratios), and represent the most important BCP ceramics for dental and medical applications (Piattelli et al., 1996b; Mangano et al., 2013a, 2015b, 2019). In literature, successful bone regeneration using biphasic calcium phosphate materials, both granules and blocks, has been reported in some clinical applications for maxillary sinus elevation (Mangano et al., 2013a; Giuliani et al., 2014; Ohayon, 2014). However, most of these reported studies are based on a single time point (6 months), not allowing an accurate assessment of the kinetics of bone growth on the long-term and thus inhibiting a detailed comparison between different morphologies of the scaffold (Scarano et al., 2000; Giuliani et al., 2016). Moreover, most of the existing studies report on 60% HA and 40% TCP, which is characterized by two types of porosity: macroporosity (pores with diameters range 300–600 micron) leads the colonization of ceramic by osteogenic cells, and microporosity (pores with diameters <10 micron) permits biological fluids circulation (Iezzi et al., 2012; Mangano et al., 2019). TCP dissolution leads to more space available for new bone formation, while the HA maintains its role as a scaffold (Mangano et al., 2015b). 3DP offers several advantages over other SFF techniques for scaffold production:

1. 3DP can make scaffolds with high consistency and precise structural anisotropy.
2. 3DP does not implicate high temperature, strong chemicals, and support structures.
3. The high constructing speed of the print head makes the mass production of scaffolds feasible.
4. It is possible to include biological mediators into the scaffolds if the binder is water.

Besides its chemical structure, one of the key parameters in 3D scaffolds is its internal configuration. Pore size would be directly associated to bone formation, since it offers surface for cell adhesion and space for bone ingrowth; pore interconnection would provide the way for cell distribution/migration and permit an efficient *in vivo* blood vessel development, suitable for bone tissue neo-formation and remodeling. Studies on non-human primates have shown bone formation by bioactive biomimetic matrices scaffolds (Ripamonti et al., 2008). Geometry is a series of recurring concavities that biomimetizes the remodeling cycle of the primate osteonic bone.

Recent studies have shown that microCT is a powerful tool for studying not only the microarchitecture of the jaw (Mangano et al., 2013b; Giuliani et al., 2016, 2018b), but also its osteocyte lacunar morphology and density (Giuliani et al., 2018b,c; Iezzi et al., 2020). In this context, it was observed in the BCP-based Test-sample an augmented specific volume and trabecular thickness, together with decreased specific surface and trabecular spacing, with respect to the unloaded control, and the peridental sites.

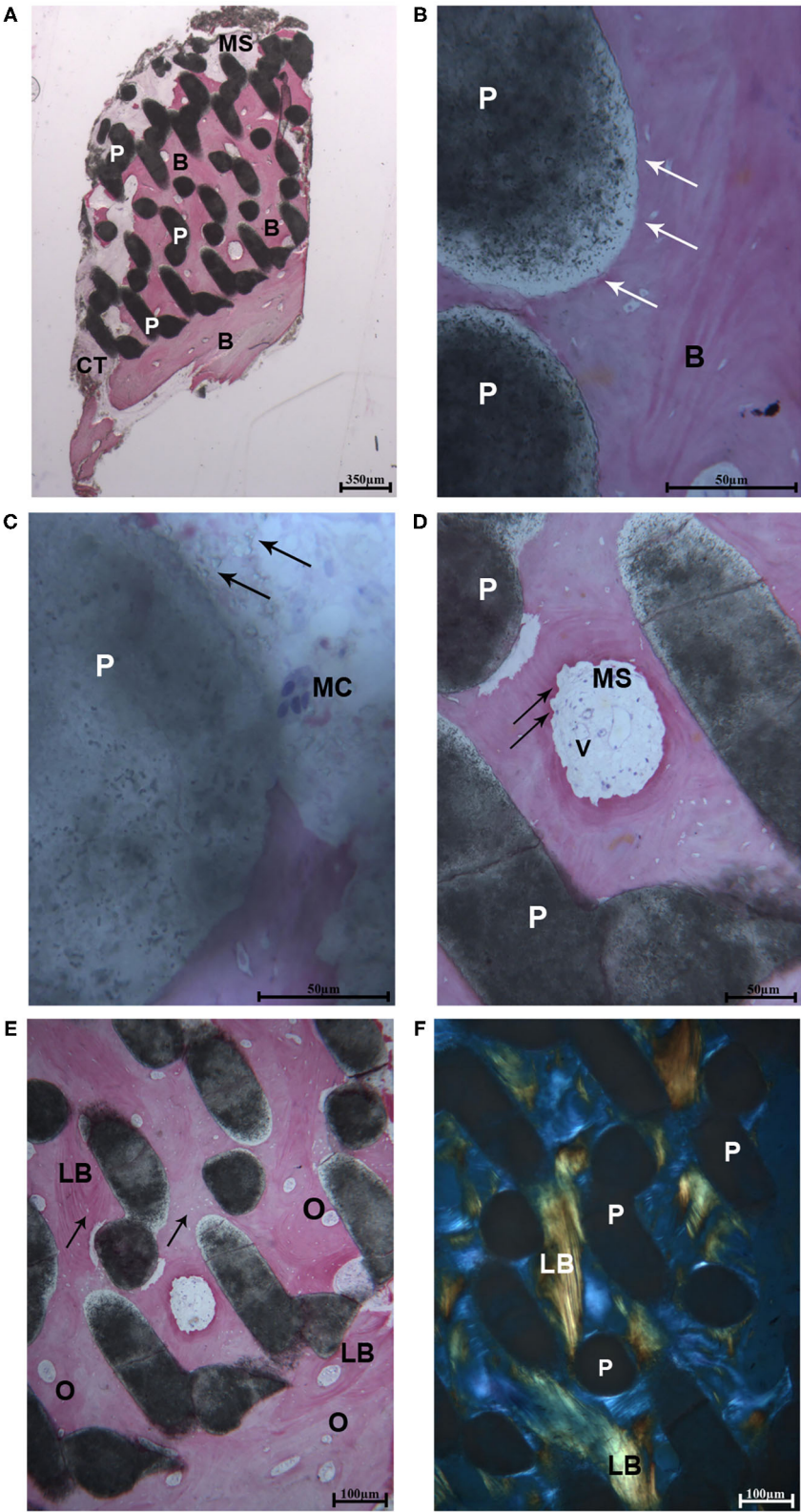


FIGURE 2 | (A) Light microscopic ground sections of the specimen showed the residual biomaterial block (P) surrounded by mature bone (B). The bone marrow (MB) and a small portion of connective tissue (CT) were present. At the bottom of the samples (occlusal region), mature bone with very small marrow spaces was shown
(Continued)

FIGURE 2 | (B) (Acid fuchsin-Toluidine blue 12X). **(B)** At higher-power magnification, the biomaterial particles (P) were in tight contact with the mature bone **(B)**. At the bone-biomaterial particles interface, the particles showed a lower density (black arrows) compared to their central portion (Acid fuchsin-Toluidine blue 40X). **(C)** Close to the residual biomaterial, which revealed signs of resorption (black arrows), a multinucleated giant cell was observed (MC). **(D)** In the small marrow spaces (MS), some blood vessels (V), and signs of bone remodeling were present (black arrows) (Acid fuchsin-Toluidine blue 200 and 100X). **(E)** Mature lamellar bone (LB) with small osteocyte lacunae were observed (black arrows) and many secondary osteons were detected (O). **(F)** Histological section under polarized light. The collagen fibers of the lamellar bone (LB) was oriented in a parallel way in many fields, and close to the biomaterial particles (P) (Acid fuchsin-Toluidine blue 40X).

CONCLUSIONS

Within the limitations of this study, based on only one patient, results indicate that while the usual unloaded jaw sites, the BCP-based Test-sample preserved a correct microarchitecture even after 7 years without masticatory loading. However, our investigation of the lacunar mean data indicated that the fact that the present specimen was unloaded for 7 years did not affect the mean volume and size of the osteocyte lacunae, but a lower lacunar density was found with respect to the peri-dental biopsies, confirming previous data (Iezzi et al., 2020).

More studies on human, with higher number of patients and with long follow up should be conducted to confirm data presented in the present paper.

DATA AVAILABILITY STATEMENT

The raw data supporting the conclusions of this article will be made available by the authors, without undue reservation.

REFERENCES

- Abramoff, M. D., Magalhães, P. J., and Ram, S. J. (2004). Image processing with ImageJ. *Biophoton. Int.* 11, 36–42. Available online at: <https://imagescience.org/meijering/publications/download/bio2004.pdf> (accessed March 25, 2020).
- Araújo, M. G., and Lindhe, J. (2005). Dimensional ridge alterations following tooth extraction. An experimental study in the dog. *J. Clin. Periodontol.* 32, 212–218. doi: 10.1111/j.1600-051X.2005.00642.x
- Asa'ad, F., Pagni, G., Pilipchuk, S. P., Giannì, A. B., Giannobile, W. V., and Rasperini, G. (2016). 3D-printed scaffolds and biomaterials: review of alveolar bone augmentation and periodontal regeneration applications. *Int. J. Dent.* 2016:1239842. doi: 10.1155/2016/1239842
- Bose, S., Vahabzadeh, S., and Bandyopadhyay, A. (2013). Bone tissue engineering using 3D printing. *Mater. Today* 16, 496–504. doi: 10.1016/j.mattod.2013.11.017
- Carrel, J.-P., Wiskott, A., Moussa, M., Rieder, P., Scherrer, S., and Durual, S. (2016). A 3D printed TCP/HA structure as a new osteoconductive scaffold for vertical bone augmentation. *Clin. Oral Implants Res.* 27, 55–62. doi: 10.1111/clr.12503
- Castilho, M., Moseke, C., Ewald, A., Gbureck, U., Groll, J., Pires, I., et al. (2014). Direct 3D powder printing of biphasic calcium phosphate scaffolds for substitution of complex bone defects. *Biofabrication* 6:015006. doi: 10.1088/1758-5082/6/1/015006
- Chung, J. J., Im, H., Kim, S. H., Park, J. W., and Jung, Y. (2020). Toward biomimetic scaffolds for tissue engineering: 3D printing techniques in regenerative medicine. *Front. Bioeng. Biotechnol.* 8:586406. doi: 10.3389/fbioe.2020.586406
- Danesh-Sani, S. A., Loomer, P. M., and Wallace, S. S. (2016). A comprehensive clinical review of maxillary sinus floor elevation: anatomy, techniques, biomaterials and complications. *Br. J. Oral Maxillofac. Surg.* 54, 724–730. doi: 10.1016/j.bjoms.2016.05.008
- Deisinger, U., Hamisch, S., Schumacher, M., Uhl, F., Detsch, R., and Ziegler, G. (2008). Fabrication of tailored hydroxyapatite scaffolds: comparison between a direct and an indirect rapid prototyping technique. *Key Eng. Mater.* 361–363, 915–918. doi: 10.4028/www.scientific.net/KEM.361-363.915

ETHICS STATEMENT

The studies involving human participants were reviewed and approved by The Ethical Committee of the Hospital of Varese, Italy approved the study protocol (N°826 del 03/10/2013). The patients/participants provided their written informed consent to participate in this study. Written informed consent was obtained from the individual(s) for the publication of any potentially identifiable images or data included in this article.

AUTHOR CONTRIBUTIONS

AP and CM: conceptualization. AP, CM, and GI: methodology. AG and MR: software. AG and GI: formal analysis. AG, MR, and GI: investigation and data curation. CM, AG, IDT, and GI: writing—original draft preparation. AP: writing—review and editing. AP and IDT: supervision. All authors have read and agreed to the published version of the manuscript.

- Doube, M., Klosowski, M. M., Arganda-Carreras, I., Cordelières, F. P., Dougherty, R. P., Jackson, J. S., et al. (2010). BoneJ: free and extensible bone image analysis in ImageJ. *Bone* 47, 1076–1079. doi: 10.1016/j.bone.2010.08.023
- Figliuzzi, M., Mangano, F. G., Fortunato, L., De Fazio, R., Macchi, A., Iezzi, G., et al. (2013). Vertical ridge augmentation of the atrophic posterior mandible with custom-made, computer-aided design/computer-aided manufacturing porous hydroxyapatite scaffolds. *J. Craniofac. Surg.* 24, 856–859. doi: 10.1097/SCS.0b013e31827ca3a7
- Giuliani, A., Iezzi, G., Mazzoni, S., Piattelli, A., Perrotti, V., and Barone, A. (2018a). Regenerative properties of collagenated porcine bone grafts in human maxilla: demonstrative study of the kinetics by synchrotron radiation microtomography and light microscopy. *Clin. Oral Investig.* 22, 505–513. doi: 10.1007/s00784-017-2139-6
- Giuliani, A., Iezzi, G., Mozzati, M., Gallezio, G., Mazzoni, S., Tromba, G., et al. (2018b). Bisphosphonate-related osteonecrosis of the human jaw: a combined 3D assessment of bone descriptors by histology and synchrotron radiation-based microtomography. *Oral Oncol.* 82, 200–202. doi: 10.1016/j.oraloncology.2018.04.026
- Giuliani, A., Iezzi, G., Mozzati, M., Gallezio, G., Mazzoni, S., Tromba, G., et al. (2018c). Three-dimensional microarchitecture and local mineralization of human jaws affected by bisphosphonate-related osteonecrosis. *Oral Oncol.* 84, 128–130. doi: 10.1016/j.oraloncology.2018.07.008
- Giuliani, A., Manescu, A., Larsson, E., Tromba, G., Luongo, G., Piattelli, A., et al. (2014). *In vivo* regenerative properties of coralline-derived (biocoral) scaffold grafts in human maxillary defects: demonstrative and comparative study with Beta-tricalcium phosphate and biphasic calcium phosphate by synchrotron radiation x-ray microtomography. *Clin. Implant. Dent. Relat. Res.* 16, 736–750. doi: 10.1111/cid.12039
- Giuliani, A., Manescu, A., Mohammadi, S., Mazzoni, S., Piattelli, A., Mangano, F., et al. (2016). Quantitative kinetics evaluation of blocks versus granules of biphasic calcium phosphate scaffolds (HA/β-TCP 30/70) by synchrotron radiation x-ray microtomography: a human study. *Implant. Dent.* 25, 6–15. doi: 10.1097/ID.0000000000000363

- Guralnick, W. C. (1968). *Textbook of Oral Surgery*, 1st edn. Boston: Boston Little.
- Harrigan, T., and Mann, R. W. (1984). Characterization of microstructural anisotropy in orthotropic materials using a second rank tensor. *J. Mater. Sci.* 19, 761–767. doi: 10.1007/BF00540446
- Hwang, K.-S., Choi, J.-W., Kim, J.-H., Chung, H. Y., Jin, S., Shim, J.-H., et al. (2017). Comparative efficacies of collagen-based 3D printed PCL/PLGA/ β -TCP composite block bone grafts and biphasic calcium phosphate bone substitute for bone regeneration. *Materials* 10:40421. doi: 10.3390/ma10040421
- Iezzi, G., Degidi, M., Piattelli, A., Mangano, C., Scarano, A., Shibli, J. A., et al. (2012). Comparative histologic results of different biomaterials used in sinus augmentation procedures: a human study at 6 months. *Clin. Oral Implants Res.* 23, 1369–1376. doi: 10.1111/j.1600-0501.2011.02308.x
- Iezzi, G., Mangano, C., Barone, A., Tirone, F., Baggi, L., Tromba, G., et al. (2020). Jawbone remodeling: a conceptual study based on Synchrotron High-resolution Tomography. *Sci. Rep.* 10, 1–12. doi: 10.1038/s41598-020-60718-8
- Jahangiri, L., Devlin, H., Ting, K., and Nishimura, I. (1998). Current perspectives in residual ridge remodeling and its clinical implications: a review. *J. Prosthet. Dent.* 80, 224–237. doi: 10.1016/S0022-3913(98)70116-7
- John, H.-D., and Wenz, B. (2004). Histomorphometric analysis of natural bone mineral for maxillary sinus augmentation. *Int. J. Oral Maxillofac. Implants* 19, 199–207.
- Kim, J.-W., Yang, B.-E., Hong, S.-J., Choi, H.-G., Byeon, S.-J., Lim, H.-K., et al. (2020). Bone regeneration capability of 3D printed ceramic scaffolds. *Int. J. Mol. Sci.* 21:4837. doi: 10.3390/ijms21144837
- Landi, L., Pretel, R. W., Hakimi, N. M., and Setayesh, R. (2000). Maxillary sinus floor elevation using a combination of DFDBA and bovine-derived porous hydroxyapatite: a preliminary histologic and histomorphometric report. *Int. J. Periodontics Restorative Dent.* 20, 574–583.
- Liu, F., Liu, Y., Li, X., Wang, X., Li, D., Chung, S., et al. (2019). Osteogenesis of 3D printed macro-pore size biphasic calcium phosphate scaffold in rabbit calvaria. *J. Biomater. Appl.* 33, 1168–1177. doi: 10.1177/0885328218825177
- Luongo, F., Mangano, F. G., Macchi, A., Luongo, G., and Mangano, C. (2016). Custom-made synthetic scaffolds for bone reconstruction: a retrospective, multicenter clinical study on 15 patients. *Biomed. Res. Int.* 2016:5862586. doi: 10.1155/2016/5862586
- Mangano, C., Mangano, F., Gobbi, L., Admakin, O., Iketani, S., and Giuliani, A. (2019). Comparative study between laser light stereo-lithography 3D-printed and traditionally sintered biphasic calcium phosphate scaffolds by an integrated morphological, morphometric and mechanical analysis. *Int. J. Mol. Sci.* 20:13318. doi: 10.3390/ijms20133118
- Mangano, C., Perrotti, V., Shibli, J. A., Mangano, F., Ricci, L., Piattelli, A., et al. (2013a). Maxillary sinus grafting with biphasic calcium phosphate ceramics: clinical and histologic evaluation in man. *Int. J. Oral Maxillofac. Implants* 28, 51–56. doi: 10.11607/jomi.2667
- Mangano, C., Piattelli, A., Mangano, F., Rustichelli, F., Shibli, J. A., Iezzi, G., et al. (2013b). Histological and synchrotron radiation-based computed microtomography study of 2 human-retrieved direct laser metal formed titanium implants. *Implant. Dent.* 22, 175–181. doi: 10.1097/ID.0b013e318282817d
- Mangano, C., Sinjari, B., Shibli, J. A., Mangano, F., Hamisch, S., Piattelli, A., et al. (2015a). A human clinical, histological, histomorphometrical, and radiographical study on biphasic HA-Beta-TCP 30/70 in maxillary sinus augmentation. *Clin. Implant. Dent. Relat. Res.* 17, 610–618. doi: 10.1111/cid.12145
- Mangano, F. G., Zecca, P. A., van Noort, R., Apresyan, S., Iezzi, G., Piattelli, A., et al. (2015b). Custom-made computer-aided-design/computer-aided-manufacturing biphasic calcium-phosphate scaffold for augmentation of an atrophic mandibular anterior ridge. *Case Rep. Dent.* 2015:941265. doi: 10.1155/2015/941265
- Mazor, Z., Horowitz, R. A., Del Corso, M., Prasad, H. S., Rohrer, M. D., and Dohan Ehrenfest, D. M. (2009). Sinus floor augmentation with simultaneous implant placement using Choukroun's platelet-rich fibrin as the sole grafting material: a radiologic and histologic study at 6 months. *J. Periodontol.* 80, 2056–2064. doi: 10.1902/jop.2009.090252
- Ohayon, L. (2014). Maxillary sinus floor augmentation using biphasic calcium phosphate: a histologic and histomorphometric study. *Int. J. Oral Maxillofac. Implants* 29, 1143–1148. doi: 10.11607/jomi.3422
- Paganin, D., Mayo, S. C., Gureyev, T. E., Miller, P. R., and Wilkins, S. W. (2002). Simultaneous phase and amplitude extraction from a single defocused image of a homogeneous object. *J. Microscopy* 206, 33–40. doi: 10.1046/j.1365-2818.2002.01010.x
- Paré, A., Charbonnier, B., Tournier, P., Vignes, C., Veziers, J., Lesoeur, J., et al. (2020). Tailored three-dimensionally printed triply periodic calcium phosphate implants: a preclinical study for craniofacial bone repair. *ACS Biomater. Sci. Eng.* 6, 553–563. doi: 10.1021/acsbomaterials.9b01241
- Parfitt, A. M., Drezner, M. K., Glorieux, F. H., Kanis, J. A., Malluche, H., Meunier, P. J., et al. (1987). Bone histomorphometry: standardization of nomenclature, symbols, and units. Report of the ASBMR Histomorphometry Nomenclature Committee. *J. Bone Miner. Res.* 2, 595–610. doi: 10.1002/jbmr.5650020617
- Pettinichio, M., Traini, T., Murmura, G., Caputi, S., Degidi, M., Mangano, C., et al. (2012). Histologic and histomorphometric results of three bone graft substitutes after sinus augmentation in humans. *Clin. Oral Investig.* 16, 45–53. doi: 10.1007/s00784-010-0484-9
- Piattelli, A., Scarano, A., Corigliano, M., and Piattelli, M. (1996a). Comparison of bone regeneration with the use of mineralized and demineralized freeze-dried bone allografts: a histological and histochemical study in man. *Biomaterials* 17, 1127–1131. doi: 10.1016/0142-9612(96)85915-1
- Piattelli, A., Scarano, A., and Mangano, C. (1996b). Clinical and histologic aspects of biphasic calcium phosphate ceramic (BCP) used in connection with implant placement. *Biomaterials* 17, 1767–1770. doi: 10.1016/0142-9612(95)00342-8
- Rasband, W. S. (2019). *ImageJ*. Bethesda, MD: U.S.: National Institute of Health. Available online at: <http://imagej.nih.gov/ij> (accessed May 14, 2019).
- Raymond, S., Maazouz, Y., Montufar, E. B., Perez, R. A., González, B., Konka, J., et al. (2018). Accelerated hardening of nanotextured 3D-plotted self-setting calcium phosphate inks. *Acta Biomater.* 75, 451–462. doi: 10.1016/j.actbio.2018.05.042
- Renghini, C., Giuliani, A., Mazzoni, S., Brun, F., Larsson, E., Bairo, F., et al. (2013). Microstructural characterization and *in vitro* bioactivity of porous glass-ceramic scaffolds for bone regeneration by synchrotron radiation X-ray microtomography. *J. Eur. Ceramic Soc.* 33, 1553–1565. doi: 10.1016/j.jeurceramsoc.2012.10.016
- Ripamonti, U., Richter, P. W., Nilen, R. W. N., and Renton, L. (2008). The induction of bone formation by smart biphasic hydroxyapatite tricalcium phosphate biomimetic matrices in the non-human primate *Papio ursinus*. *J. Cell Mol. Med.* 12, 2609–2621. doi: 10.1111/j.1582-4934.2008.00312.x
- Scarano, A., Di Domizio, P., Petrone, G., Iezzi, G., and Piattelli, A. (2000). Implant periapical lesion: a clinical and histologic case report. *J. Oral Implantol.* 26, 109–113. doi: 10.1563/1548-1336(2000)026<0109:IPLACA>2.3.CO;2
- Scarano, A., Piattelli, A., Perrotti, V., Manzoni, L., and Iezzi, G. (2011). Maxillary sinus augmentation in humans using cortical porcine bone: a histological and histomorphometrical evaluation after 4 and 6 months. *Clin. Implant. Dent. Relat. Res.* 13, 13–18. doi: 10.1111/j.1708-8208.2009.00176.x
- Schneider, C. A., Rasband, W. S., and Eliceiri, K. W. (2012). NIH Image to ImageJ: 25 years of image analysis. *Nat. Methods* 9, 671–675. doi: 10.1038/nmeth.2089
- Yamamichi, N., Itoe, T., Neiva, R., and Wang, H.-L. (2008). Long-term evaluation of implant survival in augmented sinuses: a case series. *Int. J. Periodontics Restorative Dent.* 28, 163–169.
- Zeng, H., Pathak, J. L., Shi, Y., Ran, J., Liang, L., Yan, Q., et al. (2020). Indirect selective laser sintering-printed microporous biphasic calcium phosphate scaffold promotes endogenous bone regeneration via activation of ERK1/2 signaling. *Biofabrication* 12:025032. doi: 10.1088/1758-5090/ab78ed

Conflict of Interest: The authors declare that the research was conducted in the absence of any commercial or financial relationships that could be construed as a potential conflict of interest.

The reviewer AS declared a shared affiliation, with no collaboration, with the authors, IDT, AP and GI, to the handling editor at the time of the review.

Copyright © 2021 Mangano, Giuliani, De Tullio, Raspanti, Piattelli and Iezzi. This is an open-access article distributed under the terms of the Creative Commons Attribution License (CC BY). The use, distribution or reproduction in other forums is permitted, provided the original author(s) and the copyright owner(s) are credited and that the original publication in this journal is cited, in accordance with accepted academic practice. No use, distribution or reproduction is permitted which does not comply with these terms.



Enlightenment of Growth Plate Regeneration Based on Cartilage Repair Theory: A Review

Xianggang Wang^{1,2†}, Zuhao Li^{1,2†}, Chenyu Wang³, Haotian Bai^{1,2}, Zhonghan Wang^{1,2}, Yuzhe Liu^{1,2}, Yirui Bao⁴, Ming Ren^{1,2*}, He Liu^{1,2*} and Jincheng Wang^{1,2*}

¹ Orthopaedic Medical Center, The Second Hospital of Jilin University, Changchun, China, ² Orthopaedic Research Institute of Jilin Province, Changchun, China, ³ Department of Plastic and Reconstructive Surgery, The First Hospital of Jilin University, Changchun, China, ⁴ Department of Orthopedics, Chinese PLA 965 Hospital, Jilin, China

OPEN ACCESS

Edited by:

Barbara Zavan,
University of Padua, Italy

Reviewed by:

Zigang GE,
Peking University, China
Fengxuan Han,
Soochow University, China

*Correspondence:

Ming Ren
renming2014@jlu.edu.cn
He Liu
heliu@jlu.edu.cn
Jincheng Wang
wangjinc@jlu.edu.cn

[†] These authors have contributed
equally to this work

Specialty section:

This article was submitted to
Tissue Engineering and Regenerative
Medicine,
a section of the journal
Frontiers in Bioengineering and
Biotechnology

Received: 15 January 2021

Accepted: 10 May 2021

Published: 03 June 2021

Citation:

Wang X, Li Z, Wang C, Bai H,
Wang Z, Liu Y, Bao Y, Ren M, Liu H
and Wang J (2021) Enlightenment
of Growth Plate Regeneration Based
on Cartilage Repair Theory: A Review.
Front. Bioeng. Biotechnol. 9:654087.
doi: 10.3389/fbioe.2021.654087

The growth plate (GP) is a cartilaginous region situated between the epiphysis and metaphysis at the end of the immature long bone, which is susceptible to mechanical damage because of its vulnerable structure. Due to the limited regeneration ability of the GP, current clinical treatment strategies (e.g., bone bridge resection and fat engraftment) always result in bone bridge formation, which will cause length discrepancy and angular deformity, thus making satisfactory outcomes difficult to achieve. The introduction of cartilage repair theory and cartilage tissue engineering technology may encourage novel therapeutic approaches for GP repair using tissue engineered GPs, including biocompatible scaffolds incorporated with appropriate seed cells and growth factors. In this review, we summarize the physiological structure of GPs, the pathological process, and repair phases of GP injuries, placing greater emphasis on advanced tissue engineering strategies for GP repair. Furthermore, we also propose that three-dimensional printing technology will play a significant role in this field in the future given its advantage of bionic replication of complex structures. We predict that tissue engineering strategies will offer a significant alternative to the management of GP injuries.

Keywords: growth plate, cartilage tissue engineering, scaffold, bone marrow mesenchymal stem cells, three-dimensional printing

INTRODUCTION

The growth plate (GP), or the physis, is a cartilaginous region situated between the epiphysis and metaphysis at the end of immature long bones. It acts as the primary center for longitudinal growth in children's long bones (Kronenberg, 2003; Mackie et al., 2011). Being cartilaginous, the GP is the weakest region in the pediatric skeleton, and is vulnerable to injuries including infections, fractures, bone tumors, and iatrogenic damage. The most common sites of GP injuries are the ankle, the distal femur, and the distal radius (MacIntyre and Dewan, 2016). According to the epidemiological data, GP injuries account for 15–30% among all pediatric skeletal injuries (Shen et al., 2019). The major problem with GP injuries is that the injured GP cartilage will be replaced by undesirable bony tissue, forming a bone bridge, which may cause length discrepancies and angular deformities (Gigante and Martinez, 2019). This result can be detrimental to children who are still in the growth phase. Current clinical treatments often include the use of interpositional materials as fillers at the site of the defect after resection of the bone bridge, these materials include autogenous fat, muscle, and

cement. Conversely, when the bone bridge occupies less than 50% of the GP, it will require surgical intervention to resect the bone bridge to insert different interpositional materials including fat, bone wax, muscle, or polymeric silicone materials. However, the clinical success of this surgery is less than 35%, as currently available interpositional materials do not integrate well with host tissues and often lead to subsequent complications. Conversely, when the bone bridge occupies over 50% of the GP, it will necessitate corrective surgeries and limb lengthening procedures in clinic. Similarly, outcomes are unsatisfactory (Ladenhauf et al., 2020). Unfortunately, clinical efforts will lead to secondary damage or result in the recurrence of bone bridge formation (Shaw et al., 2018). It is critical to identify new approaches to prevent bone bridge formation and to promote tissue regeneration.

In recent years, due to the introduction of cartilage repair theory, cartilage tissue engineering has been considered a potential alternative treatment for GP injuries (Diaz-Payno et al., 2020). This technology mainly involves seed cells, growth factors, and scaffolds. The seed cells are expanded *in vitro* and are implanted into the scaffolds to form a cell-based scaffold (Zhao et al., 2019). Although seed cells are influenced by the microenvironment *in situ*, growth factors are still critical to inducing cells to differentiate into desired lineages. Scaffolds fabricated by biocompatible and biodegradable materials, with three-dimensional (3D) structures and suitable mechanical strength, can serve as a substitute for GP defects (Li et al., 2017). After being implanted in the GP defects, the scaffold is degraded gradually during the formation of the new cartilage tissue (Liu J. Y. et al., 2020). Although many studies have been carried out and have achieved good results, there is no consensus on the most suitable materials, seed cells, or growth factors (Erickson et al., 2018). Hence, cartilage tissue engineering still requires more intensive studies in the future.

In this review, we will summarize the histological structure of the GP and pathological processes occurring during bone bridge formation. We will review the progress achieved in tissue engineering for treatment of GP injuries, the challenges in clinical application, and the prospect for the future development will also be analyzed (Scheme 1).

THE MECHANISM OF THE GP DAMAGE

Physiological Characteristics of the GP

The Histological Structure of the GP

The differentiation stages of chondrocytes divide the GP into three distinct zones, from the epiphysis to metaphysis: the resting zone, proliferation zone, and hypertrophic zone (Liu et al., 2019; Figure 1A). Because of the cell types and locations, the composition of the extracellular matrix (ECM) also differs in terms of mechanical strength. Furthermore, the proportions between the three zones also differs among species.

Adjacent to the epiphysis, the resting zone forms a reservoir of stem cells or progenitor cells for chondrocytes in the proliferative zone. Each cell can differentiate into chondrocytes and forms a cell column parallel to the axis of

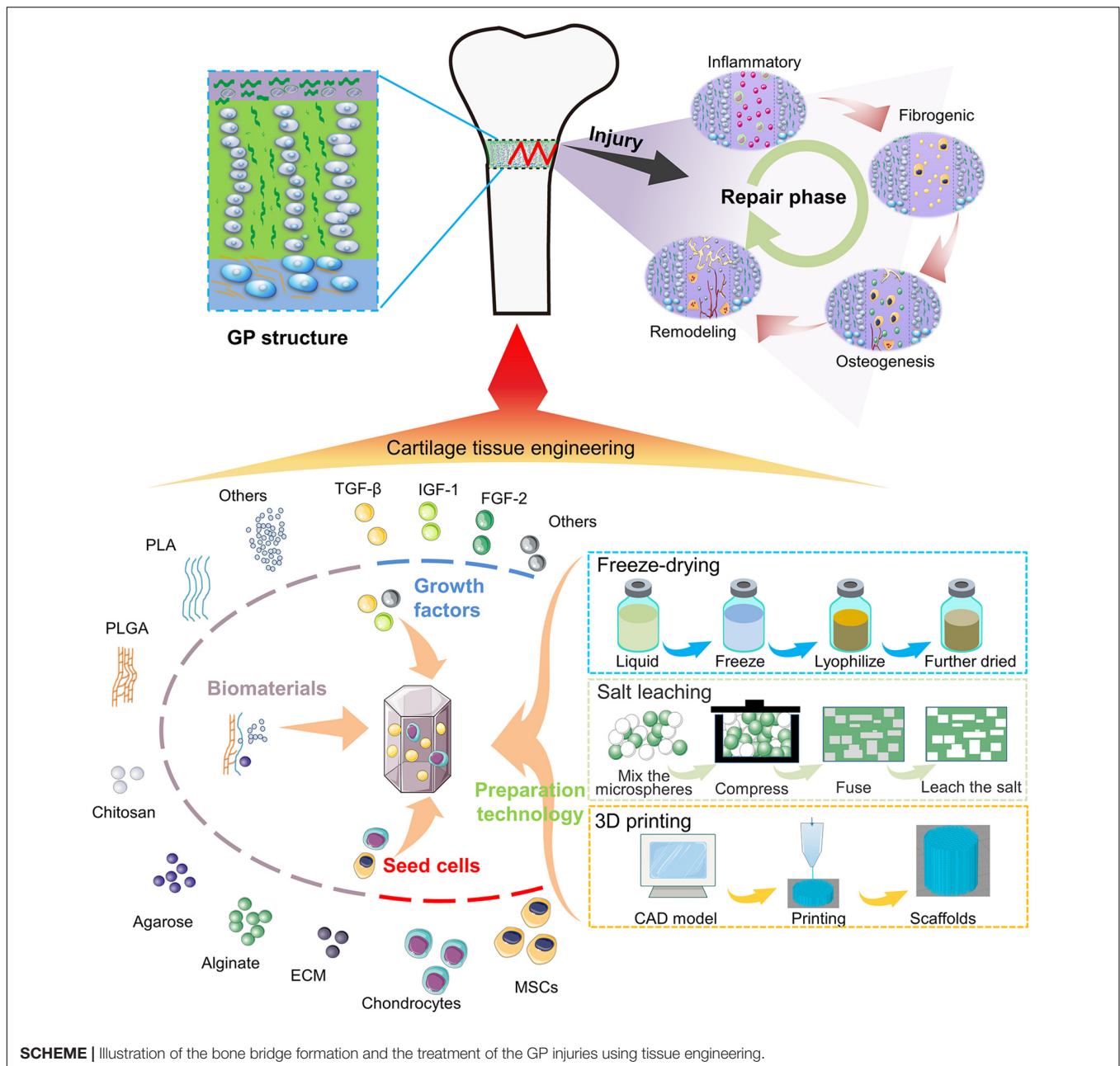
long bones (Newton et al., 2019). Cells located here also secrete parathyroid hormone-related protein (PTHrP), which modulates GP homeostasis by interacting with a growth factor called the Indian hedgehog (Ihh) secreted by hypertrophic chondrocytes (Mizuhashi et al., 2018). PTHrP mainly preserves the population of resting cells and promotes chondrocyte proliferation at the upper region of the GPs. Conversely, Ihh directly antagonizes PTHrP signaling and promotes chondrocyte hypertrophy at the lower region of the GPs (Lee D. et al., 2019). Although these resting cells possess the ability to produce cartilaginous matrix, they tend to remain inactive with lower collagen II (Col II) and proteoglycan production. The main composition of the ECM in this zone is horizontally aligned Col II (Mizuhashi et al., 2019).

Located adjacent to the resting zone, the proliferative zone is vital for cellular division and matrix production, it contains vertically arranged chondrocytes. These longitudinal columns of chondrocytes are separated by the cartilage matrix surrounding them. The ECM is mainly produced in this zone and is enriched in vertically aligned Col II and aggrecan (Lui et al., 2014; Shaw et al., 2018).

In addition, regulated by different growth factors, including bone morphogenic protein (BMP), fibroblast growth factor (FGF), insulin-like growth factor-1 (IGF-1), and tumor necrosis factor (TNF), chondrocytes in the hypertrophic zone stop proliferating, and swell in size (Chung and Xian, 2014). By analyzing the relationship between different parameters and bone growth, the enlargement of chondrocytes is mostly associated with the longitude growth (44–59%) (Cooper et al., 2013). The hypertrophic zone is mainly associated with matrix mineralization, where the ECM is mostly composed of Col X (Pazzaglia et al., 2020). Under the influence of low oxygen tension and in the presence of vascular endothelial growth factor (VEGF), the hypertrophic zone allows blood vessels invasion from the metaphysis. The vessels bring osteoblasts, osteoclasts, and mineralized cartilage-resorptive cells to the zone, and thus convert the mineralized matrix into a bone trabecular-like metaphysis (Cheng et al., 2019). As for hypertrophic chondrocytes in this zone, hypertrophic cells were originally believed to be the final state of chondrocyte differentiation. However, recent fate-mapping studies have altered this view since some hypertrophic chondrocytes differentiate into osteoblasts or progenitor cells instead of undergoing apoptosis. Thus, it is tempting to investigate how resting stem cells establish the fate of hypertrophic cells (Yang et al., 2014; Zhou et al., 2014; Park et al., 2015).

Mechanical Properties of the GP

In the past, studies were limited by ethical concerns and access to materials, and only a few experiments tested the mechanical properties of human GPs. Most studies were based on animal testing, including piglets (Shen et al., 2019), bovine (Cohen et al., 1992), and sheep models (Celarek et al., 2014). In general, for 10-year-old children, with a loading rate of 0.003 s^{-1} , the mean human ultimate stress is $0.98 \pm 0.29 \text{ MPa}$, the mean human ultimate strain is $31 \pm 7\%$, and the mean human tangent modulus is $4.26 \pm 1.22 \text{ MPa}$ (Williams et al., 2001). Animal studies have demonstrated that the lateral region of the proximal tibial GPs

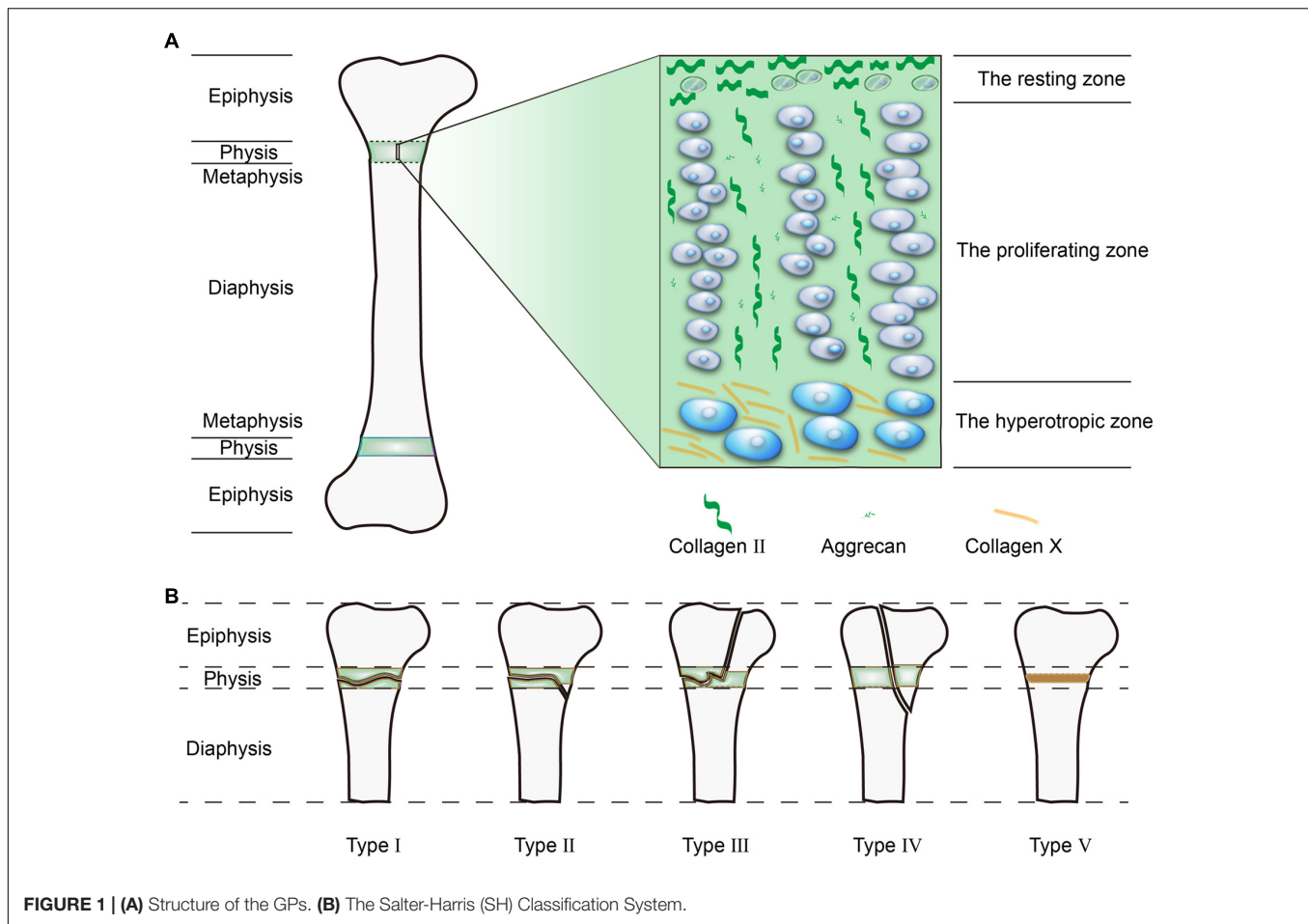


was stronger than the central region and the ultimate tensile strength was similar in different parts of the body. However, the tensile strength is largely affected by the GP thickness. For example, the capital femoral GPs in humans is twice as thick as the bovine proximal tibial GPs, but the tensile strength is only half bovine GPs (Cohen et al., 1992; Williams et al., 2001; Sylvestre et al., 2007). Thus, the GP tends to be weakened as it thickens.

It is important to imitate the natural mechanical properties of GPs in order to successfully engineer cartilage tissue scaffolds. However, to date these characteristics have not been clearly elucidated and additional in-depth studies are required.

Biomechanics plays important role in GP formation and function as well. By varying the loading frequency, amplitude,

or duration, it is shown to affect the height, morphology, gene expression, and matrix mineralization of the GP (D'Andrea et al., 2020). Stokes et al. (2007) demonstrated that intermittent static loading increased GP height while persistent static loading decreased it. As for chondrocyte count in proliferative zone, it is shown to increase in tension, but decrease under compression using persistent static load. Similarly, persistent static tension is reported to stimulate hypertrophic zone height while compression is found to reduce it (Killion et al., 2017). Except for the mechanical loads on GPs, the mechanical properties of biomaterials used in scaffolds are reported to affect chondrogenesis as well. For instance, cells exposed to stiffer substrates showed a more organized cytoskeleton and faster



proliferation rate. Moreover, on softer substrates, cells tended to migrate faster than stiffer one (Ghosh et al., 2007). In conclusion, intermittent tension loading with stiffer scaffolds may benefit GP reconstruction. It is important to figure out the effects of different forms of mechanical stimulation on engineered GPs and to find the optimized stimulus for GP reconstruction. Understanding the effects of mechanical stimulation may help find targets for mechanical strategies for GP repair as well.

Differences Between GP and Other Cartilages

The key for GP regeneration is to reconstruct the gradient differentiation states of chondrocytes in a columnar structure. Enlighten by cartilage regeneration, in order to promote GP regeneration based on cartilage repair theory, it is important to dig up the difference and similarity between GP and other cartilage, especially with articular cartilage.

In cartilage, the GP is the most unique. Among all cartilage in human, articular cartilage is the most similar to GPs. Both of them are composed of chondrocytes and cartilage matrix, they are divided into different zones according to the different state of chondrocytes. Their main components of ECM are Col II, Col X, and glycosaminoglycans (GAGs). However, there are also some differences between GPs and articular cartilage. Firstly, from the perspective of developmental biology, the GP

is most affected by age. In short bones, like phalanges, the GP will close early, while in long bones, it will close later (Lui et al., 2018). When people reach adulthood, all GPs will be replaced by bone plates. In traditional assumptions, it is eventually programmed to cease at the age of 14 in girls and 16 in boys (Little and Milewski, 2016). However, articular cartilage will maintain function and degenerate until people get old. Secondly, in terms of tissue structure, GPs have three distinct zones while articular cartilage is divided into four zones: the superficial zone, the middle zone, the deep zone, and the calcified zone (Qiao et al., 2021). Meanwhile, the arrangement of chondrocytes in GPs are more regular in a columnar structure. Unlike the junction between bone and articular cartilage, GPs have two chondro-osseous junctions because of their anatomical locations (Kazemi and Williams, 2020). In addition, the ECM between GPs and articular cartilage are different as well. As Diaz-Payno et al. (2020) reported, GP specific ECM could be used to promote osteogenesis of BMSCs while articular cartilage derived ECM was potent for chondrogenesis. The spatial distribution of growth factors was also different. In the GP, expression of BMP2 and BMP6 are increased from resting zone to hypertrophic zone. But in articular cartilage, they are decreased from superficial to calcified zones (Garrison et al., 2017). Finally, the functions of GPs and articular cartilage are totally different. The GP is mainly responsible for

longitudinal growth, which is vulnerable and cannot bear much compression, especially for the hypertrophic zone (Xie et al., 2020). Articular cartilage is located in joints, which plays the role of lubrication and buffering (Matsuzaki et al., 2018).

Pathological Characteristics of the GP Damage

Classification of GP Injuries

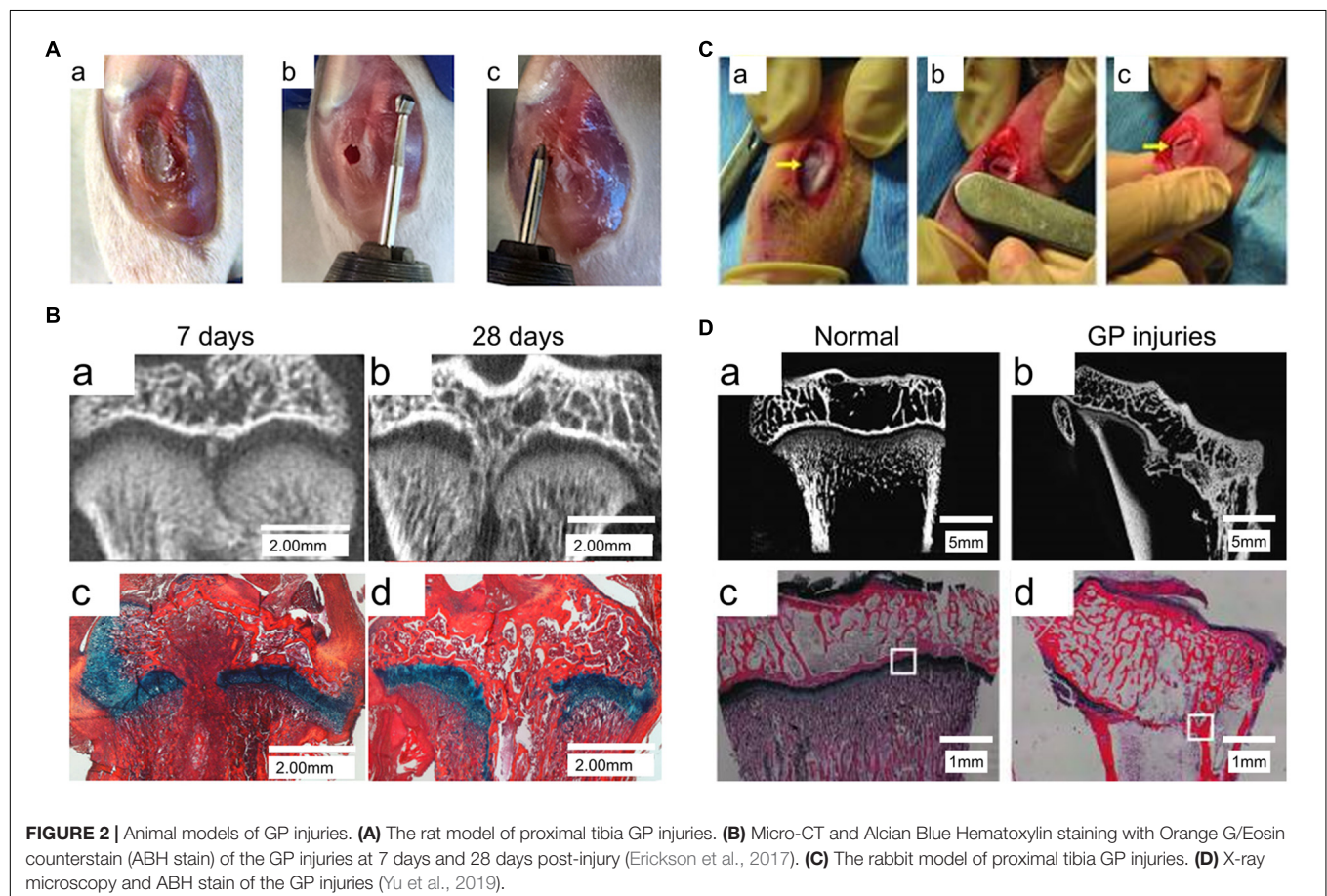
The Salter-Harris (SH) Classification System is most commonly used classification in clinical use that classifies GP injuries into five patterns (**Figure 1B**). About 5% of GP injuries are SH type I, where the injuries affect the whole GP and produces fragmentation. SH type II is the most common type of injury and accounts for 75% of observed injuries, whereby the injuries not only occur transversely across the GP, but also obliquely penetrate the metaphysis. In SH type III, the injuries cross the GP and obliquely penetrate the epiphysis, although this type only accounts for 10% of injuries. In SH type IV, the injuries occur longitudinally through the GP from the articular surface to the metaphysis, this type occurs in 10% of all GP injuries. SH type V, the compressional type, is the least common injury, but is the most likely type to result in bone bridge formation (Chung and Xian, 2014; Sferopoulos, 2014). Among these patterns, the more superficial injuries (SH type III, IV, and V) that destroy both the

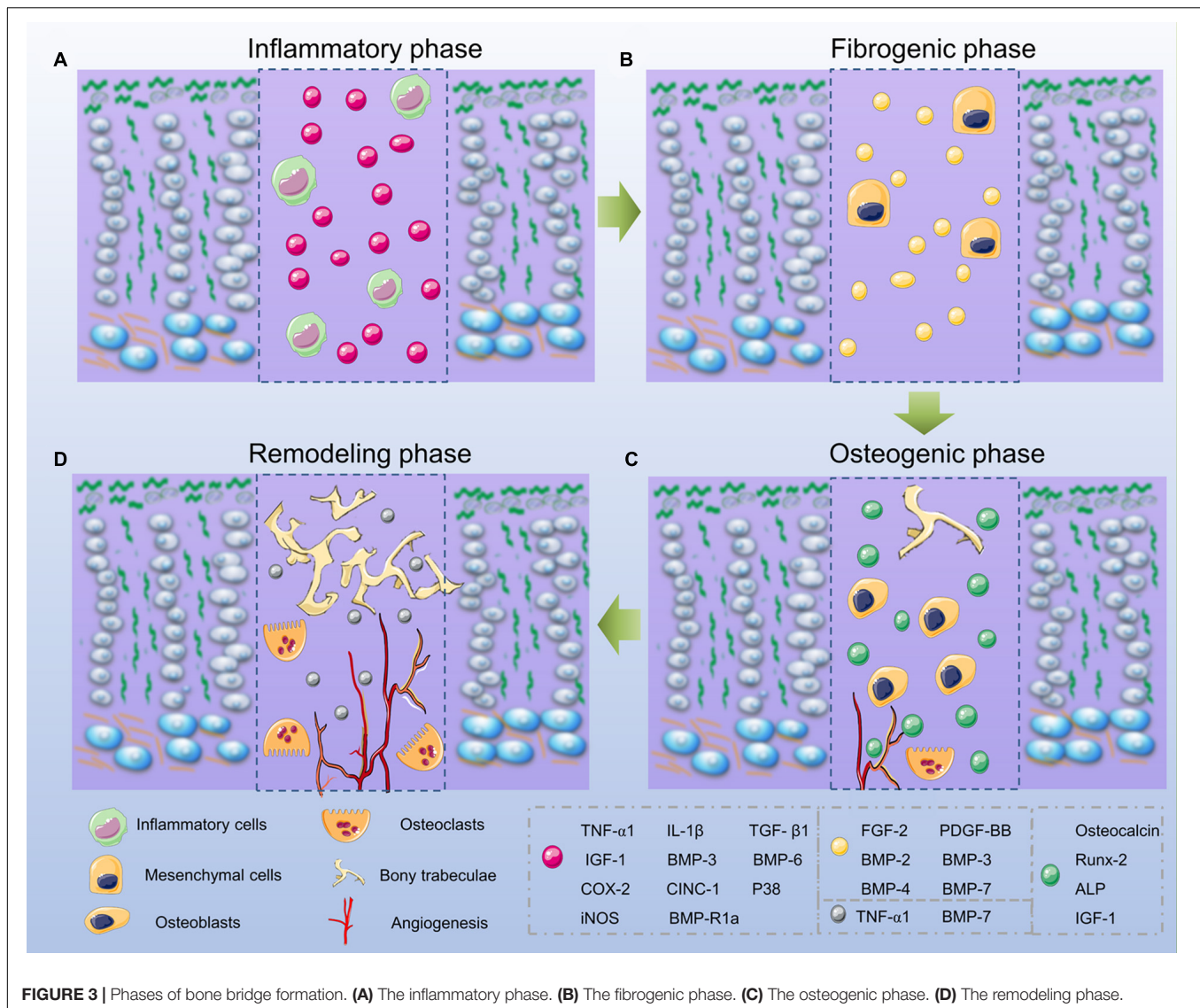
GP and its blood supply often lead to growth arrest and bone bridge formation, the deeper injuries (SH type I and II) which do not disturb the blood supply usually achieve a better prognosis (Yukata et al., 2018; Watanabe et al., 2019).

Phases of GP Injuries

In previous studies, numerous animal models have been used to elucidate the pathophysiology involved in bone repair in GP injuries (**Figure 2**). These animal models included immature mice (Erickson et al., 2017), the miniature pig (Ding et al., 2018), and sheep models (Knapik et al., 2018). These studies identified four phases of injury responses leading to bone repair, namely, the inflammatory phase, the fibrogenic phase, the osteogenic phase, and the remodeling phase (Zhou et al., 2004, 2006).

As for common bone fracture and soft tissue injuries, the first phase after GP injuries is the inflammatory phase, and involves an initial influx of inflammatory cells including neutrophils, macrophages/monocytes, and lymphocytes (**Figure 3A**). Consistent with this infiltration, the rat neutrophil chemokine CINC-1, equivalent to human interleukin (IL)-8, peaks on day 1 and decreases to basal levels on day 4 (Chung et al., 2006, 2011; Chung and Xian, 2014). In order to confirm the importance of the neutrophil-mediated inflammatory responses in bone repair, Chung et al. (2006) utilized a neutrophil-neutralizing antiserum in rats, and their results showed an





increase of osteogenesis-related genes like osteocalcin and core binding factor α -1, a decrease of chondrogenesis-related genes like sex determining region Y box-9 (Sox-9) and Col II, which suggested the inflammatory phase was vital for downstream bone repair events. In addition, TNF- α and IL-1 α also increase significantly on day 1 (Wang et al., 2017). Using a TNF- α antagonist, Zhou et al. (2006) found a clear delay of mesenchymal infiltration, which means TNF- α is required for the migration and proliferation of mesenchymal cells. Other studies also highlighted that TNF- α is a critical factor for healing and tissue repair (Birkel et al., 2019). Overall, the inflammatory phase plays a significant role in the repair of GP injuries as it modulates the cascade downstream of the healing responses.

After the initial inflammatory response, the fibrogenic phase appears on days 3–7 after the GP injuries and involves the fibrous vimentin-immunopositive mesenchymal cells gathering at the injured site. These cells may contain mesenchymal

stem cells (MSCs), osteoprogenitor, and chondroprogenitor cells, which are confirmed to be vital for the fracture repair process (Macasai et al., 2011; Neumayer et al., 2017; **Figure 3B**). In the fibrogenic phase, growth factors, such as FGF-2 and platelet derived growth factor (PDGF) play an important role (Zhou et al., 2004; Shaw et al., 2018). FGF-2 in particular acts by stimulating osteoprogenitor and mesenchymal cell proliferation, migration, alkaline phosphatase (ALP) activity, as well as inhibiting chondrocyte differentiation (Nasrabadi et al., 2018). During wound healing, PDGF functions to enhance cell migration, proliferation, and angiogenesis. During repair of GP injuries, PDGF is essential for the proliferation and migration of fibroblasts and osteoblasts (Zhou et al., 2004; Chung et al., 2009, 2011).

Around day 7, the subsequent osteogenic phase occurs with the appearance of trabecular bone. The Runt-related transcription factor 2 (Runx-2) and ALP-positive stained cells are observed. Additional bone matrix proteins including osteocalcin

(OCN) are produced (Xian et al., 2004). Similarly, Col I production is observed by the presence of regenerated bone tissue at the injury site. During this phase, the bone bridge begins to form (Chung and Xian, 2014; **Figure 3C**).

The remodeling phase can be observed from day 14 onwards, since there are more mesenchymal cells and osteoclasts present in the bone trabeculae (Chung et al., 2009). During this phase, chondrogenesis-related genes like Sox-9 and Col II are expressed at a low level, while the osteogenesis-related genes like OCN are highly expressed (Zhou et al., 2004). In addition, growth factors, such as TNF- α , IGF-1, and BMP-7, increase as well, and they promote differentiation and recruitment of the osteoclasts, thus promoting bone remodeling (Fischer et al., 2018; Kim et al., 2018; **Figure 3D**).

Responses to GP Injuries in Different Anatomical Locations

After the GP injury, chondrocyte columns become disorganized at the injury site (Hajdu et al., 2011). Throughout the whole section, the thickness of the injured area was always higher than non-injured area. As more hypertrophic chondrocytes occurred after the fibrogenic phase, the height of resting zone and hypertrophic zone increased while proliferative zone height relatively reduced. Immunohistochemistry of Col X staining also reported that Col X extends throughout the entire injury site (Drenkard et al., 2017). Furthermore, the GP injury also affects the adjacent non-injured region because injuries destroyed the controlled endochondral ossification process. For example, Macsai et al. (2011) detected bone bridge formation at the uninjured area of GPs on day 60 in rats. Further analysis revealed there was a decrease in expression of chondrogenic factors including Sox-9, transforming growth factor- β 1 (TGF- β 1), and IGF-1, and an increase of apoptotic factors like caspase-3 in the adjacent non-injured area (Musumeci et al., 2013). Studies have demonstrated there are different responses in varied locations after GP injuries, but the detailed evidence is limited. It requires more studies to elucidate how the three distinct zones response in varied phases and how these contributions change the outcomes after GP injuries.

CARTILAGE TISSUE ENGINEERING FOR GP INJURIES

The engineering of cartilage tissue is a comprehensive approach that utilizes various cell types and growth factors, including bone marrow mesenchymal stem cells (BMSCs), chondrocytes, and TGF- β , IGF-1, and FGF-2 (Chen et al., 2020; Wei et al., 2020), as well as different scaffolds constructed with natural or synthetic materials (Abdollahiyan et al., 2020). In this section, we will discuss the progress of cartilage tissue engineering in the treatment of GP injuries.

Seed Cells

Because of the limited microenvironment for cartilage regeneration, seed cells are widely used to fill defects following bone bridge resections. By promoting cell proliferation and ECM

excretion, the seed cells will restore the cartilage tissue of the GP. Extensively used seed cells, such as MSCs and chondrocytes in GP repair are discussed below.

Mesenchymal Stem Cells

MSCs have been widely used in cartilage tissue engineering due to their capability for self-renewal and potential for multiple differentiation. MSCs can secrete diverse growth factors and differentiate into various cellular types, such as osteocytes, chondrocytes, and adipocytes, which play an important role in cell-based therapies (Isobe et al., 2016; Gultekin et al., 2020). As mentioned earlier, during the fibrogenic phase, there is an influx of MSCs in the injured site, indicating that MSCs are vital in the repair process of GP injuries (Zhou et al., 2004).

In previous studies, MSCs from multifarious sources were utilized in the treatment of GP injuries and achieved excellent results (Sananta et al., 2020). Li et al. (2017) fabricated an oriented ECM scaffold incorporating BMSCs to cure the injured GPs in rabbits, and results showed that compared to ECM scaffolds alone, ECM scaffolds with BMSCs prevented the bone bridge formation, reduced the length discrepancy and consequently the angular deformity. To further examine the role of periosteum MSCs, Chen et al. (2003) transferred the periosteum together with harvested MSCs embedded agarose to the site of GP defects, the transferred group receiving agarose alone showed poor results, while the angular deformity and growth arrest were corrected in the MSCs embedded group. In another study, Ando et al. produced a 6-week-old rabbit growth arrest model by disrupting the medial half of the proximal tibias, in order to test the effect of synovial derived MSCs, a scaffold-free construct was used, and results showed that the MSCs proliferated and differentiated into cells similar to chondrocytes, suggesting that the MSC-based therapy could be an effective method for curing GP injuries (Yoshida et al., 2012).

In addition to MSCs derived from bone marrow, periosteum, and synovium, MSCs can also be obtained from adipose tissue, umbilical cord, placenta, and skeletal muscle (Uder et al., 2018). Previous studies have demonstrated that MSCs derived from various compartments possess different regenerative potentials (Kaviani et al., 2019). Therefore, it is necessary to define the most practical way to promote the GP repair for clinical applications among all the available sources. Therefore, Isobe et al. (2016) examined the multipotentiality of MSCs derived from adult dental pulp, synovial fluid, exfoliated deciduous teeth, and bone marrow, and concluded that bone marrow- and synovial fluid-derived MSCs were most suitable for osteogenesis while synovial fluid-derived cells produced the highest levels of chondrogenesis. Similarly, Sakaguchi et al. (2005) also compared the properties of MSCs derived from bone marrow, periosteum, adipose tissue, and skeletal muscle, and also verified that MSC features differed significantly according to their sources, and MSCs isolated from synovium were superior in both osteogenesis and chondrogenesis. Although synovium-derived MSCs seemed to have more potential for GP repair, they are more difficult to obtain and purify, which limits their application. Meanwhile, BMSCs can be isolated easily and are expanded efficiently (Yee et al., 2018). Furthermore, it has been demonstrated that BMSCs

can stimulate angiogenesis, suppress the immunoreaction, and inhibit fiber tissue formation (An et al., 2018). Altogether, the evidence suggests that BMSCs maybe more suitable as seed cells in the treatment of GP injuries (Planka et al., 2009).

As for MSCs, another problem that has been addressed is whether autogenous MSCs are superior to allogeneic MSCs. In one clinical study, patients with Hurler syndrome (MPS-IH) infused allogeneic BMSCs for treatment of patients with metachromatic leukodystrophy (MLD). The results indicated an improvement in bone mineral density and nerve function among all patients, indicating that allogeneic MSCs could survive and function in host tissue (Koc et al., 2002). Furthermore, Planka et al. (2008) transplanted autogenous and allogeneic MSCs in rabbits with distal femoral GP injuries, and found there was no significant difference either in femur length discrepancy or in angular deformity between these two procedures. It seems there is a high tolerance of allogeneic MSCs in host immune rejection. Studies have elucidated that allogeneic MSCs escape from the host immune response by altering cytokine secretion, and thus modulate immune cells including dendritic cells, natural killer cells, and effector T cells (Bocelli-Tyndall et al., 2007; Cequier et al., 2019). Therefore, the effects of allogeneic MSCs are equal to those of autogenous MSCs.

Chondrocytes

Since the most abundant cell type in the GP is chondrocytes, it is quite rational to implant chondrocytes in cartilage tissue engineered scaffolds for treatment of GP injuries (Lee et al., 2016; Tomaszewski et al., 2016). Chondrocytes can also be obtained from different compartments in autograft or allograft. In an autologous chondrocyte experiment, Tomaszewski et al. (2014) resected the medial part of the proximal tibia GP in rabbits and then implanted it in the GP defects. Histological and radiological results demonstrated that implanting of autologous chondrocytes significantly prevented the bone bridge formation and growth arrest. In another study, Jin et al. (2006) investigated autologous chondrocytes obtained from the iliac crest, seeded on the demineralized bone matrix (DBM) scaffold for the treatment of rabbit GP injuries. This type of autologous tissue engineered scaffold not only prevented the angular deformity and bone formation, but also built the columnar structure at the injured site. Although the autologous chondrocytes can avoid the immune rejection and show good results both *in vitro* and *in vivo*, they are limited in number and may cause additional damage (Boopalan et al., 2019). From this standpoint, allogeneic chondrocytes may represent a better alternative if they present good results in future studies. Li et al. (2013) used allogeneic chondrocytes harvested from distal femoral GPs, microencapsulated by semipermeable membranes, and transplant the preparations in a GP injury model. Sixteen weeks later, the chondrocytes-treated group showed less length discrepancy and angular deformity than other groups, the histological results also exhibited columnar arrangement formed by neogenetic chondrocytes at the injured site, which indicated that the allogeneic chondrocytes could prevent bone formation to the same extent as autologous chondrocytes. Since there is no significant difference between allogeneic and autologous

chondrocytes, it is tempting to speculate how allogeneic chondrocytes escape from the immune response. Several studies have proposed that the avascular nature in cartilage and the surrounding ECM may provide a protective immune barrier for embedded chondrocytes (Zhao et al., 2019).

Allogeneic and autologous chondrocytes may have a similar treatment effect, but when determining the body sites for chondrocyte derivations, it is difficult to define the most suitable site. Although Jin et al. (2006) indicated that chondrocytes derived from the iliac crest GP had more advantages than chondrocytes from joint cartilage as the former still had the potential for proliferation and differentiation (Jin et al., 2006). More studies are needed to elucidate the different effects between chondrocytes isolated from various sources.

As for proliferative and differentiation abilities, *in vitro* studies have shown that three dimensional (3D) cultures can retain the chondrogenic potential better than monolayer cultures (Chow et al., 2011). Parreno et al. (2017) demonstrated that the monolayer culture of chondrocytes could alter their phenotype and produce more Col I secretion and less Col II secretion, which indicated the primitive feature of chondrocytes was lost. Meanwhile, several studies have demonstrated that 3D culture of chondrocytes can promote cellular proliferation without changing phenotypes. For example, rabbit articular chondrocytes cultured on poly(ethylene glycol)/poly(ϵ -caprolactone) (PEG/PCL) hydrogel led to the up-regulated expression of chondrogenic genes such as Sox-9, aggrecan, and Col II in 2 weeks, and increased proteoglycans and Col II accumulation after 4 weeks (Chang et al., 2018). Therefore, in order to retain the phenotype of implanted chondrocytes, a favorable strategy is to incubate them in a 3D culture environment before seeding.

Growth Factors

Cartilage-stimulating growth factors are bioactive peptides that bind to specific receptors and trigger a series of cell activities including cell migration, proliferation, and differentiation (Chen et al., 2020). In order to ameliorate the microenvironment for cartilage tissue formation, it is necessary to use chondrogenic factors such as IGF-1, FGF-2, and TGF- β 1, to stimulate the chondrogenic differentiation of chondrocyte-related progenitor cells.

TGF- β

TGF- β is produced in an inactive form and is activated via signaling pathways, it plays an important role during the chondrogenesis of MSCs (Chen et al., 2018). *In vivo*, TGF- β has two forms, and mostly accumulates by binding to the ECM, while the other form is a soluble free form, which is present in only small amounts, but plays a predominant role. Previous studies have demonstrated that TGF- β functions differently and has opposite effects on GP through TGF- β /Smad2/3 or BMP/Smad1/5/8 signals. The TGF- β /Smad2/3 signaling pathway stimulates chondrogenesis and ECM synthesis while the BMP/Smad1/5/8 signaling pathway inhibits chondrogenesis and promotes osteogenesis (Thielen et al., 2019). As a short-lived cytokine, TGF- β is only active for a few minutes in response to GP inflammation or ECM damage (Liu W. et al., 2020).

Since TGF- β is a critical factor in cartilaginous differentiation, cartilage tissue engineered scaffolds have used TGF- β in the treatment of GP repair. An *in vitro* study indicated that MSCs induced by TGF- β 1 presented significantly higher levels of aggrecan, Col II, and Sox-9 in a high-density monolayer culture (Coleman et al., 2013). In an ovine animal model, McCarty et al. (2010) utilized a gelfoam scaffold containing autologous BMSCs and TGF- β 1, implanted in the proximal ovine tibial GP defect, and results showed that the scaffold containing TGF- β 1 inhibited bone bridge formation.

Two strategies have been described for using TGF- β to stimulate MSC differentiation or proliferation: one involves the secretion of TGF- β by chondrocytes through co-culture of MSCs and chondrocytes, the other involves the addition of exogenous TGF- β . Chen et al. (2018) used a mathematical model to compare these two distinct strategies and proposed a hybrid strategy. The authors reported that in cocultures of chondrocytes and MSCs, a critical value of chondrocyte density was to be achieved before the complete differentiation of MSCs could be induced. For the *in vitro* environment, the critical density was between 5 and 25%. With regard to the exogenous administration of TGF- β , there were two critical values, a_{crit1} and a_{crit2} : below the concentration of a_{crit1} , no cells were produced, and above the initial concentration of a_{crit2} , all MSCs would be driven to differentiation. The value of a_{crit2} was slightly lower than 10 ng/mL. Moreover, by combining these two strategies, fewer chondrocytes were required and less exogenous TGF- β was needed to induce MSCs differentiation, and a lower concentration of a_{crit2} was needed, requiring about 10% chondrocytes co-culture (Chen et al., 2018). Similarly, Dahlin et al. (2014) also observed that co-culture of articular chondrocytes and MSCs required less TGF- β 3 to achieve an equivalent chondrogenesis level compared to MSCs cultured alone. In conclusion, it is more effective to use chondrocyte co-cultures and less exogenous TGF- β to stimulate MSCs differentiation or proliferation.

IGF-1

Being vital in cartilage homeostasis and repair, IGF-1 is an anabolic growth factor which has been extensively studied (Lo et al., 2020). Previous studies have confirmed that IGF-1 can not only stimulate chondrocytes to synthesis matrix proteins like Col II and proteoglycan, but it can also inhibit chondrocytes degradation and apoptosis during cartilage damage by blocking the function of IL-1 or TNF- α (Mahran et al., 2019). In a clinical trial, IGF-1 was used to treat short stature children for 1 year. No adverse events were reported, which indicated that IGF-1 may have potential for clinical application (Midyett et al., 2010).

Over the past 20 years, several studies have been conducted to investigate the effects of IGF-1 on loaded scaffolds in GP regeneration. In an *in vitro* study, Mullen et al. (2015) utilized a porous collagen-glycosaminoglycan scaffold containing chondrocytes and different concentrations of IGF-1, and testing the amount of proteoglycan and Col II products. The results showed that the most suitable IGF-1 loading concentration was 50 μ g/mL, and IGF-1 loaded groups synthesized more ECM than the empty group (Mullen et al., 2015). An *in vivo*

study also indicated that a collagen sponge impregnated with exogenous IGF-1 induced higher chondrocytes influx and ECM production in immature cartilage defects, which means that IGF-1 is beneficial to cartilage repair (Tuncel et al., 2005). In another study, porous PLGA scaffolds loaded with IGF-1 were used in the treatment of a rabbit model with proximal tibial GP defects, after implantation in the GP defects, regenerated cartilage was observed in the IGF-1 releasing group, while there was only bone formation in the empty group and in the scaffolds alone group (Figure 4), all the results indicated that IGF-1 was suitable for GP regeneration (Sundararaj et al., 2015). As for the biphasic pattern of IGF-1 release in PLGA scaffolds, initially, due to the rapid surface diffusion, a burst in IGF-1 release is observed within 24–48 h, this burst can be therapeutic for it initiates early MSCs differentiation, proliferation, and ECM deposition. Afterward, IGF-1 is released to a much lower degree with erosion of the scaffold matrix, thus maintaining a certain concentration of IGF-1 in the injured site (Giteau et al., 2008; Mullen et al., 2015; Sundararaj et al., 2015).

FGF-2

The family of the FGF has been demonstrated to be critical for a wide range of cell types regarding differentiation, proliferation, migration, and growth. Among the FGF family members, FGF-2, FGF-8, and FGF-18 have recently been proposed to be the most important contributing factors in cartilage modulation (Lee et al., 2018). As for GP-related MSCs differentiation and proliferation, FGF-2 has been extensively investigated. Interestingly, previous studies have shown contradictory effects for FGF-2 in the expansion and differentiation phases (Jin et al., 2020). During MSCs expansion, FGF-2 enhances the proliferation potential and retards the differentiation process by regulating the expression of FGF receptor 1 (Yang et al., 2008). Moreover, by upregulating FGF receptor 3, it also promotes matrix deposition (Furusho et al., 2020). During the differentiation phase, the FGF receptor 1 is poorly expressed, and thus inhibits differentiation and matrix deposition (Han et al., 2020).

FGF-2 is effective when applied to cartilage tissue engineered scaffolds for GP repair which mainly exist in the resting and proliferating zones (Krejci et al., 2007). An *in vitro* study indicated that MSCs expanded and maintained high viability of FGF-2 levels, but showed minimal matrix deposition (Coleman et al., 2013). Other MSCs culture experiments also demonstrated that MSCs express FGF receptors, and FGF-2 treatment increased the mitogenic ability of MSCs, thus promoting their proliferation rate during expansion (Xu et al., 2017). In the application of engineered cartilage tissue, FGF-2 was usually used with other growth factors. In an experiment of rat BMSCs culture, Coleman et al. (2007) demonstrated that BMSCs produced greater amounts of sulfated glycosaminoglycans in the presence of FGF-2 and TGF- β 1 than with TGF- β 1 treated alone, which indicates that FGF-2 plays a role in GP regeneration.

Other Growth Factors

In addition to the growth factors described above, (i.e., TGF- β , IGF-1, and FGF-2) there are many other growth factors that have also been validated to be associated with GP repair.

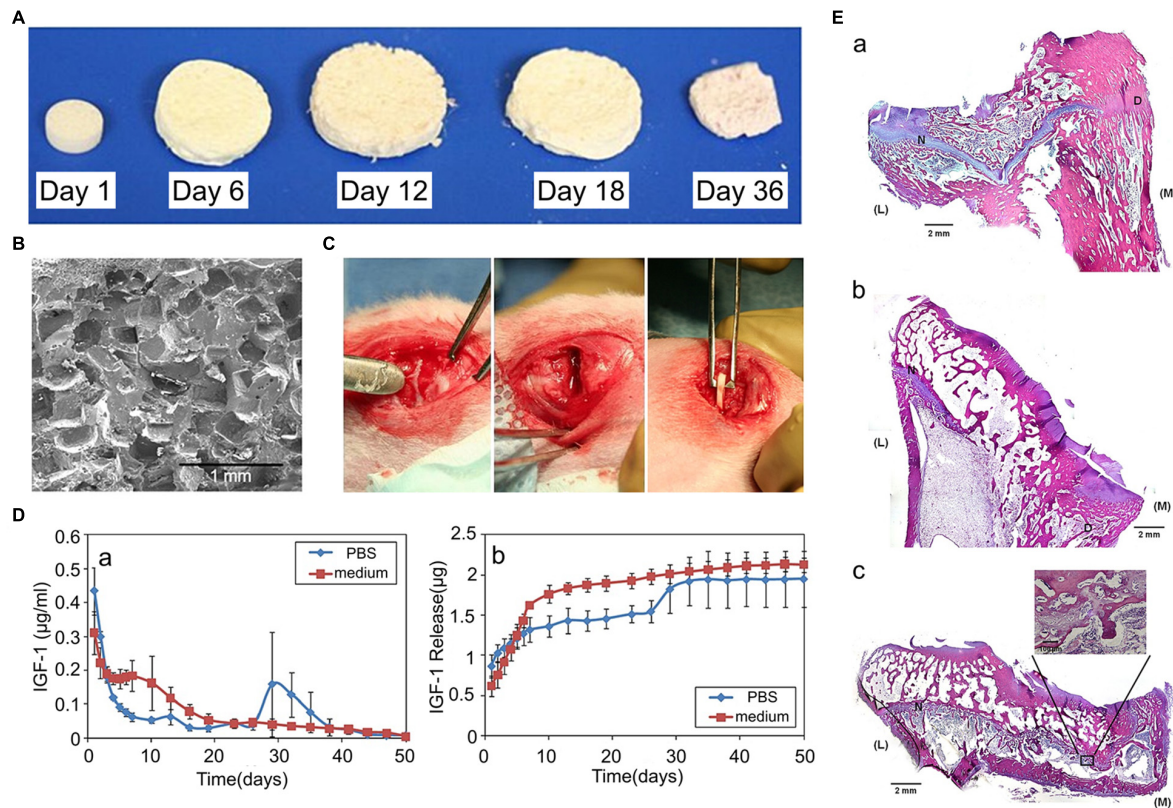


FIGURE 4 | Effects of IGF-1 loaded scaffolds in GP injuries. **(A)** Morphology of the PLGA scaffold and its degradation in the cell culture medium. **(B)** The transverse plane of PLGA scaffolds observed using a scanning electron microscope (SEM). **(C)** The proximal tibial GP defects of rabbits. **(D)** The biphasic pattern of IGF-1 release. **(E)** Hematoxylin and eosin (H&E) staining of the GP repair. (a) control group without implantation, (b) the blank scaffold group, (c) the IGF-1 loaded scaffold group (reproduced with permission from Sundararaj et al., 2015).

Using a rat tibial GP injury model, Chung et al. (2014) found that treatment with anti-VEGF antibody inhibited the activity of VEGF, which decreased bone formation, OCN, and Runx-2 expression, indicating that VEGF-promoted angiogenesis plays an important role in undesired bone repair. Another study found that neurotrophin-3 enhanced osteogenesis and angiogenesis by upregulating BMP-2 and VEGF in bone formation, indicating that neurotrophin-3 may be a potential target to inhibit bone repair in GP injuries (Su et al., 2016). Similar to VEGF and BMP-2, BMP-6, and BMP receptor-1a were also shown to contribute to bone formation (Fischerauer et al., 2013). However, Zhou et al. (2006) demonstrated that TNF- α could inhibit bone formation at the injured GP site in rats by stimulating p38 MAP kinase activity. In conclusion, these growth factors are positively or negatively associated with unwanted bone formation during GP repair, they are potential targets for curing GP injuries. However, the therapeutic application of these growth factors in cartilage tissue engineering have not been fully explored. Further studies are required to elucidate their roles for GP regeneration.

Scaffolds

Since the GP is a functional area responsible for longitudinal growth and withstands weight-bearing between the metaphysis

and diaphysis, it is important for cartilage scaffolds to exhibit good biocompatibility, biodegradability, suitable porosity, as well as appropriate mechanical properties. Currently, a wide range of biomaterials have been used for GP repair, including natural and synthetic materials.

Fabrication Methods

In cartilage tissue engineering, various preparation methods have been applied while fabricating scaffolds. These methods include the freeze-drying technique, the salt leaching technique, 3D printing technique, the gas foaming technique, electrospinning technique, crosslinking methods for hydrogel scaffolds preparation and so on. In this section, we will present the most commonly used technique in GP scaffold fabrication.

The Freeze-Drying Technique

The freeze-drying technique has been commonly used for fabricating porous scaffolds in previous investigations. It contains three major phases: first, the material solutions are infused into a cylindrical mold, which is then allowed to freeze in a freezer at -20°C for 1 or 2 h. Then, the mold is transferred into a freeze dryer to allow lyophilization under vacuum for approximately 48 h. Finally, the scaffold is then dried and stored

in a refrigerator at 4°C (Suphasiriroj et al., 2009; Zheng et al., 2011). Scaffolds manufactured using this method have significant advantages, generating pore sizes of around 100 μm and porosity of more than 90%, and with some improvements, it can also produce structured scaffolds, which not only improve mechanical properties, but also exhibit a biomimetic columnar structure to stimulate chondrocytes proliferation in GPs (Mohammady et al., 2020). However, freeze-drying is a complex and time consuming process with harsh environmental requirements and the need for expensive equipment limit its applications. Nonetheless it is still challenging to find new techniques with simpler procedure and cheaper cost.

The Salt Leaching Technique

The salt leaching technique is mainly used to fabricate scaffolds using materials in the form of microspheres. The procedure can be illustrated briefly as follows: initially the microspheres are mixed with salt particles, mostly NaCl. Afterward, the mixture is placed in a cast (according to the diameter of scaffolds) and is consolidated by compressing at a load of 2.5 tons (tons increase with diameters) for a few minutes. Then, the disc is heated near the melting point (T_g) of the material for about 48 h in order to fuse the microspheres. After that, the salt is leached in deionized water overnight to create porous scaffolds. Finally, the porous scaffolds are lyophilized in a vacuum (Das et al., 2018). Following these steps, the scaffolds are ready to use. The pore size achieved by this method is between 1 and 700 μm , the porosity is around 60% (Ravi et al., 2012). Although scaffolds made in this way have good mechanical properties, the procedure is also time consuming and complex, the available materials are limited and the pore sizes are randomly distributed. Therefore, it is necessary to find another technique which can control the pore size in a more accurate way.

3D Printing Technique

Application of 3D printing, or additive manufacturing, also known as solid-freeform technology or rapid prototyping, is a promising technology developed since the mid-1980s, and has been applied in various fields including construction, automation, and aerospace. The additive manufacturing techniques include stereolithography (SLA), fused deposition modeling (FDM), selective laser sintering (SLS), inkjet bioprinting, and extrusion bioprinting (Reeser and Doiron, 2019). Compared to traditional techniques used to make scaffolds for the treatment of GP injuries, 3D printing has the following advantages. (1) Few equipment and technical requirements: to complete the scaffold, all that is needed are prepared materials, a 3D printer, and a computer-aided design (CAD) software (Mikolajczyk et al., 2019). There is no need to modify temperature or time, the 3D printer automatically adjusts these parameters (Siller et al., 2019). (2) Lower costs and time saving: with minimal use of materials and printing requires only a few hours or even a few minutes, thus demanding less labor and material resources, the 3D printing technique can maximally cut the cost (Ballard et al., 2020). (3) A wide range of available materials: unlike conventional fabricating techniques, 3D printing uses a variety of materials, including metals, alloys,

polymers, and bioceramics (Tardajos et al., 2018). (4) Precise individual customization: through a CAD software monitor, the pore size and porosity are made highly consistent with expectations, consequently, it is possible to fabricate gradient scaffolds with accurately designed pore sizes (Wo et al., 2020).

Hydrogel Scaffolds Preparation Techniques

Nowadays, hydrogels are immensely used in cartilage tissue engineering because of their excellent biocompatible properties. They have three dimensional networks which are formed from crosslinked polymer. They provide desired structure by absorbing water, which mimic the natural ECM of cartilage (Choi et al., 2020b). Various hydrogel scaffolds have been used in cartilage tissue engineering, their composition include natural materials (e.g., alginate, chitosan, Col and gelatin), synthetic materials [e.g., polyether, poly(vinyl pyrrolidone), and poly(acrylate acid)] and composite materials.

As for preparation of hydrogels, they are crosslinked by physical or chemical crosslinking methods. Physical crosslinking is a way to produce network of polymer chains by physical treatments like heating, cooling, freeze-drying, or ultrasonication. In this way, the polymer networks are connected by reversible bonds such as ionic interaction, hydrogen bonds, or crystallization (Zhang et al., 2021). The advantage of physical crosslinking methods is that each component does not produce chemical reaction during crosslinking. It avoids the production of new substances which may be toxic. Its deficiency is obvious as well. Hydrogels made in this way are deficient in mechanical strength and thermal stability (Wang Y. X. et al., 2020). Materials suitable for physical crosslinking are chitosan, Col I, alginates, and polyvinyl alcohol. Chemical crosslinking is another gelation method which creates covalent linkage among polymer chains by using proper crosslinking reagents (Kong et al., 2020). These crosslinking reagents include glutaric dialdehyde, tannic acid, genipin and so on. Because of the strong connections, chemical crosslinking not only enhances mechanical strengths of hydrogels, but also improves the resistance to degeneration. Moreover, the biomechanical strengths can be adjusted by altering the type or concentration of reagents (Fathi-Achachelouei et al., 2020). The main disadvantage of chemical crosslinking method is the potential usage of cytotoxic reagents, catalysts, or initiators (Oryan et al., 2018).

For preparation of hydrogel scaffolds, various techniques have been used, such as bioprinting technique, microfluidic technique, photolithography technique and so on. Among these techniques, bioprinting technique is a 3D printing technique using hydrogels as a bioink (Antich et al., 2020). Besides bioprinting, microfluidic technology is another efficient method to fabricate hydrogel scaffolds with precision. Through droplet production methods like dielectrophoresis and electrowetting on dielectric, microfluidic systems can produce microparticles in a highly monodispersed pattern and manipulate these nanoliter of liquids through microchannels. Because of the production of tiny droplets, this technique is a powerful tool for preparing scaffolds with complex 3D structure, as well as hydrogel scaffolds with mechanical or chemical gradients (Moreira et al., 2021). The photolithography technique is mainly used in hydrogel that

crosslinked via ultraviolet light. After fabricate hydrogel in a plane pattern, the light will transmit through the hydrogels in designed pathway. The mechanical strength of scaffolds can be altered by changing the intensity or irradiation time of ultraviolet light (Vedaghavami et al., 2017).

Materials

Natural Materials

Thanks to the superior biocompatibility and suitable biodegradability, natural materials like ECM, alginate, agarose, and chitosan are appropriate to initiate chondrocyte regeneration and cartilaginous ECM secretion (Choi et al., 2020a).

ECM Derived From GPs. As a natural material derived from GP, ECM is an alternative matrix used to make scaffolds for treatment of GP injuries, since it is not only composed of cartilage matrix such as GAGs and Col II which can best imitate the microenvironment for chondrocyte regeneration (Cunniffe et al., 2019), but it is also known to contain various growth factors that modulate angiogenesis, cell migration, differentiation, proliferation, and the immune response (Horton et al., 2020).

Previous studies have shown that GP-derived ECM containing diverse growth factors, such as VEGF and IGF- β 1, not only supported vascularization, but also enhanced the regeneration of BMSCs (Cunniffe et al., 2017). These results suggested that this type of ECM was a multipotential substrate and its function would change based on the transplantation site. For treatment of GP injuries, Li et al. (2017) collected the ECM from GPs and constructed the structured ECM scaffolds loaded with BMSCs. Sixteen weeks after transplantation into the tibial GP defects, the histological results showed regeneration of new chondrocytes, and the radiographic results showed reduced length and angular deformities (Figure 5), indicating this GP generated a structured ECM scaffold with the potential for GP repair (Li et al., 2017). Although GP-derived ECM was biocompatible with the porous structure and proved superior to artificial polymer materials, the restricted accessibility limits its application (Lee S. et al., 2019). For clinical usage, it is necessary to find materials that are more accessible, inexpensive, biocompatible, and biodegradable.

Alginate. With ideal biocompatibility and low toxicity, alginate is one of the most extensively used materials for hydrogel-based cartilage tissue engineering (Sturivant and Callanan, 2020). Since alginate hydrogels are able to provide a 3D environment with a wide range of pore sizes, scaffolds made by alginate facilitate MSCs distribution and provide efficient nutrient transport (Farokhi et al., 2020). Furthermore, it can also be used to deliver growth factors with adjustable release rates by changing the molecular weight (Jiao et al., 2019). In order to enhance the chondrogenesis of MSCs in alginate, several studies have successfully delivered growth factor or genes to local MSCs, thus directs the fate of MSCs and increases sGAG and Col II production (Davis et al., 2018; Khatab et al., 2020). As for GP cartilage regeneration, using an *in vitro* model of the GP chondrocytes seeded on alginate hydrogel scaffolds with exogenous factors also resulted in high viability, low level hypertrophy, and cartilage matrix deposition (Coleman et al., 2007; Erickson et al., 2018). In a GP injuries

model, alginate-polylysinealginate semipermeable membranes were used for chondrocyte encapsulation. After 16 weeks of implantation into defects, the radiological results showed less angular deformity and length discrepancies, indicating this alginate material was suitable for GP reconstruction (Li et al., 2013). However, alginate hydrogel is negatively charged, which results in a dissimilar environment for encapsulated cells (Freeman and Kelly, 2017). Nonetheless, alginate hydrogel is still a suitable material for constructing scaffolds for GP regeneration.

Agarose. Agarose is another popular material for cartilage tissue engineering. As a natural polysaccharide polymer, agarose is composed of repetitions of D-galactose and 3, 6-anhydro-L-galactopyranose (Choi et al., 2020a; Salati et al., 2020). Similar to alginate, it is commonly used for hydrogel due to its excellent biodegradability and biocompatibility as well (Bonhome-Espinosa et al., 2020). Moreover, agarose has a similar structure to ECM, and possess great capacity of water absorbing, both features make it particularly suitable for cell adhesion, cell growth, differentiation, and nutrient permeation (Grolman et al., 2019). When applied to treatment of GP defects with MSCs, both *in vitro* and *in vivo* studies presented chondrogenesis and correction of limb deformity, indicating agarose scaffolds could support cell growth and delivery growth factors (Chen et al., 2003; Coleman et al., 2013). Most importantly, its thermal reversible gelation behavior and internal networks allow it to composite with other polymers, which makes it possible to fabricate scaffolds with higher strength (Lee Y. et al., 2019).

Chitosan. Chitosan, made of β (1–4) glycosidic bonds and D-glucosamine residues, is a natural polymer found in the exoskeleton of crustaceans (Ribeiro et al., 2020). It contains different amounts of N-acetyl-D-glucosamine (NAG) groups. When the chitosan has more than 50% NAG, it is called chitin, and when it has more than 50% N-glucosamine, it is called chitosan (Saravanan et al., 2016). With the characteristics of excellent mechanical stability, biocompatibility, biodegradability, and a hydrophilic surface, chitosan is thought to be a suitable material to fabricate porous scaffolds (Ishikawa et al., 2020). When applied to cartilage tissue engineering, it has shown to promote hyaluronic acid synthesis, which benefits cartilage regeneration (Kashi et al., 2018). To restore the damaged GP, the chitosan scaffold alone showed poor results, but when combined with a large concentration of MSCs, it resulted in less angular deformity in rabbits (Azarpira et al., 2015). Therefore, MSCs based chitosan scaffolds may be a good combination in treatment of GP injuries (Erickson et al., 2020).

Synthetic Materials

Synthetic materials, such as PLGA, PLA, and PCL, are widely used to make scaffolds in cartilage tissue engineering, they have tunable properties in terms of mechanics and degradation rates can be artificially regulated by changing the degree of polymerization (Uz et al., 2019). Compared to natural materials, they possess more suitable mechanical strength for load bearing and drug delivery.

PLGA. PLGA is a promising synthetic polymer material suitable for the treatment of GP damage. It has alterable mechanical

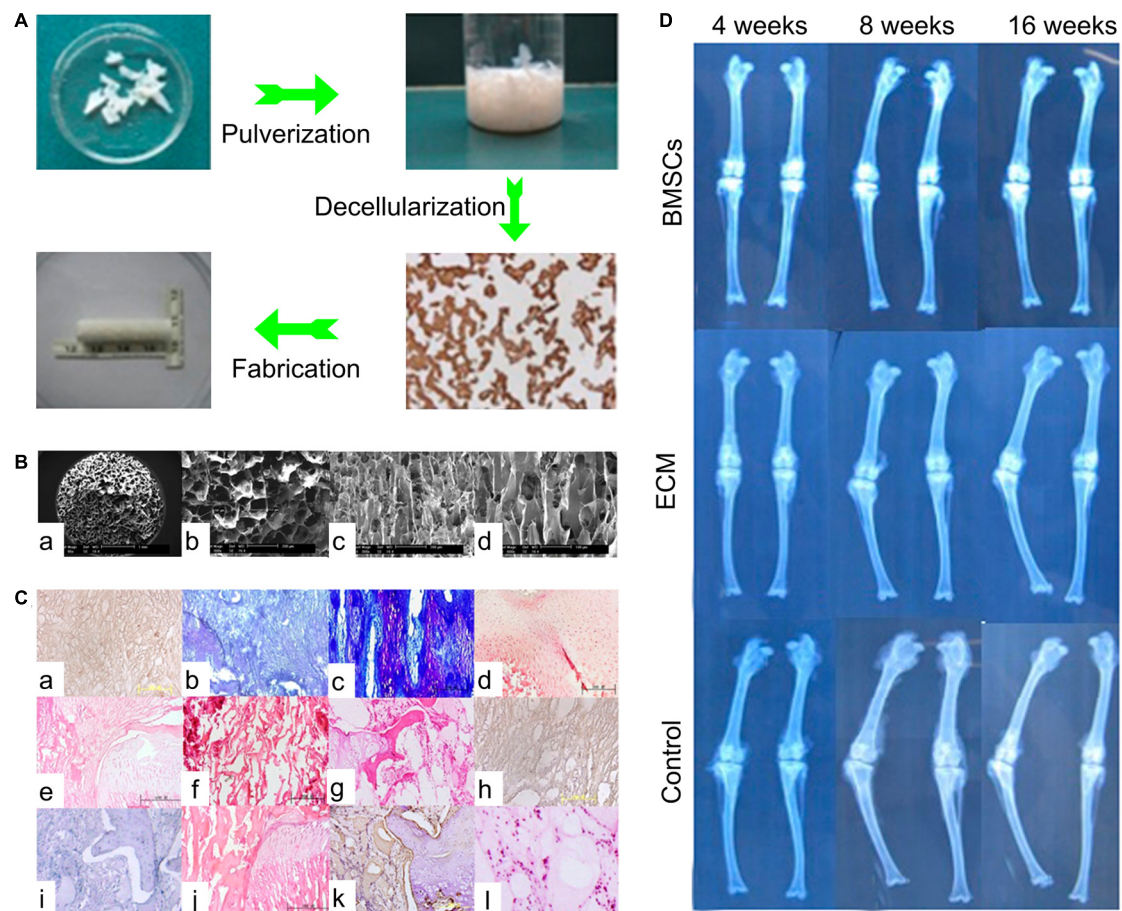


FIGURE 5 | The ECM scaffold in treatment of GP injuries. **(A)** The process of ECM scaffold fabrication. **(B)** SEM micrograph of ECM scaffolds. **(C)** The histological results of ECM based scaffolds. (a–d) In the ECM + BMSCs group, from 4 to 16 weeks, neogenetic chondrocytes increased gradually and were arranged in a columnar structure. (e–h) In the ECM alone group, from 4 to 16 weeks, fibrous tissue and bone tissue gradually come into being. (i–l) In the control group, from 4 to 16 weeks, fibrous tissue and bone tissue covered the defects early. **(D)** The radiological results of three groups [Reproduced with permission from Li et al. (2017)].

properties by controlling the proportion of lactic acid and glycolic acid, which makes it suitable for cartilage tissue implantation (Yan et al., 2017). When implanted *in vivo*, PLGA scaffolds will be degraded into lactic acid and glycolic acid which will be eliminated through GP metabolic pathway (Fathi-Achachelouei et al., 2020). Moreover, thanks to its controllable drug release kinetics, PLGA microspheres have also been approved for drug delivery by the Food and Drug Administration (FDA) (Zuo et al., 2016). Certainly, when utilized as a drug delivery vehicle of IGF-1, more chondrocytes and Col II were observed both *in vitro* and *in vivo* (Sundararaj et al., 2015). In a detailed study, Clark et al. (2015) used PLGA scaffolds alone or loaded with IGF-1 and cells for the treatment of GP injuries, PLGA alone had therapeutical effects as it showed more chondrocytes accumulation compared to fat grafts used in the clinic. Moreover, in our study BMSCs loaded with IGF-1 improved chondrocyte proliferation with more chondrocyte accumulation, and inhibited bone formation than scaffolds alone or IGF-1 delivered alone (Figure 6). All these results unravel that the PLGA scaffold is a good interpositional material and an appropriate carrier for GPs reconstruction.

Poly(lactic Acid). Poly(lactic acid) (PLA) is also a hydrophobic polyester used in biomedical applications (Yao et al., 2020). As a semicrystalline polymer, its crystallinity is approximately 37%, its glass transition temperature is approximately 67°C, and its melting temperature is approximately 180°C (Wan and Zhang, 2018). In addition, PLA is a thermoplastic polymer with high mechanical strength and low degradation rate (Georgiopoulos et al., 2018). Similar to PLGA, PLA is degraded in the form of oligomers, and its degradation products are lactic acid which is present in human body and can be metabolized *via* natural pathways (Gremare et al., 2018). The disadvantages of PLA are its poor thermal stability, high hydrophobicity, and brittleness (Vroman and Tighzert, 2009; Saini et al., 2016). However, there are only a few studies available using PLA scaffolds in the treatment of GP injuries. Implanted in proximal tibial GP defects in rabbits, the treatment of PLA scaffolds combined with chondrocytes resulted in new columnar chondrocytes formation, indicating that PLA is an appropriate material to fabricate scaffolds in GP related cartilage tissue engineering (Zhou et al., 2000, 2003).

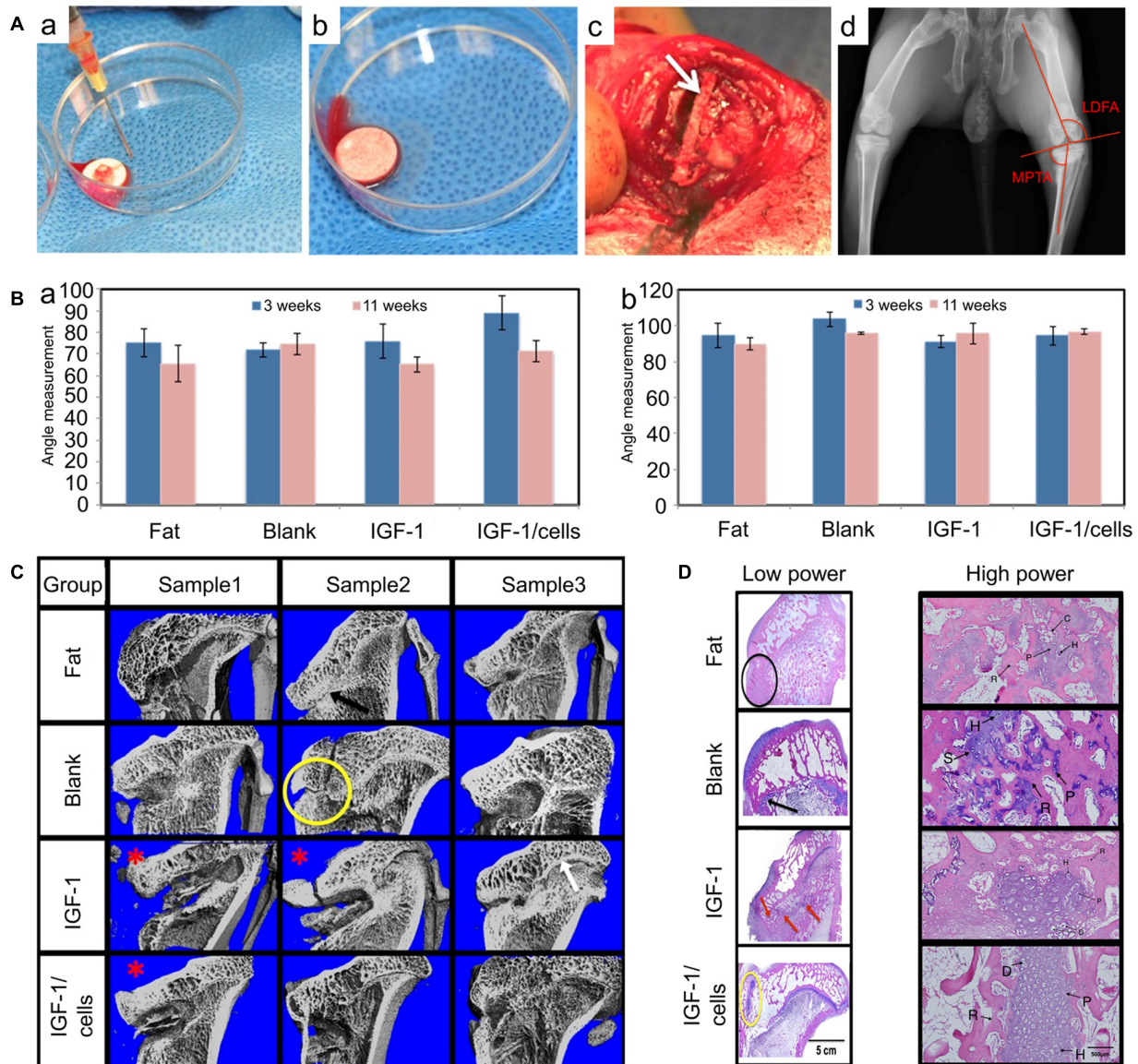


FIGURE 6 | PLGA scaffolds in the treatment of GP injuries. **(A)** (a–c) The morphology of PLGA scaffolds *in vitro* and *in vivo*. **(d)** Measurements of the lateral distal femoral angle (LDFA) and the medial proximal tibial angle (MPTA). **(B)** (a) MPTA and (b) LDFA results of GP injuries at 3 weeks (without bone bridge resection) and 11 weeks (8 weeks after scaffolds implantation). **(C)** Micro-CT of the tibia in four treatment groups. **(D)** The histological results of GP repair with low power and high power in different groups (reproduced with permission from Clark et al., 2015).

Composite Materials

Scaffolds made by composite materials are currently increasingly used. Given the disadvantages of single materials, it is reasonable to mix materials with complementary advantages together when fabricating a scaffold (Keplinger et al., 2019; Trakoolwannahchai et al., 2019). As described above, the remarkable ECM material derived from GP is a typical composite material mainly composed of GAGs and Col II (Horton et al., 2020). With tunable mechanical properties and excellent biocompatibility, composite materials can suitably simulate the internal environment and exhibit good cell affinity. For example, agarose hydrogel is

a biocompatible material with poor mechanical properties, and is rapidly degraded *in vivo* (Zarrintaj et al., 2018). To overcome these limitations, agarose based composite materials are necessary. Kumar et al. (2018) synthesized a composite material with agarose and chitosan, and this new material-based scaffolds showed more suitable degradation rates and higher mechanical strength which may be more suitable for cartilage tissue engineering. Not only do natural composite materials have better characteristics, but also composite materials made by natural and synthetic materials are advantageous. For example, Wang et al. (2016) utilized a composite scaffold

synthesized by PLGA, Col, and silk fibroin for cartilage repair, by altering the ratio of constituents. The *in vitro* studies indicated this composite scaffold promoted MSCs proliferation and differentiation without side effects, and the *in vivo* results showed enhanced cartilage regeneration in cartilage defects (Wang et al., 2016). In another study treating GP arrest in pigs, a scaffold consisting of chitosan and Col I was investigated. The composite material was more stable in the simulated body environment and the mechanical properties were significantly better than the single materials (Planka et al., 2012). In conclusion, scaffolds made by composite materials will be a promising solution for GP repair and regeneration (Table 1).

THE POTENTIAL APPLICATIONS OF 3D PRINTING

Utilization of 3D Printing in Cartilage Tissue Engineering

Over the last two decades, the technology of 3D printing has played a crucial role in the development of cartilage tissue engineering. A significant breakthrough has involved the utilization of biomimetic materials. As described above, ECM is an excellent material that provides a suitable microenvironment for chondrocytes growth and proliferation. Recently, several studies have explored its strengths for fabricating scaffolds. After removing all the cellular materials the ECM can be obtained from fat, cartilage, heart, or muscle tissue. The decellularized ECM has successfully been transformed into bioink for 3D printing (Fahimipour et al., 2019). Pati et al. (2014) produced 3D printed

scaffolds with a porous 3D structure using cartilage derived ECM with a PCL framework. When cultured with MSCs, high cell viability and cartilage-related gene expression were observed, suggesting the 3D printed scaffolds would provide critical stimuli for MSCs growth, engraftment, and long-term functions (Pati et al., 2014). Another study printed an alginate reinforced ECM scaffold for cartilage regeneration, the ECM based scaffold was capable of supporting MSCs and could deliver growth factors to promote robust chondrogenesis with a high level of Col II expression (Rathan et al., 2019). A different method used to achieve biomimetic materials involves using composite materials. Many studies have prepared cartilage imitating materials with chitosan-PCL/silk fibroin composite (Thunsiri et al., 2020), chitosan-gelatin hydrogel/PLGA composite (Schneider et al., 2018), or chitosan/gelatin/sodium β -glycerophosphate composite (Hu et al., 2019). Scaffolds printed by these chondro-inductive materials have been shown to stimulate chondrocytes survival and proliferation (Muller et al., 2017).

Thanks to the accurate control of 3D printing, another breakthrough achieved is the production of gradient scaffolds with distinct regions (Daly et al., 2017). Because gradient structures are present in human cartilage, it is reasonable to use scaffolds with various pore sizes. The heterogeneous interspace has a direct impact on nutrient distribution, which determines the chondrogenesis (Li et al., 2020). Through 3D fiber deposition technology, Di Luca et al. (2016) prepared a gradient scaffold with four distinct pore sizes of 326, 540, 744, and 968 μ m. MSCs seeded in the gradient scaffold observed enhanced chondrogenesis with more GAG deposition compared with non-gradient scaffolds

TABLE 1 | Recently published experimental studies.

References	Seed cells	Growth factors	Scaffolds	Technique	Animal models	Results
Li et al. (2017)	BMSCs		ECM	New freeze-drying technique	Rabbits	Reduced the angular deformity and length discrepancy, observed neogenetic GPs
Gultekin et al. (2020)	BMSCs or Chondrocytes		Cell sheets		Rabbits	Prevented endochondral ossification, promoted bone growth
Lee et al. (2016)	Chondrocytes		Cell synthesized ECM	Cell culture	Rabbits	Minimized the deformity of rabbits
Tomaszewski et al. (2016)	Chondrocytes		A cartilago-fibrous construct		Rabbits	Satisfactory graft integration and fair restitution of GP architecture
Sundararaj et al. (2015)		IGF-1	PLGA	The salt leaching technique	Rabbits	Observed neogenetic cartilage
Clark et al. (2015)	BMSCs	IGF-1	PLGA	The salt leaching technique	Rabbits	Increased chondrocyte density and inhibited bone bridge formation
Azarpira et al. (2015)	BMSCs		Chitosan	The freeze-drying technique	Albino rabbits	Less angular deformity with more MSCs concentration
Erickson et al. (2020)			Alginate/chitosan hydrogels		Rats	50:50 of irradiated alginate and chitosan produced the most cartilage tissue
Erickson et al. (2017)			A chitosan microgel		Rats	Neogenetic cartilage was observed
Lee D. et al. (2019)	Chondrocytes		Allogeneic decalcified bone matrix		Rabbits	Prevent limb deformity
Sananta et al. (2020)	Adipose-derived cells		Bone wax		Rat	Prevented bone bridge formation

(Di Luca et al., 2016). Therefore, scaffolds with gradient structure are considered as a good strategy to promote chondrogenic differentiation of MSCs.

Potential Superiorities of 3D Printing in GP Repair

Since the GP has three distinct zones with diverse differentiation stages of chondrocytes and different ECM components, the mechanical properties of each region are also distinctive (Shaw et al., 2018). From this standpoint, a 3D printing technique will be a fitting method as it produces scaffolds with gradient pore sizes possessing heterogeneous mechanical strength (Montazerian et al., 2019). Moreover, when printing different regions of a scaffold, using bioink with distinct strengths will also change the mechanical properties in different parts of the scaffold, which will best imitate the physiological structure of the GP.

Furthermore, chondrocytes with gradient density in scaffolds could be achieved by 3D bioprinting technology. Ren et al. (2016) bioprinted a cell gradient scaffold using Col II and chondrocytes and cultured it for several weeks. The gradient chondrocyte density resulted in a gradient deposition of ECM, making it possible to achieve the distinct GP ECM through variable cell density bioprinting (Ren et al., 2016).

Previous investigations have also suggested that more scaffolds improve the restore the physical structure, the better enhance of cartilage regeneration (Pati et al., 2014; Di Luca et al., 2016). Therefore, we expect the 3D printing technology will be applied widely in cartilage tissue engineering to treat GP injuries.

FUTURE DIRECTIONS

Due to the avascular and hypoxic characteristics of cartilage tissue, healing is difficult after a severe injury (Wang D. Q. et al., 2020). Based on this shortcoming, cell-based cartilage tissue engineering technology has been proposed for the treatment of cartilage damage. In this cartilage repair system, seed cells are provided directly, and scaffolds made of biomaterials are used as carriers to fill the defects (Munir et al., 2020). Inspired by this system, the same method can be applied to GP injuries because of the limited self-healing capacity. Tissue engineered GPs have been explored in many studies; however, many problems remain unresolved as well.

Mechanism of GP Development

At present, the precise regulatory mechanism of the GP is not clear. It is critical to unravel how different cytokines interact to precisely regulate the growth of long bones. In the future, a deeper understanding of the regulatory signaling pathways in skeletal development will make it possible to inhibit bone bridge formation with medicines that modulate specific signaling pathways. Moreover, additional studies are needed to clarify the specific phenotype of GP cells. Differences between chondrocytes in the GPs and chondrocytes in articular cartilage should also be elucidated. Recently, stem cells in the resting zone have been identified (Newton et al., 2019), but how these cells proliferate and differentiate

into hypertrophic chondrocytes, and what determines the fate of hypertrophic chondrocytes still remains unknown. The essential physiology of GP chondrocytes needs to be further deepened.

Repair Cells

Recently, much progress has been achieved in the area of tissue engineered cartilage repair in GP injuries. The most extensively used seed cells are BMSCs and chondrocytes. However, other stem cells like embryonic stem cells and induced pluripotent stem cells (iPSCs) are also frequently used in cartilage tissue engineering. Thus, it is worth investigating the application of other types of stem cells in the treatment of GP injuries. Given the proficient application of iPSCs in cartilage repair system, it would be easier to apply iPSCs for the treatment of GP injuries in the future. Thanks to the easy accessibility and multiple differentiation potentials, iPSCs will likely play a critical role in clinical applications (Swaroop et al., 2018). In addition, due to the current limitations in basic research, the methods used to identify regenerated GP chondrocytes relies on histological observation and immunological detection of cartilage-related proteins (Fernandez-Iglesias et al., 2020). Nonetheless, these methods can only evaluate chondrocytes in general, while the identification of GP-specific chondrocytes still remains an unsolved problem. It is expected that in the future, we can find a specific protein related to the GP chondrocytes in order to accurately identify GP reconstruction.

Local Bioactive Microenvironment

At present, a self-healing system of tissue engineered GPs is widely used for damaged GPs. Experimental results show that cartilage repair is successful, a large number of chondrocytes are regenerated, and cartilaginous ECM is synthesized in large quantities (Hong Y. P. et al., 2020). Following bone bridge resection, defects can be filled with scaffolds, which are loaded with seed cells (Erickson et al., 2018). If necessary, growth factors could also be added to enrich the regeneration microenvironment (Sundararaj et al., 2015). As for the selection of growth factors, during the process of development to maturity, there are a variety of regulatory factors involved in GP regulation, such as Ihh, PTHrP, and BMP-2 (Hallett et al., 2019). But unfortunately, the application of these bioactive substances has not been fully explored. Future studies should assess the therapeutic effects of these active factors.

Structure Design of Scaffolds

The scaffold materials used currently have many shortcomings. Considering the numerous composite materials available for cartilage tissue engineering exhibiting excellent performance, 3D printing technology will allow to achieve a precise control in fabrication technology, which has been widely used to produce scaffolds with complex and gradient structures (Hong H. et al., 2020). It is foreseeable that bionic scaffolds fabricated by composite materials will play an important role in treatment of GP injuries in the near future. Currently, scaffolds with various

structures are used in cartilage tissue engineering, for example, to generate pores of different shapes and orientations, such as in grid, triangular, rectangular, or circular. Further, porous scaffolds having different porosity and pore sizes, with interconnected or unconnected pores, have all been applied to cartilage tissue engineering, but there is still no consensus on the best structure. Additional studies will be required to identify the most suitable parameters for GP reconstruction.

CONCLUSION

The GP plays an important role in the longitudinal growth of long bones. Considering damage to GPs will result in limb length discrepancies and angular deformities, it is critical to identify more effective ways to address these problems. Inspired by the advances in the cartilage repair system, tissue engineered GPs have received greater attention as a potential therapy for GP regeneration. The construction of the implants theoretically should include repair seed cells for cartilaginous tissue reconstruction, growth factors to induce chondrogenesis, as well as scaffolds for load bearing, active substance delivery, and enhancing the regenerative microenvironment. This review mainly focused on the developments of tissue engineered GPs in the treatment of GP injuries. The unsolved problems and challenges that impede its clinical application were unraveled. Moreover, combined with the advantages of 3D bioprinting

technology to fabricate scaffolds with gradient bionic structure, tissue engineered GPs will help overcome the challenges in the treatment of GP injuries in the future.

AUTHOR CONTRIBUTIONS

XW and ZL conceived the study and wrote the manuscript. CW and HB carried out the analysis with the help of ZW, YL, and YB. MR, HL, and JW contributed intellectually throughout the study. All of the authors critically reviewed this manuscript and approved the final draft.

FUNDING

This study was supported by the National Natural Science Foundation of China (82001971 and 81701811); National Key R&D Program of China (2018YFB1105100); Scientific Development Program of Jilin Province (20200403088SF, 20200802008GH, 20200404202YY, 20200404140YY, 20190304123YY, 20200404190YY, 20190103087JH, 20180201041SF, and 20180623050TC); Program of Jilin Provincial Health Department (2019SCZT001, 2019SCZT014, and 2019SRCJ001); the Youth Talents Promotion Project of Jilin Province (192004); and the Interdisciplinary Research Funding Program for Doctoral candidates of Jilin University (No. 41900200861).

REFERENCES

- Abdollahiyan, P., Oroojalian, F., Mokhtarzadeh, A., and de la Guardia, M. (2020). Hydrogel-based 3D bioprinting for bone and cartilage tissue engineering. *Biotechnol. J.* 15:e2000095. doi: 10.1002/biot.202000095
- An, Y., Liu, W. J., Xue, P., Ma, Y., Zhang, L. Q., Zhu, B., et al. (2018). Autophagy promotes MSC-mediated vascularization in cutaneous wound healing via regulation of VEGF secretion. *Cell Death Dis.* 9:58. doi: 10.1038/s41419-017-0082-8
- Antich, C., de Vicente, J., Jimenez, G., Chocarro, C., Carrillo, E., Montanez, E., et al. (2020). Bio-inspired hydrogel composed of hyaluronic acid and alginate as a potential bioink for 3D bioprinting of articular cartilage engineering constructs. *Acta Biomater.* 106, 114–123. doi: 10.1016/j.actbio.2020.01.046
- Azarpira, M. R., Shahcheraghi, G. H., Ayatollahi, M., and Geramizadeh, B. (2015). Tissue engineering strategy using mesenchymal stem cell-based chitosan scaffolds in growth plate surgery: a preliminary study in rabbits. *Orthop. Traumatol. Surg. Res.* 101, 601–605. doi: 10.1016/j.otsr.2015.04.010
- Ballard, D. H., Mills, P., Duszak, R., Weisman, J. A., Rybicki, F. J., and Woodard, P. K. (2020). Medical 3D printing cost-savings in orthopedic and maxillofacial surgery: cost analysis of operating room time saved with 3D printed anatomic models and surgical guides. *Acad. Radiol.* 27, 1103–1113. doi: 10.1016/j.acra.2019.08.011
- Birkel, D., Quiros, M., Garcia-Hernandez, V., Zhou, D. W., Brazil, J. C., Hilgarth, R., et al. (2019). TNF α promotes mucosal wound repair through enhanced platelet activating factor receptor signaling in the epithelium. *Mucos. Immunol.* 12, 909–918. doi: 10.1038/s41385-019-0150-8
- Bocelli-Tyndall, C., Bracci, L., Spagnoli, G., Braccini, A., Bouchenaki, M., Ceredig, R., et al. (2007). Bone marrow mesenchymal stromal cells (BM-MSCs) from healthy donors and auto-immune disease patients reduce the proliferation of autologous- and allogeneic-stimulated lymphocytes in vitro. *Rheumatology* 46, 403–408.
- Bonhome-Espinosa, A. B., Campos, F., Durand-Herrera, D., Sanchez-Lopez, J. D., Schaub, S., Duran, J. D. G., et al. (2020). In vitro characterization of a novel magnetic fibrin-agarose hydrogel for cartilage tissue engineering. *J. Mech. Behav. Biomed. Mater.* 104:103619. doi: 10.1016/j.jmbbm.2020.103619
- Boopalan, P., Varghese, V. D., Sathishkumar, S., Arumugam, S., and Amarnath, V. (2019). Similar regeneration of articular cartilage defects with autologous & allogenic chondrocytes in a rabbit model. *Indian J. Med. Res.* 149, 650–655. doi: 10.4103/ijmr.IJMR_1233_17
- Celarek, A., Fischerauer, S. F., Weinberg, A. M., and Tschegg, E. K. (2014). Fracture patterns of the growth plate and surrounding bone in the ovine knee joint at different ages. *J. Mech. Behav. Biomed. Mater.* 29, 286–294. doi: 10.1016/j.jmbbm.2013.09.010
- Cequier, A., Barrachina, L., Romero, A., Vitoria, A., Zaragoza, P., Vazquez, F. J., et al. (2019). Humoral immune response against allogeneic equine mesenchymal stem cells (MSCs) mediated by the major histocompatibility complex (MHC): an issue to take into account for the safety and efficacy of treatment with MSCs. *Hum. Gene Ther.* 30, A164–A164.
- Chang, C. S., Yang, C. Y., Hsiao, H. Y., Chen, L., Chu, I. M., Cheng, M. H., et al. (2018). Cultivation of auricular chondrocytes in poly(ethylene glycol)/poly(epsilon-caprolactone) hydrogel for tracheal cartilage tissue engineering in a rabbit model. *Eur. Cells Mater.* 35, 350–364. doi: 10.22203/eCm.v035a24
- Chen, F., Hui, J. H., Chan, W. K., and Lee, E. H. (2003). Cultured mesenchymal stem cell transfers in the treatment of partial growth arrest. *J. Pediatr. Orthop.* 23, 425–429.
- Chen, L., Liu, J. X., Guan, M., Zhou, T. Q., Duan, X., and Xiang, Z. (2020). Growth factor and its polymer scaffold-based delivery system for cartilage tissue engineering. *Int. J. Nanomed.* 15, 6097–6111. doi: 10.2147/IJn.S249829
- Chen, M. J., Whiteley, J. P., Please, C. P., Schwab, A., Ehlicke, F., Waters, S. L., et al. (2018). Inducing chondrogenesis in MSC/chondrocyte co-cultures using exogenous TGF- β : a mathematical model. *J. Theor. Biol.* 439, 1–13. doi: 10.1016/j.jtbi.2017.11.024

- Cheng, X., Li, P. Z., Wang, G., Yan, Y., Li, K., Brand-Saber, B., et al. (2019). Microbiota-derived lipopolysaccharide retards chondrocyte hypertrophy in the growth plate through elevating Sox9 expression. *J. Cell Physiol.* 234, 2593–2605. doi: 10.1002/jcp.27025
- Choi, J. H., Kim, J. S., Kim, W. K., Lee, W., Kim, N., Song, C. U., et al. (2020a). Evaluation of hyaluronic acid/agarose hydrogel for cartilage tissue engineering biomaterial. *Macromol. Res.* 28, 979–985. doi: 10.1007/s13233-020-8137-6
- Choi, J. H., Park, A., Lee, W., Youn, J., Rim, M. A., Kim, W., et al. (2020b). Preparation and characterization of an injectable dexamethasone-cyclodextrin complexes-loaded gellan gum hydrogel for cartilage tissue engineering. *J. Control. Rel.* 327, 747–765. doi: 10.1016/j.jconrel.2020.08.049
- Chow, S. K. H., Lee, K. M., Qin, L., Leung, K. S., and Cheung, W. H. (2011). Restoration of longitudinal growth by bioengineered cartilage pellet in physeal injury is not affected by low intensity pulsed ultrasound. *J. Biomed. Mater. Res. Part B Appl. Biomater.* 99B, 36–44. doi: 10.1002/jbm.b.31869
- Chung, R. S., and Xian, C. J. (2014). Recent research on the growth plate mechanisms for growth plate injury repair and potential cell-based therapies for regeneration. *J. Mol. Endocrinol.* 53, T45–T61. doi: 10.1530/jme-14-0062
- Chung, R., Cool, J. C., Scherer, M. A., Foster, B. K., and Xian, C. J. (2006). Roles of neutrophil-mediated inflammatory response in the bony repair of injured growth plate cartilage in young rats. *J. Leukoc. Biol.* 80, 1272–1280. doi: 10.1189/jlb.0606365
- Chung, R., Foster, B. K., and Xian, C. J. (2011). Injury responses and repair mechanisms of the injured growth plate. *Front. Biosci.* 3:117–125. doi: 10.2741/s137
- Chung, R., Foster, B. K., and Xian, C. J. (2014). The potential role of VEGF-induced vascularisation in the bony repair of injured growth plate cartilage. *J. Endocrinol.* 221, 63–75. doi: 10.1530/JOE-13-0539
- Chung, R., Foster, B. K., Zannettino, A. C., and Xian, C. J. (2009). Potential roles of growth factor PDGF-BB in the bony repair of injured growth plate. *Bone* 44, 878–885. doi: 10.1016/j.bone.2009.01.377
- Clark, A., Hilt, J. Z., Milbrandt, T. A., and Puleo, D. A. (2015). Treating proximal tibial growth plate injuries using poly(Lactic-co-Glycolic Acid) scaffolds. *Biores. Open Access* 4, 65–74. doi: 10.1089/biores.2014.0034
- Cohen, B., Chorney, G. S., Phillips, D. P., Dick, H. M., Buckwalter, J. A., Ratcliffe, A., et al. (1992). The microstructural tensile properties and biochemical composition of the bovine distal femoral growth plate. *J. Orthop. Res.* 10, 263–275. doi: 10.1002/jor.1100100214
- Coleman, R. M., Case, N. D., and Guldberg, R. E. (2007). Hydrogel effects on bone marrow stromal cell response to chondrogenic growth factors. *Biomaterials* 28, 2077–2086. doi: 10.1016/j.biomaterials.2007.01.010
- Coleman, R. M., Schwartz, Z., Boyan, B. D., and Guldberg, R. E. (2013). The therapeutic effect of bone marrow-derived stem cell implantation after epiphyseal plate injury is abrogated by chondrogenic predifferentiation. *Tissue Eng. Part A* 19, 475–483. doi: 10.1089/ten.tea.2012.0125
- Cooper, K. L., Oh, S., Sung, Y., Dasari, R. R., Kirschner, M. W., and Tabin, C. J. (2013). Multiple phases of chondrocyte enlargement underlie differences in skeletal proportions. *Nature* 495, 375–378.
- Cunniffe, G. M., Diaz-Payno, P. J., Ramey, J. S., Mahon, O. R., Dunne, A., Thompson, E. M., et al. (2017). Growth plate extracellular matrix-derived scaffolds for large bone defect healing. *Eur. Cell Mater.* 33, 130–142. doi: 10.22203/eCM.v033a10
- Cunniffe, G. M., Diaz-Payno, P. J., Sheehy, E. J., Critchley, S. E., Almeida, H. V., Pitacco, P., et al. (2019). Tissue-specific extracellular matrix scaffolds for the regeneration of spatially complex musculoskeletal tissues. *Biomaterials* 188, 63–73. doi: 10.1016/j.biomaterials.2018.09.044
- Dahlin, R. L., Ni, M., Meretoja, V. V., Kasper, F. K., and Mikos, A. G. (2014). TGF-beta3-induced chondrogenesis in co-cultures of chondrocytes and mesenchymal stem cells on biodegradable scaffolds. *Biomaterials* 35, 123–132. doi: 10.1016/j.biomaterials.2013.09.086
- Daly, A. C., Freeman, F. E., Gonzalez-Fernandez, T., Critchley, S. E., Nulty, J., and Kelly, D. J. (2017). 3D bioprinting for cartilage and osteochondral tissue engineering. *Adv. Healthc. Mater.* 6:1700298. doi: 10.1002/adhm.201700298
- D'Andrea, C. R., Alfraihat, A., Singh, A., Anari, J. B., Cahill, P. J., Schaer, T., et al. (2020). Part 1. Review and meta-analysis of studies on modulation of longitudinal bone growth and growth plate activity: a macro-scale perspective. *J. Orthop. Res.* 39, 907–918. doi: 10.1002/jor.24976
- Das, A., Ghosh, P., Ganguly, S., Banerjee, D., and Kargupta, K. (2018). Salt-leaching technique for the synthesis of porous poly(2,5-benzimidazole) (ABPBI) membranes for fuel cell application. *J. Appl. Poly. Sci.* 135:45773. doi: 10.1002/app.45773
- Davis, M. S., Marrero-Berrios, I., Perez, X. I., Maguire, T., Radhakrishnan, P., Manchikalapati, D., et al. (2018). Alginate-liposomal construct for bupivacaine delivery and MSC function regulation. *Drug Deliv. Transl. Res.* 8, 226–238. doi: 10.1007/s13346-017-0454-8
- Di Luca, A., Szlczak, K., Lorenzo-Moldero, I., Ghebes, C. A., Lepedda, A., Swieszkowski, W., et al. (2016). Influencing chondrogenic differentiation of human mesenchymal stromal cells in scaffolds displaying a structural gradient in pore size. *Acta Biomater.* 36, 210–219. doi: 10.1016/j.actbio.2016.03.014
- Diaz-Payno, P. J., Browe, D. C., Cunniffe, G. M., and Kelly, D. J. (2020). The identification of articular cartilage and growth plate extracellular matrix-specific proteins supportive of either osteogenesis or stable chondrogenesis of stem cells. *Biochem. Biophys. Res. Commun.* 528, 285–291. doi: 10.1016/j.bbrc.2020.05.074
- Ding, J., He, J., Zhang, Z. Q., Wu, Z. K., and Jin, F. C. (2018). Effect of hemiepiphyseal osteotomy on the growth plate: the histopathological changes and mechanism exploration of recurrence in mini pig model. *Biomed Res. Int.* 2018:6348171. doi: 10.1155/2018/6348171
- Drenkard, L. M. M., Kupratis, M. E., Li, K., Gerstenfeld, L. C., and Morgan, E. F. (2017). Local changes to the distal femoral growth plate following injury in mice. *J. Biomech. Eng.* 139:071010. doi: 10.1115/1.4036686
- Erickson, A. G., Laughlin, T. D., Romereim, S. M., Sargus-Patino, C. N., Pannier, A. K., and Dudley, A. T. (2018). A tunable, three-dimensional in vitro culture model of growth plate cartilage using alginate hydrogel scaffolds. *Tissue Eng. Part A* 24, 94–105. doi: 10.1089/ten.tea.2017.0091
- Erickson, C. B., Newsom, J. P., Fletcher, N. A., Feuer, Z. M., Yu, Y., Rodriguez-Fontan, F., et al. (2020). In vivo degradation rate of alginate-chitosan hydrogels influences tissue repair following physeal injury. *J. Biomed. Mater. Res. B Appl. Biomater.* 108, 2484–2494. doi: 10.1002/jbm.b.34580
- Erickson, C. B., Shaw, N., Hadley-Miller, N., Riederer, M. S., Krebs, M. D., and Payne, K. A. (2017). A rat tibial growth plate injury model to characterize repair mechanisms and evaluate growth plate regeneration strategies. *J. Visual. Exp.* 125:e55571. doi: 10.3791/55571
- Fahimipour, F., Dashtimoghadam, E., Hasani-Sadrabadi, M. M., Vargas, J., Vashae, D., Lobner, D. C., et al. (2019). Enhancing cell seeding and osteogenesis of MSCs on 3D printed scaffolds through injectable BMP2 immobilized ECM-Mimetic gel. *Dent. Mater.* 35, 990–1006. doi: 10.1016/j.dental.2019.04.004
- Farokhi, M., Shariatzadeh, F. J., Solouk, A., and Mirzadeh, H. (2020). Alginate based scaffolds for cartilage tissue engineering: a review. *Int. J. Polym. Mater. Polym. Biomater.* 69, 230–247. doi: 10.1080/00914037.2018.1562924
- Fathi-Achachelouei, M., Keskin, D., Bat, E., Vrana, N. E., and Tezcaner, A. (2020). Dual growth factor delivery using PLGA nanoparticles in silk fibroin/PEGDMA hydrogels for articular cartilage tissue engineering. *J. Biomed. Mater. Res. Part B Appl. Biomater.* 108, 2041–2062. doi: 10.1002/jbm.b.34544
- Fernandez-Iglesias, A., Fuente, R., Gil-Pena, H., Alonso-Duran, L., Garcia-Bengoa, M., Santos, F., et al. (2020). A simple method based on confocal microscopy and thick sections recognizes seven subphases in growth plate chondrocytes. *Sci. Rep.* 10:6935. doi: 10.1038/s41598-020-63978-6
- Fischer, C., Reiner, C., Schmidmaier, G., Doll, J., Child, C., Grutzner, P. A., et al. (2018). Safety study: is there a pathologic IGF-1, PDGF and TGF-beta cytokine expression caused by adjunct BMP-7 in tibial and femoral non-union therapy? *Ther. Clin. Risk Manag.* 14, 691–697. doi: 10.2147/TCRM.S160064
- Fischerauer, E. E., Manninger, M., Seles, M., Janezic, G., Pichler, K., Ebner, B., et al. (2013). BMP-6 and BMP-1a are up-regulated in the growth plate of the fractured tibia. *J. Orthop. Res.* 31, 357–363. doi: 10.1002/jor.22238
- Freeman, F. E., and Kelly, D. J. (2017). Tuning alginate bioink stiffness and composition for controlled growth factor delivery and to spatially direct MSC fate within bioprinted tissues. *Sci. Rep.* 7:17042. doi: 10.1038/s41598-017-17286-1
- Furusko, M., Ishii, A., Hebert, J. M., and Bansal, R. (2020). Developmental stage-specific role of Frs adapters as mediators of FGF receptor signaling in the oligodendrocyte lineage cells. *Glia* 68, 617–630. doi: 10.1002/glia.23743
- Garrison, P., Yue, S., Hanson, J., Baron, J., and Lui, J. C. (2017). Spatial regulation of bone morphogenetic proteins (BMPs) in postnatal articular and growth plate cartilage. *PLoS One* 12:e0176752. doi: 10.1371/journal.pone.0176752

- Georgiopoulos, P., Kontou, E., and Georgousis, G. (2018). Effect of silane treatment loading on the flexural properties of PLA/flax unidirectional composites. *Compos. Commun.* 10, 6–10. doi: 10.1016/j.coco.2018.05.002
- Ghosh, K., Pan, Z., Guan, E., Ge, S. R., Liu, Y. J., Nakamura, T., et al. (2007). Cell adaptation to a physiologically relevant ECM mimic with different viscoelastic properties. *Biomaterials* 28, 671–679. doi: 10.1016/j.biomaterials.2006.09.038
- Gigante, C., and Martinez, A. I. C. (2019). Desepiphysiodesis and reconstruction of the distal radial growth plate with an autologous iliac crest cartilage graft: a case report and review of literature. *J. Orthop. Case Rep.* 10, 70–73. doi: 10.13107/jocr.2019.v10.i01.1642
- Giteau, A., Venier-Julienne, M. C., Aubert-Pouessel, A., and Benoit, J. P. (2008). How to achieve sustained and complete protein release from PLGA-based microparticles? *Int. J. Pharm.* 350, 14–26. doi: 10.1016/j.ijpharm.2007.11.012
- Gremare, A., Guduric, V., Bareille, R., Heroguez, V., Latour, S., L'Heureux, N., et al. (2018). Characterization of printed PLA scaffolds for bone tissue engineering. *J. Biomed. Mater. Res. A* 106, 887–894. doi: 10.1002/jbm.a.36289
- Grolman, J. M., Singh, M., Mooney, D. J., Eriksson, E., and Nuutila, K. (2019). Antibiotic-containing agarose hydrogel for wound and burn care. *J. Burn Care Res.* 40, 900–906. doi: 10.1093/jbcr/irz113
- Gultekin, A., Agirdil, Y., Oncel Duman, B., Subasi, C., and Karaoz, E. (2020). Comparison of mesenchymal stem cell sheets and chondrocyte sheets in a rabbit growth plate injury model. *Turk. J. Med. Sci.* 50, 1082–1094. doi: 10.3906/sag-1902-228
- Hajdu, S., Schwendenwein, E., Kaltenecker, G., Laszlo, I., Lang, S., Vecsei, V., et al. (2011). The effect of drilling and screw fixation of the growth plate—an experimental study in rabbits. *J. Orthop. Res.* 29, 1834–1839. doi: 10.1002/jor.21463
- Hallett, S. A., Ono, W., and Ono, N. (2019). Growth plate chondrocytes: skeletal development, growth and beyond. *Int. J. Mol. Sci.* 20:6009. doi: 10.3390/ijms20236009
- Han, D., Lee, S. M., Kwon, M., Noh, H., Lee, J. H., Yoon, Y., et al. (2020). YAP enhances FGF2-dependent neural stem cell proliferation by induction of FGF receptor expression. *Stem Cells Dev.* 29, 1240–1246. doi: 10.1089/scd.2019.0281
- Hong, H., Seo, Y. B., Kim, D. Y., Lee, J. S., Lee, Y. J., Lee, H., et al. (2020). Digital light processing 3D printed silk fibroin hydrogel for cartilage tissue engineering. *Biomaterials* 232:119679. doi: 10.1016/j.biomaterials.2019.119679
- Hong, Y. P., Liu, N., Zhou, R., Zhao, X. X., Han, Y. G., Xia, F. F., et al. (2020). Combination therapy using kartogenin-based chondrogenesis and complex polymer scaffold for cartilage defect regeneration. *ACS Biomater. Sci. Eng.* 6, 6276–6284. doi: 10.1021/acsbomaterials.0c00724
- Horton, E. R., Vallmajo-Martin, Q., Martin, I., Snedeker, J. G., Ehrbar, M., and Blache, U. (2020). Extracellular matrix production by mesenchymal stromal cells in hydrogels facilitates cell spreading and is inhibited by FGF-2. *Adv. Healthc. Mater.* 9:e1901669. doi: 10.1002/adhm.201901669
- Hu, X., Li, W., Li, L., Lu, Y., Wang, Y., Parungao, R., et al. (2019). A biomimetic cartilage gradient hybrid scaffold for functional tissue engineering of cartilage. *Tissue Cell* 58, 84–92. doi: 10.1016/j.tice.2019.05.001
- Ishikawa, S., Iijima, K., Matsukuma, D., Iijima, M., Osawa, S., and Otsuka, H. (2020). Enhanced function of chondrocytes in a chitosan-based hydrogel to regenerate cartilage tissues by accelerating degradability of the hydrogel via a hydrolysable crosslinker. *J. Appl. Polymer Sci.* 137:48893. doi: 10.1002/app.48893
- Isobe, Y., Koyama, N., Nakao, K., Osawa, K., Ikeno, M., Yamanaka, S., et al. (2016). Comparison of human mesenchymal stem cells derived from bone marrow, synovial fluid, adult dental pulp, and exfoliated deciduous tooth pulp. *Int. J. Oral Maxillofac. Surg.* 45, 124–131. doi: 10.1016/j.ijom.2015.06.022
- Jiao, W. X., Chen, W. X., Mei, Y. Q., Yun, Y. H., Wang, B. Q., Zhong, Q. P., et al. (2019). Effects of molecular weight and guluronic acid/mannuronic acid ratio on the rheological behavior and stabilizing property of sodium alginate. *Molecules* 24:4374. doi: 10.3390/molecules24234374
- Jin, S., Yang, C., Huang, J., Liu, L., Zhang, Y., Li, S., et al. (2020). Conditioned medium derived from FGF-2-modified GMSCs enhances migration and angiogenesis of human umbilical vein endothelial cells. *Stem Cell Res. Ther.* 11:68. doi: 10.1186/s13287-020-1584-3
- Jin, X. B., Luo, Z. J., and Wang, J. (2006). Treatment of rabbit growth plate injuries with an autologous tissue-engineered composite - an experimental study. *Cells Tissues Organs* 183, 62–67. doi: 10.1159/000095510
- Kashi, M., Baghbani, F., Mortazadeh, F., Mobasheri, H., and Kowsari, E. (2018). Green synthesis of degradable conductive thermosensitive oligopyrrole/chitosan hydrogel intended for cartilage tissue engineering. *Int. J. Biol. Macromol.* 107, 1567–1575. doi: 10.1016/j.ijbiomac.2017.10.015
- Kaviani, M., Azarpira, N., Aghdaie, M. H., Esfandiari, E., Geramizadeh, B., Nikeghbalian, S., et al. (2019). Comparison of human mesenchymal stem cells derived from various compartments of human adipose tissue and tunica adventitia layer of the arteries subsequent to organ donation. *Int. J. Organ Transpl. Med.* 10, 65–73.
- Kazemi, M., and Williams, J. L. (2020). Properties of cartilage-subchondral bone junctions: a narrative review with specific focus on the growth plate. *Cartilage* 1947603520924776. doi: 10.1177/1947603520924776
- Keplinger, T., Wang, X. Q., and Burgert, I. (2019). Nanofibrillated cellulose composites and wood derived scaffolds for functional materials. *J. Mater. Chem. A* 7, 2981–2992. doi: 10.1039/c8ta10711d
- Khatib, S., Leijts, M. J., van Buul, G., Haeck, J., Kops, N., Nieboer, M., et al. (2020). MSC encapsulation in alginate microcapsules prolongs survival after intra-articular injection, a longitudinal in vivo cell and bead integrity tracking study. *Cell Biol. Toxicol.* 36, 553–570. doi: 10.1007/s10565-020-09532-6
- Killion, C. H., Mitchell, E. H., Duke, C. G., and Serra, R. (2017). Mechanical loading regulates organization of the actin cytoskeleton and column formation in postnatal growth plate. *Mol. Biol. Cell* 28, 1862–1870. doi: 10.1091/mbc.E17-02-0084
- Kim, Y., Kang, B. J., Kim, W. H., Yun, H. S., and Kweon, O. K. (2018). Evaluation of mesenchymal stem cell sheets overexpressing BMP-7 in canine critical-sized bone defects. *Int. J. Mol. Sci.* 19:2073. doi: 10.3390/ijms19072073
- Knapik, D. M., Zirkle, L. G., and Liu, R. W. (2018). Consequences following distal femoral growth plate violation in an ovine model with an intramedullary implant: a pilot study. *J. Pediatr. Orthop.* 38, e640–e645. doi: 10.1097/BPO.0000000000001234
- Koc, O. N., Day, J., Nieder, M., Gerson, S. L., Lazarus, H. M., and Krivit, W. (2002). Allogeneic mesenchymal stem cell infusion for treatment of metachromatic leukodystrophy (MLD) and Hurler syndrome (MPS-IH). *Bone Marrow Transplant* 30, 215–222. doi: 10.1038/sj.bmt.1703650
- Kong, W. L., Gao, Y. L., Liu, Q. L., Dong, L. P., Guo, L. K., Fan, H. S., et al. (2020). The effects of chemical crosslinking manners on the physical properties and biocompatibility of collagen type I/hyaluronic acid composite hydrogels. *Int. J. Biol. Macromol.* 160, 1201–1211. doi: 10.1016/j.ijbiomac.2020.05.208
- Krejci, P., Krakow, D., Mekikian, P. B., and Wilcox, W. R. (2007). Fibroblast growth factors 1, 2, 17, and 19 are the predominant FGF ligands expressed in human fetal growth plate cartilage. *Pediatr. Res.* 61, 267–272. doi: 10.1203/pdr.0b013e318030d157
- Kronenberg, H. M. (2003). Developmental regulation of the growth plate. *Nature* 423, 332–336. doi: 10.1038/nature01657
- Kumar, N., Desagani, D., Chandran, G., Ghosh, N. N., Karthikeyan, G., Waigaonkar, S., et al. (2018). Biocompatible agarose-chitosan coated silver nanoparticle composite for soft tissue engineering applications. *Artif. Cells Nanomed. Biotechnol.* 46, 637–649. doi: 10.1080/21691401.2017.1337021
- Ladenhauf, H. N., Jones, K. J., Potter, H. G., Nguyen, J. T., and Green, D. W. (2020). Understanding the undulating pattern of the distal femoral growth plate: implications for surgical procedures involving the pediatric knee: a descriptive MRI study. *Knee* 27, 315–323. doi: 10.1016/j.knee.2020.02.003
- Lee, D., Erickson, A., Dudley, A. T., and Ryu, S. (2019). Mechanical stimulation of growth plate chondrocytes: previous approaches and future directions. *Exp. Mech.* 59, 1261–1274. doi: 10.1007/s11340-018-0424-1
- Lee, S. U., Lee, J. Y., Joo, S. Y., Lee, Y. S., and Jeong, C. (2016). Transplantation of a scaffold-free cartilage tissue analogue for the treatment of physeal cartilage injury of the proximal tibia in rabbits. *Yonsei Med. J.* 57, 441–448. doi: 10.3349/ymj.2016.57.2.441
- Lee, S., Choi, J., Mohanty, J., Sousa, L. P., Tome, F., Pardon, E., et al. (2018). Structures of beta-klotho reveal a 'zip code'-like mechanism for endocrine FGF signalling. *Nature* 553, 501–505. doi: 10.1038/nature25010
- Lee, S., Kim, J. E., Seo, H. J., and Jang, J. H. (2019). Design of fibronectin type III domains fused to an elastin-like polypeptide for the osteogenic differentiation

- of human mesenchymal stem cells. *Acta Biochim. Biophys. Sin.* 51, 856–863. doi: 10.1093/abbs/gmz063
- Lee, Y., Kim, S. K., Park, Y. J., Cho, J., and Koo, H. J. (2019). A humidity-sensing composite microfiber based on moisture-induced swelling of an agarose polymer matrix. *Polymer Composit.* 40, 3582–3587. doi: 10.1002/pc.25220
- Li, S. W., Tallia, F., Mohammed, A. A., Stevens, M. M., and Jones, J. R. (2020). Scaffold channel size influences stem cell differentiation pathway in 3-D printed silica hybrid scaffolds for cartilage regeneration. *Biomater. Sci.* 8, 4458–4466. doi: 10.1039/c9bm01829h
- Li, W. C., Xu, R. J., Huang, J. X., Bao, X., and Zhao, B. (2017). Treatment of rabbit growth plate injuries with oriented ECM scaffold and autologous BMSCs. *Sci. Rep.* 7:44140. doi: 10.1038/srep44140
- Li, W. C., Xu, R. J., Xue, Y. L., Huang, J. X., and Gao, Y. H. (2013). Treatment of growth plate injury with microencapsulated chondrocytes. *Biotechnol. Bioprocess Eng.* 18, 655–662. doi: 10.1007/s12257-012-0451-1
- Little, R. M., and Milewski, M. D. (2016). Physal fractures about the knee. *Curr. Rev. Musculoskel. Med.* 9, 478–486. doi: 10.1007/s12178-016-9370-7
- Liu, J. Y., Fang, Q., Lin, H., Yu, X. F., Zheng, H., and Wan, Y. (2020). Alginate-polyoxamer/silk fibroin hydrogels with covalently and physically cross-linked networks for cartilage tissue engineering. *Carbohydr. Polym.* 247:116593. doi: 10.1016/j.carbpol.2020.116593
- Liu, W., Feng, M., Jayasuriya, C. T., Peng, H., Zhang, L., Guan, Y., et al. (2020). Human osteoarthritis cartilage-derived stromal cells activate joint degeneration through TGF-beta lateral signaling. *FASEB J.* 34, 16552–16566. doi: 10.1096/fj.202001448R
- Liu, Z. M., Shen, P. C., Lu, C. C., Chou, S. H., and Tien, Y. C. (2019). Characterization of the proliferating layer chondrocytes of growth plate for cartilage regeneration. *Tissue Eng. Part A* 25, 364–378. doi: 10.1089/ten.TEA.2018.0110
- Lo, W. C., Dubey, N. K., Tsai, F. C., Lu, J. H., Peng, B. Y., Chiang, P. C., et al. (2020). Amelioration of nicotine-induced osteoarthritis by platelet-derived biomaterials through modulating IGF-1/AKT/IRS-1 signaling axis. *Cell Transplant* 29:963689720947348. doi: 10.1177/0963689720947348
- Lui, J. C., Jee, Y. H., Garrison, P., Iben, J. R., Yue, S., Ad, M., et al. (2018). Differential aging of growth plate cartilage underlies differences in bone length and thus helps determine skeletal proportions. *PLoS Biol.* 16:e2005263. doi: 10.1371/journal.pbio.2005263
- Lui, J. C., Nilsson, O., and Baron, J. (2014). Recent research on the growth plate: recent insights into the regulation of the growth plate. *J. Mol. Endocrinol.* 53, T1–T9. doi: 10.1530/JME-14-0022
- MacIntyre, N. J., and Dewan, N. (2016). Epidemiology of distal radius fractures and factors predicting risk and prognosis. *J. Hand Ther.* 29, 136–144.
- Mackie, E. J., Tatarczuch, L., and Mirams, M. (2011). The skeleton: a multi-functional complex organ: the growth plate chondrocyte and endochondral ossification. *J. Endocrinol.* 211, 109–121. doi: 10.1530/JOE-11-0048
- Macsa, C. E., Hopwood, B., Chung, R., Foster, B. K., and Xian, C. J. (2011). Structural and molecular analyses of bone bridge formation within the growth plate injury site and cartilage degeneration at the adjacent uninjured area. *Bone* 49, 904–912. doi: 10.1016/j.bone.2011.07.024
- Mahran, Y. F., Badr, A. M., Aldosari, A., Bin-Zaid, R., and Alotaibi, H. N. (2019). Carvacrol and thymol modulate the cross-talk between TNF-alpha and IGF-1 signaling in radiotherapy-induced ovarian failure. *Oxid. Med. Cell Longev.* 2019:3173745. doi: 10.1155/2019/3173745
- Matsuzaki, T., Alvarez-Garcia, O., Mokuda, S., Nagira, K., Olmer, M., Gamin, R., et al. (2018). FoxO transcription factors modulate autophagy and proteoglycan 4 in cartilage homeostasis and osteoarthritis. *Sci. Transl. Med.* 10:eaan0746. doi: 10.1126/scitranslmed.aan0746
- McCarty, R. C., Xian, C. J., Gronthos, S., Zannettino, A. C., and Foster, B. K. (2010). Application of autologous bone marrow derived mesenchymal stem cells to an ovine model of growth plate cartilage injury. *Open Orthop. J.* 4, 204–210. doi: 10.2174/1874325001004010204
- Midyett, L. K., Rogol, A. D., Van Meter, Q. L., Frane, J., Bright, G. M., and Group, M. S. S. (2010). Recombinant insulin-like growth factor (IGF)-I treatment in short children with low IGF-I levels: first-year results from a randomized clinical trial. *J. Clin. Endocrinol. Metab.* 95, 611–619. doi: 10.1210/jc.2009-0570
- Mikolajczyk, T., Malinowski, T., Moldovan, L., Hu, F. W., Paczkowski, T., and Ciobanu, I. (2019). “CAD CAM system for manufacturing innovative hybrid design using 3D printing” in *Proceedings of the 12th International Conference Interdisciplinarity in Engineering (Inter-Eng 2018)*, Tirgu Mures, 22–28. doi: 10.1016/j.promfg.2019.02.178
- Mizuhashi, K., Nagata, M., Matsushita, Y., Ono, W., and Ono, N. (2019). Growth plate borderline chondrocytes behave as transient mesenchymal precursor cells. *J. Bone Miner. Res.* 34, 1387–1392. doi: 10.1002/jbmr.3719
- Mizuhashi, K., Ono, W., Matsushita, Y., Sakagami, N., Takahashi, A., Saunders, T. L., et al. (2018). Resting zone of the growth plate houses a unique class of skeletal stem cells. *Nature* 563, 254–258. doi: 10.1038/s41586-018-0662-5
- Mohammady, M., Mohammadi, Y., and Yousefi, G. (2020). Freeze-drying of pharmaceutical and nutraceutical nanoparticles: the effects of formulation and technique parameters on nanoparticles characteristics. *J. Pharmaceut. Sci.* 109, 3235–3247. doi: 10.1016/j.xphs.2020.07.015
- Montazerian, H., Mohamed, M. G. A., Montazeri, M. M., Kheiri, S., Milani, A. S., Kim, K., et al. (2019). Permeability and mechanical properties of gradient porous PDMS scaffolds fabricated by 3D-printed sacrificial templates designed with minimal surfaces. *Acta Biomater.* 96, 149–160. doi: 10.1016/j.actbio.2019.06.040
- Moreira, A., Carneiro, J., Campos, J. B. L. M., and Miranda, J. M. (2021). Production of hydrogel microparticles in microfluidic devices: a review. *Microfluid. Nanofluid.* 25:10. doi: 10.1007/s10404-020-02413-8
- Mullen, L. M., Best, S. M., Ghose, S., Wardale, J., Rushton, N., and Cameron, R. E. (2015). Bioactive IGF-1 release from collagen-GAG scaffold to enhance cartilage repair in vitro. *J. Mater. Sci. Mater. Med.* 26:5325. doi: 10.1007/s10856-014-5325-y
- Muller, M., Ozturk, E., Arlov, O., Gatenholm, P., and Zenobi-Wong, M. (2017). Alginate sulfate-nanocellulose bioinks for cartilage bioprinting applications. *Ann. Biomed. Eng.* 45, 210–223.
- Munir, N., McDonald, A., and Callanan, A. (2020). Integrational technologies for the development of three-dimensional scaffolds as platforms in cartilage tissue engineering. *ACS Omega* 5, 12623–12636. doi: 10.1021/acsomega.9b04022
- Musumeci, G., Castrogiovanni, P., Loreto, C., Castorina, S., Pichler, K., and Weinberg, A. M. (2013). Post-traumatic caspase-3 expression in the adjacent areas of growth plate injury site: a morphological study. *Int. J. Mol. Sci.* 14, 15767–15784. doi: 10.3390/ijms140815767
- Nasrabadi, D., Rezaeiani, S., Eslaminejad, M. B., and Shabani, A. (2018). Improved protocol for chondrogenic differentiation of bone marrow derived mesenchymal stem cells -effect of PTHrP and FGF-2 on TGFbeta1/BMP2-induced chondrocytes hypertrophy. *Stem Cell Rev. Rep.* 14, 755–766. doi: 10.1007/s12015-018-9816-y
- Neumayer, B., Amerstorfer, E., Diwok, C., Lindtner, R. A., Wadl, E., Scheurer, E., et al. (2017). Assessment of pharmacokinetics for microvessel proliferation by DCE-MRI for early detection of physal bone bridge formation in an animal model. *MAGMA* 30, 417–427. doi: 10.1007/s10334-017-0615-2
- Newton, P. T., Li, L., Zhou, B., Schweingruber, C., Hovorakova, M., Xie, M., et al. (2019). A radical switch in clonality reveals a stem cell niche in the epiphyseal growth plate. *Nature* 567, 234–238. doi: 10.1038/s41586-019-0989-6
- Oryan, A., Kamali, A., Moshiri, A., Baharvand, H., and Daemi, H. (2018). Chemical crosslinking of biopolymeric scaffolds: current knowledge and future directions of crosslinked engineered bone scaffolds. *Int. J. Biol. Macromol.* 107, 678–688. doi: 10.1016/j.ijbiomac.2017.08.184
- Park, J., Gebhardt, M., Golovchenko, S., Perez-Branguli, F., Hattori, T., Hartmann, C., et al. (2015). Dual pathways to endochondral osteoblasts: a novel chondrocyte-derived osteoprogenitor cell identified in hypertrophic cartilage. *Biol. Open* 4, 608–621. doi: 10.1242/bio.201411031
- Parreno, J., Niaki, M. N., Andrejevic, K., Jiang, A., Wu, P. H., and Kandel, R. A. (2017). Interplay between cytoskeletal polymerization and the chondrogenic phenotype in chondrocytes passaged in monolayer culture. *J. Anat.* 230, 234–248. doi: 10.1111/joa.12554
- Pati, F., Jang, J., Ha, D. H., Won Kim, S., Rhie, J. W., Shim, J. H., et al. (2014). Printing three-dimensional tissue analogues with decellularized extracellular matrix bioink. *Nat. Commun.* 5:3935. doi: 10.1038/ncomms4935
- Pazzaglia, U. E., Reguzzoni, M., Casati, L., Sibilia, V., Zarattini, G., and Raspanti, M. (2020). New morphological evidence of the ‘fate’ of growth plate hypertrophic

- chondrocytes in the general context of endochondral ossification. *J. Anat.* 236, 305–316. doi: 10.1111/joa.13100
- Planka, L., Gal, P., Kecova, H., Klima, J., Hlucilova, J., Filova, E., et al. (2008). Allogeneic and autogenous transplantations of MSCs in treatment of the physal bone bridge in rabbits. *BMC Biotechnol.* 8:70. doi: 10.1186/1472-6750-8-70
- Planka, L., Srnc, R., Rauser, P., Sary, D., Filova, E., Jancar, J., et al. (2012). Nanotechnology and mesenchymal stem cells with chondrocytes in prevention of partial growth plate arrest in pigs. *Biomed. Pap. Med. Fac. Univ. Palacky Olomouc Czech Repub.* 156, 128–134. doi: 10.5507/bp.2012.041
- Planka, L., Sary, D., Hlucilova, J., Klima, J., Jancar, J., Kren, L., et al. (2009). Comparison of preventive and therapeutic transplantations of allogeneic mesenchymal stem cells in healing of the distal femoral growth plate cartilage defects in miniature pigs. *Acta Veter. Brno* 78, 293–U122. doi: 10.2754/avb200978020293
- Qiao, Z. G., Lian, M. F., Han, Y., Sun, B. B., Zhang, X., Jiang, W. B., et al. (2021). Bioinspired stratified electrowritten fiber-reinforced hydrogel constructs with layer-specific induction capacity for functional osteochondral regeneration. *Biomaterials* 266, 1–14. doi: 10.1016/j.biomaterials.2020.120385
- Rathan, S., Dejob, L., Schipani, R., Haffner, B., Mobius, M. E., and Kelly, D. J. (2019). Fiber reinforced cartilage ECM functionalized bioinks for functional cartilage tissue engineering. *Adv. Healthc. Mater.* 8:e1801501. doi: 10.1002/adhm.201801501
- Ravi, N., Gupta, G., Milbrandt, T. A., and Puleo, D. A. (2012). Porous PLGA scaffolds for controlled release of naked and polyethyleneimine-complexed DNA. *Biomed. Mater.* 7:055007. doi: 10.1088/1748-6041/7/5/055007
- Reeser, K., and Doiron, A. L. (2019). Three-dimensional printing on a rotating cylindrical mandrel: a review of additive-lathe 3D printing technology. *3d Print. Addit. Manufact.* 6, 293–307. doi: 10.1089/3dp.2019.0058
- Ren, X., Wang, F. Y., Chen, C., Gong, X. Y., Yin, L., and Yang, L. (2016). Engineering zonal cartilage through bioprinting collagen type II hydrogel constructs with biomimetic chondrocyte density gradient. *Bmc Musculoskeletal Disorders* 17:301. doi: 10.1186/s12891-016-1130-8
- Ribeiro, E. F., de Barros-Alexandrino, T. T., Assis, O. B. G., Cruz, A., Quiles, A., Hernando, I., et al. (2020). Chitosan and crosslinked chitosan nanoparticles: synthesis, characterization and their role as Pickering emulsifiers. *Carbohydr. Polym.* 250:116878. doi: 10.1016/j.carbpol.2020.116878
- Saini, P., Arora, M., and Kumar, M. (2016). Poly(lactic acid) blends in biomedical applications. *Adv. Drug Deliv. Rev.* 107, 47–59. doi: 10.1016/j.addr.2016.06.014
- Sakaguchi, Y., Sekiya, I., Yagishita, K., and Muneta, T. (2005). Comparison of human stem cells derived from various mesenchymal tissues - Superiority of synovium as a cell source. *Arthritis Rheumat.* 52, 2521–2529. doi: 10.1002/art.21212
- Salati, M. A., Khazai, J., Tahmuri, A. M., Samadi, A., Taghizadeh, A., Taghizadeh, M., et al. (2020). Agarose-based biomaterials: opportunities and challenges in cartilage tissue engineering. *Polymers* 12:1150. doi: 10.3390/polym12051150
- Sananta, P., Oka, R. I. G. M., Dradjat, S. R., Suroto, H., Mustamsir, E., Kalsum, U., et al. (2020). Adipose-derived stromal vascular fraction prevent bone bridge formation on growth plate injury in rat (in vivo studies) an experimental research. *Ann. Med. Surg.* 60, 211–217. doi: 10.1016/j.amsu.2020.09.026
- Saravanan, S., Leena, R. S., and Selvamurugan, N. (2016). Chitosan based biocomposite scaffolds for bone tissue engineering. *Int. J. Biol. Macromol.* 93(Pt B), 1354–1365. doi: 10.1016/j.ijbiomac.2016.01.112
- Schneider, M., Gunter, C., and Taubert, A. (2018). Co-deposition of a hydrogel/calcium phosphate hybrid layer on 3D printed poly(Lactic Acid) scaffolds via dip coating: towards automated biomaterials fabrication. *Polymers* 10:275. doi: 10.3390/polym10030275
- Sferopoulos, N. K. (2014). Classification of distal radius physal fractures not included in the salter-harris system. *Open Orthop. J.* 8, 219–224. doi: 10.2174/1874325001408010219
- Shaw, N., Erickson, C., Bryant, S. J., Ferguson, V. L., Krebs, M. D., Hadley-Miller, N., et al. (2018). Regenerative medicine approaches for the treatment of pediatric physal injuries. *Tissue Eng. Part B Rev.* 24, 85–97. doi: 10.1089/ten.TEB.2017.0274
- Shen, M., Liu, S., Jin, X., Mao, H., Zhu, F., Saif, T., et al. (2019). Porcine growth plate experimental study and estimation of human pediatric growth plate properties. *J. Mech. Behav. Biomed. Mater.* 101:103446. doi: 10.1016/j.jmbbm.2019.103446
- Siller, I. G., Enders, A., Steinwedel, T., Epping, N. M., Kirsch, M., Lavrentieva, A., et al. (2019). Real-time live-cell imaging technology enables high-throughput screening to verify in vitro biocompatibility of 3D printed materials. *Materials* 12:2125. doi: 10.3390/ma12132125
- Stokes, I. A. F., Clark, K. C., Farnum, C. E., and Aronsson, D. D. (2007). Alterations in the growth plate associated with growth modulation by sustained compression or distraction. *Bone* 41, 197–205. doi: 10.1016/j.bone.2007.04.180
- Sturtivant, A., and Callanan, A. (2020). The use of antifreeze proteins to modify pore structure in directionally frozen alginate sponges for cartilage tissue engineering. *Biomed. Phys. Eng. Express* 6:055016. doi: 10.1088/2057-1976/aba7aa
- Su, Y. W., Chung, R., Ruan, C. S., Chim, S. M., Kuek, V., Dwivedi, P. P., et al. (2016). Neurotrophin-3 induces BMP-2 and VEGF activities and promotes the bony repair of injured growth plate cartilage and bone in rats. *J. Bone Miner. Res.* 31, 1258–1274. doi: 10.1002/jbmr.2786
- Sundararaj, S. K. C., Cieply, R. D., Gupta, G., Milbrandt, T. A., and Puleo, D. A. (2015). Treatment of growth plate injury using IGF-I-loaded PLGA scaffolds. *J. Tissue Eng. Regen. Med.* 9, E202–E209. doi: 10.1002/term.1670
- Suphasirroj, W., Yotnuengnit, P., Surarit, R., and Pichyangkura, R. (2009). The fundamental parameters of chitosan in polymer scaffolds affecting osteoblasts (MC3T3-E1). *J. Mater. Sci. Mater. Med.* 20, 309–320. doi: 10.1007/s10856-008-3575-2
- Swaroop, M., Brooks, M. J., Gieser, L., Swaroop, A., and Zheng, W. (2018). Patient iPSC-derived neural stem cells exhibit phenotypes in concordance with the clinical severity of mucopolysaccharidosis I. *Hum. Mol. Genet.* 27, 3612–3626. doi: 10.1093/hmg/ddy259
- Sylvestre, P. L., Villemure, I., and Aubin, C. E. (2007). Finite element modeling of the growth plate in a detailed spine model. *Med. Biol. Eng. Comput.* 45, 977–988. doi: 10.1007/s11517-007-0220-z
- Tardajos, M. G., Cama, G., Dash, M., Misseeuw, L., Gheysens, T., Gorzelanny, C., et al. (2018). Chitosan functionalized poly-epsilon-caprolactone electrospun fibers and 3D printed scaffolds as antibacterial materials for tissue engineering applications. *Carbohydr. Polym.* 191, 127–135. doi: 10.1016/j.carbpol.2018.02.060
- Thielen, N. G. M., van der Kraan, P. M., and van Caam, A. P. M. (2019). TGFbeta/BMP signaling pathway in cartilage homeostasis. *Cells* 8:969. doi: 10.3390/cells8090969
- Thunsiri, K., Pitjamit, S., Pothacharoen, P., Pruksakorn, D., Nakkiew, W., and Wattanachariya, W. (2020). The 3D-printed bilayer's bioactive-biomaterials scaffold for full-thickness articular cartilage defects treatment. *Materials* 13:3417. doi: 10.3390/ma13153417
- Tomaszewski, R., Bohosiewicz, J., Gap, A., Bursig, H., and Wysocka, A. (2014). Autogenous cultured growth plate chondrocyte transplantation in the treatment of physal injury in rabbits. *Bone Joint Res.* 3, 310–316. doi: 10.1302/2046-3758.311.2000207
- Tomaszewski, R., Wiktor, Ł., and Gap, A. (2016). Orthotopic autologous chondrocyte grafting as a method of treatment of growth plate damage in rabbits. *Ortop. Traumatol. Rehabil.* 18, 485–496. doi: 10.5604/15093492.1226594
- Trakoolwannachai, V., Kheolamai, P., and Ummartyotin, S. (2019). Characterization of hydroxyapatite from eggshell waste and polycaprolactone (PCL) composite for scaffold material. *Composit. Part B Eng.* 173:106974. doi: 10.1016/j.compositesb.2019.106974
- Tuncel, M., Halici, M., Canoz, O., Yildirim Turk, C., Oner, M., Ozturk, F., et al. (2005). Role of insulin like growth factor-I in repair response in immature cartilage. *Knee* 12, 113–119. doi: 10.1016/j.knee.2004.04.003
- Uder, C., Bruckner, S., Winkler, S., Tautenhahn, H. M., and Christ, B. (2018). Mammalian MSC from selected species: features and applications. *Cytomet. A* 93, 32–49. doi: 10.1002/cyto.a.23239
- Uz, U., Gunhan, K., Vatansever, S., Kivanc, M., and Yuceturk, A. V. (2019). Novel simple strategy for cartilage tissue engineering using stem cells and synthetic polymer scaffold. *J. Craniofac. Surg.* 30, 940–943. doi: 10.1097/Scs.00000000000005374
- Vedadghavami, A., Minooei, F., Mohammadi, M. H., Khetani, S., Kolahchi, A. R., Mashayekhan, S., et al. (2017). Manufacturing of hydrogel biomaterials with controlled mechanical properties for tissue engineering applications. *Acta Biomater.* 62, 42–63. doi: 10.1016/j.actbio.2017.07.028

- Vroman, I., and Tighertz, L. (2009). Biodegradable polymers. *Materials* 2, 307–344. doi: 10.3390/ma2020307
- Wan, L., and Zhang, Y. H. (2018). Jointly modified mechanical properties and accelerated hydrolytic degradation of PLA by interface reinforcement of PLA-WF. *J. Mech. Behav. Biomed. Mater.* 88, 223–230. doi: 10.1016/j.jmbbm.2018.08.016
- Wang, C., Xu, C. X., Alippe, Y., Qu, C., Xiao, J., Schipani, E., et al. (2017). Chronic inflammation triggered by the NLRP3 inflammasome in myeloid cells promotes growth plate dysplasia by mesenchymal cells. *Sci. Rep.* 7:4880. doi: 10.1038/s41598-017-05033-5
- Wang, D. Q., Xu, H., Liu, J. M., Chen, Z. X., Li, Y. Y., Hu, B. H., et al. (2020). Bio-inspired cellulose reinforced anisotropic composite hydrogel with zone-dependent complex mechanical adaptability and cell recruitment characteristics. *Composit. Part B Eng.* 202:108418. doi: 10.1016/j.compositesb.2020.108418
- Wang, J., Yang, Q., Cheng, N., Tao, X., Zhang, Z., Sun, X., et al. (2016). Collagen/silk fibroin composite scaffold incorporated with PLGA microsphere for cartilage repair. *Mater. Sci. Eng. C Mater. Biol. Appl.* 61, 705–711. doi: 10.1016/j.msec.2015.12.097
- Wang, Y. X., Chen, Y. F., Xu, Y., Chen, M. Y., Lu, Y., Liang, J., et al. (2020). Effects of the bonding intensity between hyaluronan and gelatin on chondrogenic phenotypic maintenance. *J. Mater. Chem. B* 8, 9062–9074. doi: 10.1039/d0tb01816c
- Watanabe, H., Majima, T., Takahashi, K., Iizawa, N., Oshima, Y., and Takai, S. (2019). Posterior tibial slope angle is associated with flexion-type Salter-Harris II and Watson-Jones type IV fractures of the proximal tibia. *Knee Surg. Sports Traumatol. Arthrosc.* 27, 2994–3000. doi: 10.1007/s00167-018-5319-2
- Wei, P. R., Xu, Y., Gu, Y., Yao, Q. Q., Li, J. Y., and Wang, L. M. (2020). IGF-1-releasing PLGA nanoparticles modified 3D printed PCL scaffolds for cartilage tissue engineering. *Drug Deliv.* 27, 1106–1114. doi: 10.1080/10717544.2020.1797239
- Williams, J. L., Do, P. D., Eick, J. D., and Schmidt, T. L. (2001). Tensile properties of the physis vary with anatomic location, thickness, strain rate and age. *J. Orthop. Res.* 19, 1043–1048. doi: 10.1016/S0736-0266(01)00040-7
- Wo, J., Huang, S. S., Wu, D. Y., Zhu, J., Li, Z. Z., and Yuan, F. (2020). The integration of pore size and porosity distribution on Ti-6Al-4V scaffolds by 3D printing in the modulation of osteo-differentiation. *J. Appl. Biomater. Funct. Mater.* 18:2280800020934652. doi: 10.1177/2280800020934652
- Xian, C. J., Zhou, F. H., McCarty, R. C., and Foster, B. K. (2004). Intramembranous ossification mechanism for bone bridge formation at the growth plate cartilage injury site. *J. Orthop. Res.* 22, 417–426. doi: 10.1016/j.orthres.2003.08.003
- Xie, M., Gol'din, P., Herdina, A. N., Estefa, J., Medvedeva, E. V., Li, L., et al. (2020). Secondary ossification center induces and protects growth plate structure. *eLife* 9:e55212. doi: 10.7554/eLife.55212
- Xu, R., Zhao, H., Muhammad, H., Dong, M., Besenbacher, F., and Chen, M. (2017). Dual-delivery of FGF-2/CTGF from silk fibroin/PLCL-PEO coaxial fibers enhances MSC proliferation and fibrogenesis. *Sci. Rep.* 7:8509. doi: 10.1038/s41598-017-08226-0
- Yan, B. Y., Zhang, Z. P., Wang, X. P., Ni, Y. F., Liu, Y. S., Liu, T., et al. (2017). PLGA-PTMC-cultured bone mesenchymal stem cell scaffold enhances cartilage regeneration in tissue-engineered tracheal transplantation. *Artif. Organs* 41, 461–469. doi: 10.1111/aor.12805
- Yang, H. J., Xia, Y. Y., Lu, S. Q., Soong, T. W., and Feng, Z. W. (2008). Basic fibroblast growth factor-induced neuronal differentiation of mouse bone marrow stromal cells requires FGFR-1, MAPK/ERK, and transcription factor AP-1. *J. Biol. Chem.* 283, 5287–5295. doi: 10.1074/jbc.M706917200
- Yang, L., Tsang, K. Y., Tang, H. C., Chan, D., and Cheah, K. S. E. (2014). Hypertrophic chondrocytes can become osteoblasts and osteocytes in endochondral bone formation. *Proc. Natl. Acad. Sci. U.S.A.* 111, 12097–12102. doi: 10.1073/pnas.1302703111
- Yao, Q. R., Song, Z. Y., Li, J., and Zhang, L. (2020). Micromorphology, mechanical, crystallization and permeability properties analysis of HA/PBAT/PLA (HA, hydroxyapatite; PBAT, poly(butylene adipate-co-butylene terephthalate); PLA, polylactide) degradability packaging films. *Polymer Int.* 69, 301–307. doi: 10.1002/pi.5953
- Yee, C. S., Manilay, J. O., Chang, J. C., Hum, N. R., Muruges, D. K., Bajwa, J., et al. (2018). Conditional deletion of sost in MSC-derived lineages identifies specific cell-type contributions to bone mass and B-Cell development. *J. Bone Miner. Res.* 33, 1748–1759. doi: 10.1002/jbmr.3467
- Yoshida, K., Higuchi, C., Nakura, A., Nakamura, N., and Yoshikawa, H. (2012). Treatment of partial growth arrest using an in vitro-generated scaffold-free tissue-engineered construct derived from rabbit synovial mesenchymal stem cells. *J. Pediatr. Orthopaed.* 32, 314–321. doi: 10.1097/BPO.0b013e31824afee3
- Yu, Y., Rodriguez-Fontan, F., Eckstein, K., Muralidharan, A., Uzcategui, A. C., Fuchs, J. R., et al. (2019). Rabbit model of physal injury for the evaluation of regenerative medicine approaches. *Tissue Eng. Part C Methods* 25, 701–710. doi: 10.1089/ten.TEC.2019.0180
- Yukata, K., Nakai, S., Ikeda, M., and Hamawaki, J. I. (2018). Isolated salter-harris Type III physal fracture of the distal ulna. *J. Hand Surg. Asian Pac.* 23, 125–127. doi: 10.1142/S2424835518720049
- Zarrintaj, P., Manouchehri, S., Ahmadi, Z., Saeb, M. R., Urbanska, A. M., Kaplan, D. L., et al. (2018). Agarose-based biomaterials for tissue engineering. *Carbohydr. Polym.* 187, 66–84. doi: 10.1016/j.carbpol.2018.01.060
- Zhang, X., Liu, Y., Luo, C. Y., Zhai, C. J., Li, Z. X., Zhang, Y., et al. (2021). Crosslinker-free silk/decellularized extracellular matrix porous bioink for 3D bioprinting-based cartilage tissue engineering. *Mater. Sci. Eng. C Mater. Biol. Appl.* 118:111388. doi: 10.1016/j.msec.2020.111388
- Zhao, Z., Fan, C., Chen, F., Sun, Y., Xia, Y., Ji, A., et al. (2019). Progress in articular cartilage tissue engineering: a review on therapeutic cells and macromolecular scaffolds. *Macromol. Biosci.* 20:e1900278. doi: 10.1002/mabi.201900278
- Zheng, X., Yang, F., Wang, S., Lu, S., Zhang, W., Liu, S., et al. (2011). Fabrication and cell affinity of biomimetic structured PLGA/articular cartilage ECM composite scaffold. *J. Mater. Sci. Mater. Med.* 22, 693–704. doi: 10.1007/s10856-011-4248-0
- Zhou, F. H., Foster, B. K., Sander, G., and Xian, C. J. (2004). Expression of proinflammatory cytokines and growth factors at the injured growth plate cartilage in young rats. *Bone* 35, 1307–1315. doi: 10.1016/j.bone.2004.09.014
- Zhou, F. H., Foster, B. K., Zhou, X. F., Cowin, A. J., and Xian, C. J. (2006). TNF-alpha mediates p38 MAP kinase activation and negatively regulates bone formation at the injured growth plate in rats. *J. Bone Miner. Res.* 21, 1075–1088. doi: 10.1359/jbmr.060410
- Zhou, Q., Li, Q. H., and Dai, G. (2003). [Repair of upper tibial epiphyseal defect with engineered epiphyseal cartilage in rabbits]. *Zhongguo Xiu Fu Chong Jian Wai Ke Za Zhi* 17, 488–492.
- Zhou, X., von der Mark, K., Henry, S., Norton, W., Adams, H., et al. (2014). Chondrocytes transdifferentiate into osteoblasts in endochondral bone during development, postnatal growth and fracture healing in mice. *PLoS Genet.* 10:e1004820. doi: 10.1371/journal.pgen.1004820
- Zhou, Y., Lu, S., Wang, J., Zhang, Y., and Huang, J. (2000). [The treatment of premature arrest of growth plate with a novel engineered growth plate: experimental studies]. *Zhonghua Wai Ke Za Zhi* 38, 742–744.
- Zuo, Q., Cui, W. D., Liu, F., Wang, Q., Chen, Z. F., and Fan, W. M. (2016). Utilizing tissue-engineered cartilage or BMNC-PLGA composites to fill empty spaces during autologous osteochondral mosaicplasty in porcine knees. *J. Tissue Eng. Regen. Med.* 10, 916–926. doi: 10.1002/term.1872

Conflict of Interest: The authors declare that the research was conducted in the absence of any commercial or financial relationships that could be construed as a potential conflict of interest.

Copyright © 2021 Wang, Li, Wang, Bai, Wang, Liu, Bao, Ren, Liu and Wang. This is an open-access article distributed under the terms of the Creative Commons Attribution License (CC BY). The use, distribution or reproduction in other forums is permitted, provided the original author(s) and the copyright owner(s) are credited and that the original publication in this journal is cited, in accordance with accepted academic practice. No use, distribution or reproduction is permitted which does not comply with these terms.



Positive Effects of Three-Dimensional Collagen-Based Matrices on the Behavior of Osteoprogenitors

Zhikai Lin^{1,2,3}, Cristina Nica^{1,2}, Anton Sculean² and Maria B. Asparuhova^{1,2*}

¹Laboratory of Oral Cell Biology, Dental Research Center, School of Dental Medicine, University of Bern, Bern, Switzerland, ²Department of Periodontology, School of Dental Medicine, University of Bern, Bern, Switzerland, ³Department of Periodontology, Shanghai Ninth People's Hospital, Shanghai Jiao Tong University School of Medicine, College of Stomatology, Shanghai Jiao Tong University, National Center for Stomatology, National Clinical Research Center for Oral Diseases, Shanghai Key Laboratory of Stomatology, Shanghai, China

OPEN ACCESS

Edited by:

Nikos Donos,
Queen Mary University of London,
United Kingdom

Reviewed by:

Olivier Huck,
Université de Strasbourg, France
Asaf Wilensky,
Hadassah Medical Center, Israel

*Correspondence:

Maria B. Asparuhova
mariya.asparuhova@zmk.unibe.ch

Specialty section:

This article was submitted to
Tissue Engineering and
Regenerative Medicine,
a section of the journal
Frontiers in Bioengineering and
Biotechnology

Received: 12 May 2021

Accepted: 05 July 2021

Published: 21 July 2021

Citation:

Lin Z, Nica C, Sculean A and
Asparuhova MB (2021) Positive Effects
of Three-Dimensional Collagen-Based
Matrices on the Behavior
of Osteoprogenitors.
Front. Bioeng. Biotechnol. 9:708830.
doi: 10.3389/fbioe.2021.708830

Recent research has demonstrated that reinforced three-dimensional (3D) collagen matrices can provide a stable scaffold for restoring the lost volume of a deficient alveolar bone. In the present study, we aimed to comparatively investigate the migratory, adhesive, proliferative, and differentiation potential of mesenchymal stromal ST2 and pre-osteoblastic MC3T3-E1 cells in response to four 3D collagen-based matrices. Dried acellular dermal matrix (DADM), hydrated acellular dermal matrix (HADM), non-crosslinked collagen matrix (NCM), and crosslinked collagen matrix (CCM) did all enhance the motility of the osteoprogenitor cells. Compared to DADM and NCM, HADM and CCM triggered stronger migratory response. While cells grown on DADM and NCM demonstrated proliferative rates comparable to control cells grown in the absence of a biomaterial, cells grown on HADM and CCM proliferated significantly faster. The pro-proliferative effects of the two matrices were supported by upregulated expression of genes regulating cell division. Increased expression of genes encoding the adhesive molecules fibronectin, vinculin, CD44 antigen, and the intracellular adhesive molecule-1 was detected in cells grown on each of the scaffolds, suggesting excellent adhesive properties of the investigated biomaterials. In contrast to genes encoding the bone matrix proteins collagen type I (Col1a1) and osteopontin (Spp1) induced by all matrices, the expression of the osteogenic differentiation markers Runx2, Alpl, Dlx5, Ibsp, Bglap2, and Phex was significantly increased in cells grown on HADM and CCM only. Short/clinically relevant pre-coating of the 3D biomaterials with enamel matrix derivative (EMD) or recombinant bone morphogenetic protein-2 (rBMP-2) significantly boosted the osteogenic differentiation of both osteoprogenitor lines on all matrices, including DADM and NCM, indicating that EMD and BMP-2 retained their biological activity after being released from the matrices. Whereas EMD triggered the expression of all osteogenesis-related genes, rBMP-2 upregulated early, intermediate, and late osteogenic differentiation markers except for Col1a1 and Spp1. Altogether, our results support favorable influence of HADM and CCM on the recruitment, growth, and osteogenic differentiation of the osteoprogenitor cell types. Furthermore, our data strongly support the biofunctionalization of the collagen-based matrices with EMD or rBMP-2 as a potential treatment modality for bone defects in the clinical practice.

Keywords: three-dimensional biomaterials, xenografts, bone regeneration, periodontal regeneration, osteogenesis, growth factors, gene expression, transcription

INTRODUCTION

Augmentation of bone defects remains a major challenge in reconstructive orthopedic, periodontal, and maxillofacial surgeries. Bone atrophy often results from trauma, infection, neoplasm, congenital disorder, or tooth extraction. Periodontal disease, endodontic lesions, severe tooth decay, or fracture can necessitate a tooth extraction. The majority of treatment modalities include the use of autogenous bone as a gold standard as well as xenogenic, allogenic, or alloplastic bone substitutes (Doonquah et al., 2021). The ideal biomaterial for the purpose of bone regeneration should be biocompatible, volume stable (space-making), osteoconductive, and osteoinductive (Yamada and Egusa, 2018). Furthermore, it should possess a predictable pattern of biodegradability, be easy for manufacturing and handling, and highly cost effective. As a primary component of the bone matrix that plays a role in numerous cellular processes, collagen appears a potential candidate for the design of three-dimensional (3D) scaffolds for bone regeneration (Pawelec et al., 2016; Pabst and Kämmerer, 2020). However, it is well known that collagen biomaterials have high biodegradability and low mechanical strength. Therefore, attempts have been made to improve the collagen scaffolds for bone tissue engineering, e.g., collagen-based composite scaffolds with bioceramic, carbon, and polymer components have been proposed (Zhang et al., 2018). Furthermore, non-enzymatic or enzymatic crosslinking procedures have been utilized in order to reduce the naturally high biodegradability and to increase the mechanical stability of the collagen matrices by establishing intermolecular bonds (Adamiak and Sionkowska, 2020). The combination of 3D collagen matrices with bone substitute materials (Basudan et al., 2016; Papi et al., 2021) or bioactive substances (Herford and Cicciù, 2012; Herford et al., 2012; Ramseier et al., 2012; Jin and Giannobile, 2014; Edelmayer et al., 2020; França-Grohmann et al., 2020) for the repair of periodontal hard tissue loss and severe alveolar ridge deficiencies have appeared as promising strategies.

In a recent study, we have demonstrated that four commercially available 3D collagen-based matrices of porcine origin can be efficiently loaded with enamel matrix derivative (EMD) or recombinant growth factors such as the transforming growth factor- β 1 (TGF- β 1), fibroblast growth factor-2 (FGF-2), platelet-derived growth factor-BB (PDGF-BB), growth and differentiation factor-5 (GDF-5), or the bone morphogenetic protein-2 (BMP-2) (Nica et al., 2020). Except for recombinant GDF-5, the loading efficiency of the investigated growth factors was close to 100%. Furthermore, the matrices have exhibited sustained growth factor release over 13 days with kinetics that will likely favor the long-term tissue regeneration following surgical reconstructive periodontal therapies. We have further demonstrated that the investigated collagen-based matrices successfully promote migration, adhesion, and proliferation of cell types involved in oral soft tissue regeneration, namely primary human oral fibroblasts and periodontal ligament cells (Lin et al., 2020). The current study extends the *in vitro*

investigations on the four 3D matrices in relation to their ability to trigger osteogenic differentiation.

Osteogenesis is a complex multistep process that requires a biomaterial with excellent physicochemical and biological properties in order to support the migration, attachment, proliferation, and differentiation of osteoprogenitor cells at the defect site. The biomaterials under investigation in the current study were selected based on their commercial availability, easy supply, excellent characteristics declared by the manufacturers, and limited (if any) data for their potential utilization in supporting bone regeneration. Therefore, one of the examined biomaterials is a dry-supplied acellular dermal matrix (mucoderm®; botiss biomaterials GmbH, Zossen, Germany), labelled DADM. *In vitro* and *in vivo* cell-matrix interaction studies have shown that DADM supports the metabolic activity and proliferation of various cell types including osteoblasts (Pabst et al., 2014). Furthermore, a successful biofunctionalization of DADM with EMD or platelet-rich fibrin have positively influenced the behavior of primary human endothelial cells *in vitro* (Park et al., 2018; Blatt et al., 2020) as well as the angiogenesis *in vivo* (Blatt et al., 2020). A novel tissue-engineered acellular dermal matrix provided in a hydrated form, labeled HADM (NovoMatrix™ Reconstructive Tissue Matrix; BioHorizons, Birmingham, AL, United States), has shown consistent favorable effects on the behavior of primary human oral fibroblasts and periodontal ligament cells *in vitro* (Lin et al., 2020) as well as in treating gingival recession defects in an *in vivo* animal model (Suárez-López Del Amo et al., 2019). The third examined xenograft is a non-crosslinked collagen matrix, labeled NCM (Geistlich Mucograft®; Geistlich, Wolhusen, Switzerland) and composed of native collagen types I and III (Nevins et al., 2003; Ghanaati et al., 2011). Interestingly, the addition of PDGF-BB to the NCM was shown to accelerate soft tissue healing and promote bone formation in bilateral mandibular alveolar defects of a minipig model (Herford and Cicciù, 2012; Herford et al., 2012). Furthermore, similar to the effects of adsorbed BMP-7, vascular endothelial growth factor and PDGF, the stromal-derived factor-1 as a potent chemoattractant of circulating stem cells was successfully adsorbed on NCM, resulting in improved bone healing at calvarial critical-sized defects in a pre-clinical murine model (Jin and Giannobile, 2014). The final forth xenograft included in the study is a novel ribose-crosslinked collagen matrix, labeled CCM (Ossix® Volumax; Datum Dental Ltd., Lod, Israel). This thick resorbable collagen scaffold, reinforced by a novel proprietary crosslinking technology (Glymatrix®), was able to restore the lost volume of a deficient ridge between existing teeth (Smidt et al., 2019). The authors of the study commented that the augmentation procedure using CCM was simpler to perform compared to procedures with bone substitute materials and/or an interpositional connective tissue graft harvested from a remote donor site. Reinforced collagen membranes of the same product family have been shown to induce bone regeneration in critical-sized alveolar ridge defects in a dog model (Zubery et al., 2007) as well as in humans with direct mineral apposition on the glycosylated collagen (Zubery et al., 2008). On a cellular level, the glycosylated collagen membrane promoted the attachment and proliferation

of human periodontal ligament fibroblasts and human SaOs-2 osteoblasts (Rothamel et al., 2004). However, thorough analyses of the responses of osteoprogenitor cells to each of the listed 3D collagen-based matrices are entirely lacking.

The aim of the present study was to investigate the migratory, proliferative, and adhesive properties as well as the osteogenic differentiation potential of mesenchymal stromal and pre-osteoblastic cells cultured on each of the four collagen-based matrices. The study further aimed to investigate whether the biological activity of EMD or BMP-2 can be transferred onto the biomaterials *in vitro*, leading to enhanced osteogenic properties of the two cell types.

MATERIALS AND METHODS

Cell Culture and 3D Xenogenic Collagen-Based Matrices

Two types of osteoprogenitors of mouse origin were used throughout the study: bone marrow-derived mesenchymal stromal ST2 cells were obtained from the RIKEN Cell Bank (Tsukuba, Japan) and calvaria-derived pre-osteoblastic MC3T3-E1 cells were obtained from the ECACC collection (Sigma, Buchs, Switzerland). Both cell lines were characterized as osteoprogenitors by well-documented past (Franceschi and Iyer, 1992; Quarles et al., 1992; Franceschi et al., 1994; Torii et al., 1996; Otsuka et al., 1999) and recent studies (Cui et al., 2016; Parisi et al., 2021), and considered good models for studying osteogenesis *in vitro*. Both lines were grown in Dulbecco's Modified Eagle Medium (DMEM) supplemented with 10% fetal calf serum (FCS; Invitrogen, Zug, Switzerland) and 1% antibiotics/antimycotics (ThermoFisher Scientific, Basel, Switzerland). Cells were starved in 0.3% FCS/DMEM for 24 h before their culturing under experimental conditions.

DADM [kindly provided by botiss biomaterials GmbH (Berlin, Germany)], HADM [kindly provided by Camlog Biotechnologies GmbH (Basel, Switzerland)], NCM, and CCM [kindly provided by Datum Dental Ltd., (Lod, Israel)] were cut sterile into 10 × 10 mm pieces, washed in serum-free DMEM for 10 min and placed on the bottom of 24-well ultra-low attachment plates (Corning, NY, United States). Cells grown in tissue culture-treated 24-well plates (Greiner Bio-One, St. Gallen, Switzerland) in the absence of a biomaterial were used as control (Ctrl).

In some cases, the collagen matrices were coated for 10 min at room temperature with 1 mg/ml of EMD (Straumann® Emdogain®; botiss biomaterials GmbH, Zossen, Germany) or 100 ng/ml of recombinant (r) BMP-2 (Peprotech, London, United Kingdom). The EMD and rBMP-2 were diluted in serum-free DMEM from a 10 mg/ml and 10 µg/ml stock solutions, respectively. Collagen-based matrices incubated in serum-free DMEM, in the absence of EMD or rBMP-2, were used as controls. To remove unbound proteins after the 10-min incubation, the collagen matrices were extensively washed in serum-free DMEM for three cycles of 5 min each. The quantities of TGF-β1 [as a measure for the release of EMD (Stähli et al., 2014; Stähli et al., 2016)] and BMP-2 in culture supernatants of cells grown on EMD- or BMP-2-coated collagen matrices,

respectively, were determined by using colorimetric enzyme-linked immunosorbent assay (ELISA; R&D Systems, Minneapolis, MN, United States) as described (Nica et al., 2020) and following the manufacturer's protocol.

For differentiation experiments followed by gene expression analyses, 10% FCS/DMEM medium was supplemented with 50 µg/ml ascorbic acid (Invitrogen) and 2 mM β-glycerophosphate (Invitrogen) as described (Parisi et al., 2021).

Cell Migration Assay

Cell migration was analyzed by a Boyden chamber assay utilizing ThinCert® transwell polyethylene terephthalate (PET) membrane supports (8 µm pore size; Greiner Bio-One, St. Gallen, Switzerland) as described (Asparuhova et al., 2021). After 24 h of starvation, 3×10^4 cells were cultured in the top insert chamber with 200 µl 0% FCS/DMEM. Each of the collagen matrices was placed in the low chamber with 800 µl 10% FCS/DMEM. Cells were allowed to migrate across the capillary pore PET membrane for 18 h at 37°C before fixation in Shandon™ Formal-Fixx™ (ThermoFisher Scientific), and staining in 0.1% crystal violet solution (Sigma). Images of duplicate inserts were acquired on an Olympus CKX41 microscope using a ProgResCT3 camera. Migration was quantified by using the ImageJ software (Schneider et al., 2012) as described (Gurbuz et al., 2014). Data represent means ± SD from three independent experiments performed with each of the two cell lines.

Cell Proliferation Assay

Growth rates of ST2 and MC3T3-E1 cells cultured on the collagen-based matrices were determined by trypan blue dye exclusion cell counting performed in a Countess™ II instrument (Invitrogen) according to the manufacturer's instructions. After 24 h of starvation, 2×10^3 cells/well were plated in 3% FCS/DMEM and allowed to proliferate for 1, 3, and 6 days before staining with 0.4% trypan blue (Invitrogen) solution. The culture media was replaced every 2 days. Data represent means ± SD from four independent experiments performed with each of the two cell lines.

Gene Expression Analysis

Quantitative reverse transcription-polymerase chain reaction (qRT-PCR) was used to investigate the expression of three groups of genes: 1) proliferative markers (Mybl2, Bub1, Plk1, Mki67, Pcna, Ccne1, Ccnd1, and Ccnb1), 2) adhesive markers (Fn1, Vcl, Cd44, and Icam1), and 3) osteogenesis markers (Col1a1, Spp1, Runx2, Alpl, Dlx5, Ibsp, Bglap2, and Phex) as described (Lin et al., 2020; Parisi et al., 2021).

After 24 h of starvation, 2.5×10^5 cells/well were cultured in 3% FCS/DMEM or osteogenic supplements-containing 10% FCS/DMEM in the absence (control) or in the presence of each of the four collagen matrices. Proliferative or osteogenesis markers, respectively, were analyzed on day 3 post-seeding. In addition, osteogenesis marker gene expression was analyzed in cells grown for 3 days on native/uncoated matrices (control groups) or matrices coated with either EMD or rBMP-2 (test groups), according to the coating procedure described in *Cell Culture and 3D Xenogenic Collagen-Based Matrices*.

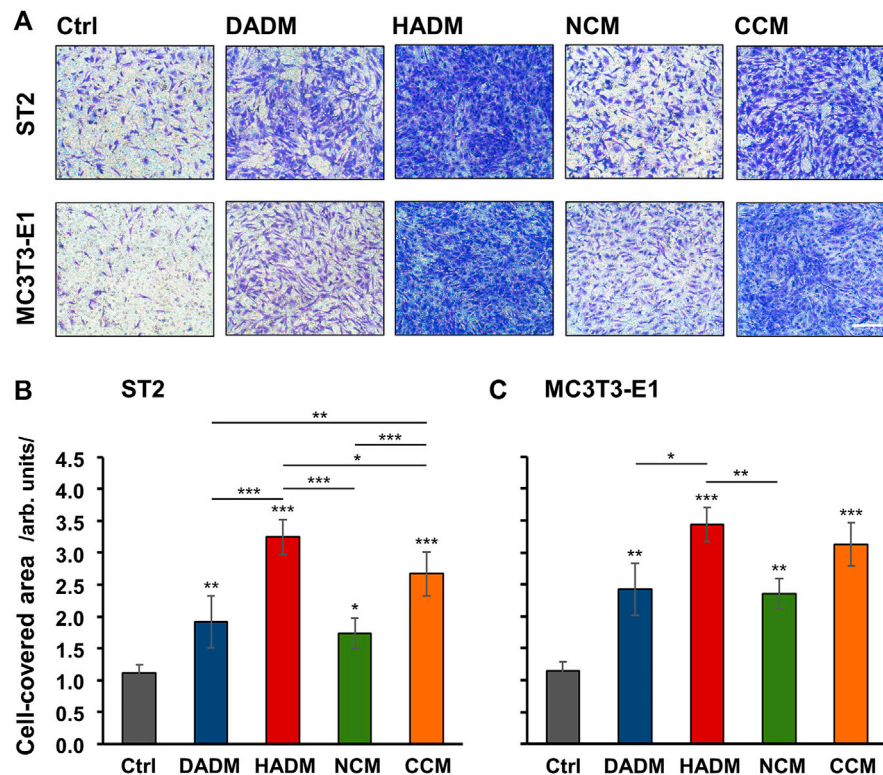


FIGURE 1 | Increased migratory potential of osteoprogenitor cell lines toward four different collagen-based matrices. Migration of mesenchymal stromal ST2 (A, B) and pre-osteoblastic MC3T3-E1 (A, C) cells toward DADM, HADM, NCM, and CCM matrices was evaluated by a modified Boyden chamber migration assay utilizing ThinCert® transwell PET membrane supports with 8 μ m pore size. (A) Representative images of fixed and stained cells that have migrated to the lower side of the membrane in each of the experimental groups. Scale bar, 500 μ m. (B, C) Quantification of the cell migration in the absence (Ctrl) or presence of collagen-based matrices by using the Image J software measuring the area on the lower side of the membrane support covered with migrated cells. Data represent means \pm SD from three independent experiments performed with each of the two cell lines. Significant differences to the respective controls unless otherwise indicated, *** p < 0.001, ** p < 0.01, * p < 0.05.

For analysis of adhesive marker gene expression, 6×10^5 cells/well were seeded in 10% FCS/DMEM in the absence (control) or in the presence of each of the four matrices and allowed to adhere for 10 h. After removal of the culture medium and before cell lysis, control cells and collagen matrices seeded with cells were extensively rinsed three times in phosphate-buffered solution (PBS) for complete removal of nonadherent cells.

Total RNA from cells of each experimental group was isolated using TRIzol (ThermoFisher Scientific) according to the manufacturer's instructions. The extracted RNA was additionally purified by using the RNeasy MinElute Cleanup Kit (Qiagen, Basel, Switzerland). RNA, spectrophotometrically quantified on a NanoDrop 2000c instrument (ThermoFisher Scientific), was reverse transcribed using the Applied Biosystems™ High-Capacity cDNA Reverse Transcription Kit (ThermoFisher Scientific). Subsequently, relative transcripts for the above listed genes, normalized to the internal control Gapdh, were quantified using FastStart Universal SYBR Green Master ROX (Roche, Basel, Switzerland) and the primer sequences listed in **Supplementary Tables 1–3**. Quantitative PCR was carried out in a QuantStudio 3 instrument (Applied Biosystems, Rotkreuz, Switzerland) using a standard thermal cycling profile. The efficiency $\Delta\Delta C_t$ method was

used to calculate gene expression levels normalized to Gapdh values and calibrated to values of controls. Samples were run in duplicates. Data represent means \pm SD from four independent experiments performed with each of the two cell lines.

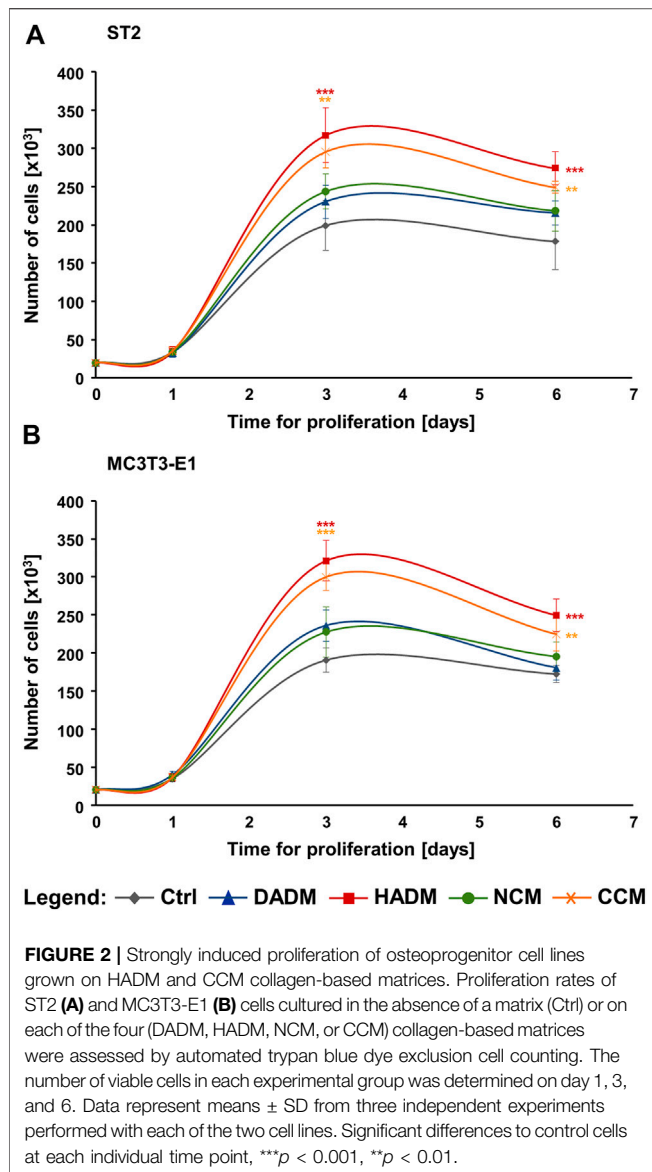
Statistical Analysis

Grouped data is represented by means \pm SD. Differences between groups were assessed by one-way analysis of variance (ANOVA) with Tukey's post-hoc test using GraphPad InStat Software (GraphPad, La Jolla, CA, United States), version 3.05. Significance was indicated using the scale, *** p < 0.001, ** p < 0.01, and * p < 0.05.

RESULTS

Increased Migratory Potential of Osteoprogenitor Cell Lines Toward Four Different Collagen-Based Matrices

Migratory properties of mesenchymal stromal ST2 and pre-osteoblastic MC3T3-E1 cells toward the investigated 3D



matrices were examined *in vitro* by using a modified Boyden chamber migration assay. Each of the four matrices caused significant (p < 0.05) induction in the migration rate of the two cell lines compared to control cells, where the migration occurred in the absence of a matrix (Figure 1). Compared to control cells, HADM caused the highest (3-fold) and most significant (p < 0.001) increase in the migration rate of the two cell lines. By effectiveness, HADM was immediately followed by CCM, which induced strongly significant (p < 0.001) cell migration by 2.4-fold in ST2 and 2.7-fold in MC3T3-E1 cells compared to the respective controls.

Compared to DADM and NCM, the pro-migratory properties of HADM and CCM were significantly better pronounced in ST2 cells only (Figure 1B). In MC3T3-E1 cells, HADM triggered significantly higher migration compared to DADM (p < 0.05) and NCM (p < 0.01) whereas the pro-migratory effect of CCM was stronger but not significantly different than the effect caused by

DADM and NCM (Figure 1C). Furthermore, a significant difference in the effects caused by CCM and HADM, in favor of the latter, was observed in ST2 (p < 0.05; Figure 1B) but not in MC3T3-E1 (Figure 1C) cells.

Strongly Induced Proliferation of Osteoprogenitor Cell Lines Grown on the Hydrated Acellular Dermal Matrix and the Ribose-Crosslinked Collagen Matrix

The proliferative rates of ST2 and MC3T3-E1 cells grown on each of the four collagen-based matrices were assessed by trypan blue dye exclusion cell counting performed in a Countess™ II instrument on days 1, 3, and 6 post-seeding. The four matrices remained compact and showed no signs of degradation during the 6-day culture period. After day 1, differences in the growth of the two cell lines on each of the matrices were detected. Both ST2 and MC3T3-E1 cells exhibited significantly higher (>1.5-fold) proliferative rates on HADM and CCM compared to control cells, with p < 0.01 between day 3 and 6 (Figure 2). In contrast, ST2 and MC3T3-E1 cells grew slightly but not significantly faster on DADM and NCM compared to the growth of control cells.

In addition, compared to DADM and NCM, the pro-proliferative effect of HADM appeared to be significantly better pronounced in both osteoprogenitor lines between day 3 and 6 (Figures 2A,B). In contrast, CCM did not exhibit a consistently higher effect on the proliferative rate of the two cell lines compared to DADM and NCM. ST2 and MC3T3-E1 cells grew with a significantly higher rate on CCM compared to DADM on day 3 (Figures 2A,B) but only the pre-osteoblastic MC3T3-E1 cells were faster growing on CCM compared to NCM on the same time point (Figure 2B). In the sake of a clearer visualization, symbols for significance are depicted for each collagen matrix tested compared to the control group only.

Increased Expression of Proliferative Marker Genes in Osteoprogenitor Cells Grown on the Hydrated Acellular Dermal Matrix and the Ribose-Crosslinked Collagen Matrix

To confirm the increased proliferative rates of osteoprogenitors grown on HADM and CCM matrices and to investigate further, how these two collagen-based scaffolds exhibit their effect on the growth of the ST2 and MC3T3-E1 cells, we performed a screen for the expression of genes involved in the regulation of the cell cycle progression (Whitfield et al., 2006). These are Mybl2 encoding the Myb-related protein B, Bub1 encoding a mitotic checkpoint serine/threonine-protein kinase, Plk1 encoding the polo-like kinase 1, Mki67 encoding the Ki-67 proliferative marker, PcnA encoding the proliferating cell nuclear antigen, and Ccn1, Ccn2, and Ccn3 encoding cyclin-E1, -D1, and -B1, respectively. The expression of the listed proliferative markers was analyzed by qRT-PCR. In agreement with the proliferation data as seen in Figure 2, on day 3, we observed a general trend of

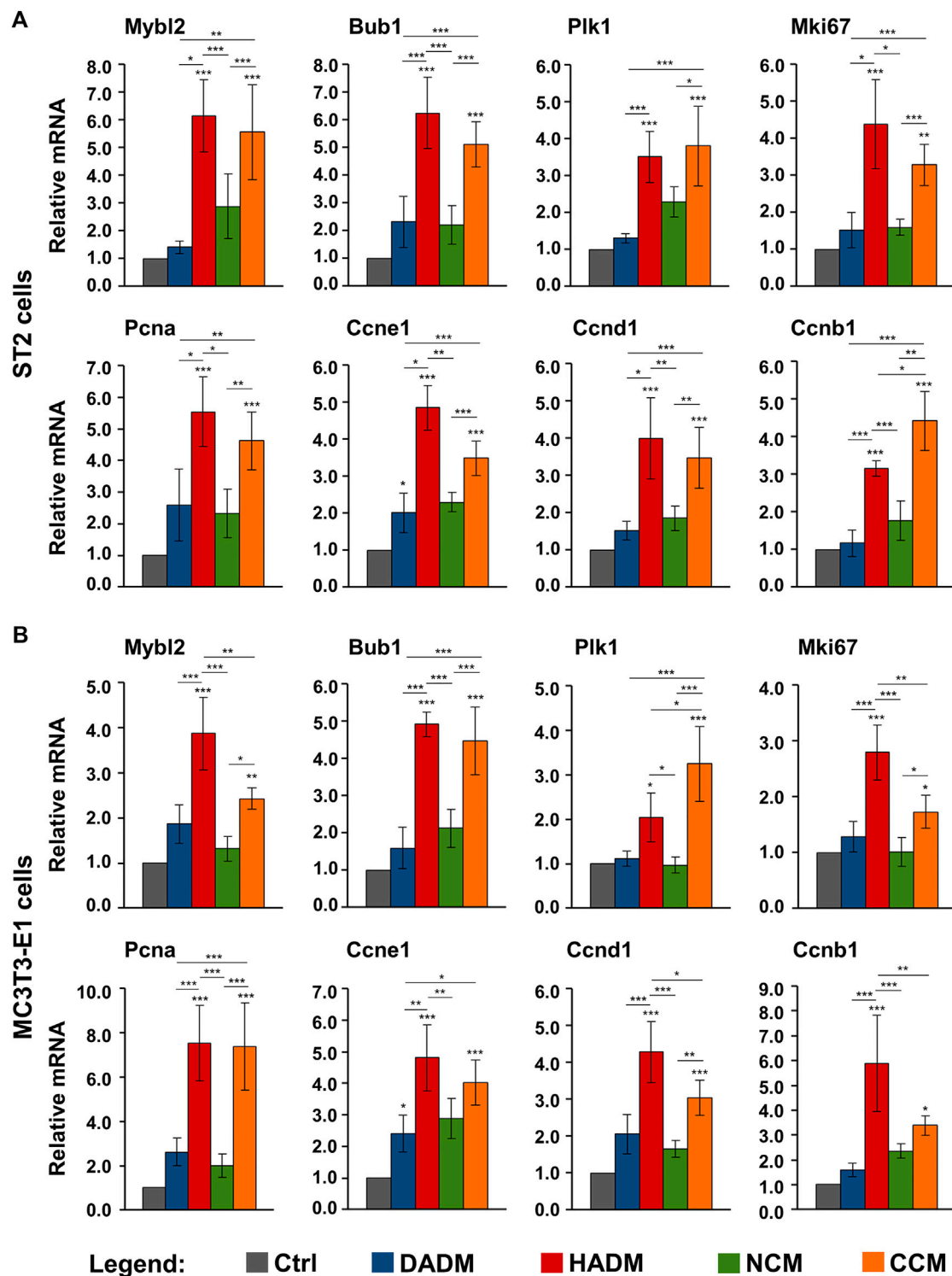


FIGURE 3 | Increased expression of proliferate marker genes in osteoprogenitor cells grown on HADM and CCM collagen-based matrices. ST2 (A) and MC3T3-E1 (B) cells were grown on DADM, HADM, NCM, or CCM collagen-based matrices for 3 days before total cellular RNA was extracted and analyzed for the expression of Mybl2, Bub1, Plk1, Mki67, Pcna, Ccne1, Ccnd1, and Ccnb1 proliferative marker genes by qRT-PCR. Controls (Ctrl) represent cells of each cell type grown in the absence of a collagen matrix. Values normalized to Gapdh are expressed relative to the values of control cells. Data represent means \pm SD from four independent experiments performed with each of the two cell lines. Significant differences to the respective controls unless otherwise indicated, *** $p < 0.001$, ** $p < 0.01$, * $p < 0.05$.

induced expression of the majority of the investigated proliferative marker genes in ST2 and MC3T3-E1 cells cultured on each of the collagen-based matrices compared to the expression levels detected in control cells (**Figure 3**). However, among the four investigated matrices, only HADM and CCM caused statistically significant ($p < 0.05$) upregulation of all proliferative markers in both osteoprogenitor cell lines, in the range of 2.0–7.5-fold, compared to control cells cultured in the absence of a matrix. In both cell lines, the *Ccne1* was the only gene that appeared significantly ($p < 0.05$) induced in cells grown on DADM compared to control cells (**Figures 3A,B**).

Interestingly, two cell type-specific differences in the effects of the investigated matrices on the proliferative marker gene expression were detected. In the ST2 cells, the HADM and CCM matrices performed significantly ($p < 0.01$) better than DADM and NCM matrices (**Figure 3A**). The only exception was seen for the *Plk1* gene expression that did not significantly differ between cells cultured on HADM and NCM. Moreover, except for *Ccnb1* gene, which was significantly ($p < 0.05$) stronger induced in ST2 cells cultured on CCM than on HADM matrix, no further differences in the effects caused by HADM and CCM were observed and the two matrices performed equally well. In contrast to ST2 cells, four out of the eight investigated proliferative marker genes were significantly ($p < 0.05$) stronger upregulated in MC3T3-E1 cells cultured on HADM compared to CCM (**Figure 3B**). These were *Mybl2*, *Mki67*, *Ccnd1*, and *Ccnb1*. In these four cases, the difference in the effect caused by CCM and HADM, in favour of the latter, was also accompanied by no significant difference in the performance between CCM and DADM or CCM and NCM (in the case of *Ccnb1*). *Plk1* was the only gene that was significantly ($p < 0.05$) better expressed in MC3T3-E1 cells cultured on CCM compared to its expression in cells cultured on HADM and respectively, no difference in the effects caused by HADM and DADM were observed.

In summary, the increased expression of genes regulating the cell cycle progression in the two osteoprogenitor cell lines grown on HADM and CCM matrices supports at least in part the strong pro-proliferative effect of HADM and CCM.

Increased Expression of Adhesive Marker Genes in Osteoprogenitor Cells Grown on Four Different Collagen-Based Matrices

Cellular adhesion precedes functional differentiation of osteoprogenitors (Biggs and Dalby, 2010). Therefore, we performed a screen for the expression of several adhesive marker genes, such as *Fn1*, *Vcl*, *Cd44*, and *Icam1*, in ST2 and MC3T3-E1 cells grown on the collagen-based scaffolds. *Fn1* gene encodes fibronectin, which is a ubiquitously expressed, non-collagenous extracellular matrix (ECM) protein with a major role in regulating cell adhesion and differentiation (Newby et al., 2020). *Vcl* encodes vinculin, which is an essential component of the focal adhesions and associated with both cell-cell and cell-matrix interactions (Bays and DeMali, 2017). *Cd44* and *Icam1* encode the CD44 antigen and the intercellular adhesion molecule-1, respectively. Both are cell surface glycoprotein receptors that promote not only cell-cell and cell-matrix

adhesion but also the migration and retention of inflammatory cells to various tissues (Hosokawa et al., 2006; Leonardi et al., 2006; Lucarini et al., 2009).

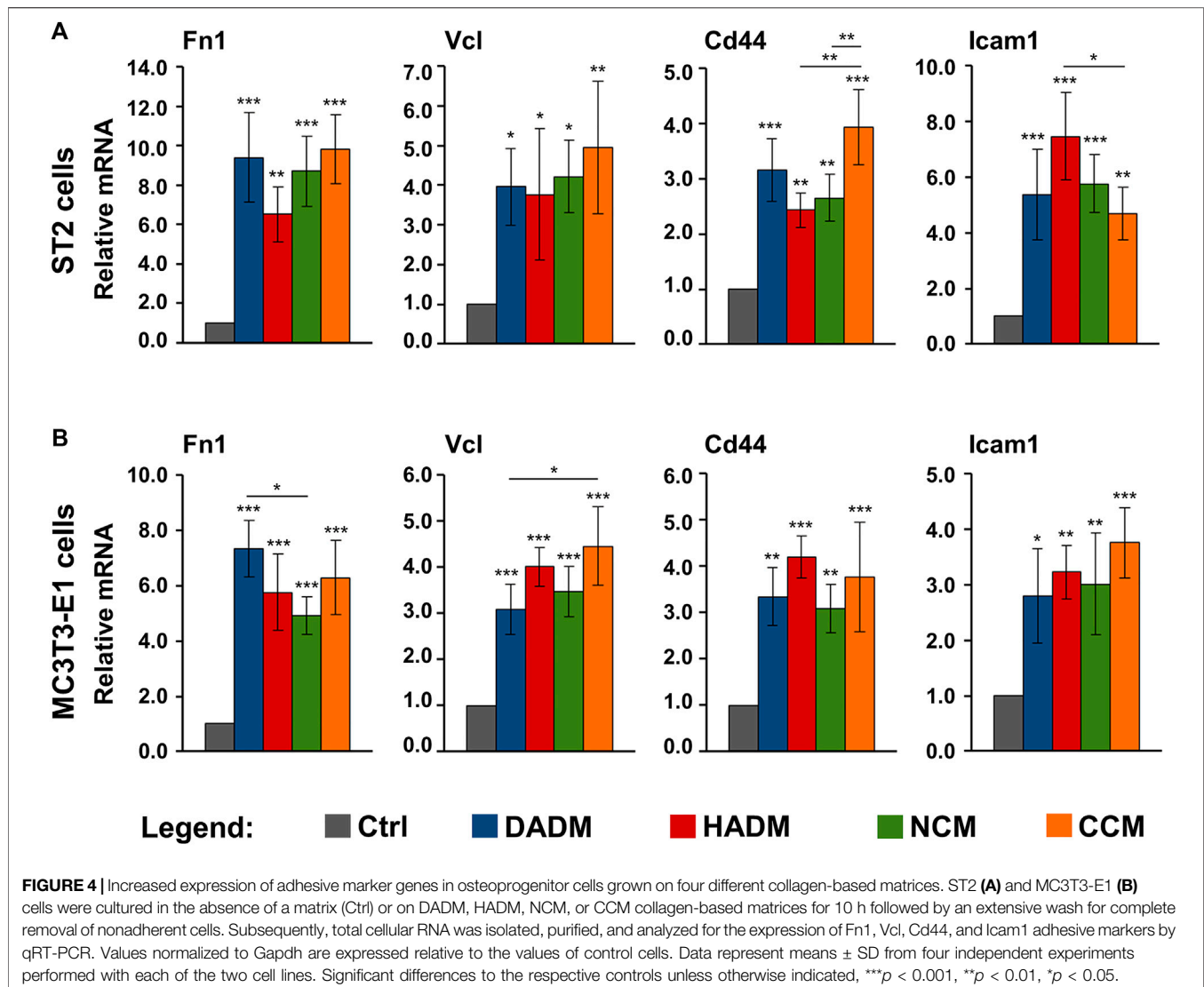
Quantification of the expression of the above listed adhesive marker genes by means of qRT-PCR revealed a significant ($p < 0.05$) induction of all four mRNA levels in both ST2 (**Figure 4A**) and MC3T3-E1 (**Figure 4B**) cells grown on each of the four collagen matrices above the expression levels detected in control cells. The observed upregulation in the expression of *Fn1*, *Vcl*, *Cd44*, and *Icam1* was comparable in both osteoprogenitor lines and in the range of 2.4–9.8-fold (**Figures 4A,B**). *Cd44* was characterized with a significantly ($p < 0.01$) higher expression in ST2 cells grown on CCM compared to its expression in ST2 cells grown on HADM and NCM (**Figure 4A**). On contrary, HADM caused a significantly ($p < 0.05$) higher upregulation of *Icam1* expression than CCM in the ST2 cells. Isolated cases of a more potent effect of DADM compared to NCM as well as of CCM compared to DADM on the induction of *Fn1* and *Vcl* in MC3T3-E1 cells, respectively, were also observed (**Figure 4B**).

Taken together, our data demonstrate a potent pro-adhesive capacity of the four collagen matrices with no clear trend for a difference in their potency.

Increased Expression of Osteogenic Differentiation Markers in Osteoprogenitor Cells Grown on the Hydrated Acellular Dermal Matrix and the Ribose-Crosslinked Collagen Matrix

As a next step, a screen for the expression of osteogenesis-related genes was performed. Therefore, ST2 and MC3T3-E1 cells grown on each of the investigated scaffolds were analyzed for the expression of 1) genes encoding bone matrix proteins such as collagen type I (*Col1a1*) and osteopontin (also known as secreted phosphoprotein 1, *Spp1*); 2) genes encoding early osteogenic markers such as the runt-related transcription factor 2 (*Runx2*) and alkaline phosphatase (*Alpl*); and 3) genes encoding intermediate and late osteogenic markers such as distal-less homeobox 5 (*Dlx5*), integrin-binding sialoprotein (*Ibsp*), osteocalcin (or bone gamma-carboxyglutamate protein 2, *Bglap2*), and phosphate regulating endopeptidase homolog, X-linked (*PheX*).

The qRT-PCR analyses showed that cells from each of the two lines grown on each of the four collagen-based scaffolds exhibited strongly induced expression of *Col1a1* and *Spp1* mRNAs above the expression levels detected in the respective control cells (**Figure 5**). The effects of DADM and HADM on the expression of *Col1a* and *Spp1* in ST2 cells (**Figure 5A**) as well as on the expression of *Spp1* in MC3T3-E1 cells (**Figure 5B**) were comparable and significantly ($p < 0.05$) better pronounced than the effects of NCM and CCM. Interestingly, HADM and CCM caused a strong ($p < 0.01$) upregulation of early, intermediate and late osteogenic differentiation markers whereas DADM and NCM had no effect on these transcripts. In isolated cases, the pro-osteogenic effects of HADM appeared superior compared to CCM. This was evident for the expression of *Runx2* and *Bglap2* in ST2 cells (**Figure 5A**) as well as for the expression of *Alpl* and *Ibsp* in MC3T3-E1 cells (**Figure 5B**). In contrast, the *Bglap2*



transcript in MC3T3-E1 cells was significantly ($p < 0.01$) better induced by CCM compared to HADM (Figure 5B).

These results suggest a stimulating effect of all investigated collagen-based scaffolds on the early stages of osteogenic differentiation, namely production of ECM that will later enable mineral deposition. Among the four investigated matrices, only HADM and CCM may be able to contribute to the osteogenesis progression by triggering the expression of osteogenic factors characterizing the advanced differentiation stages.

Enhancing Effect of Collagen-Based Matrices Biofunctionalized With Enamel Matrix Derivative or Recombinant Bone Morphogenetic Protein-2 on the Expression of Osteogenic Differentiation Markers in Osteoprogenitor Cells

In the light of a limited modulation of the osteogenic process by only two of the four investigated collagen-based matrices, we

investigated whether a short, clinically relevant coating of the scaffolds with either EMD or rBMP-2 can positively influence the osteogenic process. Earlier studies identified TGF- β 1 in EMD by immunoassays (Stähli et al., 2014) and had shown that TGF- β -like activity can be passively released from EMD-coated collagen products (Stähli et al., 2016). To ensure proper technical performance of the coating experiments, on day 3, we measured the amounts of TGF- β 1 and BMP-2 released in culture supernatants of cells cultured on EMD- and BMP-2-coated collagen matrices, respectively, by using ELISAs. The TGF- β 1 was in the range of $2,140 \pm 230$ pg/ml \div $3,168 \pm 220$ pg/ml, and BMP-2 was in the range of 660 ± 55 pg/ml \div 940 ± 42 pg/ml.

In comparison with control conditions consisting of ST2 or MC3T3-E1 cells grown on the respective native/uncoated matrices, the expression levels of *Col1a1* and *Spp1* were significantly ($p < 0.01$) upregulated in osteoprogenitors cultured on all EMD-coated collagen matrices (Figure 6A). No effect of rBMP-2 was observed on the expression of these

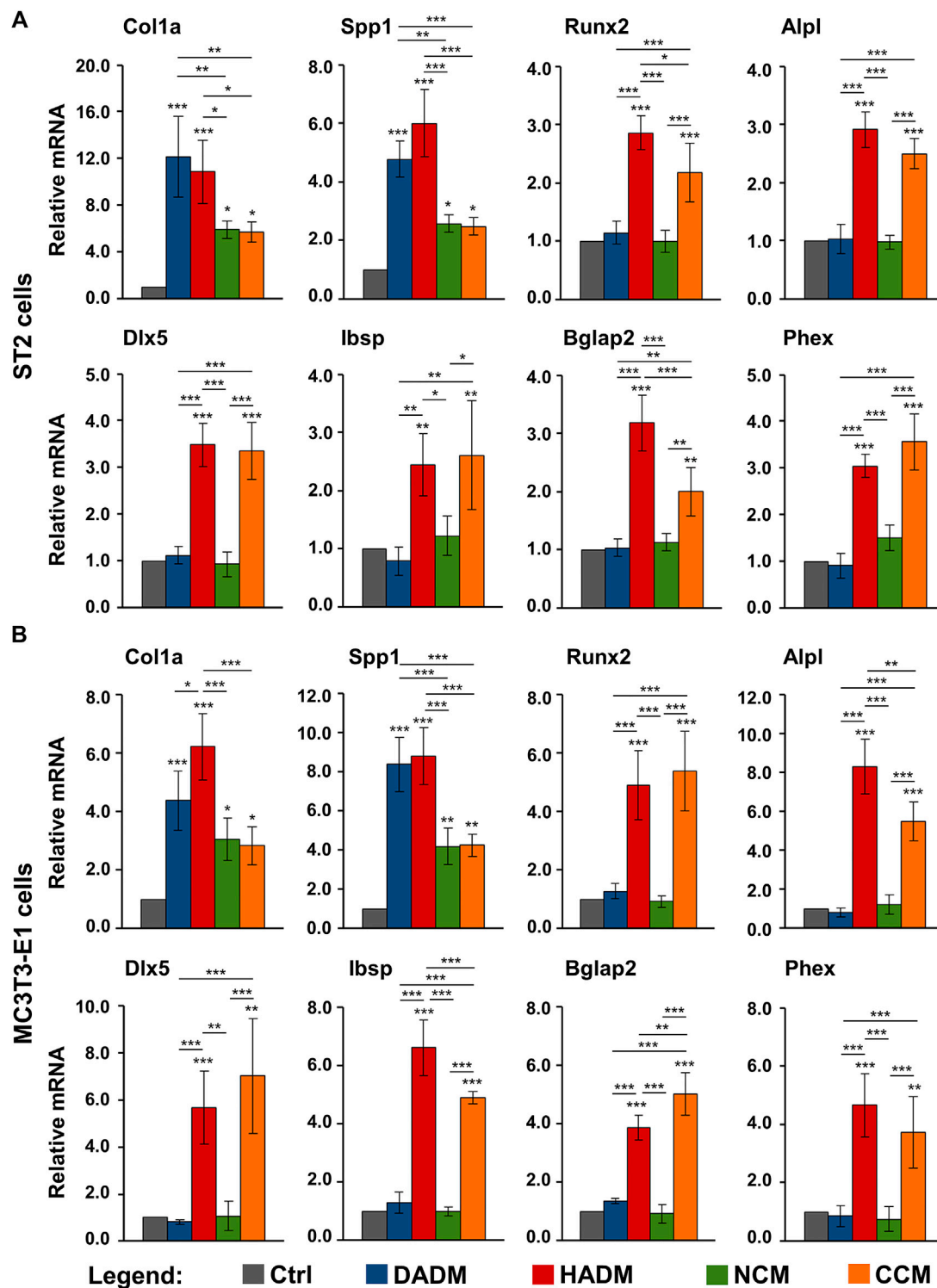


FIGURE 5 | Increased expression of osteogenic differentiation markers in osteoprogenitor cells grown on HADM and CCM collagen-based matrices. ST2 (A) and MC3T3-E1 (B) cells were cultured in the absence of a collagen matrix (Ctrl) or on DADM, HADM, NCM, or CCM collagen-based matrices for 3 days before total cellular RNA was extracted, purified, and analyzed for the expression of Col1a1, Spp1, Runx2, Alpl, Dlx5, Ibsp, Bglap2, and PheX osteogenic markers by qRT-PCR. Values normalized to Gapdh are expressed relative to the values of control cells. Data represent means \pm SD from four independent experiments performed with each of the two cell lines. Significant differences to the respective controls unless otherwise indicated, *** $p < 0.001$, ** $p < 0.01$, * $p < 0.05$.

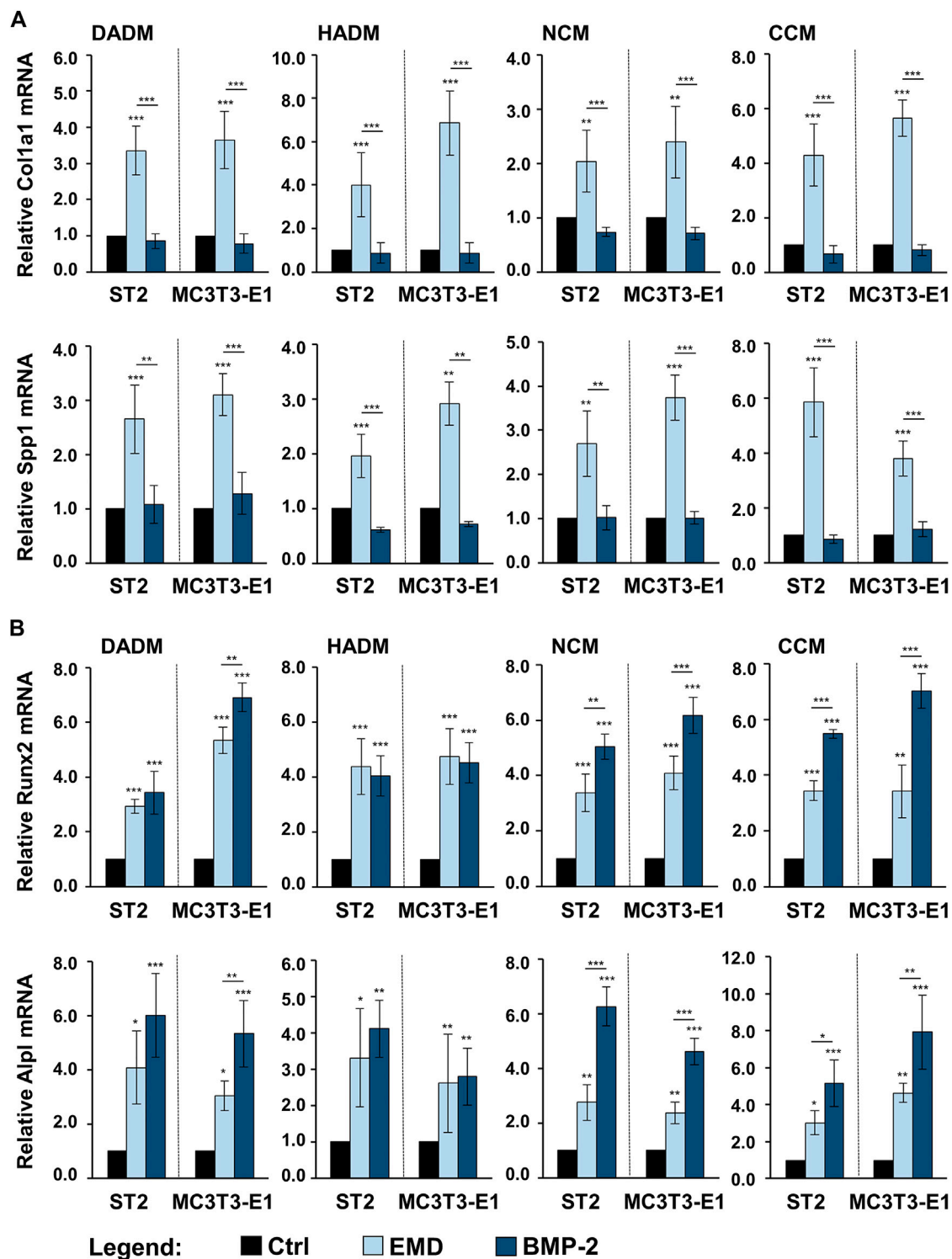


FIGURE 6 | Enhancing effect of collagen-based matrices biofunctionalized with EMD or rBMP-2 on the expression of genes characterizing the early stages of osteogenic differentiation. Each of the two osteoprogenitor cell lines, ST2 and MC3T3-E1, were cultured on DADM, HADM, NCM, or CCM collagen-based matrices under three different conditions: 1) control condition (Ctrl), consisting of cells grown on native/uncoated matrices, 2) cells grown on matrices coated with EMD, and 3) cells grown on matrices coated with rBMP-2. For conditions 2) and 3), collagen matrices were coated for 10 min at room temperature in serum-free DMEM containing 1 mg/ml of EMD or 100 ng/ml of rBMP-2, respectively, followed by extensive wash of the matrices as described in the Materials and Methods section. Cells were grown under the above listed conditions for 3 days before total RNA was extracted and analyzed by qRT-PCR for the expression of Col1a1 and Spp1 (A), Runx2 and Alpl (B). Values normalized to Gapdh are expressed relative to the values of the respective control cells. Means \pm SD from four independent experiments performed with each of the two cell lines and significant differences to the control unless otherwise indicated, *** p < 0.001, ** p < 0.01, * p < 0.05 are shown.

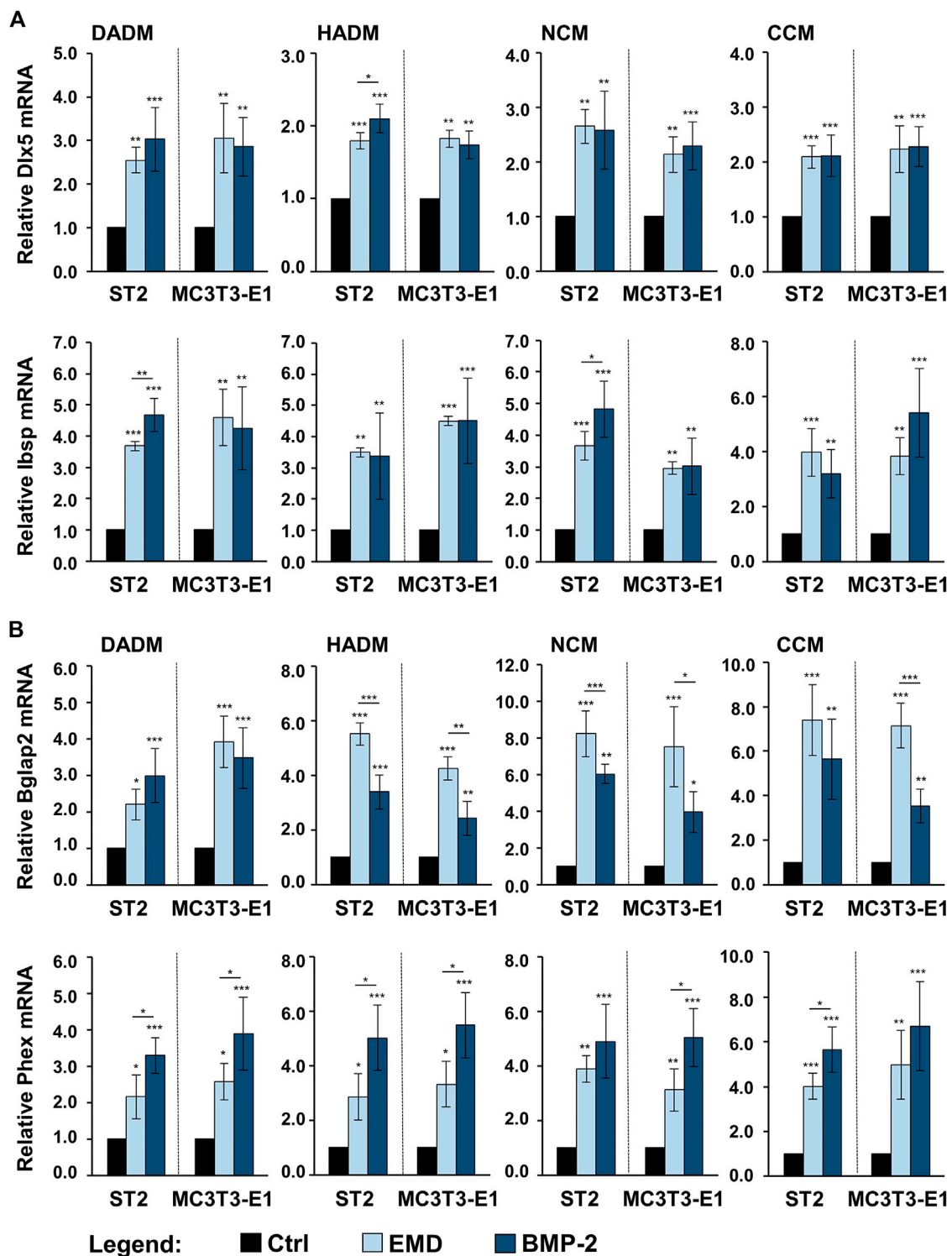


FIGURE 7 | Enhancing effect of collagen-based matrices biofunctionalized with EMD or rBMP-2 on the expression of genes characterizing intermediate and late stages of osteogenic differentiation. Each of the two osteoprogenitor cell lines, ST2 and MC3T3-E1, were cultured on DADM, HADM, NCM, or CCM collagen-based matrices under three different conditions: 1) control condition (Ctrl), consisting of cells grown on native/uncoated matrices, 2) cells grown on matrices coated with EMD, and 3) cells grown on matrices coated with rBMP-2. For conditions 2) and 3), collagen matrices were coated for 10 min at room temperature in serum-free DMEM containing 1 mg/ml of EMD or 100 ng/ml of rBMP-2, respectively, followed by extensive wash of the matrices as described in the Materials and Methods section. Cells were grown under the above listed conditions for 3 days before total RNA was extracted and analyzed by qRT-PCR for the expression of Dlx5 and Ibsp (**A**), Bglap2 and Phex (**B**). Values normalized to Gapdh are expressed relative to the values of the respective control cells. Means \pm SD from four independent experiments performed with each of the two cell lines and significant differences to the control unless otherwise indicated, *** p < 0.001, * p < 0.01, p < 0.05 are shown.

two genes. The expression of the early osteogenic marker genes Runx2 and Alpl was significantly ($p < 0.05$) induced by both EMD and rBMP-2 on each of the collagen-based matrices with a trend of a better pronounced effect of rBMP-2 in both ST2 and MC3T3-E1 cells cultured on NCM or CCM as well as in MC3T3-E1 cells cultured on DADM (Figure 6B).

In comparison with the respective uncoated matrices, all four matrices coated with either EMD or rBMP-2 were able to cause prominent upregulation of the intermediate and late osteogenic markers *Dlx5*, *Ibsp*, *Bglap2*, and *Phex* in each of the two cell lines (Figures 7A,B). The induction was in the range of 1.7–8.2-fold ($p < 0.05$). Interestingly, whereas on some of the scaffolds *Dlx5*, *Ibsp*, and *Phex* transcripts were characterized with a higher induction caused by rBMP-2 compared to EMD, the expression of *Bglap2* mRNA was significantly better induced by EMD applied as a coating to HADM, NCM, and CCM. However, no clear pattern of better functionalization of the collagen matrices with one or the other bioactive substance could be identified.

The observed changes in the osteogenic marker gene expression indicate preserved biological activity of EMD and rBMP-2 adsorbed and released from each of the investigated collagen-based matrices as well as a clear stimulatory effect of each of the two substances on the osteogenic differentiation of the two osteoprogenitor lines. Whereas BMP-2 did not influence the expression of genes encoding bone matrix proteins, the effect of EMD was ubiquitous and spread over the entire range of genes regulating the osteogenic process.

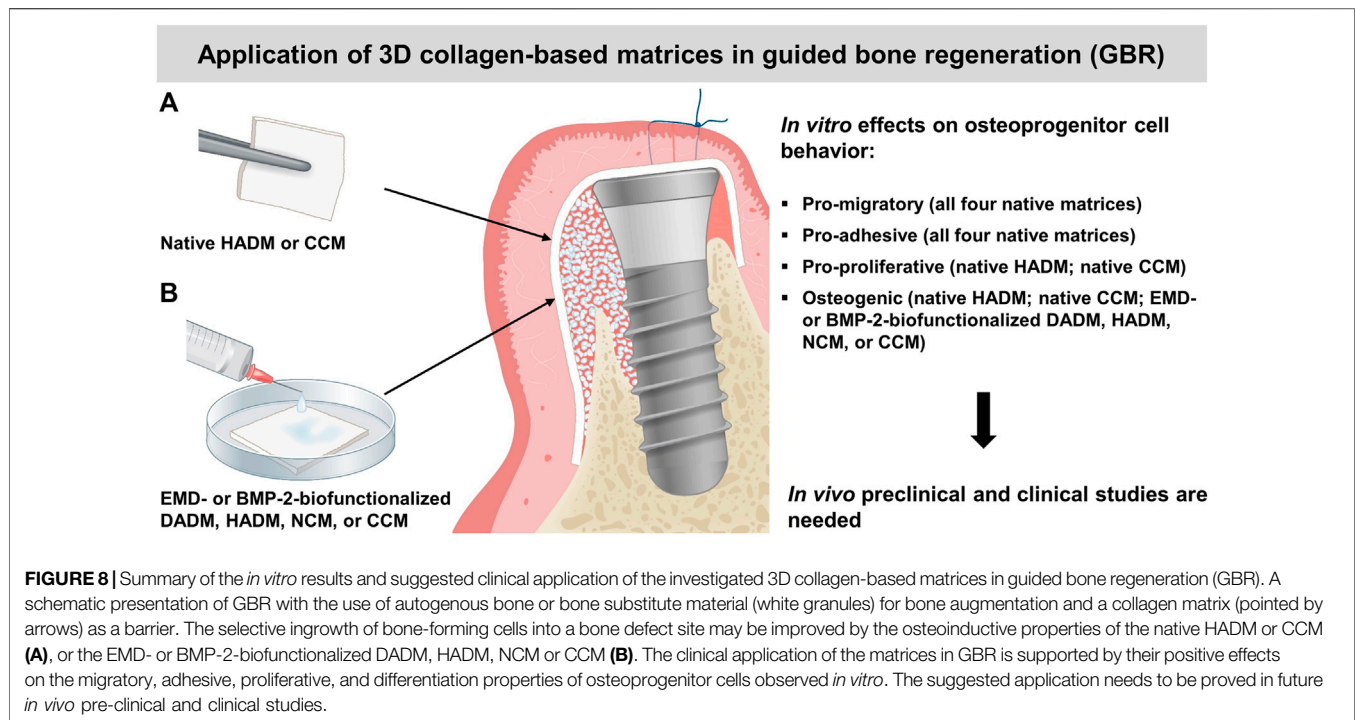
DISCUSSION

Collagen-based biomaterials are shown to have advantages over other biomaterials and are therefore used in various tissue-engineering applications (Patil and Masters, 2020). Since collagen is the most abundant protein in the human body and a major component of bone and periodontal connective tissue, it appears chemotactic for various cell types (Farndale et al., 2004; Rothamel et al., 2004; Thibault et al., 2007; Lin et al., 2020), in addition to its prominent role in coagulum formation (Farndale et al., 2004; Kumar et al., 2014; Asparuhova et al., 2021) and angiogenesis at wounded sites (Twardowski et al., 2007). Clinically, collagen-based scaffolds are mostly utilized for guided tissue regeneration and soft tissue augmentation (Pabst and Kämmerer, 2020). The aim of the current study was to investigate the biocompatibility of different collagen-based scaffolds in cultures of mesenchymal stromal and pre-osteoblastic cells as well as to evaluate their potential to induce osteogenic cell differentiation *in vitro*. To the best of our knowledge, only one of the four matrices, namely the glycated CCM, has been previously tested in the context of osteogenesis, more specifically for restoring lost tissue volume of a deficient ridge (Smidt et al., 2019). Therefore, the current study appears to be the only one comparing the effects of the four different scaffolds on the behavior of cells involved in hard tissue regeneration.

The osteogenic process is characterized by recruitment of osteoprogenitor cells, their attachment, growth, and differentiation into mature osteoblasts (Teti, 2011). Following

the sequence of events accompanying the osteogenesis, our data have clearly demonstrated increased migratory, adhesive, proliferative, and osteogenic properties of mesenchymal stromal ST2 and pre-osteoblastic MC3T3-E1 cells grown on each of the four (for migration and adhesion) or on some (for proliferation and osteogenesis) matrices. Indeed, while all investigated 3D matrices exhibited favorable effects on the motility and attachment of the two osteoprogenitor cell lines, only the hydrated matrix of new generation, HADM and the crosslinked matrix, CCM were able to induce significant cell proliferation and to boost the expression of differentiation markers characterizing both early and late stages of the osteogenesis. However, the osteogenic potential of the other two matrices, DADM and NCM, was significantly boosted by EMD and rBMP-2 applied as a coating to the biomaterials. Taken together, the obtained results suggest an application of the 3D collagen-based matrices in guided bone regeneration (GBR). A summary of the results and suggested clinical application is depicted in Figure 8.

Interestingly, often chemically-induced crosslinking, e.g., the intra- and/or intermolecular crosslinking of collagen molecules with glutaraldehyde, has been proposed as a possible reason for a decreased biocompatibility of collagen-based materials (Marinucci et al., 2003; Adamiak and Sionkowska, 2020). In our study, the sugar-crosslinked CCM, which has been generated by a crosslinking method resembling the naturally occurring glycation process in mammalian cells, did not show any signs of reduced biocompatibility. On contrary, both the mesenchymal stromal and pre-osteoblastic cells showed increased proliferative rates on the CCM matrix that were comparable to the cell growth rates on the non-crosslinked HADM and superior compared with the natural NCM and DADM matrices. The impact of the four collagen-based matrices on the migratory, adhesive, and proliferative properties of ST2 and MC3T3-E1 cells, with a better pronounced pro-proliferative effect of HADM and CCM, resembled the impact of the matrices on the functionality of primary human periodontal ligament cells and oral fibroblasts investigated in a recently published study (Lin et al., 2020). This suggests that the difference in the potency of the four matrices to induce changes in the cellular behavior is not cell-specific but rather depends on their physicochemical characteristics. Numerous investigations have demonstrated that the matrix composition, pore size and degree of porosity, and surface motifs involved in the cell recognition and cell-matrix interactions are in the basis of the differential behavior of cells grown on the different matrices (Stevens and George, 2005; Yeung et al., 2005; Chen et al., 2013; Rodina et al., 2016; Rodina et al., 2017). It has been shown that mesenchymal stem cells are prone to undergo osteospecific differentiation and functional bone tissue formation when cultured on topographies that increase the focal adhesion frequency and reinforcement (Biggs et al., 2009; Sjöström et al., 2009; Biggs and Dalby, 2010). Whereas fibroblasts prefer smooth or finely textured surfaces, osteoprogenitor cells attach better to rough or textured porous surfaces that would also enhance mineralization at the advanced stages of the osteoblast differentiation (Bowers et al., 1992; Rausch et al., 2021). Topographical analyses of the 3D matrices as well as



investigations of the cell-matrix interactions in a direct way, by means of microscopy, have not been performed in the current investigation and deserve special attention.

Furthermore, focal adhesion reinforcement has been directly correlated with the expression of the transcription factor Runx2 as a master regulator of osteogenic marker gene expression (Salasznyk et al., 2007; Gordon et al., 2009). Upregulation of Runx2 expression has been documented in mesenchymal populations cultured on a variety of next generation biomaterials including 3D fibrous scaffolds (Woo et al., 2007), nanostructures (Mendonça et al., 2009), biofunctionalized titanium (Lim et al., 2009), and hydroxyapatite/tricalcium phosphate scaffolds (Sun et al., 2008). In our study, Runx2 as well as Alpl, Dlx5, Ibsp, Bglap2, and Phex transcripts were all significantly induced in osteoprogenitors cultured on native/non-functionalized HADM and CCM matrices only. This suggests that among the four investigated matrices, native HADM and CCM carry the greatest osteoinductive capacity. It remains to be elucidated whether native, unmodified HADM and CCM would have the ability to ossify when placed in proximity to bone *in vivo*. It is well known that collagen itself has a limited ability to induce apatite formation. Therefore, we investigated the possibility to use bioactive substances such as EMD, known to exhibit growth factor activities (Wyganowska-Świątkowska et al., 2015), or the highly osteogenic BMP-2 (Wozney et al., 1988) for biofunctionalization of the investigated biomaterials.

Recombinant growth factors are generally characterized with short half-lives, instability and fast degradation rates when applied in solution, side effects, and poor cost-effectiveness (Bowen-Pope et al., 1984; Anusaksathien and Giannobile, 2002; Carreira et al., 2014; Rocque et al., 2014). In a recent study, we have examined the adsorption and release of EMD and

rBMP-2 from the four investigated collagen-based matrices (Nica et al., 2020). BMP-2 was characterized with relatively low release from all four matrices during the entire 13-day test period and several time points at which a burst release was observed. Based on findings demonstrating that TGF- β -like activity can be passively released from EMD-coated collagen products (Stähli et al., 2016), the EMD release kinetics was investigated by the means of TGF- β 1 release and demonstrated a burst release within 24 h from HADM, DADM, NCM, and within 3 days from CCM, followed by a sustained slow release over 13 days. Both types of release kinetics were suggested as advantageous for the slow process of bone regeneration following implant placement or periodontal reconstruction. These findings prompted us to choose namely EMD and rBMP-2 as coatings in the present study.

EMD is an extract from fetal teeth composed of a mixture of enamel matrix proteins. Amelogenin proteins, including their enzymatically cleaved and alternatively spliced fragments, dominate this protein mixture by more than 90% (Grandin et al., 2012). The ability of EMD to regulate osteoblast proliferation and differentiation has been described as cell-specific and dependent on the stage of cell differentiation. More specifically, EMD has been shown to stimulate proliferation in the early stages of osteoblastic maturation and to enhance osteogenic differentiation in committed osteoblasts only (Schwartz et al., 2000). In our study, we have not detected any inverse relation between differentiation triggered by EMD-coated collagen matrices in the mesenchymal stromal ST2 and pre-osteoblastic MC3T3-E1 cells, likely due to the very close differentiation status of the two cell lines. Moreover, in agreement with earlier studies showing that EMD significantly upregulates Col1 (Du et al., 2005; Mroziak et al., 2012), Spp1

(Rincon et al., 2005), *Alpl* (Du et al., 2005; Fukae et al., 2006; Nagano et al., 2006), and *Bglap2* (Iwata et al., 2002; Du et al., 2005) gene expression, we have demonstrated a stimulatory effect of EMD-coated matrices on the expression of the above listed genes. Indeed, various *in vitro* studies reported on the capacity of EMD to induce osteogenic gene expression in alveolar bone proper-derived stem cells (Fawzy El-Sayed et al., 2014) and dental follicle cells (Hakki et al., 2001) as well as to increase collagen, fibronectin, and TGF- β 1 production in periodontal ligament cells (Van der Pauw et al., 2000). In addition to these *in vitro* studies, a number of clinical studies have reported a prominent regenerative effect of EMD in treating intrabony and furcation defects (Velasquez-Plata et al., 2002; Windisch et al., 2002; Donos et al., 2003; Sculean et al., 2003; Sculean et al., 2004; Losada et al., 2017).

BMP-2, on the other hand, belongs to the BMP subgroup of the TGF- β superfamily of proteins. The BMPs were first identified as factors able to induce ectopic bone formation *in vivo* (Wozney et al., 1988). Numerous studies on BMP-2 have shown that it strongly enhances the expression of osteogenic markers in cultures of bone marrow-derived stromal cells (Thies et al., 1992; Rickard et al., 1994; Asparuhova et al., 2018), myoblasts (Katagiri et al., 1994), alveolar bone proper-derived stem cells (Fawzy El-Sayed et al., 2014), and dental pulp stem cells (Hrubi et al., 2018). However, treatment of cells with BMP-2 have resulted in various outcomes and its osteogenic effects have appeared strongly dependent on the cell type, the applied dose, the treatment duration, and the local microenvironment, namely the presence of other osteoinductive molecules (Zhao et al., 2003; Hrubi et al., 2018). In this respect, it was not surprising that we observed no effect of BMP-2-coated matrices on the expression of genes encoding bone matrix proteins (Col1a1 and Spp1) but strongly induced expression of genes encoding early (Runx2 and *Alpl*), intermediate (Dlx5, *Ibsp*, and *Bglap2*), and late (Phex) osteogenic differentiation markers. On the one hand, the differential effects of EMD- and rBMP-2-coated matrices on the expression of Col1a1 and Spp1 transcripts can be explained by the proven TGF- β 1 activity of EMD (Stähli et al., 2014; Wyganowska-Świątkowska et al., 2015; Stähli et al., 2016). TGF- β 1 stimulates the synthesis of ECM proteins such as collagen, osteopontin, osteonectin, fibronectin, and integrins, and inhibits matrix degradation by stimulating the production of protease inhibitors and suppressing the production of proteases (Roberts et al., 1988). On the other hand, the observed similarities in the effects of EMD- and rBMP-2-coated matrices on the expression of the rest of osteogenic marker genes can be attributed to an existing relation between EMD and BMPs. It has been reported that 1) EMD upregulates the endogenous cellular production of BMPs (Parkar and Tonetti, 2004), and 2) EMD can be contaminated with trace amounts of active BMP-2 during the manufacturing process (Saito et al., 2008; Johnson et al., 2009).

The strategy of combining the investigated 3D collagen-based matrices with bioactive substances has the potential to enhance the bone regenerative process and to shed further light onto the underlying mechanisms of bone regeneration. In recent years, collagen-based matrices have been loaded not only with diverse bioactive substances but also with various cell types, drugs such as bisphosphonates, or vectors/nucleic acids encoding growth

factors (Zhang et al., 2018). However, a composite collagen-based scaffold with ideal physicochemical and biological properties is still not available. Moreover, *in vivo* pre-clinical and clinical studies validating the utility of engineered composite scaffolds are largely missing. *In vitro* cell culture investigations carry the inherited limitation of testing biomaterials in the context of specific cell lines, which often do not fully represent the primary cells and are placed outside of their natural environment (in the case of two-dimensional culture models).

Within the limitations of the current *in vitro* study, it can be concluded that two of the four investigated collagen-based 3D scaffolds, namely the HADM and CCM, have the potential to be applied in GBR procedures (Figure 8A), in addition to their well-documented use as soft tissue substitute materials. With their pro-migratory, pro-adhesive, pro-proliferative, and osteogenic potential, HADM and CCM may allow osteoprogenitor cells to populate the protected space and to progress further into the differentiation process. Moreover, the presented study extends on the possibility to transfer osteoinductive properties onto the osteoconductive 3D collagen scaffolds by their short-term, clinically relevant pre-activation with EMD or rBMP-2 (Figure 8B). Such biofunctionalization may appear an optimal treatment modality for bone defects in periodontal and implant surgery.

DATA AVAILABILITY STATEMENT

The original contributions presented in the study are included in the article/Supplementary Material, further inquiries can be directed to the corresponding author.

AUTHOR CONTRIBUTIONS

MA and AS conceived the study. MA designed and supervised the experiments. ZL and CN performed the experiments. ZL and MA analyzed and interpreted the data. MA wrote the paper, assisted by ZL, CN, and AS. All authors approved the final version of the manuscript.

FUNDING

The study was funded by a grant received from the Oral Reconstruction Foundation ORF11803 to MA and AS.

ACKNOWLEDGMENTS

We thank Larissa Hofmann for excellent technical assistance.

SUPPLEMENTARY MATERIAL

The Supplementary Material for this article can be found online at: <https://www.frontiersin.org/articles/10.3389/fbioe.2021.708830/full#supplementary-material>

REFERENCES

- Adamiak, K., and Sionkowska, A. (2020). Current Methods of Collagen Cross-Linking: Review. *Int. J. Biol. Macromolecules* 161, 550–560. doi:10.1016/j.jbiomac.2020.06.075
- Anusaksathien, O., and Giannobile, W. (2002). Growth Factor Delivery to Re-engineer Periodontal Tissues. *Curr. Pharm. Biotechnol.* 3 (2), 129–139. doi:10.2174/1389201023378391
- Asparuhova, M. B., Caballé-Serrano, J., Buser, D., and Chappuis, V. (2018). Bone-conditioned Medium Contributes to Initiation and Progression of Osteogenesis by Exhibiting Synergistic TGF- β 1/bmp-2 Activity. *Int. J. Oral Sci.* 10 (2), 20. doi:10.1038/s41368-018-0021-2
- Asparuhova, M. B., Stähli, A., Guldener, K., and Sculean, A. (2021). A Novel Volume-Stable Collagen Matrix Induces Changes in the Behavior of Primary Human Oral Fibroblasts, Periodontal Ligament, and Endothelial Cells. *Int. J. Mol. Sci.* 22 (8), 4051. doi:10.3390/ijms22084051
- Basudan, A., Babay, N., Ramalingam, S., Nooh, N., AlKindi, M., Al-Rasheed, A., et al. (2016). Efficacy of Mucograft vs Conventional Resorbable Collagen Membranes in Guided Bone Regeneration Around Standardized Calvarial Defects in Rats: An *In Vivo* Microcomputed Tomographic Analysis. *Int. J. Periodontics Restorative Dent* 36 (Suppl. 1), s109–s121. doi:10.11607/prd.2261
- Bays, J. L., and DeMali, K. A. (2017). Vinculin in Cell-Cell and Cell-Matrix Adhesions. *Cell. Mol. Life Sci.* 74 (16), 2999–3009. doi:10.1007/s00018-017-2511-3
- Biggs, M. J. P., and Dalby, M. J. (2010). Focal Adhesions in Osteoneogenesis. *Proc. Inst. Mech. Eng. H* 224 (12), 1441–1453. doi:10.1243/09544119jeim775
- Biggs, M. J. P., Richards, R. G., Gadegaard, N., McMurray, R. J., Affrossman, S., Wilkinson, C. D. W., et al. (2009). Interactions with Nanoscale Topography: Adhesion Quantification and Signal Transduction in Cells of Osteogenic and Multipotent Lineage. *J. Biomed. Mater. Res.* 91A (1), 195–208. doi:10.1002/jbm.a.32196
- Blatt, S., Burkhardt, V., Kämmerer, P. W., Pabst, A. M., Sagheb, K., Heller, M., et al. (2020). Biofunctionalization of Porcine-Derived Collagen Matrices with Platelet Rich Fibrin: Influence on Angiogenesis *In Vitro* and *In Vivo*. *Clin. Oral Invest.* 24 (10), 3425–3436. doi:10.1007/s00784-020-03213-8
- Bowen-Pope, D., Malpass, T., Foster, D., and Ross, R. (1984). Platelet-derived Growth Factor *In Vivo*: Levels, Activity, and Rate of Clearance. *Blood* 64 (2), 458–469. doi:10.1182/blood.v64.2.458.bloodjournal642458
- Bowers, K. T., Keller, J. C., Randolph, B. A., Wick, D. G., and Michaels, C. M. (1992). Optimization of Surface Micromorphology for Enhanced Osteoblast Responses *In Vitro*. *Int. J. Oral Maxillofac. Implants* 7 (3), 302–310.
- Carreira, A. C., Lojudice, F. H., Halcsik, E., Navarro, R. D., Sogayar, M. C., and Granjeiro, J. M. (2014). Bone Morphogenetic Proteins. *J. Dent Res.* 93 (4), 335–345. doi:10.1177/0022034513518561
- Chen, A. K., Delrio, F. W., Peterson, A. W., Chung, K.-H., Bhadiraju, K., and Plant, A. L. (2013). Cell Spreading and Proliferation in Response to the Composition and Mechanics of Engineered Fibrillar Extracellular Matrices. *Biotechnol. Bioeng.* 110 (10), 2731–2741. doi:10.1002/bit.24921
- Cui, Y., Luan, J., Li, H., Zhou, X., and Han, J. (2016). Exosomes Derived from Mineralizing Osteoblasts Promote ST2 Cell Osteogenic Differentiation by Alteration of microRNA Expression. *FEBS Lett.* 590 (1), 185–192. doi:10.1002/1873-3468.12024
- Donos, N., Sculean, A., Glavind, L., Reich, E., and Karring, T. (2003). Wound Healing of Degree III Furcation Involvements Following Guided Tissue Regeneration And/or Emdogain. *J. Clin. Periodontol.* 30 (12), 1061–1068. doi:10.1046/j.0303-6979.2003.00429.x
- Doonquah, L., Holmes, P.-J., Ranganathan, L. K., and Robertson, H. (2021). Bone Grafting for Implant Surgery. *Oral Maxillofac. Surg. Clin. North America* 33 (2), 211–229. doi:10.1016/j.coms.2021.01.006
- Du, C., Schneider, G. B., Zaharias, R., Abbott, C., Seabold, D., Stanford, C., et al. (2005). Apatite/Amelogenin Coating on Titanium Promotes Osteogenic Gene Expression. *J. Dent Res.* 84 (11), 1070–1074. doi:10.1177/154405910508401120
- Edelmayer, M., Wehner, C., Ulm, C., Zechner, W., Shafer, D., and Agis, H. (2020). Which Substances Loaded onto Collagen Scaffolds Influence Oral Tissue Regeneration?—An Overview of the Last 15 Years. *Clin. Oral Invest.* 24 (10), 3363–3394. doi:10.1007/s00784-020-03520-0
- Farndale, R. W., Sixma, J. J., Barnes, M. J., and de Groot, P. G. (2004). The Role of Collagen in Thrombosis and Hemostasis. *J. Thromb. Haemost.* 2 (4), 561–573. doi:10.1111/j.1538-7836.2004.00665.x
- Fawzy El-Sayed, K. M., Dörfer, C., Ungefroren, H., Kassem, N., Wiltfang, J., and Paris, S. (2014). Effect of Emdogain Enamel Matrix Derivative and BMP-2 on the Gene Expression and Mineralized Nodule Formation of Alveolar Bone Proper-Derived Stem/progenitor Cells. *J. Craniomaxillofac. Surg.* 42 (5), 568–576. doi:10.1016/j.jcms.2013.07.028
- Franceschi, R. T., Iyer, B. S., and Cui, Y. (1994). Effects of Ascorbic Acid on Collagen Matrix Formation and Osteoblast Differentiation in Murine MC3T3-E1 Cells. *J. Bone Miner Res.* 9 (6), 843–854. doi:10.1002/jbmr.5650090610
- Franceschi, R. T., and Iyer, B. S. (1992). Relationship between Collagen Synthesis and Expression of the Osteoblast Phenotype in MC3T3-E1 Cells. *J. Bone Miner Res.* 7 (2), 235–246. doi:10.1002/jbmr.5650070216
- França-Grohmann, I. L., Sangiorgio, J. P. M., Bueno, M. R., Casarin, R. C. V., Silvério Ruiz, K. G., Nociti, F. H., Jr., et al. (2020). Treatment of Dehiscence-type Defects With Collagen Matrix And/or Enamel Matrix Derivative: Histomorphometric Study in Minipigs. *J. Periodontol.* 91 (7), 967–974. doi:10.1002/jper.19-0107
- Fukae, M., Kanazashi, M., Nagano, T., Tanabe, T., Oida, S., and Gomi, K. (2006). Porcine Sheath Proteins Show Periodontal Ligament Regeneration Activity. *Eur. J. Oral Sci.* 114 (Suppl. 1), 212–218. discussion 254–216, 381–212. doi:10.1111/j.1600-0722.2006.00309.x
- Ghanaati, S., Schlee, M., Webber, M. J., Willershausen, I., Barbeck, M., Balic, E., et al. (2011). Evaluation of the Tissue Reaction to a New Bilayered Collagen Matrix *In Vivo* and its Translation to the Clinic. *Biomed. Mater.* 6 (1), 015010. doi:10.1088/1748-6041/6/1/015010
- Gordon, J. A. R., Hunter, G. K., and Goldberg, H. A. (2009). Activation of the Mitogen-Activated Protein Kinase Pathway by Bone Sialoprotein Regulates Osteoblast Differentiation. *Cells Tissues Organs* 189 (1–4), 138–143. doi:10.1159/000151728
- Grandin, H. M., Gemperli, A. C., and Dard, M. (2012). Enamel Matrix Derivative: a Review of Cellular Effects *In Vitro* and a Model of Molecular Arrangement and Functioning. *Tissue Eng. B: Rev.* 18 (3), 181–202. doi:10.1089/ten.TEB.2011.0365
- Gurbuz, I., Ferralli, J., Roloff, T., Chiquet-Ehrismann, R., and Asparuhova, M. B. (2014). SAP Domain-dependent Mkl1 Signaling Stimulates Proliferation and Cell Migration by Induction of a Distinct Gene Set Indicative of Poor Prognosis in Breast Cancer Patients. *Mol. Cancer* 13, 22. doi:10.1186/1476-4598-13-22
- Hakki, S. S., Berry, J. E., and Somerman, M. J. (2001). The Effect of Enamel Matrix Protein Derivative on Follicle Cells *In Vitro*. *J. Periodontol.* 72 (5), 679–687. doi:10.1902/jop.2001.72.5.679
- Herford, A. S., and Cicciù, M. (2012). Bone Resorption Analysis of Platelet-Derived Growth Factor Type BB Application on Collagen for Bone Grafts Secured by Titanium Mesh over a Pig Jaw Defect Model. *Natl. J. Maxillofac. Surg.* 3 (2), 172–179. doi:10.4103/0975-5950.111374
- Herford, A. S., Lu, M., Akin, L., and Cicciù, M. (2012). Evaluation of a Porcine Matrix with and without Platelet-Derived Growth Factor for Bone Graft Coverage in Pigs. *Int. J. Oral Maxillofac. Implants* 27 (6), 1351–1358.
- Hosokawa, Y., Hosokawa, I., Ozaki, K., Nakae, H., and Matsuo, T. (2006). Cytokines Differentially Regulate ICAM-1 and VCAM-1 Expression on Human Gingival Fibroblasts. *Clin. Exp. Immunol.* 144 (3), 494–502. doi:10.1111/j.1365-2249.2006.03064.x
- Hrubí, E., Imre, L., Robaszkiewicz, A., Virág, L., Kerényi, F., Nagy, K., et al. (2018). Diverse Effect of BMP-2 Homodimer on Mesenchymal Progenitors of Different Origin. *Hum. Cel* 31 (2), 139–148. doi:10.1007/s13577-018-0202-5
- Iwata, T., Morotome, Y., Tanabe, T., Fukae, M., Ishikawa, I., and Oida, S. (2002). Noggin Blocks Osteoinductive Activity of Porcine Enamel Extracts. *J. Dent Res.* 81 (6), 387–391. doi:10.1177/0810387
- Jin, Q., and Giannobile, W. V. (2014). SDF-1 Enhances Wound Healing of Critical-Sized Calvarial Defects beyond Self-Repair Capacity. *PLoS One* 9 (5), e97035. doi:10.1371/journal.pone.0097035
- Johnson, D. L., Carnes, D., Steffensen, B., and Cochran, D. L. (2009). Cellular Effects of Enamel Matrix Derivative Are Associated with Different Molecular Weight Fractions Following Separation by Size-Exclusion Chromatography. *J. Periodontol.* 80 (4), 648–656. doi:10.1902/jop.2009.070420
- Katagiri, T., Yamaguchi, A., Komaki, M., Abe, E., Takahashi, N., Ikeda, T., et al. (1994). Bone Morphogenetic Protein-2 Converts the Differentiation Pathway of

- C2C12 Myoblasts into the Osteoblast Lineage [published Erratum Appears in J Cell Biol 1995 Feb;128(4):following 713]. *J. Cell Biol.* 127 (6 Pt 1), 1755–1766. doi:10.1083/jcb.127.6.1755
- Kumar, V. A., Taylor, N. L., Jalan, A. A., Hwang, L. K., Wang, B. K., and Hartgerink, J. D. (2014). A Nanostructured Synthetic Collagen Mimic for Hemostasis. *Biomacromolecules* 15 (4), 1484–1490. doi:10.1021/bm500091e
- Leonardi, R., Loreto, C., Caltabiano, R., and Caltabiano, C. (2006). Immunolocalization of CD44s in Human Teeth. *Acta Histochem.* 108 (6), 425–429. doi:10.1016/j.acthis.2006.06.006
- Lim, T. Y., Wang, W., Shi, Z., Poh, C. K., and Neoh, K. G. (2009). Human Bone Marrow-Derived Mesenchymal Stem Cells and Osteoblast Differentiation on Titanium with Surface-Grafted Chitosan and Immobilized Bone Morphogenetic Protein-2. *J. Mater. Sci. Mater. Med.* 20 (1), 1–10. doi:10.1007/s10856-008-3528-9
- Lin, Z., Nica, C., Sculean, A., and Asparuhova, M. B. (2020). Enhanced Wound Healing Potential of Primary Human Oral Fibroblasts and Periodontal Ligament Cells Cultured on Four Different Porcine-Derived Collagen Matrices. *Materials* 13 (17), 3819. doi:10.3390/ma13173819
- Losada, M., González, R., García, Á. P., Santos, A., and Nart, J. (2017). Treatment of Non-Contained Infrabony Defects with Enamel Matrix Derivative Alone or in Combination With Biphasic Calcium Phosphate Bone Graft: A 12-Month Randomized Controlled Clinical Trial. *J. Periodontol.* 88 (5), 426–435. doi:10.1902/jop.2016.160459
- Lucarini, G., Zizzi, A., Aspriello, S. D., Ferrante, L., Tosco, E., Lo Muzio, L., et al. (2009). Involvement of Vascular Endothelial Growth Factor, CD44 and CD133 in Periodontal Disease and Diabetes: an Immunohistochemical Study. *J. Clin. Periodontol.* 36 (1), 3–10. doi:10.1111/j.1600-051X.2008.01338.x
- Marinucci, L., Lilli, C., Guerra, M., Belcastro, S., Becchetti, E., Stabellini, G., et al. (2003). Biocompatibility of Collagen Membranes Crosslinked with Glutaraldehyde or Diphenylphosphoryl Azide: An In Vitro Study. *J. Biomed. Mater. Res.* 67 (2), 504–509. doi:10.1002/jbm.a.10082
- Mendonça, G., Mendonça, D. B. S., Simões, L. G. P., Araújo, A. L., Leite, E. R., Duarte, W. R., et al. (2009). The Effects of Implant Surface Nanoscale Features on Osteoblast-specific Gene Expression. *Biomaterials* 30 (25), 4053–4062. doi:10.1016/j.biomaterials.2009.04.010
- Mrozik, K. M., Gronthos, S., Menicanin, D., Marino, V., and Bartold, P. M. (2012). Effect of Coating Straumann Bone Ceramic with Emdogain on Mesenchymal Stromal Cell Hard Tissue Formation. *Clin. Oral Invest.* 16 (3), 867–878. doi:10.1007/s00784-011-0558-3
- Nagano, T., Oida, S., Suzuki, S., Iwata, T., Yamakoshi, Y., Ogata, Y., et al. (2006). Porcine Enamel Protein Fractions Contain Transforming Growth Factor- β 1. *J. Periodontol.* 77 (10), 1688–1694. doi:10.1902/jop.2006.050352
- Nevins, M., Camelo, M., Nevins, M. L., Schenk, R. K., and Lynch, S. E. (2003). Periodontal Regeneration in Humans Using Recombinant Human Platelet-Derived Growth Factor-BB (rhPDGF-BB) and Allogenic Bone. *J. Periodontol.* 74(9), 1282–1292. doi:10.1902/jop.2003.74.9.1282
- Newby, S. D., Masi, T., Griffin, C. D., King, W. J., Chipman, A., Stephenson, S., et al. (2020). Functionalized Graphene Nanoparticles Induce Human Mesenchymal Stem Cells to Express Distinct Extracellular Matrix Proteins Mediating Osteogenesis. *Int. J. Nanomedicine* 15, 2501–2513. doi:10.2147/ijn.S245801
- Nica, C., Lin, Z., Sculean, A., and Asparuhova, M. B. (2020). Adsorption and Release of Growth Factors from Four Different Porcine-Derived Collagen Matrices. *Materials* 13 (11), 2635. doi:10.3390/ma13112635
- Otsuka, E., Yamaguchi, A., Hirose, S., and Hagiwara, H. (1999). Characterization of Osteoblastic Differentiation of Stromal Cell Line ST2 that Is Induced by Ascorbic Acid. *Am. J. Physiology-Cell Physiol.* 277 (1), C132–C138. doi:10.1152/ajpcell.1999.277.1.C132
- Pabst, A., and Kämmerer, P. W. (2020). Collagen Matrices: Opportunities and Perspectives in Oral Hard and Soft Tissue Regeneration. *Quintessence Int.* 51 (4), 318–327. doi:10.3290/j.qi.a44149
- Pabst, A. M., Happe, A., Callaway, A., Ziebart, T., Stratul, S. I., Ackermann, M., et al. (2014). In Vitro and In Vivo Characterization of Porcine Acellular Dermal Matrix for Gingival Augmentation Procedures. *J. Periodont Res.* 49 (3), 371–381. doi:10.1111/jre.12115
- Papi, P., Pranno, N., Di Murro, B., and Pompa, G. (2021). Early Implant Placement and Peri-Implant Augmentation with a Porcine-Derived Acellular Dermal Matrix and Synthetic Bone in the Aesthetic Area: a 2-year Follow-Up Prospective Cohort Study. *Int. J. Oral Maxillofac. Surg.* 50 (2), 258–266. doi:10.1016/j.ijom.2020.07.002
- Parisi, L., Buser, D., Chappuis, V., and Asparuhova, M. B. (2021). Cellular Responses to Deproteinized Bovine Bone mineral Biofunctionalized with Bone-Conditioned Medium. *Clin. Oral Invest.* 25 (4), 2159–2173. doi:10.1007/s00784-020-03528-6
- Park, J. S., Pabst, A. M., Ackermann, M., Moergel, M., Jung, J., and Kasaj, A. (2018). Biofunctionalization of Porcine-Derived Collagen Matrix Using Enamel Matrix Derivative and Platelet-Rich Fibrin: Influence on Mature Endothelial Cell Characteristics In Vitro. *Clin. Oral Invest.* 22 (2), 909–917. doi:10.1007/s00784-017-2170-7
- Parkar, M. H., and Tonetti, M. (2004). Gene Expression Profiles of Periodontal Ligament Cells Treated with Enamel Matrix Proteins In Vitro: Analysis Using cDNA Arrays. *J. Periodontol.* 75 (11), 1539–1546. doi:10.1902/jop.2004.75.11.1539
- Patil, V. A., and Masters, K. S. (2020). Engineered Collagen Matrices. *Bioengineering* 7 (4), 163. doi:10.3390/bioengineering7040163
- Pawelec, K. M., Best, S. M., and Cameron, R. E. (2016). Collagen: a Network for Regenerative Medicine. *J. Mater. Chem. B* 4 (40), 6484–6496. doi:10.1039/c6tb00807k
- Quarles, L. D., Yohay, D. A., Lever, L. W., Caton, R., and Wenstrup, R. J. (1992). Distinct Proliferative and Differentiated Stages of Murine MC3T3-E1 Cells in Culture: an In Vitro Model of Osteoblast Development. *J. Bone Miner Res.* 7 (6), 683–692. doi:10.1002/jbmr.5650070613
- Ramseier, C. A., Rasperini, G., Batia, S., and Giannobile, W. V. (2012). Advanced Reconstructive Technologies for Periodontal Tissue Repair. *Periodontol.* 2000 59 (1), 185–202. doi:10.1111/j.1600-0757.2011.00432.x
- Rausch, M. A., Shokoobi-Tabrizi, H., Wehner, C., Pippenger, B. E., Wagner, R. S., Ulm, C., et al. (2021). Impact of Implant Surface Material and Microscale Roughness on the Initial Attachment and Proliferation of Primary Human Gingival Fibroblasts. *Biology* 10 (5), 356. doi:10.3390/biology10050356
- Rickard, D. J., Sullivan, T. A., Shenker, B. J., Leboy, P. S., and Kazhdan, I. (1994). Induction of Rapid Osteoblast Differentiation in Rat Bone Marrow Stromal Cell Cultures by Dexamethasone and BMP-2. *Develop. Biol.* 161 (1), 218–228. doi:10.1006/dbio.1994.1022
- Rincon, J. C., Xiao, Y., Young, W. G., and Bartold, P. M. (2005). Enhanced Proliferation, Attachment and Osteopontin Expression by Porcine Periodontal Cells Exposed to Emdogain. *Arch. Oral Biol.* 50 (12), 1047–1054. doi:10.1016/j.archoralbio.2005.04.006
- Roberts, A. B., Flanders, K. C., Kondaiah, P., Thompson, N. L., Van Obberghen-Schilling, E., Wakefield, L., et al. (1988). Transforming Growth Factor β : Biochemistry and Roles in Embryogenesis, Tissue Repair and Remodeling, and Carcinogenesis. *Recent Prog. Horm. Res.* 44, 157–197. doi:10.1016/b978-0-12-571144-9.50010-7
- Rocque, B. G., Kelly, M. P., Miller, J. H., Li, Y., and Anderson, P. A. (2014). Bone Morphogenetic Protein-Associated Complications in Pediatric Spinal Fusion in the Early Postoperative Period: an Analysis of 4658 Patients and Review of the Literature. *J. Neurosurg. Pediatr.* 14 (6), 635–643. doi:10.3171/2014.8.Peds13665
- Rodina, A. V., Tenchurin, T. K., Saprykin, V. P., Shepelev, A. D., Mamagulashvili, V. G., Grigor'ev, T. E., et al. (2016). Migration and Proliferative Activity of Mesenchymal Stem Cells in 3D Polylactide Scaffolds Depends on Cell Seeding Technique and Collagen Modification. *Bull. Exp. Biol. Med.* 162 (1), 120–126. doi:10.1007/s10517-016-3560-6
- Rodina, A. V., Tenchurin, T. K., Saprykin, V. P., Shepelev, A. D., Mamagulashvili, V. G., Grigor'ev, T. E., et al. (2017). Proliferative and Differentiation Potential of Multipotent Mesenchymal Stem Cells Cultured on Biocompatible Polymer Scaffolds with Various Physicochemical Characteristics. *Bull. Exp. Biol. Med.* 162 (4), 488–495. doi:10.1007/s10517-017-3646-9
- Rothamel, D., Schwarz, F., Sculean, A., Herten, M., Scherbaum, W., and Becker, J. (2004). Biocompatibility of Various Collagen Membranes in Cultures of Human PDL Fibroblasts and Human Osteoblast-Like Cells. *Clin. Oral Implants Res.* 15 (4), 443–449. doi:10.1111/j.1600-0501.2004.01039.x
- Saito, K., Konishi, I., Nishiguchi, M., Hoshino, T., and Fujiwara, T. (2008). Amelogenin Binds to Both Heparan Sulfate and Bone Morphogenetic Protein 2 and Pharmacologically Suppresses the Effect of Noggin. *Bone* 43 (2), 371–376. doi:10.1016/j.bone.2008.03.029

- Salasznyk, R. M., Klees, R. F., Williams, W. A., Boskey, A., and Plopper, G. E. (2007). Focal Adhesion Kinase Signaling Pathways Regulate the Osteogenic Differentiation of Human Mesenchymal Stem Cells. *Exp. Cel Res.* 313 (1), 22–37. doi:10.1016/j.yexcr.2006.09.013
- Schneider, C. A., Rasband, W. S., and Eliceiri, K. W. (2012). NIH Image to ImageJ: 25 Years of Image Analysis. *Nat. Methods* 9 (7), 671–675. doi:10.1038/nmeth.2089
- Schwartz, Z., Carnes, D. L., Jr., Pulliam, R., Lohmann, C. H., Sylvia, V. L., Liu, Y., et al. (2000). Porcine Fetal Enamel Matrix Derivative Stimulates Proliferation but Not Differentiation of Pre-osteoblastic 2T9 Cells, Inhibits Proliferation and Stimulates Differentiation of Osteoblast-like MG63 Cells, and Increases Proliferation and Differentiation of normal Human Osteoblast NHOst Cells. *J. Periodontol.* 71 (8), 1287–1296. doi:10.1902/jop.2000.71.8.1287
- Sculean, A., Donos, N., Schwarz, F., Becker, J., Brex, M., and Arweiler, N. B. (2004). Five-year Results Following Treatment of Intra-bony Defects with Enamel Matrix Proteins and Guided Tissue Regeneration. *J. Clin. Periodontol.* 31 (7), 545–549. doi:10.1111/j.1600-051X.2004.00518.x
- Sculean, A., Junker, R., Donos, N., Windisch, P., Brex, M., and Dünker, N. (2003). Immunohistochemical Evaluation of Matrix Molecules Associated with Wound Healing Following Treatment with an Enamel Matrix Protein Derivative in Humans. *Clin. Oral Invest.* 7 (3), 167–174. doi:10.1007/s00784-003-0212-9
- Sjöström, T., Dalby, M. J., Hart, A., Tare, R., Oreffo, R. O. C., and Su, B. (2009). Fabrication of Pillar-like Titania Nanostructures on Titanium and Their Interactions with Human Skeletal Stem Cells. *Acta Biomater.* 5 (5), 1433–1441. doi:10.1016/j.actbio.2009.01.007
- Smidt, A., Gutmacher, Z., and Sharon, E. (2019). A Nouveau Collagen Scaffold to Simplify Lateral Augmentation of Deficient Ridges between Natural Teeth. *Quintessence Int.* 50 (7), 576–582. doi:10.3290/j.qi.a42652
- Stähli, A., Bosshardt, D., Sculean, A., and Gruber, R. (2014). Emdogain-Regulated Gene Expression in Palatal Fibroblasts Requires TGF- β RI Kinase Signaling. *PLoS One* 9 (9), e105672. doi:10.1371/journal.pone.0105672
- Stähli, A., Miron, R. J., Bosshardt, D. D., Sculean, A., and Gruber, R. (2016). Collagen Membranes Adsorb the Transforming Growth Factor- β Receptor I Kinase-Dependent Activity of Enamel Matrix Derivative. *J. Periodontol.* 87, 583–590. doi:10.1902/jop.2016.150538
- Stevens, M. M., and George, J. H. (2005). Exploring and Engineering the Cell Surface Interface. *Science* 310 (5751), 1135–1138. doi:10.1126/science.1106587
- Suárez-López Del Amo, F., Rodriguez, J. C., Asa'ad, F., and Wang, H.-L. (2019). Comparison of Two Soft Tissue Substitutes for the Treatment of Gingival Recession Defects: an Animal Histological Study. *J. Appl. Oral Sci.* 27, e20180584. doi:10.1590/1678-7757-2018-0584
- Sun, H., Ye, F., Wang, J., Shi, Y., Tu, Z., Bao, J., et al. (2008). The Upregulation of Osteoblast Marker Genes in Mesenchymal Stem Cells Prove the Osteoinductivity of Hydroxyapatite/tricalcium Phosphate Biomaterial. *Transplant. Proc.* 40 (8), 2645–2648. doi:10.1016/j.transproceed.2008.07.096
- Teti, A. (2011). Bone Development: Overview of Bone Cells and Signaling. *Curr. Osteoporos. Rep.* 9 (4), 264–273. doi:10.1007/s11914-011-0078-8
- Thibault, M. M., Hoemann, C. D., and Buschmann, M. D. (2007). Fibronectin, Vitronectin, and Collagen I Induce Chemotaxis and Haptotaxis of Human and Rabbit Mesenchymal Stem Cells in a Standardized Transmembrane Assay. *Stem Cell Develop.* 16 (3), 489–502. doi:10.1089/scd.2006.0100
- Thies, R. S., Bauduy, M., Ashton, B. A., Kurtzberg, L., Wozney, J. M., and Rosen, V. (1992). Recombinant Human Bone Morphogenetic Protein-2 Induces Osteoblastic Differentiation in W-20-17 Stromal Cells. *Endocrinology* 130 (3), 1318–1324. doi:10.1210/endo.130.3.131123610.1210/en.130.3.1318
- Torii, Y., Hitomi, K., and Tsukagoshi, N. (1996). Synergistic Effect of BMP-2 and Ascorbate on the Phenotypic Expression of Osteoblastic MC3T3-E1 Cells. *Mol. Cel Biochem* 165 (1), 25–29. doi:10.1007/bf00229742
- Twardowski, T., Fertala, A., Orgel, J., and San Antonio, J. (2007). Type I Collagen and Collagen Mimetics as Angiogenesis Promoting Superpolymers. *Curr. Pharm. Des.* 13 (35), 3608–3621. doi:10.2174/138161207782794176
- Van der Pauw, M. T., Van den Bos, T., Everts, V., and Beertsen, W. (2000). Enamel Matrix-Derived Protein Stimulates Attachment of Periodontal Ligament Fibroblasts and Enhances Alkaline Phosphatase Activity and Transforming Growth Factor β 1Release of Periodontal Ligament and Gingival Fibroblasts. *J. Periodontol.* 71 (1), 31–43. doi:10.1902/jop.2000.71.1.31
- Velasquez-Plata, D., Todd Scheyer, E., and Mellonig, J. T. (2002). Clinical Comparison of an Enamel Matrix Derivative Used Alone or in Combination with a Bovine-Derived Xenograft for the Treatment of Periodontal Osseous Defects in Humans. *J. Periodontol.* 73 (4), 433–440. doi:10.1902/jop.2002.73.4.433
- Whitfield, M. L., George, L. K., Grant, G. D., and Perou, C. M. (2006). Common Markers of Proliferation. *Nat. Rev. Cancer* 6 (2), 99–106. doi:10.1038/nrc1802
- Windisch, P., Sculean, A., Klein, F., Tóth, V., Gera, I., Reich, E., et al. (2002). Comparison of Clinical, Radiographic, Histometric Measurements Following Treatment with Guided Tissue Regeneration or Enamel Matrix Proteins in Human Periodontal Defects. *J. Periodontol.* 73 (4), 409–417. doi:10.1902/jop.2002.73.4.409
- Woo, K. M., Jun, J.-H., Chen, V. J., Seo, J., Baek, J.-H., Ryoo, H.-M., et al. (2007). Nano-fibrous Scaffolding Promotes Osteoblast Differentiation and Biomaterialization. *Biomaterials* 28 (2), 335–343. doi:10.1016/j.biomaterials.2006.06.013
- Wozney, J., Rosen, V., Celeste, A., Mitsock, L., Whitters, M., Kriz, R., et al. (1988). Novel Regulators of Bone Formation: Molecular Clones and Activities. *Science* 242 (4885), 1528–1534. doi:10.1126/science.3201241
- Wyganowska-Świątkowska, M., Urbaniak, P., Nohawica, M. M., Kotwicka, M., and Jankun, J. (2015). Enamel Matrix Proteins Exhibit Growth Factor Activity: A Review of Evidence at the Cellular and Molecular Levels. *Exp. Ther. Med.* 9 (6), 2025–2033. doi:10.3892/etm.2015.2414
- Yamada, M., and Egusa, H. (2018). Current Bone Substitutes for Implant Dentistry. *J. Prosthodontic Res.* 62 (2), 152–161. doi:10.1016/j.jpor.2017.08.010
- Yeung, T., Georges, P. C., Flanagan, L. A., Marg, B., Ortiz, M., Funaki, M., et al. (2005). Effects of Substrate Stiffness on Cell Morphology, Cytoskeletal Structure, and Adhesion. *Cell Motil. Cytoskeleton* 60 (1), 24–34. doi:10.1002/cm.20041
- Zhang, D., Wu, X., Chen, J., and Lin, K. (2018). The Development of Collagen Based Composite Scaffolds for Bone Regeneration. *Bioactive Mater.* 3 (1), 129–138. doi:10.1016/j.bioactmat.2017.08.004
- Zhao, M., Berry, J. E., and Somerman, M. J. (2003). Bone Morphogenetic Protein-2 Inhibits Differentiation and Mineralization of Cementoblasts *In Vitro*. *J. Dent Res.* 82 (1), 23–27. doi:10.1177/154405910308200106
- Zubery, Y., Goldlust, A., Alves, A., and Nir, E. (2007). Ossification of a Novel Cross-Linked Porcine Collagen Barrier in Guided Bone Regeneration in Dogs. *J. Periodontol.* 78 (1), 112–121. doi:10.1902/jop.2007.060055
- Zubery, Y., Nir, E., and Goldlust, A. (2008). Ossification of a Collagen Membrane Cross-Linked by Sugar: a Human Case Series. *J. Periodontol.* 79 (6), 1101–1107. doi:10.1902/jop.2008.070421

Conflict of Interest: The authors declare that the research was conducted in the absence of any commercial or financial relationships that could be construed as a potential conflict of interest.

The handling editor declared a past co-authorship with one of the authors AS.

Copyright © 2021 Lin, Nica, Sculean and Asparuhova. This is an open-access article distributed under the terms of the Creative Commons Attribution License (CC BY). The use, distribution or reproduction in other forums is permitted, provided the original author(s) and the copyright owner(s) are credited and that the original publication in this journal is cited, in accordance with accepted academic practice. No use, distribution or reproduction is permitted which does not comply with these terms.



Regenerative Medicine Technologies to Treat Dental, Oral, and Craniofacial Defects

Jessica M. Latimer¹, Shogo Maekawa^{1,2}, Yao Yao^{3,4}, David T. Wu^{1,5,6}, Michael Chen¹ and William V. Giannobile^{1*}

¹ Department of Oral Medicine, Infection, and Immunity, Harvard School of Dental Medicine, Boston, MA, United States,

² Department of Periodontology, Graduate School of Medical and Dental Sciences, Tokyo Medical and Dental University,

Tokyo, Japan, ³ Department of Periodontics & Oral Medicine, University of Michigan School of Dentistry, Ann Arbor, MI,

United States, ⁴ Biointerfaces Institute, University of Michigan, Ann Arbor, MI, United States, ⁵ Laboratory for Cell and Tissue

Engineering, Harvard John A. Paulson School of Engineering and Applied Sciences, Boston, MA, United States, ⁶ Wyss

Institute for Biologically Inspired Engineering, Harvard University, Boston, MA, United States

OPEN ACCESS

Edited by:

Barbara Zavan,
University of Padua, Italy

Reviewed by:

Vamsi Yadavalli,
Virginia Commonwealth University,
United States
Shinn-Jyh Ding,
Chung Shan Medical University,
Taiwan

*Correspondence:

William V. Giannobile
William_Giannobile@hsdm.harvard.edu

Specialty section:

This article was submitted to
Tissue Engineering and Regenerative
Medicine,
a section of the journal
Frontiers in Bioengineering and
Biotechnology

Received: 01 May 2021

Accepted: 29 June 2021

Published: 06 August 2021

Citation:

Latimer JM, Maekawa S, Yao Y,
Wu DT, Chen M and Giannobile WV
(2021) Regenerative Medicine
Technologies to Treat Dental, Oral,
and Craniofacial Defects.
Front. Bioeng. Biotechnol. 9:704048.
doi: 10.3389/fbioe.2021.704048

Additive manufacturing (AM) is the automated production of three-dimensional (3D) structures through successive layer-by-layer deposition of materials directed by computer-aided-design (CAD) software. While current clinical procedures that aim to reconstruct hard and soft tissue defects resulting from periodontal disease, congenital or acquired pathology, and maxillofacial trauma often utilize mass-produced biomaterials created for a variety of surgical indications, AM represents a paradigm shift in manufacturing at the individual patient level. Computer-aided systems employ algorithms to design customized, image-based scaffolds with high external shape complexity and spatial patterning of internal architecture guided by topology optimization. 3D bioprinting and surface modification techniques further enhance scaffold functionalization and osteogenic potential through the incorporation of viable cells, bioactive molecules, biomimetic materials and vectors for transgene expression within the layered architecture. These computational design features enable fabrication of tissue engineering constructs with highly tailored mechanical, structural, and biochemical properties for bone. This review examines key properties of scaffold design, bioresorbable bone scaffolds produced by AM processes, and clinical applications of these regenerative technologies. AM is transforming the field of personalized dental medicine and has great potential to improve regenerative outcomes in patient care.

Keywords: bone regeneration, 3D printing, biocompatibility, regenerative medicine, tissue engineering, periodontal diseases/therapy, bioresorbable scaffolds

INTRODUCTION – REGENERATIVE MEDICINE IN DENTISTRY

Etiology of Dental and Craniomaxillofacial Bone Deformities

Hard tissue deficiencies in the maxillofacial region are the result of numerous diseases, disorder and injuries, and appropriate rehabilitative therapies are necessary to restore quality-of-life for affected individuals. The Global Burden of Diseases, Injuries, and Risk Factors Study 2017 (GBD 2017) revealed that oral disorders had the greatest age-standardized prevalence and incidence in the world

(Spencer et al., 2018). Periodontal disease is a significant contributor to oral disease burden; in 2017, the reported global prevalence was 796 million and the percentage change in age-standardized rates for this high impact disease has continued to increase (Spencer et al., 2018). Periodontitis is a chronic, multifactorial inflammatory disease associated with host-microbiome dysbiosis (Papapanou et al., 2018). The disease pathogenesis involves a complex, immunoinflammatory response, modulated by individual microbial, environmental, and genetic factors (Kornman, 2008). Further, periodontal disease is strongly interrelated with overall health, as evidenced by the vast number of oral manifestations in systemic diseases (Kornman et al., 2017; Albandar et al., 2018). Consequences of periodontitis include progressive deterioration of the periodontal attachment apparatus and alveolar bone, ultimately resulting in tooth loss and oral dysfunction (Page and Kornman, 1997; Pihlstrom et al., 2005). The disease may be further characterized by continuous progression, intermittent periods of disease activity (Goodson et al., 1982), or an “asynchronous multiple burst” model (Socransky et al., 1984), to which older adults are more susceptible (Page and Kornman, 1997; Marcenes et al., 2013).

Similar to trends for periodontal disease, incidence rates for cancers of the lip and oral cavity are also increasing (Spencer et al., 2018). Squamous cell carcinoma (SCC) is the leading form of head and neck cancer and the recent surge in prevalence is primarily attributed to oncogenic types of human papillomavirus (HPV) infection (Gillison et al., 2015; Menezes et al., 2021). High level evidence implicates HPV in a quarter of oral cavity cancers and well over half of cases in the oropharynx (Abogunrin et al., 2014; Rodrigo et al., 2014). Malignant tumors involving the oral cavity are often treated by surgical resection, accompanied by other treatment modalities such as radiotherapy, chemotherapy, or immunotherapy. Remission may be attained at the expense of a substantial loss of tissue and large residual bone defects in the maxillofacial region (Muzaffar et al., 2021). Another common cause of hard tissue deficiencies include craniomaxillofacial trauma resulting from motor vehicular collisions, falls, and other accidents (Manodh et al., 2016). According to the GBD 2017, head injuries had a global prevalence and incidence of 47 and 21.6 million, respectively (Spencer et al., 2018). Ultimately, craniomaxillofacial bone defects have a wide range of etiologies including infection, periodontal disease, oral cancer, tooth extraction or tooth loss, and trauma (Bodic et al., 2005). These bone deficiencies can detrimentally affect facial esthetics and important oral functions such as mastication, speech, and nutrition, thereby significantly impairing patient quality-of-life.

Clinical Treatment of Periodontal Defects

The regeneration of periodontal defects in humans is case-sensitive due to the involvement of multiple tissue types and variability in defect morphology (Kao et al., 2015; Yu et al., 2019). For instance, a single defect in the periodontium may consist of all four of its major anatomical components: the gingiva, cementum, periodontal ligament (PDL), and alveolar bone (Smith et al., 2015). The regeneration of these tissues

and their unique interfaces is necessary to restore full function as a supportive structure for the teeth (Melcher, 1976). Generally, vertical intrabony defects progress more rapidly than horizontal defects and are at an increased risk for tooth loss (Papapanou and Wennstrom, 1991). Moreover, a residual probing pocket depth (PPD) ≥ 7 mm after periodontal treatment represents risk for tooth loss at a 64.2 odds ratio compared to a PPD of ≤ 3 mm (Matuliene et al., 2008). In turn, tooth loss initiates anatomic remodeling processes which precede the formation of localized deficiencies in alveolar bone (Araujo et al., 2005). Considering the dramatic decrease in prognosis associated with defect progression and imminent ridge resorption after tooth loss, periodontal defects require timely intervention in order to maintain teeth and their associated bone volume.

The prognosis of regenerative periodontal therapy is dictated by the defect morphology, which primarily considers the number of remaining bone walls and the defect angle (Klein et al., 2001; Reynolds et al., 2015). 3-wall intrabony defects and class II furcations are well-contained spaces that offer the most predictable indications for periodontal regeneration. Defects with fewer bony walls or wider angles tend to be more difficult to treat and the results are often unpredictable (Klein et al., 2001; Reynolds et al., 2015). Other factors that decrease prognosis include an unfavorable vertical sub-classification of furcation involvement, root proximity and root concavities (Aichelmann-Reidy et al., 2015; Tonetti et al., 2017). Following complete debridement to reduce bacterial load and remove granulomatous tissue, periodontal regeneration can be achieved with or without biologics. In dental regenerative medicine, the most commonly used biologics are enamel matrix derivative (EMD) (Hammarstrom et al., 1997; Tsai et al., 2020) and recombinant human platelet-derived growth factor (rhPDGF-BB) (Nevins et al., 2003). rhPDGF-BB has demonstrated acceleration of clinical attachment level (CAL) gain and improved bone fill in the reconstruction of periodontal defects (Nevins et al., 2005; Nevins et al., 2013; Tavelli et al., 2021b). Recently, the second-generation platelet concentrate, platelet-rich fibrin (PRF), has attracted widespread attention for its regenerative potential in soft tissues, however, influence on bone healing and periodontal regeneration is not well established (Tsai et al., 2020). Also of note, clinical trials using fibroblast growth factor-2 (FGF2) have demonstrated promising results for the regeneration of periodontal defects (Cochran et al., 2016; Kitamura et al., 2016) and this biologic currently has approval for use in Japan.

The key elements of periodontal regeneration are cells, scaffolds, growth factors, and blood supply (Larsson et al., 2016). Improved knowledge of how these components interact to promote periodontal tissue formation (**Figure 1**), accompanied by the advancement of microsurgical techniques and modern biomaterials, has led to the development of minimally invasive treatment approaches with improved clinical outcomes (Cortellini and Tonetti, 2011; Cortellini, 2012; Schincaglia et al., 2015; Moreno Rodriguez et al., 2019; Aslan et al., 2020; Barbato et al., 2020). While clinical standards for regeneration are usually well-achieved, true, histologic periodontal regeneration,

involving formation of new cementum, PDL, and alveolar bone, remains elusive and instead, periodontal repair is often observed (Sculean et al., 2008). Animal studies have revealed that conventional guided tissue regeneration (GTR) results in long junctional epithelium and connective tissue (Sculean et al., 2015a), rather than an anatomic, periodontal attachment apparatus. In humans, EMD application paired with the coronally advanced flap (CAF) technique promoted new bone and cementum formation in the apical region of Miller class I and II (Miller, 1985) gingival recession defects (McGuire et al., 2016). Overall, periodontal regeneration requires technical surgeries and judicious, decision-making strategies to adapt a broad range of biomaterials, either in combination or alone, to achieve desired biologic and clinical results (Tavelli et al., 2020).

Clinical Approaches in the Treatment of Alveolar Ridge Deficiencies

Dental implant therapy is often the treatment of choice to replace missing teeth, offering patients high satisfaction and improved oral health-related quality-of-life following treatment (Feine et al., 2018). The suitability of an edentulous site for implant placement is contingent on a sufficient, available bone volume (Avila-Ortiz et al., 2014). With advanced computer-aided design (CAD), virtual planning of the restorative position can accurately guide preoperative assessments of the residual ridge. Alveolar ridge augmentation with hard and soft tissue is frequently required to support a functional and esthetic result. In larger defects, guided bone regeneration (GBR) using barrier membranes and bone grafts may be performed, followed by implant placement and peri-implant soft tissue phenotype modification, if indicated (Tavelli et al., 2021a). Mounting evidence supports the augmentation of the peri-implant soft tissue volume and keratinized mucosa width to promote peri-implant health and stability of the marginal bone level (Giannobile et al., 2018; Longoni et al., 2019; Tavelli et al., 2021a). Autologous grafts remain the most effective treatment for soft tissue augmentation (Zucchelli et al., 2020). However, xenografts may offer similar clinical results with improved patient-reported outcomes in terms of pain and satisfaction (McGuire et al., 2020). With regards to hard tissue augmentation, autogenous bone grafts impart osteogenic influence and are often considered as the “Gold Standard” for regeneration (Al-Moraissi et al., 2020). Their disadvantage is that large quantities of graft material necessitate a secondary surgical site, such as the mandibular ramus or symphysis, in which donor-site morbidity and limited available bone volume for harvest are important considerations (Sculean et al., 2015b). As GBR requires substantial amounts of bone graft material compared to periodontal defects, a mixture of autograft and xenograft is commonly used (Urban et al., 2011, 2013).

Alveolar ridge deficiencies are categorized by their severity and defect type, generally described as horizontal, vertical, or combined (Seibert, 1983; Allen et al., 1985; Seibert and Salama, 1996; Wang and Al-Shammari, 2002). More severe and combined defects may require multiple surgical procedures

for augmentation and are difficult to regenerate. Reported survival rates of dental implants placed in resultant bone from GBR procedures is comparable to rates in native bone (Jensen and Terheyden, 2009; Clementini et al., 2012). According to a recent systematic review, weighted means of clinical vertical bone gain were 8.04 mm for distraction osteogenesis, 4.18 mm for GBR, and 3.46 mm for bone block grafts, and post-operative complication rates were 47.3, 12.1, and 23.9%, respectively (Urban et al., 2019). GBR is technique-sensitive as surgical success relies upon adequate flap release to achieve primary closure and proper membrane application to prevent ingrowth of connective tissues into the bone compartment (Eskan et al., 2017; Soldatos et al., 2017). Non-resorbable membrane exposure, which is the predominant post-operative complication, occurs at rates of 13.8% in horizontal augmentation and 18% in vertical augmentation (Jensen and Terheyden, 2009). The development of dense, polytetrafluoroethylene (PTFE) membranes has enabled ridge preservation without primary closure, facilitating comparable results to GBR using e-PTFE membranes while reducing complications (Urban et al., 2019).

Current Research Gaps

The clinical limitations, implications of invasive reconstructive surgical procedures, and prognostic uncertainty are current challenges in regenerative dental medicine. Clinical scenarios in which predictable treatments have yet to be achieved include ridge defects with severe horizontal or vertical components of alveolar bone loss, class III furcations, papilla deficiencies, and advanced peri-implant defects (McGuire and Scheyer, 2007; Reynolds et al., 2015; Monje et al., 2019). Additionally, few clinical strategies emphasize bone regeneration in the craniofacial complex. Defects in the calvaria, facial bones, and temporomandibular joint (TMJ) are often reconstructed with customized metal plates and implants with varying degrees of success. However, anatomic regeneration of functional craniomaxillofacial bone structures has yet to be achieved (Zhang and Yelick, 2018). Current regenerative biomaterials for bone commonly present issues related to early resorption or persistence, and limited capacity to reconstruct large or uncontained defects (Giannobile et al., 2019; Tao et al., 2019). Since 2000, regenerative medicine research, mainly in the field of bioengineering, has made significant progress. A broad range of research has been conducted using stem cells (Kaigler et al., 2013, 2015; Iwata et al., 2018; Xuan et al., 2018; Park J. Y. et al., 2020; Sanchez et al., 2020), gene delivery (Jin et al., 2003; Dunn et al., 2005; Chang et al., 2009, 2010; Sugano et al., 2014; Zhang Y. et al., 2015), surface modification with microstructures (Pilipchuk et al., 2016; Zhang Z. et al., 2016; Pilipchuk et al., 2018), three-dimensional (3D) bioprinting (Rasperini et al., 2015; Raveendran et al., 2019), and whole tooth regeneration (Kim et al., 2010; Oshima et al., 2011, 2017; Oshima and Tsuji, 2015). Additionally, clinical trials of microstructure-applied scaffolds (Rasperini et al., 2015; Raveendran et al., 2019) and PDL-derived cell sheets or PDL-derived mesenchymal stem cells (MSCs) have been conducted in humans (Iwata et al., 2018; Sanchez et al., 2020). The

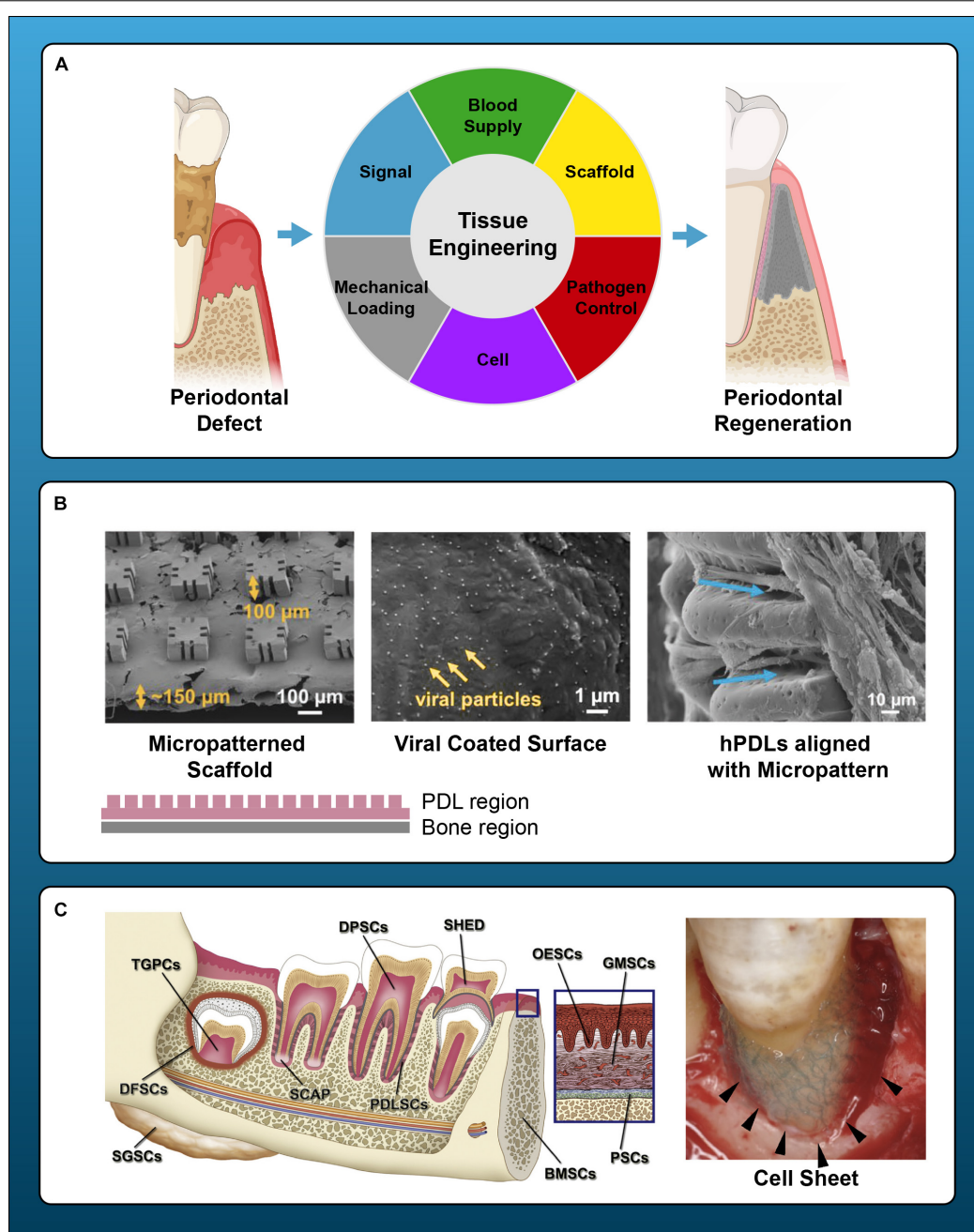


FIGURE 1 | Principles and current endeavors for periodontal regeneration with tissue bioengineering. **(A)** Key components of periodontal regeneration with tissue engineering. Cells, growth factors, scaffold, mechanical loading, pathogen control, and ideal blood supply are the key for periodontal regeneration. **(B)** Examples of micropatterned scaffold, which enhances the orientation of fiber in periodontal regeneration. Left panel: SEM image of a micropatterned scaffold with grooves. Center: Viral Gene delivery (Ad-BMP-7) with chemical vapor deposition. Right: human PDL cells aligned along with the grooves of micropattern. **(C)** Left: prospective sources of stem cells in dental and maxillofacial region. BMSCs, bone marrow-derived mesenchymal stem cells from orofacial bone; DPSCs, dental pulp stem cells; SHED, stem cells from human exfoliated deciduous teeth; PDLSCs, periodontal ligament stem cells; DFSCs, dental follicle stem cells; TGPCs, tooth germ progenitor cells; SCAP, stem cells from the apical papilla; OESCs, oral epithelial progenitor/stem cells; GMSCs, gingiva-derived MSCs; PSCs, periosteum-derived stem cells; SGSCs, salivary gland-derived stem cells. Right: autologous PDL-derived a three-layered cell sheet with woven PGA. Adapted with permission from Egusa et al. (2012), Iwata et al. (2018), Pilipchuk et al. (2018), and Yu et al. (2019).

clinical regeneration of oral, dental, and craniofacial structures has advanced tremendously in recent years but there are still considerable needs for improving the customization of scaffolds

to complex architectures to gain more predictable outcomes. Usage of modern scaffold fabrication techniques in coordination with biologic agents and novel cellular and molecular therapies

are expected to develop the next generation of biomaterials in bone tissue engineering.

KEY PROPERTIES OF SCAFFOLD DESIGN

Biomaterial Compatibility With the Manufacturing Process

Material selection is critical in the design of scaffolds produced by additive manufacturing (AM) techniques. Suitable biomaterials must demonstrate process compatibility with the specific AM technique applied, as well as appropriate biochemical and physical characteristics to function successfully *in vivo* (Bourell et al., 2017). Although optimal processing parameters vary between the different forms of AM, typical features of a suitable material include buildability of the incrementally deposited layers, adequate densification after chemical or thermal treatments, and structural tolerance of other post-processing steps (Gu, 2015). Certain combinations of materials and AM processes may not facilitate adequate process accuracy, thus detrimentally affecting the consistency of a scaffold's internal architecture, overall part quality, and reproducibility (Leong et al., 2003). Additionally, techniques involving processing steps that employ high temperatures (Han et al., 2017; Ligon et al., 2017), ultraviolet light irradiation (Bagheri and Jin, 2019), or organic solvents (Mikos and Temenoff, 2000) may preclude the simultaneous incorporation of cells and other biological factors.

AM technology enables scaffold production with a diverse array of materials, including polymers, metals, ceramics, hydrogels, and carbon-based nanomaterials (Guvendiren et al., 2016). Thermoplastic polymers are often used in extrusion-based technologies whereas ceramic, metal, or polymer powders are typically processed at higher temperatures in laser-based methods (Zhang S. et al., 2015; Yang et al., 2019). Recently, biodegradable metal alloys containing magnesium (Mg) or Zinc (Zn) are of increasing interest due to their improved corrosion resistance and biomimicry (Li et al., 2018; Wen et al., 2018; Hernández-Escobar et al., 2019). However, these materials present unique challenges such as high melting points, flammability, and generation of metallic vapors that compromise process stability (Grasso et al., 2018). Numerous synthetic polymers are practical material choices for AM fabrication of biomedical implants due to their high biocompatibility, biodegradability, bioresorption, and processability (Puppi et al., 2010). Polycaprolactone (PCL) is the most commonly used biomaterial in AM due to its excellent mechanical properties, low cost, ease of processability, and low melting point.

While polymers are excellent materials in their ability to accommodate AM processing parameters, singular material groups are limited in their capacity to mutually satisfy requirements for both AM processing and clinical utility in biomedical applications. For instance, polylactides have high tensile strength accompanied by a slow degradation rate, which may persist longer than desirable *in vivo*. In contrast, although polyglycolic acid (PGA) and poly lactic-co glycolic acid (PLGA)

offer superior mechanical properties, they degrade quickly when used as a bioresorbable scaffold and within 2 weeks, their tensile strength is reduced by half (Ikada, 2006). To address this obstacle, ceramics are often combined with polymers to form composite materials with improved mechanical characteristics and biologic properties (Nyberg et al., 2017; Zhang et al., 2018).

Bone itself is a composite tissue by nature, consisting of a mineral phase predominated by nanocrystalline hydroxyapatite (HA) and an organic phase, consisting of extracellular matrix proteins, of which approximately 90% is collagen type 1 (Paschalis et al., 2003). The presence of mineralized collagen fibers affords bone both high elasticity and strength to prevent fracture during weight-bearing activities (Nair et al., 2013). In the periodontium, alveolar bone houses the dentition in fibrous joints classified as gomphoses. The tooth-bone interface is mediated by the PDL, a well-vascularized structure constituted by collagenous sheets of extracellular matrix, extending from alveolar bone and embedding into the root cementum (Naveh et al., 2013). Fibers of the PDL exhibit region-specific orientation that participate in physiologic loading, nutrient transport, and bone remodeling (Connizzo et al., 2021). Due to complex organization and composition required for function, multi-material constructs have superior capability to replicate hybrid tissue structures and promote scaffold performance (Jakus and Shah, 2017; Kim et al., 2018).

Tailored Biomechanical Properties of Materials for Use in Alveolar Bone Reconstruction

By mimicking the physiologic characteristics of native bone, material property tailoring enhances the regenerative capacity of tissue engineered constructs in the presence of biomechanical stresses (Palmer et al., 2008). This is especially relevant for dental applications as the bone that comprises the periodontium and jaws is regularly subject to extrinsic forces (Korioth et al., 1992) that result in a physiologic degree of elastic deformation (Daegling et al., 1992; Korioth and Hannam, 1994). Consequently, alveolar bone is anisotropic in nature, meaning that it demonstrates a non-linear, elastic symmetry (Giesen et al., 2001; Peterson et al., 2006). This regional and directional variation in modulus is imparted by the structural orientation of mineralized collagen fibers and aids proper stress distribution (Lettry et al., 2003; Wang and Ural, 2018). The elastic modulus of trabecular and cortical bone have been reported to be in the ranges of 3.5–125.6 MPa (Misch et al., 1999) and 6.9–16.0 GPa, respectively (Dechow et al., 2010). AM techniques can produce versatile scaffolds with mechanical properties within these physiologic ranges for craniofacial and dentoalveolar reconstruction. This has been demonstrated in degradable polymers, calcium phosphate ceramics, and composite ceramic-polymer scaffolds fabricated with both direct and indirect means of solid free-form fabrication (SFF) (Hollister et al., 2005).

The layered construction process utilized in AM is advantageous for the production of lightweight and porous constructs that can support tissue regeneration in an irregular defect. CAD files can be used to generate scaffold configurations

that accurately replicate the overall defect shape and dimensions. Further, customized 3D surface topology can be generated by using standard triangle language (STL) files to topologically subtract defects from a digital scaffold design (Park et al., 2012). This promotes anatomical scaffold adaptation to the defect boundaries, minimizing dead space and micromotion (Grottkau et al., 2002). An effective scaffold should also provide sufficient rigidity to sustain matrix deposition until newly formed tissue has developed the mechanical integrity to withstand normal load bearing conditions. Resistance to deformation is largely dictated by material selection, degradation rate, internal geometry and porosity. Cell seeding can further reinforce scaffolds through enhanced extracellular matrix production while also compensating for the gradual decline in structural integrity that accompanies degradation (Spalazzi et al., 2006a). Finally, modulus matching of the scaffold material to bone is essential to prevent disadvantageous mechanoregulation of anatomic remodeling (Sandino and Lacroix, 2011), as well as other adverse sequelae, such as scaffold fragmentation and stress shielding. Stress shielding occurs when an implanted substrate has a higher modulus than the surrounding host bone, creating areas of differential strain distribution on the adjacent tissue (Orr et al., 2001) and resulting in a localized decrease in density of the surrounding bone (Spector, 1994; Van Lenthe et al., 1997).

Mechanical cues provided by scaffold materials can regulate the fate of stem and progenitor cells (Vining and Mooney, 2017). In 2D culture, mechanical properties of the extracellular matrix (ECM) such as stiffness dictate the differentiation of MSCs derived from bone marrow or adipose tissues (Engler et al., 2006). In 3D systems, Huebsch et al. (2010) showed that the elasticity of the substrate or matrix appears to direct MSCs differentiation to the cell fate that best matches the elasticity of the native physiological ECM; stiffer matrix (11–30 kPa) stimulates osteogenic differentiation while softer matrix (2.5–5 kPa) promotes adipogenic or neuronal differentiation. Furthermore, variations in matrix stiffness can regulate MSC behaviors such as cell fate and migration (Tse and Engler, 2011). MSCs may be more responsive to a gradient of stiffness established by tunable levels of crosslinking along a spatial axis in a hydrogel scaffold (Sunyer et al., 2016).

Viscoelasticity, a key property of living tissues, is another regulator of MSC behavior. Viscoelastic materials exhibit a combination of storage of elastic energy as a solid, and loss of mechanical energy as a fluid. These materials exhibit stress relaxation and hysteresis in the stress-strain relationship during loading and unloading. When a mechanical load is applied then removed, viscoelastic materials can dissipate energy (Chaudhuri et al., 2020). Chaudhuri et al. (2016) demonstrated that MSC cell fate and activity is regulated by tuning the stress relaxation of the alginate hydrogel scaffold, independently of the hydrogel's initial elastic modulus, degradation and cell-adhesion ligand density. More specifically, MSC cell spreading, proliferation, and osteogenic differentiation, and bone matrix production are enhanced when encapsulated in hydrogels with faster stress relaxation. When implanting alginate hydrogels with tunable stress relaxation to deliver human MSCs into rodent calvaria defects, animals receiving fast-relaxing hydrogels

showed significantly enhanced new bone growth, extensive matrix remodeling and hydrogel disappearance compared to the group that received slow relaxing, stiffness-matched hydrogels (Darnell et al., 2017).

Mechanistically, the effect of scaffold mechanics is mediated by adhesion-ligand binding via integrin, actin-myosin contractility and activation of mechanosensing and mechanotransduction pathways. For instance, matrix elasticity directed stem cell lineage specification is non-muscle myosin II dependent (Engler et al., 2006). In addition, when stiffness matched, stress relaxation led to increased nuclear translocation of the YAP transcription factor, a key transcription factor mediating mechanotransduction (Chaudhuri et al., 2016). In tissue engineering and regenerative medicine, synthetic matrices with defined mechanical and biophysical properties are useful to guide stem cells *ex vivo* prior to transplantation, and to tune stem cell behavior *in vivo* following transplantation in order to improve their regenerative capacity (Huebsch et al., 2015; Darnell et al., 2017; Vining and Mooney, 2017).

Architectural and Topographical Determinants of Cell-Scaffold Interactions

AM can be used to produce sophisticated scaffolds with optimized macroscale architecture, internal geometry, and topographical features that enhance the requisite cellular processes for new tissue formation (Figure 2). The precise control of scaffold design afforded by AM techniques is a valuable feature for dental and craniofacial bone applications, as defects in these regions often involve multiple tissues that require complex spatiotemporal regulation for development (Lee et al., 2016). This presents the unique challenge of guiding the differentiation and maintenance of multiple, cellular phenotypes, as well as achieving synthesis of distinct but continuous tissues in a single construct. Triphasic scaffolds consisting of stratified compartments with unique material compositions mimic the organization of native tissues and enable tri-culture of chondrocytes, fibroblasts, and osteoblasts (Spalazzi et al., 2006b). This scaffold architecture efficaciously mediates phase-specific cellular proliferation and phenotypic matrix production (Spalazzi et al., 2006a, 2008).

Modern AM techniques have driven the evolution of hybrid scaffold systems designed for the regeneration of fibrous articulations within the craniofacial complex (Vaquette et al., 2018). 3D printed wax molds have been used to indirectly fabricate polymeric scaffolds with fiber-guiding microchannels to align fibroblasts and their subsequent connective tissue formation in a novel tooth to PDL interface (Park et al., 2010). Fused deposition modeling (FDM) and electrospinning techniques have been combined to produce biphasic periodontal scaffolds with well-integrated compartments for PDL and bone (Vaquette et al., 2012; Costa et al., 2014). Electrospinning methods have also produced functionally graded scaffolds with seamless transition zones (Eriskien et al., 2008) and gradients in scaffold features such as pore size (Abbasi et al., 2019; Zhou et al., 2020).

It has been well established that pore characteristics mediate important cell-scaffold interactions that dictate cell morphology,

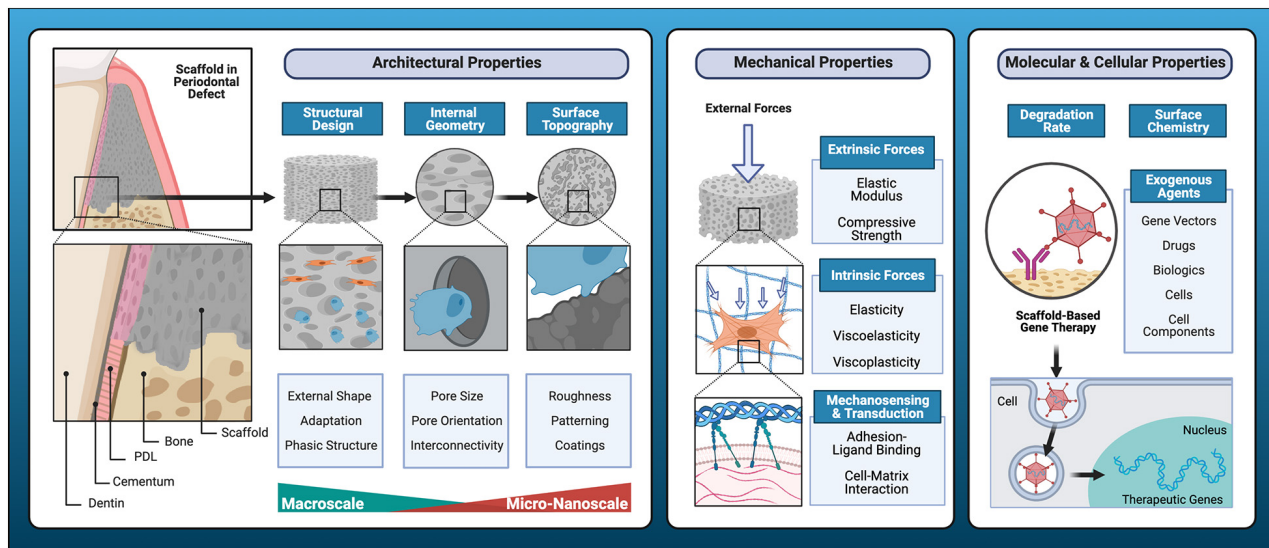


FIGURE 2 | Key determinants of cell-scaffold interactions. Resorbable scaffolds for the regeneration of functional dental, oral, and craniofacial tissues require tailored, biomimetic features that consider structural design, internal geometry, and surface topography to promote cell-scaffold interactions. Additive manufacturing facilitates optimization of physical properties of scaffold substrates to promote overall mechanical performance and fine tune biomechanical regulation of cell behavior. Intrinsic material properties such as degradation rate and surface chemistry are key biochemical considerations, and various exogenous agents with bioactive properties may be incorporated for scaffold functionalization to further enhance regenerative outcomes.

phenotype maintenance, and biosynthetic activity (Nehrer et al., 1997). The recommended pore size for bone scaffolds ranges from 300 to 800 μm (Ishaug et al., 1997; Tsuruga et al., 1997), with the optimal size depending on the selected biomaterial composition and intended regional application of the scaffold. Larger pores are thought to facilitate vascularization, oxygenation, and direct osteogenesis while smaller pores may favor osteochondral ossification (Karageorgiou and Kaplan, 2005). Although the significance of pore size within this range may be minimal (Roosa et al., 2010), it is universally acknowledged that pores less than 100 μm in size prevent cellular infiltration and result in the formation of undesirable, non-mineralized osteoid or fibrous tissue (Hulbert et al., 1970). Further, small pores <125 μm in diameter prevent differentiation of MSCs (Swanson et al., 2021). As long as the selected pore size permits adequate cell migration for tissue ingrowth and osteogenic cell phenotypes, other features affecting fluid conductance (Hui et al., 1996), such as pore interconnectivity and orientation may be of greater influence. While conventional, porogen-leached scaffolds exhibit variable microarchitecture consisting of random interconnections, indirect SFF allows for controlled introduction of porosity, pore interconnectivity, and surface topography at the microscale (Taboas et al., 2003), resulting in superior distribution and quality of mineralized tissue formation *in vivo* (Park et al., 2012, 2014).

With increasingly advanced AM processes, high resolution features can be incorporated into the internal microarchitecture of a scaffold. Modern image rendering technology can develop biomimetic surface topographies that positively influence osteoblast behavior and local production of osteogenic factors such as osteocalcin (OCN), vascular endothelial growth factor

(VEGF), osteoprotegerin (OPG), and bone morphogenetic protein (BMP)-2 (Cheng et al., 2016). Computer-directed deposition can produce micropores with customized orientation and interconnecting channels (Lim et al., 2010; Park et al., 2017). These features improve nutrient and oxygen diffusion throughout larger defect volumes and may also play a role in cell-cell communication. Microscale features such as patterning and surface roughness further enhance cell migration, adhesion, proliferation, and osteogenic differentiation (Zhu et al., 2020). This topographical influence on cell response is derived from effects on surface energy and protein adsorption, interactions that are recapitulated on the submicron (Wang et al., 2015) and nanoscales (Khang et al., 2012). Additionally, nanotopographical features can upregulate expression of genes known to be important for osteoblast adhesion, such as intercellular adhesion molecule 1 (ICAM1), integrin αM (ITGAM), integrin α1 (ITGA1) (Dalby et al., 2007), integrin α5 (ITGA5) and integrin β1 (ITGB1) (Liu et al., 2017).

Scaffold Functionalization With Bioactive Molecules

Regenerative medicine is based upon the manipulation of known physiologic processes to create a microenvironment that simulates a desired stage of tissue development, thus inducing tissue formation and renewal. Not only must tissue dynamics be replicated at a macroscopic organ or tissue scale, but on the cellular and molecular levels as well. Scaffolds primarily serve to provide an osteoconductive matrix and benefit from the addition of growth factors that exert osteoinductive influence on cellular activity. Biologics such as recombinant

human BMP-2 and BMP-7, growth differential factor-5 (GDF-5), EMD, and rhPDGF-BB, have all been well-studied for their capacities to promote osteogenic differentiation and enhance bone formation in regenerative dental medicine (Suárez-López Del Amo et al., 2015). Growth factor delivery strategies frequently take advantage of bioresorbable, polymer-based scaffolds as a carrier (Schliephake, 2010). The simplest method is scaffold immersion in a growth factor solution. However, drawbacks of physical adsorption include an initial burst release in the first 24 h followed by rapid attenuation (Caballé-Serrano et al., 2019). Post-processing, polyelectrolyte nanolayer coatings can deliver physiologically relevant quantities of active biologics with tunable release, however, this modification reduces pore area (Wei et al., 2007; Jin et al., 2008; Shah et al., 2014). Common strategies to simultaneously incorporate growth factors during the AM process include physical entrapment, which involves direct-loading of growth factor solution into structural reservoirs with a multi-head deposition system, or pre-loading, using a growth factor loaded paste as raw material in extrusion-based printing. In a study that compared these approaches, direct-loading exhibited similar issues to adsorption, in that it had diminished capability for sustained growth factor release (Huang et al., 2018).

Limitations in conventional growth factor delivery may be mitigated by the use of gene-activated scaffolds, in which a scaffold is utilized as a gene delivery device to facilitate controlled gene transduction upon implantation (Fang et al., 1996; Jin et al., 2004). Common methods of vector-based gene delivery may utilize peptides, viruses (adenovirus, baculovirus, or lentivirus), or non-viral vectors to deliver genes that induce expression of growth factors (Yan et al., 2019). Gene therapy has been further enhanced with treatments such as chemical vapor deposition (CVD) polymerization (Lahann et al., 2001), in which antibodies conjugated to adenoviral vectors for transgene expression (Hao et al., 2016) are immobilized onto a scaffold surface. This delivery mechanism allows for multi-growth factor gene expression to promote regenerative activities in target cells, as previously demonstrated with rhPDGF-BB and BMP-7 in human PDL fibroblasts (Hao et al., 2016). The same CVD-mediated, adenoviral vector treatment using adPDGF-BB and adBMP-7 was assessed in micropatterned, biphasic PLGA/PCL scaffolds implanted into alveolar bone defects *in vivo* (Pilipchuk et al., 2018). The results confirmed the ability to control the localization of multiple growth factors within a single scaffold construct to improve the formation and quality of regenerated periodontal tissues. Gene expression may be further altered by leveraging the epigenetic capabilities of microRNA (miRNA). MiRNA are small non-coding RNAs that regulate post-transcriptional modifications of a target messenger RNA and can inhibit translation of multiple genes by sequence-pairing homology (Larsson et al., 2015). Epigenetic functionalization of scaffolds to impart anti-inflammatory, immunomodulatory, or osteogenic influence may be achieved through incorporation of miRNA-transfected cells or direct loading of miRNA into the biomaterials (Asa'ad et al., 2020).

Finally, AM offers great capability to produce bioresorbable, scaffold-based drug delivery systems, incorporating

pharmacologic agents that confer antimicrobial properties or other therapeutic effects. New bone formation occurs slowly over a period of several months and the scaffold material must persist for a relatively long duration of time. Biofilm colonization, localized tissue infection, and chronic inflammatory processes pose serious risks to the final regenerative outcome. Scaffolds produced by AM processes may address these concerns through the addition of antibiotics and corticosteroids, while enhancing the regenerative outcome. A 0.5 mg/ml concentration of doxycycline has been demonstrated to promote osteoblast differentiation *in vitro* (Almazin et al., 2009) and other research has identified anti-osteoclastic (Bettany et al., 2000) and anti-collagenase (Holmes et al., 2004) activity. It should be noted that pre-loading methods involving high temperatures can significantly reduce the efficacy of specific types of antibiotic compounds (Shim et al., 2015). Additionally, controlled release is essential, otherwise excessive dosages of antibiotics will confer cytotoxic effects on osteogenic cell populations (Feng et al., 2010; Park, 2011). Use of nanocoatings or nanofiber delivery mechanisms (Han et al., 2017; Li Z. et al., 2020) to convey antimicrobial properties should be further explored (Kumar et al., 2020). Scaffold modifications with anti-fouling, zwitterionic polymer coatings (Chen et al., 2019) and antimicrobial peptides (Liang et al., 2021) represent promising alternative strategies to discourage biofilm formation or microbial infections.

ADDITIVE MANUFACTURING FOR BONE TISSUE ENGINEERING

Paradigm Shift in Scaffold Production for Regenerative Medicine

AM is a layer-by-layer construction process used to create 3D constructs with CAD and computer-aided manufacturing (CAM) technology. It is often used interchangeably with SFF, which also implies the use of a fixture-less platform without part-specific tooling or human intervention, or rapid prototyping (RP), often used in contexts that describe fast fabrication of scale models or parts. AM processes first emerged in the 1980's and have rapidly evolved to become a powerful tool for biomedical scaffold design, capturing particular interest from the research community in bone tissue engineering. Research involving bone-related applications account for approximately 20% of the existing publications in searches for articles with the terms "additive manufacturing" and "3D printing."

AM fabrication of personalized biomedical constructs begins with the acquisition of high resolution, 3D datasets, typically with computed tomography (CT) or magnetic resonance imaging (MRI), from an individual patient. The images are then converted to a common medical file format referred to as digital imaging and communication in medicine (DICOM). The DICOM file is then imported into a software package that performs segmentation to produce serial sectional data (slices) and reconstruction of a volumetric model composed of voxels. A voxel is a single unit of volume within a 3D grid as opposed to

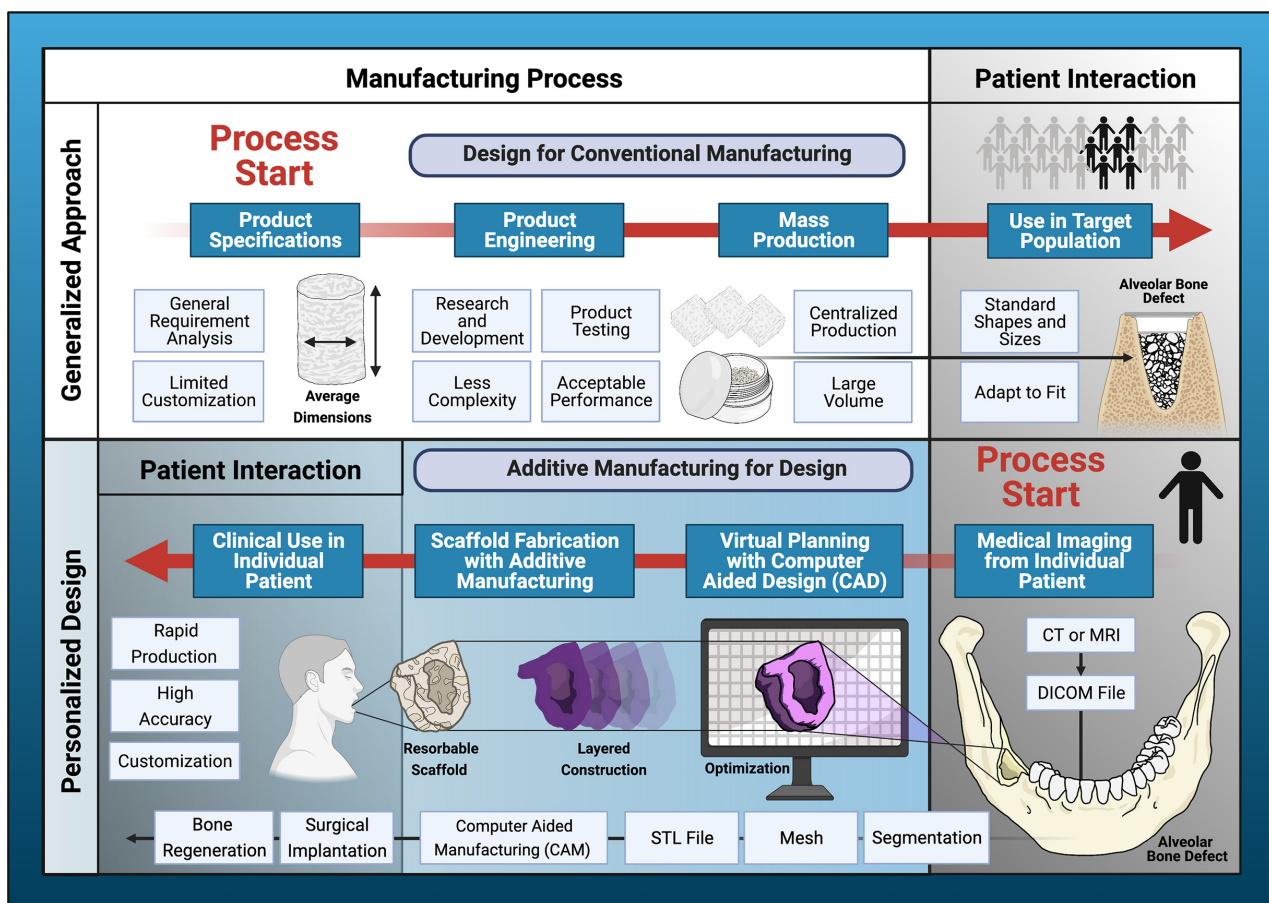
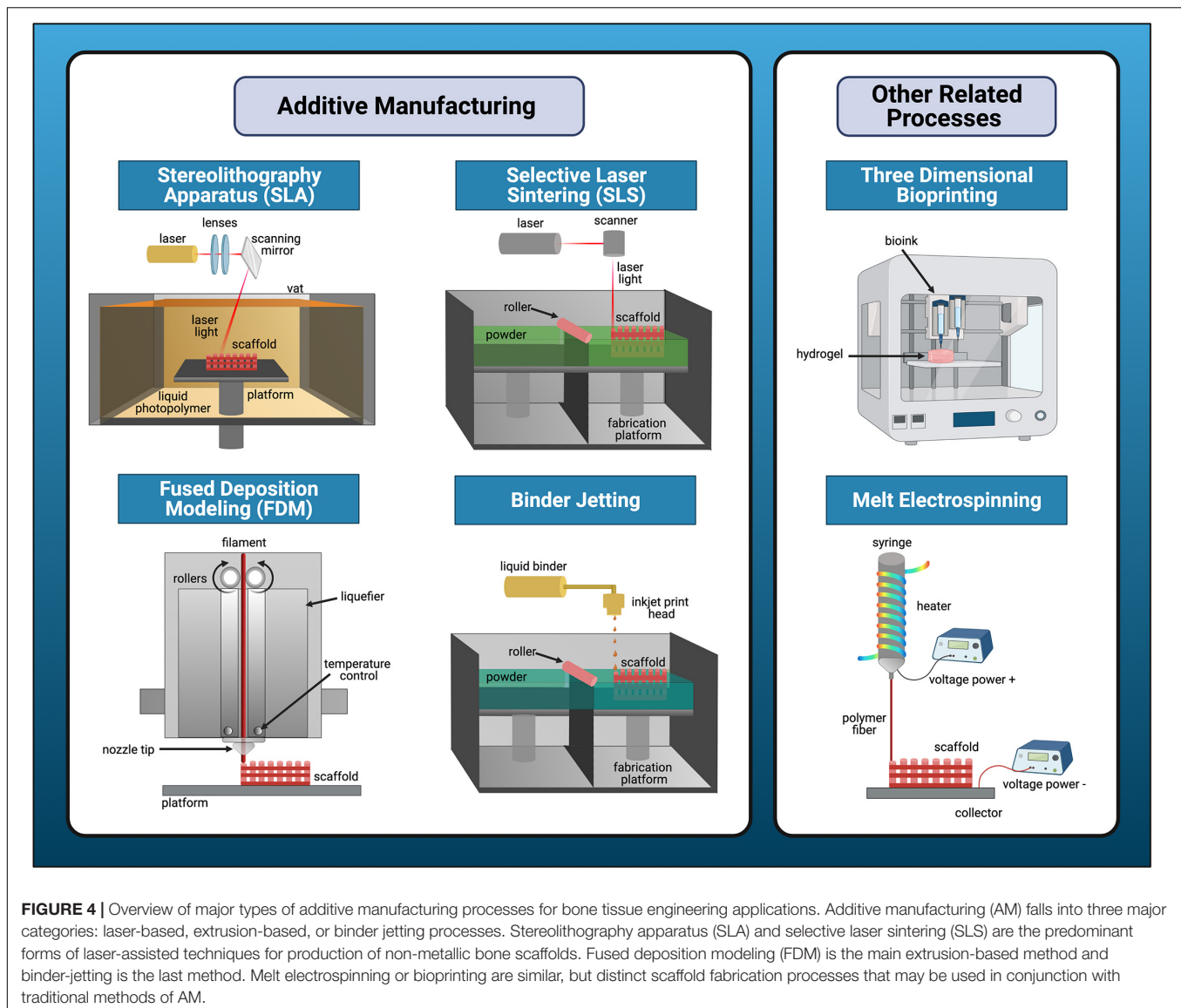


FIGURE 3 | Paradigm shift in scaffold production. Additive manufacturing has introduced a departure from design for conventional manufacturing processes to additive manufacturing driven by design for the individual patient. The generalized design approach utilizes traditional product specification and engineering processes to facilitate large-scale production for distribution to a target population. Disadvantages of conventional manufacturing include limited capacity for complex designs and less customization. Additive manufacturing (AM) utilizes individual patient data processed by computer-aided design (CAD)/computer-aided manufacturing (CAM) software to perform virtual planning, design optimization, and fabrication of highly personalized scaffolds for bone regeneration. This design process begins and ends with direct patient interaction. AM has enormous potential to improve accessibility to personalized regenerative medicine in everyday clinical dentistry.

a 2D pixel. A density threshold is then established and the signal intensity of point data is used to determine which points will be included. Surface polygons are then extracted to reconstruct a tessellated, polyhedral model, also known as a mesh which can be exported as an STL file. Surface refinement is performed with algorithms such as non-uniform rational B-spline (NURBS) functions; this can occur either before the creation of the STL-triangulated surface, known as reverse modeling or after, which is the STL-triangulated model converting approach (Sun et al., 2005). With these steps, a CAD-based solid model is available for further optimization and digital manipulation.

Dentistry is a field that has embraced AM techniques and frequently uses commercially available equipment to fabricate patient-specific constructs in everyday practice. AM is considered a technologic hallmark of the 4th industrial revolution and has resulted in a paradigm shift from design for manufacturing to manufacturing for design (Figure 3). In the

next decade, AM is expected to drastically reduce the utilization of conventional manufacturing techniques and consequently transform employment dynamics in numerous industries (Pérez-Pérez et al., 2018). AM will give rise to new fields and technical occupations, as it has already done with the advent of computer-aided tissue engineering (Sun et al., 2005), and eliminate tasks that can be performed by automated processes. The future of clinical regenerative procedures will possibly involve biomedical laboratories staffed with bioengineers and computer technicians dedicated to the fabrication of personalized bone scaffolds, similar to the current scenario in which dental laboratories produce customized prosthetic components like dentures and crowns. While ongoing research has yet to produce a reliable AM protocol to create custom, bioresorbable scaffolds for bone reconstruction, this pending scientific development signifies untapped potential for unprecedented regenerative outcomes, as well as commercialization and economic growth.



Types of Additive Manufacturing

Depending on the specific tissue and critical defect size, there are numerous options for AM regenerative scaffolds in the oral and craniofacial arena. The predominant methods for non-metallic bone scaffold production can be categorized broadly into extrusion-based, laser-assisted, or binder jetting type processes (Figure 4). The details regarding the primary compatible materials and specific advantages and disadvantages of each AM technique is summarized in Table 1. The main extrusion-based method for non-metallic scaffold production is FDM. First developed in 1988, FDM is commonly used in the oral and craniofacial regeneration research areas. Materials are extruded as a filament through an output (nozzle or syringe) that is directed by CAD files obtained via radiology or similar imaging techniques (Mota et al., 2015). FDM's main advantages include greater mechanical strengths and simpler processes relative to other AM techniques. When considering some of the

complex oral internal structures, such as the intricate geometry of the periodontal ligament, the lack of resolution needed to create detailed features via FDM is a disadvantage when compared to other AM techniques (George et al., 2017). FDM enables high production rate at a low cost, which has positive implications for FDM's ability to be used widely in the clinical setting. Additionally, FDM may be used in conjunction with other scaffold fabrication techniques such as electrospinning; preclinical research has shown potential of this combined approach for biphasic constructs employed in vertical bone augmentation (Sudheesh Kumar et al., 2018; Vaquette et al., 2021) and regeneration of the periodontal complex and supporting alveolar bone (Vaquette et al., 2012).

Stereolithography apparatus (SLA) and selective laser sintering (SLS) are the primary laser-assisted techniques for non-metallic bone scaffold production. First developed in 1983, SLA utilizes photochemical reactions with UV lasers to produce

TABLE 1 | Types of additive manufacturing processes and their general features.

AM technique	Process	Compatible materials	Advantages	Disadvantages
Fused deposition modeling (FDM)	Extrusion-based	PLA PCL β -TCP	High mechanical strength. No excess material inside scaffold.	Thermal processing. Low printing resolution ($>100\ \mu\text{m}$).
Stereolithography apparatus (SLA)	Laser-assisted	HA CA	Cell and bioink carrier potential. Internal resolution.	Limited material diversity.
Selective laser sintering (SLS)	Laser-assisted	PCL PLA HA	No support structure necessary	Thermal processing
Three-dimensional printing (3DP)	Binder jetting	PCL	No heat or support structure necessary.	Low mechanical strength.
Melt electrospinning	Fiber-based	PCL	Tunable fiber thickness ($<20\ \mu\text{m}$). High architectural control.	Limited material diversity.

PLA, polylactic acid; PCL, polycaprolactone; TCP, tricalcium phosphate; HA, hydroxyapatite; CA, ceramic acrylate.

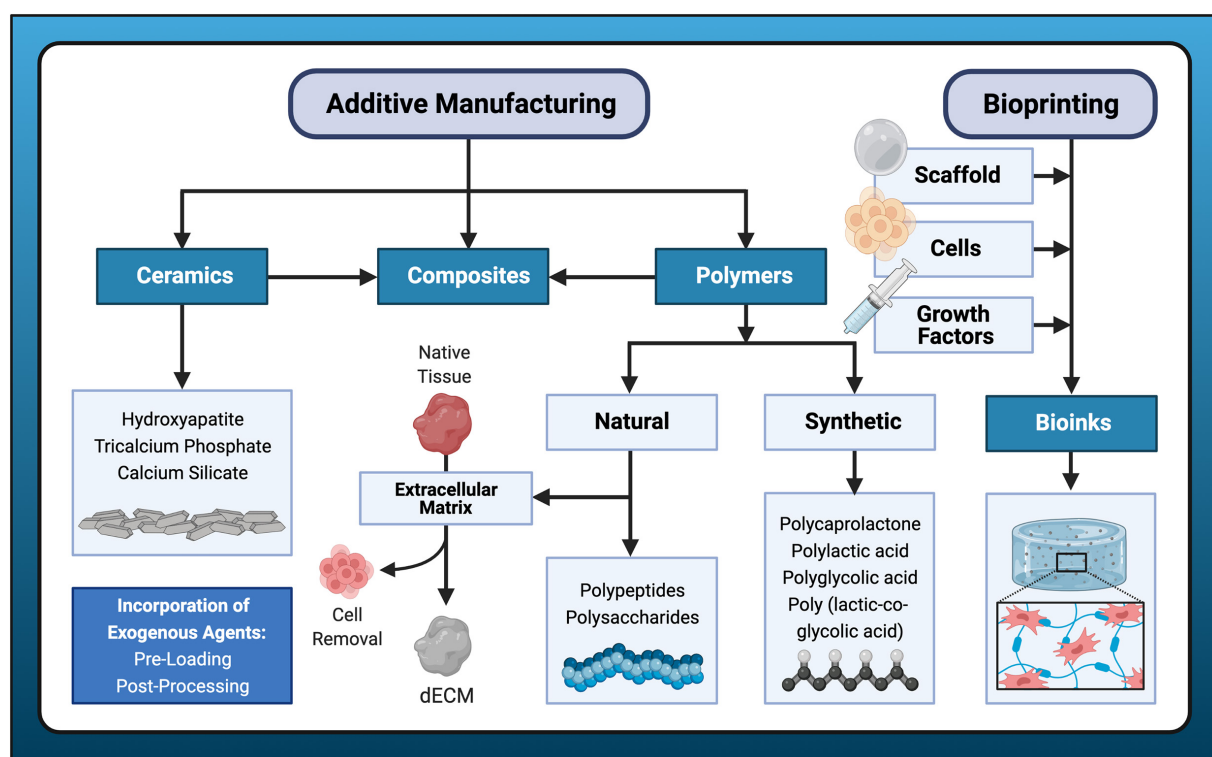


FIGURE 5 | Biomaterials for bone scaffold fabrication. A variety of candidate materials are available for scaffold fabrication using additive manufacturing or bioprinting processes. Additive manufacturing typically employs polymers, to which ceramic materials may be added to form composites. Bioprinting incorporates all three elements of the tissue engineering triad: cells, scaffold (hydrogel), and growth factors. Exogenous agents are often incorporated either with pre-loading or post-processing methods.

scaffolds out of photosensitive polymers. Because of specific material and post-processing requirements associated with toxicity concerns, SLA is not as commonly used for craniofacial regeneration. The main advantage of SLA is its capability for high accuracy and refined internal resolution relative to other AM techniques (Msallam et al., 2020). First developed and then subsequently commercialized in 1992, SLS is a powder-based technique which utilizes a laser to sinter powder spread across a rolling plate. Scaffolds developed with SLS have strong mechanical properties suitable for bone and can be designed with complex geometries (Sudarmadji et al., 2011). SLS is especially useful for fabricating porous, bioactive bone scaffolds consisting

of polymer-ceramic composites, most commonly involving the combination of HA and PCL (Xia et al., 2013; Du et al., 2015).

Melt electrospinning is a distinct processing technique often used in conjunction with AM. In general, this technique allows for the introduction of micro- and nano-scale features into regenerative scaffolds. The technique is similar to FDM, with the main difference being a high-voltage power supply to extrude precise droplets with a refined resolution. Electrospun fibers and scaffolds are particularly advantageous for drug or small molecule loading because of its nanoscale morphological structure (Chew et al., 2006). Biomaterials with antimicrobial properties offer a significant advantage in the regeneration

of periodontal structures affected by periodontal disease, in which oral-biofilm is a key component in the dysregulated inflammatory response. An electrospun gelatin and low molecular weight chitosan scaffold demonstrated antimicrobial efficacy against *Aggregatibacter actinomycetemcomitans*, a facultative anaerobe commonly implicated in periodontal infections (Budai-Szűcs et al., 2021). Further, an ibuprofen-functionalized, nanofibrous PCL scaffold improved CAL and reduced expression of inflammatory mediators COX-2 and IL-8 in seeded human oral epithelial cells and fibroblasts challenged by *Porphyromonas gingivalis* lipopolysaccharide, a key pathogenic factor in periodontitis (Jain and Darveau, 2010). Alternatively, solution electrospinning involves polymer solutions and solvents to solubilize the solutions into materials in the scaffold design (Xue et al., 2019). This technique is still used with improved alignment, although melt electrospinning offers more detailed control over the architecture and less toxicity concerns for craniofacial regenerative purposes.

Bioresorbable Scaffolds for Bone Reconstruction

Bioresorbable scaffolds are materials that may be degraded into moieties *in vivo*, undergoing subsequent elimination through natural pathways resulting in total removal of the initial material without adverse biologic effects (Vert et al., 1992). A large variety of bioresorbable materials with unique material properties and degradation rates are available for scaffold fabrication (Figure 5). The mechanism of degradation occurs either through highly specific enzymatic cleavage, as is the case for natural polymers such as collagen, or passive hydrolysis, which induces chain scission of synthetic polymers under physiologic conditions. The degradation rate is influenced by a multitude of factors including but not limited to the molecular weight, chain configuration, comonomer ratio, residual monomer content, and crystallinity, as well as annealing and sterilization procedures and incorporation of drugs or other additives (Yannas, 2015). Bioresorbable materials are advantageous in bone tissue engineering due to their ability to facilitate regeneration while eliminating the need for removal by a secondary surgical procedure. This is an essential feature for periodontal tissue regeneration, in which delicate connective tissue structures and their interfaces must be restored; removal of a non-resorbable material would traumatize the site and disrupt healing. A principal challenge in formulating bioresorbable materials is matching the degradation rate to the intrinsic pace of native tissue remodeling, while maintaining sufficient mechanical properties of the scaffold. Failure to do so poses a high risk of scaffold exposure in periodontal surgery due to inflammatory complications in the thin gingival tissues that overlay alveolar bone, however, this risk is also present in the use of non-resorbable, metallic scaffolds. Careful flap design and suturing technique must also be employed to obtain primary closure and promote normal wound healing.

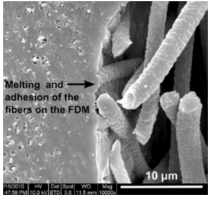
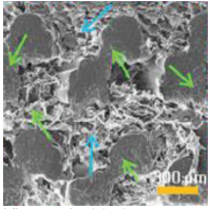
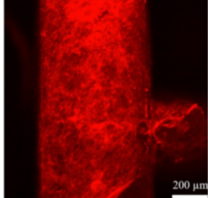
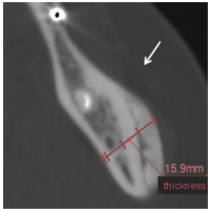
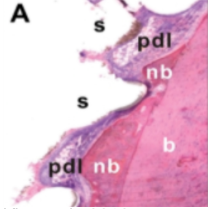
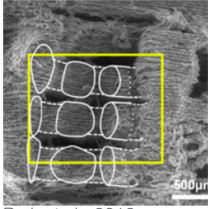
Scaffolds for bone tissue engineering can be typically assigned to one of the following categories: natural biopolymers, synthetic polymers, ceramics, acellular tissue matrices, and composite

materials composed of two or more material groups (Akter and Ibanez, 2016). Natural polymers are biologically active and can be further categorized into polypeptides or polysaccharides, which are both frequently used in 3D bioprinting techniques (covered in section “Three Dimensional Bioprinting”). Polypeptide-based materials in particular possess amino acid sequences associated with integrin-binding domains conducive to cell adhesion and growth (Filippi et al., 2020). Another notable advantage is their biodegradability, which facilitates host cell production of extracellular matrix to replace the degrading scaffold (Akter and Ibanez, 2016). Disadvantageous features of some natural materials include risk of immunogenicity, possibility for disease transmission, and relatively low mechanical strength.

Synthetic polymers are the largest group of biodegradable polymers and include poly(α -ester)s, polyurethanes, polyacetals, poly(ester amide)s, polyanhydrides, polyphosphazenes, and pseudo poly(amino acids) (Filippi et al., 2020). Their use are highly prevalent in AM techniques due to characteristic low melting points and versatile physical properties that accommodate a wide range of processing parameters. Due to their high biocompatibility, numerous synthetic polymers are FDA-approved and can be employed in a broad range of biomedical applications. The poly(α -ester) family is the most common bioresorbable material choice compatible with AM production of scaffolds for bone tissue engineering and includes PCL, PLGA, polylactic acid (PLA), and polyglycolic acid (PGA) (Burg, 2014). These polymers are also frequently combined with ceramic biomaterials, which not only enhance mechanical properties and osteoconductivity, but also confer osteoinductive and osteogenic potential due to their similar composition to the inorganic phase of bone (Ducheyne and Qiu, 1999; Chai et al., 2012). Incorporation of other bioactive compounds such as calcium-silicate, can improve polymer surface hydrophilicity (Lin et al., 2017) and provide osteostimulation (Zhai et al., 2017). Representative *in vivo* studies of bioresorbable polymeric and polymeric-composite scaffolds produced by AM techniques for bone regeneration are featured in Table 2.

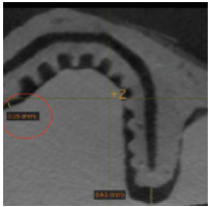
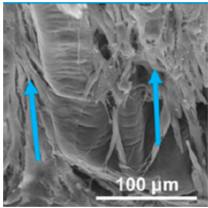
Cell-derived, decellularized extracellular matrix (dECM) may also be combined with synthetic polymeric scaffolds to provide appropriate molecular cues for osteogenic activity. AM-printed constructs have been coated with dECM obtained from bone cells (Wu et al., 2019) or non-bone cells such as human lung fibroblasts (Kim et al., 2018) and MSCs from nasal inferior turbinate tissue (Pati et al., 2015). dECM has also been obtained from dental pulp (Sangkert et al., 2016). Preclinical experiments have demonstrated superior ability of dECM coatings to enhance new bone formation *in vivo* compared to bare scaffold controls (Pati et al., 2015; Kim et al., 2018; Wu et al., 2019). Further, dECM coatings downregulate expression of pro-inflammatory cytokines tumor necrosis factor α (TNF- α) and interleukin-1 (IL-1) and improve MSC adhesion, proliferation, and osteogenic differentiation through induction of attachment protein expression *in vitro* (Wu et al., 2019). Application of dECM coatings to scaffolds produced by AM addresses the need for balance between biologic and mechanical properties while overcoming limitations of tissue-derived ECM which consists of decellularized tissues or organs (Zhang W. et al., 2016).

TABLE 2 | Representative *in vivo* studies using additive manufacturing (AM) to produce resorbable scaffolds for dental, oral, and craniofacial-related bone regeneration from 2010 to 2020.

Material	Added biologic components	AM method	Model; tissue types	Notable design features	Key outcomes	Illustration
PCL + β -TCP	Human osteoblasts + human PDLCs	Fused deposition modeling + electrospinning	Rat; periodontal complex	Biphasic scaffold with bone and PDL compartments combined with use of cell sheets.	The mixed-methods approach created well integrated but distinct compartments. Presence of cell sheets facilitated periodontal fiber attachment and cementum-like tissue.	 Vaquette et al., 2012
PCL + β -TCP	dECM from porcine bone + MC3T3 preosteoblast cells	Extrusion-based	Rabbit; calvaria	Composite polymer-ceramic material immersed in bone dECM solution.	Bone dECM imparted high quantities of BMP-2 and BMP-7 and enhanced MC3T3 differentiation <i>in vitro</i> . Bone volume fraction and bone mineral density was highest in PCL/ β -TCP/dECM group <i>in vivo</i> .	 Kim et al., 2018
PCL + CS powder	dECM from MG64 cells	Extrusion-based	Rat; calvaria	dECM coating was applied to the scaffold to improve biocompatibility and cellular response.	CS/PCL/dECM improved cellular adhesion, proliferation, and differentiation of human MSCs, expression of osteogenic genes increased and pro-inflammatory genes decreased.	 Wu et al., 2019
α -TCP powder + hardening liquid (5% sodium chondroitin sulfate, 12% disodium succinate, 83% distilled water).		3D inkjet printing	Human; maxilla, mandible, and frontal bone	Unsintered calcium phosphate was selected to promote replacement rate by native bone in large alloplastic grafts.	Satisfactory bone union occurred in 18 of 21 remaining sites at 1 year. Bone union was missing in the other three sites. Some host sites experienced resorption and no scaffolds underwent complete replacement.	 Kanno et al., 2016
Poly- ϵ -caprolactone + hydroxyapatite	SDF-1 + BMP-7	Extrusion-based	Rat; mandibular incisor	3D microstrands with interconnecting microchannels.	Orthotopic implantation showed tissue ingrowth and scaffold interface with fibrous tissue reminiscent of PDL and newly formed bone.	 Kim et al., 2010
PCL	Human PDLCs + AdCMV-BMP-7	3D printing and indirect mold casting	Rat; periodontal complex	Controlled pore orientation and distinct tissue compartments with fiber-guiding channels.	Novel scaffold architecture directed spatial bone growth and enhanced bone volume fraction and tissue mineral density outcomes <i>in vivo</i> compared to control with random porous architecture.	 Park et al., 2012

(Continued)

TABLE 2 | Continued

Material	Added biologic components	AM method	Model; tissue types	Notable design features	Key outcomes	Illustration
PCL powder + 4% hydroxyapatite	rhPDGF-BB	Selective laser sintering	Human; periodontal complex	Internal port for growth factor delivery and fiber guiding pegs for periodontal ligament PDL orientation.	Initial 3 mm gain of clinical attachment and partial root coverage was achieved without inflammatory reaction at 12 months. Scaffold exposure occurred at 13 months due to slow degradation rate of PCL and ultimately necessitated removal.	 Rasperini et al., 2015
PLGA/PCL + amorphous PCL	AdPDGF-BB + AdBMP-7 + human PDLs	Photolithography and indirect mold casting	Rat; periodontal complex	Micropatterned pillars and chemical vapor deposition to immobilize adenoviral gene vectors for PDGF-BB and BMP-7 expression.	Micropatterning promoted PDL maturation similar to the width of native PDL. Gene delivery groups showed increased expression of collagen III and periostin, as well as greater bone fill maintenance. Minimal cementum formation observed.	 Pilipchuk et al., 2018

PCL, polycaprolactone; TCP, tricalcium phosphate; PDLs, periodontal ligament cells; dECM, decellularized extracellular matrix; BMP, bone morphogenetic protein; CS, calcium silicate; MSCs, mesenchymal stem cells; 3D, three-dimensional; SDF, stromal-derived factor; rhPDGF-BB, recombinant human platelet derived growth factor-BB; PLGA, poly lactic-co glycolic acid.

Three Dimensional Bioprinting

Bioprinting, generally defined as “the use of computer-aided transfer processes for patterning and assembly of living and non-living materials with a prescribed 2D or 3D organization to produce bioengineered structures” (Daly et al., 2021b), is a promising field in regenerative medicine, providing precise and controlled deposition of cells, hormones, drugs, and growth factors, etc. thus directing improved tissue regeneration (Aljohani et al., 2018). Among the broad range of 3D printing techniques, the most common and accessible bioprinting method is extrusion bioprinting, where the pressure-driven extrusion of a bioink from a printer head is used to print filaments following a defined design or pattern (Ozbolat and Hospodiuk, 2016). Inkjet printing falls under the umbrella of extrusion printing but involves the deposition of bioink droplets through the printhead rather than continuous filaments (Li X. et al., 2020). For extrusion-based or extrusion-related bioprinting, the bioink is a unique feature compared with cell-free 3D printing. Bioinks can generally be described as “a formulation of cells that is suitable to be processed by an automated biofabrication technology” (Groll et al., 2018), which usually has a hydrogel formulation as the main component containing cell-suspensions or cell aggregates (Daly et al., 2021b).

The selection of bioinks is one of the most critical steps in the process of bioprinting, mainly relying on two important aspects: biofabrication and biocompatibility. Biofabrication usually refers to the printability of the ink, such as the compatibility with

the printer and printing resolution, which is highly related to the rheological properties of the bioink. Viscous and shear-thinning hydrogels, such as gelatin and methylcellulose (Ahlfeld et al., 2020), are often considered suitable for many bioprinting scenarios, as these materials can flow smoothly during extrusion, avoid the formation of clogging within the printhead, and stabilize after deposition. Biocompatibility involves the impact of the bioink on cell behaviors including short-term cell viability and long-term cell proliferation, migration, differentiation and organization. The cellular interactions with the bioink can be influenced by multiple factors simultaneously such as the gelation and deposition processes, as well as the biological and biophysical properties. Of note, a desired bioink might be specifically related to limited cell types and biological scenarios.

Dental, oral and craniofacial tissues are organized with complex 3D architectures involving multiple types of cells and tissues. Mimicking their 3D complexity and multicellular interactions represents one of the main barriers in dental and craniofacial regeneration (Obregon et al., 2015). 3D bioprinting holds great potential for creating 3D defect-specific constructs with multiple cell sources for use in regenerative medicine. 3D bioprinting studies applied to dental and craniofacial regeneration can be divided into three general focuses including the periodontal complex, pulp-dentin complex and craniomaxillofacial bone (Table 3). As periodontal ligament cells (PDLs) contain stem cells that harbor the potential to generate cementum/PDL-like tissue (Seo et al., 2004),

PDLs are one of the most frequently-employed cell types for periodontal regeneration-oriented bioprinting. A previous study systematically investigated the printability of various concentrations of GelMA hydrogels and the influence of different 3DP parameters such as photoinitiator concentration, UV exposure, pressure and needle diameter on the viability of PDLs in order to achieve high printing resolution, dimension ability and cell viability simultaneously for periodontal regeneration (Raveendran et al., 2019).

The regeneration of pulp-dentin complex or the whole tooth has attracted great attention in dentistry. It is known that dental pulp stem cells (DPSCs) can differentiate into several cell types, including odontoblasts, neural progenitors, osteoblasts, chondrocytes, and adipocytes with high proliferative capability (Casagrande et al., 2011). Therefore, various studies have combined DPSCs with modified bioinks to establish 3D-bioprinted dental constructs. In previous research, a dentin matrix was isolated and combined with alginate to fabricate hydrogel blends as the bioink (Athirasala et al., 2018). The printability of the bioinks was greater in the formulations containing higher concentrations of alginate, whereas a higher proportion of dentin matrix proteins significantly improved cell viability and a 1:1 ratio of alginate and dentin was determined to be most suitable. Further, addition of acid-soluble dentin molecules into hydrogels enhanced odontogenic differentiation. Besides naturally derived molecules, synthetic biomolecules such as BMP-mimetic peptide have been incorporated into bioink as well. Park J. H. et al. (2020) developed a novel BMP peptide-tethering bioink formulation and found 50% of the peptides remained in the bioprinted construct after 3 weeks in an *in vitro* cell culture. The BMP peptide construct group exhibited the highest calcification as compared to the growth medium, osteogenic medium, and control groups with robust expression of osteogenic genes. In addition to pulp-dentin complex, the feasibility of whole tooth bioprinting has been studied by co-printing the hDPSCs-laden bioinks with PCL. The results not only achieved localized differentiation of hDPSCs in the outer region of the 3D cellular construct but also successfully produced 3D patient-specific cellular constructs for tooth tissue engineering in a predefined pattern (Han et al., 2019).

Engineering craniomaxillofacial bone tissue is a unique challenge due to the complex architecture of bone, consisting of organized calcified regions with interpenetrated vasculature (Salgado et al., 2004). In order to support osteogenesis, stem cells with osteogenic potential such as bone marrow-derived MSCs or DPSCs were frequently used. Moreover, various bioactive components have been incorporated into bioinks to enhance the osteogenic ability including amorphous magnesium phosphate (Dubey et al., 2020), bioactive glass (Ojansivu et al., 2019) and silicate nanoplatelets (Byambaa et al., 2017). To further promote vascularization, human umbilical vein endothelial cells (HUVECs) have been encapsulated into GelMA hydrogel bioinks to engineer vasculogenic niches. Moreover, to promote vascular spreading, chemically conjugated VEGF were introduced in the surrounding bone niches (Byambaa et al., 2017).

Although extrusion bioprinting is a common and accessible bioprinting technology compatible with a large variety of

bioinks, other bioprinting technologies have been developed to overcome the main limitations of extrusion-based printing including lithography bioprinting and spheroid bioprinting (Daly et al., 2021b). Lithography bioprinting technology can create physical features at the scale of 10–100 μm , which is a significant advantage over extrusion bioprinting in which the minimum resolution is $\sim 100 \mu\text{m}$ (Bertlein et al., 2017; Lim et al., 2018). Spheroid bioprinting, which processes self-organized tissues (often cell spheroids) into 3D constructs to scale and direct self-organization, can mimic tissue-like features and achieve high cell densities to promote cell-cell contacts (Skylar-Scott et al., 2019; Daly et al., 2021a). There are numerous interesting and promising applications of lithography and spheroid bioprinting techniques to fabricate complicated *in vitro* systems that would otherwise be challenging for extrusion-based processes to realize, including a liver lobule model (Ma et al., 2016), alveolar lung model (Grigoryan et al., 2019), and other organ and tissue models (Grigoryan et al., 2019; Daly et al., 2021a). Until now, dental, oral, and craniofacial applications using these novel bioprinting technologies for repair and regeneration have been scarce.

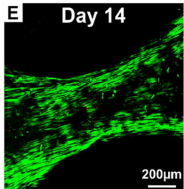
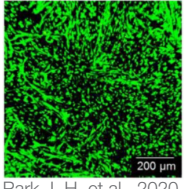
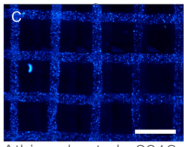
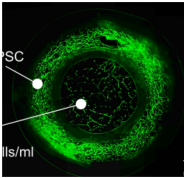
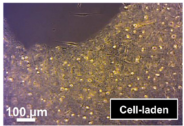
CLINICAL APPLICATIONS FOR DENTAL REGENERATIVE MEDICINE

Personalized Reconstruction With Image-Based Scaffolds

The numerous bones of the craniofacial skeleton exhibit variable anatomical forms and exist in intimate relation to one another, as well as to abundant nerves and vessels. As such, bony reconstruction within this region often entails labor-intensive, multi-step operations with limited surgical access to morphologically complex defects. In the early stage of AM, stereolithographic models were introduced as an adjunct to standard diagnostic imaging and casts. These 3D models improved surgeon visualization of bony defects and their spatial relationship to adjacent structures, thus enhancing accuracy in preoperative evaluation, diagnosis, and treatment planning (D'Urso et al., 1999). With significant advancements in high resolution medical imaging and CAD-CAM software, AM processes are now employed to fabricate personalized constructs for a vast range of applications in all phases of craniomaxillofacial surgery (Levine et al., 2012; Yu et al., 2019).

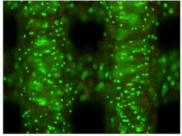
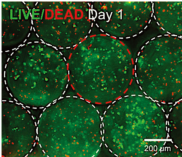
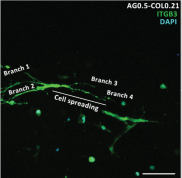
In a recent systematic review of customized objects used in 3D printing-assisted craniofacial and maxillofacial operations, four major categories of personalized constructs were identified: (1) contour models; (2) guides; (3) splints; and (4) implants (Jacobs and Lin, 2017). Contour models facilitate accurate prebending of reconstruction meshes or plates, eliminating the need for extensive intraoperative manipulation and significantly reducing operating time (Sumida et al., 2015; von Wilmowsky et al., 2020). Guides utilize negative space relative to patient anatomy to provide intraoperative reference for precise osteotomy preparation and controlled positioning of dental (Ersoy et al., 2008) and zygomatic (Wang et al., 2020) implants. Splints are similar to guides; however, they are fabricated to align structures

TABLE 3 | Representative studies on 3D bioprinting for dental, oral, and craniofacial-related regeneration from 2016 to 2020.

Bioink	Bioprinting method	Tissue types	Cells/growth factors encapsulated	Key outcomes	Illustration
GelMA	Microextrusion-based	Periodontal complex	PDLCS	The optimized printing conditions supported a high level of PDLCS viability and facilitated cellular proliferation within the construct over 14 days.	 <p>Day 14</p> <p>200 μm</p> <p>Raveendran et al., 2019</p>
GelMA	Microextrusion-based	Pulp-dentin complex	hDPSCs + BMP-mimetic peptide	BMP-GelMA bioink formulation provided proper printability and dental specific microenvironment to support hDPSCs high viability, proliferation, and differentiation.	 <p>200 μm</p> <p>Park J. H. et al., 2020</p>
Dentin-derived ECM + Alginate	Extrusion-based	Pulp-dentin complex	Odontoblast-like cell line (OD21) + acid-soluble dentin molecules	Dentin-derived ECM hybrid cell-laden hydrogel bioink showed high printability and cell survival. This hybrid hydrogel embedded with acid-soluble dentin molecules can enhance odontogenic differentiation.	 <p>Athirasala et al., 2018</p>
Fibrinogen + Gelatin + Hyaluronic acid + Glycerol	Custom-made syringe bioprinting	Whole tooth	hDPSCs	A dentin pulp complex with patient-specific shape was successfully produced by co-printing the bio-inks with polycaprolactone. After culturing for 15 days, localized differentiation of hDPSCs in the outer region of the construct was achieved with localized mineralization.	 <p>SC</p> <p>cells/ml</p> <p>Han et al., 2019</p>
ECM bioink (2% octapeptide) + AMP	Microvalve bioprinting	Craniofacial bone tissue	hDPSCs	The cell-laden bioprinted constructs modified with AMP exhibited a high level of mineralization and osteogenic gene expression <i>in vitro</i> and the ECM/1.0AMP composition displayed excellent bone regeneration capability <i>in vivo</i> .	 <p>100 μm</p> <p>Cell-laden</p> <p>Dubey et al., 2020</p>

(Continued)

TABLE 3 | Continued

Bioink	Bioprinting method	Tissue types	Cells/growth factors encapsulated	Key outcomes	Illustration
Gelatin-alginate + cellulose nanofibrils + bioactive glass	Extrusion-based	Bone	(i) Human osteoblast-like cells (Saos-2). (ii) hBMSCs	The addition of bioactive glass and cellulose nanofibrils to gelatin-alginate system enhanced their printability and osteogenic activity but resulted in the death of Saos-2 cells due to increased viscosity.	 Ojansivu et al., 2019
GelMA + silicate nanoplatelets	Extrusion-based direct-writing bioprinting	Bone	HUVECs + hBMSCs + VEGF	Two GelMA hydrogels containing different concentrations of VEGF were optimized and bioprinted into well-defined 3D architectures, which resulted in the formation of a perfusable lumen, maturation of vascular vessels, and induced osteogenic differentiation.	 Byambaa et al., 2017
Agarose + collagen I	Inkjet	Bone	hBMSCs	Increased solids concentrations of collagen in the 3D-bioprinted hydrogel blend enhanced cell spreading, that ultimately contribute to enhanced and directed MSC osteogenic differentiation.	 Duarte Campos et al., 2016

GelMA, gelatin methacryloyl; PDLs, periodontal ligament cells; hDPSCs, human dental pulp stem cells; ECM, extracellular matrix; AMP, amorphous magnesium phosphate; hBMSCs, human bone marrow-derived mesenchymal stem cells; HUVECs, human umbilical vein endothelial cells; VEGF, vascular endothelial growth factor; 3D, three-dimensional.

in virtually planned, postoperative positions. Finally, implants are medical devices surgically placed patient tissues. Customized CAD-CAM devices have been employed for human clinical use in the reconstruction of structures such as the temporomandibular joint (Ackland et al., 2018), maxilla and mandible (Lethaus et al., 2012; Ma et al., 2017; Chiapasco et al., 2021), paranasal sinuses, nasal bone (Horn et al., 2012), orbit (Bachelet et al., 2018), and cranial vault (Jardini et al., 2014; Park et al., 2016; Unterhofer et al., 2017). Use of components produced by AM can also minimize discrepancies between planned and actual surgical outcomes. For example, in a case series documenting nine patients undergoing orthognathic surgery or distraction osteogenesis procedures, the use of custom templates and reconstruction microplates enabled accurate repositioning of the maxillary segment within 1 mm of the digitally planned centroid position and 1° orientation in all linear and axial directions, respectively (He et al., 2015).

Additive manufacturing is now widely employed in dentistry for a variety of purposes, including fabrication of dentures,

occlusal splints, temporary crowns and bridges, orthodontic appliances, and surgical guides. More recently, customized, non-resorbable titanium metal cages intended for extraosseous alveolar ridge augmentation have become available to clinicians as well. Despite prolific use of commercially available AM equipment to create custom dental devices in every day clinical practice, attempts to utilize bioresorbable bone scaffolds produced by this technology have only recently begun in academic, clinical settings. In 2015, the first dental use of a personalized, bioresorbable scaffold produced with AM in humans was reported. A PCL scaffold fabricated by selective laser sintering was loaded with rhPDGF-BB solution and implanted into a periosseous defect in the periodontium localized to a mandibular canine site (Rasperini et al., 2015). The design incorporated novel, cylindrical-shaped, PDL fiber-guiding architecture previously reported in a rodent model (Park et al., 2012). At 1 year, a modest 3 mm gain in clinical attachment and partial root coverage was achieved but graft exposure culminated in scaffold failure (Rasperini et al., 2015).

This complication also occurred in a case series assessing the use of prefabricated, FDM-printed, PCL scaffolds for alveolar ridge preservation (Goh et al., 2015). The scaffolds remained largely intact within the healing extraction sockets for 6 months and 2/13 patients experienced manageable graft exposure, highlighting the challenges posed by the slow resorption rate of PCL.

Customized, bioresorbable bone scaffolds created by AM processes have been tested more extensively in the fields of maxillofacial and craniofacial surgery. In 2016, a clinical case series described 20 patients who received artificial bone constructed with 3D inkjet printing to graft non-weight bearing, maxillofacial bone deformities in 23 sites (Saijo et al., 2009; Kanno et al., 2016). These scaffolds were fabricated in 0.1 mm layers by spraying hardening liquid composed of 5% sodium chondroitin sulfate, 12% disodium succinate, and 83% distilled water onto an α -TCP powder. At 1 year, 18 of 21 remaining grafted sites demonstrated CT values indicative of satisfactory bone union. Bacterial infection necessitated removal in 4 sites within a period of 1 – 5 years postoperatively. Failures tended to occur in grafts spanning larger missing bone volume or in one case, a patient that was a carrier of MRSA. With the longest follow-up period occurring just over 7 years, none of the artificial bones demonstrated complete replacement and only partial new bone formation was observed within the scaffold. Despite the limited success observed in these initial translational studies, these efforts represent the emergence of image-based, bioresorbable scaffold technology in the clinical arenas of dental and craniomaxillofacial surgery.

Clinical Impact

Bone grafting is a routine procedure in clinical dentistry and may occur in approximately half of all dental implant sites (Cha et al., 2016). Augmentation of the alveolar ridge through procedures such as guided bone regeneration and maxillary sinus lifts, are often necessary to create adequate bone volume prior to implant placement. Due to a high frequency of bone grafting procedures in the healthcare field overall and a limited pool of musculoskeletal tissue donors, increased use of bone graft substitutes relative to autogenous grafts is a precipitating trend (Kinaci et al., 2014). This is reflected in the global market for dental bone graft substitutes, which had an estimated value of \$450 million in 2020 and is projected to reach \$659 million by 2025 (Markets and Markets, 2020). In the future, AM may yield a new generation of bone graft substitutes that achieve improved regenerative outcomes by uniting the versatility of CAD-CAM technology with modern tissue engineering principles and a personalized medicine treatment approach.

Contemporary biomedical research is steadily approaching a reliable AM strategy to create bioresorbable bone scaffolds for clinical use and the implications for patient care are enormous. Recently, a workflow for AM fabrication of porous, bioresorbable scaffolds consisting of medical grade PCL for the reconstruction of large, posterior mandibular defects was demonstrated (Bartnikowski et al., 2020). The resultant porosity (83.91%) and mean pore size ($590 \pm 243 \mu\text{m}$) were

within suitable ranges for bone regeneration and the mean discrepancy between the template implant model and the scanned scaffold was found to be $74 \pm 14 \mu\text{m}$, representing a level of accuracy adequate for clinical application. Pending further preclinical validation and clinical trials, rapid in-house fabrication and deployment of personalized bone scaffolds with accurate replication of individual patient anatomy could revolutionize trauma care in the fields of maxillofacial and craniofacial surgery. Esthetics, form, and function could also be restored in patients that have undergone massive tumor resection in craniofacial structures. In implant dentistry, substantial augmentation or reconstruction of the alveolar ridge could be accomplished with personalized constructs rather than adapting universal materials to anatomically diverse defects. Invasive procedures, such as autogenous harvesting of large, block grafts from secondary surgical sites or the placement of zygomatic implants, which are reserved for severely atrophic maxillae, may also be avoided. Finally, AM offers new strategies to employ scaffolds as carriers for exogenous agents that not only enhance regeneration but offer therapeutic benefit to the patient as well. This may be especially valuable for modulation of the destructive, biochemical mechanisms inherent to tissues affected by chronic inflammation, such as in periodontal disease.

FUTURE DIRECTIONS

Challenges in Additive Manufacturing

AM holds tremendous promise for the advancement of regenerative medicine; however, this impressive technology must overcome several obstacles before it can be extensively introduced to clinical settings for the purpose of fabricating personalized bone tissue scaffolds. First, AM has historically been limited by relatively low production speed. In 2017, the average build time to create a personalized object constructed by AM techniques in the field of craniomaxillofacial surgery is approximately 18.9 h but can be as high as 96 h per object (Jacobs and Lin, 2017). Practical utilization requires faster manufacturing processes that maintain adequate print resolution, surface quality, and mechanical integrity, especially to hold relevance for applications in urgent care. Use of modern multi-extrusion printing systems is swiftly rising in tissue engineering for bone and periodontal structures due to its one-step printing approach, improved speeds, and ability to use versatile material formulations (Porta et al., 2020). Second, variations in part quality can occur due to errors introduced during the digital manipulation of virtual models or during the physical construction process. Third, decentralization of bioresorbable scaffold fabrication from commercial biomaterial manufacturing facilities to local centers of production may complicate safety assessments and reporting of adverse events. Last, the use of customized scaffolds with innumerable variations in composition and design may present significant challenges for standardized regulation in the clinical dental practice setting. Development and oversight of appropriate guidelines for post-manufacturing

quality assurance and sterilization would be required. In the case of implantable scaffolds, sterilization is especially critical to prevent infection. Scaffolds constructed with certain polymeric materials may not be able to withstand the high temperatures necessary for autoclave sterilization and would require alternative sterilization methods.

Despite these potential limitations, the technologic infrastructure necessary to produce bioresorbable scaffolds for bone regeneration by AM is available for implementation. Successful translation to clinical use now relies upon the ability to manipulate biomaterials and precisely coordinate their architectural and biochemical features with known physiologic mechanisms of tissue formation. This process is further complicated by the addition of exogenous agents, such as viable cells, growth factors, gene vectors, drugs, and other bioactive components, which must be present in appropriate quantities to simulate a suitable microenvironment for regeneration. Simultaneous incorporation of viable cells during scaffold fabrication remains a preeminent challenge. Ensuring cell survival during the AM process and preserving their phenotype and morphology post-processing will require continued development of cell-deposition techniques and cell-carrier systems. Improved control of cellular responses will benefit from the progressive advancement of scaffold-based gene therapy techniques. Finally, innovation in the use of hydrogel bioinks and 3D bioprinting processes will further refine spatiotemporal regulation of biomolecular signaling and progress efforts to regenerate bone tissue with bioresorbable, biomimetic scaffolds *in vivo*.

Emerging Additive Manufacturing Research With Potential for Dentistry

A successful, alloplastic bone substitute biomaterial fabricated by AM is a treatment concept just on the horizon of realistic clinical practice and there are many exciting implications for the future. AM has given rise to a new manufacturing concept termed four-dimensional (4D) printing, in which time is the fourth dimension of the printed construct (Saska et al., 2021). 4D printing aims to create scaffolds fabricated with advanced or “smart” materials that react to external stimuli such as pH, humidity, light, and temperature, allowing dynamic responses to *in vivo* conditions (Valvez et al., 2021). Potential applications of these sensitive materials include utilizing environmental stimuli to induce appropriate release patterns of angiogenic and osteogenic factors during wound healing and tissue formation processes, thus enhancing regenerative capability. Even further, shape-morphing (Gladman et al., 2016) and shape-memory materials (Zhou and Sheiko, 2016; Liu et al., 2020) are setting the stage for scaffold materials capable of controlled self-assembly or even self-repair (Zhang et al., 2019), which may offer pivotal advantages for the regeneration of weight-bearing structures, such as the jaws or temporomandibular joint. Lastly, *in situ* bioprinting, which entails real-time scaffold fabrication directly within the defect (O’Connell et al., 2016; Di Bella et al., 2018), is an interesting development of AM technology with clinical potential for bone regeneration (Keriquel et al., 2010; Keriquel

et al., 2017), especially in defect sites with complex morphologies, significant undercuts, or limited surgical access; examples of potential applications include bone grafting of the maxillary sinuses, intrabony defects, and peri-implant defects.

CONCLUSION

The treatment of dental, oral, and craniofacial bone defects is currently restricted by available biomaterials, which have limited capacity to facilitate true regeneration of new tissues that exhibit native physiologic form, function and esthetics. Further research efforts are needed to optimize AM for the production of bioresorbable scaffolds that yield safe, predictable, and efficacious clinical outcomes in the reconstruction of bony defects. More preclinical studies are needed to improve the material properties and clinical performance of polymer-ceramic composite scaffolds for bone reconstruction and to refine understanding of the architectural features that promote formation of an anatomic periodontal ligament compartment. Additionally, tremendous opportunity exists to functionalize scaffolds for therapeutic purposes, especially with regards to gene therapy. As the understanding of multifaceted biomaterial interactions and tissue dynamics improves within the scientific community, AM offers a promising future in which a superior generation of sustainable regenerative biomaterials will become accessible for everyday clinical use. Commercialization of custom scaffold technology will dramatically accelerate the trend toward increased usage of synthetic bone substitutes and expand their existing market share within the multibillion dollar industry for biomaterials. Successful adaptation of AM technology for bone tissue engineering will expose a new realm of regenerative possibilities within dental medicine, thus expanding treatment options for patients and significantly improving their oral health related quality-of-life. Eventually, personalized bone constructs for dental regenerative medicine will evolve from state-of-the-art technology to a new standard in patient care.

AUTHOR CONTRIBUTIONS

WG and JL contributed to conception and design. JL led the writing of the manuscript. SM, YY, DW, and MC wrote sections of the manuscript. All authors contributed to manuscript revision. All authors read and approved the submitted version.

FUNDING

This work was supported by U24 DE026915 and U24 DE029462 from the NIDCR (WG) and the Osteology Foundation (SM).

ACKNOWLEDGMENTS

The authors thank James Sugai for critically reviewing the manuscript. All figures were made in BioRender (biorender.com).

REFERENCES

- Abbasi, N., Abdal-Hay, A., Hamlet, S., Graham, E., and Ivanovski, S. (2019). Effects of gradient and offset architectures on the mechanical and biological properties of 3-D Melt Electrowritten (MEW) scaffolds. *ACS Biomater. Sci. Eng.* 5, 3448–3461. doi: 10.1021/acsbiomaterials.8b01456
- Abogunrin, S., Di Tanna, G. L., Keeping, S., Carroll, S., and Iheanacho, I. (2014). Prevalence of human papillomavirus in head and neck cancers in European populations: a meta-analysis. *BMC Cancer* 14:968.
- Ackland, D., Robinson, D., Lee, P., and Dimitroulis, G. (2018). Design and clinical outcome of a novel 3D-printed prosthetic joint replacement for the human temporomandibular joint. *Clin. Biomech.* 56, 52–60. doi: 10.1016/j.clinbiomech.2018.05.006
- Ahlfeld, T., Guduric, V., Duin, S., Akkineni, A., Schütz, K., Kilian, D., et al. (2020). Methylcellulose—a versatile printing material that enables biofabrication of tissue equivalents with high shape fidelity. *Biomater. Sci.* 8, 2102–2110. doi: 10.1039/d0bm00027b
- Aichelmann-Reidy, M. E., Avila-Ortiz, G., Klokkevold, P. R., Murphy, K. G., Rosen, P. S., Schallhorn, R. G., et al. (2015). Periodontal regeneration - furcation defects: practical applications from the AAP regeneration workshop. *Clin. Adv. Periodontics* 5, 30–39. doi: 10.1902/cap.2015.140068
- Akter, F., and Ibanez, J. (2016). Chapter 8 - bone and cartilage tissue engineering. *Tissue Eng. Made Easy* 2016, 77–97. doi: 10.1016/b978-0-12-805361-4.00008-4
- Albandar, J. M., Susin, C., and Hughes, F. J. (2018). Manifestations of systemic diseases and conditions that affect the periodontal attachment apparatus: case definitions and diagnostic considerations. *J. Periodontol.* 89(Suppl. 1), S183–S203.
- Aljohani, W., Ullah, M. W., Zhang, X., and Yang, G. (2018). Bioprinting and its applications in tissue engineering and regenerative medicine. *Int. J. Biol. Macromol.* 107, 261–275.
- Allen, E. P., Gainza, C. S., Farthing, G. G., and Newbold, D. A. (1985). Improved technique for localized ridge augmentation. a report of 21 cases. *J. Periodontol.* 56, 195–199. doi: 10.1902/jop.1985.56.4.195
- Almazin, S. M., Dziak, R., Andreana, S., and Ciancio, S. G. (2009). The effect of doxycycline hyclate, chlorhexidine gluconate, and minocycline hydrochloride on osteoblastic proliferation and differentiation in vitro. *J. Periodontol.* 80, 999–1005. doi: 10.1902/jop.2009.080574
- Al-Moraissi, E. A., Alkhutari, A. S., Abotaleb, B., Altairi, N. H., and Del Fabbro, M. (2020). Do osteoconductive bone substitutes result in similar bone regeneration for maxillary sinus augmentation when compared to osteogenic and osteoinductive bone grafts? a systematic review and frequentist network meta-analysis. *Int. J. Oral. Maxillofac. Surg.* 49, 107–120. doi: 10.1016/j.ijom.2019.05.004
- Araujo, M. G., Sukekava, F., Wennstrom, J. L., and Lindhe, J. (2005). Ridge alterations following implant placement in fresh extraction sockets: an experimental study in the dog. *J. Clin. Periodontol.* 32, 645–652. doi: 10.1111/j.1600-051x.2005.00726.x
- Asa'ad, F., Pelanye, G., Philip, J., Dahlin, C., and Larsson, L. (2020). The role of epigenetic functionalization of implants and biomaterials in osseointegration and bone regeneration—a review. *Molecules* 25:5879. doi: 10.3390/molecules25245879
- Aslan, S., Buduneli, N., and Cortellini, P. (2020). Clinical outcomes of the entire papilla preservation technique with and without biomaterials in the treatment of isolated intrabony defects: a randomized controlled clinical trial. *J. Clin. Periodontol.* 47, 470–478. doi: 10.1111/jcpe.13255
- Athirasala, A., Tahayeri, A., Thirivikraman, G., França, C. M., Monteiro, N., Tran, V., et al. (2018). A dentin-derived hydrogel bioink for 3D bioprinting of cell laden scaffolds for regenerative dentistry. *Biofabrication* 10:024101. doi: 10.1088/1758-5090/aa9b4e
- Avila-Ortiz, G., Elangovan, S., Kramer, K. W., Blanchette, D., and Dawson, D. V. (2014). Effect of alveolar ridge preservation after tooth extraction: a systematic review and meta-analysis. *J. Dent. Res.* 93, 950–958. doi: 10.1177/0022034514541127
- Bachelet, J. T., Cordier, G., Porcheray, M., Bourlet, J., Gleizal, A., and Foletti, J. M. (2018). Orbital reconstruction by patient-specific implant printed in porous titanium: a retrospective case series of 12 patients. *J. Oral Maxillofac. Surg.* 76, 2161–2167. doi: 10.1016/j.joms.2018.04.006
- Bagheri, A., and Jin, J. (2019). Photopolymerization in 3D Printing. *ACS Appl. Polym. Mater.* 1, 593–611. doi: 10.1021/acsapm.8b00165
- Barbato, L., Selvaggi, F., Kalemaj, Z., Buti, J., Bendinelli, E., Marca, M., et al. (2020). Clinical efficacy of minimally invasive surgical (MIS) and non-surgical (MINST) treatments of periodontal intra-bony defect. A systematic review and network meta-analysis of RCT's. *Clin. Oral Investig.* 24, 1125–1135. doi: 10.1007/s00784-020-03229-0
- Bartnikowski, M., Vaquette, C., and Ivanovski, S. (2020). Workflow for highly porous resorbable custom 3D printed scaffolds using medical grade polymer for large volume alveolar bone regeneration. *Clin. Oral Implants Res.* 31, 431–441. doi: 10.1111/clr.13579
- Bertlein, S., Brown, G., Lim, K. S., Jungst, T., Boeck, T., Blunk, T., et al. (2017). Thiol–ene clickable gelatin: a platform bioink for multiple 3D biofabrication technologies. *Adv. Mater.* 29:1703404. doi: 10.1002/adma.201703404
- Bettany, J. T., Peet, N. M., Wolowacz, R. G., Skerry, T. M., and Grabowski, P. S. (2000). Tetracyclines induce apoptosis in osteoclasts. *Bone* 27, 75–80. doi: 10.1016/s8756-3282(00)00297-0
- Bodic, F., Hamel, L., Lerouxel, E., Baslé, M. F., and Chappard, D. (2005). Bone loss and teeth. *Joint Bone Spine* 72, 215–221. doi: 10.1016/j.jbspin.2004.03.007
- Bourell, D., Kruth, J., Leu, M., Levy, G., Rosen, D., Beese, A., et al. (2017). Materials for additive manufacturing. *CIRP Ann.* 66, 659–681.
- Budai-Szűcs, M., Ruggeri, M., Faccendini, A., Léber, A., Rossi, S., Varga, G., et al. (2021). Electrospun scaffolds in periodontal wound healing. *Polymers* 13:307. doi: 10.3390/polym13020307
- Burg, K. (2014). “Poly(α-ester)s,” in *Natural and Synthetic Biomedical Polymers*, ed. S. G. Kum (London: Newnes).
- Byambaa, B., Annabi, N., Yue, K., Trujillo-de Santiago, G., Alvarez, M. M., Jia, W., et al. (2017). Bioprinted osteogenic and vasculogenic patterns for engineering 3D bone tissue. *Adv. Healthc. Mater.* 6:1700015. doi: 10.1002/adhm.201700015
- Caballé-Serrano, J., Abdeslam-Mohamed, Y., Munar-Frau, A., Fujioka-Kobayashi, M., Hernández-Alfaro, F., and Miron, R. (2019). Adsorption and release kinetics of growth factors on barrier membranes for guided tissue/bone regeneration: a systematic review. *Arch. Oral Biol.* 100, 57–68. doi: 10.1016/j.archoralbio.2019.02.006
- Casagrande, L., Cordeiro, M. M., Nör, S. A., and Nör, J. E. (2011). Dental pulp stem cells in regenerative dentistry. *Odontology* 99, 1–7. doi: 10.1007/978-3-319-55645-1_1
- Cha, H. S., Kim, J. W., Hwang, J. H., and Ahn, K. M. (2016). Frequency of bone graft in implant surgery. *Maxillofac. Plast. Reconstr. Surg.* 38:19. doi: 10.1007/978-1-4471-1934-0_4
- Chai, Y. C., Carlier, A., Bolander, J., Roberts, S. J., Geris, L., Schrooten, J., et al. (2012). Current views on calcium phosphate osteogenicity and the translation into effective bone regeneration strategies. *Acta Biomater.* 8, 3876–3887. doi: 10.1016/j.actbio.2012.07.002
- Chang, P. C., Cirelli, J. A., Jin, Q., Seol, Y. J., Sugai, J. V., D'Silva, N. J., et al. (2009). Adenovirus encoding human platelet-derived growth factor-B delivered to alveolar bone defects exhibits safety and biodistribution profiles favorable for clinical use. *Hum. Gene Ther.* 20, 486–496. doi: 10.1089/hum.2008.114
- Chang, P. C., Seol, Y. J., Cirelli, J. A., Pellegrini, G., Jin, Q., Franco, L. M., et al. (2010). PDGF-B gene therapy accelerates bone engineering and oral implant osseointegration. *Gene Ther.* 17, 95–104. doi: 10.1038/gt.2009.117
- Chaudhuri, O., Cooper-White, J., Janmey, P. A., Mooney, D. J., and Shenoy, V. B. (2020). Effects of extracellular matrix viscoelasticity on cellular behaviour. *Nature* 584, 535–546. doi: 10.1038/s41586-020-2612-2
- Chaudhuri, O., Gu, L., Klumpers, D., Darnell, M., Bencherif, S. A., Weaver, J. C., et al. (2016). Hydrogels with tunable stress relaxation regulate stem cell fate and activity. *Nat. Mater.* 15, 326–334. doi: 10.1038/nmat4489
- Chen, X., Lin, Z., Feng, Y., Tan, H., Xu, X., Luo, J., et al. (2019). Zwitterionic PMCP-Modified polycaprolactone surface for tissue engineering: antifouling, cell adhesion promotion, and osteogenic differentiation properties. *Small* 15:e1903784. doi: 10.1002/smll.201903784
- Cheng, A., Humayun, A., Boyan, B. D., and Schwartz, Z. (2016). Enhanced osteoblast response to porosity and resolution of additively manufactured Ti-6Al-4V constructs with trabeculae-inspired porosity. *3D Print. Addit. Manuf.* 3, 10–21. doi: 10.1089/3dp.2015.0038

- Chew, S. Y., Wen, Y., Dzenis, Y., and Leong, K. W. (2006). The role of electrospinning in the emerging field of nanomedicine. *Curr. Pharm. Des.* 12, 4751–4770. doi: 10.2174/138161206779026326
- Chiapasco, M., Casentini, P., Tommasato, G., Dellavia, C., and Del Fabbro, M. (2021). Customized CAD/CAM Titanium meshes for the guided bone regeneration of severe alveolar ridge defects: preliminary results of a retrospective clinical study in humans. *Clin. Oral Implants Res.* 32, 498–510. doi: 10.1111/clr.13720
- Clementini, M., Morlupi, A., Canullo, L., Agrestini, C., and Barlattani, A. (2012). Success rate of dental implants inserted in horizontal and vertical guided bone regenerated areas: a systematic review. *Int. J. Oral Maxillofac. Surg.* 41, 847–852. doi: 10.1016/j.ijom.2012.03.016
- Cochran, D. L., Oh, T. J., Mills, M. P., Clem, D. S., McClain, P. K., Schallhorn, R. A., et al. (2016). A randomized clinical trial evaluating rh-FGF-2/beta-TCP in periodontal defects. *J. Dent. Res.* 95, 523–530. doi: 10.1177/0022034516632497
- Connizzo, B. K., Sun, L., Lacin, N., Gendelman, A., Solomonov, I., Sagi, I., et al. (2021). Nonuniformity in periodontal ligament: mechanics and matrix composition. *J. Dent. Res.* 100, 179–186. doi: 10.1177/0022034520962455
- Cortellini, P. (2012). Minimally invasive surgical techniques in periodontal regeneration. *J. Evid. Based Dent. Pract.* 12, 89–100. doi: 10.1016/s1532-3382(12)70021-0
- Cortellini, P., and Tonetti, M. S. (2011). Clinical and radiographic outcomes of the modified minimally invasive surgical technique with and without regenerative materials: a randomized-controlled trial in intra-bony defects. *J. Clin. Periodontol.* 38, 365–373. doi: 10.1111/j.1600-051x.2011.01705.x
- Costa, P. F., Vaquette, C., Zhang, Q., Reis, R. L., Ivanovski, S., and Hutmacher, D. W. (2014). Advanced tissue engineering scaffold design for regeneration of the complex hierarchical periodontal structure. *J. Clin. Periodontol.* 41, 283–294. doi: 10.1111/jcpe.12214
- Daegling, D. J., Ravosa, M. J., Johnson, K. R., and Hylander, W. L. (1992). Influence of teeth, alveoli, and periodontal ligaments on torsional rigidity in human mandibles. *Am. J. Phys. Anthropol.* 89, 59–72. doi: 10.1002/ajpa.1330890106
- Dalby, M. J., Gadegaard, N., Tare, R., Andar, A., Riehle, M. O., Herzyk, P., et al. (2007). The control of human mesenchymal cell differentiation using nanoscale symmetry and disorder. *Nat. Mater.* 6, 997–1003. doi: 10.1038/nmat2013
- Daly, A. C., Davidson, M. D., and Burdick, J. A. (2021a). 3D bioprinting of high cell-density heterogeneous tissue models through spheroid fusion within self-healing hydrogels. *Nat. Commun.* 12:753
- Daly, A. C., Prendergast, M. E., Hughes, A. J., and Burdick, J. A. (2021b). Bioprinting for the biologist. *Cell* 184, 18–32. doi: 10.1016/j.cell.2020.12.002
- Darnell, M., Young, S., Gu, L., Shah, N., Lippens, E., Weaver, J., et al. (2017). Substrate stress-relaxation regulates scaffold remodeling and bone formation in vivo. *Adv. Healthc. Mater.* 6:1601185.
- Dechow, P. C., Wang, Q., and Peterson, J. (2010). Edentulation alters material properties of cortical bone in the human craniofacial skeleton: functional implications for craniofacial structure in primate evolution. *Anat. Rec.* 293, 618–629. doi: 10.1002/ar.21124
- Di Bella, C., Duchi, S., O'Connell, C. D., Blanchard, R., Augustine, C., Yue, Z., et al. (2018). In situ handheld three-dimensional bioprinting for cartilage regeneration. *J. Tissue Eng. Regen. Med.* 12, 611–621. doi: 10.1002/term.2476
- Du, Y., Liu, H., Shuang, J., Wang, J., Ma, J., and Zhang, S. (2015). Microsphere-based selective laser sintering for building macroporous bone scaffolds with controlled microstructure and excellent biocompatibility. *Colloids Surf. B Biointerfaces* 135, 81–89. doi: 10.1016/j.colsurfb.2015.06.074
- Duarte Campos, D. F., Blaeser, A., Buellesbach, K., Sen, K. S., Xun, W., Tillmann, W., et al. (2016). Bioprinting organotypic hydrogels with improved mesenchymal stem cell remodeling and mineralization properties for bone tissue engineering. *Adv. Healthc. Mater.* 5, 1336–1345. doi: 10.1002/adhm.201501033
- Dubey, N., Ferreira, J. A., Malda, J., Bhaduri, S. B., and Bottino, M. C. (2020). Extracellular matrix/amorphous magnesium phosphate bioink for 3D bioprinting of Craniomaxillofacial bone tissue. *ACS Appl. Mater. Interfaces* 12, 23752–23763. doi: 10.1021/acsami.0c05311
- Ducheyne, P., and Qiu, Q. (1999). Bioactive ceramics: the effect of surface reactivity on bone formation and bone cell function. *Biomaterials* 20, 2287–2303. doi: 10.1016/s0142-9612(99)00181-7
- Dunn, C. A., Jin, Q., Taba, M., Franceschi, R. T., Bruce Rutherford, R., et al. (2005). BMP gene delivery for alveolar bone engineering at dental implant defects. *Mol. Ther.* 11, 294–299. doi: 10.1016/j.ymt.2004.10.005
- D'Urso, P. S., Barker, T. M., Earwaker, W. J., Bruce, L. J., Atkinson, R. L., Lanigan, M. W., et al. (1999). Stereolithographic biomodelling in cranio-maxillofacial surgery: a prospective trial. *J. Craniomaxillofac. Surg.* 27, 30–37. doi: 10.1016/s1010-5182(99)80007-9
- Egusa, H., Sonoyama, W., Nishimura, M., Atsuta, I., and Akiyama, K. (2012). Stem cells in dentistry—part I: stem cell sources. *J. Prosthodont. Res.* 56, 151–165. doi: 10.1016/j.jpor.2012.06.001
- Engler, A. J., Sen, S., Sweeney, H. L., and Discher, D. E. (2006). Matrix elasticity directs stem cell lineage specification. *Cell* 126, 677–689. doi: 10.1016/j.cell.2006.06.044
- Erisken, C., Kalyon, D. M., and Wang, H. (2008). Functionally graded electropun polycaprolactone and beta-tricalcium phosphate nanocomposites for tissue engineering applications. *Biomaterials* 29, 4065–4073. doi: 10.1016/j.biomaterials.2008.06.022
- Ersoy, A. E., Turkyilmaz, I., Ozan, O., and McGlumphy, E. A. (2008). Reliability of implant placement with stereolithographic surgical guides generated from computed tomography: clinical data from 94 implants. *J. Periodontol.* 79, 1339–1345. doi: 10.1902/jop.2008.080059
- Eskan, M. A., Girouard, M. E., Morton, D., and Greenwell, H. (2017). The effect of membrane exposure on lateral ridge augmentation: a case-controlled study. *Int. J. Implant Dent.* 3:26.
- Fang, J., Zhu, Y. Y., Smiley, E., Bonadio, J., Rouleau, J. P., Goldstein, S. A., et al. (1996). Stimulation of new bone formation by direct transfer of osteogenic plasmid genes. *Proc. Natl. Acad. Sci. U. S. A.* 93, 5753–5758. doi: 10.1073/pnas.93.12.5753
- Feine, J., Abou-Ayash, S., Al Mardini, M., de Santana, R. B., Bjelke-Holtermann, T., Bornstein, M. M., et al. (2018). Group 3 ITI consensus report: patient-reported outcome measures associated with implant dentistry. *Clin. Oral Implants Res.* 29(Suppl. 16), 270–275. doi: 10.1111/clr.13299
- Feng, K., Sun, H., Bradley, M. A., Dupler, E. J., Giannobile, W. V., and Ma, P. X. (2010). Novel antibacterial nanofibrous PLLA scaffolds. *J. Control. Release* 146, 363–369. doi: 10.1016/j.jconrel.2010.05.035
- Filippi, M., Born, G., Chaaban, M., and Scherberich, A. (2020). Natural polymeric scaffolds in bone regeneration. *Front. Bioeng. Biotechnol.* 8:474.
- George, E., Liacouras, P., Rybicki, F. J., and Mitsouras, D. (2017). Measuring and establishing the accuracy and reproducibility of 3D printed medical models. *Radiographics* 37, 1424–1450. doi: 10.1148/rq.2017160165
- Giannobile, W. V., Berglundh, T., Al-Nawas, B., Araujo, M., Bartold, P. M., Bouchard, P., et al. (2019). Biological factors involved in alveolar bone regeneration: consensus report of Working Group 1 of the 15(th) european workshop on periodontology on bone regeneration. *J. Clin. Periodontol.* 46(Suppl. 21), 6–11. doi: 10.1111/jcpe.13130
- Giannobile, W. V., Jung, R. E., Schwarz, F., and Groups of the 2nd Osteology Foundation Consensus Meeting. (2018). Evidence-based knowledge on the aesthetics and maintenance of peri-implant soft tissues: osteology foundation consensus report Part 1-effects of soft tissue augmentation procedures on the maintenance of peri-implant soft tissue health. *Clin. Oral Implants Res.* 29, 7–10. doi: 10.1111/clr.13110
- Giesen, E. B. W., Ding, M., Dalstra, M., and van Eijden, T. M. G. J. (2001). Mechanical properties of cancellous bone in the human mandibular condyle are anisotropic. *J. Biomech.* 34, 799–803. doi: 10.1016/s0021-9290(01)00030-6
- Gillison, M. L., Chaturvedi, A. K., Anderson, W. F., and Fakhry, C. (2015). Epidemiology of human papillomavirus-positive head and neck squamous cell carcinoma. *J. Clin. Oncol.* 33, 3235–3242. doi: 10.1200/jco.2015.61.6995
- Gladman, A. S., Matsumoto, E. A., Nuzzo, R. G., Mahadevan, L., and Lewis, J. A. (2016). Biomimetic 4D printing. *Nat. Mater.* 15, 413–418.
- Goh, B. T., Teh, L. Y., Tan, D. B., Zhang, Z., and Teoh, S. H. (2015). Novel 3D polycaprolactone scaffold for ridge preservation—a pilot randomised controlled clinical trial. *Clin. Oral Implants Res.* 26, 271–277. doi: 10.1111/clr.12486
- Goodson, J. M., Tanner, A. C., Haffajee, A. D., Sornberger, G. C., and Socransky, S. S. (1982). Patterns of progression and regression of advanced destructive periodontal disease. *J. Clin. Periodontol.* 9, 472–481. doi: 10.1111/j.1600-051x.1982.tb02108.x

- Grasso, M., Demir, A. G., Previtali, B., and Colosimo, B. M. (2018). In situ monitoring of selective laser melting of zinc powder via infrared imaging of the process plume. *Robot. Comput. Integr. Manuf.* 49, 229–239. doi: 10.1016/j.rcim.2017.07.001
- Grigoryan, B., Paulsen, S. J., Corbett, D. C., Sazer, D. W., Fortin, C. L., Zaita, A. J., et al. (2019). Multivascular networks and functional intravascular topologies within biocompatible hydrogels. *Science* 364, 458–464. doi: 10.1126/science.aav9750
- Groll, J., Burdick, J. A., Cho, D.-W., Derby, B., Gelinsky, M., Heilshorn, S. C., et al. (2018). A definition of bioinks and their distinction from biomaterial inks. *Biofabrication* 11:013001. doi: 10.1088/1758-5090/aec52
- Grottka, B. E., Noordin, S., Shortkroff, S., Schaffer, J. L., Thornhill, T. S., and Spector, M. (2002). Effect of mechanical perturbation on the release of PGE(2) by macrophages in vitro. *J. Biomed. Mater. Res.* 59, 288–293. doi: 10.1002/jbm.1244
- Gu, D. (2015). *Laser Additive Manufacturing of High-Performance Materials*. Berlin: Springer.
- Guvendiren, M., Molde, J., Soares, R. M., and Kohn, J. (2016). Designing biomaterials for 3D printing. *ACS Biomater. Sci. Eng.* 2, 1679–1693. doi: 10.1021/acsbomaterials.6b00121
- Hammarstrom, L., Heijl, L., and Gestrelus, S. (1997). Periodontal regeneration in a buccal dehiscence model in monkeys after application of enamel matrix proteins. *J. Clin. Periodontol.* 24, 669–677. doi: 10.1034/j.1600-051x.1997.00669.x
- Han, C., Yao, Y., Cheng, X., Luo, J., Luo, P., Wang, Q., et al. (2017). Electrophoretic deposition of gentamicin-loaded silk fibroin coatings on 3D-printed porous cobalt–chromium–molybdenum bone substitutes to prevent orthopedic implant infections. *Biomacromolecules* 18, 3776–3787. doi: 10.1021/acsbomac.7b01091
- Han, J., Kim, D. S., Jang, H., Kim, H.-R., and Kang, H.-W. (2019). Bioprinting of three-dimensional dentin–pulp complex with local differentiation of human dental pulp stem cells. *J. Tissue Eng.* 10:2041731419845849.
- Hao, J., Cheng, K. C., Kruger, L. G., Larsson, L., Sugai, J. V., Lahann, J., et al. (2016). Multigrowth factor delivery via immobilization of gene therapy vectors. *Adv. Mater.* 28, 3145–3151. doi: 10.1002/adma.201600027
- He, W., Tian, K., Xie, X., Wang, X., Li, Y., and Li, Z. (2015). Individualized surgical templates and titanium microplates for Le Fort I osteotomy by computer-aided design and computer-aided manufacturing. *J. Craniofac. Surg.* 26, 1877–1881. doi: 10.1097/scs.0000000000001938
- Hernández-Escobar, D., Champagne, S., Yilmazer, H., Dikici, B., Boehlert, C. J., and Hermawan, H. (2019). Current status and perspectives of zinc-based absorbable alloys for biomedical applications. *Acta Biomater.* 97, 1–22. doi: 10.1016/j.actbio.2019.07.034
- Hollister, S. J., Lin, C. Y., Saito, E., Schek, R. D., Taboas, J. M., Williams, J. M., et al. (2005). Engineering craniofacial scaffolds. *Orthod. Craniofac. Res.* 8, 162–173.
- Holmes, S. G., Still, K., Buttle, D. J., Bishop, N. J., and Grabowski, P. S. (2004). Chemically modified tetracyclines act through multiple mechanisms directly on osteoclast precursors. *Bone* 35, 471–478. doi: 10.1016/j.bone.2004.02.028
- Horn, D., Engel, M., Bodem, J. P., Hoffmann, J., and Freudlsperger, C. (2012). Reconstruction of a near-total nasal defect using a precontoured titanium mesh with a converse scalping flap. *J. Craniofac. Surg.* 23, e410–e412.
- Huang, K. H., Lin, Y. H., Shie, M. Y., and Lin, C. P. (2018). Effects of bone morphogenic protein-2 loaded on the 3D-printed MesoCS scaffolds. *J. Formos. Med. Assoc.* 117, 879–887. doi: 10.1016/j.jfma.2018.07.010
- Huebsch, N., Arany, P. R., Mao, A. S., Shvartsman, D., Ali, O. A., Bencherif, S. A., et al. (2010). Harnessing traction-mediated manipulation of the cell/matrix interface to control stem-cell fate. *Nat. Mater.* 9, 518–526. doi: 10.1038/nmat2732
- Huebsch, N., Lippens, E., Lee, K., Mehta, M., Koshy, S. T., Darnell, M. C., et al. (2015). Matrix elasticity of void-forming hydrogels controls transplanted-stem-cell-mediated bone formation. *Nat. Mater.* 14, 1269–1277. doi: 10.1038/nmat4407
- Hui, P. W., Leung, P. C., and Sher, A. (1996). Fluid conductance of cancellous bone graft as a predictor for graft–host interface healing. *J. Biomech.* 29, 123–132. doi: 10.1016/0021-9290(95)00010-0
- Hulbert, S. F., Young, F. A., Mathews, R. S., Klawitter, J. J., Talbert, C. D., and Stelling, F. H. (1970). Potential of ceramic materials as permanently implantable skeletal prostheses. *J. Biomed. Mater. Res.* 4, 433–456. doi: 10.1002/jbm.820040309
- Ikada, Y. (2006). Challenges in tissue engineering. *J. R. Soc. Interface* 3, 589–601.
- Ishaug, S. L., Crane, G. M., Miller, M. J., Yasko, A. W., Yaszemski, M. J., and Mikos, A. G. (1997). Bone formation by three-dimensional stromal osteoblast culture in biodegradable polymer scaffolds. *J. Biomed. Mater. Res.* 36, 17–28. doi: 10.1002/(sici)1097-4636(199707)36:1<17::aid-jbm3>3.0.co;2-o
- Iwata, T., Yamato, M., Washio, K., Yoshida, T., Tsumanuma, Y., Yamada, A., et al. (2018). Periodontal regeneration with autologous periodontal ligament-derived cell sheets - a safety and efficacy study in ten patients. *Regen. Ther.* 9, 38–44. doi: 10.1016/j.reth.2018.07.002
- Jacobs, C. A., and Lin, A. Y. (2017). A new classification of three-dimensional printing technologies: systematic review of three-dimensional printing for patient-specific craniomaxillofacial surgery. *Plast. Reconstr. Surg.* 139, 1211–1220. doi: 10.1097/prs.0000000000003232
- Jain, S., and Darveau, R. P. (2010). Contribution of *Porphyromonas gingivalis* lipopolysaccharide to periodontitis. *Periodontol* 2000 54, 53–70. doi: 10.1111/j.1600-0757.2009.00333.x
- Jakus, A. E., and Shah, R. N. (2017). Multi and mixed 3D-printing of graphene-hydroxyapatite hybrid materials for complex tissue engineering. *J. Biomed. Mater. Res. A* 105, 274–283. doi: 10.1002/jbm.a.35684
- Jardini, A. L., Larosa, M. A., Maciel Filho, R., Zavaglia, C. A., Bernardes, L. F., Lambert, C. S., et al. (2014). Cranial reconstruction: 3D biomodel and custom-built implant created using additive manufacturing. *J. Craniofac. Surg.* 42, 1877–1884. doi: 10.1016/j.jcms.2014.07.006
- Jensen, S. S., and Terheyden, H. (2009). Bone augmentation procedures in localized defects in the alveolar ridge: clinical results with different bone grafts and bone-substitute materials. *Int. J. Oral Maxillofac. Implants* 24(Suppl.), 218–236.
- Jin, Q. M., Anusaksathien, O., Webb, S. A., Rutherford, R. B., and Giannobile, W. V. (2003). Gene therapy of bone morphogenetic protein for periodontal tissue engineering. *J. Periodontol.* 74, 202–213. doi: 10.1902/jop.2003.74.2.202
- Jin, Q., Anusaksathien, O., Webb, S. A., Printz, M. A., and Giannobile, W. V. (2004). Engineering of tooth-supporting structures by delivery of PDGF gene therapy vectors. *Mol. Ther.* 9, 519–526. doi: 10.1016/j.ymthe.2004.01.016
- Jin, Q., Wei, G., Lin, Z., Sugai, J. V., Lynch, S. E., Ma, P. X., et al. (2008). Nanofibrous scaffolds incorporating PDGF-BB microspheres induce chemokine expression and tissue neogenesis in vivo. *PLoS One* 3:e1729. doi: 10.1371/journal.pone.0001729
- Kaigler, D., Avila-Ortiz, G., Travan, S., Taut, A. D., Padial-Molina, M., Rudek, L., et al. (2015). Bone engineering of maxillary sinus bone deficiencies using Enriched CD90+ Stem cell therapy: a randomized clinical trial. *J. Bone Miner. Res.* 30, 1206–1216. doi: 10.1002/jbmr.2464
- Kaigler, D., Pagni, G., Park, C. H., Braun, T. M., Holman, L. A., Yi, E., et al. (2013). Stem cell therapy for craniofacial bone regeneration: a randomized, controlled feasibility trial. *Cell Transplant.* 22, 767–777. doi: 10.3727/096368912x652968
- Kanno, Y., Nakatsuka, T., Saijo, H., Fujihara, Y., Atsuhiko, H., Chung, U., et al. (2016). Computed tomographic evaluation of novel custom-made artificial bones, “CT-bone”, applied for maxillofacial reconstruction. *Regen. Ther.* 5, 1–8. doi: 10.1016/j.reth.2016.05.002
- Kao, R. T., Nares, S., and Reynolds, M. A. (2015). Periodontal regeneration - intrabony defects: a systematic review from the AAP regeneration Workshop. *J. Periodontol.* 86, S77–S104.
- Karageorgiou, V., and Kaplan, D. (2005). Porosity of 3D biomaterial scaffolds and osteogenesis. *Biomaterials* 26, 5474–5491. doi: 10.1016/j.biomaterials.2005.02.002
- Keriquel, V., Guillemot, F., Arnault, I., Guillotin, B., Miraux, S., Amédée, J., et al. (2010). In vivo bioprinting for computer- and robotic-assisted medical intervention: preliminary study in mice. *Biofabrication* 2:014101. doi: 10.1088/1758-5082/2/1/014101
- Keriquel, V., Oliveira, H., Rémy, M., Ziane, S., Delmond, S., Rousseau, B., et al. (2017). In situ printing of mesenchymal stromal cells, by laser-assisted bioprinting, for in vivo bone regeneration applications. *Sci. Rep.* 7:1778.
- Khang, D., Choi, J., Im, Y. M., Kim, Y. J., Jang, J. H., Kang, S. S., et al. (2012). Role of subnano-, nano- and submicron-surface features on osteoblast differentiation of bone marrow mesenchymal stem cells. *Biomaterials* 33, 5997–6007. doi: 10.1016/j.biomaterials.2012.05.005

- Kim, J. Y., Ahn, G., Kim, C., Lee, J. S., Lee, I. G., An, S. H., et al. (2018). Synergistic effects of beta tri-calcium phosphate and porcine-derived decellularized bone extracellular matrix in 3D-printed polycaprolactone scaffold on bone regeneration. *Macromol. Biosci.* 18:e1800025.
- Kim, K., Lee, C. H., Kim, B. K., and Mao, J. J. (2010). Anatomically shaped tooth and periodontal regeneration by cell homing. *J. Dent. Res.* 89, 842–847. doi: 10.1177/0022034510370803
- Kinaci, A., Neuhaus, V., and Ring, D. C. (2014). Trends in bone graft use in the United States. *Orthopedics* 37, e783–e788.
- Kitamura, M., Akamatsu, M., Kawanami, M., Furuichi, Y., Fujii, T., Mori, M., et al. (2016). Randomized placebo-controlled and controlled non-inferiority Phase III trials comparing trafermin, a recombinant human fibroblast growth Factor 2, and enamel matrix derivative in periodontal regeneration in intrabony defects. *J. Bone Miner. Res.* 31, 806–814. doi: 10.1002/jbmr.2738
- Klein, F., Kim, T. S., Hassfeld, S., Staehle, H. J., Reitmeir, P., Holle, R., et al. (2001). Radiographic defect depth and width for prognosis and description of periodontal healing of infrabony defects. *J. Periodontol.* 72, 1639–1646. doi: 10.1902/jop.2001.72.12.1639
- Korioth, T. W., and Hannam, A. G. (1994). Deformation of the human mandible during simulated tooth clenching. *J. Dent. Res.* 73, 56–66. doi: 10.1177/00220345940730010801
- Korioth, T. W., Romilly, D. P., and Hannam, A. G. (1992). Three-dimensional finite element stress analysis of the dentate human mandible. *Am. J. Phys. Anthropol.* 88, 69–96. doi: 10.1002/ajpa.1330880107
- Kornman, K. S. (2008). Mapping the pathogenesis of periodontitis: a new look. *J. Periodontol.* 79, 1560–1568. doi: 10.1902/jop.2008.080213
- Kornman, K. S., Giannobile, W. V., and Duff, G. W. (2017). Quo vadis: what is the future of periodontics? how will we get there? *Periodontol.* 2000 75, 353–371. doi: 10.1111/prd.12217
- Kumar, S., Nehra, M., Kedia, D., Dilbaghi, N., Tankeshwar, K., and Kim, K. H. (2020). Nanotechnology-based biomaterials for orthopaedic applications: recent advances and future prospects. *Mater. Sci. Eng. C Mater. Biol. Appl.* 106:110154. doi: 10.1016/j.msec.2019.110154
- Lahann, J., Klee, D., Plueter, W., and Hoecker, H. (2001). Bioactive immobilization of r-hirudin on CVD-coated metallic implant devices. *Biomaterials* 22, 817–826. doi: 10.1016/s0142-9612(00)00244-1
- Larsson, L., Castilho, R. M., and Giannobile, W. V. (2015). Epigenetics and its role in periodontal diseases: a state-of-the-art review. *J. Periodontol.* 86, 556–568. doi: 10.1902/jop.2014.140559
- Larsson, L., Decker, A. M., Nibali, L., Pilipchuk, S. P., Berglundh, T., and Giannobile, W. V. (2016). Regenerative medicine for periodontal and peri-implant diseases. *J. Dent. Res.* 95, 255–266. doi: 10.1177/0022034515618887
- Lee, N., Robinson, J., and Lu, H. (2016). Biomimetic strategies for engineering composite tissues. *Curr. Opin. Biotechnol.* 40, 64–74. doi: 10.1016/j.copbio.2016.03.006
- Leong, K. F., Cheah, C. M., and Chua, C. K. (2003). Solid freeform fabrication of three-dimensional scaffolds for engineering replacement tissues and organs. *Biomaterials* 24, 2363–2378. doi: 10.1016/s0142-9612(03)00030-9
- Lethaus, B., Poort, L., Böckmann, R., Smeets, R., Tolba, R., and Kessler, P. (2012). Additive manufacturing for microvascular reconstruction of the mandible in 20 patients. *J. Craniomaxillofac. Surg.* 40, 43–46. doi: 10.1016/j.jcms.2011.01.007
- Lettry, S., Seedhom, B., Berry, E., and Cuppone, M. (2003). Quality assessment of the cortical bone of the human mandible. *Bone* 32, 35–44. doi: 10.1016/s8756-3282(02)00921-3
- Levine, J. P., Patel, A., Saadeh, P. B., and Hirsch, D. L. (2012). Computer-aided design and manufacturing in craniomaxillofacial surgery: the new state of the art. *J. Craniofac. Surg.* 23, 288–293. doi: 10.1097/scs.0b013e318241ba92
- Li, X., Liu, B., Pei, B., Chen, J., Zhou, D., Peng, J., et al. (2020). Inkjet bioprinting of biomaterials. *Chem. Rev.* 120, 10793–10833. doi: 10.1021/acs.chemrev.0c00008
- Li, Y., Zhou, J., Pavanram, P., Leeflang, M. A., Fockaert, L. I., Pouran, B., et al. (2018). Additively manufactured biodegradable porous magnesium. *Acta Biomater.* 67, 378–392.
- Li, Z., Mei, S., Dong, Y., She, F., Li, Y., Li, P., et al. (2020). Functional nanofibrous biomaterials of tailored structures for drug delivery—a critical review. *Pharmaceutics* 12:522. doi: 10.3390/pharmaceutics12060522
- Liang, C., Chen, J., Zhang, Y., Wei, F., Ling, Y., and Li, X. (2021). Construction of novel antimicrobial peptide-modified extracellular matrix biologic scaffold material. *Biochem. Biophys. Res. Commun.* 546, 162–168. doi: 10.1016/j.bbrc.2021.02.002
- Ligon, S. C., Liska, R., Stampfl, J., Gurr, M., and Mülhaupt, R. (2017). Polymers for 3D printing and customized additive manufacturing. *Chem. Rev.* 117, 10212–10290.
- Lim, K. S., Levato, R., Costa, P. F., Castilho, M. D., Alcalá-Orozco, C. R., Van Dorenmalen, K. M., et al. (2018). Bio-resin for high resolution lithography-based biofabrication of complex cell-laden constructs. *Biofabrication* 10:034101. doi: 10.1088/1758-5090/aac00c
- Lim, T. C., Chian, K. S., and Leong, K. F. (2010). Cryogenic prototyping of chitosan scaffolds with controlled micro and macro architecture and their effect on in vivo neo-vascularization and cellular infiltration. *J. Biomed. Mater. Res. A* 94, 1303–1311.
- Lin, Y. H., Chiu, Y. C., Shen, Y. F., Wu, Y. A., and Shie, M. Y. (2017). Bioactive calcium silicate/poly-ε-caprolactone composite scaffolds 3D printed under mild conditions for bone tissue engineering. *J. Mater. Sci. Mater. Med.* 29:11.
- Liu, T., Liu, L., Zeng, C., Liu, Y., and Leng, J. (2020). 4D printed anisotropic structures with tailored mechanical behaviors and shape memory effects. *Compos. Sci. Technol.* 186:107935. doi: 10.1016/j.compscitech.2019.107935
- Liu, Y., Ma, Y., Zhang, J., Xie, Q., Wang, Z., Yu, S., et al. (2017). MBG-modified β-TCP scaffold promotes mesenchymal stem cells adhesion and osteogenic differentiation via a FAK/MAPK signaling pathway. *ACS Appl. Mater. Interfaces* 9, 30283–30296. doi: 10.1021/acsami.7b02466
- Longoni, S., Tinto, M., Pacifico, C., Sartori, M., and Andreano, A. (2019). Effect of peri-implant keratinized tissue width on tissue health and stability: systematic review and meta-analysis. *Int. J. Oral Maxillofac. Implants* 34, 1307–1317. doi: 10.11607/jomi.7622
- Ma, J., Ma, L., Wang, Z., Zhu, X., and Wang, W. (2017). The use of 3D-printed titanium mesh tray in treating complex comminuted mandibular fractures: a case report. *Medicine* 96:e7250. doi: 10.1097/md.00000000000007250
- Ma, X., Qu, X., Zhu, W., Li, Y.-S., Yuan, S., Zhang, H., et al. (2016). Deterministically patterned biomimetic human iPSC-derived hepatic model via rapid 3D bioprinting. *Proc. Natl. Acad. Sci. U. S. A.* 113, 2206–2211. doi: 10.1073/pnas.1524510113
- Manodh, P., Prabhu Shankar, D., Pradeep, D., Santhosh, R., and Murugan, A. (2016). Incidence and patterns of maxillofacial trauma—a retrospective analysis of 3611 patients—an update. *Oral Maxillofac. Surg.* 20, 377–383. doi: 10.1007/s10006-016-0576-z
- Marcenes, W., Kassebaum, N. J., Bernabe, E., Flaxman, A., Naghavi, M., Lopez, A., et al. (2013). Global burden of oral conditions in 1990–2010: a systematic analysis. *J. Dent. Res.* 92, 592–597. doi: 10.1177/0022034513490168
- Markets and Markets (2020). *Dental Bone Graft Substitute Market by Type (Synthetic Bone Grafts, Xenograft, Allograft, Alloplast), Application (Sinus Lift, Ridge Augmentation, Socket Preservation), Product (Bio-OSS, OsteoGraft, Grafton), End User (Hospital)- Global Forecast to 2025* [Online]. Available online at: <https://www.marketsandmarkets.com/Market-Reports/dental-bone-graft-substitutes-market-159678690.html> (accessed March 25, 2021).
- Matulienė, G., Pjetursson, B. E., Salvi, G. E., Schmidlin, K., Bragger, U., Zwahlen, M., et al. (2008). Influence of residual pockets on progression of periodontitis and tooth loss: results after 11 years of maintenance. *J. Clin. Periodontol.* 35, 685–695. doi: 10.1111/j.1600-051x.2008.01245.x
- McGuire, M. K., and Scheyer, E. T. (2007). A randomized, double-blind, placebo-controlled study to determine the safety and efficacy of cultured and expanded autologous fibroblast injections for the treatment of interdental papillary insufficiency associated with the papilla priming procedure. *J. Periodontol.* 78, 4–17. doi: 10.1902/jop.2007.060105
- McGuire, M. K., Scheyer, E. T., and Schubach, P. (2016). A Prospective, case-controlled study evaluating the use of enamel matrix derivative on human buccal recession defects: a human histologic examination. *J. Periodontol.* 87, 645–653. doi: 10.1902/jop.2016.150459
- McGuire, M. K., Scheyer, E. T., Lipton, D. I., and Gunsolley, J. C. (2020). Randomized, controlled clinical trial to evaluate a xenogeneic collagen matrix as an alternative to free gingival grafting for oral soft tissue augmentation: 6 to 8 year follow-up. *J. Periodontol.* doi: 10.1002/JPER.20-0627 [Online ahead of print].
- Melcher, A. H. (1976). On the repair potential of periodontal tissues. *J. Periodontol.* 47, 256–260. doi: 10.1902/jop.1976.47.5.256

- Menezes, F. D. S., Fernandes, G. A., Antunes, J. L. F., Villa, L. L., and Toporcov, T. N. (2021). Global incidence trends in head and neck cancer for HPV-related and -unrelated subsites: a systematic review of population-based studies. *Oral Oncol.* 115:105177. doi: 10.1016/j.oraloncology.2020.105177
- Mikos, A. G., and Temenoff, J. S. (2000). Formation of highly porous biodegradable scaffolds for tissue engineering. *Electronic J. Biotechnol.* 3, 114–119.
- Miller, P. D. (1985). A classification of marginal tissue recession. *Int. J. Periodontics Restorative Dent.* 5, 8–13.
- Misch, C. E., Qu, Z., and Bidez, M. W. (1999). Mechanical properties of trabecular bone in the human mandible: implications for dental implant treatment planning and surgical placement. *J. Oral Maxillofac. Surg.* 57, 700–706. doi: 10.1016/s0278-2391(99)90437-8
- Monje, A., Pons, R., Insua, A., Nart, J., Wang, H. L., and Schwarz, F. (2019). Morphology and severity of peri-implantitis bone defects. *Clin. Implant. Dent. Relat. Res.* 21, 635–643.
- Moreno Rodriguez, J. A., Ortiz Ruiz, A. J., and Caffesse, R. G. (2019). Supra-alveolar attachment gain in the treatment of combined intra-suprabony periodontal defects by non-incised papillae surgical approach. *J. Clin. Periodontol.* 46, 927–936. doi: 10.1111/jcpe.13158
- Mota, C., Puppi, D., Chiellini, F., and Chiellini, E. (2015). Additive manufacturing techniques for the production of tissue engineering constructs. *J. Tissue Eng. Regen. Med.* 9, 174–190. doi: 10.1002/term.1635
- Msallem, B., Sharma, N., Cao, S., Halbeisen, F. S., Zeilhofer, H. F., and Thieringer, F. M. (2020). Evaluation of the dimensional accuracy of 3D-printed anatomical mandibular models using FFF, SLA, SLS, MJ, and BJ printing technology. *J. Clin. Med.* 9:817. doi: 10.3390/jcm9030817
- Muzaffar, J., Bari, S., Kirtane, K., and Chung, C. H. (2021). Recent advances and future directions in clinical management of head and neck squamous cell carcinoma. *Cancers* 13:338. doi: 10.3390/cancers13020338
- Nair, A. K., Gautieri, A., Chang, S. W., and Buehler, M. J. (2013). Molecular mechanics of mineralized collagen fibrils in bone. *Nat. Commun.* 4:1724.
- Naveh, G., Brumfeld, V., Shahar, R., and Weiner, S. (2013). Tooth periodontal ligament: direct 3D microCT visualization of the collagen network and how the network changes when the tooth is loaded. *J. Struct. Biol.* 181, 108–115. doi: 10.1016/j.jsb.2012.10.008
- Nehrer, S., Breinan, A., Ramappa, A., Young, G., Shortkroff, S., Louie, L., et al. (1997). Matrix collagen type and pore size influence behaviour of seeded canine chondrocytes. *Biomaterials* 18, 769–776. doi: 10.1016/s0142-9612(97)00001-x
- Nevins, M., Camelo, M., Nevins, M. L., Schenk, R. K., and Lynch, S. E. (2003). Periodontal regeneration in humans using recombinant human platelet-derived growth factor-BB (rhPDGF-BB) and allogenic bone. *J. Periodontol.* 74, 1282–1292. doi: 10.1902/jop.2003.74.9.1282
- Nevins, M., Giannobile, W. V., McGuire, M. K., Kao, R. T., Mellonig, J. T., Hinrichs, J. E., et al. (2005). Platelet-derived growth factor stimulates bone fill and rate of attachment level gain: results of a large multicenter randomized controlled trial. *J. Periodontol.* 76, 2205–2215. doi: 10.1902/jop.2005.76.12.2205
- Nevins, M., Kao, R. T., McGuire, M. K., McClain, P. K., Hinrichs, J. E., McAllister, B. S., et al. (2013). Platelet-derived growth factor promotes periodontal regeneration in localized osseous defects: 36-month extension results from a randomized, controlled, double-masked clinical trial. *J. Periodontol.* 84, 456–464. doi: 10.1902/jop.2012.120141
- Nyberg, E., Rindone, A., Dorafshar, A., and Grayson, W. L. (2017). Comparison of 3D-Printed Poly-ε-caprolactone scaffolds functionalized with tricalcium phosphate, hydroxyapatite, Bio-Oss, or decellularized bone matrix. *Tissue Eng. Part A* 23, 503–514. doi: 10.1089/ten.tea.2016.0418
- Obregon, F., Vaquette, C., Ivanovski, S., Huttmacher, D., and Bertassoni, L. (2015). Three-dimensional bioprinting for regenerative dentistry and craniofacial tissue engineering. *J. Dent. Res.* 94, 1435–1525.
- O'Connell, C. D., Di Bella, C., Thompson, F., Augustine, C., Beirne, S., Cornock, R., et al. (2016). Development of the Biopen: a handheld device for surgical printing of adipose stem cells at a chondral wound site. *Biofabrication* 8:015019. doi: 10.1088/1758-5090/8/1/015019
- Ojansivu, M., Rashad, A., Ahlinder, A., Massera, J., Mishra, A., Syverud, K., et al. (2019). Wood-based nanocellulose and bioactive glass modified gelatin-alginate bioinks for 3D bioprinting of bone cells. *Biofabrication* 11:035010. doi: 10.1088/1758-5090/ab0692
- Orr, T. E., Villars, P. A., Mitchell, S. L., Hsu, H. P., and Spector, M. (2001). Compressive properties of cancellous bone defects in a rabbit model treated with particles of natural bone mineral and synthetic hydroxyapatite. *Biomaterials* 22, 1953–1959. doi: 10.1016/s0142-9612(00)00370-7
- Oshima, M., and Tsuji, T. (2015). Whole tooth regeneration as a future dental treatment. *Adv. Exp. Med. Biol.* 881, 255–269. doi: 10.1007/978-3-319-22345-2_14
- Oshima, M., Mizuno, M., Imamura, A., Ogawa, M., Yasukawa, M., Yamazaki, H., et al. (2011). Functional tooth regeneration using a bioengineered tooth unit as a mature organ replacement regenerative therapy. *PLoS One* 6:e21531. doi: 10.1371/journal.pone.0021531
- Oshima, M., Ogawa, M., and Tsuji, T. (2017). Functional tooth regeneration. *Methods Mol. Biol.* 1597, 97–116. doi: 10.1007/978-1-4939-6949-4_8
- Ozolat, I. T., and Hospodiuk, M. (2016). Current advances and future perspectives in extrusion-based bioprinting. *Biomaterials* 76, 321–343. doi: 10.1016/j.biomaterials.2015.10.076
- Page, R. C., and Kornman, K. S. (1997). The pathogenesis of human periodontitis: an introduction. *Periodontol.* 2000 14, 9–11. doi: 10.1111/j.1600-0757.1997.tb00189.x
- Palmer, L., Newcomb, C., Kaltz, S., Spoerke, E., and Stupp, S. (2008). Biomimetic systems for hydroxyapatite mineralization inspired by bone and enamel. *Chem. Rev.* 108, 4754–4783. doi: 10.1021/cr8004422
- Papapanou, P. N., and Wennstrom, J. L. (1991). The angular bony defect as indicator of further alveolar bone loss. *J. Clin. Periodontol.* 18, 317–322. doi: 10.1111/j.1600-051x.1991.tb00435.x
- Papapanou, P. N., Sanz, M., Buduneli, N., Dietrich, T., Feres, M., Fine, D. H., et al. (2018). Periodontitis: consensus report of workgroup 2 of the 2017 world workshop on the classification of periodontal and peri-implant diseases and conditions. *J. Periodontol.* 89(Suppl. 1), S173–S182.
- Park, C. H., Kim, K. H., Lee, Y. M., Giannobile, W. V., and Seol, Y. J. (2017). 3D printed, microgroove pattern-driven generation of oriented ligamentous architectures. *Int. J. Mol. Sci.* 18:1927. doi: 10.3390/ijms18091927
- Park, C. H., Rios, H. F., Jin, Q., Bland, M. E., Flanagan, C. L., Hollister, S. J., et al. (2010). Biomimetic hybrid scaffolds for engineering human tooth-ligament interfaces. *Biomaterials* 31, 5945–5952. doi: 10.1016/j.biomaterials.2010.04.027
- Park, C. H., Rios, H. F., Jin, Q., Sugai, J. V., Padiol-Molina, M., Taut, A. D., et al. (2012). Tissue engineering bone-ligament complexes using fiber-guiding scaffolds. *Biomaterials* 33, 137–145. doi: 10.1016/j.biomaterials.2011.09.057
- Park, C. H., Rios, H. F., Taut, A. D., Padiol-Molina, M., Flanagan, C. L., Pilipchuk, S. P., et al. (2014). Image-based, fiber guiding scaffolds: a platform for regenerating tissue interfaces. *Tissue Eng. Part C Methods* 20, 533–542. doi: 10.1089/ten.tec.2013.0619
- Park, E. K., Lim, J. Y., Yun, I. S., Kim, J. S., Woo, S. H., Kim, D. S., et al. (2016). Cranioplasty enhanced by three-dimensional printing: custom-made three-dimensional-printed titanium implants for skull defects. *J. Craniofac. Surg.* 27, 943–949. doi: 10.1097/scs.00000000000002656
- Park, J. B. (2011). Effects of doxycycline, minocycline, and tetracycline on cell proliferation, differentiation, and protein expression in osteoprecursor cells. *J. Craniofac. Surg.* 22, 1839–1842. doi: 10.1097/SCS.0b013e31822e8216
- Park, J. H., Gillispie, G. J., Copus, J. S., Zhang, W., Atala, A., Yoo, J. J., et al. (2020). The effect of BMP-mimetic peptide tethering bioinks on the differentiation of dental pulp stem cells (DPSCs) in 3D bioprinted dental constructs. *Biofabrication* 12:035029. doi: 10.1088/1758-5090/ab9492
- Park, J. Y., Park, C. H., Yi, T., Kim, S. N., Iwata, T., and Yun, J. H. (2020). rhBMP-2 pre-treated human periodontal ligament stem cell sheets regenerate a mineralized layer mimicking dental cementum. *Int. J. Mol. Sci.* 21:3767. doi: 10.3390/ijms21113767
- Paschalis, E. P., Recker, R., DiCarlo, E., Doty, S. B., Atti, E., and Boskey, A. L. (2003). Distribution of collagen cross-links in normal human trabecular bone. *J. Bone Miner. Res.* 18, 1942–1946. doi: 10.1359/jbmr.2003.18.11.1942
- Pati, F., Song, T. H., Rijal, G., Jang, J., Kim, S. W., and Cho, D. W. (2015). Ornamenting 3D printed scaffolds with cell-laid extracellular matrix for bone tissue regeneration. *Biomaterials* 37, 230–241. doi: 10.1016/j.biomaterials.2014.10.012
- Pérez-Pérez, M. P., Gómez, E., and Sebastián, M. A. (2018). Delphi prospecton on additive manufacturing in 2030: implications for education and employment in Spain. *Materials* 11:1500. doi: 10.3390/ma11091500

- Peterson, J., Wang, Q., and Dechow, P. C. (2006). Material properties of the dentate maxilla. *Anat. Rec. A Discov. Mol. Cell Evol. Biol.* 288, 962–972. doi: 10.1002/ar.a.20358
- Pihlstrom, B. L., Michalowicz, B. S., and Johnson, N. W. (2005). Periodontal diseases. *Lancet* 366, 1809–1820.
- Pilipchuk, S. P., Fretwurst, T., Yu, N., Larsson, L., Kavanagh, N. M., Asa'ad, F., et al. (2018). Micropatterned scaffolds with immobilized growth factor genes regenerate bone and periodontal ligament-like tissues. *Adv. Healthc. Mater.* 7:e1800750.
- Pilipchuk, S. P., Monje, A., Jiao, Y., Hao, J., Kruger, L., Flanagan, C. L., et al. (2016). Integration of 3D printed and micropatterned polycaprolactone scaffolds for guidance of oriented collagenous tissue formation in vivo. *Adv. Healthc. Mater.* 5, 676–687. doi: 10.1002/adhm.201500758
- Porta, M., Tonda-Turo, C., Pierantozzi, D., Ciardelli, G., and Mancuso, E. (2020). Towards 3D multi-layer scaffolds for periodontal tissue engineering applications: addressing manufacturing and architectural challenges. *Polymers* 12:2233. doi: 10.3390/polym12102233
- Puppi, D., Chiellini, F., Piras, A. M., and Chiellini, E. (2010). Polymeric materials for bone and cartilage repair. *Prog. Polym. Sci.* 35, 403–440. doi: 10.1016/j.progpolymsci.2010.01.006
- Rasperini, G., Pilipchuk, S. P., Flanagan, C. L., Park, C. H., Pagni, G., Hollister, S. J., et al. (2015). 3D-printed bioresorbable scaffold for periodontal repair. *J. Dent. Res.* 94, 153S–157S.
- Raveendran, N. T., Vaquette, C., Meinert, C., Ipe, D. S., and Ivanovski, S. (2019). Optimization of 3D bioprinting of periodontal ligament cells. *Dent. Mater.* 35, 1683–1694. doi: 10.1016/j.dental.2019.08.114
- Reynolds, M. A., Kao, R. T., Nares, S., Camargo, P. M., Caton, J. G., Clem, D. S., et al. (2015). Periodontal regeneration - intrabony defects: practical applications from the AAP regeneration workshop. *Clin. Adv. Periodontics* 5, 21–29. doi: 10.1902/cap.2015.140062
- Rodrigo, J. P., Heideman, D. A., Garcia-Pedrero, J. M., Fresno, M. F., Brakenhoff, R. H., Díaz Molina, J. P., et al. (2014). Time trends in the prevalence of HPV in oropharyngeal squamous cell carcinomas in northern Spain (1990–2009). *Int. J. Cancer* 134, 487–492. doi: 10.1002/ijc.28355
- Roosa, S. M., Kemppainen, J. M., Moffitt, E. N., Krebsbach, P. H., and Hollister, S. J. (2010). The pore size of polycaprolactone scaffolds has limited influence on bone regeneration in an in vivo model. *J. Biomed. Mater. Res. A* 92, 359–368. doi: 10.1002/jbm.a.32381
- Saijo, H., Igawa, K., Kanno, Y., Mori, Y., Kondo, K., Shimizu, K., et al. (2009). Maxillofacial reconstruction using custom-made artificial bones fabricated by inkjet printing technology. *J. Artif. Organs* 12, 200–205. doi: 10.1007/s10047-009-0462-7
- Salgado, A. J., Coutinho, O. P., and Reis, R. L. (2004). Bone tissue engineering: state of the art and future trends. *Macromol. Biosci.* 4, 743–765. doi: 10.1002/mabi.200400026
- Sanchez, N., Fierravanti, L., Nunez, J., Vignoletti, F., Gonzalez-Zamora, M., Santamaria, S., et al. (2020). Periodontal regeneration using a xenogeneic bone substitute seeded with autologous periodontal ligament-derived mesenchymal stem cells: a 12-month quasi-randomized controlled pilot clinical trial. *J. Clin. Periodontol.* 47, 1391–1402. doi: 10.1111/jcpe.13368
- Sandino, C., and Lacroix, D. (2011). A dynamical study of the mechanical stimuli and tissue differentiation within a CaP scaffold based on micro-CT finite element models. *Biomech. Model. Mechanobiol.* 10, 565–576. doi: 10.1007/s10237-010-0256-0
- Sangkert, S., Meesane, J., Kamonmattayakul, S., and Chai, W. (2016). Modified silk fibroin scaffolds with collagen/decellularized pulp for bone tissue engineering in cleft palate: morphological structures and biofunctionalities. *Mater. Sci. Eng. C* 58, 1138–1149. doi: 10.1016/j.msec.2015.09.031
- Saska, S., Pilatti, L., Blay, A., and Shibli, J. A. (2021). Bioresorbable polymers: advanced materials and 4d printing for tissue engineering. *Polymers* 13:563. doi: 10.3390/polym13040563
- Schincaglia, G. P., Hebert, E., Farina, R., Simonelli, A., and Trombelli, L. (2015). Single versus double flap approach in periodontal regenerative treatment. *J. Clin. Periodontol.* 42, 557–566. doi: 10.1111/jcpe.12409
- Schliephake, H. (2010). Application of bone growth factors—the potential of different carrier systems. *Oral Maxillofac. Surg.* 14, 17–22. doi: 10.1007/s10006-009-0185-1
- Sculean, A., Chapple, I. L., and Giannobile, W. V. (2015a). Wound models for periodontal and bone regeneration: the role of biologic research. *Periodontol.* 2000 68, 7–20. doi: 10.1111/prd.12091
- Sculean, A., Nikolidakis, D., and Schwarz, F. (2008). Regeneration of periodontal tissues: combinations of barrier membranes and grafting materials - biological foundation and preclinical evidence: a systematic review. *J. Clin. Periodontol.* 35, 106–116. doi: 10.1111/j.1600-051x.2008.01263.x
- Sculean, A., Nikolidakis, D., Nikou, G., Ivanovic, A., Chapple, I. L., and Stavropoulos, A. (2015b). Biomaterials for promoting periodontal regeneration in human intrabony defects: a systematic review. *Periodontol.* 2000 68, 182–216. doi: 10.1111/prd.12086
- Seibert, J. S. (1983). Reconstruction of deformed, partially edentulous ridges, using full thickness onlay grafts. Part I. technique and wound healing. *Compend. Contin. Educ. Dent.* 4, 437–453.
- Seibert, J. S., and Salama, H. (1996). Alveolar ridge preservation and reconstruction. *Periodontol* 2000 11, 69–84. doi: 10.1111/j.1600-0757.1996.tb00185.x
- Seo, B.-M., Miura, M., Gronthos, S., Bartold, P. M., Batouli, S., Brahimi, J., et al. (2004). Investigation of multipotent postnatal stem cells from human periodontal ligament. *Lancet* 364, 149–155. doi: 10.1016/s0140-6736(04)16627-0
- Shah, N. J., Hyder, M. N., Quadir, M. A., Dorval Courchesne, N.-M., Seeherman, H. J., Nevins, M., et al. (2014). Adaptive growth factor delivery from a polyelectrolyte coating promotes synergistic bone tissue repair and reconstruction. *Proc. Natl. Acad. Sci. U. S. A.* 111, 12847–12852. doi: 10.1073/pnas.1408035111
- Shim, J.-H., Kim, M.-J., Park, J. Y., Pati, R. G., Yun, Y.-P., Kim, S. E., et al. (2015). Three-dimensional printing of antibiotics-loaded poly-ε-caprolactone/poly(lactic-co-glycolic acid) scaffolds for treatment of chronic osteomyelitis. *Tissue Eng. Regen. Med.* 12, 283–293. doi: 10.1007/s13770-015-0014-6
- Skylar-Scott, M. A., Uzel, S. G., Nam, L. L., Ahrens, J. H., Truby, R. L., Damaraju, S., et al. (2019). Biomaterials for organ-specific tissues with high cellular density and embedded vascular channels. *Sci. Adv.* 5:eaaw2459. doi: 10.1126/sciadv.aaw2459
- Smith, P. C., Martinez, C., Caceres, M., and Martinez, J. (2015). Research on growth factors in periodontology. *Periodontol.* 2000 67, 234–250. doi: 10.1111/prd.12068
- Socransky, S. S., Haffajee, A. D., Goodson, J. M., and Lindhe, J. (1984). New concepts of destructive periodontal disease. *J. Clin. Periodontol.* 11, 21–32. doi: 10.1111/j.1600-051x.1984.tb01305.x
- Soldatos, N. K., Stylianou, P., Koidou, V. P., Angelov, N., Yukna, R., and Romanos, G. E. (2017). Limitations and options using resorbable versus nonresorbable membranes for successful guided bone regeneration. *Quintessence Int.* 48, 131–147.
- Spalazzi, J. P., Dagher, E., Doty, S. B., Guo, X. E., Rodeo, S. A., and Lu, H. H. (2006a). In vivo evaluation of a tri-phasic composite scaffold for anterior cruciate ligament-to-bone integration. *Conf. Proc. IEEE Eng. Med. Biol. Soc.* 2006, 525–528.
- Spalazzi, J. P., Dagher, E., Doty, S. B., Guo, X. E., Rodeo, S. A., and Lu, H. H. (2008). In vivo evaluation of a multiphased scaffold designed for orthopaedic interface tissue engineering and soft tissue-to-bone integration. *J. Biomed. Mater. Res. A* 86, 1–12. doi: 10.1002/jbm.a.32073
- Spalazzi, J. P., Doty, S. B., Moffat, K. L., Levine, W. N., and Lu, H. H. (2006b). Development of controlled matrix heterogeneity on a triphasic scaffold for orthopedic interface tissue engineering. *Tissue Eng.* 12, 3497–3508. doi: 10.1089/ten.2006.12.3497
- Spector, M. (1994). Anorganic bovine bone and ceramic analogs of bone mineral as implants to facilitate bone regeneration. *Clin. Plast. Surg.* 21, 437–444. doi: 10.1016/s0094-1298(20)31021-x
- Spencer, L. J., Degu, A., Kalkidan, H. A., Solomon, M. A., Cristiana, A., Nooshin, A., et al. (2018). Global, regional, and national incidence, prevalence, and years lived with disability for 354 diseases and injuries for 195 countries and territories, 1990–2017: a systematic analysis for the Global Burden of Disease Study 2017. *Lancet* 392, 1789–1858.
- Suárez-López Del Amo, F., Monje, A., Padial-Molina, M., Tang, Z., and Wang, H. L. (2015). Biologic agents for periodontal regeneration and implant site development. *Biomed. Res. Int.* 2015:957518.

- Sudarmadji, N., Tan, J. Y., Leong, K. F., Chua, C. K., and Loh, Y. T. (2011). Investigation of the mechanical properties and porosity relationships in selective laser-sintered polyhedral for functionally graded scaffolds. *Acta Biomater.* 7, 530–537. doi: 10.1016/j.actbio.2010.09.024
- Sudheesh Kumar, P. T., Hashimi, S., Saifzadeh, S., Ivanovski, S., and Vaquette, C. (2018). Additively manufactured biphasic construct loaded with BMP-2 for vertical bone regeneration: a pilot study in rabbit. *Mater. Sci. Eng. C Mater. Biol. Appl.* 92, 554–564. doi: 10.1016/j.msec.2018.06.071
- Sugano, M., Negishi, Y., Endo-Takahashi, Y., Hamano, N., Usui, M., Suzuki, R., et al. (2014). Gene delivery to periodontal tissue using Bubble liposomes and ultrasound. *J. Periodontol. Res.* 49, 398–404. doi: 10.1111/jre.12119
- Sumida, T., Otawa, N., Kamata, Y. U., Kamakura, S., Mtsushita, T., Kitagaki, H., et al. (2015). Custom-made titanium devices as membranes for bone augmentation in implant treatment: clinical application and the comparison with conventional titanium mesh. *J. Craniomaxillofac. Surg.* 43, 2183–2188. doi: 10.1016/j.jcms.2015.10.020
- Sun, W., Starly, B., Nam, J., and Darling, A. (2005). Bio-CAD modeling and its applications in computer-aided tissue engineering. *Comput. Aided Des.* 37, 1097–1114. doi: 10.1016/j.cad.2005.02.002
- Sunyer, R., Conte, V., Escribano, J., Elosegui-Artola, A., Labernadie, A., Valon, L., et al. (2016). Collective cell durotaxis emerges from long-range intercellular force transmission. *Science* 353, 1157–1161. doi: 10.1126/science.aaf7119
- Swanson, W. B., Omi, M., Zhang, Z., Nam, H., Jung, Y., Wang, G., et al. (2021). Macropore design of tissue engineering scaffolds regulates mesenchymal stem cell differentiation fate. *Biomaterials* 272:120769. doi: 10.1016/j.biomaterials.2021.120769
- Taboas, J. M., Maddox, R. D., Krebsbach, P. H., and Hollister, S. J. (2003). Indirect solid free form fabrication of local and global porous, biomimetic and composite 3D polymer-ceramic scaffolds. *Biomaterials* 24, 181–194. doi: 10.1016/s0142-9612(02)00276-4
- Tao, O., Kort-Mascort, J., Lin, Y., Pham, H. M., Charbonneau, A. M., ElKashty, O. A., et al. (2019). The applications of 3D printing for craniofacial tissue engineering. *Micromachines* 10:480. doi: 10.3390/mi10070480
- Tavelli, L., Barootchi, S., Avila-Ortiz, G., Urban, I. A., Giannobile, W. V., and Wang, H. L. (2021a). Peri-implant soft tissue phenotype modification and its impact on peri-implant health: a systematic review and network meta-analysis. *J. Periodontol.* 92, 21–44. doi: 10.1002/jper.19-0716
- Tavelli, L., McGuire, M. K., Zucchelli, G., Rasperini, G., Feinberg, S. E., Wang, H. L., et al. (2020). Biologics-based regenerative technologies for periodontal soft tissue engineering. *J. Periodontol.* 91, 147–154. doi: 10.1002/jper.19-0352
- Tavelli, L., Ravidà, A., Barootchi, S., Chambrone, L., and Giannobile, W. V. (2021b). Recombinant human platelet-derived growth factor: a systematic review of clinical findings in oral regenerative procedures. *JDR Clin. Trans. Res.* 6, 161–173. doi: 10.1177/2380084420921353
- Tonetti, M. S., Christiansen, A. L., and Cortellini, P. (2017). Vertical subclassification predicts survival of molars with class II furcation involvement during supportive periodontal care. *J. Clin. Periodontol.* 44, 1140–1144. doi: 10.1111/jcpe.12789
- Tsai, S. J., Ding, Y. W., Shih, M. C., and Tu, Y. K. (2020). Systematic review and sequential network meta-analysis on the efficacy of periodontal regenerative therapies. *J. Clin. Periodontol.* 47, 1108–1120. doi: 10.1111/jcpe.13338
- Tse, J. R., and Engler, A. J. (2011). Stiffness gradients mimicking in vivo tissue variation regulate mesenchymal stem cell fate. *PLoS One* 6:e15978. doi: 10.1371/journal.pone.0015978
- Tsuruga, E., Takita, H., Itoh, H., Wakisaka, Y., and Kuboki, Y. (1997). Pore size of porous hydroxyapatite as the cell-substratum controls BMP-induced osteogenesis. *J. Biochem.* 121, 317–324. doi: 10.1093/oxfordjournals.jbchem.a021589
- Unterhofer, C., Wipplinger, C., Verius, M., Recheis, W., Thomé, C., and Ortler, M. (2017). Reconstruction of large cranial defects with poly-methyl-methacrylate (PMMA) using a rapid prototyping model and a new technique for intraoperative implant modeling. *Neurol. Neurochir. Pol.* 51, 214–220. doi: 10.1016/j.pjnns.2017.02.007
- Urban, I. A., Montero, E., Monje, A., and Sanz-Sanchez, I. (2019). Effectiveness of vertical ridge augmentation interventions: a systematic review and meta-analysis. *J. Clin. Periodontol.* 46(Suppl. 21), 319–339. doi: 10.1111/jcpe.13061
- Urban, I. A., Nagursky, H., and Lozada, J. L. (2011). Horizontal ridge augmentation with a resorbable membrane and particulated autogenous bone with or without anorganic bovine bone-derived mineral: a prospective case series in 22 patients. *Int. J. Oral Maxillofac. Implants* 26, 404–414.
- Urban, I. A., Nagursky, H., Lozada, J. L., and Nagy, K. (2013). Horizontal ridge augmentation with a collagen membrane and a combination of particulated autogenous bone and anorganic bovine bone-derived mineral: a prospective case series in 25 patients. *Int. J. Periodontics Restorative Dent.* 33, 299–307. doi: 10.11607/prd.1407
- Valvez, S., Reis, P. N. B., Susmel, L., and Berto, F. (2021). Fused filament fabrication-4D-printed shape memory polymers: a review. *Polymers* 13:701. doi: 10.3390/polym13050701
- Van Lenthe, G. H., de Waal Malefijt, M. C., and Huisjes, R. (1997). Stress shielding after total knee replacement may cause bone resorption in the distal femur. *J. Bone. Joint. Surg. Br.* 79, 117–122. doi: 10.1302/0301-620x.79b1.0790117
- Vaquette, C., Fan, W., Xiao, Y., Hamlet, S., Huttmacher, D. W., and Ivanovski, S. (2012). A biphasic scaffold design combined with cell sheet technology for simultaneous regeneration of alveolar bone/periodontal ligament complex. *Biomaterials* 33, 5560–5573. doi: 10.1016/j.biomaterials.2012.04.038
- Vaquette, C., Mitchell, J., Fernandez-Medina, T., Kumar, S., and Ivanovski, S. (2021). Resorbable additively manufactured scaffold imparts dimensional stability to extraskeletally regenerated bone. *Biomaterials* 269:120671. doi: 10.1016/j.biomaterials.2021.120671
- Vaquette, C., Pilipchuk, S. P., Bartold, P. M., Huttmacher, D. W., Giannobile, W. V., and Ivanovski, S. (2018). Tissue engineered constructs for periodontal regeneration: current status and future perspectives. *Adv. Healthc. Mater.* 7:e1800457.
- Vert, M., Li, S. M., Spenlehauer, G., and Guerin, P. (1992). Bioresorbability and biocompatibility of aliphatic polyesters. *J. Mater. Sci. Mater. Med.* 3, 432–446. doi: 10.1007/bf00701240
- Vining, K. H., and Mooney, D. J. (2017). Mechanical forces direct stem cell behaviour in development and regeneration. *Nat. Rev. Mol. Cell Biol.* 18, 728–742. doi: 10.1038/nrm.2017.108
- von Wilmowsky, C., Schwertner, M. G., Nkenke, E., Moest, T., Adler, W., and Ebker, T. (2020). Use of CAD-based pre-bent implants reduces theatre time in orbital floor reconstruction: results of a prospective study. *Br. J. Oral Maxillofac. Surg.* 58, 753–758. doi: 10.1016/j.bjoms.2019.11.020
- Wang, C. I., Cho, S. H., Cho, D., Ducote, C., Reddy, L. V., and Sinada, N. (2020). A 3D-printed guide to assist in sinus slot preparation for the optimization of zygomatic implant axis trajectory. *J. Prosthodontics* 29, 179–184. doi: 10.1111/jopr.13139
- Wang, H. L., and Al-Shammari, K. (2002). HVC ridge deficiency classification: a therapeutically oriented classification. *Int. J. Periodontics Restorative Dent.* 22, 335–343.
- Wang, X., Schwartz, Z., Gittens, R. A., Cheng, A., Olivares-Navarrete, R., Chen, H., et al. (2015). Role of integrin $\alpha 2 \beta 1$ in mediating osteoblastic differentiation on three-dimensional titanium scaffolds with submicron-scale texture. *J. Biomed. Mater. Res. A* 103, 1907–1918. doi: 10.1002/jbm.a.35323
- Wang, Y., and Ural, A. (2018). Effect of modifications in mineralized collagen fibril and extra-fibrillar matrix material properties on submicroscale mechanical behavior of cortical bone. *J. Mech. Behav. Biomed. Mater.* 82, 18–26. doi: 10.1016/j.jmbbm.2018.03.013
- Wei, G., Jin, Q., Giannobile, W. V., and Ma, P. X. (2007). The enhancement of osteogenesis by nano-fibrous scaffolds incorporating rhBMP-7 nanospheres. *Biomaterials* 28, 2087–2096. doi: 10.1016/j.biomaterials.2006.12.028
- Wen, P., Jauer, L., Voshage, M., Chen, Y., Poprawe, R., and Schleifenbaum, J. H. (2018). Densification behavior of pure Zn metal parts produced by selective laser melting for manufacturing biodegradable implants. *J. Mater. Process. Technol.* 258, 128–137. doi: 10.1016/j.jmatprotec.2018.03.007
- Wu, Y. A., Chiu, Y. C., Lin, Y. H., Ho, C. C., Shie, M. Y., and Chen, Y. W. (2019). 3D-printed bioactive calcium Silicate/Poly- ϵ -Caprolactone bioscaffolds modified with biomimetic extracellular matrices for bone regeneration. *Int. J. Mol. Sci.* 20:942. doi: 10.3390/ijms20040942
- Xia, Y., Zhou, P., Cheng, X., Xie, Y., Liang, C., Li, C., et al. (2013). Selective laser sintering fabrication of nano-hydroxyapatite/poly- ϵ -caprolactone scaffolds for bone tissue engineering applications. *Int. J. Nanomed.* 8, 4197–4213. doi: 10.2147/ijn.s50685

- Xuan, K., Li, B., Guo, H., Sun, W., Kou, X., He, X., et al. (2018). Deciduous autologous tooth stem cells regenerate dental pulp after implantation into injured teeth. *Sci. Transl. Med.* 10:eaf3227. doi: 10.1126/scitranslmed.aaf3227
- Xue, J., Wu, T., Dai, Y., and Xia, Y. (2019). Electrospinning and electrospun nanofibers: methods, materials, and applications. *Chem. Rev.* 119, 5298–5415.
- Yan, X., Chen, Y. R., Song, Y. F., Yang, M., Ye, J., Zhou, G., et al. (2019). Scaffold-based gene therapeutics for osteochondral tissue engineering. *Front. Pharmacol.* 10:1534.
- Yang, Y., Wang, G., Liang, H., Gao, C., Peng, S., Shen, L., et al. (2019). Additive manufacturing of bone scaffolds. *Int. J. Bioprint* 5:148.
- Yannas, I. (2015). *Tissue and Organ Regeneration in Adults*. Berlin: Springer.
- Yu, N., Nguyen, T., Cho, Y. D., Kavanagh, N. M., Ghassib, I., and Giannobile, W. V. (2019). Personalized scaffolding technologies for alveolar bone regenerative medicine. *Orthod. Craniofac. Res.* 22(Suppl. 1), 69–75. doi: 10.1111/ocr.12275
- Zhai, D., Xu, M., Liu, L., Chang, J., and Wu, C. (2017). Silicate-based bioceramics regulating osteoblast differentiation through a BMP2 signalling pathway. *J. Mater. Chem. B* 5, 7297–7306. doi: 10.1039/c7tb01931a
- Zhang, B., Zhang, W., Zhang, Z., Zhang, Y. F., Hingorani, H., Liu, Z., et al. (2019). Self-healing four-dimensional printing with an ultraviolet curable double-network shape memory polymer system. *ACS Appl. Mater. Interfaces* 11, 10328–10336. doi: 10.1021/acsami.9b00359
- Zhang, D., Wu, X., Chen, J., and Lin, K. (2018). The development of collagen based composite scaffolds for bone regeneration. *Bioact. Mater.* 3, 129–138. doi: 10.1016/j.bioactmat.2017.08.004
- Zhang, S., Cheng, X., Yao, Y., Wei, Y., Han, C., Shi, Y., et al. (2015). Porous niobium coatings fabricated with selective laser melting on titanium substrates: preparation, characterization, and cell behavior. *Mater. Sci. Eng. C* 53, 50–59. doi: 10.1016/j.msec.2015.04.005
- Zhang, W., and Yelick, P. C. (2018). Craniofacial tissue engineering. *Cold Spring Harb. Perspect. Med.* 8:a025775.
- Zhang, W., Zhu, Y., Li, J., Guo, Q., Peng, J., Liu, S., et al. (2016). Cell-Derived extracellular matrix: basic characteristics and current applications in orthopedic tissue engineering. *Tissue Eng. Part B Rev.* 22, 193–207. doi: 10.1089/ten.teb.2015.0290
- Zhang, Y., Miron, R. J., Li, S., Shi, B., Sculean, A., and Cheng, X. (2015). Novel MesoPorous BioGlass/silk scaffold containing adPDGF-B and adBMP7 for the repair of periodontal defects in beagle dogs. *J. Clin. Periodontol.* 42, 262–271. doi: 10.1111/jcpe.12364
- Zhang, Z., Cheng, X., Yao, Y., Luo, J., Tang, Q., Wu, H., et al. (2016). Electrophoretic deposition of chitosan/gelatin coatings with controlled porous surface topography to enhance initial osteoblast adhesive responses. *J. Mater. Chem. B* 4, 7584–7595. doi: 10.1039/c6tb02122k
- Zhou, J., and Sheiko, S. S. (2016). Reversible shape-shifting in polymeric materials. *J. Polym. Sci. Part B Polym. Phys.* 54, 1365–1380. doi: 10.1002/polb.24014
- Zhou, X., Jin, Y., and Du, J. (2020). Functionally graded scaffolds with programmable pore size distribution based on triply periodic minimal surface fabricated by selective laser melting. *Materials* 13:5046. doi: 10.3390/ma13215046
- Zhu, L., Luo, D., and Liu, Y. (2020). Effect of the nano/microscale structure of biomaterial scaffolds on bone regeneration. *Int. J. Oral Sci.* 12:6.
- Zucchelli, G., Tavelli, L., McGuire, M. K., Rasperini, G., Feinberg, S. E., and Wang, H. L. (2020). Autogenous soft tissue grafting for periodontal and peri-implant plastic surgical reconstruction. *J. Periodontol.* 91, 9–16. doi: 10.1002/jper.19-0350

Conflict of Interest: The authors declare that the research was conducted in the absence of any commercial or financial relationships that could be construed as a potential conflict of interest.

Publisher's Note: All claims expressed in this article are solely those of the authors and do not necessarily represent those of their affiliated organizations, or those of the publisher, the editors and the reviewers. Any product that may be evaluated in this article, or claim that may be made by its manufacturer, is not guaranteed or endorsed by the publisher.

Copyright © 2021 Latimer, Maekawa, Yao, Wu, Chen and Giannobile. This is an open-access article distributed under the terms of the Creative Commons Attribution License (CC BY). The use, distribution or reproduction in other forums is permitted, provided the original author(s) and the copyright owner(s) are credited and that the original publication in this journal is cited, in accordance with accepted academic practice. No use, distribution or reproduction is permitted which does not comply with these terms.



Tissue Engineering in Stomatology: A Review of Potential Approaches for Oral Disease Treatments

Lilan Cao^{1‡}, Huiying Su^{1‡}, Mengying Si¹, Jing Xu¹, Xin Chang¹, Jiajia Lv^{1,2} and Yuankun Zhai^{1,2*†}

¹School of Stomatology, Henan University, Kaifeng, China, ²Henan International Joint Laboratory for Nuclear Protein Regulation, Kaifeng, China

OPEN ACCESS

Edited by:

Stefano Sivoletta,
University Hospital of Padua, Italy

Reviewed by:

Giovanna Orsini,
Marche Polytechnic University, Italy
Luca Sbricoli,
University of Padua, Italy

*Correspondence:

Yuankun Zhai
zhaiyuankun@henu.edu.cn

†ORCID:

Yuankun Zhai
orcid.org/0000-0001-8156-1368

[‡]These authors have contributed
equally to this work

Specialty section:

This article was submitted to
Tissue Engineering and Regenerative
Medicine,
a section of the journal
Frontiers in Bioengineering and
Biotechnology

Received: 01 February 2021

Accepted: 01 October 2021

Published: 08 November 2021

Citation:

Cao L, Su H, Si M, Xu J, Chang X, Lv J
and Zhai Y (2021) Tissue Engineering in
Stomatology: A Review of Potential
Approaches for Oral
Disease Treatments.
Front. Bioeng. Biotechnol. 9:662418.
doi: 10.3389/fbioe.2021.662418

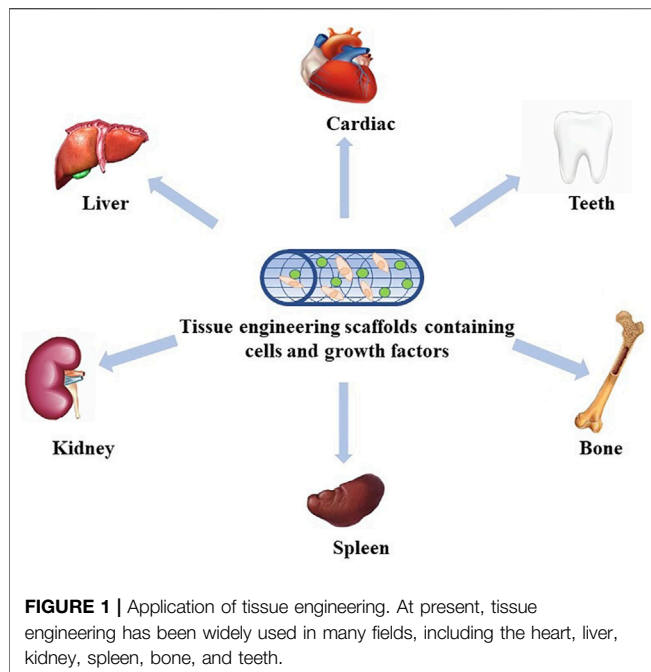
Tissue engineering is an emerging discipline that combines engineering and life sciences. It can construct functional biological structures *in vivo* or *in vitro* to replace native tissues or organs and minimize serious shortages of donor organs during tissue and organ reconstruction or transplantation. Organ transplantation has achieved success by using the tissue-engineered heart, liver, kidney, and other artificial organs, and the emergence of tissue-engineered bone also provides a new approach for the healing of human bone defects. In recent years, tissue engineering technology has gradually become an important technical method for dentistry research, and its application in stomatology-related research has also obtained impressive achievements. The purpose of this review is to summarize the research advances of tissue engineering and its application in stomatology. These aspects include tooth, periodontal, dental implant, cleft palate, oral and maxillofacial skin or mucosa, and oral and maxillofacial bone tissue engineering. In addition, this article also summarizes the commonly used cells, scaffolds, and growth factors in stomatology and discusses the limitations of tissue engineering in stomatology from the perspective of cells, scaffolds, and clinical applications.

Keywords: tissue engineering, scaffolds, growth factors, periodontal, dental implants, cleft palate, oral and maxillofacial skin or mucosa, oral and maxillofacial bone

INTRODUCTION

In the 1980s, Professor Joseph P. Vacanti and Robert Langer from the United States first explored tissue engineering research (Vacanti et al., 1988). In 1993, they defined tissue engineering in an article as “an interdisciplinary field that applies the principles of engineering and the life sciences toward the development of biological substitutes that restore, maintain, or improve tissue function” (Langer and Vacanti, 1993).

Nowadays, tissue engineering technology is booming and has become a popular research method for the reconstruction of damaged or missing tissues and organs (Fang et al., 2021; Farhat et al., 2021; Shang et al., 2021), and breakthroughs have been made in many fields (**Figure 1**) (Gosselin et al., 2018; Anandakrishnan and Azeloglu, 2020; Mirdamadi et al., 2020; Berbéri et al., 2021; Li et al., 2021; Scott et al., 2021). Therefore, we believe that tissue engineering technology will create extensive innovation in the field of stomatology. The basic principle of tissue engineering is to collect functionally related cells and plant them on a natural or synthetic scaffold with a certain spatial structure and induce cell proliferation through the influence of growth factors, thereby regenerating tissues or organs (**Figure 2**) (Han et al., 2014; Dzobo et al., 2018; Dey et al., 2020).



Cells are the source of biological activity in tissue engineering. Embryonic stem cells (ESCs) and adult mesenchymal stem cells (MSCs) are two types of stem cells classified according to their differentiation potential (Kolagar et al., 2020; Haghighat et al., 2021). Because of the ethical issues that limit the use of ESCs, multiple sources of MSCs have been more widely used in tissue engineering (Nancarrow-Lei et al., 2017). Induced pluripotent stem cells (iPSCs), which are obtained by artificially inducing somatic cells to express some specific genes, have the ability to divide indefinitely and hold a pluripotent differentiation capacity that enables them to differentiate into any human cells (Deicher and Seeger, 2021). In addition to bone mesenchymal stem cells

(BMSCs) (Nakamura et al., 2013; Yoo et al., 2013; Selvasandran et al., 2018; Li Y. et al., 2019; Xu M. et al., 2019) and adipose-derived stromal cells (ADSCs) (Yoon et al., 2011; Yao et al., 2012; Mihaila et al., 2014; Zhu et al., 2019; Xu et al., 2020), various MSCs have also been derived from teeth in recent years (Volponi et al., 2010), such as dental pulp stem cells (DPSCs) (Chen Y.-Y. et al., 2016; Lambrechts et al., 2017), stem cells from human exfoliated deciduous teeth (SHEDs) (Alkai et al., 2013; Alipour et al., 2014; Behnia et al., 2014; Sugimura-Wakayama et al., 2015), periodontal ligament stem cells (PDLSCs) (Kim et al., 2010; Chen F.-M. et al., 2016; Panduwawala et al., 2017), stem cells from apical papilla (SCAPs) (Bakopoulou et al., 2011; Somoza et al., 2017; Yang et al., 2018; Yang et al., 2020; Shen et al., 2021), dental follicle cells (DFCs) (Tian et al., 2015; Yildirim et al., 2016; Lima et al., 2017), and gingival mesenchymal stem cells (GMSCs) (Zhang et al., 2009; Ansari et al., 2016; Shi et al., 2017; Rao et al., 2019; Liu X. et al., 2020) (Table 1). Scaffolds provide a suitable space for cell growth and functions. There are two main categories of scaffolding material used in tissue engineering research: natural and synthetic materials, such as ceramics, proteins, and polymers (Table 2) (Rai et al., 2015). Due to the limitations of single-type materials, composite scaffolds composed of two or more different materials have gradually attracted attention (Mogoşanu and Grumezescu, 2014). In recent years, the third-generation scaffolds are capable of promoting angiogenesis and inducing osteogenesis (Thein-Han and Xu, 2011). As carriers, scaffolds can provide sustained-release growth factors, which are soluble polypeptides that bind to cell membrane receptors (Pilipchuk et al., 2015). Some of these growth factors can promote epithelial regeneration, such as epidermal growth factor (EGF) (Zhao et al., 2010), and some induce bone formation such as bone morphogenetic protein (BMP), transforming growth factor- β (TGF- β), and basic fibroblast growth factor (bFGF). (Park et al., 2015), while others such as platelet-derived growth factor (PDGF) and vascular endothelial growth factor (VEGF) are beneficial in

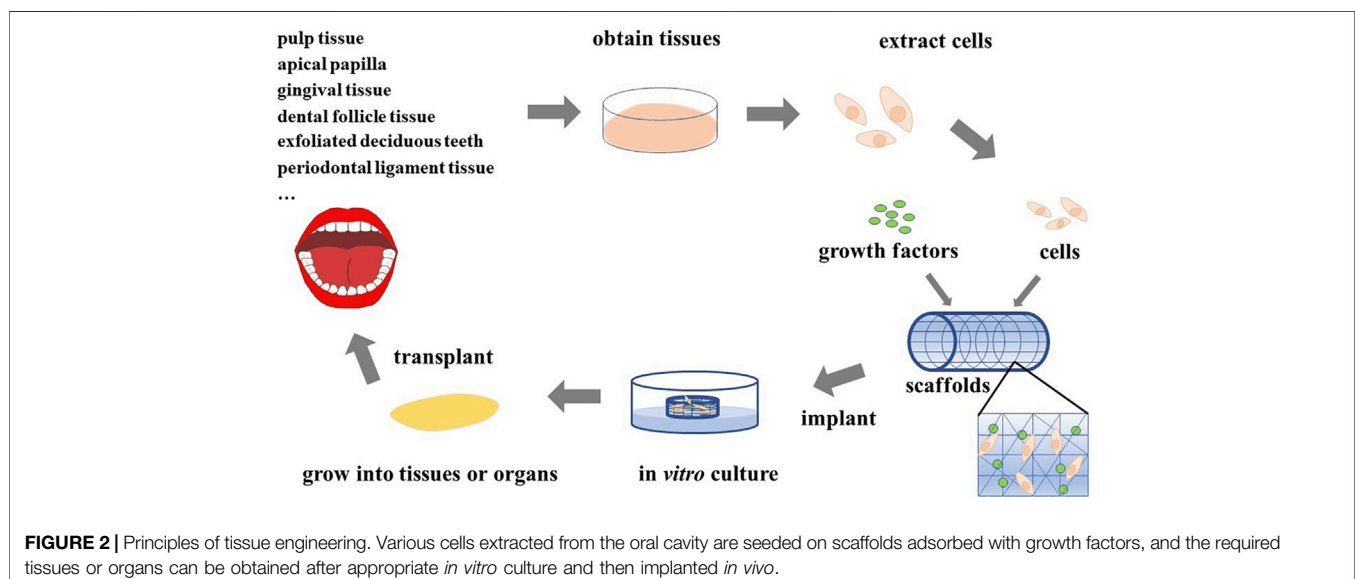


TABLE 1 | Cells commonly used in oral tissue engineering.

Cell	Sources	Functions	References
DPSCs	Pulp tissue	(1) Multidirectional differentiation potential; (2) play a paracrine effect on nerve cells and endothelial cells; (3) promote pulp regeneration; (4) expression of tendon markers under mechanical load	Chen et al. (2016b); Lambrechts et al. (2017)
SHED	Exfoliated deciduous teeth	(1) Extensive proliferation and differentiation ability; (2) enhance osteogenesis ability and repair bone defect; (3) inhibit the proliferation of T lymphocytes; (4) enhance peripheral nerve regeneration	Alkaiasi et al. (2013); Alipour et al. (2014); Behnia et al. (2014); Sugimura-Wakayama et al. (2015)
PDLSCs	Periodontal ligament tissue	(1) Immunomodulatory effect on peripheral blood mononuclear cells of the same and heterogeneous species; (2) multidirectional differentiation potential and promotion of periodontal tissue regeneration; (3) treatment of periodontal bone defects	Kim et al. (2010); Chen et al. (2016a); Panduwawala et al. (2017)
SCAP	Apical papilla	(1) High proliferation rate and mineralization potential; (2) renewable dentin paste complex; (3) secrete TGF- β 3; (4) capable of cloning and multiline differentiation; (5) express mesenchymal stem cell markers; (6) possesses the ability of cartilage differentiation and the potential to promote cartilage tissue regeneration	Bakopoulou et al. (2011); Somoza et al. (2017); Yang et al. (2018); Yang et al. (2020); Shen et al. (2021)
DFCs	Dental follicle tissue	(1) High proliferation potential; (2) excellent bone formation, fat formation and cartilage formation ability; (3) inhibit lymphocyte proliferation and apoptosis; (4) promote regeneration of dentin tissue; (5) express embryo, mesenchymal, and neural stem cell markers	Tian et al. (2015); Yildirim et al. (2016); Lima et al. (2017)
GMSCs	Gingival tissue	(1) Exhibit clonogenicity, self-renewal, and multipotent differentiation capacities; (2) immunomodulatory and anti-inflammatory component of the immune system <i>in vivo</i> ; (3) promote tissue regeneration; (4) derived exosomes can promote wound healing and nerve regeneration; (5) regulate lipid metabolism and inflammation	Zhang et al. (2009); Ansari et al. (2016); Shi et al. (2017); Rao et al. (2019); Liu et al. (2020a)
ABMSCs	Alveolar bone	(1) Proliferation and differentiation ability; (2) improve the phagocytic activity of THP-1 macrophages; (3) inhibit the activation and proliferation of T lymphocytes; (4) excellent osteogenic differentiation ability and bone defect reconstruction ability	Liu et al. (2020b); Cao et al. (2020)
TGSCs	Tooth germ	(1) Affect the formation of new blood vessels, bone, fat and neurogenesis; (2) odontogenesis and osteogenesis	Yalvac et al. (2010); Taşlı et al. (2014); Ercal et al. (2017)
BMSCs	Bone marrow tissue	(1) The potential for self-renewal and multidirectional differentiation; (2) possesses fat-forming ability, bone-forming ability and angiogenesis ability; (3) promote wound healing; (4) secrete TGF- β and weaken the immune response in ischemic brain; (5) promote myocardial healing and improve heart function	Nakamura et al. (2013); Yoo et al. (2013); Selvasandran et al. (2018); Li et al. (2019b); Xu et al. (2019b)
ADSCs	Adipose tissue	(1) Good proliferation ability and cartilage differentiation potential; (2) promote fat formation; (3) osteogenic capacity; (4) paracrine function promotes blood vessel formation; (5) reduce the production of active oxygen and inflammation and improve skin photoaging	Yoon et al. (2011); Yao et al. (2012); Mihaila et al. (2014); Zhu et al. (2019); Xu et al. (2020)
NSCs	Primary tissues, somatic cells, and pluripotent stem cells	(1) Self-renewal and multidirectional differentiation ability; (2) potential to promote nerve regeneration	Bonaguidi et al. (2011); Ng et al. (2019)
ESCs	The early mammalian embryo	(1) Produce functional anterior pituitary gland; (2) excellent osteogenesis and angiogenesis ability; (3) rebuild epithelial tissue; (4) augment cardiomyocyte-driven heart regeneration	Ozone et al. (2016); Chen et al. (2018); Bargehr et al. (2019); Zhao et al. (2019)
iPSCs	SCAP, DPSCs, and SHED, gingival and periodontal ligament fibroblasts, and buccal mucosa fibroblasts	(1) Excellent osteogenesis and angiogenesis ability; (2) promote the formation of cementum, alveolar bone, and periodontal ligament to help PDL regeneration; (3) anti-inflammatory effects	Duan et al. (2011); Yang et al. (2014); Chen et al. (2018)

Abbreviations: DPSCs, dental pulp stem cells; SHED, stem cells from exfoliated deciduous teeth; PDLSCs, periodontal ligament stem cells; SCAP, stem cells from apical papilla; DFCs, dental follicle cells; GMSCs, gingival mesenchymal stem cells; ABMSCs, alveolar bone-derived mesenchymal stem cells; TGSCs, tooth germ stem cells; BMSCs, bone marrow stromal stem cells; ADSCs, adipose-derived stromal cells; NSCs, neural stem cells; ESCs, embryonic stem cells; iPSCs, induced pluripotent stem cells.

TABLE 2 | Scaffolds commonly used in oral tissue engineering.

Type	Scaffolds	Advantages	Disadvantages	References
Naturally, derived polymeric scaffolds	Collagen	Favorable biocompatibility Major protein of connective tissue Low antigenicity	Poor mechanical properties Unmanageable biodegradation rate	Chattopadhyay and Raines (2014); Chang et al. (2016)
	Alginate	Excellent biocompatibility Low cost Low immunogenicity	Not conducive to cell adhesion Low cell adhesion	Lambricht et al. (2014); Liao et al. (2017)
	Chitosan	Favorable bioactivity Low cytotoxicity Sterilizable; enhance bone and cartilage formation	Slow degradation rate Inferior mechanical strength	Bhardwaj and Kundu (2012); Muzzarelli et al. (2015); Vishwanath et al. (2016)
	Hyaluronic acid	Participate in various biological processes Turn over quickly Bioactivity	Low mechanical strength Complex structure	Lataillade et al. (2010); Ferroni et al. (2015); Chang et al. (2017)
	Bioceramic	Excellent biocompatibility Non-immunogenic Stable; high porosity	Low biodegradability Inherent brittleness	Chang et al., (2017); Yu et al. (2017)
	PEG	Favorable biocompatibility Low cytotoxicity Great hydrophilicity	Low cell reactivity Inert bioactivity Non-biodegradability	Zhu and Marchant (2011); Singh et al. (2013)
Synthetic scaffolds	PLLA	Great mechanical strength Non-toxic biodegradable	Rapid degradation Poor toughness	Amjadi et al. (2016)
	PLGA	Favorable biocompatibility Non-toxic biodegradable Allow to control the degradation rate	Inferior cell affinity Poor hydrophilicity Swelling reaction of polymer	Gentile et al. (2014); Zhao et al. (2016b); Martins et al. (2018)
	PCL	Excellent thermal stability Good mechanical properties	Inferior cell affinity Poor hydrophilicity	Siddiqui et al. (2018)
	Collagen and chitosan	Good flexibility	Chitosan is insoluble in water and most organic solvents	Fu et al. (2017); Lauritano et al. (2020); Wang et al. (2020)
Composite scaffolds	HA-PLGA	Reinforce the structure Increase pore size Reduce the brittleness of the ceramics	Poor potentiality in cell adhesion/migration and proliferation Low degradation rates which cause exists longer time in cellular environment	Namini et al. (2018); Brassolatti et al. (2021)
	PEG-PLGA	Better cell adhesion Accelerate periapical bone repair Biodegrade to carbon dioxide and water	Cellular responses are not sufficient. Prohibitive cost Premix with autologous SCAP	Shiehzhadeh et al. (2014); Raddall et al. (2019)

Abbreviations: PEG, polyethylene glycol; PLLA, poly(L-lactide) acid; PLGA, poly(lactic-co-glycolic acid); PCL, polycaprolactone; HA, hydroxyapatite.

forming a functional vascular network (Table 3) (Yang et al., 2012). In conclusion, the core of tissue engineering lies in the establishment of a perfect three-dimensional spatial complex that consists of scaffolds, seed cells, and growth factors (Table 4).

TOOTH TISSUE ENGINEERING

The tooth, an indispensable organ to humans, consists of soft connective tissues, namely, the pulp in the pulp cavity, and three outer layers of mineralized hard tissue, such as enamel, cementum, and dentin, playing an important role in mastication, pronunciation, and aesthetics. Tooth development is accomplished by a series of epithelial-mesenchymal interactions and reciprocal inductions, which ultimately lead to cell differentiation and developmental space formation (Yuan and Chai, 2019). Tooth

loss, which is caused by many reasons, such as dental caries, tooth agenesis, or trauma, is a common oral disease that seriously affects physiological functions and even increases the morbidity of gastrointestinal cancer (Ma et al., 2018), cardiovascular disease, and stroke (Cheng et al., 2018). Moreover, permanent teeth are not renewable once they fall off. At present, removable dentures and fixed dentures are commonly used in the clinic to repair missing teeth, but these traditional restorative methods suffer some flaws, such as causing discomfort and inefficient mastication (Hejazi et al., 2021). Hence, the construction of biological tissue-engineered teeth has emerged to solve these disadvantages. Tooth regeneration therapy for dental tissue repair and whole-tooth replacement has been a long-term goal to achieve in dentistry.

Researchers have already made some progress during the regeneration of partial dental tissues. Regenerative endodontics (RE) mostly utilize the strategy of cell homing and

TABLE 3 | Growth factors commonly used in oral tissue engineering.

Inducibility	Growth factors	Features	Oral applications	References
Pro-epithelialization	EGF	Induce stem cells to differentiate into epidermal cells Promote the fibroblast proliferation	Promote the early healing of acute oral soft tissue wounds	Xing et al. (2013); Ben Amara et al. (2019)
Pro-osteogenesis	BMP	Induce mineralization Bone and cartilage regeneration Belong to TGF- β family	Induce the differentiation of SHED into odontoblasts	Casagrande et al. (2010); Kim et al. (2012b); Agrawal and Sinha (2017)
	IGF	Initiate cell growth Induce cell proliferation Combined with BMP2 can synergistically promote osteogenic differentiation	IGF-1 family participate in the process of pulpal differentiation	Caviedes-Bucheli et al. (2009); Kim et al. (2012a); Magnucki et al. (2013)
	TGF- β	Regulate extracellular matrix synthesis Induce fundamental cell processes such as proliferation, chemotaxis and apoptosis	Stimulate odontoblast to secrete matrix Promote osteogenic differentiation of DPSCs	Wang et al. (2017); Weiss and Attisano (2013); Wang et al. (2017); Niwa et al. (2018)
Pro-angiogenesis	VEGF	The major factor for angiogenesis Regulate endothelial cell secretion and proliferation	Enhance proliferation and osteogenic differentiation of DPSCs <i>in vitro</i>	D' Alimonte et al. (2011); Shibuya (2013)
	PDGF	Induce VSMCs proliferation and migration Promote osteogenic differentiation Induce MSCs chemotaxis and proliferation	A combination of collagen membrane and bone graft material mixed with rhPDGF-BB achieved alveolar ridge augmentation A collagen matrix infused with rhPDGF-BB increased the soft tissue volume in esthetic peri-implant sites	Simion et al. (2012); Funato et al. (2013); Jin et al. (2014); Tan et al. (2015); Zhao et al. (2016a)
		Stimulate proliferation of fibroblasts and capillary endothelial cells Promote angiogenesis and wound healing	bFGF contributed to pulp cells proliferation and dentin matrix formation	
Pro-neurogenic	NGF	Regulate the growth and development of neurons Facilitate axonal regrowth	Induce the differentiation of immortalized dental papilla cells into odontoblasts <i>in vitro</i>	Arany et al. (2009)

Abbreviations: EGF, epidermal growth factor; BMP, bone morphogenetic protein; IGF, insulin-like growth factor; TGF- β , transforming growth factor- β ; VEGF, vascular endothelial growth factor; PDGF, platelet-derived growth factor; VSMCs, vascular smooth muscle cells; bFGF, basic fibroblast growth factor; NGF, nerve growth factor.

transplantation to repair or replace necrotic tissue and regenerate dentine–pulp complex (DPC) (Morotomi et al., 2019). First, the main principle of cell homing is that the body's stem cells are recruited and induced to accumulate at the defective site, leading to endogenous tissue regeneration (Wang X. et al., 2018), but the mechanism and application prospects still require much research to clarify. In addition, cell transplantation is currently the main approach for achieving pulp tissue regeneration. A study combining pulp stem cells with granulocyte colony-stimulating factor (G-CSF) in a canine pulpectomy model found that pulp tissue containing vasculature and innervation filled the entire root canal, thereby achieving successful regeneration in pulp tissue (Iohara et al., 2013). There have also been some researchers attempting to develop a biomimetic tooth bud model with dental cells encapsulated within gelatin methacrylate (GelMA) hydrogel scaffolds to obtain a mineralized crown (Smith et al., 2017).

Simultaneously, whole-tooth bioengineering using embryonic tooth bud cells has been established in several animal models, including mice, rats, pigs, and dogs (Zhang and Chen, 2014). Cai et al. found that integration-free human urine-induced pluripotent stem cell (iFhU-iPSC)-derived epithelial sheets recombined with mouse dental

mesenchyme could successfully regenerate tooth-like structures (Cai et al., 2013). Wang et al. proved the feasibility of whole-tooth regeneration in large animals by reconstructing single cells from the fourth deciduous molar tooth germ (p4) of pigs to bioengineer tooth buds in *in vitro* culture and *in vivo* transplantation in mouse subrenal capsules and jawbones. As a result, pig bioengineered tooth buds restore odontogenesis and develop into large tooth sizes (Wang F. et al., 2018). Ono et al. dissected canine permanent premolar (P2, P3, and P4) tooth germs from the mandible of beagles and then transplanted them into the alveolar bone socket of the same mandible to gain functional whole-tooth restoration by autologous transplantation of bioengineered tooth germ in a large animal model (Ono et al., 2017). Zhang et al. used decellularized tooth bud (dTB) scaffolds created from natural porcine tooth buds (TBs) and successfully formed mineralized whole teeth in miniature pig jaws *in vivo* (Zhang et al., 2017).

These results indicate that tissue-engineered teeth have bright prospects in tooth regeneration and can effectively solve the oral problems posed by tooth loss. In future, emerging technologies will provide increasingly advanced ideas for tooth regeneration.

TABLE 4 | Tissue engineering in stomatology.

Tissue engineering	Cells	Scaffolds	Growth factors	Applications	References
Tooth tissue engineering	DPSCs IPSC DFCs PDLSCs;SCAP	PLLA PLGA-PEG; alginate Collagen-hydroxyapatite	BMP FGF IGF CGF	Obtain the mineralized crown Achieve pulp tissue regeneration Form biological root Achieve functional whole-tooth restoration	Cai et al. (2013); Iohara et al. (2013); Shiehzhadeh et al. (2014); Baba et al. (2015); Tian et al. (2015); Wang et al. (2016a); Athirasala et al. (2018); Xu et al. (2019a); Nosrat et al. (2019); Oyanagi et al. (2019)
Periodontal tissue engineering	PDLSCs SHED SCAP	PCL PRF PLGA HA/TCP; alginate; chitosan/ABB	CGF IGF BMP	Promote periodontal ligament, cementum, and alveolar bone regeneration; effectively repair periodontal defects	Dan et al. (2014); Fu et al. (2014); Zang et al. (2016); Duruel et al. (2017); Khodakaram-Tafti et al. (2017); Panduwawala et al. (2017); Yang et al. (2018); Aghamohamadi et al. (2020)
Dental implant tissue engineering	DPSCs; UCMSCs PDLSCs	HA Collagen Bioceramic	PRF TGF- β PDGF	Change the alveolar bone and soft tissue environment; achieve good osseointegration and soft tissue augmentation	Wang et al. (2017); Simion et al. (2012); Funato et al. (2013); Hao et al. (2014); Yun et al. (2014); Wang et al. (2017); Iwasaki et al. (2019); Schorn et al. (2021)
Cleft palate repair tissue engineering	iPSCs CBSCs BMSCs	PP PU; fibrin Alginate Collagen Polyesters; polyisocyanopeptide hydrogel	BMP CTGF EGF FGF TGF- β	Closure of oronasal fistula; effectively guide palatal soft and hard tissue regeneration	Lipska et al. (2011); Kagami et al. (2014); Tarr et al. (2018); Von den Hoff et al. (2019); Schreurs et al. (2020); Tetè et al. (2020); Adhikari et al. (2021)
Oral and maxillofacial skin or mucosal tissue engineering	ESCs; skin keratinocytes Oral mucosal epithelial cells	PCL SPS PLGA; collagen Tissue-engineered 3D cultures	EGF FGF PDGF VEGF	Promote the epithelial regeneration of oral wounds; reconstruct oral skin and mucosa; improve aesthetics	Lubkowska et al. (2012); Peramo et al. (2012); Bayar et al. (2016); Nikoloudaki et al. (2020); Oliva et al. (2020); Toma et al. (2021)
Oral and maxillofacial bone tissue engineering	ADSCs; BMSCs; ABMSCs	Fibrin BioMax HA/TCP- β Nanoporous HA	HGF VEGF SDF-1 TGF- β 1	Repair alveolar bone defect, maxillary bone defect, and mandibular defect; revascularization around maxillofacial bone	Khodakaram-Tafti et al. (2018); Redondo et al. (2018); Shahnaseri et al. (2020); Zhang et al. (2020); Liu et al. (2021)

Abbreviations: ABMSCs, alveolar bone-derived mesenchymal stem cells; ADSCs, adipose-derived stromal cells; BMSCs, bone marrow stromal stem cells; CBSCs, cord blood stem cells; DFCs, dental follicle cells; DPSCs, dental pulp stem cells; ESCs, embryonic stem cells; iPSCs, induced pluripotent stem cells; PDLSCs, periodontal ligament stem cells; SHED, stem cell from exfoliated deciduous teeth; UCMSCs, human umbilical cord mesenchymal stem cells; PEG, polyethylene glycol; PLLA, poly(L-lactide) acid; PLGA, poly(lactic-co-glycolic acid); PCL, polycaprolactone; HA, hydroxyapatite; PP, polypropylene; PU, polyurethanes; SPS, synthetic polymeric scaffolds; TCP, tricalcium phosphate; ABB, anorganic bovine bone; PRF, the patient-derived fibrin scaffold; EGF, epidermal growth factor; BMP, bone morphogenetic protein; IGF, insulin-like growth factor; TGF- β , transforming growth factor- β ; VEGF, vascular endothelial growth factor; PDGF, platelet-derived growth factor; FGF, fibroblast growth factor; HGF, hepatocyte growth factor; SDF-1, stromal cell-derived factor.

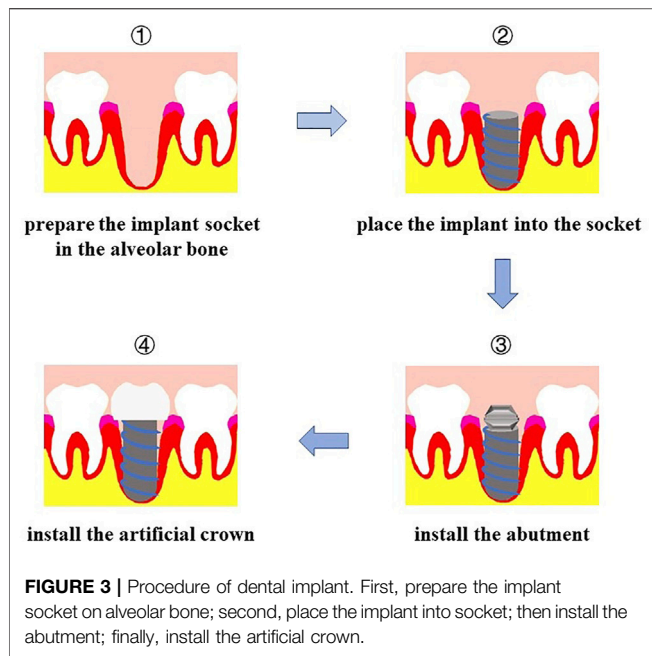
PERIODONTAL TISSUE ENGINEERING

Periodontal tissue diseases are usually involved in periodontal inflammation and trauma, including destruction of the cementum, gingiva, periodontal ligament, and alveolar bone. The formation of periodontal pockets and the resorption of alveolar bone are typical manifestations of periodontitis and eventually develop into tooth loss. The most ideal periodontal treatment is to achieve complete functional regeneration of alveolar bone, cementum, and periodontal ligament to obtain new periodontal attachment (Iwata et al., 2014). Traditional periodontal therapy only removes bacteria and delays the disease process, but it is difficult to achieve periodontal regeneration. Different from traditional periodontal therapy, periodontal tissue engineering is a new concept for reconstructing defective periodontal tissues and organs and has already made rapid development in recent years.

The traditional tissue engineering methods are based on combining scaffolding materials with seed cells. Mrozik et al.

cultured and purified sheep PDLSCs *in vitro*, combined them with gelatin sponges, and implanted them into the periodontal defect of the second premolar, and the newly formed alveolar bone, cementum, and Sharpey fibers were significantly more abundant than those in the control group without stem cell inoculation (Mrozik et al., 2013). Fu et al. treated animal models of periodontitis with stem cells isolated from miniature pig deciduous teeth (SPDs) plus hydroxyapatite/tricalcium phosphate (HA/TCP), and the loss of soft and hard tissue showed significant restoration after 12 weeks (Fu et al., 2014).

However, there are still differences between regenerated tissue and natural periodontal tissue in clinical applications (Matichescu et al., 2020). Therefore, newer techniques need to be introduced into the field of periodontal tissue engineering. Wu et al. inoculated gingival fibroblasts into Bio-Gide collagen membranes bilaterally and induced their mineralization, then constructed a tissue-engineered sandwich membrane to repair periodontal defects in premolar regions of beagles, and found that



new alveolar bone, cementum, and periodontal ligament eventually formed (Wu et al., 2018). In terms of the processing and manufacturing of scaffolds, electrospinning technology is expected to provide more appropriate materials for tissue engineering. Higuchi et al. produced biodegradable membranes for the regeneration of periodontal tissue defects by electrospinning and sonocoating with nanohydroxyapatite particles (Higuchi et al., 2019). Sprio et al. fabricated hybrid superparamagnetic 3-layer scaffolds simulating the 3D environment of periodontium, which is conducive to boosting osteogenic and osteoconductive stimulation (Sprio et al., 2018). Regarding cell culture, cell sheet technology (CST) is defined as a cell transplantation method that does not require scaffolding materials and can preserve intact extracellular matrix (Sprio et al., 2018). Some researchers transplanted cell sheets supported by electrospun polycaprolactone (CaP-PCL) scaffolds, and denuded root and alveolar bone formation occurred at the defect site after 4 weeks, confirming that the combination of PCL and CaP-PCL scaffolds can promote periodontal regeneration (Dan et al., 2014). All these results provide important insights into advancements in periodontal tissue engineering, and it is believed that with the development of periodontal tissue engineering, complete realization of periodontal regeneration will be full of infinite possibilities.

DENTAL IMPLANT TISSUE ENGINEERING

We have mentioned the importance of teeth to humans and some related studies on the use of tooth tissue engineering to repair tooth loss. Dental implantation is another common method to restore tooth loss. Implant restoration is performed in the alveolar bone of the edentulous area to implant the artificial tooth root, which replaces the natural tooth root, and

subsequently repair the absent the tooth, which includes the artificial crown of the upper part and lower part of the support of implants (Figure 3). Although dental implants overcome some disadvantages of dentures and effectively repair defects caused by tooth loss, two conditions still hinder the development of dental implant technology: 1) insufficient local bone mass in the implants (Pardal-Peláez et al., 2021) and 2) insufficient soft tissue around the implants (Noh et al., 2021). Dental implant tissue engineering mainly uses tissue engineering technology and changes the alveolar bone and soft tissue environment before the implant is implanted into the alveolar bone in the edentulous area to achieve good osseointegration (Hao et al., 2021) and soft tissue augmentation.

On the one hand, tissue engineering contributes to overcoming the obstacles encountered with bone regeneration during dental implants. Yun et al. applied platelet-rich plasma (PRP) and human bone marrow mesenchymal stem cells (BMMSCs) to the bone defect area around the dental implant with porous hydroxyapatite (HA) as the scaffold and determined the bone regeneration ability of BMMSCs and PRP histologically. The data showed that the HA + BMMSC + PRP group had a higher bone density between 6 and 12 weeks (Yun et al., 2014). To investigate the role of umbilical cord mesenchymal stem cells (UCMSCs) in bone defects around the implant after immediate implantation, Hao et al. filled the defect on one side with platelet-rich fibrin (PRF) and UCMSCs, while the other side was filled with PRF only as the control group and placed a titanium implant into the extraction socket. The results showed that UCMSCs can promote the formation of new bone in the bone defect area around implants; hence, UCMSCs can be used as excellent cells in the regeneration of bone defects after implantation (Hao et al., 2014).

On the other hand, concerning the problem of insufficient soft tissue, Simion et al. used a resorbable collagen matrix as a scaffold to carry recombinant human platelet-derived growth factor BB (rhPDGF-BB), and the results indicated that the soft tissue volume around implants increased moderately when applying a collagen matrix infused with rhPDGF-BB (Simion et al., 2012). Liu et al. employed acellular dermal matrix grafts conducive to increasing the attached gingiva and resin splint conducive to facilitating the healing of soft tissue attached to dental implants, and patients were satisfied with the reconstruction effects of dense connective tissue surrounding the implants after the operation (Liu et al., 2014). The patients with maxillary gingival recessions were treated with autologous fibroblast cell culture (AFCC) on a collagen scaffold placed under a coronally advanced flap (CAF), and soft tissues were significantly improved, suggesting that AFCC is a novel tissue engineering concept and a reliable therapy to solve the problem of insufficient soft tissues during defect repair caused by tooth loss (Milinkovic et al., 2015).

In summary, through the aid of tissue engineering technology, an increasing number of cells and scaffolds have been used for bone regeneration after dental implants, providing novel ideas for solving the problem of insufficient local bone mass in implants.

Through the advantages of tissue engineering, such as less damage to the tissue around implants and good aesthetic effects, the development of oral implantology will be more vigorous in the future.

Cleft Palate Repair Tissue Engineering

Cleft palate is one of the congenital malformations with the highest probability of occurrence in oral and maxillofacial regions and can occur alone or together with cleft lip. Cleft palate not only manifests as soft tissue deformity but also bone tissue defects and deformities and may be accompanied by disorders of jaw development. In other words, the occurrence of cleft palate will have a huge impact on facial esthetics, and it will also cause dysfunction in language, eating, and breathing. Therefore, the repair of cleft palate is crucial, and surgery is one of the most important therapy methods. Traditional palatoplasty usually applies a loose incision to reduce tension, but bone surface trauma exposed after surgery will be scarred and can even lead to the restriction of development and deformity of the jawbone (Cantarella and Mazzola, 2020; Choi et al., 2021).

To solve or avoid the problems caused by traditional surgical methods during the healing of cleft palate, researchers have tried to find better ways to resolve cleft palate. Tissue engineering technology has been applied to repair cleft palate and has already obtained some results in many studies. Bajestan et al. explored the use of *ex vivo* expanded stem cell populations to treat large alveolar bone defects in patients with a history of cleft palate or craniofacial trauma. The results indicated that stem cell population therapy is safe, but the ability to completely reconstruct large alveolar defects is finite, so further optimization is needed to satisfy the requirements of cleft palate treatment (Bajestan et al., 2017). Sharif et al. developed a plasma-functionalized electrospun composite polymer membrane, modified the fabricated membranes by plasma polymerization, and then implanted them in rats subcutaneously. The results showed that these membranes were biocompatible and angiogenic, providing the possibility for permanent closure of oronasal fistula (Sharif et al., 2019). Lee et al. created cell sheets derived from hMSCs and SHEDs for bone repair of cleft palate and found that the cell sheets led to calcification *in vitro*, which indicated that osteogenic stem cell sheets may become a new choice for the reconstruction of cleft palate (Lee J.-M. et al., 2019). Li et al. developed a tissue-engineered graft for the repair of cleft palate in young rats by incorporating and integrating a synthetic polymer with a human decellularized amniotic membrane (DAM). This cell-free and absorbable graft could effectively guide soft and hard tissue regeneration and support palate regeneration and tissue growth (Li W. et al., 2019).

In summary, the use of tissue engineering techniques to repair cleft palate not only avoids scar tissue formation, wound contraction, and facial deformity caused by traditional cleft palate repair surgery but also effectively reconstructs and stimulates the healing of defects. In other words, we believe that there may be a new breakthrough for the repair of cleft

palate through the in-depth study of tissue engineering technology.

Oral and Maxillofacial Skin or Mucosal Tissue Engineering

Skin and mucosal lesions caused by inflammation, trauma, tumors, or autoimmune diseases are very common in the clinical treatment of dentistry. Traditional autologous skin or mucosal flap transplantation is a popular method to treat lesions, but this method still has some disadvantages because the surgery causes donor site injury. Meanwhile, the source of homogenous skin or mucosal flap for transplantation is too limited, and the characteristics of exogenous tissue flap are different from oral and maxillofacial skin and mucosa. Even if the mucosal flap is successfully transplanted, it is difficult to maintain the secretion and lubrication function of the oral mucosa (Wang Z.-S. et al., 2016). To repair oral skin and mucosa lesions, an important task for researchers is to find alternatives to replace the traditional transplantation of autologous skin and mucosa, and the application of tissue engineering technology may provide a new direction in this research area.

Peramo et al. reported a three-dimensional tissue structure that can be used to repair lip defects, consisting of a continuous layer that contains the morphological features of lips: epidermal skin, vermilion, and oral mucosa, plus can produce tissues with similar anatomy as native human lips (Peramo et al., 2012). Yoshizawa et al. found that grafting *ex vivo*-produced oral mucosa equivalent (EVPOME) with live oral keratinocytes onto an intraoral mucosal wound can effectively promote epithelial regeneration in oral wounds (Yoshizawa et al., 2012). Bayar et al. created a construct containing a mucocutaneous junction with a transitional zone (vermilion) *in vitro*, which can produce a microvascular prelaminated flap in lip reconstruction, and the results showed that this construct could promote the phenotypic expression of regenerated tissue closer to native tissue (Bayar et al., 2016).

Some researchers preferred to combine flap surgery and tissue engineering technology to enhance the therapeutic effects in clinical treatment. Sieira et al. proposed a new approach to obtain keratinized mucosa over a fibula flap using full-thickness, tissue-engineered, autologous oral mucosa and found that this oral mucosa can restore native tissue and avoid peri-implant tissue complications during the repair of mucosal oral defects (Sieira Gil et al., 2015). Some research builds an oral mucosal model by using tissue engineering technology and evaluates the changes in the interface in implant soft tissue because the biotightness formed by the soft tissue around implants can impact the prognosis after dental implant treatments. Chai et al. developed a tissue-engineered three-dimensional oral mucosal model (3D OMM) by using primary human oral keratinocytes, fibroblasts, and a skin-derived scaffold. The titanium implant was then inserted into the engineered oral mucosa, and the results showed that the tissue-engineered oral mucosa was similar to the normal oral mucosa. 3D OMM can form epithelial attachments on the titanium surface (Chai et al., 2010). Trichloroacetic acid

(TCA) has attracted the focus of dental researchers due to its pivotal role during skin regeneration. Lee et al. injected TCA into open wound defects of the palatal mucosa in beagles and found that TCA promoted the healing and regeneration of wound defects in oral soft tissue by upregulating cell cycle progression, cell growth, and cell viability (Lee K. et al., 2019).

The aforementioned studies demonstrated that tissue engineering technology can more easily repair defects in oral and maxillofacial skin or mucosa. If tissue-engineered skin and mucosa are widely used in oral and maxillofacial clinical surgery, it can effectively avoid the challenges caused by the transplantation of traditional autologous skin or mucosal flaps.

Oral and Maxillofacial Bone Tissue Engineering

Oral and maxillofacial bone defects are diseases caused by congenital deformity, trauma, tumors, inflammation, or periodontal disease and mainly include alveolar, maxillary, and mandibular bone defects (Bangun et al., 2021; Lin and Kudva, 2021). Bone transplantation, guided bone regeneration membrane technology, stimulation of osteogenesis, and prosthetic repair are the main methods for the healing of defects. In the clinic, autologous bone is regarded as the “gold standard” for bone transplantation, but it also has some disadvantages. For example, autologous bone cannot be shaped randomly, which will impact the recovery and appearance of prognostic functions. Furthermore, the source is limited, and some complications may still occur after autologous bone transplantation. Recently, there have been many studies related to the healing of oral and maxillofacial bone defects by using bone tissue engineering technologies.

Khodakaram et al. compared the effects of fibrin glue scaffolds and autologous bone grafts during the healing of rabbit mandibular defects and found that they have similar osteogenic effects, so fibrin glue may be a good bone graft substitute and can be used to reconstruct maxillofacial bone defects (Khodakaram-Tafti et al., 2018). Shahnasari et al. created a maxillary defect to simulate a human alveolar cleft model. One side of the defect was filled with hydroxyapatite/ β -tricalcium phosphate scaffolds that contained mesenchymal stem cells from the subcutaneous adipose tissue of dogs, and the other side was filled with autologous bone grafts collected from the tibia. The results showed that both grafts had good bone formation effects, so tissue engineering can be used as an alternative method to reconstruct bone defects (Shahnasari et al., 2020). Redondo et al. inoculated mesenchymal stem cells from alveolar bone into BioMax scaffolds prepared from autologous serum and treated maxillary cystic bone defects under GMP conditions. The results showed that BioMax cross-linked serum scaffolds containing osteogenic differentiated MSCs gained a good effect during the repair of maxillary defects (Redondo et al., 2018). Zhang et al. constructed tissue-engineered bones by using 3D printing molds and high-temperature sintering and produced nanoporous hydroxyapatite scaffolds that can convincingly repair *in situ* bone defects in experimental dogs (Zhang et al., 2020).

The reconstruction of bone defects (especially critical sized bone defects) is difficult because the survival and growth of bone require the surrounding and internal blood vessels to provide oxygen and nutrients. Therefore, the vascularization of tissue-engineered bone is very important during the repair of oral and maxillofacial bone defects. Matthias et al. successfully reconstructed large posttraumatic mandibular defects by using fresh frozen humeral allografts seeded with autologous bone marrow aspirate and vascularized them with a radial forearm flap (Matthias et al., 2019).

There are four main methods to reconstruct the blood supply of tissue-engineered bones: 1) using growth factors to promote the formation of new blood vessels (Omorphos et al., 2021); 2) culturing vascular endothelial cells as seed cells with the scaffold to form a complex unit and then implanting them *in vivo* to promote angiogenesis (Hancock et al., 2021); 3) combining microsurgery technology with bone tissue engineering to promote blood vessel formation (Vidal et al., 2020); and 4) using genetic engineering technology to promote blood vessel formation (Est-Witte et al., 2020). Selecting the appropriate tissue-engineered bone and constructing a good blood supply system will accelerate the healing of critical-sized bone defects. We believe that with the support of osteogenic cells, scaffolds, and growth factors, increasingly more tissue-engineered bone will be developed, and oral and maxillofacial bone defects will be repaired easily.

Limitations

We mentioned that the basic elements of tissue engineering technology are cells, scaffolds, and growth factors. Current relevant studies also obtained satisfactory reconstruction results, but there are still some disadvantages that limit the development of tissue engineering. If researchers can understand these limitations of tissue engineering correctly, it will contribute to the further research and application of tissue engineering and will be helpful for solving problems during the healing of defective tissues or organs.

Limitations of Cells

At present, the cells used for tissue engineering research mainly include xenogeneic cells, allogeneic cells, and autologous cells. Xenogeneic cells are taken from non-human body tissues and can be derived from animals such as pigs and dogs, which means that the use of xenogeneic cells may cause immune rejection. Although some researchers have overcome this immune rejection (Mohiuddin et al., 2014; Iwase et al., 2015), the safety and long-term therapeutic effects of xenogeneic cells still need to be further verified (Sun et al., 2019). Compared with xenogeneic cells, allogeneic cells can better overcome immune rejection (Goyer et al., 2019), but they may have some other disadvantages. In recent years, research on allogeneic cells has mainly focused on human embryonic stem cells derived from 1) naturally or artificially aborted embryos and 2) *in vitro* fertilized embryos. However, the application of human embryos is considered extremely cruel, immoral, and illegal in many countries. Autologous cells are taken from their own tissues and have the potential to regenerate various tissues and organs.

Autologous cells, unlike xenogeneic and allogeneic cells, will not cause immune rejection and have no ethics problems, but their application is restricted by their limited source and traumas caused during cell harvesting.

Limitations of Scaffolds

As previously summarized, natural biomaterials, synthetic polymer materials, or hydrogel scaffolds, all have some limitations. Because most natural biomaterials are derived from animal and have good biocompatibility during *in vivo* and *in vitro* experiments, they are still judged as non-autologous and labeled foreign bodies by the immune system and may eventually induce serious immunogenic responses after long-term use (Gilmartin et al., 2013). In addition, we should also pay attention to the instability of these biomaterials and the variability of molecular structures among different batches (Ige et al., 2012). Synthetic polymer materials generally exhibit poor cell affinity in previous studies (Zhao W. et al., 2016). The major disadvantage of electrospun scaffolds is the complexity of electrospinning and lack of defined control, so more reliable data from animal experiments are needed to support future practical applications (McClellan and Landis, 2016). Rasperini et al. reported the first human case in which a 3D-printed bioresorbable polymer scaffold was used to treat a periodontal osseous defect; however, the scaffold was exposed at 13 months and removed at 14 months because of a larger dehiscence and failure of wound healing (Rasperini et al., 2015). How to control the degradation rate of scaffolds to match the speed of defect healing and how to prepare layered scaffolds that can guide coordinated tissue regeneration may be the main directions of improvement approaches in the future.

Limitations of Clinical Application

Constructing a tissue engineering complex rich in living cells *in vitro* and then implanting it *in vivo* is the main process of transplantation of engineered tissue or organs. However, it also has some potential risks to the recipients of implanted engineered tissues or organs. When culturing the engineered complex *in vitro*, it is necessary to add fetal bovine serum, streptomycin, or other substances that can promote cell growth, but most substances are not derived from humans themselves, so the engineered complex may cause allergic reactions after implantation *in vivo*. On the other hand, absorbable polymer materials and some other types of materials are often selected as scaffolding materials to support

seeding cells. Although most of these materials show no toxic effects, the long-term safety and immunological rejection of these materials are still major concerns for clinical application. For example, people prefer using allogeneic bone as a scaffold material, but it still has little antigenicity even when treated at extremely low temperatures. Therefore, we should further consider the safety and validity of engineered tissue or organs before they are applied in the clinic.

CONCLUSION

In summary, tissue engineering has broad prospects in stomatology and provides a valuable direction for future research on tooth loss, periodontal defects, dental implants, cleft palate defects, oral and maxillofacial skin or mucosal defects, and bone defects. It is believed that with the in-depth exploration of tissue engineering, ideal seed cell, better scaffold materials, and growth factors will be discovered and applied in effective clinical management of oral diseases in the future.

AUTHOR CONTRIBUTIONS

LC, HS, and XC collected data of seed cells, scaffolds, and growth factors; drew figures and made tables; and also drafted the overview of the manuscript. MS and JX collected the data on dental implant tissue engineering, cleft palate tissue engineering, and oral and maxillofacial skin, and mucosal tissue engineering. JL reviewed the manuscript. YZ conceived the presented idea, reviewed, and revised the manuscript, and also approved the final version. All authors agreed to be accountable for all aspects of the work.

FUNDING

This work was supported by grants from the Foundation of Science and Technology Department of Henan Province, China (No. 212102310103); the Natural Science Foundation of Education Department of Henan Province, China (No. 21A320004); the Foundation of National Health Commission of Henan Province, China (No. Wjlx2020017); and the Foundation of Science and Technology Department of Luoyang City, Henan Province, China (No. 2101065A).

REFERENCES

- Adhikari, J., Roy, A., Das, A., Ghosh, M., Thomas, S., Sinha, A., et al. (2021). Effects of Processing Parameters of 3D Bioprinting on the Cellular Activity of Bioinks. *Macromol. Biosci.* 21 (1), 2000179. doi:10.1002/mabi.202000179
- Adib, M., Alipour, R., Hashemi-Beni, B., and Sadeghi, F. (2014). The Effect of Stem Cell from Human Exfoliated Deciduous Teeth on T Lymphocyte Proliferation. *Adv. Biomed. Res.* 3, 202. doi:10.4103/2277-9175.142312
- Aghamohamadi, Z., Kadkhodazadeh, M., Torshabi, M., and Tabatabaei, F. (2020). A Compound of Concentrated Growth Factor and Periodontal Ligament Stem Cell-Derived Conditioned Medium. *Tissue and Cell* 65, 101373. doi:10.1016/j.tice.2020.101373
- Agrawal, V., and Sinha, M. (2017). A Review on Carrier Systems for Bone Morphogenetic Protein-2. *J. Biomed. Mater. Res.* 105 (4), 904–925. doi:10.1002/jbm.b.33599
- Alkai, A., Ismail, A. R., Mutum, S. S., Rifin Ahmad, Z. A., Masudi, S. a., and Razak, N. H. A. (2013). Transplantation of Human Dental Pulp Stem Cells: Enhance Bone Consolidation in Mandibular Distraction Osteogenesis. *J. Oral Maxillofacial Surg.* 71 (10), e1–1758. doi:10.1016/j.joms.2013.05.0161713
- Amjadian, S., Seyedjafari, E., Zeynali, B., and Shabani, I. (2016). The Synergistic Effect of Nano-Hydroxyapatite and Dexamethasone in the Fibrous Delivery

- System of Gelatin and Poly(l-Lactide) on the Osteogenesis of Mesenchymal Stem Cells. *Int. J. Pharmaceutics* 507 (1–2), 1–11. doi:10.1016/j.iijpharm.2016.04.032
- Anandakrishnan, N., and Azeloglu, E. U. (2020). Kidney Tissue Engineering for Precision Medicine. *Nat. Rev. Nephrol.* 16 (11), 623–624. doi:10.1038/s41581-020-00355-6
- Ansari, S., Chen, C., Xu, X., Annabi, N., Zadeh, H. H., Wu, B. M., et al. (2016). Muscle Tissue Engineering Using Gingival Mesenchymal Stem Cells Encapsulated in Alginate Hydrogels Containing Multiple Growth Factors. *Ann. Biomed. Eng.* 44 (6), 1908–1920. doi:10.1007/s10439-016-1594-6
- Arany, S., Koyota, S., and Sugiyama, T. (2009). Nerve Growth Factor Promotes Differentiation of Odontoblast-like Cells. *J. Cell. Biochem.* 106 (4), 539–545. doi:10.1002/jcb.22006
- Athirasala, A., Tahayeri, A., Thrivikraman, G., França, C. M., Monteiro, N., Tran, V., et al. (2018). A Dentin-Derived Hydrogel Bioink for 3D Bioprinting of Cell Laden Scaffolds for Regenerative Dentistry. *Biofabrication* 10 (2), 024101. doi:10.1088/1758-5090/aa9b4e
- Baba, O., Ota, M. S., Terashima, T., Tabata, M. J., and Takano, Y. (2015). Expression of Transcripts for Fibroblast Growth Factor 18 and its Possible Receptors during Postnatal Dentin Formation in Rat Molars. *Odontology* 103 (2), 136–142. doi:10.1007/s10266-013-0147-9
- Bajestan, M. N., Rajan, A., Edwards, S. P., Aronovich, S., Cevdanes, L. H. S., Polymeri, A., et al. (2017). Stem Cell Therapy for Reconstruction of Alveolar Cleft and Trauma Defects in Adults: A Randomized Controlled, Clinical Trial. *Clin. Implant Dent Relat. Res.* 19 (5), 793–801. doi:10.1111/cid.12506
- Bakopoulou, A., Leyhausen, G., Volk, J., Tsiotsoglou, A., Garefis, P., Koidis, P., et al. (2011). Comparative Analysis of *In Vitro* Osteo/odontogenic Differentiation Potential of Human Dental Pulp Stem Cells (DPSCs) and Stem Cells from the Apical Papilla (SCAP). *Arch. Oral Biol.* 56 (7), 709–721. doi:10.1016/j.archoralbio.2010.12.008
- Bangun, K., Sukasah, C. L., Dilogio, I. H., Indrani, D. J., Siregar, N. C., Pandelaki, J., et al. (2021). Bone Growth Capacity of Human Umbilical Cord Mesenchymal Stem Cells and BMP-2 Seeded into Hydroxyapatite/Chitosan/Gelatin Scaffold in Alveolar Cleft Defects: An Experimental Study in Goat. *Cleft Palate-Craniofacial J.* 58 (6), 707–717. doi:10.1177/1055665620962360
- Bargehr, J., Ong, L. P., Colzani, M., Davaapil, H., Hofsteen, P., Bhandari, S., et al. (2019). Epicardial Cells Derived from Human Embryonic Stem Cells Augment Cardiomyocyte-Driven Heart Regeneration. *Nat. Biotechnol.* 37 (8), 895–906. doi:10.1038/s41587-019-0197-9
- Bayar, G. R., Kuo, S., Marcelo, C. L., and Feinberg, S. E. (2016). *In Vitro* Development of a Mucocutaneous Junction for Lip Reconstruction. *J. Oral Maxillofacial Surg.* 74 (11), 2317–2326. doi:10.1016/j.joms.2016.04.002
- Behnia, A., Haghighat, A., Talebi, A., Nourbakhsh, N., and Heidari, F. (2014). Transplantation of Stem Cells from Human Exfoliated Deciduous Teeth for Bone Regeneration in the Dog Mandibular Defect. *Wjsc* 6 (4), 505–510. doi:10.4252/wjsc.v6.i4.505
- Ben Amara, H., Thoma, D. S., Schwarz, F., Song, H. Y., Capetillo, J., and Koo, K.-T. (2019). Healing Kinetics of Oral Soft Tissue Wounds Treated with Recombinant Epidermal Growth Factor: Translation from a Canine Model. *J. Clin. Periodontol.* 46 (1), 105–117. doi:10.1111/jcpe.13035
- Berbéri, A., Fayyad-Kazan, M., Ayoub, S., Bou Assaf, R., Sabbagh, J., Ghassibe-Sabbagh, M., et al. (2021). Osteogenic Potential of Dental and Oral Derived Stem Cells in Bone Tissue Engineering Among Animal Models: An Update. *Tissue and Cell* 71, 101515. doi:10.1016/j.tice.2021.101515
- Bhardwaj, N., and Kundu, S. C. (2012). Chondrogenic Differentiation of Rat MSCs on Porous Scaffolds of Silk Fibroin/chitosan Blends. *Biomaterials* 33 (10), 2848–2857. doi:10.1016/j.biomaterials.2011.12.028
- Bonaguidi, M. A., Wheeler, M. A., Shapiro, J. S., Stadel, R. P., Sun, G. J., Ming, G.-L., et al. (2011). *In Vivo* clonal Analysis Reveals Self-Renewing and Multipotent Adult Neural Stem Cell Characteristics. *Cell* 145 (7), 1142–1155. doi:10.1016/j.cell.2011.05.024
- Brassolatti, P., Bossini, P. S., Andrade, A. L. M. d., Luna, G. L. F., Silva, J. V. d., Almeida-Lopes, L., et al. (2021). Comparison of Two Different Biomaterials in the Bone Regeneration (15, 30 and 60 Days) of Critical Defects in Rats. *Acta Cir. Bras.* 36 (6), e360605. doi:10.1590/acb360605
- Cai, J., Zhang, Y., Liu, P., Chen, S., Wu, X., Sun, Y., et al. (2013). Generation of Tooth-like Structures from Integration-free Human Urine Induced Pluripotent Stem Cells. *Cell Regen.* 2 (1), 2–6. doi:10.1186/2045-9769-2-6
- Cantarella, G., and Mazzola, R. F. (2020). Adding Nanofat to Fat Grafting to Treat Velar Scarring in Velopharyngeal Incompetence. *J. Craniofac. Surg.* 31 (7), 1925–1927. doi:10.1097/scs.00000000000006698
- Cao, C., Tarlé, S., and Kaigler, D. (2020). Characterization of the Immunomodulatory Properties of Alveolar Bone-Derived Mesenchymal Stem Cells. *Stem Cell Res Ther* 11 (1), 102. doi:10.1186/s13287-020-01605-x
- Casagrande, L., Demarco, F. F., Zhang, Z., Araujo, F. B., Shi, S., and Nör, J. E. (2010). Dentin-derived BMP-2 and Odontoblast Differentiation. *J. Dent Res.* 89 (6), 603–608. doi:10.1177/0022034510364487
- Caviedes-Bucheli, J., Canales-Sánchez, P., Castrillón-Sarria, N., Jovel-García, J., Alvarez-Vázquez, J., Rivero, C., et al. (2009). Expression of Insulin-like Growth Factor-1 and Proliferating Cell Nuclear Antigen in Human Pulp Cells of Teeth with Complete and Incomplete Root Development. *Int. Endod. J.* 42 (8), 686–693. doi:10.1111/j.1365-2591.2009.01568.x
- Chai, W. L., Moharamzadeh, K., Brook, I. M., Emanuelsson, L., Palmquist, A., and van Noort, R. (2010). Development of a Novel Model for the Investigation of Implant-Soft Tissue Interface. *J. Periodontol.* 81 (8), 1187–1195. doi:10.1902/jop.2010.090648
- Chang, B., Ahuja, N., Ma, C., and Liu, X. (2017). Injectable Scaffolds: Preparation and Application in Dental and Craniofacial Regeneration. *Mater. Sci. Eng. R: Rep.* 111, 1–26. doi:10.1016/j.mser.2016.11.001
- Chattopadhyay, S., and Raines, R. T. (2014). Collagen-based Biomaterials for Wound Healing. *Biopolymers* 101 (8), 821–833. doi:10.1002/bip.22486
- Chen, F.-M., Gao, L.-N., Tian, B.-M., Zhang, X.-Y., Zhang, Y.-J., Dong, G.-Y., et al. (2016a). Treatment of Periodontal Intrabony Defects Using Autologous Periodontal Ligament Stem Cells: a Randomized Clinical Trial. *Stem Cell Res Ther* 7, 33. doi:10.1186/s13287-016-0288-1
- Chen, W., Liu, X., Chen, Q., Bao, C., Zhao, L., Zhu, Z., et al. (2018). Angiogenic and Osteogenic Regeneration in Rats via Calcium Phosphate Scaffold and Endothelial Cell Co-culture with Human Bone Marrow Mesenchymal Stem Cells (MSCs), Human Umbilical Cord MSCs, Human Induced Pluripotent Stem Cell-Derived MSCs and Human Embry. *J. Tissue Eng. Regen. Med.* 12 (1), 191–203. doi:10.1002/term.2395
- Chen, Y.-Y., He, S.-T., Yan, F.-H., Zhou, P.-F., Luo, K., Zhang, Y.-D., et al. (2016b). Dental Pulp Stem Cells Express Tendon Markers under Mechanical Loading and Are a Potential Cell Source for Tissue Engineering of Tendon-like Tissue. *Int. J. Oral Sci.* 8 (4), 213–222. doi:10.1038/ijos.2016.33
- Cheng, F., Zhang, M., Wang, Q., Xu, H., Dong, X., Gao, Z., et al. (2018). Tooth Loss and Risk of Cardiovascular Disease and Stroke: A Dose-Response Meta Analysis of Prospective Cohort Studies. *PLoS One* 13 (3), e0194563. doi:10.1371/journal.pone.0194563
- Choi, J. M., Park, H., and Oh, T. S. (2021). Use of a Buccinator Myomucosal Flap and Bilateral Pedicled Buccal Fat Pad Transfer in Wide Palatal Fistula Repair: a Case Report. *Arch. Craniofac. Surg.* 22 (4), 209–213. doi:10.7181/acfs.2021.00269
- D'Alimonte, I., Nargi, E., Mastrangelo, F., Falco, G., Lanuti, P., Marchisio, M., et al. (2011). Vascular Endothelial Growth Factor Enhances *In Vitro* Proliferation and Osteogenic Differentiation of Human Dental Pulp Stem Cells. *J. Biol. Regul. Homeost. Agents* 25 (1), 57–69.
- Dan, H., Vaquette, C., Fisher, A. G., Hamlet, S. M., Xiao, Y., Huttmacher, D. W., et al. (2014). The Influence of Cellular Source on Periodontal Regeneration Using Calcium Phosphate Coated Polycaprolactone Scaffold Supported Cell Sheets. *Biomaterials* 35 (1), 113–122. doi:10.1016/j.biomaterials.2013.09.074
- Deicher, A., and Seeger, T. (2021). Human Induced Pluripotent Stem Cells as a Disease Model System for Heart Failure. *Curr. Heart Fail. Rep.* 18 (1), 1–11. doi:10.1007/s11897-020-00497-5
- Dey, K., Roca, E., Ramorino, G., and Sartore, L. (2020). Progress in the Mechanical Modulation of Cell Functions in Tissue Engineering. *Biomater. Sci.* 8 (24), 7033–7081. doi:10.1039/d0bm01255f
- Duan, X., Tu, Q., Zhang, J., Ye, J., Sommer, C., Mostoslavsky, G., et al. (2011). Application of Induced Pluripotent Stem (iPS) Cells in Periodontal Tissue Regeneration. *J. Cell. Physiol.* 226 (1), 150–157. doi:10.1002/jcp.22316
- Duruel, T., Çakmak, A. S., Akman, A., Nohutcu, R. M., and Gümüşderelioglu, M. (2017). Sequential IGF-1 and BMP-6 Releasing Chitosan/alginate/PLGA Hybrid Scaffolds for Periodontal Regeneration. *Int. J. Biol. Macromolecules* 104 (Pt A), 232–241. doi:10.1016/j.jbiomac.2017.06.029

- Dzobo, K., Thomford, N. E., Senthebane, D. A., Shipanga, H., Rowe, A., Dandara, C., et al. (2018). Advances in Regenerative Medicine and Tissue Engineering: Innovation and Transformation of Medicine. *Stem Cell Int.* 2018, 1–24. doi:10.1155/2018/2495848
- Ercal, P., Pekozer, G. G., Gumru, O. Z., Kose, G. T., and Ramazanoglu, M. (2017). Influence of STRO-1 Selection on Osteogenic Potential of Human Tooth Germ Derived Mesenchymal Stem Cells. *Arch. Oral Biol.* 82, 293–301. doi:10.1016/j.archoralbio.2017.06.028
- Est-Witte, S. E., Farris, A. L., Tzeng, S. Y., Hutton, D. L., Gong, D. H., Calabresi, K. G., et al. (2020). Non-viral Gene Delivery of HIF-1 α Promotes Angiogenesis in Human Adipose-Derived Stem Cells. *Acta Biomater.* 113, 279–288. doi:10.1016/j.actbio.2020.06.042
- Fang, J., Chen, F., Liu, D., Gu, F., and Wang, Y. (2021). Adipose Tissue-Derived Stem Cells in Breast Reconstruction: a Brief Review on Biology and Translation. *Stem Cell Res Ther* 12 (1), 8. doi:10.1186/s13287-020-01955-6
- Farhat, W., Chatelain, F., Marret, A., Faivre, L., Arakelian, L., Cattani, P., et al. (2021). Trends in 3D Bioprinting for Esophageal Tissue Repair and Reconstruction. *Biomaterials* 267, 120465. doi:10.1016/j.biomaterials.2020.120465
- Ferroni, L., Gardin, C., Sivoletta, S., Brunello, G., Berengo, M., Piattelli, A., et al. (2015). A Hyaluronan-Based Scaffold for the *In Vitro* Construction of Dental Pulp-like Tissue. *Ijms* 16 (3), 4666–4681. doi:10.3390/ijms16034666
- Fu, X., Jin, L., Ma, P., Fan, Z., and Wang, S. (2014). Allogeneic Stem Cells from Deciduous Teeth in Treatment for Periodontitis in Miniature Swine. *J. Periodontol.* 85 (6), 845–851. doi:10.1902/jop.2013.130254
- Funato, A., Ishikawa, T., Kitajima, H., Yamada, M., and Moroi, H. (2013). A Novel Combined Surgical Approach to Vertical Alveolar ridge Augmentation with Titanium Mesh, Resorbable Membrane, and rhPDGF-BB: a Retrospective Consecutive Case Series. *Int. J. Periodontics Restorative Dent* 33 (4), 437–445. doi:10.11607/prd.1460
- Gentile, P., Chiono, V., Carmagnola, I., and Hatton, P. (2014). An Overview of Poly(lactic-Co-Glycolic) Acid (PLGA)-based Biomaterials for Bone Tissue Engineering. *Ijms* 15 (3), 3640–3659. doi:10.3390/ijms15033640
- Gilmartin, D. J., Alexaline, M. M., Thrassivoulou, C., Phillips, A. R. J., Jayasinghe, S. N., and Becker, D. L. (2013). Integration of Scaffolds into Full-Thickness Skin Wounds: the Connexin Response. *Adv. Healthc. Mater.* 2 (8), 1151–1160. doi:10.1002/adhm.201200357
- Gosselin, E. A., Eppler, H. B., Bromberg, J. S., and Jewell, C. M. (2018). Designing Natural and Synthetic Immune Tissues. *Nat. Mater* 17 (6), 484–498. doi:10.1038/s41563-018-0077-6
- Goyer, B., Larouche, D., Kim, D. H., Veillette, N., Pruneau, V., Bernier, V., et al. (2019). Immune Tolerance of Tissue-Engineered Skin Produced with Allogeneic or Xenogeneic Fibroblasts and Syngeneic Keratinocytes Grafted on Mice. *Acta Biomater.* 90, 192–204. doi:10.1016/j.actbio.2019.04.010
- Haghighat, M., Iranbakhsh, A., Baharara, J., Ebadi, M., and Sotoodehnejadnematalahi, F. (2021). Effect of β -carotene on the Differentiation Potential of Ciliary Epithelium-Derived MSCs Isolated from Mouse Eyes on Alginate-Based Scaffolds. *Exp. Eye Res.* 202, 108346. doi:10.1016/j.exer.2020.108346
- Han, J., Menicanin, D., Gronthos, S., and Bartold, P. (2014). Stem Cells, Tissue Engineering and Periodontal Regeneration. *Aust. Dent J.* 59 (Suppl. 1), 117–130. doi:10.1111/adj.12100
- Hancock, P. C., Koduru, S. V., Sun, M., and Ravnice, D. J. (2021). Induction of Scaffold Angiogenesis by Recipient Vasculature Precision Micropuncture. *Microvasc. Res.* 134, 104121. doi:10.1016/j.mvr.2020.104121
- Hao, C.-P., Cao, N.-J., Zhu, Y.-H., and Wang, W. (2021). The Osseointegration and Stability of Dental Implants with Different Surface Treatments in Animal Models: a Network Meta-Analysis. *Sci. Rep.* 11 (1), 13849. doi:10.1038/s41598-021-93307-4
- Hao, P. J., Wang, Z. G., Xu, Q. C., Xu, S., Li, Z. R., Yang, P. S., et al. (2014). Effect of Umbilical Cord Mesenchymal Stem Cell in Peri-Implant Bone Defect after Immediate Implant: an experiment Study in Beagle Dogs. *Int. J. Clin. Exp. Pathol.* 7 (11), 8271–8278.
- Hejazi, M., Zareshahrabadi, Z., Ashayeri, S., Saharkhiz, M. J., Iraj, A., Alishahi, M., et al. (2021). Characterization and Physical and Biological Properties of Tissue Conditioner Incorporated with Carum Copticum L. *Biomed. Res. Int.* 2021, 1–10. doi:10.1155/2021/5577760
- Higuchi, J., Fortunato, G., Woźniak, B., Chodara, A., Domaschke, S., Męczyńska-Wielgosz, S., et al. (2019). Polymer Membranes Sonocoated and Electrospayed with Nano-Hydroxyapatite for Periodontal Tissues Regeneration. *Nanomaterials* 9 (11), 1625. doi:10.3390/nano9111625
- Ige, O. O., Umoru, L. E., and Aribio, S. (2012). Natural Products: A Minefield of Biomaterials. *ISRN Mater. Sci.* 2012, 1–20. doi:10.5402/2012/983062
- Iohara, K., Murakami, M., Takeuchi, N., Osako, Y., Ito, M., Ishizaka, R., et al. (2013). A Novel Combinatorial Therapy with Pulp Stem Cells and Granulocyte colony-stimulating Factor for Total Pulp Regeneration. *Stem Cell Transl Med* 2 (7), 521–533. doi:10.5966/sctm.2012-0132
- Iwasaki, K., Washio, K., Meinzer, W., Tsumanuma, Y., Yano, K., and Ishikawa, I. (2019). Application of Cell-Sheet Engineering for New Formation of Cementum Around Dental Implants. *Heliyon* 5 (6), e01991. doi:10.1016/j.heliyon.2019.e01991
- Iwase, H., Liu, H., Wijkstrom, M., Zhou, H., Singh, J., Hara, H., et al. (2015). Pig Kidney Graft Survival in a Baboon for 136 Days: Longest Life-Supporting Organ Graft Survival to Date. *Xenotransplantation* 22 (4), 302–309. doi:10.1111/xen.12174
- Iwata, T., Yamato, M., Ishikawa, I., Ando, T., and Okano, T. (2014). Tissue Engineering in Periodontal Tissue. *Anat. Rec.* 297 (1), 16–25. doi:10.1002/ar.22812
- Jin, Y., Zhang, W., Liu, Y., Zhang, M., Xu, L., Wu, Q., et al. (2014). rhPDGF-BB via ERK Pathway Osteogenesis and Adipogenesis Balancing in ADSCs for Critical-Sized Calvarial Defect Repair. *Tissue Eng. A* 20 (23–24), 3303–3313. doi:10.1089/ten.TEA.2013.0556
- Kagami, H., Agata, H., Inoue, M., Asahina, I., Tojo, A., Yamashita, N., et al. (2014). The Use of Bone Marrow Stromal Cells (Bone Marrow-Derived Multipotent Mesenchymal Stromal Cells) for Alveolar Bone Tissue Engineering: Basic Science to Clinical Translation. *Tissue Eng. B: Rev.* 20 (3), 229–232. doi:10.1089/ten.TEB.2013.0578
- Khodakaram-Tafti, A., Mehrabani, D., and Shaterzadeh-Yazdi, H. (2017). An Overview on Autologous Fibrin Glue in Bone Tissue Engineering of Maxillofacial Surgery. *Dent Res. J. (Isfahan)* 14 (2), 79–86.
- Khodakaram-Tafti, A., Mehrabani, D., Shaterzadeh-Yazdi, H., Zamiri, B., and Omid, M. (2018). Tissue Engineering in Maxillary Bone Defects. *World J. Plast. Surg.* 7 (1), 3–11.
- Kim, H.-S., Kim, K.-H., Kim, S.-H., Kim, Y.-S., Koo, K.-T., Kim, T.-I., et al. (2010). Immunomodulatory Effect of Canine Periodontal Ligament Stem Cells on Allogenic and Xenogenic Peripheral Blood Mononuclear Cells. *J. Periodontal Implant Sci.* 40 (6), 265–270. doi:10.5051/jpis.2010.40.6.265
- Kim, S. G., Zhou, J., Solomon, C., Zheng, Y., Suzuki, T., Chen, M., et al. (2012b). Effects of Growth Factors on Dental Stem/progenitor Cells. *Dental Clin. North America* 56 (3), 563–575. doi:10.1016/j.cden.2012.05.001
- Kim, S., Kang, Y., Krueger, C. A., Sen, M., Holcomb, J. B., Chen, D., et al. (2012a). Sequential Delivery of BMP-2 and IGF-1 Using a Chitosan Gel with Gelatin Microspheres Enhances Early Osteoblastic Differentiation. *Acta Biomater.* 8 (5), 1768–1777. doi:10.1016/j.actbio.2012.01.009
- Kolagar, T. A., Farzaneh, M., Nikkar, N., and Khoshnam, S. E. (2020). Human Pluripotent Stem Cells in Neurodegenerative Diseases: Potentials, Advances and Limitations. *Cscr* 15 (2), 102–110. doi:10.2174/1574888x14666190823142911
- Lambricht, L., De Berdt, P., Vanacker, J., Leprince, J., Diogenes, A., Goldansaz, H., et al. (2014). The Type and Composition of Alginate and Hyaluronic-Based Hydrogels Influence the Viability of Stem Cells of the Apical Papilla. *Dental Mater.* 30 (12), e349–e361. doi:10.1016/j.dental.2014.08.369
- Lambrichts, L., Driesen, R. B., Dillen, Y., Gervois, P., Ratajczak, J., Vanganswinkel, T., et al. (2017). Dental Pulp Stem Cells: Their Potential in Reinnervation and Angiogenesis by Using Scaffolds. *J. Endodontics* 43 (9s), S12–s16. doi:10.1016/j.joen.2017.06.001
- Langer, R., and Vacanti, J. (1993). Tissue Engineering. *Science* 260 (5110), 920–926. doi:10.1126/science.8493529
- Lataillade, J.-J., Albanese, P., and Uzan, G. (2010). Implication de l'acide hyaluronique dans l'angiogenèse normale et pathologique, application à l'ingénierie cellulaire. *Ann. de Dermatologie de Vénérologie* 137 (Suppl. 1), S15–S22. doi:10.1016/s0151-9638(10)70004-1
- Lauritano, D., Limongelli, L., Moreo, G., Favia, G., and Carinci, F. (2020). Nanomaterials for Periodontal Tissue Engineering: Chitosan-Based

- Scaffolds. A Systematic Review. *Nanomaterials* 10 (4), 605. doi:10.3390/nano10040605
- Lee, J.-M., Kim, H.-Y., Park, J.-S., Lee, D.-J., Zhang, S., Green, D. W., et al. (2019a). Developing Palatal Bone Using Human Mesenchymal Stem Cell and Stem Cells from Exfoliated Deciduous Teeth Cell Sheets. *J. Tissue Eng. Regen. Med.* 13 (2), 319–327. doi:10.1002/term.2811
- Lee, K., Ben Amara, H., Lee, S. C., Leesungbok, R., Chung, M. A., Koo, K.-T., et al. (2019b). Chemical Regeneration of Wound Defects: Relevance to the Canine Palatal Mucosa and Cell Cycle Up-Regulation in Human Gingival Fibroblasts. *Tissue Eng. Regen. Med.* 16 (6), 675–684. doi:10.1007/s13770-019-00227-6
- Li, W., Fu, Y., Jiang, B., Lo, A. Y., Ameer, G. A., Barnett, C., et al. (2019a). Polymer-integrated Amnion Scaffold Significantly Improves Cleft Palate Repair. *Acta Biomater.* 92, 104–114. doi:10.1016/j.actbio.2019.05.035
- Li, Y., Yang, F., Gao, M., Gong, R., Jin, M., Liu, T., et al. (2019b). miR-149-3p Regulates the Switch between Adipogenic and Osteogenic Differentiation of BMSCs by Targeting FTO. *Mol. Ther. - Nucleic Acids* 17, 590–600. doi:10.1016/j.omtn.2019.06.023
- Li, Z., Du, T., Ruan, C., and Niu, X. (2021). Bioinspired Mineralized Collagen Scaffolds for Bone Tissue Engineering. *Bioactive Mater.* 6 (5), 1491–1511. doi:10.1016/j.bioactmat.2020.11.004
- Liao, J., Wang, B., Huang, Y., Qu, Y., Peng, J., and Qian, Z. (2017). Injectable Alginate Hydrogel Cross-Linked by Calcium Gluconate-Loaded Porous Microspheres for Cartilage Tissue Engineering. *ACS Omega* 2 (2), 443–454. doi:10.1021/acsomega.6b00495
- Lima, R. L., Holanda-Afonso, R. C., Moura-Neto, V., Bolognese, A. M., DosSantos, M. F., and Souza, M. M. (2017). Human Dental Follicle Cells Express Embryonic, Mesenchymal and Neural Stem Cells Markers. *Arch. Oral Biol.* 73, 121–128. doi:10.1016/j.archoralbio.2016.10.003
- Lin, C.-H., and Kudva, A. (2021). Simultaneous Reconstruction of Mandibular and Maxillary Defects Using the Single Free Fibular Osseocutaneous Flap. *Ann. Plast. Surg.* 86 (4), 428–433. doi:10.1097/sap.0000000000002436
- Lipska, B. S., Brzeskiewicz, M., Wierzb, J., Morzuchi, L., Piotrowski, A., and Limon, J. (2011). 8.6Mb Interstitial Deletion of Chromosome 4q13.3q21.23 in a Boy with Cognitive Impairment, Short Stature, Hearing Loss, Skeletal Abnormalities and Facial Dysmorphism. *Genet. Couns.* 22 (4), 353–363.
- Liu, C., Su, Y., Tan, B., Ma, P., Wu, G., Li, J., et al. (2014). Reconstruction of Attached Soft Tissue Around Dental Implants by Acellular Dermal Matrix Grafts and Resin Splint. *Int. J. Clin. Exp. Med.* 7 (12), 4666–4676.
- Liu, T., Xu, J., Pan, X., Ding, Z., Xie, H., Wang, X., et al. (2021). Advances of Adipose-Derived Mesenchymal Stem Cells-Based Biomaterial Scaffolds for Oral and Maxillofacial Tissue Engineering. *Bioactive Mater.* 6 (8), 2467–2478. doi:10.1016/j.bioactmat.2021.01.015
- Liu, X., Chang, L., Miao, Y., Fan, D., Zhang, H., Ma, H., et al. (2016). The Efficiency of Magnetic Hyperthermia and *In Vivo* Histocompatibility for Human-like Collagen Protein-Coated Magnetic Nanoparticles. *Ijn* 11, 1175–1185. doi:10.2147/ijn.S101741
- Liu, X., Wang, Z., Song, W., Sun, W., Hong, R., Pothukuchi, A., et al. (2020a). Systematically Transplanted Human Gingiva-derived Mesenchymal Stem Cells Regulate Lipid Metabolism and Inflammation in Hyperlipidemic Mice with Periodontitis. *Exp. Ther. Med.* 19 (1), 672–682. doi:10.3892/etm.2019.8256
- Liu, Y., Wang, H., Dou, H., Tian, B., Li, L., Jin, L., et al. (2020b). Bone Regeneration Capacities of Alveolar Bone Mesenchymal Stem Cells Sheet in Rabbit Calvarial Bone Defect. *J. Tissue Eng.* 11, 204173142093037. doi:10.1177/2041731420930379
- Lubkowska, A., Dolegowska, B., and Banfi, G. (2012). Growth Factor Content in PRP and Their Applicability in Medicine. *J. Biol. Regul. Homeost. Agents* 26 (2 Suppl. 1), 3s–22s.
- Ma, P., Dai, S., Jin, C., Yao, Y., and Zou, C. (2018). Tooth Loss and Risk of Colorectal Cancer: A Dose-Response Meta-Analysis of Prospective Cohort Studies. *Ott* 11, 1617–1623. doi:10.2147/ott.S151028
- Magnucki, G., Schenk, U., Ahrens, S., Navarrete Santos, A., R. Gernhardt, C., Schaller, H.-G., et al. (2013). Expression of the IGF-1, IGF-1R and IGF-1 Receptors in Dental Pulp Stem Cells and Impacted Third Molars. *J. Oral Sci.* 55 (4), 319–327. doi:10.2334/josnusd.55.319
- Martins, C., Sousa, F., Araújo, F., and Sarmiento, B. (2018). Functionalizing PLGA and PLGA Derivatives for Drug Delivery and Tissue Regeneration Applications. *Adv. Healthc. Mater.* 7 (1), 1701035. doi:10.1002/adhm.201701035
- Matichescu, A., Ardelean, L. C., Rusu, L.-C., Craciun, D., Bratu, E. A., Babucea, M., et al. (2020). Advanced Biomaterials and Techniques for Oral Tissue Engineering and Regeneration-A Review. *Materials* 13 (22), 5303. doi:10.3390/ma13225303
- Matthias, S., Nicot, R., Arnaud, Depeyre, Juma, Alkasbi, and Joël, Ferri. (2019). Reconstruction of a Large Posttraumatic Mandibular Defect Using Bone Tissue Engineering with Fresh-Frozen Humeral Allograft Seeded with Autologous Bone Marrow Aspirate and Vascularized with a Radial Forearm Flap. *J. Craniofac. Surg.* 30 (7), 2085–2087.
- McClellan, P., and Landis, W. J. (2016). Recent Applications of Coaxial and Emulsion Electrospinning Methods in the Field of Tissue Engineering. *BioResearch Open Access* 5 (1), 212–227. doi:10.1089/biores.2016.0022
- Mihaila, S. M., Gaharwar, A. K., Reis, R. L., Khademhosseini, A., Marques, A. P., and Gomes, M. E. (2014). The Osteogenic Differentiation of SSEA-4 Subpopulation of Human Adipose Derived Stem Cells Using Silicate Nanoplatelets. *Biomaterials* 35 (33), 9087–9099. doi:10.1016/j.biomaterials.2014.07.052
- Milinkovic, I., Aleksic, Z., Jankovic, S., Popovic, O., Bajic, M., Cacic, S., et al. (2015). Clinical Application of Autologous Fibroblast Cell Culture in Gingival Recession Treatment. *J. Periodont Res.* 50 (3), 363–370. doi:10.1111/jre.12215
- Mirdamadi, E. S., Kalhori, D., Zakeri, N., Azarpira, N., and Solati-Hashjin, M. (2020). Liver Tissue Engineering as an Emerging Alternative for Liver Disease Treatment. *Tissue Eng. Part B: Rev.* 26 (2), 145–163. doi:10.1089/ten.TEB.2019.0233
- Mogoșanu, G. D., and Grumezescu, A. M. (2014). Natural and Synthetic Polymers for Wounds and Burns Dressing. *Int. J. Pharmaceutics* 463 (2), 127–136. doi:10.1016/j.ijpharm.2013.12.015
- Mohiuddin, M. M., Singh, A. K., Corcoran, P. C., Hoyt, R. F., Thomas, M. L., 3rd, Lewis, B. G. T., et al. (2014). One-year Heterotopic Cardiac Xenograft Survival in a Pig to Baboon Model. *Am. J. Transpl.* 14 (2), 488–489. doi:10.1111/ajt.12562
- Morotomi, T., Washio, A., and Kitamura, C. (2019). Current and Future Options for Dental Pulp Therapy. *Jpn. Dental Sci. Rev.* 55 (1), 5–11. doi:10.1016/j.jdsr.2018.09.001
- Mrozik, K. M., Wada, N., Marino, V., Richter, W., Shi, S., Wheeler, D. L., et al. (2013). Regeneration of Periodontal Tissues Using Allogeneic Periodontal Ligament Stem Cells in an Ovine Model. *Regenerative Med.* 8 (6), 711–723. doi:10.2217/rme.13.66
- Muzzarelli, R., El Mehtedi, M., Bottegoni, C., Aquili, A., and Gigante, A. (2015). Genipin-Crosslinked Chitosan Gels and Scaffolds for Tissue Engineering and Regeneration of Cartilage and Bone. *Mar. Drugs* 13 (12), 7314–7338. doi:10.3390/md13127068
- Nakamura, Y., Ishikawa, H., Kawai, K., Tabata, Y., and Suzuki, S. (2013). Enhanced Wound Healing by Topical Administration of Mesenchymal Stem Cells Transfected with Stromal Cell-Derived Factor-1. *Biomaterials* 34 (37), 9393–9400. doi:10.1016/j.biomaterials.2013.08.053
- Namini, M. S., Bayat, N., Tajerian, R., Ebrahimi-Barough, S., Azami, M., Irani, S., et al. (2018). A Comparison Study on the Behavior of Human Endometrial Stem Cell-Derived Osteoblast Cells on PLGA/HA Nanocomposite Scaffolds Fabricated by Electrospinning and Freeze-Drying Methods. *J. Orthop. Surg. Res.* 13 (1), 63. doi:10.1186/s13018-018-0754-9
- Nancarrow-Lei, R., Mafi, P., Mafi, R., and Khan, W. (2017). A Systemic Review of Adult Mesenchymal Stem Cell Sources and Their Multilineage Differentiation Potential Relevant to Musculoskeletal Tissue Repair and Regeneration. *Curr. Stem Cell Res Ther* 12 (8), 601–610. doi:10.2174/1574888x12666170608124303
- Ng, T. K., Yang, Q., Fortino, V. R., Lai, N. Y. K., Carballosa, C. M., Greenberg, J. M., et al. (2019). MicroRNA-132 Directs Human Periodontal Ligament-derived Neural Crest Stem Cell Neural Differentiation. *J. Tissue Eng. Regen. Med.* 13 (1), 12–24. doi:10.1002/term.2759
- Nikoloudaki, G., Creber, K., and Hamilton, D. W. (2020). Wound Healing and Fibrosis: a Contrasting Role for Periostin in Skin and the Oral Mucosa. *Am. J. Physiology-Cell Physiol.* 318 (6), C1065–c1077. doi:10.1152/ajpcell.00035.2020
- Niwa, T., Yamakoshi, Y., Yamazaki, H., Karakida, T., Chiba, R., Hu, J. C.-C., et al. (2018). The Dynamics of TGF- β in Dental Pulp, Odontoblasts and Dentin. *Sci. Rep.* 8 (1), 4450. doi:10.1038/s41598-018-22823-7

- Noh, K., Thoma, D. S., Park, J.-C., Lee, D.-W., Shin, S.-Y., and Lim, H.-C. (2021). A Case Series of Profilometric Changes in Two Implant Placement Protocols at Periodontally Compromised Non-molar Sites. *Sci. Rep.* 11 (1), 1714. doi:10.1038/s41598-021-81402-5
- Nosrat, A., Kolahdouzan, A., Khatibi, A. H., Verma, P., Jamshidi, D., Nevins, A. J., et al. (2019). Clinical, Radiographic, and Histologic Outcome of Regenerative Endodontic Treatment in Human Teeth Using a Novel Collagen-Hydroxyapatite Scaffold. *J. Endodontics* 45 (2), 136–143. doi:10.1016/j.joen.2018.10.012
- Oliva, J., Bardag-Gorce, F., and Niihara, Y. (2020). Clinical Trials of Limbal Stem Cell Deficiency Treated with Oral Mucosal Epithelial Cells. *Ijms* 21 (2), 411. doi:10.3390/ijms21020411
- Omorphos, N. P., Gao, C., Tan, S. S., and Sangha, M. S. (2021). Understanding Angiogenesis and the Role of Angiogenic Growth Factors in the Vascularisation of Engineered Tissues. *Mol. Biol. Rep.* 48 (1), 941–950. doi:10.1007/s11033-020-06108-9
- Ono, M., Oshima, M., Ogawa, M., Sonoyama, W., Hara, E. S., Oida, Y., et al. (2017). Practical Whole-Tooth Restoration Utilizing Autologous Bioengineered Tooth Germ Transplantation in a Postnatal Canine Model. *Sci. Rep.* 7, 44522. doi:10.1038/srep44522
- Oyanagi, T., Takeshita, N., Hara, M., Ikeda, E., Chida, T., Seki, D., et al. (2019). Insulin-like Growth Factor 1 Modulates Bioengineered Tooth Morphogenesis. *Sci. Rep.* 9 (1), 368. doi:10.1038/s41598-018-36863-6
- Ozone, C., Suga, H., Eiraku, M., Kadoshima, T., Yonemura, S., Takata, N., et al. (2016). Functional Anterior Pituitary Generated in Self-Organizing Culture of Human Embryonic Stem Cells. *Nat. Commun.* 7, 10351. doi:10.1038/ncomms10351
- Panduwawala, C. P., Zhan, X., Dissanayaka, W. L., Samaranyake, L. P., Jin, L., and Zhang, C. (2017). *In Vivo* periodontal Tissue Regeneration by Periodontal Ligament Stem Cells and Endothelial Cells in Three-Dimensional Cell Sheet Constructs. *J. Periodont Res.* 52 (3), 408–418. doi:10.1111/jre.12405
- Pardal-Peláez, B., Flores-Fraile, J., Pardal-Refoyo, J. L., and Montero, J. (2021). Implant Loss and Crestal Bone Loss in Immediate versus Delayed Load in Edentulous Mandibles: A Systematic Review and Meta-Analysis. *The J. Prosthetic Dentistry* 125 (3), 437–444. doi:10.1016/j.prosdent.2020.01.032
- Park, J. H., Hong, J. M., Ju, Y. M., Jung, J. W., Kang, H.-W., Lee, S. J., et al. (2015). A Novel Tissue-Engineered Trachea with a Mechanical Behavior Similar to Native Trachea. *Biomaterials* 62, 106–115. doi:10.1016/j.biomaterials.2015.05.008
- Peramo, A., Marcelo, C. L., and Feinberg, S. E. (2012). Tissue Engineering of Lips and Muco-Cutaneous Junctions: *In Vitro* Development of Tissue Engineered Constructs of Oral Mucosa and Skin for Lip Reconstruction. *Tissue Eng. C: Methods* 18 (4), 273–282. doi:10.1089/ten.TEC.2011.0406
- Pilipchuk, S. P., Plonka, A. B., Monje, A., Taut, A. D., Lanis, A., Kang, B., et al. (2015). Tissue Engineering for Bone Regeneration and Osseointegration in the Oral Cavity. *Dental Mater.* 31 (4), 317–338. doi:10.1016/j.dental.2015.01.006
- Raddall, G., Mello, I., and Leung, B. M. (2019). Biomaterials and Scaffold Design Strategies for Regenerative Endodontic Therapy. *Front. Bioeng. Biotechnol.* 7, 317. doi:10.3389/fbioe.2019.00317
- Rai, R., Raval, R., Khandeparker, R. V., Chidrawar, S. K., Khan, A. A., and Ganpat, M. S. (2015). Tissue Engineering: Step Ahead in Maxillofacial Reconstruction. *J. Int. Oral Health* 7 (9), 138–142.
- Rao, F., Zhang, D., Fang, T., Lu, C., Wang, B., Ding, X., et al. (2019). Exosomes from Human Gingiva-Derived Mesenchymal Stem Cells Combined with Biodegradable Chitin Conduits Promote Rat Sciatic Nerve Regeneration. *Stem Cell Int.* 2019, 1–12. doi:10.1155/2019/2546367
- Rasperini, G., Pilipchuk, S. P., Flanagan, C. L., Park, C. H., Pagni, G., Hollister, S. J., et al. (2015). 3D-printed Bioresorbable Scaffold for Periodontal Repair. *J. Dent Res.* 94 (9 Suppl. 1), 153s–157s. doi:10.1177/0022034515588303
- Redondo, L. M., García, V., Peral, B., Verrier, A., Becerra, J., Sánchez, A., et al. (2018). Repair of Maxillary Cystic Bone Defects with Mesenchymal Stem Cells Seeded on a Cross-Linked Serum Scaffold. *J. Craniomaxillofac. Surg.* 46 (2), 222–229. doi:10.1016/j.jcms.2017.11.004
- Schorn, L., Fienitz, T., Gerstenberg, M. F., Sterner-Kock, A., Maul, A. C., Lommen, J., et al. (2021). Influence of Different Carrier Materials on Biphasic Calcium Phosphate Induced Bone Regeneration. *Clin. Oral Invest.* 25 (6), 3729–3737. doi:10.1007/s00784-020-03700-y
- Schreurs, M., Suttorp, C. M., Mutsaers, H. A. M., Kuijpers-Jagtman, A. M., den Hoff, J. W., Ongkosuwo, E. M., et al. (2020). Tissue Engineering Strategies Combining Molecular Targets against Inflammation and Fibrosis, and Umbilical Cord Blood Stem Cells to Improve Hampered Muscle and Skin Regeneration Following Cleft Repair. *Med. Res. Rev.* 40 (1), 9–26. doi:10.1002/med.21594
- Scott, L., Jurewicz, I., Jeevaratnam, K., and Lewis, R. (2021). Carbon Nanotube-Based Scaffolds for Cardiac Tissue Engineering-Systematic Review and Narrative Synthesis. *Bioengineering* 8 (6), 80. doi:10.3390/bioengineering8060080
- Selvasandran, K., Makhoul, G., Jaiswal, P. K., Jurakhan, R., Li, L., Ridwan, K., et al. (2018). A Tumor Necrosis Factor- α and Hypoxia-Induced Secretome Therapy for Myocardial Repair. *Ann. Thorac. Surg.* 105 (3), 715–723. doi:10.1016/j.athoracsur.2017.09.005
- Shang, F., Yu, Y., Liu, S., Ming, L., Zhang, Y., Zhou, Z., et al. (2021). Advancing Application of Mesenchymal Stem Cell-Based Bone Tissue Regeneration. *Bioactive Mater.* 6 (3), 666–683. doi:10.1016/j.bioactmat.2020.08.014
- Sharif, F., Roman, S., Asif, A., Gigliobianco, G., Ghafoor, S., Tariq, M., et al. (2019). Developing a Synthetic Composite Membrane for Cleft Palate Repair. *J. Tissue Eng. Regen. Med.* 13 (7), 1178–1189. doi:10.1002/term.2867
- Shen, Z., Tsao, H., LaRue, S., Liu, R., Kirkpatrick, T. C., Souza, L. C. d., et al. (2021). Vascular Endothelial Growth Factor And/or Nerve Growth Factor Treatment Induces Expression of Dentinogenic, Neuronal, and Healing Markers in Stem Cells of the Apical Papilla. *J. Endodontics* 47 (6), 924–931. doi:10.1016/j.joen.2021.02.011
- Shi, Q., Qian, Z., Liu, D., Sun, J., Wang, X., Liu, H., et al. (2017). GMSC-derived Exosomes Combined with a Chitosan/Silk Hydrogel Sponge Accelerates Wound Healing in a Diabetic Rat Skin Defect Model. *Front. Physiol.* 8, 904. doi:10.3389/fphys.2017.00904
- Shibuya, M. (2013). Vascular Endothelial Growth Factor and its Receptor System: Physiological Functions in Angiogenesis and Pathological Roles in Various Diseases. *J. Biochem.* 153 (1), 13–19. doi:10.1093/jb/mvs136
- Shiehzhadeh, V., Aghmasheh, F., Shiehzhadeh, F., Joulae, M., Kosarieh, E., and Shiehzhadeh, F. (2014). Healing of Large Periapical Lesions Following Delivery of Dental Stem Cells with an Injectable Scaffold: New Method and Three Case Reports. *Indian J. Dent Res.* 25 (2), 248–253. doi:10.4103/0970-9290.135937
- Siddiqui, N., Asawa, S., Birru, B., Baadhe, R., and Rao, S. (2018). PCL-based Composite Scaffold Matrices for Tissue Engineering Applications. *Mol. Biotechnol.* 60 (7), 506–532. doi:10.1007/s12033-018-0084-5
- Sieira Gil, R., Pagés, C. M., Díez, E. G., Llamas, S., Fuertes, A. F., and Vilagran, J. L. (2015). Tissue-engineered Oral Mucosa Grafts for Intraoral Lining Reconstruction of the Maxilla and Mandible with a Fibula Flap. *J. Oral Maxillofacial Surg.* 73 (1), e1–195. doi:10.1016/j.joms.2014.09.001
- Simion, M., Rocchietta, I., Fontana, F., and Dellavia, C. (2012). Evaluation of a Resorbable Collagen Matrix Infused with rhPDGF-BB in Peri-Implant Soft Tissue Augmentation: a Preliminary Report with 3.5 Years of Observation. *Int. J. Periodontics Restorative Dent* 32 (3), 273–282.
- Singh, R. K., Seliktar, D., and Putnam, A. J. (2013). Capillary Morphogenesis in PEG-Collagen Hydrogels. *Biomaterials* 34 (37), 9331–9340. doi:10.1016/j.biomaterials.2013.08.016
- Smith, E. E., Zhang, W., Schiele, N. R., Khademhosseini, A., Kuo, C. K., and Yelick, P. C. (2017). Developing a Biomimetic Tooth Bud Model. *J. Tissue Eng. Regen. Med.* 11 (12), 3326–3336. doi:10.1002/term.2246
- Soltani, P., Shahnaseri, S., Sheikhi, M., Hashemibeni, B., and Mousavi, S. (2020). Comparison of Autogenous Bone Graft and Tissue-Engineered Bone Graft in Alveolar Cleft Defects in Canine Animal Models Using Digital Radiography. *Indian J. Dent Res.* 31 (1), 118–123. doi:10.4103/ijdr.IJDR_156_18
- Somoza, R. A., Acevedo, C. A., Albornoz, F., Luz-Crawford, P., Carrión, F., Young, M. E., et al. (2017). TGF β 3 Secretion by Three-Dimensional Cultures of Human Dental Apical Papilla Mesenchymal Stem Cells. *J. Tissue Eng. Regen. Med.* 11 (4), 1045–1056. doi:10.1002/term.2004
- Sprio, S., Campodoni, E., Sandri, M., Preti, L., Keppler, T., Müller, F., et al. (2018). A Graded Multifunctional Hybrid Scaffold with Superparamagnetic Ability for Periodontal Regeneration. *Ijms* 19 (11), 3604. doi:10.3390/ijms19113604
- Sugimura-Wakayama, Y., Katagiri, W., Osugi, M., Kawai, T., Ogata, K., Sakaguchi, K., et al. (2015). Peripheral Nerve Regeneration by Secretomes of Stem Cells from Human Exfoliated Deciduous Teeth. *Stem Cell Development* 24 (22), 2687–2699. doi:10.1089/scd.2015.0104

- Sun, X., Liu, C., Shi, Y., Li, C., Sun, L., Hou, L., et al. (2019). The Assessment of Xenogeneic Bone Immunotoxicity and Risk Management Study. *Biomed. Eng. Online* 18 (1), 108. doi:10.1186/s12938-019-0729-z
- Tan, H. B., Giannoudis, P. V., Boxall, S. A., McGonagle, D., and Jones, E. (2015). The Systemic Influence of Platelet-Derived Growth Factors on Bone Marrow Mesenchymal Stem Cells in Fracture Patients. *BMC Med.* 13, 6. doi:10.1186/s12916-014-0202-6
- Tarr, J., Lambi, A., Bradley, J., Barbe, M., and Popoff, S. (2018). Development of Normal and Cleft Palate: A Central Role for Connective Tissue Growth Factor (CTGF)/CCN2. *Jdb* 6 (3), 18. doi:10.3390/jdb6030018
- Taşlı, P. N., Aydın, S., Yalvaç, M. E., and Şahin, F. (2014). Bmp 2 and Bmp 7 Induce Odonto- and Osteogenesis of Human Tooth Germ Stem Cells. *Appl. Biochem. Biotechnol.* 172 (6), 3016–3025. doi:10.1007/s12010-013-0706-0
- Tetè, G., D'Orto, B., Nagni, M., Agostinacchio, M., Polizzi, E., and Agliardi, E. (2020). Role of Induced Pluripotent Stem Cells (iPSCs) in Bone Tissue Regeneration in Dentistry: a Narrative Review. *J. Biol. Regul. Homeost. Agents* 34 (6 Suppl. 3), 1–10.
- Thein-Han, W., and Xu, H. H. K. (2011). Collagen-calcium Phosphate Cement Scaffolds Seeded with Umbilical Cord Stem Cells for Bone Tissue Engineering. *Tissue Eng. Part A* 17 (23–24), 2943–2954. doi:10.1089/ten.tea.2010.0674
- Tian, Y., Bai, D., Guo, W., Li, J., Zeng, J., Yang, L., et al. (2015). Comparison of Human Dental Follicle Cells and Human Periodontal Ligament Cells for Dentin Tissue Regeneration. *Regenerative Med.* 10 (4), 461–479. doi:10.2217/rme.15.21
- Toma, A. I., Fuller, J. M., Willett, N. J., and Goudy, S. L. (2021). Oral Wound Healing Models and Emerging Regenerative Therapies. *Translational Res.* 236, 17–34. doi:10.1016/j.trsl.2021.06.003
- Vacanti, J. P., Morse, M. A., Saltzman, W. M., Domb, A. J., Perez-Atayde, A., and Langer, R. (1988). Selective Cell Transplantation Using Bioabsorbable Artificial Polymers as Matrices. *J. Pediatr. Surg.* 23 (1 Pt 2), 3–9. doi:10.1016/s0022-3468(88)80529-3
- Vidal, L., Brennan, M. Á., Krissian, S., De Lima, J., Hoornaert, A., Rosset, P., et al. (2020). *In Situ* production of Pre-vascularized Synthetic Bone Grafts for Regenerating Critical-Sized Defects in Rabbits. *Acta Biomater.* 114, 384–394. doi:10.1016/j.actbio.2020.07.030
- Vishwanath, V., Pramanik, K., and Biswas, A. (2016). Optimization and Evaluation of Silk Fibroin-Chitosan Freeze-Dried Porous Scaffolds for Cartilage Tissue Engineering Application. *J. Biomater. Sci. Polym. Edition* 27 (7), 657–674. doi:10.1080/09205063.2016.1148303
- Volponi, A. A., Pang, Y., and Sharpe, P. T. (2010). Stem Cell-Based Biological Tooth Repair and Regeneration. *Trends Cell Biol.* 20 (12), 715–722. doi:10.1016/j.tcb.2010.09.012
- Von den Hoff, J. W., Carvajal Monroy, P. L., Ongkosuwito, E. M., van Kuppevelt, T. H., and Daamen, W. F. (2019). Muscle Fibrosis in the Soft Palate: Delivery of Cells, Growth Factors and Anti-fibrotics. *Adv. Drug Deliv. Rev.* 146, 60–76. doi:10.1016/j.addr.2018.08.002
- Wang, F., Wu, Z., Fan, Z., Wu, T., Wang, J., Zhang, C., et al. (2018a). The Cell Re-association-based Whole-Tooth Regeneration Strategies in Large Animal, *Sus scrofa*. *Cell Prolif* 51 (4), e12479. doi:10.1111/cpr.12479
- Wang, T., Muhetaer, H., and Li, J. (2017). Experimental Study of Transforming Growth Factor-B3 Combined with Dental Pulp Stem Cells in Promoting the Implant's Osseointegration. *Zhonghua Kou Qiang Yi Xue Za Zhi* 52 (6), 367–373. doi:10.3760/cma.j.issn.1002-0098.2017.06.009
- Wang, W., Dang, M., Zhang, Z., Hu, J., Eyster, T. W., Ni, L., et al. (2016a). Dentin Regeneration by Stem Cells of Apical Papilla on Injectable Nanofibrous Microspheres and Stimulated by Controlled BMP-2 Release. *Acta Biomater.* 36, 63–72. doi:10.1016/j.actbio.2016.03.015
- Wang, W., Meng, Q., Li, Q., Liu, J., Zhou, M., Jin, Z., et al. (2020). Chitosan Derivatives and Their Application in Biomedicine. *Ijms* 21 (2), 487. doi:10.3390/ijms21020487
- Wang, X., Chang, J., and Wu, C. (2018b). Bioactive Inorganic/organic Nanocomposites for Wound Healing. *Appl. Mater. Today* 11, 308–319. doi:10.1016/j.apmt.2018.03.001
- Wang, Z.-S., Feng, Z.-H., Wu, G.-F., Bai, S.-Z., Dong, Y., Chen, F.-M., et al. (2016b). The Use of Platelet-Rich Fibrin Combined with Periodontal Ligament and Jaw Bone Mesenchymal Stem Cell Sheets for Periodontal Tissue Engineering. *Sci. Rep.* 6, 28126. doi:10.1038/srep28126
- Weiss, A., and Attisano, L. (2013). The TGFβ Superfamily Signaling Pathway. *Wires Dev. Biol.* 2 (1), 47–63. doi:10.1002/wdev.86
- Wu, M., Wang, J., Zhang, Y., Liu, H., and Dong, F. (2018). Mineralization Induction of Gingival Fibroblasts and Construction of a Sandwich Tissue-Engineered Complex for Repairing Periodontal Defects. *Med. Sci. Monit.* 24, 1112–1123. doi:10.12659/msm.908791
- Xing, B., Wu, F., Li, T., Qi, S., Xie, J., and Ye, Z. (2013). Experimental Study of Comparing rhEGF with rhβFGF on Improving the Quality of Wound Healing. *Int. J. Clin. Exp. Med.* 6 (8), 655–661.
- Xu, F., Qiao, L., Zhao, Y., Chen, W., Hong, S., Pan, J., et al. (2019a). The Potential Application of Concentrated Growth Factor in Pulp Regeneration: an *In Vitro* and *In Vivo* Study. *Stem Cell Res Ther* 10 (1), 134. doi:10.1186/s13287-019-1247-4
- Xu, M., Li, J., Liu, X., Long, S., Shen, Y., Li, Q., et al. (2019b). Fabrication of Vascularized and Scaffold-free Bone Tissue Using Endothelial and Osteogenic Cells Differentiated from Bone Marrow Derived Mesenchymal Stem Cells. *Tissue and Cell* 61, 21–29. doi:10.1016/j.tice.2019.08.003
- Xu, P., Xin, Y., Zhang, Z., Zou, X., Xue, K., Zhang, H., et al. (2020). Extracellular Vesicles from Adipose-Derived Stem Cells Ameliorate Ultraviolet B-Induced Skin Photoaging by Attenuating Reactive Oxygen Species Production and Inflammation. *Stem Cell Res Ther* 11 (1), 264. doi:10.1186/s13287-020-01777-6
- Yalvac, M. E., Ramazanoglu, M., Rizvanov, A. A., Sahin, F., Bayrak, O. F., Salli, U., et al. (2010). Isolation and Characterization of Stem Cells Derived from Human Third Molar Tooth Germs of Young Adults: Implications in Neo-Vascularization, Osteo-, Adipo- and Neurogenesis. *Pharmacogenomics J.* 10 (2), 105–113. doi:10.1038/tpj.2009.40
- Yang, H., Apreccio, R. M., Zhou, X., Wang, Q., Zhang, W., Ding, Y., et al. (2014). Therapeutic Effect of TSG-6 Engineered iPSC-Derived MSCs on Experimental Periodontitis in Rats: a Pilot Study. *PLoS One* 9 (6), e100285. doi:10.1371/journal.pone.0100285
- Yang, H., Cao, Y., Zhang, J., Liang, Y., Su, X., Zhang, C., et al. (2020). DLX5 and HOXC8 Enhance the Chondrogenic Differentiation Potential of Stem Cells from Apical Papilla via LINC01013. *Stem Cell Res Ther* 11 (1), 271. doi:10.1186/s13287-020-01791-8
- Yang, J., Wang, W. J., Jia, W. Q., Zhao, Y. M., and Ge, L. H. (2018). Effect of Exogenous Stem Cells from Apical Papillae in the Pulp Revascularization Treatment for the Immature Permanent Tooth with Periapical Periodontitis. *Zhonghua Kou Qiang Yi Xue Za Zhi* 53 (7), 459–465. doi:10.3760/cma.j.issn.1002-0098.2018.07.006
- Yang, Y.-Q., Tan, Y.-Y., Wong, R., Wenden, A., Zhang, L.-K., and Rabie, A. B. M. (2012). The Role of Vascular Endothelial Growth Factor in Ossification. *Int. J. Oral Sci.* 4 (2), 64–68. doi:10.1038/ijos.2012.33
- Yao, R., Zhang, R., Luan, J., and Lin, F. (2012). Alginate and Alginate/gelatin Microspheres for Human Adipose-Derived Stem Cell Encapsulation and Differentiation. *Biofabrication* 4 (2), 025007. doi:10.1088/1758-5082/4/2/025007
- Yildirim, S., Zibandeh, N., Genc, D., Ozcan, E. M., Goker, K., and Akkoc, T. (2016). The Comparison of the Immunologic Properties of Stem Cells Isolated from Human Exfoliated Deciduous Teeth, Dental Pulp, and Dental Follicles. *Stem Cell Int.* 2016, 1–15. doi:10.1155/2016/4682875
- Yoo, S.-W., Chang, D.-Y., Lee, H.-S., Kim, G.-H., Park, J.-S., Ryu, B.-Y., et al. (2013). Immune Following Suppression Mesenchymal Stem Cell Transplantation in the Ischemic Brain Is Mediated by TGF-β. *Neurobiol. Dis.* 58, 249–257. doi:10.1016/j.nbd.2013.06.001
- Yoon, I.-S., Chung, C. W., Sung, J.-H., Cho, H.-J., Kim, J. S., Shim, W.-S., et al. (2011). Proliferation and Chondrogenic Differentiation of Human Adipose-Derived Mesenchymal Stem Cells in Porous Hyaluronic Acid Scaffold. *J. Biosci. Bioeng.* 112 (4), 402–408. doi:10.1016/j.jbiosc.2011.06.018
- Yoshizawa, M., Koyama, T., Kojima, T., Kato, H., Ono, Y., and Saito, C. (2012). Keratinocytes of Tissue-Engineered Human Oral Mucosa Promote Re-epithelialization after Intraoral Grafting in Athymic Mice. *J. Oral Maxillofacial Surg.* 70 (5), 1199–1214. doi:10.1016/j.joms.2011.03.057
- Yu, P., Bao, R.-Y., Shi, X.-J., Yang, W., and Yang, M.-B. (2017). Self-assembled High-Strength Hydroxyapatite/graphene Oxide/chitosan Composite Hydrogel for Bone Tissue Engineering. *Carbohydr. Polym.* 155, 507–515. doi:10.1016/j.carbpol.2016.09.001
- Yuan, Y., and Chai, Y. (2019). Regulatory Mechanisms of Jaw Bone and Tooth Development. *Curr. Top. Dev. Biol.* 133, 91–118. doi:10.1016/bs.ctdb.2018.12.013

- Yun, J.-H., Han, S.-H., Choi, S.-H., Lee, M.-H., Lee, S.-J., Song, S. U., et al. (2014). Effects of Bone Marrow-Derived Mesenchymal Stem Cells and Platelet-Rich Plasma on Bone Regeneration for Osseointegration of Dental Implants: Preliminary Study in Canine Three-wall Intrabony Defects. *J. Biomed. Mater. Res.* 102 (5), 1021–1030. doi:10.1002/jbm.b.33084
- Zang, S., Jin, L., Kang, S., Hu, X., Wang, M., Wang, J., et al. (2016). Periodontal Wound Healing by Transplantation of Jaw Bone Marrow-Derived Mesenchymal Stem Cells in Chitosan/Anorganic Bovine Bone Carrier into One-Wall Infrabony Defects in Beagles. *J. Periodontol.* 87 (8), 971–981. doi:10.1902/jop.2016.150504
- Zhang, L., Tang, J., Sun, L., Zheng, T., Pu, X., Chen, Y., et al. (2020). Three-dimensional Printed Tissue Engineered Bone for Canine Mandibular Defects. *Genes Dis.* 7 (1), 138–149. doi:10.1016/j.gendis.2019.04.003
- Zhang, Q., Shi, S., Liu, Y., Uyanne, J., Shi, Y., Shi, S., et al. (2009). Mesenchymal Stem Cells Derived from Human Gingiva Are Capable of Immunomodulatory Functions and Ameliorate Inflammation-Related Tissue Destruction in Experimental Colitis. *J. Immunol.* 183 (12), 7787–7798. doi:10.4049/jimmunol.0902318
- Zhang, W., Vazquez, B., Oreadi, D., and Yelick, P. C. (2017). Decellularized Tooth Bud Scaffolds for Tooth Regeneration. *J. Dent Res.* 96 (5), 516–523. doi:10.1177/0022034516689082
- Zhang, Y., and Chen, Y. (2014). Bioengineering of a Human Whole Tooth: Progress and challenge. *Cell Regen.* 3 (1), 3–8. doi:10.1186/2045-9769-3-8
- Zhao, H., Shao, Y., Li, H., and Zhou, H. (2019). A Novel Method to Reconstruct Epithelial Tissue Using High-Purity Keratinocyte Lineage Cells Induced from Human Embryonic Stem Cells. *Cell Cycle* 18 (3), 264–273. doi:10.1080/15384101.2018.1555118
- Zhao, J., Han, Y., Liang, Z., Zhang, Z., Lu, Q., Yan, X., et al. (2010). Sustained Local Application of Epidermal Growth Factor to Accelerate Reepithelialization of Tracheal Grafts. *J. Thorac. Cardiovasc. Surg.* 140 (1), 209–215. doi:10.1016/j.jtcvs.2009.10.036
- Zhao, J., Jian, L., Zhang, L., Ding, T., Li, X., Cheng, D., et al. (2016a). Knockdown of SCARA5 Inhibits PDGF-BB-Induced Vascular Smooth Muscle Cell Proliferation and Migration through Suppression of the PDGF Signaling Pathway. *Mol. Med. Rep.* 13 (5), 4455–4460. doi:10.3892/mmr.2016.5074
- Zhao, M.-l., Li, X.-h., Fu, F., Qin, Z., Xu, C., Chen, X.-y., et al. (2017). Magnetic Resonance Imaging-Three-Dimensional Printing Technology Fabricates Customized Scaffolds for Brain Tissue Engineering. *Neural Regen. Res.* 12 (4), 614–622. doi:10.4103/1673-5374.205101
- Zhao, W., Li, J., Jin, K., Liu, W., Qiu, X., and Li, C. (2016b). Fabrication of Functional PLGA-Based Electrospun Scaffolds and Their Applications in Biomedical Engineering. *Mater. Sci. Eng. C* 59, 1181–1194. doi:10.1016/j.msec.2015.11.026
- Zhao, Y.-Z., Tian, X.-Q., Zhang, M., Cai, L., Ru, A., Shen, X.-T., et al. (2014). Functional and Pathological Improvements of the Hearts in Diabetes Model by the Combined Therapy of bFGF-Loaded Nanoparticles with Ultrasound-Targeted Microbubble Destruction. *J. Controlled Release* 186, 22–31. doi:10.1016/j.jconrel.2014.04.054
- Zhu, J., and Marchant, R. E. (2011). Design Properties of Hydrogel Tissue-Engineering Scaffolds. *Expert Rev. Med. Devices* 8 (5), 607–626. doi:10.1586/erd.11.27
- Zhu, Z., Yuan, Z.-Q., Huang, C., Jin, R., Sun, D., Yang, J., et al. (2019). Pre-culture of Adipose-Derived Stem Cells and Heterologous Acellular Dermal Matrix: Paracrine Functions Promote post-implantation Neovascularization and Attenuate Inflammatory Response. *Biomed. Mater.* 14 (3), 035002. doi:10.1088/1748-605X/ab0355

Conflict of Interest: The authors declare that the research was conducted in the absence of any commercial or financial relationships that could be construed as a potential conflict of interest.

Publisher's Note: All claims expressed in this article are solely those of the authors and do not necessarily represent those of their affiliated organizations, or those of the publisher, the editors, and the reviewers. Any product that may be evaluated in this article, or claim that may be made by its manufacturer, is not guaranteed or endorsed by the publisher.

Copyright © 2021 Cao, Su, Si, Xu, Chang, Lv and Zhai. This is an open-access article distributed under the terms of the Creative Commons Attribution License (CC BY). The use, distribution or reproduction in other forums is permitted, provided the original author(s) and the copyright owner(s) are credited and that the original publication in this journal is cited, in accordance with accepted academic practice. No use, distribution or reproduction is permitted which does not comply with these terms.



Ectopic Bone Tissue Engineering in Mice Using Human Gingiva or Bone Marrow-Derived Stromal/Progenitor Cells in Scaffold-Hydrogel Constructs

OPEN ACCESS

Edited by:

Nikos Donos,
Queen Mary University of London,
United Kingdom

Reviewed by:

Joaquim Vives,
Banc de Sang i Teixits, Spain
Deborah Stanco,
University of Zurich, Switzerland

*Correspondence:

Siddharth Shanbhag
siddharth.shanbhag@uib.no
Kamal Mustafa
Kamal.Mustafa@uib.no

Specialty section:

This article was submitted to
Tissue Engineering and Regenerative
Medicine,
a section of the journal
Frontiers in Bioengineering and
Biotechnology

Received: 26 September 2021

Accepted: 16 November 2021

Published: 30 November 2021

Citation:

Shanbhag S, Kampleitner C,
Mohamed-Ahmed S, Yassin MA,
Dongre H, Costea DE, Tangl S,
Hassan MN, Stavropoulos A,
Bolstad AI, Suliman S and Mustafa K
(2021) Ectopic Bone Tissue
Engineering in Mice Using Human
Gingiva or Bone Marrow-Derived
Stromal/Progenitor Cells in Scaffold-
Hydrogel Constructs.
Front. Bioeng. Biotechnol. 9:783468.
doi: 10.3389/fbioe.2021.783468

Siddharth Shanbhag^{1,2*}, Carina Kampleitner^{3,4,5}, Samih Mohamed-Ahmed¹,
Mohammed Ahmad Yassin¹, Harsh Dongre^{6,7}, Daniela Elena Costea^{6,7}, Stefan Tangl^{4,5},
Mohamad Nageeb Hassan¹, Andreas Stavropoulos^{8,9}, Anne Isine Bolstad¹, Salwa Suliman¹
and Kamal Mustafa^{1*}

¹Center for Translational Oral Research (TOR), Department of Clinical Dentistry, Faculty of Medicine, University of Bergen, Bergen, Norway, ²Department of Immunology and Transfusion Medicine, Haukeland University Hospital, Bergen, Norway, ³Ludwig Boltzmann Institute for Traumatology, The Research Center in Cooperation With AUVA, Vienna, Austria, ⁴Karl Donath Laboratory for Hard Tissue and Biomaterial Research, University Clinic of Dentistry, Medical University of Vienna, Vienna, Austria, ⁵Austrian Cluster for Tissue Regeneration, Vienna, Austria, ⁶Gade Laboratory for Pathology, Department of Clinical Medicine, Faculty of Medicine, University of Bergen, Bergen, Norway, ⁷Centre for Cancer Biomarkers (CCBIO), Faculty of Medicine, University of Bergen, Bergen, Norway, ⁸Department of Periodontology, Faculty of Odontology, Malmö University, Malmö, Sweden, ⁹Division of Conservative Dentistry and Periodontology, University Clinic of Dentistry, Medical University of Vienna, Vienna, Austria

Three-dimensional (3D) spheroid culture can promote the osteogenic differentiation and bone regeneration capacity of mesenchymal stromal cells (MSC). Gingiva-derived progenitor cells (GPC) represent a less invasive alternative to bone marrow MSC (BMSC) for clinical applications. The aim of this study was to test the *in vivo* bone forming potential of human GPC and BMSC cultured as 3D spheroids or dissociated cells (2D). 2D and 3D cells encapsulated in constructs of human platelet lysate hydrogels (HPLG) and 3D-printed poly (L-lactide-co-trimethylene carbonate) scaffolds (HPLG-PLATMC) were implanted subcutaneously in nude mice; cell-free HPLG-PLATMC constructs served as a control. Mineralization was assessed using micro-computed tomography (μ CT), histology, scanning electron microscopy (SEM) and *in situ* hybridization (ISH). After 4–8 weeks, μ CT revealed greater mineralization in 3D-BMSC vs. 2D-BMSC and 3D-GPC ($p < 0.05$), and a similar trend in 2D-GPC vs. 2D-BMSC ($p > 0.05$). After 8 weeks, greater mineralization was observed in cell-free constructs vs. all 2D- and 3D-cell groups ($p < 0.05$). Histology and SEM revealed an irregular but similar mineralization pattern in all groups. ISH revealed similar numbers of 2D and 3D BMSC/GPC within and/or surrounding the mineralized areas. In summary, spheroid culture promoted ectopic mineralization in constructs of BMSC, while constructs of dissociated GPC and BMSC performed similarly. The combination of HPLG and PLATMC represents a promising scaffold for bone tissue engineering applications.

Keywords: xeno-free, platelet lysate, MSC, spheroid culture, bone tissue engineering

INTRODUCTION

Adult mesenchymal stromal cells (MSC) are increasingly being used in bone tissue engineering (BTE) for the reconstruction of clinically challenging bone defects, and to overcome the limitations of existing bone-substitute materials (Shanbhag et al., 2019). Although MSC derived from bone marrow (BMSC) are the most widely tested, progenitor cells from other tissues requiring less-invasive harvesting, e.g., oral tissues, are being explored (Sharpe, 2016; Pittenger et al., 2019). Gingiva, in particular, can be harvested with minimal morbidity and contains a subpopulation of multipotent progenitor cells (GPCs), which demonstrate an MSC-like phenotype, immunomodulatory properties, and osteogenic potential both *in vitro* and *in vivo* (Fournier et al., 2010; Mitrano et al., 2010; Tomar et al., 2010).

A critical aspect in the clinical translation of cell therapies is the use of safe and standardized culture conditions resulting in safe-to-use cell constructs. Exclusion of animal-derived supplements, e.g., fetal bovine serum (FBS), in *ex vivo* culture systems is considered important to facilitate clinical translation of cell therapies and is also a recommendation by regulatory health authorities (Bieback et al., 2019). Pooled human platelet lysate (HPL) has been identified as the optimal “xeno-free” supplement for MSC culture, with particular benefits for BTE by promoting MSC osteogenic differentiation (Fekete et al., 2012; Shanbhag et al., 2017). We have recently reported that HPL cultured GPC and BMSC demonstrate superior proliferation, osteogenic gene expression and *in vitro* mineralization vs. corresponding FBS-based cultures (Shanbhag et al., 2020a; Shanbhag et al., 2020b).

Compared to two-dimensional (2D) monolayer cultures, the self-assembly or aggregation of MSC into 3D spheroids is mediated by unique cell-cell and cell-extracellular matrix (ECM) interactions, biomechanical cues and activated signaling pathways, simulating more closely the *in vivo* microenvironment (Sart et al., 2014; Cesarz and Tamama, 2016). Several studies have reported that, compared to conventional 2D monolayers, spheroid MSC show enhanced “stemness”, differentiation capacity, paracrine activity and immunomodulatory potential (Kale et al., 2000; Follin et al., 2016; Petrenko et al., 2017). We have recently reported that the expressions of several genes associated with self-renewal and osteogenic differentiation were significantly enhanced in xeno-free 3D spheroid vs. 2D monolayer cultures of GPC and BMSC, independent of osteogenic induction via media supplements (Shanbhag et al., 2020b). GPC and BMSC spheroids also demonstrated *in situ* mineralization and ECM formation following *in vitro* osteogenic induction, altogether, suggesting a promising potential for use in BTE (Shanbhag et al., 2020b).

Traditional cell delivery methods involve direct seeding of cells on the surface of biomaterial scaffolds before *in vivo* transplantation (Shanbhag and Shanbhag, 2015). However, this may not be optimal for MSC spheroids where the 3D structure is lost by direct seeding, thus potentially compromising their efficacy. To preserve the 3D structure, encapsulation of spheroids in hydrogel scaffolds maintains their 3D assembly and represents an effective delivery system (Murphy et al.,

2014; Murphy et al., 2015; Ho et al., 2018). Since HPL is increasingly being used for clinical-grade MSC culture, extending its application as a hydrogel scaffold represents a clinically relevant and cost-effective strategy (Robinson et al., 2016). Additionally, using 3D-printing technology, pliable scaffolds of novel copolymers, e.g., poly (L-lactide-co-trimethylene carbonate) (PLATMC) (Jain et al., 2020), can be custom designed to support the cell-hydrogel constructs in non-contained critical-size bone and/or periodontal defects (Hassan et al., 2019; Yamada et al., 2021). As a preliminary step, the regenerative potential of tissue engineered constructs is frequently tested in ectopic, e.g., subcutaneous or intramuscular, sites (Scott et al., 2012). The absence of local osteogenic cells and stimuli surmises that any observed mineralization is from exogenous origins and/or stimuli. Therefore, the objective of the present study was to compare the potential of xeno-free GPC and BMSC, as dissociated cells (2D) or spheroids (3D), encapsulated in constructs of HPL hydrogels (HPLG) and PLATMC (HPLG-PLATMC), for ectopic BTE in a subcutaneous immunocompromised mouse model.

MATERIALS AND METHODS

Cell Culture

The use of human cells and tissues was approved by the Regional Committees for Medical Research Ethics (REK) in Norway (2013-1248/REK-sør-øst C and 2016-1266/REK-nord) and obtained following appropriate informed consent. Bone marrow aspirates were obtained from three donors (one female and two males; 8–10 years) undergoing corrective surgery at the Department of Plastic Surgery, Haukeland University Hospital, Bergen, Norway. Gingival biopsies were collected from three systemically healthy, non-smoking patients (two females and one male; 18–31 years) undergoing dental surgery at the Department of Clinical Dentistry, University of Bergen, Bergen, Norway. BMSC and GPC were isolated as previously described (Mohamed-Ahmed et al., 2018; Shanbhag et al., 2020b). Briefly, primary monolayer cultures of GPC and BMSC were separately established in growth media comprising Dulbecco's Modified Eagle's medium (DMEM; Invitrogen, Carlsbad, CA, United States) supplemented with 5% (v/v) HPL (Bergenlys[®], Bergen, Norway), 1% (v/v) penicillin/streptomycin (GE Healthcare, South Logan, UT, United States) and 1 IU/ml heparin (Leo Pharma AS, Lysaker, Norway). Cells were sub-cultured (4,000 cells/cm²) and expanded in humidified 5% CO₂ at 37°C. Characterization of monolayer GPC and BMSC according to the “minimal MSC criteria” (Dominici et al., 2006), i.e., plastic adherence, stromal-like immunophenotype and multi-lineage differentiation potential, has been reported elsewhere (Shanbhag et al., 2020a; Shanbhag et al., 2020b).

To generate 3D spheroids, passage-2 dissociated monolayer GPC and BMSC ($n = 3$ donors, pooled) were separately seeded in microwell-patterned 24-well plates (Kugelmeiers Ltd., Erlbach, CH); after 24 h, aggregate spheroids of ~1000 cells were formed via guided self-assembly (Shanbhag et al., 2020b).

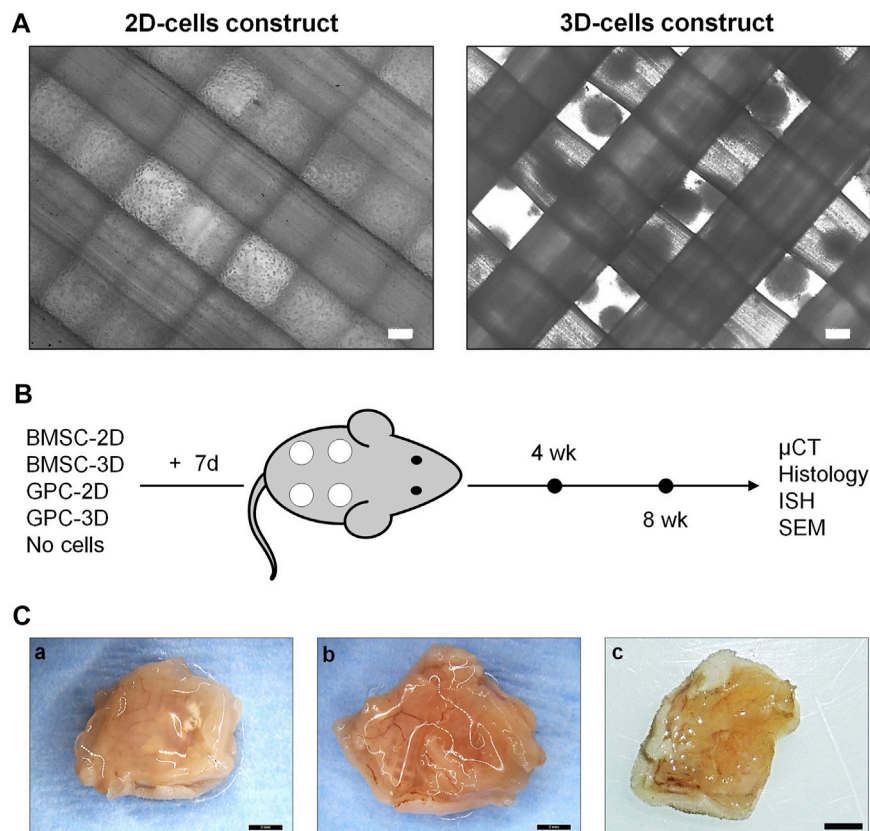


FIGURE 1 | Study design. **(A)** Representative phase microscopic images of 2D (single cells) and 3D (spheroids) cell constructs; scale bars 100 µm. **(B)** Schema of study design, experimental groups and outcomes; constructs were cultured *in vitro* in osteogenic induction medium for 7 days prior to implantation (+7 days). **(C)** Representative macroscopic images of 8-weeks tissue specimens containing BMSC (a), GPC (b) or cell-free constructs (c); scale bars 2 mm.

Characterization of GPC and BMSC spheroids based on gene expression, cytokine secretion and *in vitro* mineralization, has been reported elsewhere (Shanbhag et al., 2020b).

Fabrication of HPLG-PLATMC Constructs

PLATMC scaffolds were produced as described elsewhere (Jain et al., 2020). Briefly, a 3D CAD model was designed using the Magics® software integrated with a 3D-Bioplotter® (both from EnvisionTEC, Gladbeck, Germany). Granules of medical-grade PLATMC (RESOMER® LT-706-S 70:30, Evonik GmbH, Essen, Germany) were loaded into the printer cartridge (pre-heated to 220°C) and rectangular sheets of three layers with an orientation of 0°–90°–0° were printed at 190°C with an inner nozzle diameter of 400 µm and strand spacing of 0.7 mm. Disc-shaped scaffolds measuring 6 mm × ~1.2 mm were punched out and placed in 48-well plates. Prior to use in experiments, the scaffolds were sterilized by soaking in 70% ethanol for 30 min, followed by washing with phosphate-buffered saline (PBS, Invitrogen) and 2 h exposure to UV light.

To avoid direct seeding on scaffolds and aiming to preserve the morphology of 3D spheroids, HPLG was added to the construct. To prepare HPLG, sterile-filtered HPL (same as in growth media) was supplemented with 20 mg/ml fibrinogen (Sigma-Aldrich, St. Louis, MO, United States) to increase the stiffness and

mechanical properties of the hydrogel (Murphy et al., 2015). Gelation was achieved by adding a “thrombin solution” containing 1 IU/ml human thrombin and 1 TIU/ml aprotinin in 20 mM CaCl₂ solution (all from Sigma-Aldrich), followed by incubation at 37°C for 15 min. To prepare the (cell-free) constructs, the HPL and thrombin solutions were mixed and 50 µl were quickly seeded on pre-wetted scaffolds. To prepare cell-loaded constructs, equal numbers of passage-2 2D or 3D GPC or BMSC were uniformly suspended in fibrin supplemented HPL, mixed with thrombin solution and seeded on scaffolds (2 × 10⁶ cells in 50 µl) as described above. Cell distribution within the constructs was observed under a light microscope (Nikon Eclipse TS100, Tokyo, Japan) (Figure 1A). Constructs were cultured in osteogenic induction media, i.e., growth media supplemented with final concentrations of 0.05 mM L-ascorbic acid 2-phosphate, 10 nM dexamethasone and 10 mM β glycerophosphate (all from Sigma-Aldrich), for 1 week prior to *in vivo* implantation.

Ectopic Implantation in Nude Mice

Animal experiments were approved by the Norwegian Animal Research Authority (Mattilsynet; FOTS-18738) and reported in accordance with the ARRIVE guidelines for all relevant items (Kilkenny et al., 2010; Berglundh and Stavropoulos, 2012).

Twenty female athymic nude mice (Rj:Athym-Foxn1nu/nu, Janvier Labs, France), 7-weeks-old and weighing 19.4 ± 1.12 g, were used. Animals were housed in stable conditions ($22 \pm 2^\circ\text{C}$) with a 12 h dark/light cycle and *ad libitum* access to food and water. Animals were allowed to acclimatize for 1 week prior to experiments and were regularly monitored for signs of pain/infection, food intake and activity during the entire experimental period.

Pre-operatively, animals were anesthetized with a mixture of sevoflurane (Abbott Laboratories, Berkshire, United Kingdom) and O_2 using a custom-made mask. Following anaesthesia, two 1-cm incisions were made in the midline of the dorsum, and four subcutaneous pouches were created using blunt dissection. Next, four constructs per animal containing either suspension [2×10^6 2D-BMSC or 2D-GPC], spheroid [2×10^6 3D-BMSC or 3D-GPC] or no cells were randomly implanted in the pouches (5 groups; $n = 8$ constructs per group per time point). GPC and BMSC were never implanted in the same animals. Post-operatively, the skin was sutured (Vicryl, Ethicon, Somerville, NJ, United States) and animals were injected subcutaneously with buprenorphine (Temgesic 0.03 mg/kg, Schering-Plough, United Kingdom) for up to 2 days thereafter. After 4 or 8 weeks, the animals were euthanized with an overdose of CO_2 and constructs were harvested. The primary outcome, i.e., ectopic mineralized tissue formation, was assessed via micro-computed tomography (μCT) and histology. Secondary outcomes included identification of transplanted human cells by *in situ* hybridization (ISH) and assessment of mineralized ultrastructure by scanning electron microscopy and energy dispersive x-ray spectroscopy (SEM/EDX) analysis. Animals were coded via ear clips and identified by numbers for all subsequent handling/analyses to facilitate blinding of personnel.

μCT

Immediately after euthanasia, the specimens were harvested along with the overlying skin and underlying muscle tissues and fixed in 10% buffered formalin (Sigma-Aldrich). Specimens were scanned using a SkyScan 1172 μCT scanner (Bruker, Kontich, Belgium) with an X-ray source of 60 kV/200 μA and 0.5 mm aluminum filter for a 10 μm resolution. Scans were reconstructed by applying a standardized volume of interest (5 mm \times 1 mm to exclude the tissue margins) and a global grey threshold of 110–255 using the CTAn v.1.18 software (Bruker). Quantification of mineralization as a ratio of the total construct volume (Mdv/TV) was performed in a blinded fashion using the CTAn software (Bruker).

Histology

Specimens were processed for histology by both decalcified (paraffin-embedded) and undecalcified (resin-embedded) methods. Selected specimens were decalcified in 20% ethylenediaminetetraacetic acid solution (EDTA; Sigma-Aldrich) for 7 days. Next, formalin-fixed tissues were dehydrated in ascending grades of alcohol and embedded in paraffin (FFPE) or light-curing resin (RE; Technovit 7200 + 1% benzoyl peroxide, Kulzer & Co., Wehrheim, Germany). FFPE tissue sections were cut ($\sim 5 \mu\text{m}$) and stained with hematoxylin

and eosin, Alizarin red S (Sigma-Aldrich) or Trichrome dyes (Roche Diagnostics, Oslo, Norway); Alizarin red staining was performed on undecalcified FFPE sections. RE specimens were further processed using EXAKT cutting and grinding equipment (EXAKT Apparatebau, Norderstedt, Germany) and thin ground sections ($\sim 100 \mu\text{m}$) were stained with Levi-Lazko dye (Morphisto GmbH, Frankfurt, Germany). FFPE and RE sections were scanned and digitized using a Nanoscope XR (Hamamatsu, Photonics Ltd., Hertfordshire, United Kingdom; $\times 40$ magnification) and Olympus BX61VS system (DotSlide 2.4; Olympus, Japan, Tokyo, $\times 20$ magnification), respectively. Quantification of total collagen (area in μm^2) in Trichrome stained FFPE sections was performed using QuPath open-source image analysis software (Bankhead et al., 2017).

ISH

Detection of transplanted human cells was performed using ISH for the human specific repetitive *Alu* sequence, which comprises approximately 5% of the total human genome (Mankani et al., 2007). ISH was performed using the RNAscope 2.5 High-Definition Brown Assay according to the manufacturer's instructions (all reagents and probes from Advanced Cell Diagnostics, Newark, CA, United States). Briefly, tissue slides were baked at 60°C for 1 h followed by deparaffinization in 100% xylene twice for 5 min each and two changes of 100% ethanol. The slides were treated with an endogenous peroxidase-blocking reagent, incubated for 15 min in boiling $1\times$ target retrieval solution and treated with protease digestion buffer for 30 min at 40°C . The slides were then incubated with the target *Alu* probe for 2 h at 40°C , followed by signal amplification as detailed in the manufacturer's guide. For colorimetric detection, 3,3'-Diaminobenzidine (DAB) was applied for 5 min at RT followed by counterstaining with hematoxylin. A peptidylprolyl isomerase B (*PPIB*) Positive Control Probe was used to validate the assay. Quantification of brown stained *Alu* + cells in ISH sections was performed using the QuPath software (Bankhead et al., 2017).

SEM

Ultrastructure of mineralization in the undecalcified ground sections was analyzed using SEM and EDX. Briefly, the slides were sputter coated with carbon and imaged at a voltage of 15 kV with an electron microscope (Supra 55VP, Carl Zeiss, Oberkochen, Germany). EDX analysis was performed using the Pathfinder software (Thermo Scientific) and atomic weight percentages of various elements such as calcium (Ca) and phosphorous (P) were automatically calculated. EDX analysis was performed at least three different regions of the mineralized tissues in each section. Sections of histologically validated ectopic bone from a previous study in mouse intramuscular sites were analyzed as positive controls.

Statistical Analysis

Statistical analysis was performed using the Prism 9.0 software (GraphPad Software, San Diego, CA, United States). Data are presented as means \pm SD, unless specified. Normality testing was performed using the Shapiro-Wilk test. The student *t* test,

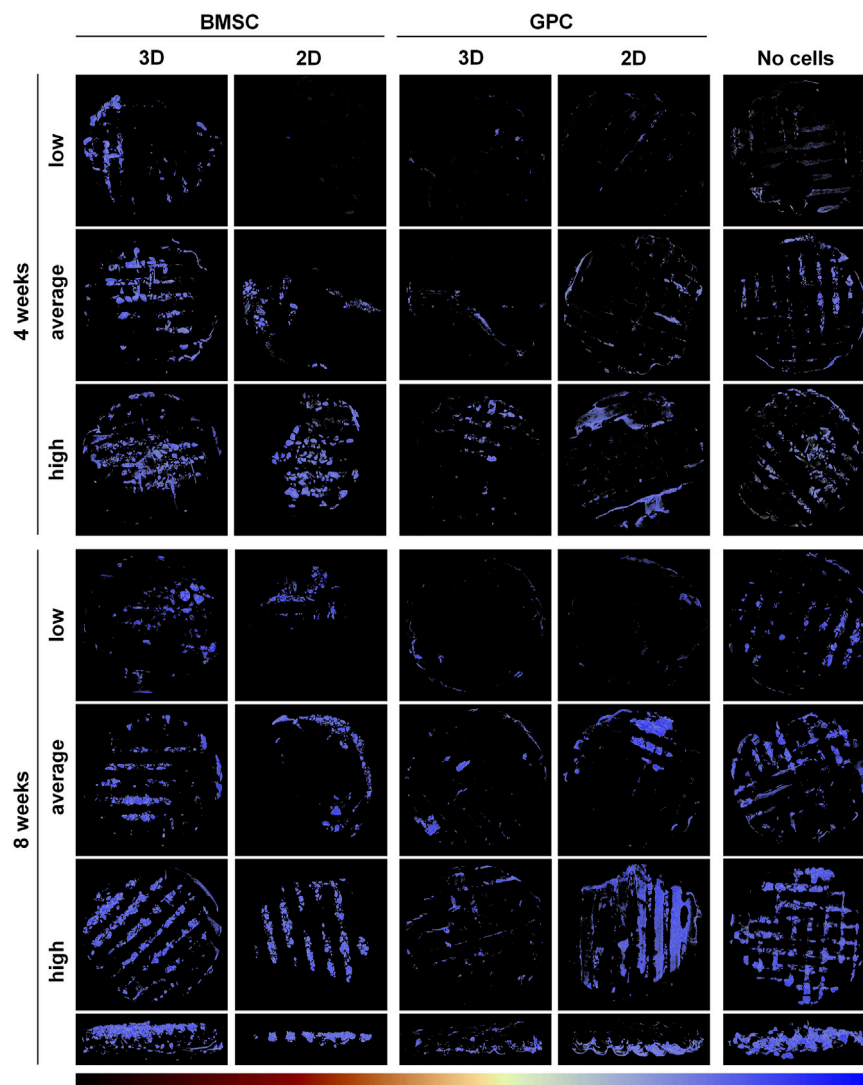


FIGURE 2 | μ CT analysis of ectopic mineralization. Representative reconstructed images showing “low, average and high” degrees of mineralization in BMSC, GPC and control constructs (no cells) after 4 and 8 weeks; the bottom row shows cross-sectional views of the corresponding “high” constructs at 8 weeks. The color bar indicates relative mineral density from minimum (black) to maximum (blue).

Mann-Whitney U test and one-way analysis of variance (ANOVA), followed by a post-hoc Tukey’s (parametric) or Dunn’s test (non-parametric) for multiple comparisons, were applied as appropriate, and $p < 0.05$ was considered statistically significant.

RESULTS

General Outcomes

HPLG-PLATMC constructs containing equal numbers of 2D or 3D GPC or BMSC were implanted subcutaneously in nude mice (Figures 1A,B). One animal died 2 days postoperatively due to an eye infection unrelated to the implants and was excluded from the analysis. All other animals recovered from surgery and no adverse events were recorded. Constructs were analyzed after 4 weeks

[2D-BMSC ($n = 8$), 3D-BMSC ($n = 8$), 2D-GPC ($n = 6$), 3D-GPC ($n = 6$), cell-free ($n = 8$)] or 8 weeks [2D-BMSC ($n = 8$), 3D-BMSC ($n = 8$), 2D-GPC ($n = 8$), 3D-GPC ($n = 8$), cell-free ($n = 8$)]. No signs of inflammation were observed on either the skin or muscle surface. Abundant blood vessels were observed in the muscle layer directly underlying the constructs in all groups.

Spheroid Culture of BMSC Promoted Ectopic Mineralization

μ CT analysis revealed mineralization of varying degrees in all groups. The pattern of mineralization typically followed the scaffold architecture, i.e., along the surface of the printed filaments in between the pores (Figure 2). Cross-sectional images demonstrated mineralization throughout the entire

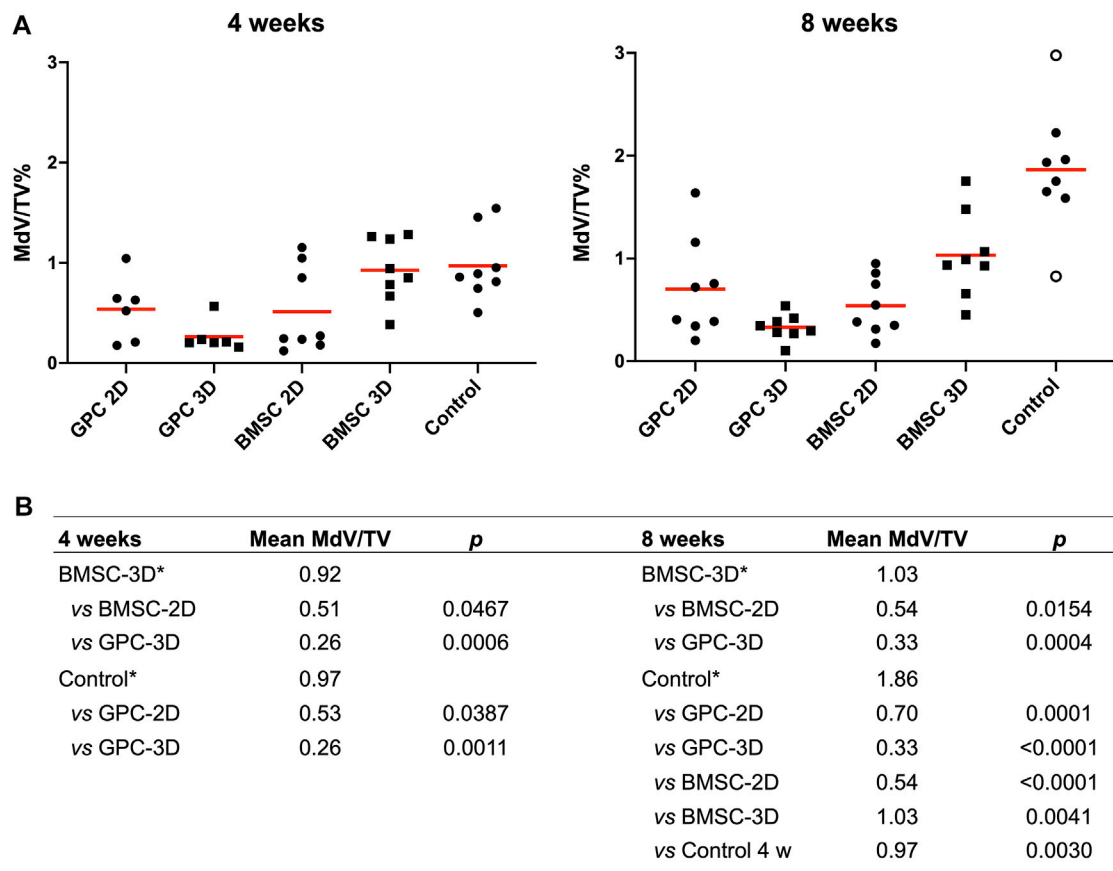


FIGURE 3 | Quantification of mineralization by μ CT. **(A)** Percentage mineralization in BMSC, GPC and control constructs (no cells) after 4 and 8 weeks; MdV/TV, mineral volume/total construct volume; data represent means; o represents outliers. **(B)** Inter-group comparisons showing statistically significant differences ($p < 0.05$); * reference group in the analysis (Kruskal-Wallis one-way ANOVA).

thickness of the construct. Significantly greater mineralization (MdV/TV) was observed in 3D-BMSC vs. 2D-BMSC constructs after 4 (0.92 ± 0.32 vs. 0.51 ± 0.42 ; $p = 0.046$) and 8 weeks (1.03 ± 0.41 vs. 0.54 ± 0.28 ; $p = 0.015$) (Figures 3A,B). In the case of GPC, a non-significant trend for greater MdV/TV was observed in 2D-GPC vs. 3D-GPC constructs at 4 (0.53 ± 0.32 vs. 0.26 ± 0.15 ; $p > 0.05$) and 8 weeks (0.70 ± 0.48 vs. 0.33 ± 0.12 ; $p > 0.05$). Comparable mineralization was observed in 2D-GPC vs. 2D-BMSC constructs at 4 and 8 weeks ($p > 0.05$). Significantly greater mineralization was observed in 3D-BMSC vs. 3D-GPC constructs at 4 and 8 weeks ($p < 0.05$).

Cell-Free Constructs Produced Robust Ectopic Mineralization

Substantial mineralization was also observed in the control, i.e., cell-free HPLG-PLATMC, constructs after 4 weeks; μ CT analysis revealed comparable MdV/TV to that of 3D-BMSC constructs at 4 weeks (0.97 ± 0.35 vs. 0.92 ± 0.32 ; $p > 0.05$). Only the cell-free group showed a significant increase in mineralization from 4 to 8 weeks (0.97 ± 0.35 to 1.86 ± 0.60 ; $p = 0.003$). After 8 weeks, mineralization in the cell-free group

was significantly greater than all other groups ($p < 0.05$) (Figures 3A,B).

Irregular Histological Appearance of Ectopic Mineralization

Generally, histological analysis of all explants (cell-loaded and cell-free) revealed fibrous encapsulation of the constructs, with little or no inflammatory cell-infiltrate around the capsules. The scaffold material within the construct was well-defined, could be clearly distinguished from the host tissues and did not indicate any signs of resorption or degradation, even after 8 weeks. The hydrogel between the scaffold pores was degraded and replaced by well-vascularized host tissues (Figures 4–6).

In paraffin-embedded (FFPE) sections, areas of diffuse mineralization were seen along the scaffold margins and between the filaments, often in direct contact with the scaffold. Alizarin red staining of undecalcified FFPE sections confirmed the presence of calcium in the tissues; *Alu* + cells were detected within/surrounding these tissues (Supplementary Figure S1). Presence of collagen was confirmed via Trichrome (blue) staining. After 8 weeks, a trend for higher collagen content

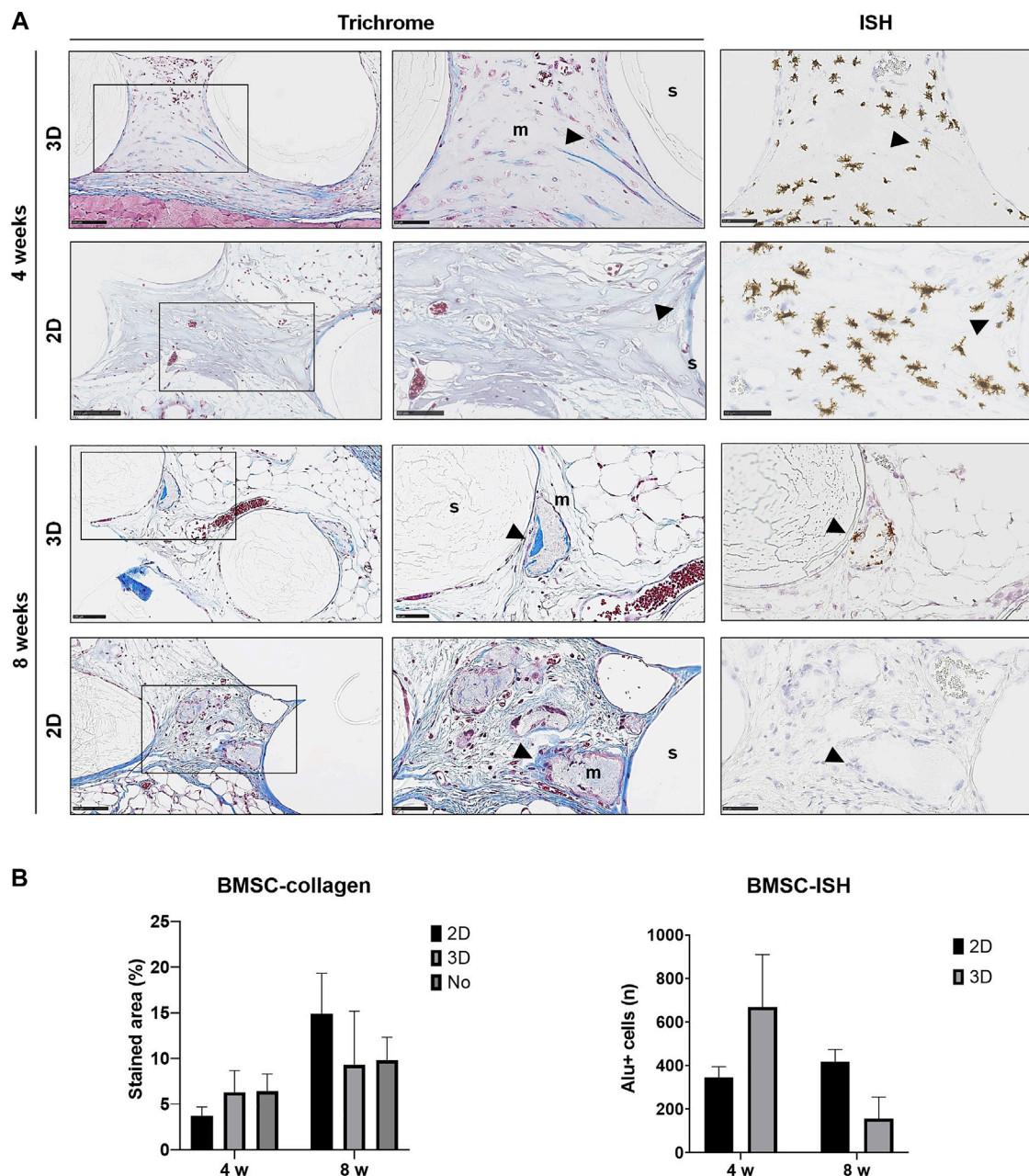


FIGURE 4 | Histology of BMSC constructs. **(A)** Representative images of Trichrome and corresponding ISH stained sections of 2D and 3D BMSC constructs after 4 and 8 weeks; m, mineralization; s, scaffold; wb, woven bone; arrows indicate dense collagen (Trichrome) and Alu + cells (ISH)—except in the ISH section of 2D-GPC at 8 weeks where dense collagen does not correlate with Alu + cells in ISH; scale bars 100 μ m. **(B)** Quantification of collagen staining (Trichrome) and Alu + cells (ISH); n, total number; data represent means \pm SD ($n = 3$).

was observed in 2D vs. 3D groups of both GPC and BMSC constructs ($p > 0.05$). Overall, no differences in morphology of the mineralized areas or collagen content were observed between cell-loaded and cell-free constructs. A trend for greater collagen and Alu + cells was observed in GPC vs. BMSC constructs ($p > 0.05$). In the 3D-BMSC and 3D-GPC groups, the spheroidal form of cell aggregates was retained after 4 weeks and often showed signs of mineralization *en masse* (**Supplementary Figure S1**).

In FFPE sections, the mineralized areas lacked the organized structure of normal bone tissue, with no evidence of embedded (osteocytes) or lining cells. Similar observations were made in undecalcified RE sections, where the mineralized areas mostly showed an irregular and acellular pattern (**Figure 7**). Only one instance of organized bone-like tissue with embedded osteocytes was observed in a single specimen from the 2D-BMSC group at 8 weeks. In this case, the new bone was seen to be formed on the

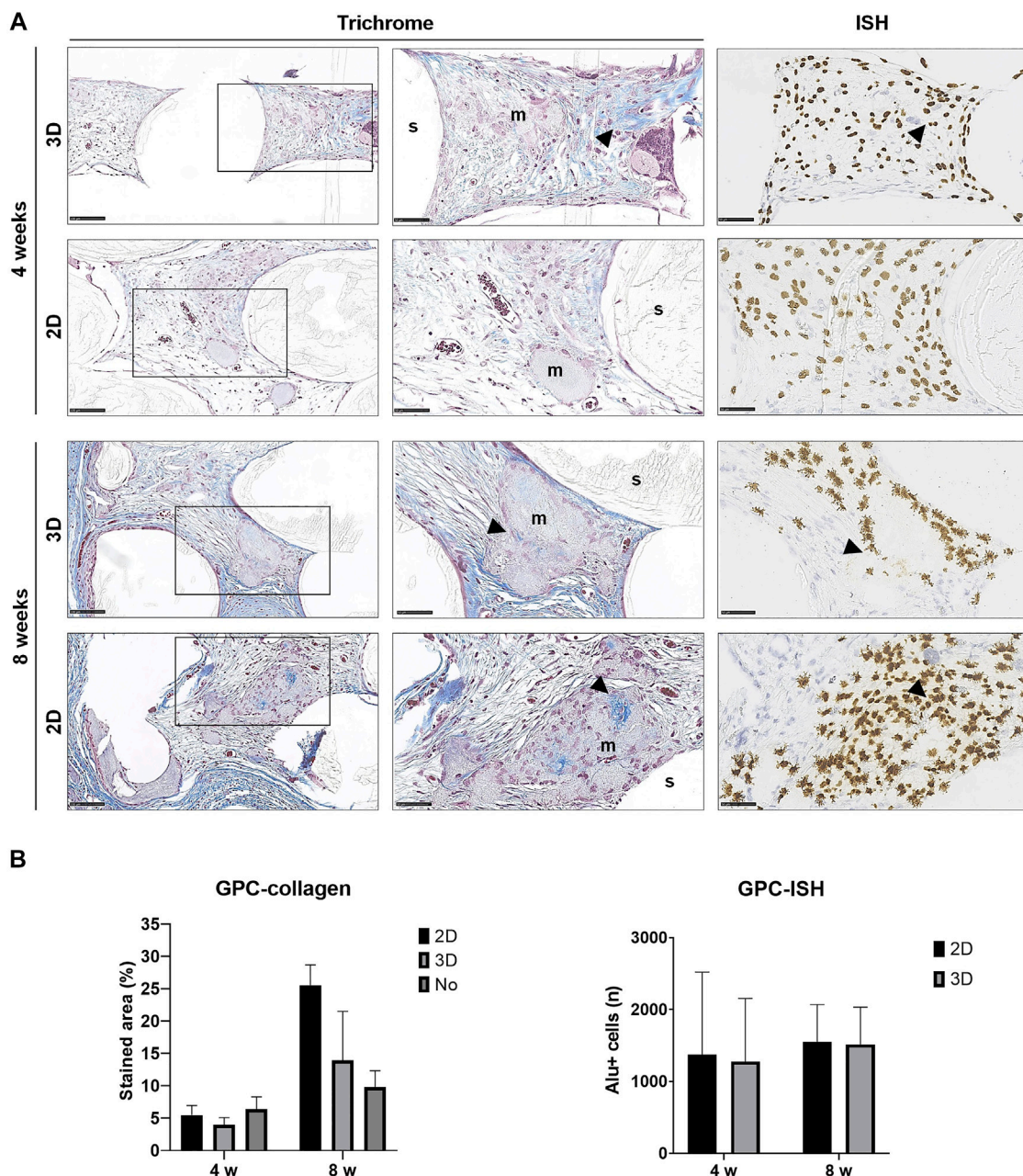


FIGURE 5 | Histology of GPC constructs. **(A)** Representative images of Trichrome and corresponding ISH stained sections of 2D and 3D GPC constructs after 4 and 8 weeks; m, mineralization; s, scaffold; arrows indicate dense collagen (Trichrome) and Alu + cells (ISH); scale bars 100 μ m. **(B)** Quantification of collagen staining (Trichrome) and Alu + cells (ISH); n, total number; data represent means \pm SD ($n = 3$).

surface of an irregular mineralization, which showed roughened borders indicative of resorption (Figure 7).

Comparable Ultrastructure of Different Mineralization Patterns

Composition of the different ectopic mineralization patterns in RE sections was further determined via SEM/EDX analysis; SEM and histological images were correlated to analyze specific regions within

the mineralized areas. Based on appearance, the different mineralization patterns were categorized as follows (in order of decreasing frequency): globular, plate-like and filament-like (Figure 8). EDX analysis revealed similar compositions in terms of Ca, P and Ca:P ratios between the different mineralization types; average values of Ca, P and Ca:P were 37.31% (range 33.46–41.12%), 17.77% (range 15.73–19.02%) and 2.10 (range 2.02–2.17), respectively. These values were comparable to historical controls of “true” ectopic bone (Supplementary Figure S2).

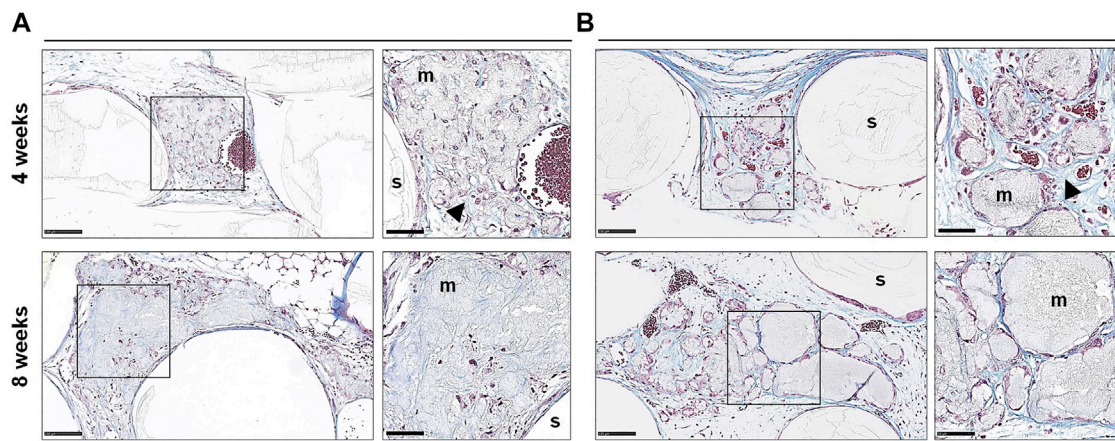


FIGURE 6 | Histology of cell-free constructs. Representative images of Trichrome stained sections of cell-free constructs showing different patterns of mineralization (A,B) after 4 and 8 weeks; m, mineralization; s, scaffold; arrows indicate dense collagen; scale bars 100 μ m (20x) and 50 μ m (40x).

Transplanted Cells Detected *in situ* After 8 weeks

Detection of transplanted human cells was performed using ISH for the human specific *Alu* sequence; no *Alu* + cells were detected in cell-free constructs (data not shown). High numbers of *Alu* + cells were detected after 4 and 8 weeks in constructs of both 2D and 3D GPC and BMSC. In 3D GPC/BMSC, cell aggregation was evident even after 8 weeks. *Alu* + cells were uniformly distributed throughout the constructs and associated with markedly denser connective tissue. In several instances, *Alu* + cells were detected within and around the areas of mineralization, although not showing the characteristic lacunae of embedded osteocytes. In BMSC constructs, a trend for greater numbers of *Alu* + cells was observed in the 3D vs. 2D group at 4 but not at 8 weeks (Figure 4B). In GPC constructs, similar numbers of *Alu* + cells were observed in the 3D vs. 2D group at both 4 and 8 weeks (Figure 5B). No significant differences in the numbers of *Alu* + cells were detected between the groups at 4 or 8 weeks ($p > 0.05$).

DISCUSSION

The present study investigated the ectopic BTE potential of HPLG-PLATMC constructs containing spheroid (3D) or dissociated (2D) BMSC or GPC in a subcutaneous mouse model. The main findings were 1) significantly greater mineralization in constructs of 3D vs. 2D BMSC, 2) comparable mineralization in 2D GPC vs. 2D BMSC, and 3) robust mineralization in cell-free constructs.

In the context of BTE, aggregation of MSC into 3D spheroids has been reported to recapitulate embryonic events during skeletal development and thereby promote their osteogenic differentiation (Hall and Miyake, 2000; Kale et al., 2000). We have recently reported significant upregulations of genes associated with self-renewal and osteogenic differentiation in xeno-free cultures of 3D vs. 2D GPC and BMSC, suggesting a

greater potential for *in vivo* osteogenesis (Shanbhag et al., 2020b). Consistently, recent studies have reported superior bone regeneration in rodent orthotopic models when using 3D vs. 2D BMSC encapsulated in Matrigel® (Corning) (Yamaguchi et al., 2014) or alginate-based hydrogels (Ho et al., 2018); similar results were reported for periodontal ligament-derived cells (PDLs) encapsulated in Matrigel® (Moritani et al., 2018). Conversely, a recent study reported no differences in the healing of mouse femoral defects treated with either 2D or 3D BMSC encapsulated in a commercial fibrin gel (Findeisen et al., 2021). In the present study, significantly greater ectopic mineralization was observed via μ CT in 3D vs. 2D BMSC constructs. To our knowledge, only one previous study has reported μ CT analysis of ectopic bone formation (Ruminski et al., 2018); another study reported conventional X-ray but not μ CT-based assessment of spheroid-hydrogel constructs (Ho et al., 2016). Nevertheless, our findings are supported by previous studies, which reported superior ectopic bone formation by 3D vs. 2D BMSC in calcium phosphate + platelet-rich plasma (PRP) complexes (Chatterjea et al., 2017) or RGD-modified alginate hydrogels (Ho et al., 2016). In the former study (Chatterjea et al., 2017), ectopic bone formation by spheroid BMSC was further enhanced in the presence of PRP, suggesting a synergistic effect of BMSC and platelet-derived growth factors (Shanbhag et al., 2017).

Fibrin- and platelet-based hydrogels, e.g., PRP, have been extensively used as scaffolds for bone regeneration (Soffer et al., 2003). In the present study, a fibrin supplemented HPLG was used to encapsulate the GPC and BMSC spheroids—to preserve their 3D architecture during *in vivo* delivery (Robinson et al., 2016). Indeed, platelet growth factors are known to promote MSC osteogenic differentiation *in vitro* (Kasten et al., 2006; Zhang et al., 2011; Huang et al., 2012; Trouillas et al., 2013; Chatterjea et al., 2017) and bone formation *in vivo* (Kasten et al., 2006; Trouillas et al., 2013; Chatterjea et al., 2017). However, an interesting (and potentially confounding) observation herein was the robust mineralization in cell-free HPLG-PLATMC constructs; after

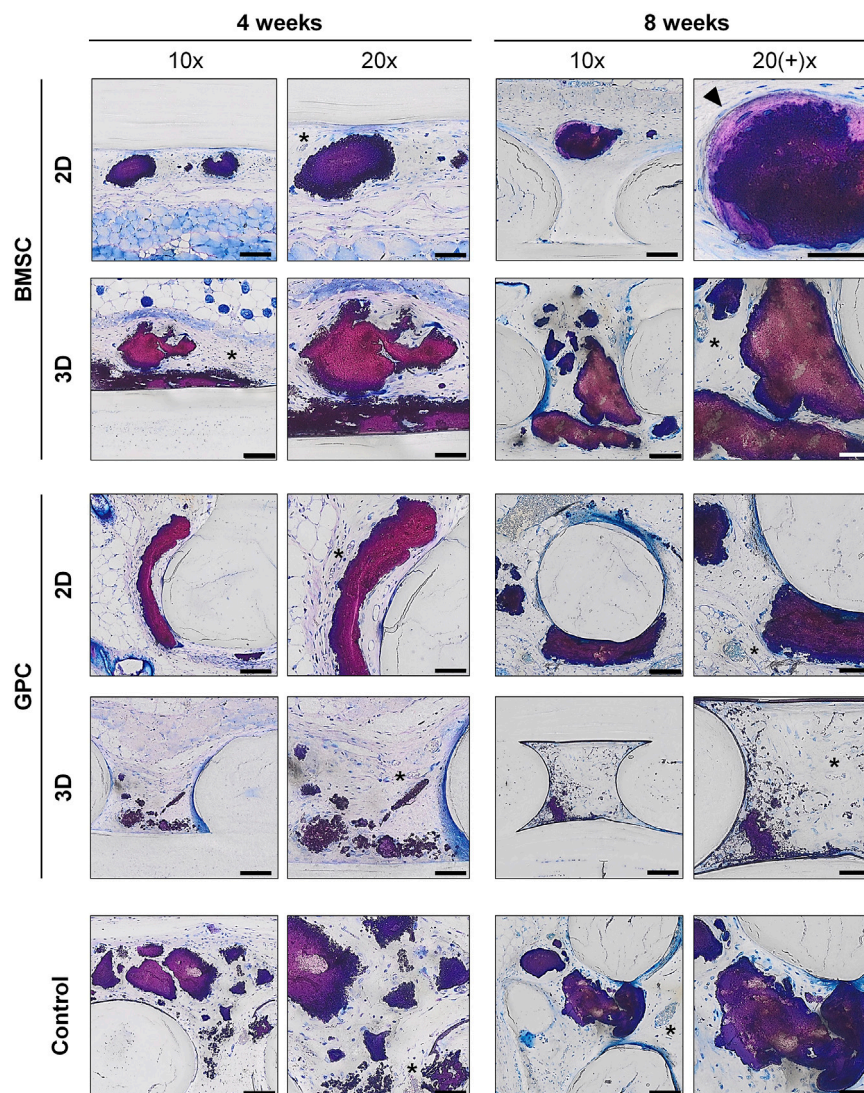


FIGURE 7 | Undecalcified histology. Representative images of BMSC, GPC and control constructs (no cells) after 4 and 8 weeks (thin ground sections, Levi Lazko staining); * indicate blood vessels; arrow indicates the only instance of “bone-like” tissue observed in the study; scale bars 100 μ m (10x) and 50 μ m (20x).

8 weeks, the greatest μ CT-based mineralization was observed in the cell-free group. Since PLATMC is biologically inert, the observed mineralization could be attributed to the HPLG. As already mentioned, although platelet growth factors (PRP) have been shown to enhance MSC-mediated ectopic bone formation, to our knowledge, no studies have detected ectopic bone formation in cell-free fibrin- or PRP-constructs alone (Yamada et al., 2003; Osathanon et al., 2008; Murphy et al., 2015). In context, previous studies have tested “HPL coated” ceramic scaffolds for ectopic and orthotopic bone formation; scaffolds were immersed in HPL for 24 h prior to experiments (Leotot et al., 2013; Bolte et al., 2019). While the HPL coating itself did not promote bone formation, it enhanced the osteogenic potential of BMSC seeded on the scaffolds (Leotot et al., 2013; Bolte et al., 2019). Therefore, whether (and if so, how) human HPL (G)

alone can lead to ectopic bone formation requires further investigation.

When comparing cell types herein, comparable ectopic mineralization was observed in constructs of 2D-GPC (Mdv/TV 0.70%) vs. 2D-BMSC (0.54%) after 8 weeks. Even constructs of 3D-BMSC (1.03%) did not significantly outperform those of 2D-GPC (0.70%), suggesting that GPC may have the potential to substitute BMSC in future BTE applications. Several studies have investigated *in vivo* bone formation by GPC; some studies have compared the ectopic bone forming potential of GPC and BMSC, of which, three (Fournier et al., 2010; Tomar et al., 2010; Zorin et al., 2014) reported comparable histological “bone formation” between GPC and BMSC (**Supplementary Table S1**). However, the morphology of mineralized tissues formed by GPC is highly variable in the reported literature—to our knowledge, only few studies have reported regular organized bone tissue with

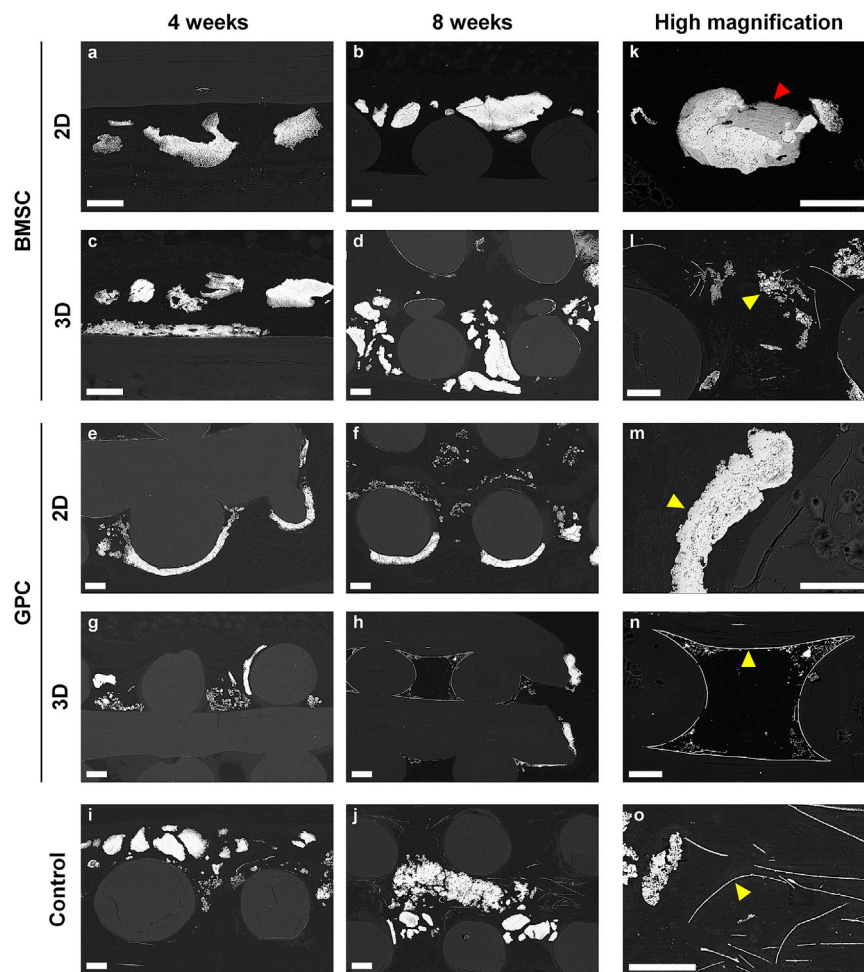


FIGURE 8 | SEM analysis. **(A–J)** Representative images of BMSC, GPC and control constructs (no cells) after 4 and 8 weeks. **(K–O)** Corresponding high magnification images from each group; yellow arrows indicate the different patterns of mineralization: **(K,M)** sheet/plate, **(L)** globular, **(N,O)** filament-like; red arrow indicates the only instance of “bone-like” tissue observed in the study; scale bars 100 μ m.

embedded (osteocytes) and/or bone forming cells (osteoblasts) (**Supplementary Table S1**). These differences in mineralization produced by GPC and BMSC may be explained by the so-called “tissue source variability” (Xu et al., 2017). BMSC are naturally resident in the bone marrow—a specialized tissue niche, and have an inherent propensity for osteogenic differentiation (Hoch and Leach, 2015). Conversely, gingiva is a connective tissue with a mainly supportive function and a large fibroblast-population. Indeed, fibroblasts from various tissues including gingiva are reported to be indistinguishable from BMSC *in vitro* based on the “minimal MSC criteria” (Denu et al., 2016), and the presence of a “true” MSC-like population in gingiva remains to be identified *in vivo* (da Silva Meirelles et al., 2008). Nevertheless, gingiva represents a promising alternative source of progenitor cells for BTE applications.

In contrast to the traditional histological picture of lamellar bone with embedded (osteocytes) and lining cells, an atypical pattern of mineral deposition/precipitation was observed in the constructs herein, regardless of the type or presence of cells. The

mineralized areas often appeared as solid masses or aggregates, with no internal lamellar structure or canals containing blood vessels. However, in several instances the mineralized areas revealed the presence of embedded cells, including transplanted BMSC and GPC; in one instance of 2D-BMSC, organized bone-like tissue with embedded osteocytes was observed. A similar pattern of atypical mineralization has previously been reported in rat calvarial defects treated with collagen membranes (Kuchler et al., 2018; Feher et al., 2021). It has been hypothesized that the collagen fibres underwent mineralization via cell-independent mechanisms and thereby served as “scaffolds” for subsequent bone formation (Nudelman et al., 2013) and may explain the observations herein. We observed organized and cellular (osteocyte containing) bone-like tissue around the mineral deposits in one specimen of the 2D-BMSC group at 8 weeks—the mineral deposits showed roughened borders characteristic of surface resorption. This finding supports the hypothesis that the mineral deposits may first undergo resorption and

subsequently serve as scaffolds for new bone formation. Other studies have reported dystrophic mineralization of biomaterials in ectopic sites, related to nucleation of calcium-phosphate complexes (Schoen and Levy, 2013; Lotsari et al., 2018). However, extending these hypotheses to the mineralization patterns observed herein is rather speculative, and the exact mechanism(s) of mineralization remains unclear.

Alu + GPC and BMSC were detected in the ectopic transplants herein. Detection of transplanted cells via ISH is well established and may assist in understanding the mechanism(s) of *in vivo* bone formation (Mankani et al., 2007; Janicki et al., 2011). It is relevant to note herein that cells (both GPC and BMSC) from pooled donors were used in the present study—to minimize donor-related variation and as a potential future strategy for allogeneic “off-the-shelf” cell therapy. The current literature is inconclusive regarding the mechanism(s) of bone formation by transplanted human MSC—either from independent or pooled donors, i.e., whether this occurs primarily via direct osteogenic differentiation of transplanted cells, paracrine stimulation of host cells, immune modulation, or a combination of factors (Moll et al., 2020). Indeed, *Alu* + cells were identified in the areas of mineralization herein; in several instances, these cells were embedded within the mineralization(s) and/or associated with areas of dense collagen deposition. However, the embedded cells did not demonstrate the well-defined surrounding lacunae characteristic of osteocytes. Previous studies have characterized the role of exogenous cells in ectopic and orthotopic bone formation. For example, transplantation of allogeneic BMSC in immunocompetent mice revealed immune modulation rather than osteoblastic differentiation in one study (Tsujigiwa et al., 2013; Takabatake et al., 2018). In another study, no transplanted human BMSC could be detected in ectopic mouse transplants beyond 2 weeks, despite robust bone formation at 8 weeks (Gamblin et al., 2014). These reports further suggest that transplanted BMSC contribute to bone formation via stimulation of tissue-resident progenitor cells rather than direct differentiation into osteoblasts (Tsujigiwa et al., 2013; Takabatake et al., 2018). Indeed, the type and immune status of the animal-model may also influence *in vivo* osteogenesis (Garske et al., 2020). Based on previous literature, we selected the athymic “nude” mouse model (Scott et al., 2012), where the absence of functional T lymphocytes (and partial defect of B cells) allows for xenogeneic transplantation of human cells without immune rejection. Others have reported favourable ectopic bone formation by human BMSC in NMRI-nude (Brennan et al., 2014; Gamblin et al., 2014) and NOD-SCID mice (Suliman et al., 2019), which present certain differences in immune status compared to our mouse model. Nevertheless, the exact mechanism(s) of osteogenesis and/or mineralization by xenotransplanted BMSC in immunocompromised rodent models remains to be elucidated.

CONCLUSION

In summary, ectopic implantation of the various HPLG-PLATMC constructs revealed significantly greater mineralization in those with 3D-BMSC vs. 2D-BMSC and comparable mineralization in those

with 2D-GPC vs. 2D-BMSC. However, the effect of cell transplantation was confounded by that of HPLG, based on the robust mineralization observed in cell-free constructs. Although transplanted GPC and BMSC were detected *in situ* after 8 weeks, their direct contribution to mineralization could neither be confirmed nor excluded. GPC represents a promising alternative to BMSC for BTE. The HPLG-PLATMC constructs herein represent promising and clinically relevant scaffolds for BTE applications.

DATA AVAILABILITY STATEMENT

The raw data supporting the conclusion of this article will be made available by the authors, without undue reservation.

ETHICS STATEMENT

The animal study was reviewed and approved by Norwegian Animal Research Authority (Mattilsynet; FOTS-18738).

AUTHOR CONTRIBUTIONS

SSH and KM conceived and designed the study. SSH performed the experiments, data collection, data analysis and drafted the manuscript. CK, SM-A, MY, HD, DE, ST, and MH assisted with data collection, data analysis/interpretation and drafting the manuscript. AS, AB, SSu, and KM assisted with data analysis/interpretation and drafting the manuscript. All authors read and approved the final version of the manuscript.

FUNDING

This work was supported by Helse Vest Strategic Research Funding, Norway (502027 and 912260/2019), Research Council of Norway (BEHANDLING-273551 and Centers of Excellence-22325), Trond Mohn Foundation, Norway (BFS2018TMT10) and the ITI Foundation, Switzerland (117/2015).

ACKNOWLEDGMENTS

We thank the Bloodbank at Haukeland University Hospital for supplying the platelets and the Molecular Imaging Center (MIC), University of Bergen, for assistance with microscopy and imaging. We also thank Bendik Nordanger, Siren Fromreide and Randi Lavik from the Department of Clinical Medicine, University of Bergen, for assistance with the histology.

SUPPLEMENTARY MATERIAL

The Supplementary Material for this article can be found online at: <https://www.frontiersin.org/articles/10.3389/fbioe.2021.783468/full#supplementary-material>

REFERENCES

- Bankhead, P., Loughrey, M. B., Fernández, J. A., Dombrowski, Y., McArt, D. G., Dunne, P. D., et al. (2017). QuPath: Open Source Software for Digital Pathology Image Analysis. *Sci. Rep.* 7 (1), 16878. doi:10.1038/s41598-017-17204-5
- Berglundh, T., and Stavropoulos, A. (2012). Preclinical *In Vivo* Research in Implant Dentistry. Consensus of the Eighth European Workshop on Periodontology. *J. Clin. Periodontol.* 39 (Suppl. 12), 1–5. doi:10.1111/j.1600-051X.2011.01827.x
- Bieback, K., Fernandez-Muñoz, B., Pati, S., and Schäfer, R. (2019). Gaps in the Knowledge of Human Platelet Lysate as a Cell Culture Supplement for Cell Therapy: a Joint Publication from the AABB and the International Society for Cell & Gene Therapy. *Int. Soc. Cell Gene Therapy Transfusion* 59, 3448–3460. doi:10.1111/trf.15483
- Bolte, J., Vater, C., Culla, A. C., Ahlfeld, T., Nowotny, J., Kasten, P., et al. (2019). Two-step Stem Cell Therapy Improves Bone Regeneration Compared to Concentrated Bone Marrow Therapy. *J. Orthop. Res.* 37 (6), 1318–1328. doi:10.1002/jor.24215
- Brennan, M. Á., Renaud, A., Amiaud, J., Rojewski, M. T., Schrezenmeier, H., Heymann, D., et al. (2014). Pre-clinical Studies of Bone Regeneration with Human Bone Marrow Stromal Cells and Biphasic Calcium Phosphate. *Stem Cell Res Ther* 5, 114. doi:10.1186/srct504
- Cesarz, Z., and Tamama, K. (2016). Spheroid Culture of Mesenchymal Stem Cells. *Stem Cell Int.* 2016, 1–11. doi:10.1155/2016/9176357
- Chatterjee, A., LaPointe, V. L., LaPointe, V., Barradas, A., Garritsen, H., Yuan, H., et al. (2017). Cell Aggregation Enhances Bone Formation by Human Mesenchymal Stromal Cells. *eCM* 33, 121–129. doi:10.22203/eCM.v033a09
- da Silva Meirelles, L., Caplan, A. I., and Nardi, N. B. (2008). In Search of the *In Vivo* Identity of Mesenchymal Stem Cells. *Stem Cells* 26 (9), 2287–2299. doi:10.1634/stemcells.2007-1122
- Denu, R. A., Nemcek, S., Bloom, D. D., Goodrich, A. D., Kim, J., Mosher, D. F., et al. (2016). Fibroblasts and Mesenchymal Stromal/stem Cells Are Phenotypically Indistinguishable. *Acta Haematol.* 136, 85–97. doi:10.1159/000445096
- Dominici, M., Le Blanc, K., Mueller, I., Slaper-Cortenbach, I., Marini, F. C., Krause, D. S., et al. (2006). Minimal Criteria for Defining Multipotent Mesenchymal Stromal Cells. The International Society for Cellular Therapy Position Statement. *Cytotherapy* 8 (4), 315–317. doi:10.1080/14653240600855905
- Feher, B., Apaza Alcayhuaman, K. A., Strauss, F. J., Lee, J.-S., Tangl, S., Kuchler, U., et al. (2021). Osteoconductive Properties of Upside-Down Bilayer Collagen Membranes in Rat Calvarial Defects. *Int. J. Implant Dent* 7 (1), 50. doi:10.1186/s40729-021-00333-y
- Fekete, N., Gadelorge, M., Fürst, D., Maurer, C., Dausend, J., Fleury-Cappellesso, S., et al. (2012). Platelet Lysate from Whole Blood-Derived Pooled Platelet Concentrates and Apheresis-Derived Platelet Concentrates for the Isolation and Expansion of Human Bone Marrow Mesenchymal Stromal Cells: Production Process, Content and Identification of Active Components. *Cytotherapy* 14 (5), 540–554. doi:10.3109/14653249.2012.655420
- Findeisen, L., Bolte, J., Vater, C., Petzold, C., Quade, M., Müller, L., et al. (2021). Cell Spheroids are as Effective as Single Cells Suspensions in the Treatment of Critical-Sized Bone Defects. *BMC Musculoskelet. Disord.* 22 (1), 401, 2021. ARTN 401. doi:10.1186/s12891-021-04264-y
- Follin, B., Juhl, M., Cohen, S., Pedersen, A. E., Kastrup, J., and Ekblond, A. (2016). Increased Paracrine Immunomodulatory Potential of Mesenchymal Stromal Cells in Three-Dimensional Culture. *Tissue Eng. B: Rev.* 22 (4), 322–329. doi:10.1089/ten.TEB.2015.0532
- Fournier, B. P. J., Ferre, F. C., Couty, L., Lataillade, J.-J., Gourven, M., Naveau, A., et al. (2010). Multipotent Progenitor Cells in Gingival Connective Tissue. *Tissue Eng. A* 16, 2891–2899. doi:10.1089/ten.tea.2009.0796
- Gamblin, A.-L., Brennan, M. A., Renaud, A., Yagita, H., Lézet, F., Heymann, D., et al. (2014). Bone Tissue Formation with Human Mesenchymal Stem Cells and Biphasic Calcium Phosphate Ceramics: the Local Implication of Osteoclasts and Macrophages. *Biomaterials* 35 (36), 9660–9667. doi:10.1016/j.biomaterials.2014.08.018
- Garske, D. S., Schmidt-Bleek, K., Ellinghaus, A., Dienelt, A., Gu, L., Mooney, D. J., et al. (2020). Alginate Hydrogels for *In Vivo* Bone Regeneration: The Immune Competence of the Animal Model Matters. *Tissue Eng. Part A* 26 (15–16), 852–862. doi:10.1089/ten.TEA.2019.0310
- Hall, B. K., and Miyake, T. (2000). All for One and One for All: Condensations and the Initiation of Skeletal Development. *Bioessays* 22, 138–147. doi:10.1002/(sici)1521-1878(200002)22:2<138::aid-bies5>3.0.co;2-4
- Hassan, M. N., Yassin, M. A., Suliman, S., Lie, S. A., Gjengedal, H., and Mustafa, K. (2019). The Bone Regeneration Capacity of 3D-Printed Templates in Calvarial Defect Models: A Systematic Review and Meta-Analysis. *Acta Biomater.* 91, 1–23. doi:10.1016/j.actbio.2019.04.017
- Ho, S. S., Hung, B. P., Heyrani, N., Lee, M. A., and Leach, J. K. (2018). Hypoxic Preconditioning of Mesenchymal Stem Cells with Subsequent Spheroid Formation Accelerates Repair of Segmental Bone Defects. *Stem Cells* 36 (9), 1393–1403. doi:10.1002/stem.2853
- Ho, S. S., Murphy, K. C., Binder, B. Y. K., Vissers, C. B., and Leach, J. K. (2016). Increased Survival and Function of Mesenchymal Stem Cell Spheroids Entrapped in Instructive Alginate Hydrogels. *STEM CELLS Translational Med.* 5 (6), 773–781. doi:10.5966/sctm.2015-0211
- Hoch, A. I., and Leach, J. K. (2015). Concise Review: Optimizing Expansion of Bone Marrow Mesenchymal Stem/stromal Cells for Clinical Applications. *Stem Cell Transl Med* 4 (4), 412. doi:10.5966/sctm.2013-0196erratum
- Huang, S., Jia, S., Liu, G., Fang, D., and Zhang, D. (2012). Osteogenic Differentiation of Muscle Satellite Cells Induced by Platelet-Rich Plasma Encapsulated in Three-Dimensional Alginate Scaffold. *Oral Surg. Oral Med. Oral Pathol. Oral Radiol.* 114 (5 Suppl. 1), S32–S40. doi:10.1016/j.tripleo.2011.07.048
- Jain, S., Yassin, M. A., Fuoco, T., Liu, H., Mohamed-Ahmed, S., Mustafa, K., et al. (2020). Engineering 3D Degradable, Pliable Scaffolds toward Adipose Tissue Regeneration; Optimized Printability, Simulations and Surface Modification. *J. Tissue Eng.* 11, 204173142095431. doi:10.1177/2041731420954316
- Janicki, P., Boeuf, S., Boeuf, S., Steck, E., Egermann, M., Kasten, P., et al. (2011). Prediction of *In Vivo* Bone Forming Potency of Bone Marrow-Derived Human Mesenchymal Stem Cells. *eCM* 21, 488–577. doi:10.22203/ecm.v021a37
- Kale, S., Biermann, S., Edwards, C., Tarnowski, C., Morris, M., and Long, M. W. (2000). Three-dimensional Cellular Development Is Essential for *Ex Vivo* Formation of Human Bone. *Nat. Biotechnol.* 18, 954–958. doi:10.1038/79439
- Kasten, P., Vogel, J., Luginbühl, R., Niemeyer, P., Weiss, S., Schneider, S., et al. (2006). Influence of Platelet-Rich Plasma on Osteogenic Differentiation of Mesenchymal Stem Cells and Ectopic Bone Formation in Calcium Phosphate Ceramics. *Cells Tissues Organs* 183 (2), 68–79. doi:10.1159/000095511
- Kilkenny, C., Browne, W. J., Cuthill, I. C., Emerson, M., and Altman, D. G. (2010). Improving Bioscience Research Reporting: the ARRIVE Guidelines for Reporting Animal Research. *Plos Biol.* 8, e1000412. doi:10.1371/journal.pbio.1000412
- Kuchler, U., Rybaczek, T., Dobask, T., Heimel, P., Tangl, S., Klehm, J., et al. (2018). Bone-conditioned Medium Modulates the Osteoconductive Properties of Collagen Membranes in a Rat Calvaria Defect Model. *Clin. Oral Impl Res.* 29 (4), 381–388. doi:10.1111/clr.13133
- Leotot, J., Coquelin, L., Bodivit, G., Bierling, P., Hernigou, P., Rouard, H., et al. (2013). Platelet Lysate Coating on Scaffolds Directly and Indirectly Enhances Cell Migration, Improving Bone and Blood Vessel Formation. *Acta Biomater.* 9, 6630–6640. doi:10.1016/j.actbio.2013.02.003
- Lotsari, A., Rajasekharan, A. K., Halvarsson, M., and Andersson, M. (2018). Transformation of Amorphous Calcium Phosphate to Bone-like Apatite. *Nat. Commun.* 9 (1), 4170. doi:10.1038/s41467-018-06570-x
- Mankani, M. H., Kuznetsov, S. A., and Robey, P. G. (2007). Formation of Hematopoietic Territories and Bone by Transplanted Human Bone Marrow Stromal Cells Requires a Critical Cell Density. *Exp. Hematol.* 35 (6), 995–1004. doi:10.1016/j.exphem.2007.01.051
- Mitrano, T. I., Grob, M. S., Carrión, F., Nova-Lamperti, E., Luz, P. A., Fierro, F. S., et al. (2010). Culture and Characterization of Mesenchymal Stem Cells from Human Gingival Tissue. *J. Periodontol.* 81, 917–925. doi:10.1902/jop.2010.090566
- Mohamed-Ahmed, S., Fristad, I., Lie, S. A., Suliman, S., Mustafa, K., Vindenes, H., et al. (2018). Adipose-derived and Bone Marrow Mesenchymal Stem Cells: a Donor-Matched Comparison. *Stem Cell Res Ther* 9 (1), 168. doi:10.1186/s13287-018-0914-1
- Moll, G., Hoogduijn, M. J., and Ankrum, J. A. (2020). Editorial: Safety, Efficacy and Mechanisms of Action of Mesenchymal Stem Cell Therapies. *Front. Immunol.* 11, 243. doi:10.3389/fimmu.2020.00243
- Moritani, Y., Usui, M., Sano, K., Nakazawa, K., Hanatani, T., Nakatomi, M., et al. (2018). Spheroid Culture Enhances Osteogenic Potential of Periodontal

- Ligament Mesenchymal Stem Cells. *J. Periodont Res.* 53, 870–882. doi:10.1111/jre.12577
- Murphy, K. C., Fang, S. Y., and Leach, J. K. (2014). Human Mesenchymal Stem Cell Spheroids in Fibrin Hydrogels Exhibit Improved Cell Survival and Potential for Bone Healing. *Cell Tissue Res* 357, 91–99. doi:10.1007/s00441-014-1830-z
- Murphy, K. C., Hughbanks, M. L., Binder, B. Y. K., Vissers, C. B., and Leach, J. K. (2015). Engineered Fibrin Gels for Parallel Stimulation of Mesenchymal Stem Cell Proangiogenic and Osteogenic Potential. *Ann. Biomed. Eng.* 43 (8), 2010–2021. doi:10.1007/s10439-014-1227-x
- Nudelman, F., Lausch, A. J., Sommerdijk, N. A. J. M., and Sone, E. D. (2013). *In Vitro* models of Collagen Biomineralization. *J. Struct. Biol.* 183 (2), 258–269. doi:10.1016/j.jsb.2013.04.003
- Osathanon, T., Linn, M. L., Rajachar, R. M., Ratner, B. D., Somerman, M. J., and Giachelli, C. M. (2008). Microporous Nanofibrous Fibrin-Based Scaffolds for Bone Tissue Engineering. *Biomaterials* 29 (30), 4091–4099. doi:10.1016/j.biomaterials.2008.06.030
- Petrenko, Y., Syková, E., and Kubinová, Š. (2017). The Therapeutic Potential of Three-Dimensional Multipotent Mesenchymal Stromal Cell Spheroids. *Stem Cell Res Ther* 8, 94. doi:10.1186/s13287-017-0558-6
- Pittenger, M. F., Discher, D. E., Péault, B. M., Phinney, D. G., Hare, J. M., and Caplan, A. I. (2019). Mesenchymal Stem Cell Perspective: Cell Biology to Clinical Progress. *NPJ Regen. Med.* 4, 22. doi:10.1038/s41536-019-0083-6
- Robinson, S. T., Douglas, A. M., Chadid, T., Kuo, K., Rajabalan, A., Li, H., et al. (2016). A Novel Platelet Lysate Hydrogel for Endothelial Cell and Mesenchymal Stem Cell-Directed Neovascularization. *Acta Biomater.* 36, 86–98. doi:10.1016/j.actbio.2016.03.002
- Rumiński, S., Ostrowska, B., Jaroszewicz, J., Skirecki, T., Włodarski, K., Świążkowski, W., et al. (2018). Three-dimensional Printed Polycaprolactone-Based Scaffolds Provide an Advantageous Environment for Osteogenic Differentiation of Human Adipose-Derived Stem Cells. *J. Tissue Eng. Regen. Med.* 12 (1), e473–e485. doi:10.1002/term.2310
- Sart, S., Tsai, A.-C., Li, Y., and Ma, T. (2014). Three-dimensional Aggregates of Mesenchymal Stem Cells: Cellular Mechanisms, Biological Properties, and Applications. *Tissue Eng. Part B: Rev.* 20, 365–380. doi:10.1089/ten.teb.2013.0537
- Schoen, F. J., and Levy, R. J. (2013). “Pathological Calcification of Biomaterials,” in *Biomaterials Science*. Editors B.D. Ratner, A.S. Hoffman, F.J. Schoen, and J.E. Lemons. Third Edition (Academic Press), 739–754. doi:10.1016/b978-0-08-087780-8.00063-2
- Scott, M. A., Levi, B., Askarinar, A., Nguyen, A., Rackohn, T., Ting, K., et al. (2012). Brief Review of Models of Ectopic Bone Formation. *Stem Cell Dev* 21 (655), 655–667. doi:10.1089/scd.2011.0517
- Shanbhag, S., Mohamed-Ahmed, S., Lunde, T. H. F., Suliman, S., Bolstad, A. I., Hervig, T., et al. (2020a). Influence of Platelet Storage Time on Human Platelet Lysates and Platelet Lysate-Expanded Mesenchymal Stromal Cells for Bone Tissue Engineering. *Stem Cell Res Ther* 11 (1), 351. doi:10.1186/s13287-020-01863-9
- Shanbhag, S., and Shanbhag, V. (2015). Clinical Applications of Cell-Based Approaches in Alveolar Bone Augmentation: a Systematic Review. *Clin. Implant Dentistry Relat. Res.* 17 (Suppl. 1), e17–e34. doi:10.1111/cid.12103
- Shanbhag, S., Stavropoulos, A., Suliman, S., Hervig, T., and Mustafa, K. (2017). Efficacy of Humanized Mesenchymal Stem Cell Cultures for Bone Tissue Engineering: a Systematic Review with a Focus on Platelet Derivatives. *Tissue Eng. Part B: Rev.* 23, 552–569. doi:10.1089/ten.teb.2017.0093
- Shanbhag, S., Suliman, S., Bolstad, A. I., Stavropoulos, A., and Mustafa, K. (2020b). Xeno-Free Spheroids of Human Gingiva-Derived Progenitor Cells for Bone Tissue Engineering. *Front. Bioeng. Biotechnol.* 8, 968. doi:10.3389/fbioe.2020.00968
- Shanbhag, S., Suliman, S., Pandis, N., Stavropoulos, A., Sanz, M., and Mustafa, K. (2019). Cell Therapy for Orofacial Bone Regeneration: A Systematic Review and Meta-Analysis. *J. Clin. Periodontol.* 46 (Suppl. 21), 162–182. doi:10.1111/jcpe.13049
- Sharpe, P. T. (2016). Dental Mesenchymal Stem Cells. *Development* 143, 2273–2280. doi:10.1242/dev.134189
- Soffer, E., Ouhayoun, J. P., and Anagnostou, F. (2003). Fibrin Sealants and Platelet Preparations in Bone and Periodontal Healing. *Oral Surg. Oral Med. Oral Pathol. Oral Radiol. Endodontology* 95 (5), 521–528. doi:10.1067/moe.2003.152
- Suliman, S., Ali, H. R. W., Karlsen, T. A., Amiaud, J., Mohamed-Ahmed, S., Layrolle, P., et al. (2019). Impact of Humanised Isolation and Culture Conditions on Stemness and Osteogenic Potential of Bone Marrow Derived Mesenchymal Stromal Cells. *Sci. Rep.* 9 (1), 16031. doi:10.1038/s41598-019-52442-9
- Takabatake, K., Tsujigiwa, H., Song, Y., Matsuda, H., Kawai, H., Fujii, M., et al. (2018). The Role of Bone Marrow-Derived Cells during Ectopic Bone Formation of Mouse Femoral Muscle in GFP Mouse Bone Marrow Transplantation Model. *Int. J. Med. Sci.* 15 (8), 748–757. doi:10.7150/ijms.24605
- Tomar, G. B., Srivastava, R. K., Gupta, N., Barhanpurkar, A. P., Pote, S. T., Jhaveri, H. M., et al. (2010). Human Gingiva-Derived Mesenchymal Stem Cells Are superior to Bone Marrow-Derived Mesenchymal Stem Cells for Cell Therapy in Regenerative Medicine. *Biochem. Biophysical Res. Commun.* 393, 377–383. doi:10.1016/j.bbrc.2010.01.126
- Trouillas, M., Prat, M., Doucet, C., Ernou, I., Laplace-Builhé, C., Blancard, P. S., et al. (2013). A New Platelet Cryoprecipitate Glue Promoting Bone Formation after Ectopic Mesenchymal Stromal Cell-Loaded Biomaterial Implantation in Nude Mice. *Stem Cell Res Ther* 4 (1), 1. doi:10.1186/scrt149
- Tsujigiwa, H., Hirata, Y., Katase, N., Buery, R. R., Tamamura, R., Ito, S., et al. (2013). The Role of Bone Marrow-Derived Cells during the Bone Healing Process in the GFP Mouse Bone Marrow Transplantation Model. *Calcif Tissue Int.* 92 (3), 296–306. doi:10.1007/s00223-012-9685-3
- Xu, L., Liu, Y., Sun, Y., Wang, B., Xiong, Y., Lin, W., et al. (2017). Tissue Source Determines the Differentiation Potentials of Mesenchymal Stem Cells: a Comparative Study of Human Mesenchymal Stem Cells from Bone Marrow and Adipose Tissue. *Stem Cell Res Ther* 8 (1), 275. doi:10.1186/s13287-017-0716-x
- Yamada, S., Shanbhag, S., and Mustafa, K. (2022). Scaffolds in Periodontal Regenerative Treatment. *Dental Clin. North America* 66, 111–130. doi:10.1016/j.cden.2021.06.004
- Yamada, Y., Seong Boo, J., Ozawa, R., Nagasaka, T., Okazaki, Y., Hata, K.-i., et al. (2003). Bone Regeneration Following Injection of Mesenchymal Stem Cells and Fibrin Glue with a Biodegradable Scaffold. *J. Craniomaxillofac. Surg.* 31 (1), 27–33. doi:10.1016/s1010-5182(02)00143-9
- Yamaguchi, Y., Ohno, J., Sato, A., Kido, H., and Fukushima, T. (2014). Mesenchymal Stem Cell Spheroids Exhibit Enhanced *In-Vitro* and *In-Vivo* Osteoregenerative Potential. *BMC Biotechnol.* 14, 105. doi:10.1186/s12896-014-0105-9
- Zhang, S., Mao, T., and Chen, F. (2011). Influence of Platelet-Rich Plasma on Ectopic Bone Formation of Bone Marrow Stromal Cells in Porous Coral. *Int. J. Oral Maxillofac. Surg.* 40 (9), 961–965. doi:10.1016/j.ijom.2011.02.037
- Zorin, V. L., Komlev, V. S., Zorina, A. I., Khromova, N. V., Solovieva, E. V., Fedotov, A. Y., et al. (2014). Octacalcium Phosphate Ceramics Combined with Gingiva-Derived Stromal Cells for Engineered Functional Bone Grafts. *Biomed. Mater.* 9 (5), 055005. doi:10.1088/1748-6041/9/5/055005

Conflict of Interest: The authors declare that the research was conducted in the absence of any commercial or financial relationships that could be construed as a potential conflict of interest.

Publisher's Note: All claims expressed in this article are solely those of the authors and do not necessarily represent those of their affiliated organizations, or those of the publisher, the editors and the reviewers. Any product that may be evaluated in this article, or claim that may be made by its manufacturer, is not guaranteed or endorsed by the publisher.

Copyright © 2021 Shanbhag, Kampleitner, Mohamed-Ahmed, Yassin, Dongre, Costea, Tangl, Hassan, Stavropoulos, Bolstad, Suliman and Mustafa. This is an open-access article distributed under the terms of the Creative Commons Attribution License (CC BY). The use, distribution or reproduction in other forums is permitted, provided the original author(s) and the copyright owner(s) are credited and that the original publication in this journal is cited, in accordance with accepted academic practice. No use, distribution or reproduction is permitted which does not comply with these terms.



Corrigendum: Ectopic Bone Tissue Engineering in Mice Using Human Gingiva or Bone Marrow-Derived Stromal/Progenitor Cells in Scaffold-Hydrogel Constructs

Siddharth Shanbhag^{1,2*}, Carina Kampeitner^{3,4,5}, Samih Mohamed-Ahmed¹, Mohammed Ahmad Yassin¹, Harsh Dongre^{6,7}, Daniela Elena Costea^{6,7}, Stefan Tangl^{4,5}, Mohamad Nageeb Hassan¹, Andreas Stavropoulos^{8,9}, Anne Isine Bolstad¹, Salwa Suliman¹ and Kamal Mustafa^{1*}

¹Center for Translational Oral Research (TOR), Department of Clinical Dentistry, Faculty of Medicine, University of Bergen, Bergen, Norway, ²Department of Immunology and Transfusion Medicine, Haukeland University Hospital, Bergen, Norway, ³Ludwig Boltzmann Institute for Traumatology, The Research Center in Cooperation with AUVA, Vienna, Austria, ⁴Karl Donath Laboratory for Hard Tissue and Biomaterial Research, University Clinic of Dentistry, Medical University of Vienna, Vienna, Austria, ⁵Austrian Cluster for Tissue Regeneration, Vienna, Austria, ⁶Gade Laboratory for Pathology, Department of Clinical Medicine, Faculty of Medicine, University of Bergen, Bergen, Norway, ⁷Centre for Cancer Biomarkers (CCBIO), Faculty of Medicine, University of Bergen, Bergen, Norway, ⁸Department of Periodontology, Faculty of Odontology, Malmö University, Malmö, Sweden, ⁹Division of Regenerative Medicine and Periodontology, University Clinics of Dental Medicine, University of Geneva, Geneva, Switzerland

OPEN ACCESS

Approved by:

Frontiers Editorial Office,
Frontiers Media SA, Switzerland

*Correspondence:

Siddharth Shanbhag
siddharth.shanbhag@uib.no
Kamal Mustafa
Kamal.Mustafa@uib.no

Specialty section:

This article was submitted to
Tissue Engineering and Regenerative
Medicine,
a section of the journal
Frontiers in Bioengineering and
Biotechnology

Received: 08 December 2021

Accepted: 15 December 2021

Published: 04 January 2022

Citation:

Shanbhag S, Kampeitner C, Mohamed-Ahmed S, Yassin MA, Dongre H, Costea DE, Tangl S, Hassan MN, Stavropoulos A, Bolstad AI, Suliman S and Mustafa K (2022) Corrigendum: Ectopic Bone Tissue Engineering in Mice Using Human Gingiva or Bone Marrow-Derived Stromal/Progenitor Cells in Scaffold-Hydrogel Constructs. *Front. Bioeng. Biotechnol.* 9:831669. doi: 10.3389/fbioe.2021.831669

Keywords: xeno-free, platelet lysate, MSC, spheroid culture, bone tissue engineering

A corrigendum on

Ectopic Bone Tissue Engineering in Mice Using Human Gingiva or Bone Marrow-Derived Stromal/Progenitor Cells in Scaffold-Hydrogel Constructs

by Shanbhag, S., Kampeitner, C., Mohamed-Ahmed, S., Yassin, M. A., Dongre, H., Costea, D. E., Tangl, S., Stavropoulos, A., Bolstad, A. I., Suliman, S., and Mustafa, K. (2021). *Front. Bioeng. Biotechnol.* 9:783468. doi:10.3389/fbioe.2021.783468

“Mohamad Nageeb Hassan” was not included as an author in the published article. The corrected **Author Contributions** Statement appears below.

“SSH and KM conceived and designed the study. SSH performed the experiments, data collection, data analysis and drafted the manuscript. CK, SM-A, MY, HD, DE, ST, and MH assisted with data collection, data analysis/interpretation and drafting the manuscript. AS, AB, SSu, and KM assisted with data analysis/interpretation and drafting the manuscript. All authors read and approved the final version of the manuscript.”

The authors apologize for this error and state that this does not change the scientific conclusions of the article in any way. The original article has been updated.

Publisher's Note: All claims expressed in this article are solely those of the authors and do not necessarily represent those of their affiliated organizations, or those of the publisher, the editors and the reviewers. Any product that may be evaluated in this article, or claim that may be made by its manufacturer, is not guaranteed or endorsed by the publisher.

Copyright © 2022 Shanbhag, Kampeitner, Mohamed-Ahmed, Yassin, Dongre, Costea, Tangl, Hassan, Stavropoulos, Bolstad, Suliman and Mustafa. This is an open-access article distributed under the terms of the Creative Commons Attribution License (CC BY). The use, distribution or reproduction in other forums is permitted, provided the original author(s) and the copyright owner(s) are credited and that the original publication in this journal is cited, in accordance with accepted academic practice. No use, distribution or reproduction is permitted which does not comply with these terms.



Recent Advances in Vertical Alveolar Bone Augmentation Using Additive Manufacturing Technologies

Cedryck Vaquette, Joshua Mitchell and Sašo Ivanovski*

School of Dentistry, Centre for Orofacial Regeneration, Reconstruction and Rehabilitation (COR3), The University of Queensland, Herston, QLD, Australia

OPEN ACCESS

Edited by:

Nikos Donos,
Queen Mary University of London,
United Kingdom

Reviewed by:

Giulia Brunello,
University Hospital of Düsseldorf,
Germany
Patrina S. P. Poh,
Charité Medical University of Berlin,
Germany

*Correspondence:

Sašo Ivanovski
s.ivanovski@uq.edu.au

Specialty section:

This article was submitted to
Tissue Engineering and Regenerative
Medicine,
a section of the journal
Frontiers in Bioengineering and
Biotechnology

Received: 20 October 2021

Accepted: 13 December 2021

Published: 07 February 2022

Citation:

Vaquette C, Mitchell J and Ivanovski S
(2022) Recent Advances in Vertical
Alveolar Bone Augmentation Using
Additive Manufacturing Technologies.
Front. Bioeng. Biotechnol. 9:798393.
doi: 10.3389/fbioe.2021.798393

Vertical bone augmentation is aimed at regenerating bone extraskeletally (outside the skeletal envelope) in order to increase bone height. It is generally required in the case of moderate to severe atrophy of bone in the oral cavity due to tooth loss, trauma, or surgical resection. Currently utilized surgical techniques, such as autologous bone blocks, distraction osteogenesis, and Guided Bone Regeneration (GBR), have various limitations, including morbidity, compromised dimensional stability due to suboptimal resorption rates, poor structural integrity, challenging handling properties, and/or high failure rates. Additive manufacturing (3D printing) facilitates the creation of highly porous, interconnected 3-dimensional scaffolds that promote vascularization and subsequent osteogenesis, while providing excellent handling and space maintaining properties. This review describes and critically assesses the recent progress in additive manufacturing technologies for scaffold, membrane or mesh fabrication directed at vertical bone augmentation and Guided Bone Regeneration and their *in vivo* application.

Keywords: extraskeletal bone, 3D-printing, BMP-2, bioceramic, polycaprolactone, bone regeneration

INTRODUCTION

Bone resorption is a phenomenon characterized by the volumetric reduction in viable bone tissue. Whilst osteoclast-mediated bone remodeling is an essential part of healthy bone metabolism, irreversible bone resorption can occur due to trauma or pathology within bone tissues (Teitelbaum, 2000). This is particularly problematic within the maxillofacial region, where surgical interventions, such as tooth extraction, can result in irreversible bone resorption leading to significant loss of bone volume. Consequently, a regenerative procedure for re-establishing the lost tissue and enabling the placement of prosthetic devices, such as dental implants, is required. Vertical bone augmentation aims to restore the previous levels of bone height, and is one of the most challenging surgical procedures in dentistry as it requires the formation and maintenance of extraskeletal bone (i.e., outside the newly established skeletal envelope) (Esposito et al., 2009; Urban et al., 2019).

Several existing techniques aimed at vertical bone augmentation, such as autologous block grafts, distraction osteogenesis, and guided bone regeneration combined with particulate grafts (GBR), have shown varying levels of success and are generally considered to be technique sensitive and clinically unpredictable (Urban et al., 2019). Indeed, whilst some commendable advances have been made in vertical bone augmentation, issues surrounding space maintenance, graft fixation, predictability of bone formation, and resorption still persist (Asa'ad et al., 2016). Other approaches are required to address these issues, and additive manufacturing (also known as three-dimensional (3D) printing)

technology has been recently shown to have considerable potential to advance the field of vertical bone augmentation (Moussa et al., 2015; Carrel et al., 2016a; Carrel et al., 2016b; Sudheesh Kumar et al., 2018; Vaquette et al., 2021). Additive manufacturing enables the fabrication of porous biomaterials with an interconnected pore network in a layer-by-layer fashion and is additionally capable of fabricating customised patient-matched constructs. Advancements in bioceramic and polymer additive manufacturing techniques have paved the way for exploration into novel techniques in vertical bone tissue regeneration (Moussa et al., 2015; Carrel et al., 2016a; Carrel et al., 2016b; Ngo et al., 2018; Sudheesh Kumar et al., 2018; Vaquette et al., 2021).

In vivo application of such scaffolds has yielded some success in pre-clinical trials and generated strong interest within the field (Melchels et al., 2012; Khojasteh et al., 2013; Asa'ad et al., 2016). This review will briefly describe the various methods of 3D-printing for the manufacturing of 3D scaffolds (bioceramic and/or polymer), membranes, and patient matched metal meshes and then critically analyze the most recent studies utilizing additive manufacturing technologies for the purpose of alveolar vertical bone augmentation.

ADDITIVE MANUFACTURING TECHNOLOGIES AND BONE REGENERATION

Significant progress in additive manufacturing technology (3D printing) has been achieved over the past twenty years. Multiple techniques ranging from powder ceramic to polymer fabrication have been developed and optimized, bringing the field to a level of technological competency whereby a diverse range of geometries can be fabricated relatively quickly, and with a high degree of dimensional accuracy and patient customization (Lipson et al., 2004; Feilden et al., 2016). Utilizing this technology in conjunction with conventional imaging techniques, such as computer tomography (CT) scanning, enables the manufacturing of scaffolds with identical geometric features to the host tissue (Melchels et al., 2011).

Synthetic scaffolds can be fabricated by a broad range of techniques, and the following **Table 1** summarizes the main additive manufacturing technologies utilized for scaffold fabrication applied in bone regeneration.

For vertical bone augmentation, scaffolds must fulfill several essential criteria. The scaffold must be biocompatible and should not induce cytotoxicity, acute inflammation or any form of rejection or fibrous encapsulation (Langer and Vacanti, 1993). The material must be capable of integrating with the native tissue by facilitating infiltration of cells, i.e., progenitor cells or osteoblasts (Asa'ad et al., 2016). The scaffold should be highly porous with an interconnected porosity to facilitate rapid vascularization to support bone formation (Cruess and Cruess, 1982). Previous research demonstrated that a porosity ranging from 60 to 90% is appropriate for bone regeneration and that a pore size above 100 microns is required for enabling cell, tissue infiltration and vascularization (Karageorgiou and Kaplan, 2005).

Interestingly, the pore size also seems to impact bone regeneration depending on the application, as a recent study reported (Ghayor et al., 2021). Indeed, it was demonstrated that a larger pore size was beneficial for vertical augmentation whereas a smaller pore size enhanced bone regeneration in a bony defect. Regardless of the internal architecture, the scaffolds must be self-supporting and mechanically robust for achieving appropriate space maintenance for bone ingrowth and to ensure it does not collapse upon mastication which force ranges from 50 to 200 N depending on age and position in the jaw (Edmonds and Glowacka, 2020). The current literature reporting on additively manufactured scaffolds for vertical bone augmentation can be divided into three major biomaterials groups: 1) bio-ceramics, 2) polymers, and 3) metals.

ADDITIVELY MANUFACTURED BIO-CERAMIC CONSTRUCTS FOR VERTICAL BONE REGENERATION

As mentioned, whilst bone grafting techniques result in desirable clinical success rates, the method is still prone to post-surgical complications, and handling can be difficult for large bone deficiencies (Nyström et al., 2002; Nyström et al., 2004). This has seen an evolution of bone grafting research into synthetic alternatives to better address resorption issues encountered with autogenous bone (Tamimi et al., 2006). Bio-ceramics are one such material group of interest due to their biocompatibility and efficacy to conduct and/or induce bone formation. Common materials of interest within this class are hydroxyapatite (HA), alpha tri-calcium phosphate (α -TCP), beta tri-calcium phosphate (β -TCP), and biphasic tricalcium phosphate (Asa'ad et al., 2016). Bio-ceramics are generally manufactured from a colloidal suspension which enables the shaping of an implant, and this part is called the “green body”. This “green body” is then subjected to high temperatures (typically 50–90% of the melting temperature) which gives the implant its final microstructure and properties (Lakhdar et al., 2021). This later step induces volumetric changes and therefore the final implant is smaller than the green body, which represents a significant challenge for the production of customized implants.

Bio-ceramics characteristically exhibit excellent osteoconductive and sometimes osteoinductive properties (Barradas et al., 2011). This is largely due to the fact that they can be fabricated with coarse topography and surfaces suitable for the release of calcium and phosphate ions known for promoting the osteo-differentiation of progenitor cells. These materials are mostly utilized in a particulate form in combination with an occlusive membrane for bone regeneration in the oral cavity. While osteoconductive, the utilization of their granular form in the clinic is a significant challenge for handling and achieving adequate stability for vertical augmentation in the case of large bone deficiencies. In addition, the packing of the granular materials results in the formation of a highly tortuous porous network, which may impede rapid vascularization of large defects and delay bone formation as previously reported (Carrel et al., 2016b). Bio-ceramic 3D-printed scaffolds could potentially

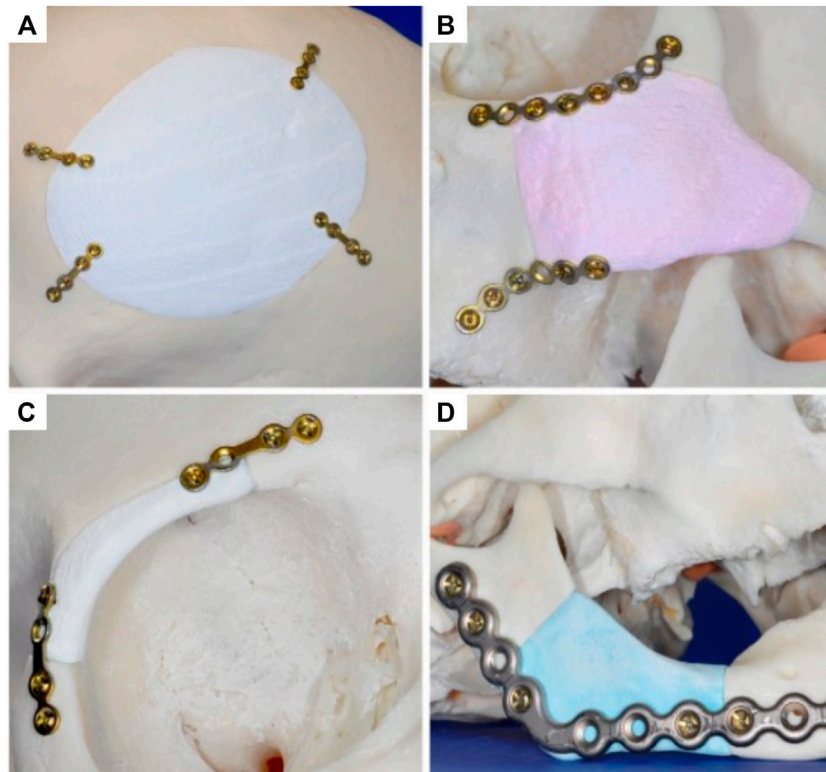


FIGURE 1 | Manufacturing of anatomically accurate 3D-printed bioceramic scaffolds for bone regeneration demonstrating the versatility of the fabrication method for various applications in the craniofacial area. Reproduced with permission from (Klammert et al., 2010) (A–D).

circumvent these issues as demonstrated in a clinical case which resulted in excellent structural maintenance and high bone formation seven years post-implantation (Mangano et al., 2021).

Bio-Ceramic Scaffolds Manufactured by 3D Powder Printing

Several research endeavors have advocated a shift away from particulate grafting to programmable 3D fabricated bio-ceramics blocks (Gbureck et al., 2007; Klammert et al., 2010). Gbureck et al. developed a 3D powder printing technique utilizing a mixture of α/β Tricalcium Phosphate (TCP) particles which were reacted and bound together by spraying a phosphoric acid solution (Gbureck et al., 2007). This enabled a curing reaction of the TCP at room temperature, resulting in the creation of biodegradable secondary calcium phosphate matrices, namely brushite and monetite [dicalcium phosphate dihydrate (Brushite), and dicalcium phosphate anhydrous monetite (Monetite)]. The final phase composition of the fabricated material was a brushite phase (67%wt) and the remaining bioceramic was the unreacted α/β -TCP phase and a small amount of monetite. Further processing via hydrothermal reaction converted brushite components to monetite. The printed brushite scaffold and the thermally converted monetite were then compared *in-vivo* in an intramuscular rodent model. Surprisingly, the monetite scaffold underwent a more rapid

degradation than the brushite. While brushite is a highly soluble phase and hence should have degraded first, a phase transition towards hydroxyapatite occurred via a dissolution/precipitation mechanism, thus rendering a proportion of the bio-ceramic block insoluble.

The versatility of this 3D-powder printing method was further demonstrated by manufacturing anatomically accurate scaffolds for potential craniofacial implantation (Figure 1) (Klammert et al., 2010). The study utilized a human cadaveric model featuring several defects that were imaged and numerically captured via computer tomography (CT), and further processed using computer aided design software (CAD) for STL file production and 3D-printing. Utilizing the 3D-powder printing technique previously described (Gbureck et al., 2007), 3D matrices of brushite (further hydrothermally converted to monetite) were fabricated matching the geometries of the defects. Although no quantitative data was provided, the study reported sound contour cohesion between the implant and defect, with some small overlapping areas which were later resolved by manual smoothing. Overall, this study demonstrated the ability of 3D-powder printed bio-ceramics to be accurately manufactured for a specific defect, which is a challenge for 3D printed bioceramics due to the significant dimensional changes occurring during the essential sintering process.

The ability of the bioceramic scaffold to support vertical bone formation was further investigated in a lapine extraskeletal model

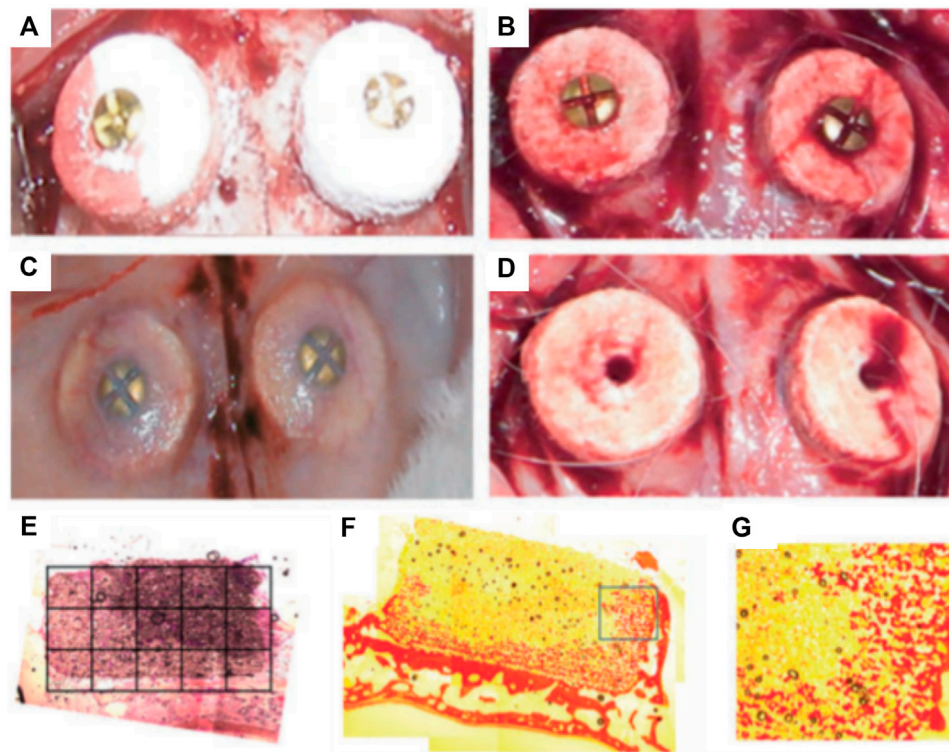


FIGURE 2 | Influence of overall height of 3D-powder printing monetite scaffold in a lapine extraskeletal model. **(A):** 3 and 4 mm high 3D-printed scaffolds were implanted and fixed using a fixation screw, **(B):** shows the blood clot stabilization within the scaffold immediately after implantation. **(C):** Specimen morphology 8 weeks post-implantation. **(D):** Removal of the fixation screws at 8 weeks post-implantation, **(E–G):** Tissue morphology as assessed by histology (picro-sirius staining) indicating a heterogenous distribution of the newly formed bone preferentially located near the resident bone and at the periphery of the scaffold. Reproduced with permission from (Torres et al., 2011).

(Tamimi et al., 2009). This study additionally evaluated the feasibility of fixing the 3D printed monetite block with craniofacial screws in an *in vivo* setting. The 3D-printed bio-ceramic scaffolds were trialed as an onlay graft and a 9 mm diameter and 2 mm thick monetite disc was compared to the performance of an autologous bone block of similar dimensions. Both structures were secured using a titanium osteosynthesis self-drilling screw placed at the center of the block. The samples were retrieved 8 weeks post-implantation and displayed no obvious signs of inflammation and were well integrated with the calvarium. However, the bone block demonstrated some resorption and histology analysis revealed intense osteoclastic activity at both the outer and inner regions of the autologous bone graft. The monetite scaffolds performed moderately well, resulting in bone formation preferentially on the lateral portions and in the area of the 3D-printed scaffold in direct contact with the calvarial bone. The bio-ceramic also displayed signs of extensive degradation and there was no significant difference in bone height when compared to the autologous bone block (Tamimi et al., 2009). A subsequent study was performed by Torres et al. using a similar 3D printed the monetite monolithic scaffold (**Figures 2A–D**) with a disc-shaped geometry, for assessing the influence of the bio-ceramic height upon vertical bone formation (3 and 4 mm

height) (Torres et al., 2011). Here again, the blocks were fixated by an osteosynthesis screw placed in a centrally located cylindrical hole and a period of 8 weeks was allowed for healing in an extraskeletal lapine model. Integration with calvarial tissue was deemed successful and histological analysis revealed that newly formed bone occupied around 40% of the blocks irrespective of their initial heights (**Figures 2E–G**) (Torres et al., 2011). Similar to the previous studies (Tamimi et al., 2009; Tamimi et al., 2014), the majority of bone was located in the proximity of the resident calvarial bone and at the periphery of the 3D-printed scaffold. This heterogeneous bone formation was attributed to the poorly interconnected porous network throughout the scaffold, which subsequently impeded vascularization and hence bone formation.

Overall, these studies highlighted the limitations of 3D-powder printing of monetite scaffolds, which despite appropriate fixation being achieved, could not support extensive bone formation, most likely due to the relatively low porosity and lack of pore interconnection preventing vascularization.

Consequently, a scaffold with increased interconnectivity by including channels within its core was developed (Tamimi et al., 2014). Several configurations were assessed as shown in **Figures 3A–C**. Design A consisted of an unmodified monetite 3D-printed

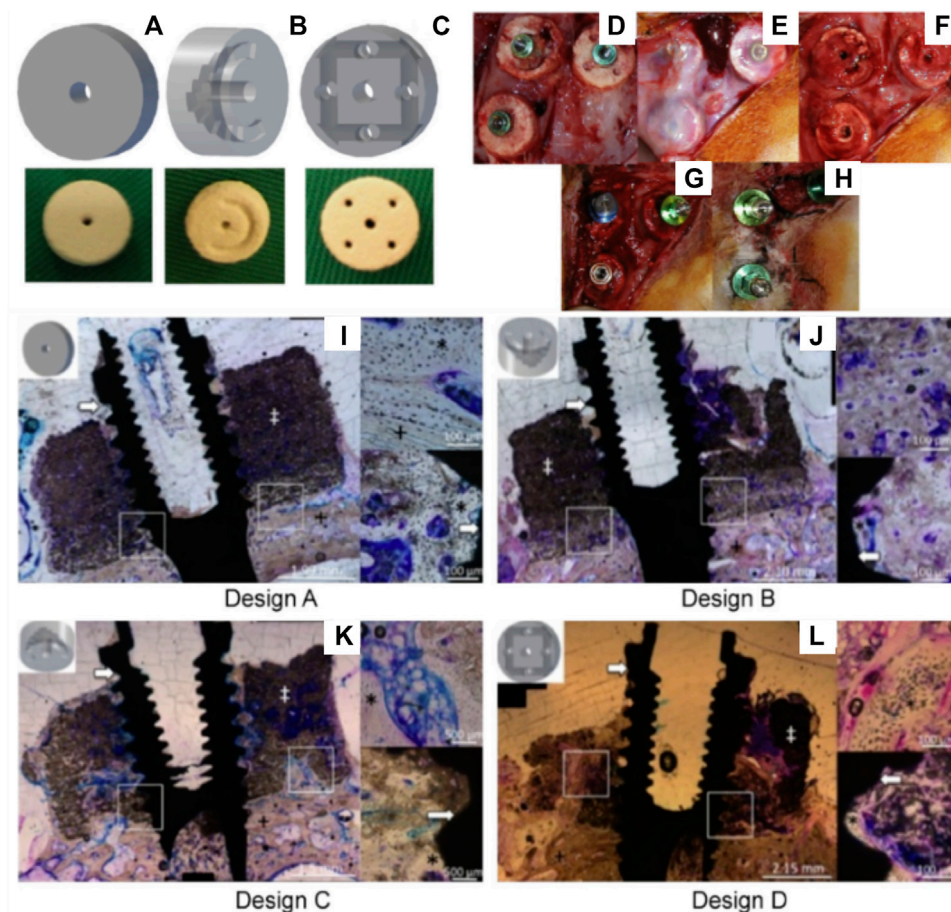


FIGURE 3 | Assessment of the bone formation performance of 3D-powder printing including various microporosity in the forms of semi-circular grooves and channels in a lapine extraskeletal model. **(A)**: Design A “control” 3D-printed monetite scaffold, **(B)**: Design B and C including a semi-circle shaped groove spanning half the diameter of the scaffold, with the semi-circle in configuration B facing away from the calvarial bone, whilst the semi-circle in configuration C faced the calvarial bone, **(C)**: Design D consisting of an array of eight interconnected channels creating multiple apertures on each surface of the scaffold, **(D)**: surgical fixation of the scaffold, **(E)**: surgical re-entry at 4 weeks post-implantation, **(F)**: removal of the fixation screws, **(G)**: Dental implant placement, **(H)**: appearance of the specimens at 4 weeks post-implant placement. **(I–L)** Tissue morphology as demonstrated by histology, indicating that the presence of the channels was beneficial to bone formation, although the overall amount of bone tissue was not greatly increased and its distribution remained heterogeneous. Reproduced with permission from (Tamimi et al., 2014).

scaffold. Designs B and C included a semi-circle shaped groove spanning half the diameter of the scaffold, with the semi-circle in configuration B facing away from the calvarial bone, whilst the semi-circle in configuration C faced the calvarial bone. Design D consisted of an array of eight interconnected channels creating multiple apertures on each surface of the scaffold. The scaffolds were implanted in a lapine model, a surgical re-entry was performed 4 weeks post-implantation for enabling the placement of titanium dental implants (Figures 3D–H), and osseointegration was allowed for a further 4 weeks. At completion of the study (8 weeks total) it was demonstrated that some bone had formed preferentially in the proximity of the host bone and in the vicinity of the channels (Figures 3I–L). However, configurations C and D that had channels in direct contact with the host bone displayed the largest amount of bone formation. Configuration A and B resulted in the lowest bone formation, demonstrating that the presence of the macroscopic channels in the other designs improved vascularization and hence

bone formation ability of the scaffolds. Histology confirmed that the dental implant was osseointegrated with any newly formed vertical bone that was present. The study concluded that modifying the geometry of the scaffolds enhanced uniform bone regeneration. However, the most medial and superior sections of all scaffold configurations exhibited little or no bone formation (Tamimi et al., 2014). While the introduction of interconnected macro-channels was beneficial for bone formation, the latter was mostly restricted to portions of the scaffold where a rapid vascularization occurred (such as in the channels or in the peripheral aspects of the scaffold). Despite the high bioactivity of bio-ceramic materials, the lack of significant bone in growth in the powder 3D printed scaffolds, featuring a low porosity, small pore size and a tortuous porous network, exemplifies the importance of the construct internal porous architecture in facilitating vascularization, and subsequent bone formation. Scaffold fabrication via a direct printing approach can circumvent these issues and produce a construct

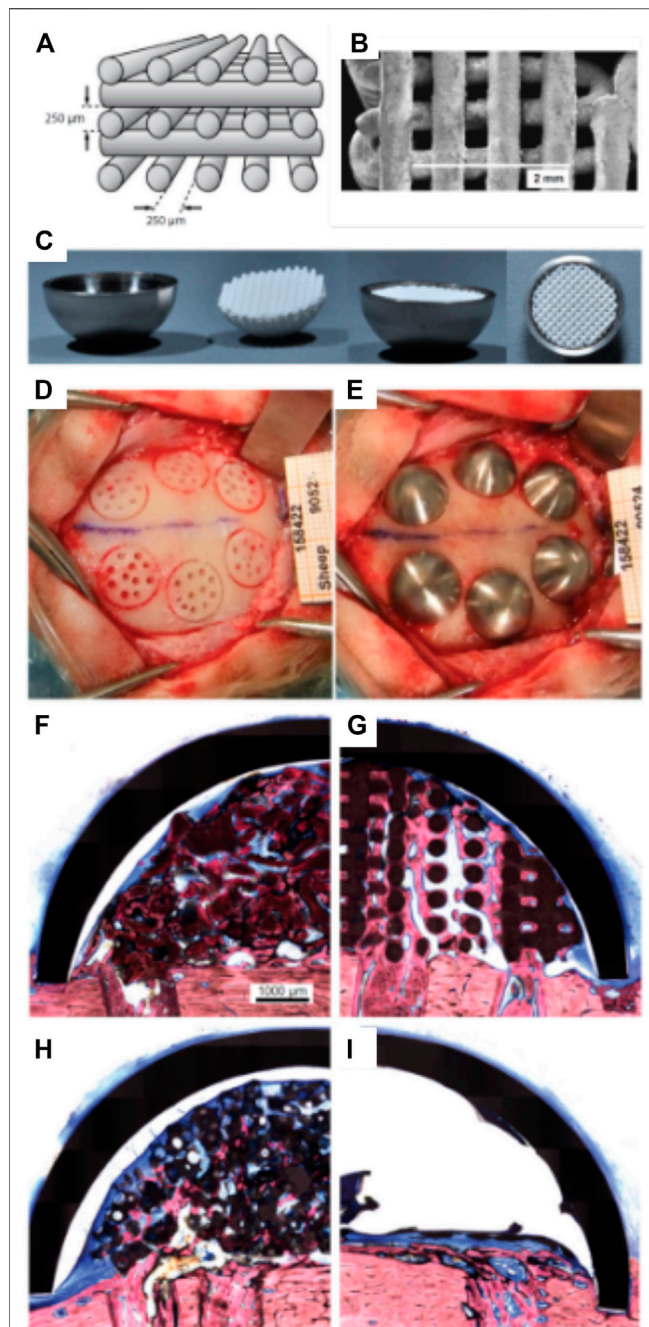


FIGURE 4 | Bio-ceramic scaffold manufacturing via direct extrusion printing. **(A):** Schematic representation of the 3D-printed Osteoflux bio-ceramic, **(B):** Morphology of the 3D-printed scaffold as imaged using Scanning Electron Microscopy. **(C):** implantation system featuring a titanium dome acting as an occlusive barrier. **(D):** Preparation of the implantation site using a sheep extraskelatal model. **(E):** pictures of the implanted domes containing the various groups. **(F–I)** histology of the specimen at 8 weeks post-implantation demonstrating the excellent bone forming ability of the 3D-printed scaffold **(F):** Bio-Oss, **(G):** 3D-printed Osteoflux, **(H):** Ceros, **(I):** empty dome (blood clot). Reproduced with permission from (Carrel et al., 2016b).

with a porous network that is more favorable for uniform bone regeneration.

Bio-Ceramic Scaffolds Manufactured by Extrusion 3D Printing

Carrel et al. confirmed that a highly porous structure, manufactured by extrusion 3D-printing and hence possessing a fully interconnected macropore network (Carrel et al., 2016b), performed better than other randomly organized geometries with lower porosities (Tamimi et al., 2006; Tamimi et al., 2009; Torres et al., 2011; Tamimi et al., 2014). This comparison was undertaken by assessing the performance of three different biomaterials: a 3D-printed bio-ceramic Osteoflux (OF), and two commercially available particulate bone grafting materials, Bio-Oss (BO) and Ceros (CO), with particle size of 0.25–1 mm, and 0.5–0.7 mm, respectively. The OF scaffolds were fabricated via 3D-printing using a calcium phosphate mixture composed of a calcium deficient hydroxyapatite and α -TCP, enabling the manufacturing of 400 μ m diameter filaments regularly ordered to form 250 μ m pores (Figures 4A,B). The scaffold or the granulate materials were housed under a titanium dome (Figure 4C) and subsequently implanted extraskelally on the skull of sheep (Figure 4D).

The specimens were retrieved 8 weeks post-implantation and histomorphometry revealed that the new bone area in the OF (Figure 4G) samples was approximately 20% of the total dome area, BO (Figure 4F), and CO (Figure 4H) displayed around 14% bone fill, while the empty dome resulted in negligible bone formation (Figure 4I). At 16 weeks post-implantation, all groups (other than the Empty group) displayed similar bone fill at around 40%, indicating that the 3D-printed scaffold enabled earlier bone formation. Interestingly, the 3D-printed scaffold also enabled increased bone height at early time points when compared to the particulate material. This was attributed to the interconnected highly porous lattice structure of the scaffold that permitted enhanced vascularization at the superior regions of the scaffold. This indicates that the 3D-printed scaffolds were architecturally designed to be conducive to both horizontal and vertical bone augmentation. In contrast, the randomly organized porous networks of particulate materials had an inferior capacity to support vascularization, resulting in delayed bone formation when compared to the 3D-printed scaffolds. These findings were confirmed in a subsequent study that assessed the performance of 3D-printed Osteoflux scaffolds in a more clinically relevant canine model (Carrel et al., 2016a). This model incorporated vertical bone augmentation in a surgically created edentulous area of a dog mandible. This was performed using a 3D-printed scaffold with dimensions of 10 mm length, 10 mm width, 5 mm height (Figures 5A,B). Four shallow bony defects were created via the removal of molars and premolars (specifically P1-4, M1, both left and right) (Figures 5C–E) and the 3D-printed scaffolds were implanted as an onlay graft. They were biomechanically secured using two Teflon loops inserted in two transcortical tunnels (1.25 mm in diameter), indicating perhaps that conventional

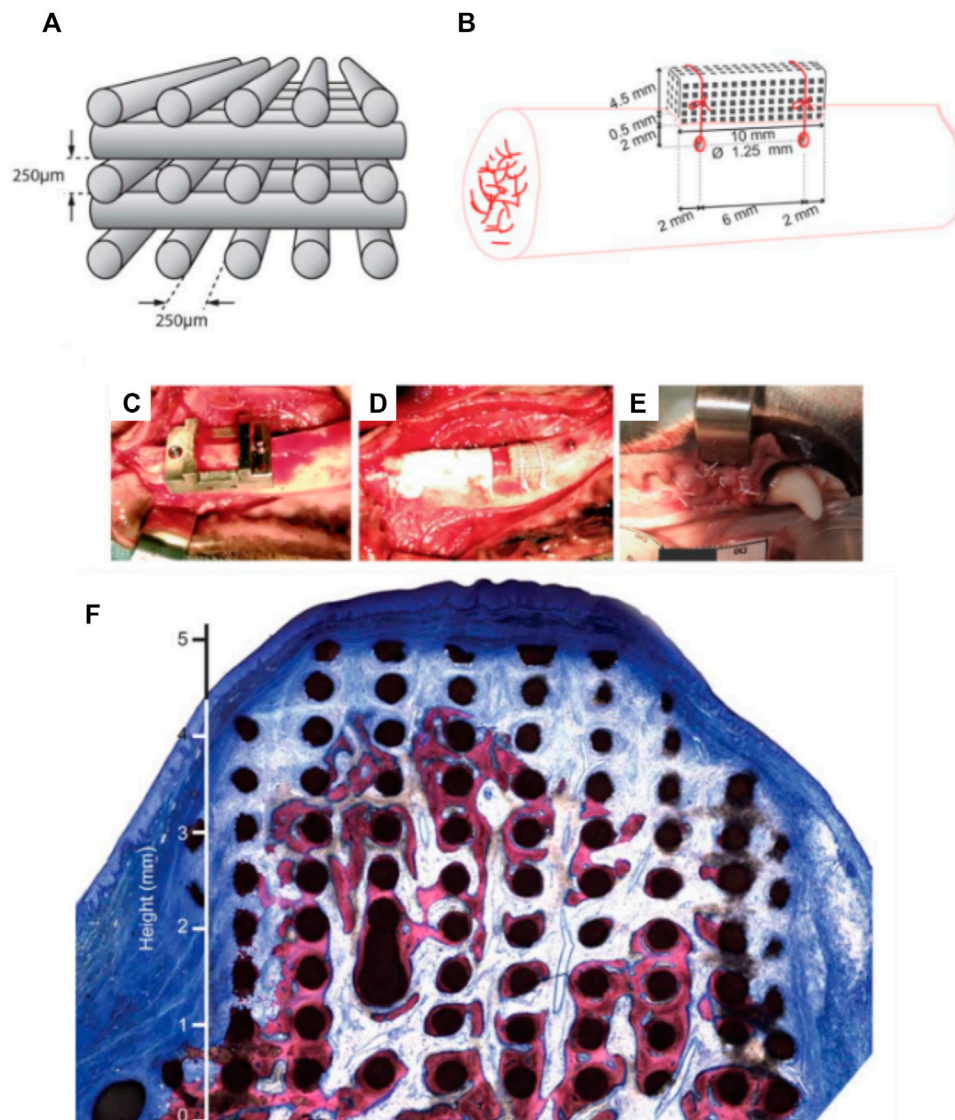


FIGURE 5 | 3D-printed bio-ceramic scaffold manufactured by a direct printing method. **(A,B):** Schematic description of the scaffold porosity and dimensions, as well as the implantation in a canine model. **(C–E):** Implantation of the 3D-printed scaffold and coverage by a collagen membrane. **(F):** histology of the vertically augmented bone 8 weeks post-implantation. Reproduced with permission from (Carrel et al., 2016a).

fixation using titanium screws was not possible. A collagen membrane covered the scaffolds for a subsequent 8-weeks healing period, consistent with standard clinical practice.

While the study utilized only one animal, the proof of concept was nevertheless established. No sites showed evidence of inflammation and the scaffolds were well integrated with the native tissue (**Figure 5F**), and the newly formed bone was highly vascularized, filling approximately one third of the elevated volume and reaching heights between 4 and 5 mm. Specifically, when compared to other ceramic scaffolds in the field, both studies by Carrel et al. demonstrated a higher volume of bone that was also more uniformly distributed throughout the scaffold. This was attributed to the superior vascularization capacity of the scaffold, particularly in its superior segments,

facilitated by the highly interconnected porous network (Carrel et al., 2016a; Carrel et al., 2016b). The main disadvantage of this bio-ceramic 3D-printed scaffold is likely to arise from its inability to be biomechanically secured using fixation screws, which would be problematic in the clinical setting (Carrel et al., 2016a; Carrel et al., 2016b).

Bio-Ceramic Scaffolds Used as Delivery Vehicles for Osteogenic Molecules

Whilst bio-ceramic grafts possess excellent osteoconduction capacity, their bone formation ability can be further improved by combining them with biological cues. The incorporation of bone morphogenetic protein 2 (BMP-2) in the scaffold is a potent

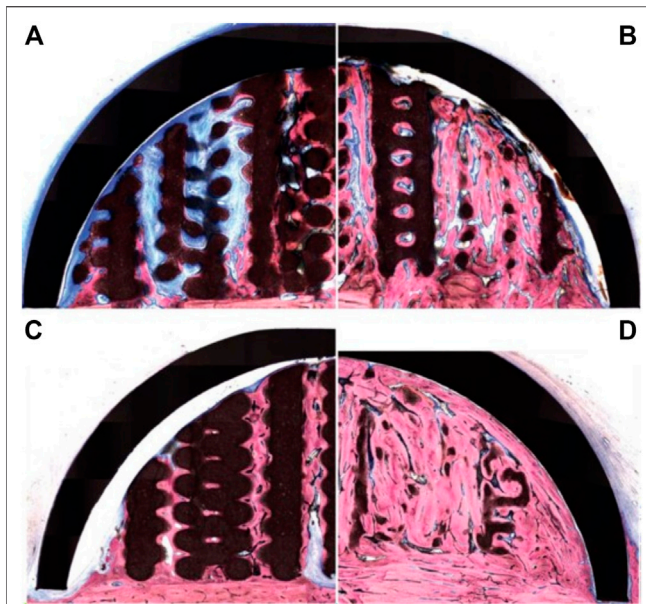


FIGURE 6 | 3D-printed bio-ceramic scaffold combined with Bone Morphogenetic Protein-2 for vertical bone formation. **(A):** pristine 3D-printed bio-ceramic scaffold and **(B):** BMP-2 loaded scaffold at 8 weeks post-implantation, **(C):** pristine 3D-printed bio-ceramic scaffold and **(D):** BMP-2 loaded scaffold at 16 weeks post-implantation demonstrating higher bone formation in the BMP-2 loaded scaffold along with advanced degradation of the bio-ceramic scaffold (in black) at the 16 weeks timepoint. Reproduced with permission from (Moussa et al., 2015).

means of increasing osteogenesis due to its ability to trigger osteoblastic differentiation in a wide range of cell types (Meejung and Senyon, 2011). This strategy was explored by Moussa et al. (2015) using the 3D-printed bio-ceramic scaffold described in the previous section. The performance of the BMP-2 loaded scaffold was assessed using the same ovine extraskeletal bone regeneration model. To this end, the scaffold, loaded with 100 μ g recombinant human BMP-2, was implanted for 8 and 16 weeks and compared to the unloaded scaffold filled with a natural blood clot. The BMP-2 primed scaffold resulted in higher bone formation at both 8- and 16-weeks post-implantation (Figures 6A–D), and degradation of the bio-ceramic scaffold was further accelerated by the presence of the growth factor (Figure 6D). Indeed, at the 16 weeks timepoint, only trace amounts of the scaffold material were observable. While the incorporation of BMP-2 results in excellent vertical bone formation, likely problems of achieving fixation of such a brittle scaffold, as highlighted in the previous section, may still hinder clinical translation.

ADDITIVELY MANUFACTURED POLYMERIC CONSTRUCTS FOR VERTICAL BONE REGENERATION

The development of more flexible polymeric scaffolds has been advocated as an alternative for circumventing the brittleness of bioceramic scaffolds and their poor fixation ability. The following

sections describe the most recent advances in the use of additively manufactured polymeric structures for vertical bone regeneration.

Polymeric Porous 3D Printed Scaffolds for Bone Regeneration

Polymer printing is capable of building a refined interconnected porous network which facilitates neo-vascularization and a provide an environment suitable for osteogenesis to occur. In addition, the utilization of flexible and ductile polymers enables adaption of the defect shape and allows usage of titanium screws for biomechanical fixation. Several proof-of-concept clinical reports using 3D-printed scaffolds for oro-dental tissue regeneration in socket preservation (Goh et al., 2015) and periodontal regeneration (Rasperini et al., 2015) have been reported, however, this approach has not been translated yet to the clinic for vertical alveolar bone formation. Pre-clinical studies using various animal models that explore the potential of additively manufactured polymeric scaffolds for vertical alveolar bone augmentation are discussed below.

An early report for vertical bone augmentation was published in 2013 by Khojasteh et al. whereby a 3D-printed β -TCP/polycaprolactone (PCL) scaffold ($20 \times 10 \times 10 \text{ mm}^3$) was implanted in the mandible of dogs (Khojasteh et al., 2013). The scaffold was seeded with bone marrow mesenchymal stem cells 24 h prior to implantation and healing was allowed for 8 weeks. The cell-laden scaffold performed significantly better when compared to the scaffold without cells with 50 and 20% bone fill, respectively. The poor performance of the scaffold without a biological additive highlights the bioinert nature of the PCL, even when blended with inorganic fillers. Interestingly, this study also reported that the scaffold was fixed using a titanium screw, demonstrating the favorable properties of the polymeric material in terms of facilitating the clinical handling and utilization of additively manufactured constructs.

Kumar et al. further explored the feasibility of a scaffold comprised entirely of polycaprolactone (PCL) and functionalized with BMP-2 in a rabbit model (Sudheesh Kumar et al., 2018). This study utilized a biphasic scaffold consisting of a 3D-printed mechanically robust outer shell, mimicking the cortical plate, into which highly porous melt electrospun scaffolds, mimicking cancellous bone, were inserted. The rationale behind this concept was to promote rapid vascularization within the interior component of the scaffold, whilst the exterior component provided mechanical integrity necessary for space maintenance. The exterior shell component was fabricated through conventional fused deposition modelling (FDM) while the interior component was fabricated through melt electrowriting (Brown et al., 2011; Brown et al., 2012) (Figure 7), producing fibres of 400 and 10 μ m in diameter, respectively. Additionally, an occlusive dome made of poly-L-lactic acid (PLLA) was utilized to prevent fibrous tissue infiltration, consistent with the principles of guided bone regeneration. The study also investigated the incorporation of a hydrogel loaded with recombinant BMP-2 within the scaffold, implanted in an extraskeletal lapine model. While a groove to

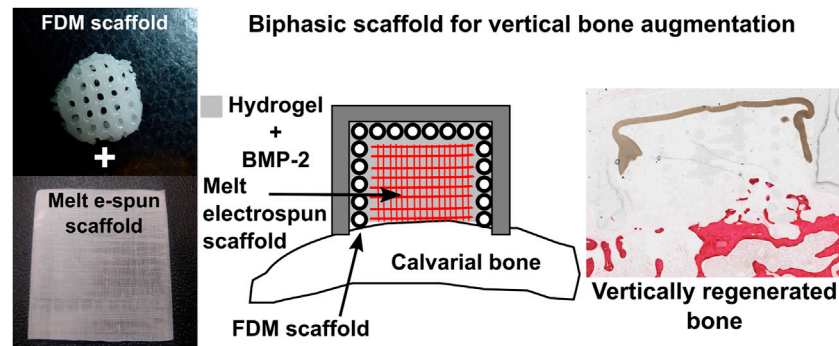


FIGURE 7 | Additively manufactured biphasic scaffold for vertical bone augmentation using a biodegradable polymer, polycaprolactone loaded with a hydrogel. Reproduced with permission from (Sudheesh Kumar et al., 2018).

accommodate the dome was prepared, no transcortical perforations were made, drastically limiting blood clot formation which delayed the initiation of the healing cascade, and therefore neovascularization and bone formation within the scaffold. Accordingly, whilst the scaffold exhibited biomechanical stability and space maintenance, it failed to result in significant new bone formation beyond the resident bony bed. Nonetheless, the concept showed sufficient potential to warrant further investigation for enhanced efficacy following optimization of both the scaffold and the *in-vivo* model.

In a follow up study performed in an extraskeletal ovine calvarium model, the regenerative potential of the PCL 3D-printed/melt electrospun biphasic scaffold was further explored for the formation and maintenance of vertically augmented bone (Vaquette et al., 2021). A 2-stage study first investigated the effect of the scaffold and BMP-2 dose on bone formation. Subsequently, bone maintenance and implant osseointegration were assessed, including surgical re-entry and placement of a dental implant. In the first step, seven configurations were examined: an empty dome, a biphasic scaffold functionalized with a gelatine hyaluronic hydrogel, a biphasic scaffold functionalized with a gelatine hyaluronic hydrogel containing 75 or 150 μg of BMP-2, the gelatine hyaluronic hydrogel alone or containing 75 or 150 μg of BMP-2. Study outcomes demonstrated that the presence of the scaffold improved vertical bone regeneration, potentially due to the hydrogel retention capacity of the scaffold, as shown in **Figure 8A**. Interestingly, the dose of BMP-2 did not make a significant difference in the volume of extraskeletally-formed bone, suggesting that there is a threshold in the dose of BMP-2 for initiating bone formation in a given defect volume, and that any addition of the growth factor may not result in enhanced bone formation. The second stage of the study involved placement of a dental implant in either bone previously formed in the BMP-2 containing hydrogel, or in the BMP-2 functionalized biphasic scaffold. Eight weeks of healing post-implantation was allowed, resulting in full resorption of the bone when the biphasic scaffold was absent (**Figure 8B**). This demonstrated with high reproducibility that the presence of a

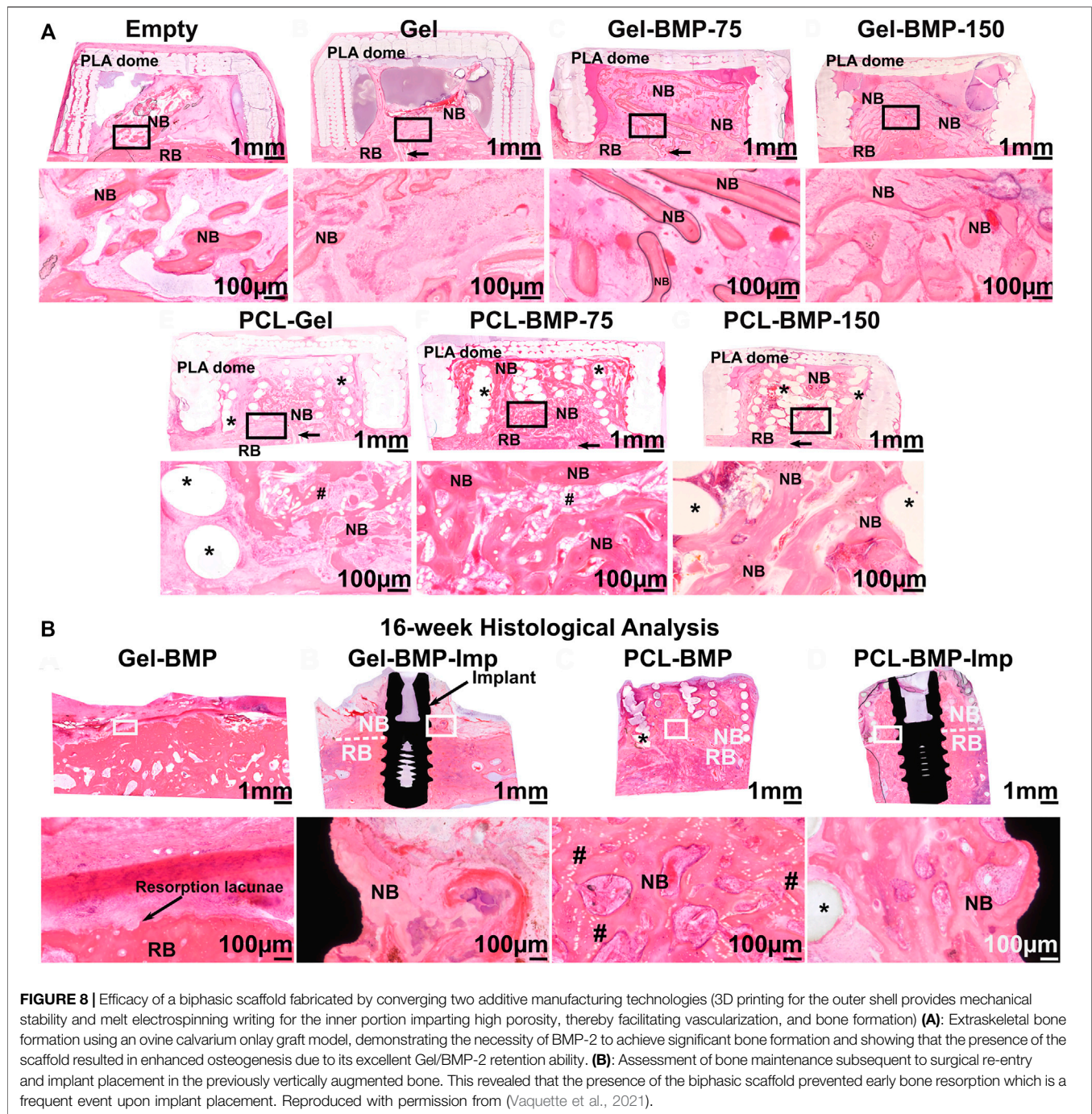
long-term space maintaining scaffold prevents early bone resorption and imparts enhanced dimensional stability to the elevated bone. A longer healing period will determine whether the elevated bone can be maintained over extended periods or after the PCL scaffold has fully degraded. This would require 3–5 years to complete degradation as PCL is a slowly degradable polymer (Lam et al., 2007; Bartnikowski et al., 2019).

Although not directly related to vertical bone augmentation, Goh et al. demonstrated in both an preclinical and a pilot clinical study that a 3D-printed PCL scaffold was capable of providing space maintenance in fresh extraction sockets (Goh et al., 2014; Goh et al., 2015). The study consisted of thirteen randomly selected patients, with seven patients acting as the control group with no space filler, whilst six patients received a PCL scaffold implanted into the tooth socket. The study assessed newly formed bone 6 months post-surgery via removal of a central segment of bone and subsequent micro-CT and histological analysis (prior to stage II surgery). Bone height, particularly at the mesio-buccal aspect, was superior in the patients that had received a polycaprolactone scaffold (Goh et al., 2015). Although both the control and PCL groups underwent bony ridge resorption, the PCL scaffold was able to limit this. This is likely attributed to the ability of the PCL scaffold to retain its geometry over the 6-month period post-surgery. Whilst this is favourable for initial space maintenance, the lack of material resorption may inhibit new bone growth and impede the long-term success of the procedure.

Other approaches have utilized additive manufacturing as a tool for fabricating guided bone regeneration membranes in conjunction with particulate materials for vertical bone augmentation. These are discussed further in the following sections.

Guided Bone Regeneration Using Additively Manufactured Polymeric Membranes

In a series of publications Shim et al. investigated the effect of 3D-printed membranes with small pore size for GBR application (Kim et al., 2014; Shim et al., 2014; Shim et al.,



2015; Shim et al., 2017). Initially, the membrane was composed of a slow degrading polymer (polycaprolactone, PCL) and a more rapidly degrading polymer [poly-lactic-co-glycolic acid, PLGA (85/15)] (Kim et al., 2014; Shim et al., 2014; Shim et al., 2015), whose half-life *in vivo* was around 9 weeks as previously reported for a porous sponge (Lu et al., 2000). Within the field of vertical bone augmentation, membranes can be utilized both as a “barrier” that mitigates against an infiltration of connective tissue and a supporting structure for space

maintenance. Shim et al. explored hybrid polymer-ceramic membrane technology in conjunction with growth factors, thus developing a bioactive membrane targeting vertical bone augmentation in a lapine calvarial defect model. These 3D-printed membranes were manufactured by blending polycaprolactone with poly(lactic-co-glycolic acid and beta tricalcium phosphate (PCL/PLGA/β-TCP) and this polymer blend was subsequently 3D-printed (Shim et al., 2014). The pores of the 3D-printed membrane were filled with a collagen

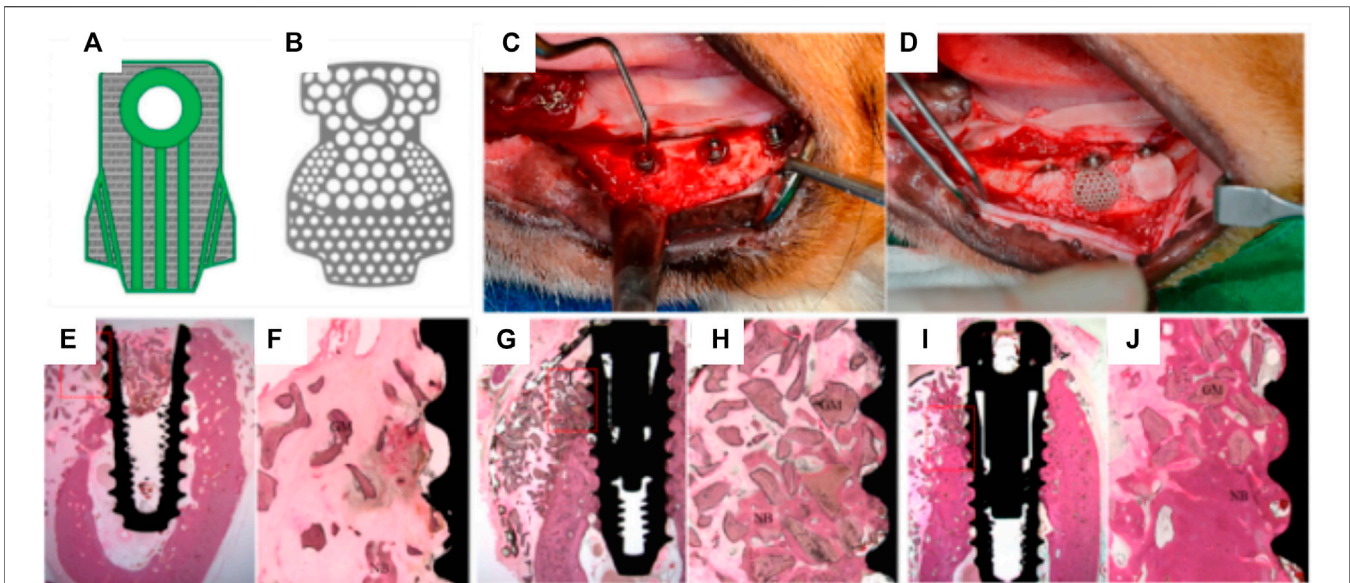


FIGURE 9 | Efficacy of 3D-printed composite GBR membranes for bone formation 8 weeks post-implantation. **(A)**: 3D CAD model design of the PCL/PLGA/β-TCP membrane; **(B)**: Design of pre-formed titanium mesh. **(C,D)**: Surgical protocol showing the placement of dental implant overlayed by the 3D-printed membrane. **(E–J)**: tissue morphology of the various groups **(E,F)**: no membrane, **(G,H)** 3D-printed membrane, **(I,J)**: Titanium membrane. Reproduced with permission from (Shim et al., 2015).

solution containing rhBMP-2. The membrane (10 mm diameter x 0.5 mm height) was then placed over an 8 mm surgically-created calvarial defect, and fixed using titanium screws. This study compared three groups: control, PCL/PLGA/β-TCP, and PCL/PLGA/β-TCP/rhBMP-2. Bone regeneration was assessed at four- and eight-weeks post-implantation, and while the control group did not exhibit any substantial bone formation, both membranes performed well, with significantly more bone formed with the BMP-2 loaded membranes (Shim et al., 2014). Interestingly, the 8-week rhBMP-2 specimens displayed almost full bone fill of the interstitial space demonstrating the effectiveness of integrating rhBMP-2 into polymeric membranes for vertical bone regeneration. Here again, the utilization of polymeric 3D printed composites may be a more advantageous choice for scaffold material due to their flexibility and enhanced handling ability compared to bio-ceramics.

Shim et al. further compared the bone forming capacity of PCL/PLGA/β-TCP membranes with that of a titanium mesh, in a canine mandibular defect model (Shim et al., 2015). Due to its high biocompatibility, mechanical and space maintaining properties, titanium fulfills most of the design criteria of an ideal scaffold for guided bone regeneration, and as such, titanium reinforced meshes are currently used for vertical bone augmentation in the clinical setting. The *in vivo* study involved placement of a dental implant, over which a pre-formed 3D-printed scaffold or titanium membrane was positioned in order to provide space maintenance and contain the particulate bone grafting biomaterials utilized in this procedure. Following an 8-weeks healing period, the degree of bone formation and overall osseointegration was reported as

being comparable between the two experimental groups (Figure 9).

However, signs of resorption were observed in the PCL/PLGA/β-TCP membrane group, likely attributed to the rapid degradation of the PLGA polymer which was the main polymer in the scaffold (the PCL:PLGA:β-TCP membrane ratio was 2:6:2). As anticipated, no material resorption was observed within the titanium mesh, and this is consistent with this structure requiring additional surgery for removal in the clinical setting. Whilst Shim et al. recorded no signs of inflammation at 8 weeks post-implantation (Shim et al., 2015), the rapid degradation of the PLGA leading to a potential burst release of acidic degradation by-products may trigger an unfavorable inflammatory reaction. In addition, PLGA degradation may also reduce the overall mechanical properties of the membrane and consequently undermine its mechanical and space maintenance properties in the longer term.

Shim et al. therefore explored two further refined versions of the polymer membranes (Shim et al., 2017); PCL only and PCL/b-TCP. As with the previous studies, the primary aim was to assess the space-maintaining capacity and overall regenerative properties of the membrane. In line with their previous study, the PCL-only and PCL/b-TCP 3D-printed membranes were implanted over a mandibular defect in a canine model (Figures 10A–D) and compared to a collagen membrane. A standardized defect geometric volume of 175 mm³ was generated in six mandibular locations, in three different animals. The membranes were fastened by titanium pins, with bovine graft particulate placed underneath each membrane and healing occurred over 8 weeks.

Interestingly, and despite the difference in initial pore size between the collagen and the 3D-printed membranes, both

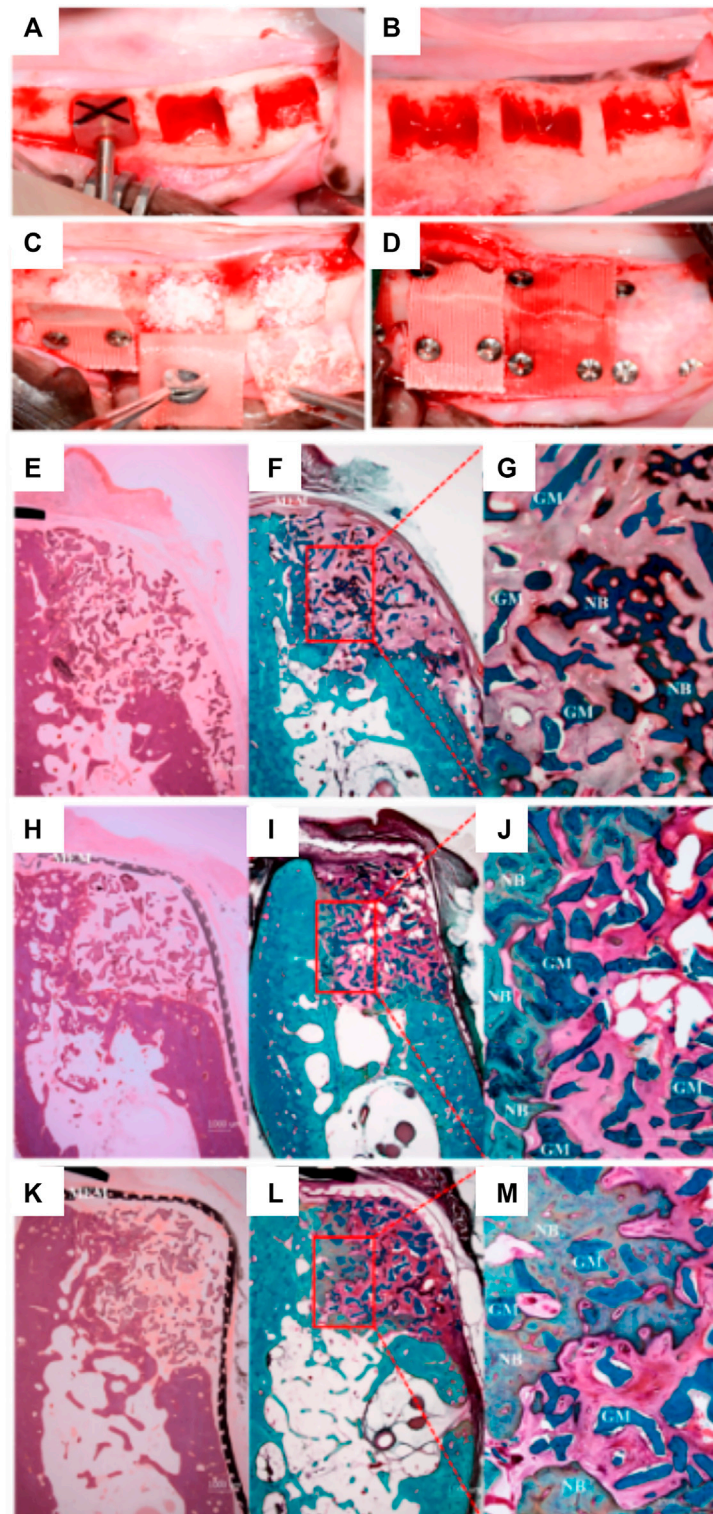


FIGURE 10 | Comparison of PCL and PLC-BTCP 3D-printed membranes to a collagen membrane in a canine mandibular defect. **(A,B)**: Surgical preparation of the site in order to create standardized defects, (length: 7 mm, height: 5 mm, depth: 5 mm) **(C)**: Implantation of the bone grafting particulate materials, **(D)**: placement of the various membranes fixed using titanium screws. Tissue morphology as demonstrated using Hematoxylin and eosin **(E, H, K)** stain and Goldner Trichrome stain **(F,G,I,J,L,M)** for collagen **(E-G)**, PCL **(H-J)**, PCL/b-TCP membrane **(K-M)**. Reproduced with permission from (Shim et al., 2017).

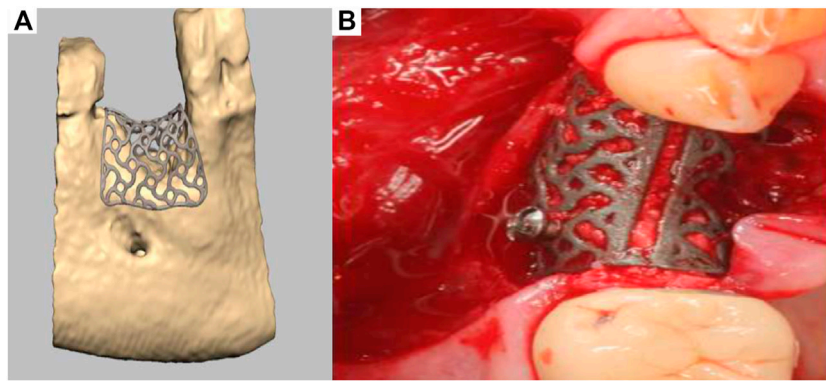


FIGURE 11 | Titanium 3D-printed mesh for vertical bone augmentation. **(A):** numerical model of the titanium mesh, **(B):** clinical placement. Reproduced with permission from (Seiler et al., 2018).

performed similarly, and no significant differences were found between the respective amount of bone formed (**Figures 10E–M**). The main advantages of the PCL or composite 3D-printed membrane is the long-term space maintenance and the enhanced handling ability when compared to a hydrated collagen membrane that loses most of its stiffness and handling ability once in contact with biological fluids. Whilst this was a promising result and effectively demonstrated the efficacy of a partially occlusive polymer/ceramic composite scaffold, the method still relied upon bone particulate grafting for ensuring bone formation and is therefore still prone to handling and stability issues. In addition, the scaffold was utilized for covering a confined defect and therefore not assessed for vertical bone augmentation, which is far more demanding. Indeed, although the handling of these polymeric membranes is enhanced by their flexibility, inadequate distribution of stresses throughout the membrane is problematic and could potentially lead to failure. Further, the shape of the resulting elevated volume is poorly controlled and may not recapitulate the original anatomical features of the jawbone.

ADDITIVELY MANUFACTURED TITANIUM MESHES FOR VERTICAL BONE REGENERATION

A recent development has seen the emergence of a patient-specific 3D-printed titanium mesh for vertical bone augmentation (Seiler et al., 2018). This system, first patented in 2013, utilizes the most recent development of CAD/CAM and metal additive manufacturing technology. This product is designed using CT or CBCT patient data and numerically processed in order to fabricate a mesh that is patient specific and therefore follows the natural contours of the patient using a workflow similar to that previously described (Bartnikowski et al., 2020). Developed by ReOss and distributed by Geistlich, this product called Yxoss CBR enables clinicians to implant patient specific, anatomically accurate titanium cages. The cage

is filled with bone grafting materials such as anorganic bone graft and/or autologous bone particles and provides the necessary space maintenance for extraskeletal bone formation to occur. Interestingly, the medical device can significantly reduce the length of the surgery and can be readily biomechanically fixed using conventional titanium screws. As shown in **Figure 11A**, a numerically created anatomical model of the scaffold is generated for 3D-printed manufacturing, then implanted in conjunction with bone grafting materials (**Figure 11B**). Upon surgical re-entry the titanium cage is removed in order to enable dental implant placement. This technology is already in clinical use, and while it represents a breakthrough for vertical bone regeneration, it is relatively recent and ongoing clinical studies to verify and quantify the efficacy of this approach for vertical bone augmentation are required. Indeed, recent case reports have shown that this approach can yield favourable clinical outcomes (Dellavia et al., 2021), although complications such as transmucosal exposure of the device (Chiapasco et al., 2021) and inaccuracies between planned and created volume and bone height (Li et al., 2021) are common. The exposure of the device is strongly related to the management of the soft tissue healing component of the vertical bone augmentation procedure. In order to mitigate this issue, the utilisation of autologous membrane fabricated from blood may provide a significant advantage as recently reported (Hartmann and Seiler, 2020). Advanced Plasma Rich Fibrin (A-PRF) membrane is obtained from low g centrifugation of blood and proven to increase soft tissue healing (Miron et al., 2017; Miron et al., 2020). As a result, the utilisation of an A-PRF membrane over the titanium patient-specific mesh significantly reduced the frequency of exposure. Therefore, the utilisation of soft tissue healing membranes in conjunction with the Yxoss system may result in better soft tissue outcome but require further investigation. In addition to the exposure of the medical device, a clear limitation of the use of these titanium meshes is the requirement for a second surgical procedure to remove the device. This could be circumvented by the utilisation of biodegradable polymers or degradable metals (Venezuela et al., 2019; Carluccio et al., 2020).

TABLE 1 | Description of the various 3D-printing technologies.

Class	Manufacturing method	Operation	Compatible printing materials
Extrusion	Fused deposition modelling (FDM)	Material is heated until molten and is extruded through a printing head using either pressurized extrusion and screw based extrusion or a combination of both. The extruded material solidifies on contact with the base plate or previous layer, forming a filament commonly called strut.	Thermoplastic polymers, rubber, eutectic metals, clay (modelling and metal) Chua et al. (2010).
	Direct ink writing/robocasting (DIW)	A polymeric ink or a binder is extruded to manufacture scaffolds with a high resolution. Objects manufactured are initially soft and fragile thus accompanying support materials are often printed simultaneously. Drying, de-binding and sintering are required post printing for optimized mechanical characteristics Feilden et al. (2017).	Ceramics, ceramic and metal matrix composites, sol-gel, polymers Xu et al. (2006).
	Continuous filament fabrication (CFF)	Identical fabrication method to FDM but uses a polymeric filament which is locally molten in the printing head. The extrusion is generated by the utilization of rollers on the filament, thereby applying extrusion forces Tekinalp et al. (2014).	Polymer and Carbon based composites, nylon and Kevlar Tekinalp et al. (2014).
Polymerization by light	Continuous liquid interface production (CLIP)	Comprised of a bath with a transparent windowpane containing a photopolymer resin. An ultraviolet beam of light cures the resin layer-by-layer as the object is extruded vertically at a constant slow velocity. A nonpermeable oxygen membrane between the windowpane and resin bath allows the laser process to be continuous Tumbleston et al. (2015).	Photopolymer Tumbleston et al. (2015).
	Stereolithography (SLA)	Comprised of a bath with a transparent windowpane containing a photopolymer resin. An ultraviolet beam of light cures the resin layer-by-layer as the object is extruded vertically at a constant slow velocity. After each layer is cured, a blade component filled with resin is swept across the windowpane, providing new resin required to cure the next layer of printing Lipson et al. (2004).	Photopolymer Lipson et al. (2004).
Powder bed	Powder bed and inkjet head 3D printing (3DP)	An inkjet head deposits a liquid fusing substance which binds particles within the powder bed. Once a single layer has been completed, a new layer of powder is added on top of the completed layer and the process is then repeated iteratively layer-by-layer until the component is completed Shirazi et al. (2015).	Plaster, metallic alloy and ceramic powders Shirazi et al. (2015).
	Electron beam additive manufacturing (EBM)	An electron beam melts metal particles together within a bed of metallic powder inside a vacuumed environment. Once a single layer has been completed, a new layer of powder is added and the process repeated iteratively until a fully dense metallic object is formed Murr et al. (2012).	Metallic alloy powders Murr et al. (2012).
	Selective laser sintering (SLS)	A high-powered pulsating carbon dioxide laser fires onto a bed of powdered material which is preheated to slightly below melting point, subsequently binding the particles together. Like other powder bed technologies, SLS requires a fresh layer of powdered material to cover the completed cross-section iteratively until the 3D object is formed Williams et al. (2005).	Metal and ceramic powders, thermoplastic B. Williams et al. (2005).

CONCLUSION

This review has described the major 3D-printing strategies for achieving extraskeletal bone formation: 3D-powder printing of bio-ceramic, bio-ceramic extrusion 3D-printing, fused deposition modelling using polymer or a mixture of polymer and inorganic filler, and metal 3D-printing. While each strategy is respectively limited by brittleness, the lack of bioactivity, and the requirement of removing non-degradable devices, it is clear that the future of the field lies with the manufacturing of patient specific geometries. The ideal anatomically accurate construct will promote extraskeletal bone formation and provide long-term space maintenance in order to allow for multiple cycles of bone remodelling,

towards preventing bone resorption upon implant placement, thus ensuring implant longevity.

AUTHOR CONTRIBUTIONS

CV and JM drafted the article and SI provided supervision and feedback.

FUNDING

This study has been supported by the Australian Dental Research Foundation (65-2015) and by National Health Medical Research Council project grant schemes (APP1043994 and APP1086181).

REFERENCES

- Asa'ad, F., Pagni, G., Pilipchuk, S. P., Gianni, A. B., Giannobile, W. V., and Rasperini, G. (2016). 3D-Printed Scaffolds and Biomaterials: Review of Alveolar Bone Augmentation and Periodontal Regeneration Applications. *Int. J. Dent.* 2016, 1239842. doi:10.1155/2016/1239842
- Barradas, A., Yuan, H., Yuan, H., van Blitterswijk, C., and Habibovic, P. (2011). Osteoinductive Biomaterials: Current Knowledge of Properties, Experimental Models and Biological Mechanisms. *eCM* 21, 407–429. doi:10.22203/ecm.v021a31
- Bartnikowski, M., Dargaville, T. R., Ivanovski, S., and Hutmacher, D. W. (2019). Degradation Mechanisms of Polycaprolactone in the Context of Chemistry, Geometry and Environment. *Prog. Polym. Sci.* 96, 1–20. doi:10.1016/j.progpolymsci.2019.05.004
- Bartnikowski, M., Vaquette, C., and Ivanovski, S. (2020). Workflow for Highly Porous Resorbable Custom 3D Printed Scaffolds Using Medical Grade Polymer for Large Volume Alveolar Bone Regeneration. *Clin. Oral Implants Res.* 31, 431. doi:10.1111/clr.13579
- Brown, T. D., Dalton, P. D., and Hutmacher, D. W. (2011). Direct Writing by Way of Melt Electrospinning. *Adv. Mater.* 23, 5651–5657. doi:10.1002/adma.201103482
- Brown, T. D., Slotsch, A., Thibaudeau, L., Taubenberger, A., Loessner, D., Vaquette, C., et al. (2012). Design and Fabrication of Tubular Scaffolds via Direct Writing in a Melt Electrospinning Mode. *Biointerphases* 7, 13–16. doi:10.1007/s13758-011-0013-7
- Carluccio, D., Xu, C., Venezuela, J., Cao, Y., Kent, D., Bermingham, M., et al. (2020). Additively Manufactured Iron-Manganese for Biodegradable Porous Load-Bearing Bone Scaffold Applications. *Acta Biomater.* 103, 346–360. doi:10.1016/j.actbio.2019.12.018
- Carrel, J. P., Wiskott, A., Scherrer, S., and Durual, S. (2016). Large Bone Vertical Augmentation Using a Three-Dimensional Printed TCP/HA Bone Graft: A Pilot Study in Dog Mandible. *Clin. Implant Dentistry Relat. Res.* 18, 1183. doi:10.1111/cid.12394
- Carrel, J.-P., Wiskott, A., Moussa, M., Rieder, P., Scherrer, S., and Durual, S. (2016). A 3D Printed TCP/HA Structure as a New Osteoconductive Scaffold for Vertical Bone Augmentation. *Clin. Oral Impl. Res.* 27, 55–62. doi:10.1111/clr.12503
- Chiapasco, M., Casentini, P., Tommasato, G., Dellavia, C., and Del Fabbro, M. (2021). Customized CAD/CAM Titanium Meshes for the Guided Bone Regeneration of Severe Alveolar ridge Defects: Preliminary Results of a Retrospective Clinical Study in Humans. *Clin. Oral Impl. Res.* 32 (4), 498–510. doi:10.1111/clr.13720
- Chua, C. K., Leong, K. F., and Lim, C. S. (2010). *Rapid Prototyping: Principles and Applications*. Singapore, London: World Scientific Publishing Company.
- Cruess, R. L. (1982). "Physiology of Bone Formation, Function, and Destruction," in *The Musculoskeletal System: Embryology, Biochemistry and Physiology*. Editor R. L. Cruess (New York, NY: Churchill Livingstone).
- Dellavia, C., Canciani, E., Pellegrini, G., Tommasato, G., Graziano, D., and Chiapasco, M. (2021). Histological Assessment of Mandibular Bone Tissue after Guided Bone Regeneration with Customized Computer-aided Design/computer-assisted Manufacture Titanium Mesh in Humans: A Cohort Study. *Clin. Implant Dent. Relat. Res.* 23 (4), 600–611. doi:10.1111/cid.13025
- Edmonds, H. M., and Glowacka, H. (2020). The Ontogeny of Maximum Bite Force in Humans. *J. Anat.* 237 (3), 529–542. doi:10.1111/joa.13218
- Esposito, M., Grusovin, M. G., Felice, P., Karatzopoulos, G., Worthington, H. V., and Coulthard, P. (2009). The Efficacy of Horizontal and Vertical Bone Augmentation Procedures for Dental Implants - a Cochrane Systematic Review. *Eur. J. Oral Implantol.* 2 (3), 167–184.
- Feilden, E., Blanca, E. G.-T., Giuliani, F., Saiz, E., and Vandeperre, L. (2016). Robocasting of Structural Ceramic Parts with Hydrogel Inks. *J. Eur. Ceram. Soc.* 36 (10), 2525–2533. doi:10.1016/j.jeurceramsoc.2016.03.001
- Feilden, E., Ferraro, C., Zhang, Q., García-Tuñón, E., D'Elia, E., Giuliani, F., et al. (2017). 3D Printing Bioinspired Ceramic Composites. *Sci. Rep.* 7 (1), 13759. doi:10.1038/s41598-017-14236-9
- Gbureck, U., Hölzel, T., Klammert, U., Würzler, K., Müller, F. A., and Barralet, J. E. (2007). Resorbable Dicalcium Phosphate Bone Substitutes Prepared by 3D Powder Printing. *Adv. Funct. Mater.* 17 (18), 3940–3945. doi:10.1002/adfm.200700019
- Ghayor, C., Bhattacharya, I., and Weber, F. E. (2021). The Optimal Microarchitecture of 3D-Printed β -TCP Bone Substitutes for Vertical Bone Augmentation Differs from that for Osteoconduction. *Mater. Des.* 204, 109650. doi:10.1016/j.matdes.2021.109650
- Goh, B. T., Chanchareonsook, N., Tideman, H., Teoh, S. H., Chow, J. K. F., and Jansen, J. A. (2014). The Use of a Polycaprolactone-Tricalcium Phosphate Scaffold for Bone Regeneration of Tooth Socket Facial wall Defects and Simultaneous Immediate Dental Implant Placement in Macaca Fascicularis. *J. Biomed. Mater. Res.* 102 (5), 1379–1388. doi:10.1002/jbm.a.34817
- Goh, B. T., Teh, L. Y., Tan, D. B. P., Zhang, Z., and Teoh, S. H. (2015). Novel 3D Polycaprolactone Scaffold for ridge Preservation - a Pilot Randomised Controlled Clinical Trial. *Clin. Oral Impl. Res.* 26 (3), 271–277. doi:10.1111/clr.12486
- Hartmann, A., and Seiler, M. (2020). Minimizing Risk of Customized Titanium Mesh Exposures - a Retrospective Analysis. *BMC Oral Health* 20 (1), 36. doi:10.1186/s12903-020-1023-y
- Karageorgiou, V., and Kaplan, D. (2005). Porosity of 3D Biomaterial Scaffolds and Osteogenesis. *Biomaterials* 26 (27), 5474–5491. doi:10.1016/j.biomaterials.2005.02.002
- Khojasteh, A., Behnia, H., Hosseini, F. S., Dehghan, M. M., Abbasnia, P., and Abbas, F. M. (2013). The Effect of PCL-TCP Scaffold Loaded with Mesenchymal Stem Cells on Vertical Bone Augmentation in Dog Mandible: A Preliminary Report. *J. Biomed. Mater. Res.* 101B (5), 848–854. doi:10.1002/jbm.b.32889
- Kim, T. H., Yun, Y. P., Park, Y. E., Lee, S. H., Yong, W., Kundu, J., et al. (2014). *In Vitro* and *In Vivo* Evaluation of Bone Formation Using Solid Freeform Fabrication-Based Bone Morphogenic Protein-2 Releasing PCL/PLGA Scaffolds. *Biomed. Mater.* 9 (2), 025008. doi:10.1088/1748-6041/9/2/025008
- Klammert, U., Gbureck, U., Vorndran, E., Röddiger, J., Meyer-Marcotty, P., and Kübler, A. C. (2010). 3D Powder Printed Calcium Phosphate Implants for Reconstruction of Cranial and Maxillofacial Defects. *J. Craniomaxillofac. Surg.* 38 (8), 565–570. doi:10.1016/j.jcms.2010.01.009
- Lakhdar, Y., Tuck, C., Binner, J., Terry, A., and Goodridge, R. (2021). Additive Manufacturing of Advanced Ceramic Materials. *Prog. Mater. Sci.* 116, 100736. doi:10.1016/j.pmatsci.2020.100736
- Lam, C. X., Teoh, S. H., and Hutmacher, D. W. (2007). Comparison of the Degradation of Polycaprolactone and Polycaprolactone-(β -Tricalcium Phosphate) Scaffolds in Alkaline Medium. *Polym. Int.* 56, 718–728. doi:10.1002/pi.2195
- Langer, R., and Vacanti, J. P. (1993). Tissue Engineering. *Science* 260, 920–926. doi:10.1126/science.8493529
- Li, L., Wang, C., Li, X., Fu, G., Chen, D., and Huang, Y. (2021). Research on the Dimensional Accuracy of Customized Bone Augmentation Combined with 3D -printing Individualized Titanium Mesh: A Retrospective Case Series Study. *Clin. Implant Dent. Relat. Res.* 23 (1), 5–18. doi:10.1111/cid.12966
- Lipson, H., Moon, F. C., Hai, J., and Paventi, C. (2004). 3-D Printing the History of Mechanisms. *J. Mech. Des.* 127 (5), 1029–1033. doi:10.1115/1.1902999
- Lu, L., Peter, S. J., D. Lyman, M., Lai, H.-L., Leite, S. M., Tamada, J. A., et al. (2000). *In Vitro* and *In Vivo* Degradation of Porous Poly(dl-Lactic-Co-Glycolic Acid) Foams. *Biomaterials* 21 (18), 1837–1845. doi:10.1016/s0142-9612(00)00047-8
- Mangano, C., Giuliani, A., De Tullio, I., Raspanti, M., Piattelli, A., and Iezzi, G. (2021). Case Report: Histological and Histomorphometrical Results of a 3-D Printed Biphasic Calcium Phosphate Ceramic 7 Years after Insertion in a Human Maxillary Alveolar Ridge. *Front. Bioeng. Biotechnol.* 9 (232), 614325. doi:10.3389/fbioe.2021.614325
- Meejung, K., and Senyon, C. (2011). BMPs and Their Clinical Potentials. *BMB Rep.* 44 (10), 619–634. doi:10.5483/BMBRep.2011.44.10.619
- Melchels, F., Wiggenshauser, P. S., Warne, D., Barry, M., Ong, F. R., Chong, W. S., et al. (2011). CAD/CAM-assisted Breast Reconstruction. *Biofabrication* 3, 034114. doi:10.1088/1758-5082/3/3/034114
- Melchels, F. P. W., Domingos, M. A. N., Klein, T. J., Malda, J., Bartolo, P. J., and Hutmacher, D. W. (2012). Additive Manufacturing of Tissues and Organs. *Prog. Polym. Sci.* 37 (8), 1079–1104. doi:10.1016/j.progpolymsci.2011.11.007
- Miron, R. J., Fujioka-Kobayashi, M., Bishara, M., Zhang, Y., Hernandez, M., and Choukroun, J. (2017). Platelet-Rich Fibrin and Soft Tissue Wound Healing: A Systematic Review. *Tissue Eng. B: Rev.* 23 (1), 83–99. doi:10.1089/ten.TEB.2016.0233
- Miron, R. J., Moraschini, V., Del Fabbro, M., Piattelli, A., Fujioka-Kobayashi, M., Zhang, Y., et al. (2020). Use of Platelet-Rich Fibrin for the Treatment of Gingival Recessions: a Systematic Review and Meta-Analysis. *Clin. Oral Invest.* 24 (8), 2543–2557. doi:10.1007/s00784-020-03400-7
- Moussa, M., Carrel, J.-P., Scherrer, S., Cattani-Lorente, M., Wiskott, A., and Durual, S. (2015). Medium-term Function of a 3D Printed TCP/HA

- Structure as a New Osteoconductive Scaffold for Vertical Bone Augmentation: A Simulation by BMP-2 Activation. *Materials* 8 (5), 2174–2190. doi:10.3390/ma8052174
- Murr, L. E., Gaytan, S. M., Ramirez, D. A., Martinez, E., Hernandez, J., Amato, K. N., et al. (2012). Metal Fabrication by Additive Manufacturing Using Laser and Electron Beam Melting Technologies. *J. Mater. Sci. Techn.* 28 (1), 1–14. doi:10.1016/s1005-0302(12)60016-4
- Ngo, T. D., Kashani, A., Imbalzano, G., Nguyen, K. T. Q., and Hui, D. (2018). Additive Manufacturing (3D Printing): A Review of Materials, Methods, Applications and Challenges. *Composites B: Eng.* 143, 172–196. doi:10.1016/j.compositesb.2018.02.012
- Nyström, E., Ahlqvist, J., Legrell, P. E., and Kahnberg, K. E. (2002). Bone Graft Remodelling and Implant success Rate in the Treatment of the Severely Resorbed Maxilla: a 5-year Longitudinal Study. *Int. J. Oral Maxillofac. Surg.* 31 (2), 158–164. doi:10.1054/ijom.2001.0197
- Nyström, E., Ahlqvist, J., Gunne, J., and Kahnberg, K.-E. (2004). 10-year Follow-Up of Onlay Bone Grafts and Implants in Severely Resorbed Maxillae. *Int. J. Oral Maxillofac. Surg.* 33 (3), 258–262. doi:10.1006/ijom.2003.0512
- Rasperini, G., Pilipchuk, S. P., Flanagan, C. L., Park, C. H., Pagni, G., Hollister, S. J., et al. (2015). 3D-printed Bioresorbable Scaffold for Periodontal Repair. *J. Dent. Res.* 94 (9 Suppl. 1), 153S–7S. doi:10.1177/0022034515588303
- Seiler, M., Kämmerer, P. W., Peetz, M., and Hartmann, A. G. (2018). Customized Titanium Lattice Structure in Three-Dimensional Alveolar Defect: An Initial Case Letter. *J. Oral Implantol.* 44 (3), 219–224. doi:10.1563/aaid-joi-d-17-00084
- Shim, J. H., Yoon, M. C., Jeong, C. M., Jang, J., Jeong, S. I., Cho, D. W., et al. (2014). Efficacy of rhBMP-2 Loaded PCL/PLGA/ β -TCP Guided Bone Regeneration Membrane Fabricated by 3D Printing Technology for Reconstruction of Calvaria Defects in Rabbit. *Biomed. Mater.* 9 (6), 065006. doi:10.1088/1748-6041/9/6/065006
- Shim, J.-H., Won, J.-Y., Sung, S.-J., Lim, D.-H., Yun, W.-S., Jeon, Y.-C., et al. (2015). Comparative Efficacies of a 3D-Printed PCL/PLGA/ β -TCP Membrane and a Titanium Membrane for Guided Bone Regeneration in Beagle Dogs. *Polymers* 7 (10), 1500. doi:10.3390/polym7101500
- Shim, J.-H., Won, J.-Y., Park, J.-H., Bae, J.-H., Ahn, G., Kim, C.-H., et al. (2017). Effects of 3D-Printed Polycaprolactone/ β -Tricalcium Phosphate Membranes on Guided Bone Regeneration. *Int. J. Mol. Sci.* 18 (5), 899. doi:10.3390/ijms18050899
- Shirazi, S. F. S., Gharehkhani, S., Mehrli, M., Yarmand, H., Metselaar, H. S. C., Adib Kadri, N., et al. (2015). A Review on Powder-Based Additive Manufacturing for Tissue Engineering: Selective Laser Sintering and Inkjet 3D Printing. *Sci. Techn. Adv. Mater.* 16 (3), 033502. doi:10.1088/1468-6996/16/3/033502
- Sudheesh Kumar, P. T., Hashimi, S., Saifzadeh, S., Ivanovski, S., and Vaquette, C. (2018). Additively Manufactured Biphasic Construct Loaded with BMP-2 for Vertical Bone Regeneration: A Pilot Study in Rabbit. *Mater. Sci. Eng. C* 92, 554–564. doi:10.1016/j.msec.2018.06.071
- Tamimi, F. M., Torres, J., Tresguerres, I., Clemente, C., López-Cabarcos, E., and Blanco, L. J. (2006). Bone Augmentation in Rabbit Calvariae: Comparative Study between Bio-Oss and a Novel β -TCP/DCPD Granulate. *J. Clin. Periodontol.* 33 (12), 922–928. doi:10.1111/j.1600-051x.2006.01004.x
- Tamimi, F., Torres, J., Gbureck, U., Lopez-Cabarcos, E., Bassett, D. C., Alkhraisat, M. H., et al. (2009). Craniofacial Vertical Bone Augmentation: a Comparison between 3D Printed Monolithic Monette Blocks and Autologous Onlay Grafts in the Rabbit. *Biomaterials* 30 (31), 6318–6326. doi:10.1016/j.biomaterials.2009.07.049
- Tamimi, F., Torres, J., Al-Abedalla, K., Lopez-Cabarcos, E., Alkhraisat, M. H., Bassett, D. C., et al. (2014). Osseointegration of Dental Implants in 3D-Printed Synthetic Onlay Grafts Customized According to Bone Metabolic Activity in Recipient Site. *Biomaterials* 35 (21), 5436–5445. doi:10.1016/j.biomaterials.2014.03.050
- Teitelbaum, S. L. (2000). Bone Resorption by Osteoclasts. *Science* 289 (5484), 1504–1508. doi:10.1126/science.289.5484.1504
- Tekinalp, H., Kunc, V., Velez-Garcia, G., Duty, C., Love, L., Naskar, A., et al. (2014). Highly Oriented Carbon Fiber-Polymer Composites via Additive Manufacturing. *Composites Sci. Techn.* 105, 144–150. doi:10.1016/j.compscitech.2014.10.009
- Torres, J., Tamimi, F., Alkhraisat, M. H., Prados-Frutos, J. C., Rastikerdar, E., Gbureck, U., et al. (2011). Vertical Bone Augmentation with 3D-Synthetic Monette Blocks in the Rabbit Calvaria. *J. Clin. Periodontol.* 38 (12), 1147–1153. doi:10.1111/j.1600-051x.2011.01787.x
- Tumbleston, J. R., Shirvanyants, D., Ermoshkin, N., Januszewicz, R., Johnson, A. R., Kelly, D., et al. (2015). Continuous Liquid Interface Production of 3D Objects. *Science* 347 (6228), 1349–1352. doi:10.1126/science.aaa2397
- Urban, I. A., Montero, E., Monje, A., and Sanz-Sánchez, I. (2019). Effectiveness of Vertical ridge Augmentation Interventions: A Systematic Review and Meta-Analysis. *J. Clin. Periodontol.* 46 (S21), 319–339. doi:10.1111/jcpe.13061
- Vaquette, C., Mitchell, J., Fernandez-Medina, T., Kumar, S., and Ivanovski, S. (2021). Resorbable Additively Manufactured Scaffold Imparts Dimensional Stability to Extraskelally Regenerated Bone. *Biomaterials* 269, 120671. doi:10.1016/j.biomaterials.2021.120671
- Venezuela, J. J. D., Johnston, S., and Dargusch, M. S. (2019). The Prospects for Biodegradable Zinc in Wound Closure Applications. *Adv. Healthc. Mater.* 8 (16), 1900408. doi:10.1002/adhm.201900408
- Williams, J. M., Adewunmi, A., Schek, R. M., Flanagan, C. L., Krebsbach, P. H., Feinberg, S. E., et al. (2005). Bone Tissue Engineering Using Polycaprolactone Scaffolds Fabricated via Selective Laser Sintering. *Biomaterials* 26 (23), 4817–4827. doi:10.1016/j.biomaterials.2004.11.057
- Xu, M., Gratson, G. M., Duoss, E. B., Shepherd, R. F., and Lewis, J. A. (2006). Biomimetic Silicification of 3D Polyamine-Rich Scaffolds Assembled by Direct Ink Writing. *Soft Matter* 2 (3), 205–209. doi:10.1039/b517278k

Conflict of Interest: The authors declare that the research was conducted in the absence of any commercial or financial relationships that could be construed as a potential conflict of interest.

Publisher's Note: All claims expressed in this article are solely those of the authors and do not necessarily represent those of their affiliated organizations, or those of the publisher, the editors and the reviewers. Any product that may be evaluated in this article, or claim that may be made by its manufacturer, is not guaranteed or endorsed by the publisher.

Copyright © 2022 Vaquette, Mitchell and Ivanovski. This is an open-access article distributed under the terms of the Creative Commons Attribution License (CC BY). The use, distribution or reproduction in other forums is permitted, provided the original author(s) and the copyright owner(s) are credited and that the original publication in this journal is cited, in accordance with accepted academic practice. No use, distribution or reproduction is permitted which does not comply with these terms.



Application of BMP in Bone Tissue Engineering

Liwei Zhu^{1,2}, Yuzhe Liu¹, Ao Wang¹, Zhengqing Zhu¹, Youbin Li¹, Chenyi Zhu¹, Zhenjia Che¹, Tengyue Liu¹, He Liu^{1,2*} and Lanfeng Huang^{1*}

¹Department of Orthopedics, The Second Hospital of Jilin University, Changchun, China, ²Orthopaedic Research Institute of Jilin Province, Changchun, China

OPEN ACCESS

Edited by:

Arnaud Scherberich,
University Hospital of Basel,
Switzerland

Reviewed by:

Janos Kanczler,
University of Southampton,
United Kingdom
Fengxuan Han,
Soochow University, China

*Correspondence:

He Liu
heliu@jlu.edu.cn
Lanfeng Huang
hlf@jlu.edu.cn

Specialty section:

This article was submitted to
Tissue Engineering and Regenerative
Medicine,
a section of the journal
Frontiers in Bioengineering and
Biotechnology

Received: 08 November 2021

Accepted: 01 March 2022

Published: 31 March 2022

Citation:

Zhu L, Liu Y, Wang A, Zhu Z, Li Y,
Zhu C, Che Z, Liu T, Liu H and Huang L
(2022) Application of BMP in Bone
Tissue Engineering.
Front. Bioeng. Biotechnol. 10:810880.
doi: 10.3389/fbioe.2022.810880

At present, bone nonunion and delayed union are still difficult problems in orthopaedics. Since the discovery of bone morphogenetic protein (BMP), it has been widely used in various studies due to its powerful role in promoting osteogenesis and chondrogenesis. Current results show that BMPs can promote healing of bone defects and reduce the occurrence of complications. However, the mechanism of BMP *in vivo* still needs to be explored, and application of BMP alone to a bone defect site cannot achieve good therapeutic effects. It is particularly important to modify implants to carry BMP to achieve slow and sustained release effects by taking advantage of the nature of the implant. This review aims to explain the mechanism of BMP action *in vivo*, its biological function, and how BMP can be applied to orthopaedic implants to effectively stimulate bone healing in the long term. Notably, implantation of a system that allows sustained release of BMP can provide an effective method to treat bone nonunion and delayed bone healing in the clinic.

Keywords: bone morphogenetic protein, BMP, biomaterials, bone tissue engineering, bone healing

1 INTRODUCTION

Bone morphogenetic proteins (BMPs) were originally discovered to promote bone growth in muscle. Since 1965, when Dr. Urist discovered that BMP can induce bone growth in muscle (Urist, 1965), multiple subsequent studies have demonstrated that BMPs function in a large variety of physiological and pathological processes. BMP is an important member of the transforming growth factor-beta (TGF- β) superfamily, a group of highly conserved homologous signalling proteins that play an important role in embryogenesis, organogenesis, cell proliferation, and stem cell differentiation (Miyazawa et al., 2002). Therefore, BMPs have been applied in a plethora of tissues and organs. To date, approximately 20 BMP family members have been identified and characterized. BMP is a dimeric molecule composed of two polypeptide chains linked by a single disulfide bond. According to the structural similarity of BMP amino acid sequences, BMP family members are generally divided into four categories: BMP2/4; BMP5/6/7/8; BMP9/10; and BMP12/13/14 (Liu et al., 1995; Gomez-Puerto et al., 2019).

In orthopaedics, BMPs are naturally secreted multifunctional proteins that play crucial roles throughout the developing skeletal system. BMPs have been proven to be key factors with significant osteogenic functions, regulating bone balance by controlling the differentiation of osteoblasts and osteoclasts (Poynton and Lane, 2002; Lavery et al., 2008). Notably, BMP-2 and BMP-7 can significantly enhance osseointegration (Dent-Acosta et al., 2012; Dolanmaz et al., 2015). Therefore, the Food and Drug Administration (FDA) has approved two factors containing recombinant human BMP (rhBMP)-2 and rhBMP-7 for a few orthopaedic disease treatments, such as open fractures, non-union fractures, vertebral fusion, and maxillofacial bone enhancement (Cecchi et al., 2016).

Fracture is a serious public health problem and is one of the diseases that most affects people's quality of life. It brings a heavy burden to patients and the medical system. Fracture also causes pain and affect a patient's exercise ability. If recovery is improper, it is very likely to reduce life-long mobility. Fracture healing is a very robust repair process that depends on many factors, including fracture type, anatomical site, and associated trauma to soft tissue and vascular structures (Hackl et al., 2017). After the fracture heals, the epiphysis can achieve structural stability, even exceeding the stability of the unfractured bone, and then undergo callus remodelling, restoring the geometry and function of the original bone. Generally, the fracture can be cured after reduction and fixation, but in some cases, severe bone defects or nonunion occur. Generally, most fracture patients will heal within a few weeks to a few months. Although most fracture patients heal quickly after timely treatment, a small number of patients will have delayed fracture union or fracture nonunion, especially patients with larger open bone injuries and non-union (Hissnauer et al., 2017). At this time, the traditional treatment method has little effect. Due to the special nature of fracture healing and fixation, the current standard of treatment for fractures includes reduction and fixation, and the requirements for clinical treatment are as follows: 1) speed up fracture healing, 2) speed up normal function recovery, and 3) reduce fracture healing complications (Goldhahn et al., 2008).

With the rapid development of orthopaedic implants, such as intramedullary nails, steel plates, joint prostheses, pedicle screws and other materials, the incidence of delayed union or nonunion of fractures has been greatly reduced when treating fractures or nonunions, shortening the healing time and reducing fixation-related complications (von Ruden et al., 2016). Notably, some patients still suffer from complications, and traditional treatment methods often cannot guarantee that the fracture will reach the complete clinical cure standard. Although device-assisted therapy is still an important part of fracture treatment, for example, reduction and fixation of the fracture site through intramedullary needles, screws, or metal plates, implants may prolong the fracture healing time and cause infection and chronic pain. Importantly, exploring new treatments for fractures has become the focus of orthopaedic research (Annis et al., 2015).

The FDA has approved rhBMP-2 and rhBMP-7 for orthopaedic treatments, such as open fractures, nonunion fractures, vertebral fusion, and maxillofacial bone enhancement (Cecchi et al., 2016). In recent years, the application of growth factors may bring new breakthroughs in the treatment of fractures. Depending on the morphology of the bone defect, rhBMP-2 and rhBMP-7 can be used in combination with bone substitutes or collagen sponges to achieve better results (Dent-Acosta et al., 2012). Importantly, with the increase in the number of treatments, retrospective studies have provided more data to analyse whether BMP can promote fracture healing. Current research advances indicate that application of biological agents may lead to significant progress in improving treatment effects.

At present, many biomaterials carrying BMP have been used in orthopaedic treatments and have achieved desired results. These implant materials should have good mechanical

properties, excellent biocompatibility, good corrosion resistance, high wear resistance, and osteointegration capability (Han et al., 2014; Chen et al., 2020). Whether implant materials are compatible with surrounding tissues and whether they can promote bone formation is a focus of orthopaedic research (Sul et al., 2002; Geetha et al., 2009). The application of BMPs on scaffolds for clinical treatment of orthopaedic diseases has initially achieved a certain effect. To achieve better therapeutic effects, people have improved biomaterials with high biocompatibility to make their design and manufacturing more perfect, which can continuously and effectively promote bone formation. This research method of bone tissue engineering shall receive more and more attention (Bosemark et al., 2015; Ding et al., 2016; Huang et al., 2018). To date, extensive research has focused on combining new biomaterials and exploring new material synthesis technologies, which can not only improve the success of surgery but also reduce the cost of surgery (Wang L. et al., 2019; Zhang X. et al., 2019). From what has been discussed above, biomaterial-loaded BMPs have become research hotspots and open up new prospects for orthopaedic disease research and treatment.

In this review, we summarize recent research advances in BMP functions in orthopaedics, including biological functions, applications in bone tissue engineering and applications in common clinical diseases.

2 ADVANCED RESEARCH PROGRESS ON THE BIOLOGICAL FUNCTION OF BMPs IN THE FIELD OF ORTHOPAEDICS

Together, the biological functions of BMP regulate the growth and development of organisms through different signalling pathways in cells. BMP signalling is transduced through serine (Ser)/threonine (Thr) protein kinase receptors, namely, type I receptors (BMPRI) and type II receptors (BMPRII) (Liu et al., 1995; Gomez-Puerto et al., 2019). These two receptor types are combined into a functional complex to initiate further signalling pathways (Koenig et al., 1994). The BMP ligand activates BMPRII, and then, BMPRII phosphorylates BMPRI. Activated BMPRI recruits and phosphorylates Smad-dependent and non-Smad-dependent signalling pathways and then transduces signals into the nucleus and controls osteogenic gene expression. On the one hand, activated BMPRI phosphorylates Smad-dependent signalling pathways, including Smad 1, Smad 5, and Smad 8 (Yamamoto et al., 1997; Nishimura et al., 1998; Kaneko et al., 2000; Pera et al., 2004), and then combines with Smad 4 to form a hybrid complex, which is transported to the nucleus and regulates target gene transcription. Smad 6 or 7 negatively regulates Smad signalling by preventing receptor-activated Smad (R-Smad) phosphorylation, inhibits the expression of osteoblast-related genes and blocks the differentiation of osteoblasts. On the other hand, BMP receptors activate non-Smad-dependent signalling pathways, namely, the p38 mitogen-activated protein kinase (MAPK), extracellular signal-regulated kinase (ERK) and c-Jun N-terminal kinase (JNK) signalling pathways (Guicheux et al., 2003). Then, BMP signalling can stimulate the expression of

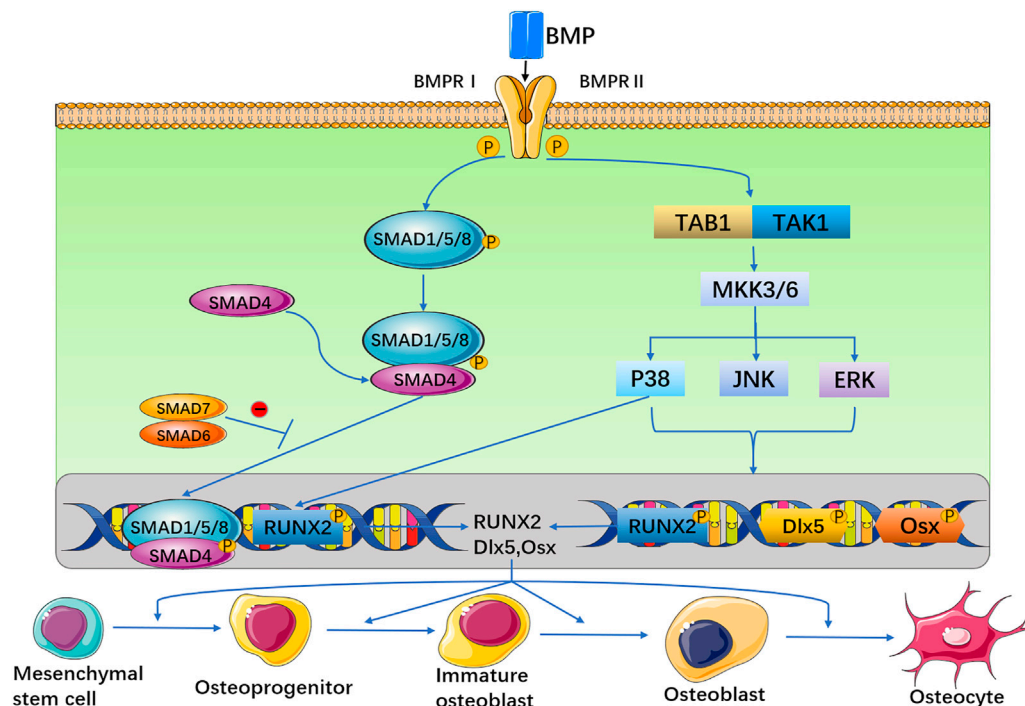


FIGURE 1 | The BMP signal is transduced through BMPRI and BMPRII receptors. These two receptors are combined into a functional complex, to initiate further signaling pathways. On the one hand, activated BMP type I receptor phosphorylates Smad-dependent signaling pathways. On the other hand, BMP receptors activate non-Smad-dependent signaling pathways, that is, activate p38 MAPK, JNK, and ERK signaling pathways. Then, BMP can stimulate the expression of three osteogenic main transcription factors Runx2, Dlx5 and Osx.

the main osteogenic transcription factors runt-related transcription factor 2 (Runx2), distal-less homeobox 5 (Dlx5), and osterix (Osx) (Lee et al., 2003), and Runx2 plays a key role in the induction of osteogenesis (Figure 1) (Celil and Campbell, 2005). In addition, TGF- β , Wnt, Hedgehog, Notch, fibroblast growth factor (FGF), and other signalling pathways also interact with the BMP signalling pathway (Wang N. et al., 2017; Zhang L. et al., 2019). At the cellular level, BMP exists as a ligand of receptors on the membrane of various cells, such as osteoblasts, osteoclasts, adipose stem cells, mesenchymal stem cells, and tendon fibroblasts, through concentration gradient diffusion. When the receptors of these cells are activated, they induce cells to differentiate and proliferate (Rawadi et al., 2003; Wu et al., 2016). Therefore, BMPs play an important role in the growth and development of bones and in homeostasis of the bone environment effect.

2.1 Cartilage Formation

Articular cartilage is often damaged by mechanical wear, inflammation, and external forces. Due to the nonvascular nature of cartilage tissue, once articular cartilage is damaged, its ability to spontaneously heal and regenerate is very weak, which reduces joint motor function. In addition, cartilage formation may also be critical for initial bridging and subsequent stabilization of a fracture and can reduce the occurrence of late complications. Compared to osteogenesis alone, timely stimulation of cartilage in fractured epiphyses

may be a more effective way to prevent delayed bone healing or nonunion of the bone (Shum et al., 2003; Hatakeyama et al., 2004; El-Magd et al., 2013; Kostenuik and Mirza, 2017; Wang T. et al., 2019; Yang et al., 2021). Therefore, cartilage formation plays a crucial role in the skeletal system. Currently, the use of tissue grafts to repair articular cartilage and other connective tissue in the joint has limited therapeutic effects. How to effectively repair and regenerate joints presents great challenges in current research.

Cartilage formation is a multistep process. At the gene level, the expression of osteogenic and cartilage-related genes is dependent on the BMP signalling pathway. Moreover, the BMP signalling pathway can directly regulate the expression of Runx2 (Akiyama et al., 2002). Runx2 is the key gene in the bone marrow mesenchymal stem cell (BMSC) differentiation process, regulating the expression of Osx, sry-related HMG-box (Sox) 9, type II collagen, aggrecan (Acan), and other genes. BMSCs form chondrocytes by maintaining Runx2 expression (Pini et al., 2018). By measuring the expression levels of BMPs in normal human cartilage, BMP-2, BMP-4, BMP-5, BMP-6, BMP-7, and BMP-9 have been found to be highly expressed in cartilage tissue (Suttapreyasri et al., 2006), suggesting that a proper proportion of BMPs may maintain normal homeostasis in normal human cartilage tissue. These BMPs have a precise impact on cartilage formation *in vivo*, but the relationship between the expression of a single BMP type and cartilage formation requires more careful *in vivo* and *in vitro* studies.

TABLE 1 | Functions of BMPs in cartilage formation.

BMP(s)	Related GENE(s)	Biological function(s)	References
BMP-2	Runx2, Sox5, Sox9, Acan, and Col2a1	Increases the expression level of Runx2, Promote chondrogenesis	Wang T. et al. (2019)
BMP-4	Sox9, type II collagen, and type X collagen	Plays a guiding role in cartilage formation. Regulation development of vertebral cartilage, pedicle of vertebral arch and proximal rib	Shum et al. (2003), Hatakeyama et al. (2004), El-Magd et al. (2013)
BMP-5	Type I collagen, type II collagen, and type X collagen	Promote cartilage formation	Guenther et al. (2008), Snelling et al. (2010)
BMP-6	Type II collagen and type X collagen	Affects cartilage development	Ye et al. (2019)
BMP-7	Col1a2, Col2a1, Col10a1, mmp13, Runx2, and Acan	Promote cartilage formation	Muller et al. (2019)
BMP-9	Type II collagen, Sox9, Acan, and ALK-1	Effectively activate Smad pathway, promote chondrocyte differentiation and osteogenic differentiation	Wang et al. (2014), van Caam et al. (2015), Ren et al. (2016)

BMP-2 increases the expression level of Runx2 at the transcriptional and posttranscriptional level by inhibiting the expression of cyclin-dependent kinase 4, ubiquitination of Runx2 and protease degradation (Shu et al., 2011). BMP-2 induces Sox9 expression, which in turn stimulates the expression of cartilage markers, such as collagen type II alpha 1 chain (Col2a1) (Zhao C. et al., 2017). BMP-4 plays a guiding role in cartilage formation. BMP-4 can not only induce mesenchymal cells to differentiate into cartilage but can also induce the expression of nodular interstitial cells, thus promoting the formation and maturation of cartilage nodules (Hatakeyama et al., 2004). BMP-5 can increase the expression of hypertrophy markers, type I collagen, type II collagen, and type X collagen (Guenther et al., 2008; Snelling et al., 2010). In one study, knockout of the BMP-6 gene in chondrocytes leads to a significant decrease in the expression of type II collagen and type X collagen (Ye et al., 2019). BMP-7 can promote the expression of cartilage markers, such as collagen type I alpha 2 chain (Col1a2), Col2a1, collagen type X alpha 1 chain (Col10a1), matrix metalloprotein (mmp) 13, Runx2 and Acan (Yan et al., 2018; Muller et al., 2019). In addition, BMP-9 can increase the expression of type II collagen, Sox 9, Acan and cartilage oligomeric protein in BMSCs (Wang et al., 2014; van Caam et al., 2015; Ren et al., 2016). Because of the overlapping biological functions of different BMPs, some combinations of BMPs may be more effective in cartilage or bone regeneration than a single BMP. **Table 1** lists the functions of BMPs in cartilage formation.

2.2 Bone Formation

There are two forms of bone formation, endomembranous and endochondral. Intramembranous osteogenesis is the differentiation of mesenchymal cells into embryonic connective tissue membranes, and then differentiation into osteoblasts for proliferation and differentiation. The parietal bone, frontal bone and clavicle of the human body occur in this way. Endochondral ossification is first formed from hyaline cartilage to form a cartilage model, which is then replaced by mineralized bone and continues to expand to both ends. Endochondral ossification occurs mainly in long bones, short bones and some irregular bones such as the base of the skull and the back of the skull. Studies have shown that there is no cartilage

tissue at an early time point in bone defect healing. Interestingly, the addition of BMP resulted in the early appearance of chondroid tissue. BMP can promote the proliferation and differentiation of chondrocytes, and can guide endochondral ossification, which plays an important role in the development of endochondral bone (Dang et al., 2017; Daly et al., 2018; Klosterhoff et al., 2022). BMP stimulates the first stage of endochondral ossification, including effective stem cell recruitment and cartilage formation. BMP plays an important role in endochondral bone development and has various functions in bone formation, including bone morphogenesis, growth plate development and osteoblast differentiation (Wu et al., 2016; Long et al., 2021; Strong et al., 2021; Yang et al., 2021). Bone remodelling is a physiological process involving absorption of old bone and formation of new bone. These two physiological processes are influenced by systemic regulation and the local release of growth factors, such as BMPs, in the body. During osteoblastic differentiation, BMSCs are controlled by Runx2 and Osx genes, which are considered to be key genes for osteoblastic differentiation. Among them, Runx2 plays a leading role in the entire differentiation process, while the BMP signalling pathway directly affects the expression of Runx2, therefore, BMPs can more effectively induce osteoblast differentiation and regulate bone formation (Yokouchi et al., 1996; Lieberman et al., 1998; Baltzer et al., 2000; Krishnan et al., 2001; Sojo et al., 2005; Bessa et al., 2008; Seo et al., 2014; Teotia et al., 2017; Pini et al., 2018; Ball et al., 2019; Chen et al., 2019; Long et al., 2021).

rhBMP-2 and rhBMP-7 are orthopaedic surgery-induced osteogenic adjuvants approved by the FDA (Cecchi et al., 2016). BMP-2 is an essential endogenous medium for fracture repair (Peng et al., 2005; Tsuji et al., 2006; Song et al., 2014). It can guide the differentiation of cells into chondrocytes in the periosteum, increase bone deposition and absorption, and plays an important role in the early stage of fracture healing (Yu et al., 2010). Consequently, BMP-2 can significantly promote the formation of mineralized nodules, osteogenic differentiation (Ball et al., 2019; Chen et al., 2019), mineralized bone length increase (Krishnan et al., 2001), bone healing (Sojo et al., 2005; Bessa et al., 2008), and limb development (Zhao C. et al., 2017). During the rapid ossification phase in the body, the mRNA expression of BMP-7 increases sharply and remains at a high level. The ability to induce Smad pathway expression is very

TABLE 2 | Functions of BMPs in bone formation.

BMP(s)	Related GENE(s)	Biological function(s)	Reference(s)
BMP-2	Runx2, Dlx5, osteopontin (OPN), osteocalcin (OCN), and type I collagen	Promote the formation of mineralized nodule and osteogenic differentiation. Bone healing and limb development	Sojo et al. (2005), Bessa et al. (2008), Seo et al. (2014), Teotia et al. (2017), Ball et al. (2019), Chen et al. (2019)
BMP-4	Sox9, Acan, and type II collagen	Activating or promoting the release of other BMPs. Bone development, reconstruction and fracture healing	Fiedler et al. (2002), Jang et al. (2016)
BMP-5	Col2a1 and Sox9	Promote fracture and soft tissue healing	Guenther et al. (2015)
BMP-6	Col1a2, Runx2, and OPN	Significant osteogenic effect. Promote the healing of vertebral defect and segmental defect	Fischerauer et al. (2013); Pelled et al. (2016); Grgurevic et al. (2019); Toprak et al. (2021)
BMP-7	Runx2, ALP, OPN, and OCN	Induces the maturation of osteoblasts, and promotes the healing of fractures	Bosemark et al. (2015), Caterini et al. (2016), Singh et al. (2016), Kim et al. (2018), Yan et al. (2018)
BMP-9	ALP, Runx2, and type I collagen	The strongest ability to induce osteogenic differentiation	Luu et al. (2007), Wang X. et al. (2017), Zhang L. et al. (2019), Zhu et al. (2021)

significant, and it is inferred that BMP-7 may be a powerful promoter of bone development (Bosemark et al., 2015; Yan et al., 2018; Zhang et al., 2018; Li et al., 2019; Zhang L. et al., 2019). In clinical applications, in patients with acute open tibial fractures, rhBMP-2 and rhBMP-7 can promote nonunion healing and shorten the recovery time of patients (Caterini et al., 2016; Singh et al., 2016). The healing effect of BMP treatment is better than conventional treatment. Therefore, rhBMP-2 is a safe and effective method for autologous bone transplantation in the treatment of tibial fractures with large-scale traumatic bone loss (Jones et al., 2006).

In osteogenic cell lines, BMP-2, BMP-4, BMP-7, and BMP-9 effectively induce Smad-mediated signalling pathways. In addition, BMP-2, BMP-4, and BMP-9 induces Runx2 expression, but interestingly, BMP-6 and BMP-7 do not significantly induce Runx2 expression (Zhang L. et al., 2019). In recent years, research progress on BMPs has revealed that BMP-9 has the strongest ability to induce osteogenic differentiation of mesenchymal stem cells (MSCs) (Luu et al., 2007; Zhang L. et al., 2019). BMP-9 can effectively promote expression of the BMP/Smad signalling pathway, increase alkaline phosphatase (ALP) activity, induce the formation of mineralized nodules, and increase expression of osteogenic related genes, thereby promoting bone and joint regeneration (Wang et al., 2014; Chen et al., 2016; Yu et al., 2019). In addition, BMP-9 activates the Wnt/ β -catenin signalling pathway, upregulates the protein level of β -catenin and promotes bone healing (Kusuyama et al., 2019; Wang H. et al., 2019). **Table 2** lists the functions of BMPs in bone formation.

2.3 Tendon/Ligament Healing

The human body needs not only the support of bones and articular cartilage but also a large number of muscles and ligaments to coordinate and pull the bones to complete various actions during daily activities. Therefore, tendons and ligaments are also important research directions in orthopaedics. However, since tendon and ligament cells are nonrenewable, only scar tissue can form, which will affect daily function. Therefore, how to fully restore tendons and ligaments is also a focus in the field of orthopaedics. In addition to cartilage formation and osteogenesis, BMPs also promote the differentiation and growth of tendons and ligaments, mainly BMP-12, BMP-13,

BMP-14, and BMP-15 (Fu et al., 2003; Chuen et al., 2004; Wang et al., 2005; Haddad-Weber et al., 2010; Henn et al., 2010; Wang et al., 2018; Zhang L. et al., 2019).

BMPs have different transcriptional regulation effects on the important mediators of BMP signal transduction in BMSCs, and the most effective upregulators of tendon related gene are BMP-11, BMP-12, BMP-13, BMP-14 and BMP-15 (Zhang L. et al., 2019). Through morphological observation and molecular biological detection, MSCs have been found to be induced to differentiate into tendon cells by BMP-12 gene transfection, leading to type I collagen mRNA and protein expression but not type III collagen mRNA and protein expression (Wang et al., 2005). Cells transfected with BMP-12 were transplanted into rat tendon defects, and the results showed that type I/III collagen, scleraxis (SCX) and tenascin-C were all upregulated (Xu et al., 2018). Adenovirus-mediated implantation of BMP-13 into the supraspinatus tendon of rats revealed that BMP-13 upregulates the expression of type III collagen and fibronectin and increases biomechanical properties (Lamplot et al., 2014). Wang et al. (2018) studied the effect of BMP-14 on BMSC differentiation *in vitro*. BMP-14 upregulated sirtuin 1 (Sirt 1) expression at the mRNA and protein level, activated the JNK and Smad pathways, and significantly increased tendon markers, such as sclerotic and tonic regulatory proteins. BMP-12 and BMP-13 were expressed in MSCs and anterior cruciate ligament (ACL) fibroblasts via an adenoviral vector, and after 21 days of culture in a type I collagen hydrogel, both the MSCs and ACL fibroblasts differentiated into ligament cells (Haddad-Weber et al., 2010). Thus, combined application of BMPs also plays an important role in tendon and ligament healing. **Table 3** lists the functions of BMPs in tendon/ligament healing.

2.4 Blood Vessel Formation

Angiogenesis is considered to be an essential key step in the process of bone regeneration because bone is highly vascularized. In the process of bone repair, newly formed blood vessels are very important for nutrition supply, macromolecular transport, cell aggregation and maintenance of the proper metabolic microenvironment. Since a defect site requires not only the continuous differentiation of MSCs but also blood vessels to provide nutrients, promotion of angiogenesis and sustained release of BMP are particularly important for promoting bone

TABLE 3 | Functions of BMPs in tendon/ligament healing.

BMP(s)	Related GENE(s)	Function(s)	References
BMP-12	Type I collagen and SCX	Induced MSCs to differentiate into tendon cells	Wang et al. (2005)
BMP-12	Type I/III collagen, tenascin-C, and SCX	Promoted window defect regeneration	Xu et al. (2018)
BMP-13	Type III collagen, fibronectin	Improve rotator cuff tendon healing and reduce the incidence of rotator cuff	Lamplot et al. (2014)
BMP-14	Sclerotic and sirtuin1	Activate JNK and Smad pathways, induce the tendon differentiation of BMSCs	Wang et al. (2018)

formation (Kempen et al., 2009). At present, vascular endothelial growth factor (VEGF) is considered to be one of the key regulators in angiogenesis (Peng et al., 2002). VEGF regulates the proliferation, vascularization and ossification of stem cells (Duan et al., 2016; Liu et al., 2020). In normal bone healing, vascular tissue development precedes bone formation. VEGF first stimulates angiogenesis, and BMP then promotes bone formation. Vascular tissue formation and bone formation are interdependent. BMP and VEGF have a regulatory coupling effect between osteogenesis and angiogenesis (Bouletreau et al., 2002; Barati et al., 2016; Zhong et al., 2016). The dual release of growth factors can promote the process of bone regeneration more effectively than either factor alone. Studies have shown that topical application of VEGF can promote bone repair in nonunion models, especially in the early stage of fracture healing (Percival and Richtsmeier, 2013; Li et al., 2021a; Li A. et al., 2021). Therefore, in order to promote bone regeneration more effectively, rapid early release of VEGF and sustained slow release of BMP-2 should be achieved, which is consistent with the law of bone growth and angiogenesis may be critical for bone tissue regeneration. VEGF and BMP-2 act together to significantly enhance osteogenesis and angiogenic differentiation (Barati et al., 2016). In the process of normal bone healing, high expression of VEGF occurs in the early stage, and high expression of BMPs occurs in the later stage. VEGF indirectly promotes bone formation by regulating formation of the vascular network. In addition, this interaction between BMP and VEGF has been confirmed in bone regeneration studies. By enhancing BMP- expression at the fracture site, the osteogenesis of osteoblasts can be directly stimulated, and the angiogenesis of endothelial cells can be promoted (Bouletreau et al., 2002; Kim et al., 2018).

2.5 BMP Derived Peptide

In general, BMP has some disadvantages such as high cost, ectopic bone formation, chemical instability, and immune response problems. BMP derived peptide has the advantages of small molecular weight, good chemical stability, flexible application and low economic cost, so it has higher application safety and biological effect (Beauvais et al., 2016; Li A. et al., 2021; Meng et al., 2021). BMP derived peptide can also activate osteogenic differentiation pathway and promote osteoblast differentiation, thus inducing differentiation and osteogenesis (Caron et al., 2021; Chao et al., 2021).

2.6 BMPs With Other Active Substances

Various biologically active substances and drug interventions have shown potential to promote fracture healing (Einhorn

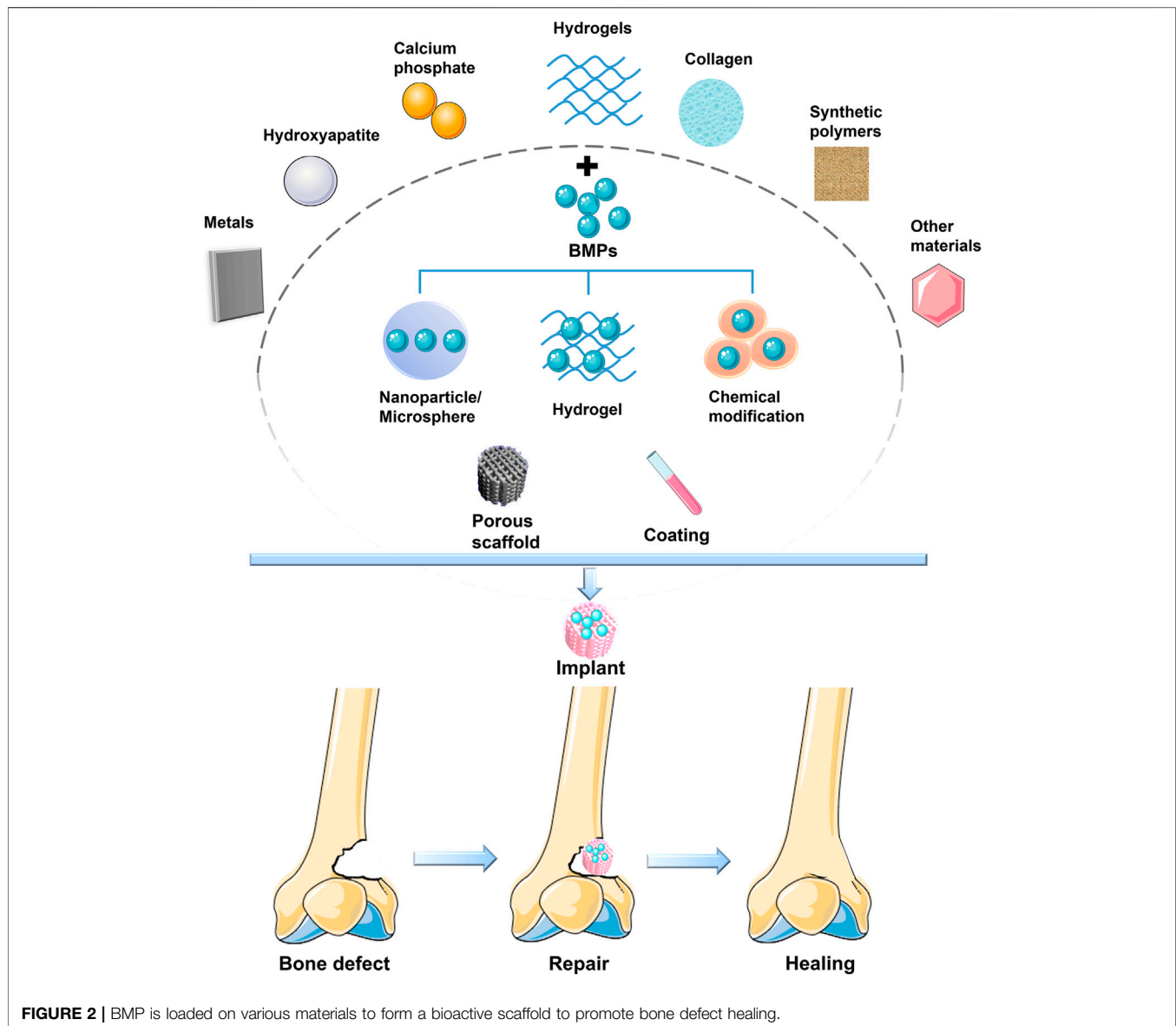
and Gerstenfeld, 2015). Bone healing relies not only on a single growth factor but also on the joint role of many biological components, such as dexamethasone (Dex), vitamin C, vitamin D, BMPs, TGF- β , VEGF, FGF, and insulin. At present, Dex is typically added to *in vitro* osteogenesis induction media. This is because Dex has a synergistic effect with BMP-2; when MSCs were cultured in basic medium supplemented with both BMP and Dex, osteoblast ALP activity was significantly increased, and osteoblast mRNA levels were increased (Rickard et al., 1994). Research shows that, the combination of BMP and FGF significantly enhanced osteogenesis than growth factor alone (Gromolak et al., 2020; Hu et al., 2021). Bmp-2 may stimulate extramedullary bone regeneration, and FGF-2 may stimulate extramedullary bone regeneration (Noshio et al., 2020). The combined use of BMP-2 and TGF-1 or TGF-3 showed stronger chondrogenic activity than BMP-2 alone (Yu et al., 2010; Sang et al., 2014). Early release of TGF-1 induces chondrogenesis, and BMP-2 promotes bone remodeling in a sustained release. TGF- β 1 and BMP-2 showed good biocompatibility and bone formation ability in bone defects, which enhanced the chondrogenic ability of bone marrow mesenchymal stem cells (Dang et al., 2017; Li et al., 2021b). The combination of TGF- β 3 and BMP-6 promoted chondrogenic differentiation of BMSCs in a synergistic manner (Taghavi et al., 2020).

3 APPLICATIONS OF BMPS IN BONE TISSUE ENGINEERING

BMPs have been shown to have strong cartilaginous, osteogenic and tendinous activity (Wang et al., 2005; Wang et al., 2018; Ball et al., 2019; Chen et al., 2019; Wang T. et al., 2019), and their applications in bone tissue engineering are promising. At present, most materials have poor retention of BMPs, leading to rapid clearance of BMPs from the site of implantation and thus to loss of the role of continuous stimulation of osteogenic differentiation of stem cells. BMPs can be slowly released in the body in several ways. The approach is to load BMPs into artificial implants, such as porous scaffolds, scaffold coatings or collagen combined with scaffolds (Figure 2) (Bouyer et al., 2016).

3.1 BMPs Combined With Scaffolds

In orthopaedic surgery, implants play a crucial role in the success of the operation, especially in bone defects that exceed a critical size and require matrix as a scaffold to guide bone regeneration. Therefore, the scaffold structure is of great significance for bone regeneration. Scaffolds are defined as special structures that allow



cells to interact with the extracellular matrix and provide mechanical support for growing cells and tissues (Li et al., 2006; Ding et al., 2016; Wu S. et al., 2018). In the field of orthopaedics, the main role of the scaffold is bone conduction, and the scaffold combines with different types of cells and adjacent tissues to promote new bone formation (Kayabasi et al., 2013; Quade et al., 2020). Moreover, scaffolds can also be used as carriers for active molecules, such as cells and drugs, in the bone regeneration process to achieve better bone healing effects and good antibacterial properties (Ren et al., 2016; Huang et al., 2018).

3.1.1 Loading and Releasing BMPs From Scaffolds

In the process of repairing bone defects, the addition of BMPs can play a significant role in promoting healing of bone defects. Although the osteogenic activity of growth factors is significant,

most orthopaedic diseases require artificial implants to assist bone healing. The quality and quantity of bone formation at the defect site depend on the dose of BMPs (Teng et al., 2019). However, a large amount of BMPs released in a short period of time not only fails to effectively promote bone formation but may also cause side effects, such as heterotopic ossification and inhibition of bone formation. Thus, slow and continuous release of BMPs at the site of implantation has an important effect on bone regeneration (Barati et al., 2016; Seo et al., 2017). At present, artificial orthopaedic implants play a stable structural role at the defect site, while the role of slow and continuous release of bioactive substances needs to be further explored. To solve the problem of BMP release, it is very important to construct a sustained BMP release system using artificial implants. Therefore, the promotion of osteogenesis by BMPs loaded in various new materials has become a research hot spot (Tao et al., 2019; Chen et al., 2020).

3.1.2 Connecting the Bone Defect Site and Promoting Bone Formation

The success of orthopaedic surgery depends on the degree of bonding between the implant and the surrounding bone. The higher the degree of osseointegration is, the higher the mechanical stability and the lower the possibility of loosening. Artificial implants can be implanted into the bone defect, connect the bone defect and combine with the surrounding bone tissue to achieve a stable mechanical structure and effectively stimulate bone formation (Rihn et al., 2009; Nam et al., 2017). However, implants have the problem of poor biocompatibility. If the implant is not specially treated, it will not combine well with the tissue in the human body, and it may cause bone nonhealing or bacterial infection, which ultimately leads to treatment failure. Modification of the implant through chemical or physical methods improves biocompatibility and helps the bone injury heal faster. In addition, bioactive molecules (such as BMPs) and drug delivery systems can be added to implants to further improve bone conductivity and antibacterial properties to promote bone healing (Liu et al., 2007; Han et al., 2014).

3.1.3 Supporting the Growth of New Blood Vessels

The osteogenic induction ability of implants also depends on their ability to induce new blood vessel formation. The necessary conditions for the survival of cells and tissues growing in scaffolds are supplied by blood vessels. The injury site is induced to form a complex vascular network in the scaffold, which can provide abundant bone progenitor cells at the bone defect site, stimulate the migration and differentiation of osteoblasts, lead to increased bone deposition, and thus promote bone healing (Kempen et al., 2009; Kim et al., 2018).

3.2 Loading Strategies of BMPs

In composite scaffold systems, bioactive proteins are usually adsorbed to the surface of porous material or encased in pores (Injamuri et al., 2020). As a biologically active substance, BMP may be inactivated or released suddenly during the process of loading into the composite scaffold. In addition, after loading BMP on the surface of the scaffold, the interaction between the BMP and the surface of the biological material may be destroyed due to the interaction between the material and the organism. These factors may cause BMP to fail to achieve the desired sustained release effect in many composite scaffolds (Rajabnejadkeleshteri et al., 2021). Therefore, the current research should focus on the development of stable composite scaffolds to achieve stable release of BMP.

3.2.1 Nanoparticle/Microsphere

Microspheres/nanoparticles can be directly used as carriers to deliver growth factors to bone defects. Growth factors were encapsulated in an intermediate delivery tool consisting of microspheres to provide a protective barrier that would not affect their biological activity during scaffold fabrication. In addition, the slow-release ability of microspheres enables BMP to be released stably and sustainably at the target site, which can effectively promote bone tissue repair. At present, microspheres

are mainly divided into natural polymer microspheres and synthetic polymer microspheres. The microspheres are wrapped with BMP through microcapsules, processed into composite scaffolds, and implanted into bone defects to achieve the purpose of continuous induction of bone regeneration (Bai et al., 2020; Injamuri et al., 2020; Kong et al., 2020; Koons et al., 2021; Rajabnejadkeleshteri et al., 2021).

3.2.2 Hydrogel

Hydrogels have been widely studied for BMP delivery due to their injectable, easy chemical modification, degradability, and permeability of macromolecules. While the hydrogel continues to degrade, BMP will also be continuously released. At the same time, because the hydrogel has better permeability, tissues and cells can also better absorb the BMP in the hydrogel (Larochette et al., 2020; Datta et al., 2021; Lee et al., 2021). The clinically approved delivery method of BMP is usually adsorbed on a collagen sponge and then implanted into the bone defect. Therefore, in orthopaedic applications, the hydrogel can be filled alone, used as a coating for implants, or used to fill porous materials to provide a greater degree of coverage in the gap between the implant and the bone, so as to better stimulate bone growth.

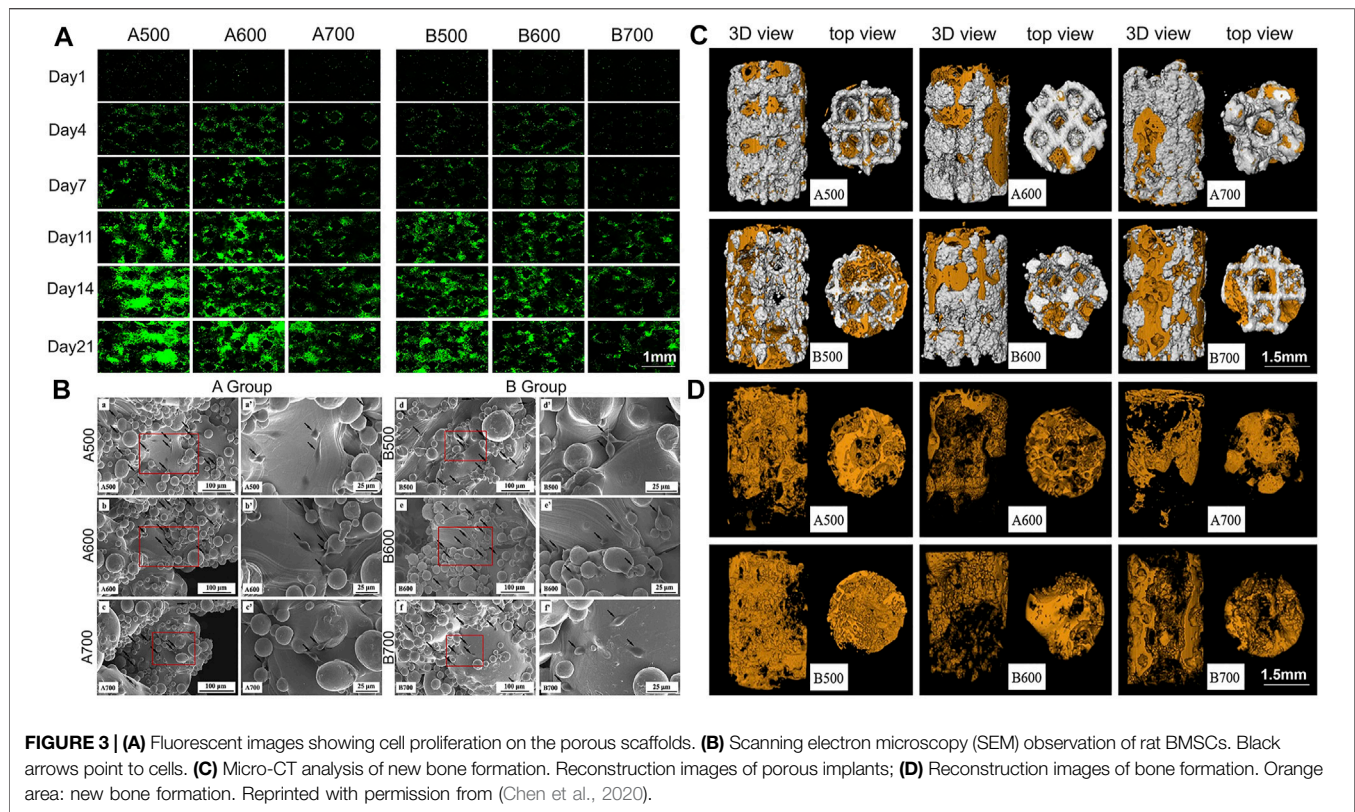
3.2.3 Chemical Modification

Due to the biological activity characteristics of BMP, it can form a more stable combination of some chemical substances through chemical bonds, thus forming a bioactive delivery system. Heparin, a natural glycosaminoglycan, is a molecule that composes the extracellular matrix (ECM), which participates in the binding and isolation of growth factors in the cell microenvironment. Heparin has a strong affinity for BMP and has the benefit of enhancing the biological activity of BMP. Heparin-binding peptides are used in drug delivery systems and show better BMP binding and controlled delivery *in vivo*. Such as heparin methacrylamide microparticles (HMPs), HMPs can be incorporated into the hydrogel to adjust the rate of release of BMP-2 from the scaffold (Hettiaratchi et al., 2020; Subbiah et al., 2020). Current research shows that compared with collagen sponges, HMPs drug delivery system has significantly increased bone formation, reduced heterotopic ossification, and regular bone formation (Vantucci et al., 2021). The heparin delivery system provides a better choice for improving the clinical use of BMP-carrying methods.

3.3 Structural Characteristics of BMP-Loaded Scaffolds

3.3.1 Porous Structure

Biomaterial scaffolds with well-connected porous structures play an important role in bone tissue engineering. The porous structure is conducive to the adhesion, proliferation and differentiation of mesenchymal stem cells, allowing the cells to interact with the extracellular matrix to provide mechanical support for growing cells and tissues (Ding et al., 2016; Li et al., 2018; Wu S. et al., 2018). On the one hand, the presence of a porous structure allows cells to quickly diffuse into the



scaffold; on the other hand, it provides a higher interface bonding area for vascularization and bone growth, which can better promote immobilization of implants and bones. More importantly, the scaffold should have interconnected pores and high porosity so that the infiltration and proliferation of cells, the growth of blood vessels, the diffusion of nutrients and the elimination of waste will achieve better results. By adjusting the pore size and porosity, an implant with the best density, strength and mechanical compatibility can be obtained, which can effectively prevent bone necrosis and bone deformity around the implant and effectively improve the success rate of orthopaedic surgery (Figure 3) (Kayabasi et al., 2013; Han et al., 2014; Nam et al., 2017; Teng et al., 2019; Zhang X. et al., 2019; Chen et al., 2020; Quade et al., 2020; Zhu et al., 2021).

3.3.2 Coating

Coating the surface of an implant reduces the gap around the implant, avoids direct contact between the implant and bone and reduces osteolysis caused by implant movement and wear at the implant site, thereby increasing opportunities for stable interface formation (Kayabasi et al., 2013; Ishack et al., 2017; Behrendt et al., 2020). Moreover, coatings can be loaded with BMPs to control their slow and long-term release to reduce the side effects of short-term overrelease of BMPs and enhance the fusion of implant bone with the surrounding bone. Therefore, a stable coating can greatly increase the success rate of implantation and osseointegration (Kayabasi et al., 2013; Shen et al., 2016; Wu S. et al., 2018; Zhu et al., 2021). At present, coating technology is developing rapidly, such as dip coating, bionic coating, sol-gel,

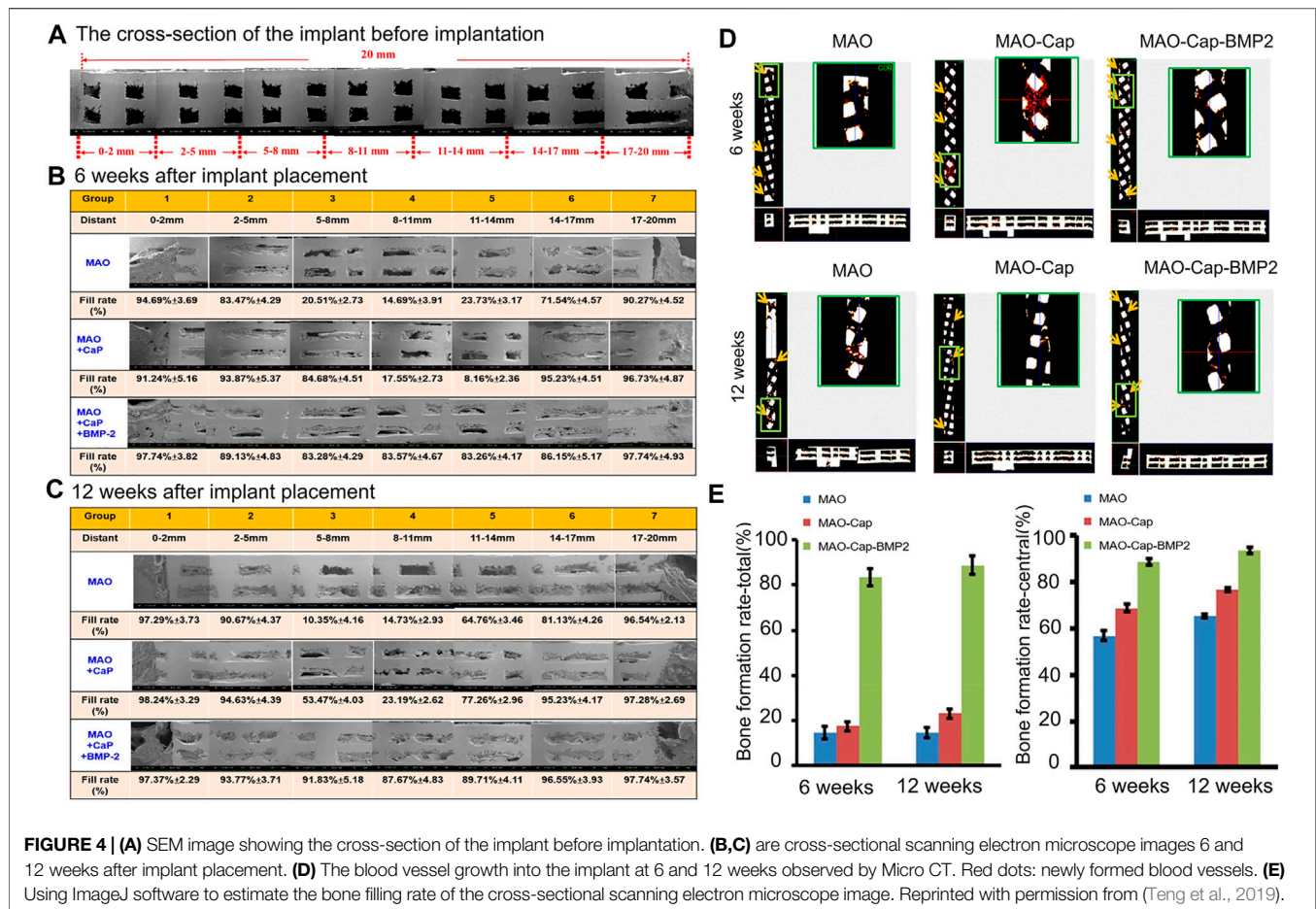
electrophoretic deposition, vapour deposition, laser processing, ion spraying and 3D printing (Teng et al., 2019; Li et al., 2021a; Koons et al., 2021).

Incorporation of BMPs into a bionic coating allows high pharmacodynamic activity at a low pharmacological level and maintenance of this activity for a long period of time. Improved implants with coatings have good bone induction and bone conduction ability, which can not only promote cell adhesion and proliferation but also effectively promote osteogenic differentiation and improve biological activity (Wu J. et al., 2018; Teng et al., 2019). The maintenance of this osteogenic activity has important clinical significance for the osseointegration of the implant (Liu et al., 2005).

3.4 Loading of BMPs in Different Biomaterials

3.4.1 Metals Based Composite Scaffolding System

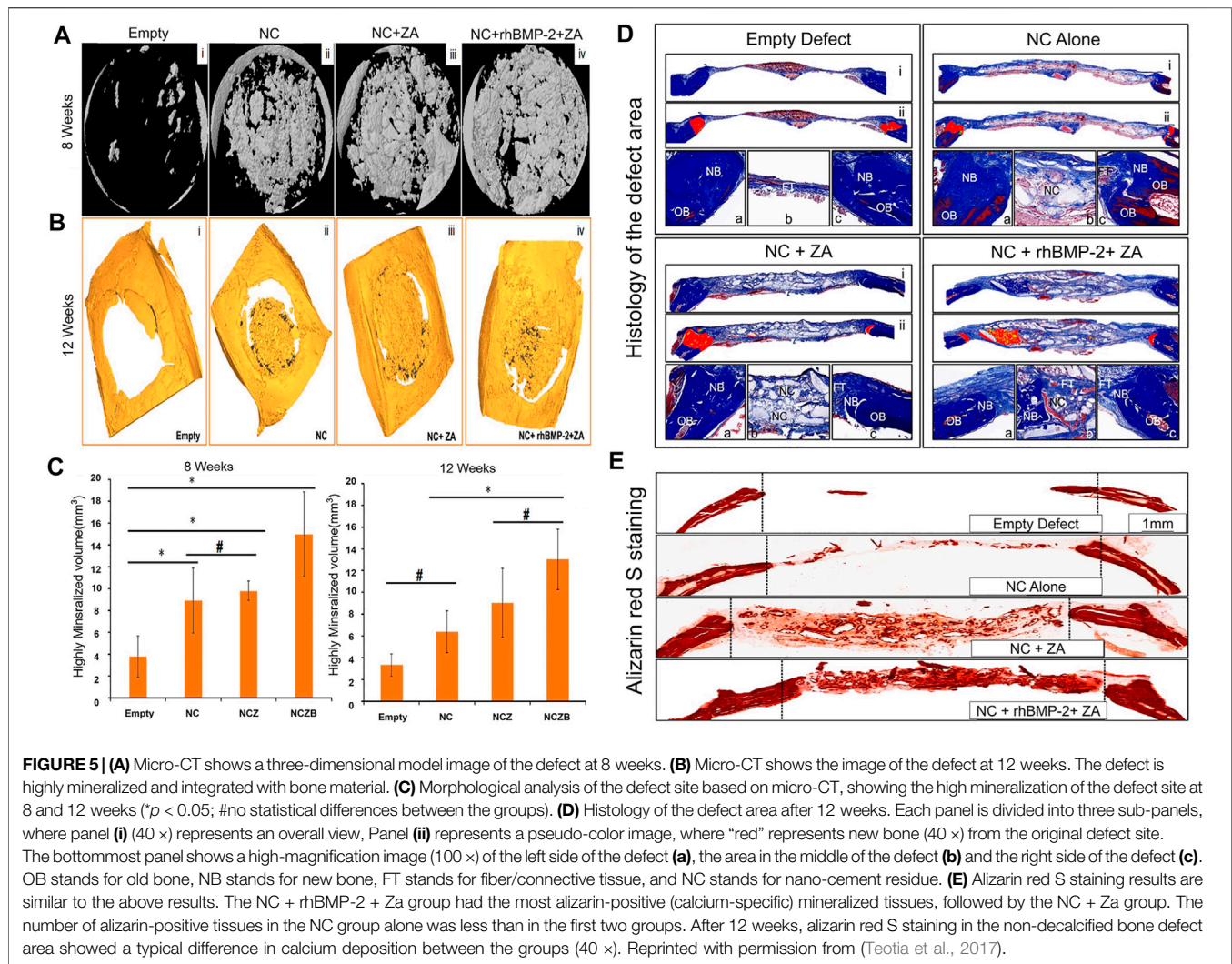
Among implant metal materials, titanium alloys are the most widely used orthopaedic implant materials due to their outstanding characteristics, such as high strength, high corrosion resistance, and biological inertness. However, due to the naturally inert nature of titanium alloys, they do not have sufficient biological activity and cannot be well combined with bone tissue; thus, there may be a gap between the bone and the implant, leading to unstable healing and resulting in failure of bone healing (Sul et al., 2002; Geetha et al., 2009; Li et al., 2021a). The porous structure of titanium alloy is constructed by 3D printing and other technologies, and surface modification of



titanium alloy is carried out using various methods, such as electrodeposition, so that biologically active molecules (such as BMP) can be loaded on the surface coating of titanium alloy to achieve slow and continuous release. Therefore, bone formation at the bone defect site is continuously stimulated, the degree of bonding between the implant and the bone interface is enhanced, and the bone healing interface is more stable (Tao et al., 2019; Teng et al., 2019; Chen et al., 2020; Zhu et al., 2021).

Titanium alloys can be optimized not only by surface modification but also by other processing techniques, including a variety of materials, porous structures, nanotechnology applications, and 3D printing technology applications. Ti6Al4V is the most widely used titanium alloy material (Chen et al., 2020). Current research shows that the pores of titanium alloy scaffolds are 400–600 μm , and the porosity is 60–80%, which can promote cell proliferation, osteogenic differentiation and bone growth and can improve the degree of bone-scaffold binding (Han et al., 2014; Taniguchi et al., 2016; Zhang T. et al., 2020). In addition, surface modification of titanium alloy can achieve faster osseointegration of bone and implants in the early stage and can achieve certain antibacterial ability to facilitate stable chemical bonds between implants and bone tissue. Increasing research has been carried out on the surface modification of titanium alloys. Through various physical

and chemical methods, materials with good biocompatibility can be stably combined on the implant surface, such as hydrogels, polymers, hydroxyapatite, calcium phosphate, and bisphosphonate (Nie and Wang, 2007; Hu et al., 2012; Han et al., 2014). Basic fibroblast growth factor (bFGF) and BMP-2 incorporated in a polydopamine (PDA) coating on a titanium surface led to an obvious improvement in surface hydrophilicity, efficient growth factor adsorption and moderate sustained release of the modified titanium matrix (Wu et al., 2020). In one study, BMP-2, calcium, and phosphorus (Ca/P) coatings were codeposited with 3D-printed porous titanium alloy implants and treated via microarc oxidation (MAO), achieving continuous release of BMP-2 over a period of 35 days. The continuous release of BMP-2 effectively improved ALP activity and *in vitro* mineralization and promoted new bone formation *in vivo*. The BMP-2 and Ca/P coating on titanium alloy produced better osseointegration and further promoted bone formation compared with pure titanium alloy or Ca/P-coated titanium alloy (Figure 4) (Teng et al., 2019). Titanium dioxide (TiO₂) nanotubes are also one of the more widely used materials. The advantage of this material is that it is receptive to loading of drugs and growth factors. Titanium dioxide was used as a carrier of BMP-2, sodium alginate, gentamicin and chitosan (CHI), and this modification improved the biocompatibility and enhanced the



antibacterial ability and bone formation ability of the composite (Tao et al., 2019).

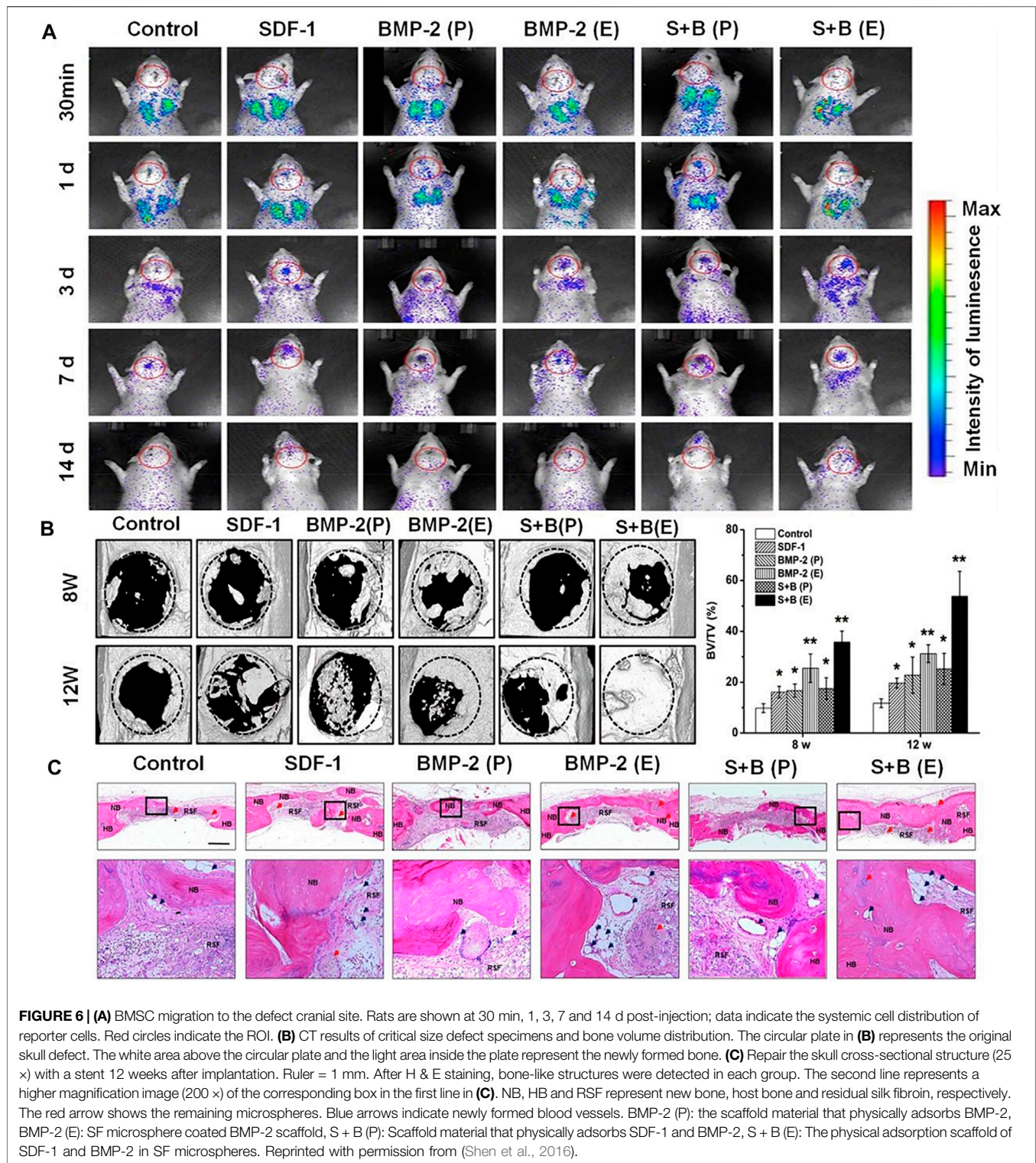
Modified titanium alloy is more suitable for implantation in multiple parts of the body, has better biocompatibility with the human body, promotes bone healing and angiogenesis, reduces the bone healing failure rate, and plays a role in healing of bone defects caused by trauma.

3.4.2 Inorganic Salts Based Composite Scaffolding System

Hydroxyapatite (HA) is the main inorganic component of human and animal bones. HA stimulates or induces bone proliferation, which can promote defective bone tissue repair. Therefore, it has excellent biocompatibility and is applied in bone tissue engineering. HA is widely used and has a good clinical effect (Kim et al., 2006; Ko et al., 2013; Bosemark et al., 2015; Wu S. et al., 2018; Li A. et al., 2021). The combined application of HA, autologous BMSCs, BMPs and autologous bone grafting (ABG) has been proven to be safe, with good stability and bone regeneration characteristics, and can be an option for

treatment of severe bone defects (Teotia et al., 2017; Dilogo et al., 2019). HA can not only be used directly as a scaffold for bone defects but can also be mixed with other materials to form a composite scaffold or fixed to an implant surface, such as a titanium alloy implant, *via* coating (Nie and Wang, 2007; Ding et al., 2016). In addition, a nanohydroxyapatite (NHA) coating has a strong adsorption capacity and can be used as a suitable coating for BMP, providing a rich active site for cell attachment, which is more conducive to stable combination of the bone and the implant (Shen et al., 2016; Deng et al., 2017; Wu S. et al., 2018; Li A. et al., 2021). NHA and calcium sulfate bone substitute (NC) were used as carriers of rhBMP-2 and zoledronic acid (Za) to repair skull defects in rats, and the results showed that it could significantly promote bone regeneration (Figure 5) (Teotia et al., 2017).

Calcium phosphate can improve the bioactivity, bioabsorbability, bone conductivity and osteoinductivity of bioceramics. Biphasic calcium phosphate (BCP) and tricalcium phosphate (TCP) have become research hotspots in the field of bioceramics. BCP and TCP scaffolds have a high degree of



biocompatibility and can support the attachment, proliferation and differentiation of osteoblasts, thereby promoting the formation of bone tissues. Thus, increasing research has been conducted on these materials (Bosemark et al., 2015; Ishack et al., 2017; Quade et al., 2020; Chao et al., 2021). Although calcium

phosphate shows a chemical composition similar to that of inorganic bone, its osteogenic performance is restricted by its low degradation rate and poor bone induction. Therefore, it is necessary to modify the material to obtain a better performance. Mixing of calcium phosphate and HA to make a scaffold has

received increasing attention. However, the delayed or rapid biodegradation rate of HA may interfere with the rate of new bone formation. The main advantage of calcium phosphate is that it has higher chemical stability, and a better biodegradation rate can improve the bone repair effect (Lee et al., 2016). Combining HA and calcium phosphate makes a composite implant more similar to bone minerals, with better biological activity, biodegradability and mechanical properties, which can achieve better therapeutic effects (Kim et al., 2006; Ko et al., 2013).

At present, due to the natural osteogenic properties of HA, more and more studies have been conducted on HA composite scaffolds. In one study, Bosemark et al. (2015) made tricalcium phosphate hydroxyapatite composite scaffolds carrying BMP-7 to study the repair of femoral defects in rats. Compared with the use of scaffolds or drugs alone, the callus characteristics of bone defects were significantly improved. In another study, the composite scaffold was made according to the ratio of 15% HA:85% β -TCP, and it has the advantages of good bone conduction and bone integration (Ishack et al., 2017). Wu S. et al. (2018) made a NHA/collagen/poly (L-lactide) composite scaffold loaded with rhBMP-2 to treat bone defects that had a positive effect on human MSCs implantation, proliferation and osteogenic differentiation. Shen, XF and others have made composite scaffolds with silk fibroin (SF) and NHA, in which BMP-2 was loaded into SF microspheres, BMP-2 can be sustained and slowly released for up to 3 weeks. Therefore, the composite scaffold can continuously and slowly release BMPs and significantly promote osteogenic differentiation of BMSCs (Figure 6) (Shen et al., 2016). In summary, HA composite systems have broad application prospects in bone tissue engineering.

3.4.3 Hydrogels Based Composite Scaffolding System

Hydrogels are extremely hydrophilic gels with a three-dimensional network structure that swell rapidly in water and can absorb a large volume of water without dissolving. The hydrogel is neither a complete solid nor a complete liquid. Under certain conditions, hydrogels can maintain a certain shape and volume, and a solute can diffuse from or penetrate the hydrogel (Li et al., 2006; Rihn et al., 2009; Jin et al., 2010; Kayabasi et al., 2013; Zhang X. et al., 2019). Therefore, in orthopaedic applications, a hydrogel can be filled separately, used as a coating for implants, or be used to fill porous materials to provide a greater degree of coverage in the gap between the implant and bone to stimulate bone growth and avoid loosening of the implant (Hu et al., 2012; Kayabasi et al., 2013; Behrendt et al., 2020). Moreover, studies have shown that hydrogels can also transfer cells, which is conducive to the growth of cells and can continuously stimulate the potential of BMSC differentiation (Ben-David et al., 2011; Hu et al., 2021). Therefore, hydrogels have been widely used in orthopaedic treatments as an implant material, coating or filling in the pore structure of a material, with the functions of controlled release and sustained release. Collagen, fibrin, CHI, agarose, hyaluronic acid, silk and sodium alginate can be configured into hydrogels to carry BMP for more convenient and effective application to bone injury sites (Ben-David et al., 2011; Kayabasi et al., 2013). In clinical

applications, combined application of hydrogels and BMPs has achieved good results (Kolambkar et al., 2011; Nam et al., 2017; Jain et al., 2019; Xu et al., 2019).

Collagen is one of the most abundant ECM proteins and the most commonly used synthetic hydrogel material. Due to its good biocompatibility, nutrition, reparability, moisture and affinity, collagen is widely used in biomedical materials (Rihn et al., 2009; Nam et al., 2017). However, due to the instability and rapid degradation of collagen, artificial collagen implants cannot maintain their structural integrity for a long time. Currently, collagen can be modified to prolong durability and mechanical strength and can be combined with other materials so that implants can achieve slow release of loaded BMPs (Li et al., 2006; Kayabasi et al., 2013). By optimizing the physical and chemical properties of collagen, the best environment for bone tissue development can be provided, greatly improving the efficiency of bone regeneration (Li et al., 2021c). To date, rhBMP-2 and rhBMP-7 has been approved by the FDA for use in combination with collagen sponges in the treatment of clinical diseases and has achieved good efficacy (Kolambkar et al., 2011; Jain et al., 2019; Xu et al., 2019).

In one study, Acellular Bioactive affinity-binding Alginate hydrogel was designed to slowly release a chondral and osteogenic inducer (TGF- β 1 and BMP-4, respectively). Hydrogel was injected into the osteochondral defect of the medial femoral condyle of miniature pigs. After 6 months, histological evaluation showed that the articular cartilage layer was effectively reconstructed with the major features of hyaluronic cartilage, such as proteoglycans and type II collagen deposition. The results showed that treatment with an affinity-binding alginate saline gel containing cell-free injectable growth factors was effective in repairing the tissue and had the main characteristics of hyaline cartilage (Ruvinov et al., 2019). CHI has a wide range of applications in bone tissue engineering and antibacterial activity. CHI scaffolds and BMP-6-transfected rat BMSCs were used to treat bone defects and promote cartilage formation (Kayabasi et al., 2013). A bioactive multilayer structure of gelatine/CHI containing BMP-2 and fibronectin was constructed on the surface of Ti6Al4V, which was beneficial to osteogenic differentiation and integration of implant and bone (Hu et al., 2012). Current research shows that composite hydrogels have more significant osteoinductive activity and better development prospects when applied together with other materials (Kolambkar et al., 2011; Dhivya et al., 2015; Ghavimi et al., 2019; Ruvinov et al., 2019).

3.4.4 Synthetic Polymers Based Composite Scaffolding System

Synthetic polymers have been widely used in bone tissue engineering because of their excellent biocompatibility and biodegradability, and they can be combined with various materials to make composite scaffolds. In recent years, synthetic polymers have been widely used in aerospace, medical, dental, automotive, and other related fields. Especially in the field of orthopaedics, because synthetic polymers have excellent biocompatibility and good mechanical properties, they are easily produced and have certain bone-like properties, which

help to extend the life of the implant (Toth et al., 2006; Wu J. et al., 2018). In terms of orthopaedic implant stents for treating disease, synthetic polymers are suitable for the manufacture of implants with high quality and high precision requirements, such as implants for joint, spine, skull, and maxillofacial surgery and other operations (Abu Bakar et al., 2003; Meisel et al., 2008; Vaidya et al., 2008). With the development of 3D printing technology, synthetic polymers can be used to manufacture implants that are highly matched to the patient according to the situation at the injury site in the patient, which can greatly improve the success rate of surgery and the long-term prognosis (Wu et al., 2015).

Polyether ether ketone (PEEK) is a thermoplastic organic polymer with excellent strength and stability, bone-like stiffness, high-temperature durability and wear resistance (Han et al., 2014). In clinical applications, patients with degenerative lumbar disease were treated with pedicle screws and PEEK cages for dorsal fixation and then treated with rhBMP-2. At 6 months of controlled evaluation, all cases met the criteria for spinal fusion (Meisel et al., 2008). PEEK can be mixed with titanium alloy, HA, TCP and other materials to improve mechanical properties and biocompatibility and achieve better therapeutic effects (Tan et al., 2003; von Wilmsky et al., 2008; Han et al., 2014). PEEK-Ti6Al4V has better osseointegration capacity (Zhang W. et al., 2020). Nano-TiO₂ can improve the biocompatibility and bone conductivity of PEEK (Han et al., 2014). Surface modification of microporous PEEK with BMP-2-loaded phosphorylated gelatine can significantly promote cell adhesion and proliferation, effectively promote osteogenic differentiation and improve biological activity (Wu J. et al., 2018). Therefore, the use of PEEK in orthopaedics has received extensive attention.

Poly(lactic acid) (PLA) is a new type of biodegradable material produced using raw starch materials obtained from renewable plant resources and subsequent synthesis of poly(lactic acid) of a certain molecular weight through chemical synthesis methods (Zhang X. et al., 2019). Poly(lactic-co-glycolic acid) (PLGA) is polymerized from lactic acid and glycolic acid according to a certain ratio (Zhao X. et al., 2017). It is a degradable organic polymer compound. The degradation rate of PLGA is faster than that of PLA. Both PLA and PLGA have good biocompatibility, degradability, and plasticity; low cost; and good medical uses. Moreover, both PLA and PLGA have been approved by the FDA for clinical treatment. Therefore, PLA and PLGA have become widely applied in recent years (Zhang X. et al., 2019). PLA and PLGA can also be mixed with other materials. PLA/PLGA composite scaffolds have good stem cell loading properties and can induce cell-cell synergy, promote bone regeneration, and achieve better therapeutic effects (Laurencin et al., 2001; Zhao X. et al., 2017; Wu S. et al., 2018; Zhang X. et al., 2019). Zhang X. et al. (2019) used 3D printing technology to print a cylindrical PLA scaffold, which was surface-modified with dopamine (DA) and equipped with BMP-2. Then, the scaffold was implanted into a rat skull defect model. At 8 weeks after surgery, bone regeneration occurred in the skull defects of rats, and the fibrous bone tended to connect to form continuous bone tissue. Wu S. et al. (2018) made a NHA/collagen/PLA scaffold loaded with rhBMP-2, and the scaffold significantly increased

phosphate content, mineral production, ALP activity and osteogenic biomarkers (OCN and Runx2). This complex had a positive effect on the proliferation and osteogenic differentiation of human MSCs. A PLGA-HA scaffold loaded with BMP-2 showed a significant promoting effect on cell adhesion and proliferation. In addition, genes related to alkaline phosphatase activity, calcium deposition and osteogenesis were highly expressed in cells (Figure 7) (Zhao X. et al., 2017). PLGA/HA composite scaffolds have good application prospects for bone regeneration (Laurencin et al., 2001; Nie and Wang, 2007). Importantly, the biological and mechanical properties of single-material scaffolds often fail to achieve the desired results. Compared with single-material scaffolds, composite material scaffolds have improved properties, show a more obvious effect on promoting bone defect healing, and can stimulate bone formation continuously, long-term and effectively (Bosemark et al., 2015; Ding et al., 2016). Table 4 lists application of BMPs in materials.

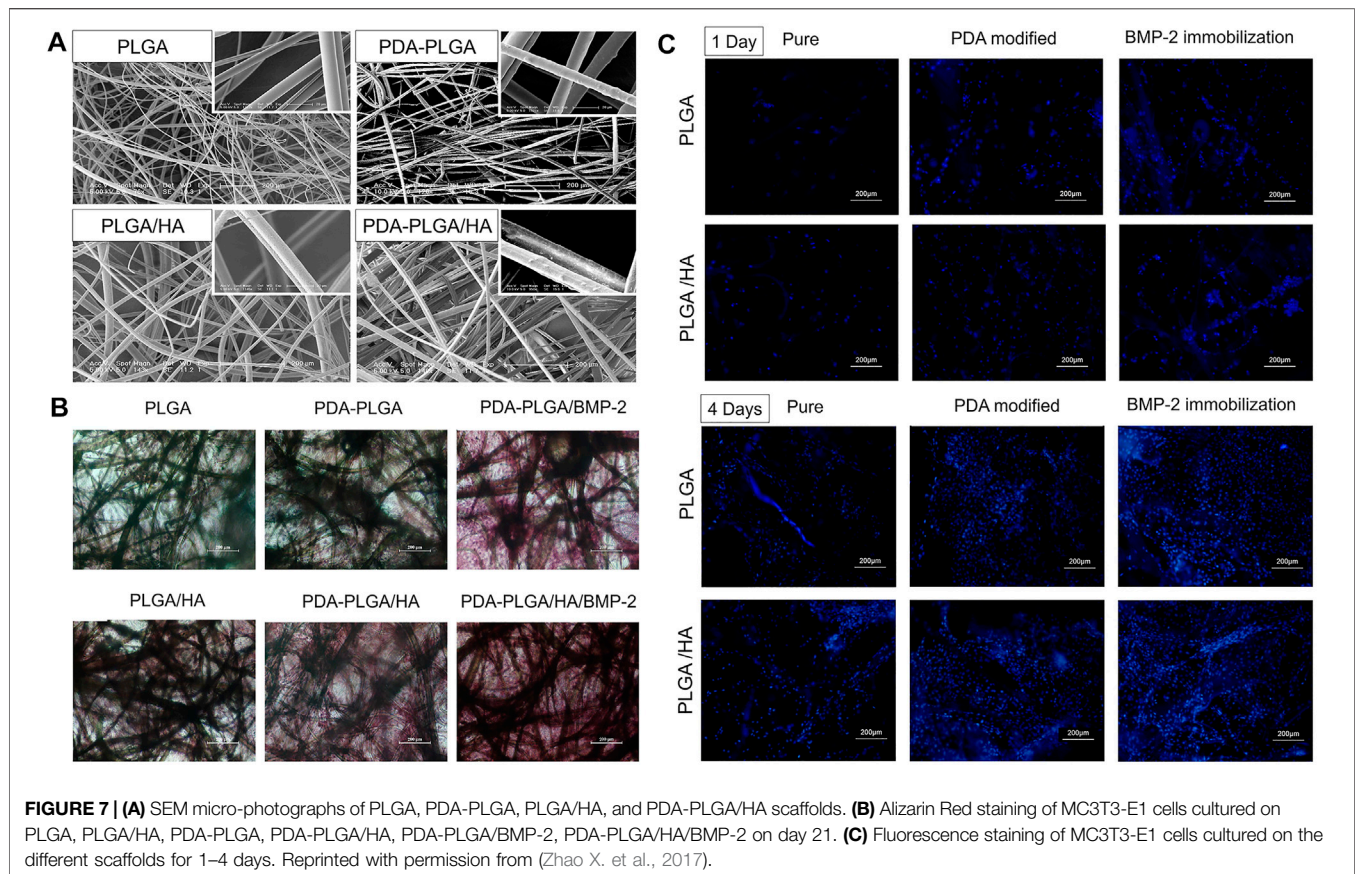
4 CLINICAL APPLICATIONS OF BMPs

4.1 Open or Nonunion Fractures

Open or nonunion fractures are a challenging complication with often unpredictable results. They can have devastating effects on patients, often require multiple surgeries and long-term recovery, and can lead to severe psychological and functional disabilities. Treatment of open or nonunion fractures is difficult. The two main principles of treatment are internal fixation to stabilize the structure and improvement of bone biology (Singh et al., 2016; Hissnauer et al., 2017).

AGB currently exhibits the best cure rate and is the safest method for treating bone defects. At present, most clinical studies have shown that BMP can achieve a faster healing time in treatment of bone nonunion, and the combination of BMP and ABG has a more significant therapeutic effect (Flierl et al., 2013; von Ruden et al., 2016). Hissnauer et al. (2017) retrospectively studied 10 children with congenital pseudarthrosis of the tibia (CPT) or tibial nonunion treated with rhBMP-2. Nine of the ten patients achieved healing after initial surgery. rhBMP-2 may provide an appropriate option for treatment of CPT or persistent tibial nonunion in children and adolescents. In a study by Singh et al. (2016), 42 patients with refractory upper limb bone nonunion who were continuously treated with rhBMP-7 were followed up. Bmp-7 was used alone in 1 case and combined with ABG in 41 cases. Forty fractures showed both clinical and radiographic healing, while the other two patients showed partial radiographic healing. Combined treatment with ABG and rhBMP-7 has achieved results in the treatment of refractory upper limb nonunion. Therefore, combined application of rhBMP and ABG may have a better effect on promoting bone nonunion healing than BMP alone.

Current studies have shown that in the treatment of bone nonunion, although rhBMP-2 and rhBMP-7 are helpful for fracture healing, the more critical factor is the method employed during the operation, which may be the most important factor affecting postoperative fracture healing



(Hackl et al., 2017; Dilogio et al., 2019). One year after rhBMP application, bone nonunion did not heal compared with the nonapplication group. Because the non-BMP group also reached the healing standard, whether there is a difference in the healing time of nonunion needs more research. Much debate remains, especially with regard to the safety and efficacy of rhBMP. At present, there are few data on adding rhBMP to the treatment for long bone nonunion, and the role and indications of rhBMP in the treatment of nonunion have not been clarified. The limitations of these studies include retrospective review, a small number of patients, and a lack of randomization. Prospective randomized controlled trials are needed to investigate the long-term efficacy and safety of rhBMP in these cases. rhBMP has been successfully used for the treatment of nonunion, and it should be warned that the use of external growth factors may bring adverse complications. However, studies have found a risk of impaired wound healing and inflammation following BMP use, but this was only a temporary problem and subsided over the course of continuous treatment, with no other complications (von Ruden et al., 2016; Hissnauer et al., 2017).

Recent studies have shown that with the development of implant materials, a variety of new implant materials equipped with BMP can continuously stimulate local bone growth. In particular, HA has been used as a material for clinical application. BMP combined with autologous bone grafts and

hydroxyapatite particles has a unique osteoinduction effect on mesenchymal cells present in autologous bone grafts and is also associated with the effect of hydroxyapatite on bone conduction at nonunion sites (Caterini et al., 2016; Dilogio et al., 2019). Caterini et al. (2016) reported 12 patients with refractory humeral nonunion who were treated with rhBMP-7, HA and ABG for nonunion. The average healing time of nonunion in all patients was 7.3 months, and function was basically restored. The patients were satisfied with the effect. This shows that the combined application of rhBMP-7 and HA is an effective method to stimulate bone healing. Dilogio et al. (2019) treated 6 patients with critical-sized defects with a combination of autologous BMSCs, HA particles, rhBMP-2 and mechanical stabilization. Follow-up for at least 12 months after surgery showed significant improvement in function in all cases (**Figure 8**).

rhBMP-2 and rhBMP-7 combined with other bone growth-promoting substances, such as HA and ABG, can significantly enhance the degree of fracture healing in patients. During treatment, the effects of the mutual promotion of various treatment methods should be evaluated in detail. To avoid complications, it is particularly important to find a treatment method suitable for combined application with rhBMP.

4.2 Vertebral Fusion

In spine surgery, nonunion is a challenging problem. Spinal instability can cause nerve damage and many sequelae, which

TABLE 4 | The application of BMPs in materials.

BMP	Material(s)	Modified	Function(s)	References
rhBMP-2	Ti6Al4V	3D printing porous structure, pore size:400–600 μm , porosity:60–80%	Improved the degree of bone-scaffold bonding	Zhang T. et al. (2020)
BMP-2	Ti6Al4V	Porous structure, pore size:600 μm , prepared by a combination of MAO, calcium-phosphorus co-precipitation and electrodeposition BMP-2 coating technology (MAO-Ca/P-BMP2)	Bone induction and bone conduction capabilities, enhances the growth of cells, enables the formation of blood vessels in the implant and has a better osteogenic effect	Teng et al. (2019)
BMP-2	TNTs	Through layer-by-layer assembly technique, the sodium alginate and gentamicin and CHI were constructed on BMP 2 loaded TNTs substrate	Enhanced antibacterial ability and bone formation ability	Tao et al. (2019)
BMP-2	HA	Combination of autologous BMSCs and ABG	Enhanced stability and bone regeneration characteristics	Teotia et al. (2017), Dilogo et al. (2019)
BMP-2	NHA	NHA coating	Providing a rich active site for cell attachment, which is more conducive to the stable combination of bone and implant	Deng et al. (2017)
BMP-7	TCP	Carried BMP-7 and bisphosphonates	Improved bone defects, promoted bone healing	Bosemark et al. (2015)
BMP-2	HA β -TCP	Composite scaffold, ratio: 15% HA: 85% β -TCP	Improve bone conduction and bone integration	Ishack et al. (2017)
rhBMP-2	NHA Collagen PLA	Composite scaffold	Positive effect on human MSCs implantation, proliferation and osteogenic differentiation	Wu S. et al. (2018)
BMP-2	SF NHA	Composite scaffold SF microspheres stromal cell-derived factor-1 (SDF-1) is bound to the scaffold	Continuously and slowly release growth factors and significantly promote the osteogenic differentiation of BMSCs	Shen et al. (2016)
BMP-2	Ti6Al4V CHI	Layer-by-layer assembly technology, construct a bioactive multilayer structure of gelatin/CHI containing BMP-2 and fibronectin on the surface of Ti6Al4V	Beneficial to osteogenic differentiation and integration of implant and bone	Hu et al. (2012)
BMP-6	CHI	CHI scaffolds and BMP-6 transfected rat BMSCs	Promote bone formation and cartilage formation	Kayabasi et al. (2013)
rhBMP-2	PEEK	Pedicle screw and PEEK cage	Spinal fusion	Meisel et al. (2008)
BMP-2	PEEK	Coated BMP-2 loaded phosphorylated gelatin on PEEK	Promote cell adhesion and proliferation, effectively promote osteogenic differentiation and improve biological activity	Wu J. et al. (2018)
BMP-2	PLA	Scaffold surface-modified with DA and BMP-2	Bone regeneration occurred in the skull defects of rats; the fibrous bone tended to connect to form continuous bone tissue	Zhang X. et al. (2019)
BMP-2	PLGA	DA and BMP-2 coatings	Significantly promoted <i>in vivo</i> bone formation in critical-sized calvarial bone defects	Ko et al. (2013)
BMP-2	PLGA HA	Modified the surface of the scaffold with DA	Significant promoting effect on cell adhesion and proliferation. Alkaline phosphatase activity, calcium deposition and osteogenesis are highly expressed	Zhao X. et al. (2017)

hinder the treatment effect. Therefore, surgery is needed to achieve fusion. The traditional surgical method has a low cure rate and can cause many complications. Therefore, whether rhBMP treatment can increase the cure rate and reduce complications has an important impact on the development of spinal surgery (Meisel et al., 2008; Annis et al., 2015; Sayama et al., 2015; Stiel et al., 2018).

The gold standard for spinal fusion is a local autogenous bone graft, with autogenous iliac crest or rib bone extracted separately. However, it can lead to complications, such as pain at the site of bone removal, haematoma, infection, and increased risk of fracture. Bone nonunion remains a challenging problem. Especially in paediatric spinal surgery, too many autogenous bone grafts will bring more serious complications due to the insufficient amount of autogenous bone in children. Therefore, it is very important to find a treatment method that can replace ABG or reduce the number or amount of bone grafts. Currently, ABG combined with BMP is used to achieve spinal fusion and has

received increasing attention (Singh et al., 2013; Sayama et al., 2015; Stiel et al., 2018). In one study, 13 children with spinal deformities were treated with rhBMP-2 during spinal fusion, with an average follow-up of 51 months. Analysis of clinical and radiographic results showed that 11 cases of spinal fusion were observed, with no significant increase in complications. The rate of spinal fusion in children treated with rhBMP-2 was high, and the incidence of complications was not significantly increased. Therefore, we consider recombinant human BMP-2 to be an option in paediatric spinal surgery, especially in cases of impaired bone healing due to congenital, systemic or local disease (Stiel et al., 2018). In one report, a retrospective review of 11 paediatric patients with L5-S1 neuromuscular spinal deformity treated with long segment fusion and rhBMP-2 was performed, and this treatment had the advantages of a lower complication rate, less bleeding, and shorter surgical duration compared to peripheral nerve fusion (Gressot et al., 2014). In another study, 17 patients with degenerative lumbar diseases were

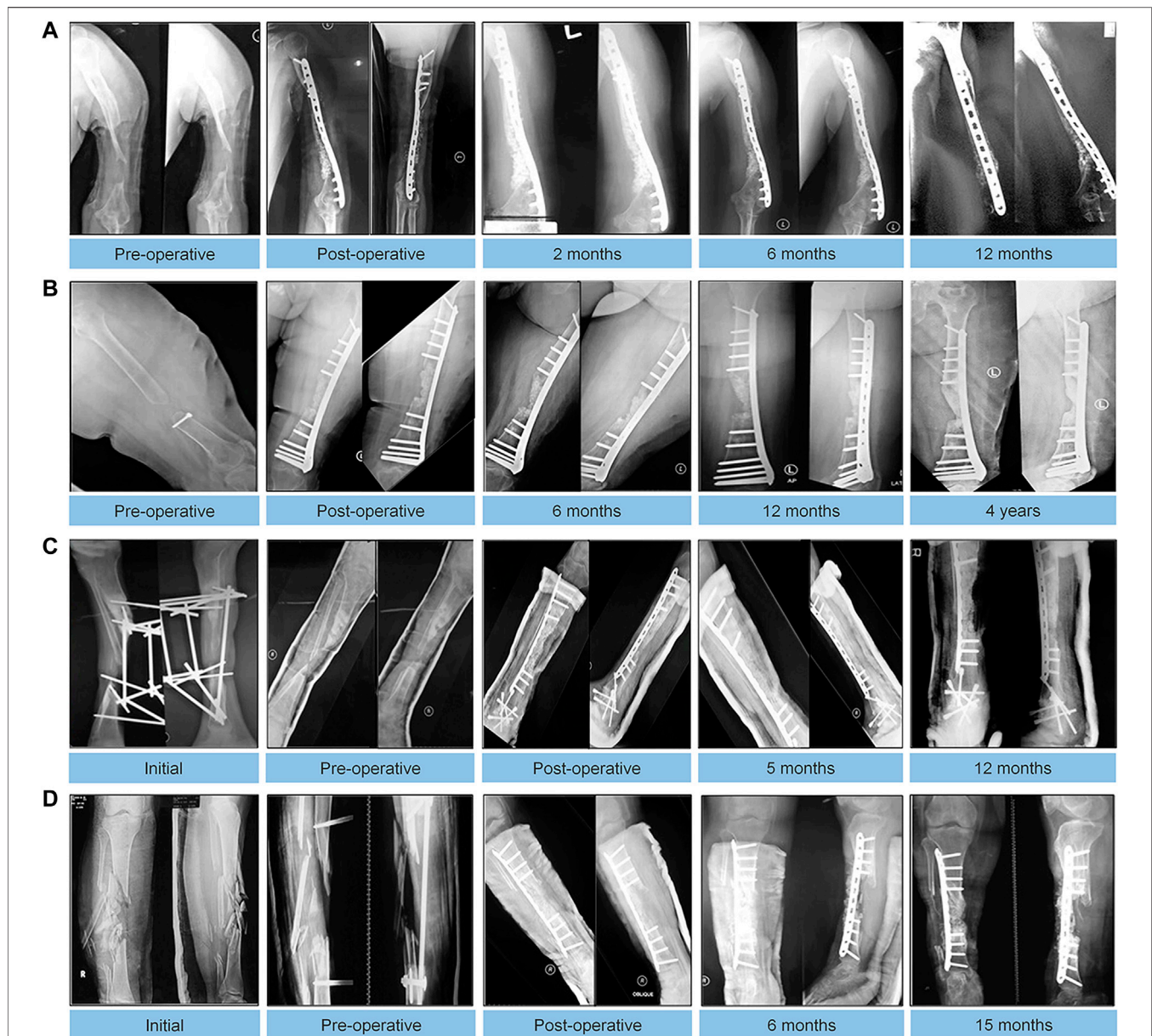


FIGURE 8 | Autologous MSC implantation, hydroxyapatite, BMP-2, and internal fixation for treating critical-sized defects. Radiographic results of follow-up visits of 4 cases. **(A):** An 18-year-old male with 5-cm bone defect of the humerus. **(B):** An 18-year-old male with 5-cm bone defect of the humerus. **(C):** A 28-year-old male with 7-year history of 8-cm bone defect of the right tibia. **(D):** A 24-year-old female with 12 cm bone defect of the tibia. Reprinted with permission from (Dilogo et al., 2019).

treated with rhBMP-2 carried in a collagen sponge. The patients were followed up for 3 and 6 months after the operation. All the patients showed signs of spinal fusion, and there were no complications, such as vertebral collapse and pain. All 17 patients reached the standard of vertebral fusion healing after 6 months (Meisel et al., 2008). In adult L5-S1 vertebral deformity surgery, BMP-2 combined with sacral internal fixation was retrospectively studied in 61 patients, and the vertebral fusion rate was 97%. A satisfactory fusion rate was obtained by combining low-dose BMP-2 with internal sacral fixation (Annis et al., 2015).

While satisfactory results have been achieved with rhBMP-2, we cannot ignore the existence of postoperative complications. The Rush University Department of Orthopaedic Surgery reviewed 573 adult patients who received rhBMP-2 during vertebral surgery. Of these patients, 91.4% achieved postoperative healing standards. However, in other cases, there were complications, and symptomatic ectopic bone formation, vertebral osteolysis, and pseudojoint complications were detected after treatment with rhBMP-2 (Singh et al., 2013). In a follow-up study of 119 patients, 33 patients received autologous iliac bone grafts, and 86 patients were treated with rhBMP-2. The data

suggest that the use of rhBMP-2 reduced the incidence of donor-site complications due to autologous bone grafts but also introduced treat-site complications, including postoperative radiculitis and ectopic bone formation. The most common complication in the rhBMP-2 group was postoperative radiculitis, and hydrogel sealing significantly reduced the incidence of postoperative radiculitis (Rihn et al., 2009). Therefore, the application of hydrogel sealant and rhBMP can reduce the incidence of postoperative complications.

The general conclusion is that the use of rhBMP-2 in adult vertebral surgery can achieve satisfactory results and reduce the incidence of complications. Although some studies in adults have shown that rhBMP-2 has a positive effect on vertebral fusion, the use of rhBMP-2 in children has shown a higher failure rate of vertebral fusion than in adults. Therefore, the application of rhBMP-2 in spinal surgery in children and in spinal fusion in adults should be studied separately. BMP affects the development of the vertebral body in children, and there should be more evaluation and research.

4.3 Maxillofacial Bone Enhancement

Maxillofacial bone enhancement is also common in head and neck surgery. As a result of congenital dysplasia or complete or partial removal of the mandible and other facial bones after tumour surgery or trauma, extensive bone defects usually appear in the oral maxillofacial region. ABG has been used to fix these defects. In addition, bone graft materials and autologous bone grafts have been used to treat other defects, such as congenital cleft palate, facial fissures, and facial asymmetry. rhBMP has also been widely used in maxillofacial bone repair. For example, a custom-made carrier based on a patient's unique CT scan can be designed to perfectly fill bone defects, resulting in accurate and low-dose BMP loading with minimal impact on surrounding tissue and reduced side effects (Herford and Boyne, 2008; Jensen et al., 2012; Nam et al., 2017; Park et al., 2017; Ayoub and Gillgrass, 2019).

The application of rhBMP without bone grafts in the treatment of mandibular defects has achieved a good therapeutic effect. In the treatment of 14 cases of bone defects caused by maxillofacial tumours or osteomyelitis, rhBMP-2 was applied to collagen, and no bone graft material was used. In all cases, the bones were successfully repaired in the toothless area, supporting the application of rhBMP-2 in facial bone regeneration or repair (Herford and Boyne, 2008). In another study to treat severe maxillary sinus atrophy, BMP-2 was added to the implant in 10 patients and successfully bound to bone a year later to form a stabilized prosthesis. In the case of severe maxillary atrophy, zygomatic implants with rhBMP-2 added are a viable option (Jensen et al., 2012). In a study treating medication-related osteonecrosis of the jaw (MRONJ), the efficacy of rhBMP-2 combined with leukocyte-rich and platelet-rich fibrin (L-PRF) was evaluated. The lesions completely resolved with the combination of L-PRF and rhBMP-2, which was significantly different from the results of treatment with L-PRF alone. Therefore, the additional use of rhBMP-2 significantly improved the healing of medication-related osteonecrosis of the jaw (Park et al., 2017). BMP-2 in combination with both

hydroxyapatite and bovine-derived xenografts can effectively enhance the alveolar ridge in treatment of augmentation of the alveolar ridge, and BMP-2 in combination with hydroxyapatite is especially effective in repairing complex bone defects (Nam et al., 2017). The use of a collagen carrier enables rhBMP-7 to be used more effectively in surgery. Collagen can be injected directly into the cleft area of the alveolar crest, which facilitates surgery because it requires a smaller incision, thus reducing complications. This provides a guarantee of the safety of BMP-7 applied to the immature area of bone. During a follow-up period of 10 years, maxillary bone growth was similar to that of autologous bone grafts in the area where rhBMP was applied, without excessive bone fusion or excessive bone growth, and rhBMP-7 has been found to be safe in the treatment of alveolar bone defect repair in children (Ayoub and Gillgrass, 2019). **Table 5** lists clinical applications of BMPs.

In clinical application of rhBMP, most previous retrospective studies have confirmed that rhBMP has the effect of repairing bone defects and can reduce the occurrence of complications. The use of rhBMP has led to preliminary achievements in the treatment of clinical orthopaedic diseases and has good efficacy in promoting bone healing and reducing complications. However, it should not be neglected that the efficacy of BMP alone is not significant, and there are other influencing factors in the process of bone healing. Combining other factors that can promote bone healing, such as ABG, HA particles, hydrogels, collagen sponges, and bone substitutes, with rhBMP can lead to a better effect. Clinical therapy is rarely based on a single bioactive molecule and almost always requires combinatorial approaches, since the combined use of bioactive molecules usually achieves greater efficacy. In the prospect of using BMPs in the treatment of orthopaedic diseases, the combined application of implants and BMPs is obviously a research trend. Because implants can be loaded with BMP, a control and continuous release system can be formed to achieve continuous and effective osteogenesis stimulation at the bone defect site. Further research progress in implants can solve a series of problems in the application of BMP.

5 CURRENT LIMITATIONS AND FUTURE PERSPECTIVES

In orthopaedics, delayed healing or nonunion of bone caused by a large bone defect area has always been a difficult treatment problem. How to promote bone regeneration and bone healing has become an important field of research. Currently, prosthesis implantation, autogenous bone transplantation, local loading of drugs or growth factors and other methods can promote bone regeneration and bone healing. Among the growth factors that have been the focus of research in recent years, BMPs have the strongest osteogenic activity. Although there is a superficial understanding of BMPs, for example, BMPs stimulate osteoblast differentiation through the Smad pathway, the signalling pathway of BMPs is still under study. What can be determined now is that BMPs do not rely on a single signalling

TABLE 5 | Clinical applications of BMPs.

Disease	Therapies	Total number of patients	Number of effective patients	Effective rate (%)	References
CPT or persistent tibial nonunion in children and adolescents	rhBMP-2	10	9	90.0	Hissnauer et al. (2017)
Refractory upper limb bone nonunion	rhBMP-7 and ABG	41	39	95.1	Singh et al. (2016)
Refractory humeral nonunion	rhBMP-7, HA, and ABG	12	12	100	Caterini et al. (2016)
Critical-sized defect	rhBMP-2, HA, and autologous BMSCs	6	6	100	Dilogo et al. (2019)
Pediatric spinal deformity	rhBMP-2	13	11	84.6	Stiel et al. (2018)
Neuromuscular spinal deformity	rh-BMP-2, segmental spinal instrumentation system	11	10	90.9	Gressot et al. (2014)
Degenerative lumbar disease	rhBMP-2 carried by collagen sponge	17	17	100	Meisel et al. (2008)
Adult L5-S1 vertebral deformity	rhBMP-2, multi-level spinal and fusion pelvic fixation	61	59	97	Annis et al. (2015)
Vertebral disease	rhBMP-2, laminectomy with bilateral facetectomy, single TLIF cage, unilateral pedicle screw fixation	573	524	91.4	Singh et al. (2013)
Bone defects caused by maxillofacial tumors or osteomyelitis	rhBMP-2 carried by collagen sponge	14	14	100	Herford and Boyne, (2008)
Severe maxillary sinus atrophy	rhBMP-2 was added to the implant	10	10	100	Jensen et al. (2012)
Medication-related osteonecrosis of the jaws	rhBMP-2 combined with L-PRF	30	30	100	Park et al. (2017)
Unilateral cleft lip and palate	rhBMP-7	9	9	100	Ayoub and Gillgrass, (2019)

pathway to function; many signalling pathways work together, and various factors affect each other, thereby stimulating osteoblasts in the body to repair bone defects. Interestingly, the individual skeleton is a composite structure, and its specific growth pattern is constructed by numerous gene lineages and domains that regulate gene expression. The individual enhancer in BMP genes provides a genome to precisely control the growth of cartilage and bone so that bone growth can be individually regulated in specific parts of the body. In addition, BMP gene expression can be found not only in the skeletal system but also in other organs and tissues. This shows that the human body is a complex overall structure that is jointly regulated by the genome to maintain homeostasis and repair damage. At present, *in vitro* studies and animal studies have shown that BMPs have an important role in cartilage differentiation, bone differentiation and tendon and ligament differentiation. BMP-2, BMP-4, BMP-5, BMP-6, BMP-7 and BMP-9 have obvious stimulating effects on cartilage formation and bone healing, while BMP-12, BMP-13 and BMP-14 have significant effects on tendon and ligament repair. In addition, BMP and other cytokines also have a synergistic effect, which can enhance the biological activity of each other and achieve better osteogenesis, chondrogenesis, tendon formation and vascular formation.

In 2002, the FDA approved rhBMP-2 and rhBMP-7 for clinical treatment of issues such as vertebral fusion, open or nonunion fractures, and maxillofacial bone reinforcement. With the increase in follow-up data in recent years, BMPs have been verified to be beneficial for the treatment of diseases. However, in the process of applying BMPs, we should pay attention to preventing complications and consider individualized treatment for adults and children. The use of local high-dose BMPs may cause various complications, such as ectopic bone formation. Slow and sustained release of BMPs at a low dose will enhance bone healing and reduce the occurrence of

complications. How to achieve slow and sustained release of BMPs at low doses is a difficulty that needs to be solved. At present, implantation of a scaffold with a porous structure and coating of the implant can achieve slow and continuous release of growth factors at the site of bone defects. However, implants made from a single material have various disadvantages in terms of strength, stability, durability, wear resistance, bone conductivity and biocompatibility. Implants made of composite materials can solve this problem and promote bone healing at the implantation site.

The development of bone tissue engineering provides a good solution for the application of BMP. At present, the research focus has been focused on the development of composite scaffolds, which have stronger biological functions. Importantly, with the development of various BMP delivery systems, BMP will be more reasonably loaded into the composite scaffold, so that BMP can continue to release slowly *in vivo*, and continue to stimulate osteoblast growth and induce bone formation in the process of fracture healing. Most notably, research on composite implant materials loaded with BMPs will provide better prospects for treatment of orthopaedic diseases.

6 CONCLUSION

BMPs have a powerful role in stimulating the differentiation of stem cells into bone, chondroblasts and tendons, which provides a new option for treatment of orthopaedic diseases. Application of BMP at the disease site requires a collagen sponge or other implant carrier to achieve slow and continuous release of BMP, thus achieving continuous and effective stimulation of bone healing. The selection of implant materials is particularly important for the degree of bone healing recovery. Composite materials can combine the advantages of various materials to endow implants with better biocompatibility, shape plasticity, antimicrobial properties

and osteogenesis capacity. This review mainly introduces the biological function of BMP in the field of orthopaedics and presents the latest progress in implant materials equipped with BMP. Further development and modification of implants would be helpful in achieving better clinical application of BMP.

AUTHOR CONTRIBUTIONS

LZ: Conceptualization, Investigation, Writing—original draft. YuL: Data curation, Writing—review and editing. AW: Validation, Methodology. ZZ: Writing—review and editing, Methodology, Conceptualization. YoL: Conceptualization, Methodology, Supervision. CZ: Conceptualization, Supervision.

REFERENCES

- Abu Bakar, M. S., Cheng, M. H. W., Tang, S. M., Yu, S. C., Liao, K., Tan, C. T., et al. (2003). Tensile Properties, Tension-Tension Fatigue and Biological Response of Polyetheretherketone-Hydroxyapatite Composites for Load-Bearing Orthopedic Implants. *Biomaterials* 24 (13), 2245–2250. doi:10.1016/s0142-9612(03)00028-0
- Akiyama, H., Chaboissier, M.-C., Martin, J. F., Schedl, A., and de Crombrughe, B. (2002). The Transcription Factor Sox9 Has Essential Roles in Successive Steps of the Chondrocyte Differentiation Pathway and Is Required for Expression of Sox5 and Sox6. *Genes Dev.* 16 (21), 2813–2828. doi:10.1101/gad.1017802
- Annis, P., Brodke, D. S., Spiker, W. R., Daubs, M. D., and Lawrence, B. D. (2015). The Fate of L5-S1 with Low-Dose BMP-2 and Pelvic Fixation, with or without Interbody Fusion, in Adult Deformity Surgery. *Spine* 40 (11), E634–E639. doi:10.1097/brs.0000000000000867
- Ayoub, A., and Gillgrass, T. (2019). The Clinical Application of Recombinant Human Bone Morphogenetic Protein 7 for Reconstruction of Alveolar Cleft: 10 years' Follow-Up. *J. Oral Maxillofac. Surg.* 77 (3), 571–581. doi:10.1016/j.joms.2018.08.031
- Bai, Y., Moeinzadeh, S., Kim, S., Park, Y., Lui, E., Tan, H., et al. (2020). Development of PLGA-PEG-COOH and Gelatin-Based Microparticles Dual Delivery System and E-Beam Sterilization Effects for Controlled Release of BMP-2 and IGF-1. *Part. Part. Syst. Charact.* 37 (10), 2000180. doi:10.1002/ppsc.202000180
- Ball, A. N., Phillips, J. N., McIlwraith, C. W., Kawcak, C. E., Samulski, R. J., and Goodrich, L. R. (2019). Genetic Modification of scAAV-equine-BMP-2 Transduced Bone-marrow-derived Mesenchymal Stem Cells before and after Cryopreservation: An "off-the-shelf" Option for Fracture Repair. *J. Orthop. Res.* 37 (6), 1310–1317. doi:10.1002/jor.24209
- Baltzer, A. W. A., Lattermann, C., Whalen, J. D., Wooley, P., Weiss, K., Grimm, M., et al. (2000). Genetic Enhancement of Fracture Repair: Healing of an Experimental Segmental Defect by Adenoviral Transfer of the BMP-2 Gene. *Gene Ther.* 7 (9), 734–739. doi:10.1038/sj.gt.3301166
- Barati, D., Shariati, S. R. P., Moeinzadeh, S., Melero-Martin, J. M., Khademhosseini, A., and Jabbari, E. (2016). Spatiotemporal Release of BMP-2 and VEGF Enhances Osteogenic and Vasculogenic Differentiation of Human Mesenchymal Stem Cells and Endothelial colony-forming Cells Co-encapsulated in a Patterned Hydrogel. *J. Controlled Release* 223, 126–136. doi:10.1016/j.jconrel.2015.12.031
- Beauvais, S., Drevelle, O., Lauzon, M.-A., Daviau, A., and Fauchoux, N. (2016). Modulation of MAPK Signalling by Immobilized Adhesive Peptides: Effect on Stem Cell Response to BMP-9-Derived Peptides. *Acta Biomater.* 31, 241–251. doi:10.1016/j.actbio.2015.12.005
- Behrendt, P., Ladner, Y., Stoddart, M. J., Lippross, S., Alini, M., Eglin, D., et al. (2020). Articular Joint-Simulating Mechanical Load Activates Endogenous TGF- β in a Highly Cellularized Bioadhesive Hydrogel for Cartilage Repair. *Am. J. Sports Med.* 48 (1), 210–221. doi:10.1177/0363546519887909
- ZC: Data curation, Validation, Visualization, Software. TL: Writing—review and editing. HL: Conceptualization, Validation, Methodology. LH: Conceptualization, Writing—review and editing.
- ## FUNDING
- This work was sponsored by the Department of Science and Technology of Jilin Province (Grant Number 20200201327JC), Health Science and Technology Capacity Improvement Project of Jilin Province (Grant Number 2021JC019), Graduate Innovation Fund of Jilin University (Grant Number 101832020CX294, 101832020CX298).
- Ben-David, D., Kizhner, T. A., Kohler, T., Müller, R., Livne, E., and Srouji, S. (2011). Cell-scaffold Transplant of Hydrogel Seeded with Rat Bone Marrow Progenitors for Bone Regeneration. *J. Craniomaxillofac. Surg.* 39 (5), 364–371. doi:10.1016/j.jcms.2010.09.001
- Bessa, P. C., Casal, M., and Reis, R. L. (2008). Bone Morphogenetic Proteins in Tissue Engineering: the Road from Laboratory to Clinic, Part II (BMP Delivery). *J. Tissue Eng. Regen. Med.* 2 (2-3), 81–96. doi:10.1002/term.74
- Bosemark, P., Perdikouri, C., Pelkonen, M., Isaksson, H., and Tägil, M. (2015). The Masquelet Induced Membrane Technique with BMP and a Synthetic Scaffold Can Heal a Rat Femoral Critical Size Defect. *J. Orthop. Res.* 33 (4), 488–495. doi:10.1002/jor.22815
- Bouletreau, P. J., Warren, S. M., Spector, J. A., Peled, Z. M., Gerrets, R. P., Greenwald, J. A., et al. (2002). Hypoxia and VEGF Up-Regulate BMP-2 mRNA and Protein Expression in Microvascular Endothelial Cells: Implications for Fracture Healing. *Plast. Reconstr. Surg.* 109 (7), 2384–2397. doi:10.1097/00006534-200206000-00033
- Bouyer, M., Guillot, R., Lavaud, J., Plettinx, C., Olivier, C., Curry, V., et al. (2016). Surface Delivery of Tunable Doses of BMP-2 from an Adaptable Polymeric Scaffold Induces Volumetric Bone Regeneration. *Biomaterials* 104, 168–181. doi:10.1016/j.biomaterials.2016.06.001
- Caron, M. M. J., Ripmeester, E. G. J., van den Akker, G., Wijnands, N. K. A. P., Steijns, J., Surtel, D. A. M., et al. (2021). Discovery of Bone Morphogenetic Protein 7-derived Peptide Sequences that Attenuate the Human Osteoarthritic Chondrocyte Phenotype. *Mol. Ther. - Methods Clin. Develop.* 21, 247–261. doi:10.1016/j.omtm.2021.03.009
- Caterini, R., Potenza, V., Ippolito, E., and Farsetti, P. (2016). Treatment of Recalcitrant Atrophic Non-union of the Humeral Shaft with BMP-7, Autologous Bone Graft and Hydroxyapatite Pellets. *Injury* 47, S71–S77. doi:10.1016/j.injury.2016.07.044
- Cecchi, S., Bennet, S. J., and Arora, M. (2016). Bone Morphogenetic Protein-7: Review of Signalling and Efficacy in Fracture Healing. *J. Orthopaedic Translation* 4, 28–34. doi:10.1016/j.jot.2015.08.001
- Celil, A. B., and Campbell, P. G. (2005). BMP-2 and Insulin-like Growth Factor-I Mediate Osterix (Ox) Expression in Human Mesenchymal Stem Cells via the MAPK and Protein Kinase D Signaling Pathways. *J. Biol. Chem.* 280 (36), 31353–31359. doi:10.1074/jbc.M503845200
- Chao, Y.-L., Lin, L.-D., Chang, H.-H., and Wang, T.-M. (2021). Preliminary Evaluation of BMP-2-Derived Peptide in Repairing a Peri-Implant Critical Size Defect: A Canine Model. *J. Formos. Med. Assoc.* 120 (5), 1212–1220. doi:10.1016/j.jfma.2020.07.023
- Chen, L., Zou, X., Zhang, R.-X., Pi, C.-J., Wu, N., Yin, L.-J., et al. (2016). IGF1 Potentiates BMP9-Induced Osteogenic Differentiation in Mesenchymal Stem Cells through the Enhancement of BMP/Smad Signaling. *Bmb Rep.* 49 (2), 122–127. doi:10.5483/BMBRep.2016.49.2.228
- Chen, X.-J., Shen, Y.-S., He, M.-C., Yang, F., Yang, P., Pang, F.-X., et al. (2019). Polydatin Promotes the Osteogenic Differentiation of Human Bone Mesenchymal Stem Cells by Activating the BMP2-Wnt/ β -Catenin Signaling Pathway. *Biomed. Pharmacother.* 112, 108746. doi:10.1016/j.biopha.2019.108746

- Chen, Z., Yan, X., Yin, S., Liu, L., Liu, X., Zhao, G., et al. (2020). Influence of the Pore Size and Porosity of Selective Laser Melted Ti6Al4V ELI Porous Scaffold on Cell Proliferation, Osteogenesis and Bone Ingrowth. *Mater. Sci. Eng. C* 106, 110289. doi:10.1016/j.msec.2019.110289
- Chuen, F. S., Chuk, C. Y., Ping, W. Y., Nar, W. W., Kim, H. L., and Ming, C. K. (2004). Immunohistochemical Characterization of Cells in Adult Human Patellar Tendons. *J. Histochem. Cytochem.* 52 (9), 1151–1157. doi:10.1369/jhc.3A6232.2004
- Daly, A. C., Pitacco, P., Nulty, J., Cuniffe, G. M., and Kelly, D. J. (2018). 3D Printed Microchannel Networks to Direct Vascularisation during Endochondral Bone Repair. *Biomaterials* 162, 34–46. doi:10.1016/j.biomaterials.2018.01.057
- Dang, P. N., Herberg, S., Varghai, D., Riaz, H., Varghai, D., McMillan, A., et al. (2017). Endochondral Ossification in Critical-Sized Bone Defects via Readily Implantable Scaffold-free Stem Cell Constructs. *Stem Cell Translational Med.* 6 (7), 1644–1659. doi:10.1002/sctm.16-0222
- Datta, S., Rameshbabu, A. P., Bankoti, K., Jana, S., Roy, S., Sen, R., et al. (2021). Microsphere Embedded Hydrogel Construct - Binary Delivery of Alendronate and BMP-2 for superior Bone Regeneration. *J. Mater. Chem. B* 9 (34), 6856–6869. doi:10.1039/d1tb00255d
- Deng, L., Li, D., Yang, Z., Xie, X., and Kang, P. (2017). Repair of the Calvarial Defect in Goat Model Using Magnesium-Doped Porous Hydroxyapatite Combined with Recombinant Human Bone Morphogenetic Protein-2. *Bme* 28 (4), 361–377. doi:10.3233/BME-171678
- Dent-Acosta, R. E., Storm, N., Steiner, R. S., and San Martin, J. (2012). The Tactics of Modern-Day Regulatory Trials. *J. Bone Jt. Surg Am* 94 (Suppl. 1), 39–44. doi:10.2106/JBJS.L.00194
- Dhivya, S., Saravanan, S., Sastry, T. P., and Selvamurugan, N. (2015). Nanohydroxyapatite-reinforced Chitosan Composite Hydrogel for Bone Tissue Repair *In Vitro* and *In Vivo*. *J. Nanobiotechnol* 13, 13. doi:10.1186/s12951-015-0099-z
- Dilogo, I. H., Phedy, P., Kholinne, E., Djaja, Y. P., Fiolin, J., Kusnadi, Y., et al. (2019). Autologous Mesenchymal Stem Cell Implantation, Hydroxyapatite, Bone Morphogenetic Protein-2, and Internal Fixation for Treating Critical-Sized Defects: a Translational Study. *Int. Orthopaedics (Sicot)* 43 (6), 1509–1519. doi:10.1007/s00264-019-04307-z
- Ding, Z., Fan, Z., Huang, X., Lu, Q., Xu, W., and Kaplan, D. L. (2016). Silk-Hydroxyapatite Nanoscale Scaffolds with Programmable Growth Factor Delivery for Bone Repair. *ACS Appl. Mater. Inter.* 8 (37), 24463–24470. doi:10.1021/acsami.6b08180
- Dolanmaz, D., Saglam, M., Inan, O., Dundar, N., Alniacik, G., Gursoy Trak, B., et al. (2015). Monitoring Bone Morphogenetic Protein-2 and -7, Soluble Receptor Activator of Nuclear Factor-Kb Ligand and Osteoprotegerin Levels in the Peri-Implant Sulcular Fluid during the Osseointegration of Hydrophilic-Modified Sandblasted Acid-Etched and Sandblasted. *J. Periodont Res.* 50 (1), 62–73. doi:10.1111/jre.12182
- Duan, X., Bradbury, S. R., Olsen, B. R., and Berendsen, A. D. (2016). VEGF Stimulates Intramembranous Bone Formation during Craniofacial Skeletal Development. *Matrix Biol.* 52–54, 127–140. doi:10.1016/j.matbio.2016.02.005
- Einhorn, T. A., and Gerstenfeld, L. C. (2015). Fracture Healing: Mechanisms and Interventions. *Nat. Rev. Rheumatol.* 11 (1), 45–54. doi:10.1038/nrrheum.2014.164
- El-Magd, M. A., Allen, S., McGonnell, I., Otto, A., and Patel, K. (2013). Bmp4 regulates chick Ebf2 and Ebf3 gene Expression in Somite Development. *Develop. Growth Differ.* 55 (8), 710–722. doi:10.1111/dgd.12077
- Fiedler, J., Röderer, G., Günther, K.-P., and Brenner, R. E. (2002). BMP-2, BMP-4, and PDGF-Bb Stimulate Chemotactic Migration of Primary Human Mesenchymal Progenitor Cells. *J. Cel. Biochem.* 87 (3), 305–312. doi:10.1002/jcb.10309
- Fischerauer, E. E., Manninger, M., Seles, M., Janezic, G., Pichler, K., Ebner, B., et al. (2013). BMP-6 and BMPR-1a Are Up-Regulated in the Growth Plate of the Fractured Tibia. *J. Orthop. Res.* 31 (3), 357–363. doi:10.1002/jor.22238
- Flierl, M. A., Smith, W. R., Mauffrey, C., Irgit, K., Williams, A. E., Ross, E., et al. (2013). Outcomes and Complication Rates of Different Bone Grafting Modalities in Long Bone Fracture Nonunions: a Retrospective Cohort Study in 182 Patients. *J. Orthop. Surg. Res.* 8, 10. doi:10.1186/1749-799x-8-33
- Fu, S. C., Wong, Y. P., Chan, B. P., Pau, H. M., Cheuk, Y. C., Lee, K. M., et al. (2003). The Roles of Bone Morphogenetic Protein (BMP) 12 in Stimulating the Proliferation and Matrix Production of Human Patellar Tendon Fibroblasts. *Life Sci.* 72 (26), 2965–2974. doi:10.1016/s0024-3205(03)00169-3
- Geetha, M., Singh, A. K., Asokamani, R., and Gogia, A. K. (2009). Ti Based Biomaterials, the Ultimate Choice for Orthopaedic Implants - A Review. *Prog. Mater. Sci.* 54 (3), 397–425. doi:10.1016/j.pmatsci.2008.06.004
- Ghavimi, S. A. A., Lungren, E. S., Faulkner, T. J., Josselet, M. A., Wu, Y., Sun, Y., et al. (2019). Inductive Co-crosslinking of Cellulose Nanocrystal/chitosan Hydrogels for the Treatment of Vertebral Compression Fractures. *Int. J. Biol. Macromolecules* 130, 88–98. doi:10.1016/j.ijbiomac.2019.02.086
- Goldhahn, J., Scheele, W. H., Mitlak, B. H., Abadie, E., Aspenberg, P., Augat, P., et al. (2008). Clinical Evaluation of Medicinal Products for Acceleration of Fracture Healing in Patients with Osteoporosis. *Bone* 43 (2), 343–347. doi:10.1016/j.bone.2008.04.017
- Gomez-Puerto, M. C., Iyengar, P. V., Garcia de Vinuesa, A., ten Dijke, P., and Sanchez-Duffhues, G. (2019). Bone Morphogenetic Protein Receptor Signal Transduction in Human Disease. *J. Pathol.* 247 (1), 9–20. doi:10.1002/path.5170
- Gressot, L. V., Patel, A. J., Hwang, S. W., Fulkerson, D. H., and Jea, A. (2014). Rh-BMP-2 for L5-S1 Arthrodesis in Long Fusions to the Pelvis for Neuromuscular Spinal Deformity in the Pediatric Age Group: Analysis of 11 Patients. *Childs Nerv Syst.* 30 (2), 249–255. doi:10.1007/s00381-013-2221-6
- Grgurevic, L., Oppermann, H., Pecin, M., Erjavec, I., Capak, H., Pauk, M., et al. (2019). Recombinant Human Bone Morphogenetic Protein 6 Delivered within Autologous Blood Coagulum Restores Critical Size Segmental Defects of Ulna in Rabbits. *J. Bone Miner Res.* 34 (5), e10085. doi:10.1002/jbm.b.140085
- Gromolak, S., Krawczyński, A., Antończyk, A., Buczak, K., Kielbowicz, Z., and Klimczak, A. (2020). Biological Characteristics and Osteogenic Differentiation of Ovine Bone Marrow Derived Mesenchymal Stem Cells Stimulated with FGF-2 and BMP-2. *Int. J. Mol. Sci.* 21 (24), 9726. doi:10.3390/ijms21249726
- Guenther, C. A., Wang, Z., Li, E., Tran, M. C., Logan, C. Y., Nusse, R., et al. (2015). A Distinct Regulatory Region of the Bmp5 Locus Activates Gene Expression Following Adult Bone Fracture or Soft Tissue Injury. *Bone* 77, 31–41. doi:10.1016/j.bone.2015.04.010
- Guenther, C., Pantalena-Filho, L., and Kingsley, D. M. (2008). Shaping Skeletal Growth by Modular Regulatory Elements in the Bmp5 Gene. *Plos Genet.* 4 (12), e1000308. doi:10.1371/journal.pgen.1000308
- Guicheux, J., Lemonnier, J., Ghayor, C., Suzuki, A., Palmer, G., and Caverzasio, J. (2003). Activation of P38 Mitogen-Activated Protein Kinase and c-Jun-NH2-terminal Kinase by BMP-2 and Their Implication in the Stimulation of Osteoblastic Cell Differentiation. *J. Bone Miner Res.* 18 (11), 2060–2068. doi:10.1359/jbmr.2003.18.11.2060
- Hackl, S., Hierholzer, C., Friederichs, J., Woltmann, A., Bühren, V., and von Rüden, C. (2017). Long-term Outcome Following Additional rhBMP-7 Application in Revision Surgery of Aseptic Humeral, Femoral, and Tibial Shaft Nonunion. *BMC Musculoskelet. Disord.* 18, 10. doi:10.1186/s12891-017-1704-0
- Haddad-Weber, M., Prager, P., Kunz, M., Seefried, L., Jakob, F., Murray, M. M., et al. (2010). BMP12 and BMP13 Gene Transfer Induce Ligamentogenic Differentiation in Mesenchymal Progenitor and Anterior Cruciate Ligament Cells. *Cytotherapy* 12 (4), 505–513. doi:10.3109/14653241003709652
- Han, C.-M., Jang, T.-S., Kim, H.-E., and Koh, Y.-H. (2014). Creation of Nanoporous TiO₂ surface onto Polyetheretherketone for Effective Immobilization and Delivery of Bone Morphogenetic Protein. *J. Biomed. Mater. Res.* 102 (3), 793–800. doi:10.1002/jbm.a.34748
- Hatakeyama, Y., Tuan, R. S., and Shum, L. (2004). Distinct Functions of BMP4 and GDF5 in the Regulation of Chondrogenesis. *J. Cel. Biochem.* 91 (6), 1204–1217. doi:10.1002/jcb.20019
- Henn, R. F., Kuo, C. E., Kessler, M. W., Razzano, P., Grande, D. P., and Wolfe, S. W. (2010). Augmentation of Zone II Flexor Tendon Repair Using Growth Differentiation Factor 5 in a Rabbit Model. *J. Hand Surg.* 35 (11), 1825–1832. doi:10.1016/j.jhsa.2010.08.031
- Herford, A. S., and Boyne, P. J. (2008). Reconstruction of Mandibular Continuity Defects with Bone Morphogenetic Protein-2 (rhBMP-2). *J. Oral Maxillofac. Surg.* 66 (4), 616–624. doi:10.1016/j.joms.2007.11.021
- Hettiaratchi, M. H., Krishnan, L., Rouse, T., Chou, C., McDevitt, T. C., and Guldberg, R. E. (2020). Heparin-mediated Delivery of Bone Morphogenetic Protein-2 Improves Spatial Localization of Bone Regeneration. *Sci. Adv.* 6 (1), eaay1240. doi:10.1126/sciadv.aay1240

- Hissnauer, T. N., Stiel, N., Babin, K., Rupprecht, M., Hoffmann, M., Rueger, J. M., et al. (2017). Bone Morphogenetic Protein-2 for the Treatment of Congenital Pseudarthrosis of the Tibia or Persistent Tibial Nonunion in Children and Adolescents: A Retrospective Study with a Minimum 2-year Follow-Up. *J. Mater. Sci. Mater. Med.* 28 (4), 8. doi:10.1007/s10856-017-5868-9
- Hu, Y., Cai, K., Luo, Z., Zhang, Y., Li, L., Lai, M., et al. (2012). Regulation of the Differentiation of Mesenchymal Stem Cells *In Vitro* and Osteogenesis *In Vivo* by Microenvironmental Modification of Titanium alloy Surfaces. *Biomaterials* 33 (13), 3515–3528. doi:10.1016/j.biomaterials.2012.01.040
- Hu, Y., Zhao, Q.-W., Wang, Z.-C., Fang, Q.-Q., Zhu, H., Hong, D.-S., et al. (2021). Co-transfection with BMP2 and FGF2 via Chitosan Nanoparticles Potentiates Osteogenesis in Human Adipose-Derived Stromal Cells *In Vitro*. *J. Int. Med. Res.* 49 (3), 030006052199767. doi:10.1177/0300060521997679
- Huang, B., Wu, Z., Ding, S., Yuan, Y., and Liu, C. (2018). Localization and Promotion of Recombinant Human Bone Morphogenetic Protein-2 Bioactivity on Extracellular Matrix Mimetic Chondroitin Sulfate-Functionalized Calcium Phosphate Cement Scaffolds. *Acta Biomater.* 71, 184–199. doi:10.1016/j.actbio.2018.01.004
- Injamuri, S., Rahaman, M. N., Shen, Y., and Huang, Y. W. (2020). Relaxin Enhances Bone Regeneration with BMP-2-loaded Hydroxyapatite Microspheres. *J. Biomed. Mater. Res.* 108 (5), 1231–1242. doi:10.1002/jbm.a.36897
- Ishack, S., Mediero, A., Wilder, T., Ricci, J. L., and Cronstein, B. N. (2017). Bone Regeneration in Critical Bone Defects Using Three-Dimensionally Printed β -tricalcium Phosphate/hydroxyapatite Scaffolds Is Enhanced by Coating Scaffolds with Either Dipyrindamole or BMP-2. *J. Biomed. Mater. Res.* 105 (2), 366–375. doi:10.1002/jbm.b.33561
- Jain, E., Chinzei, N., Blanco, A., Case, N., Sandell, L. J., Sell, S., et al. (2019). Platelet-Rich Plasma Released from Polyethylene Glycol Hydrogels Exerts Beneficial Effects on Human Chondrocytes. *J. Orthop. Res.* 37 (11), 2401–2410. doi:10.1002/jor.24404
- Jang, Y., Jung, H., Nam, Y., Rim, Y. A., Kim, J., Jeong, S. H., et al. (2016). Centrifugal Gravity-Induced BMP4 Induces Chondrogenic Differentiation of Adipose-Derived Stem Cells via SOX9 Upregulation. *Stem Cell Res Ther* 7, 10. doi:10.1186/s13287-016-0445-6
- Jensen, O. T., Cottam, J., Ringeman, J., and Adams, M. (2012). Trans-Sinus Dental Implants, Bone Morphogenetic Protein 2, and Immediate Function for All-On-4 Treatment of Severe Maxillary Atrophy. *J. Oral Maxillofac. Surg.* 70 (1), 141–148. doi:10.1016/j.joms.2011.03.045
- Jin, R., Moreira Teixeira, L. S., Krouwels, A., Dijkstra, P. J., van Blitterswijk, C. A., Karperien, M., et al. (2010). Synthesis and Characterization of Hyaluronic Acid-Poly(ethylene Glycol) Hydrogels via Michael Addition: An Injectable Biomaterial for Cartilage Repair. *Acta Biomater.* 6 (6), 1968–1977. doi:10.1016/j.actbio.2009.12.024
- Jones, A. L., Bucholz, R. W., Bosse, M. J., Mirza, S. K., Lyon, T. R., Webb, L. X., et al. (2006). Recombinant Human BMP-2 and Allograft Compared with Autogenous Bone Graft for Reconstruction of Diaphyseal Tibial Fractures with Cortical Defects. *J. Bone Jt. Surg.* 88 (7), 1431–1441. doi:10.2106/jbjs.E.00381
- Kaneko, H., Arakawa, T., Mano, H., Kaneda, T., Ogasawara, A., Nakagawa, M., et al. (2000). Direct Stimulation of Osteoclastic Bone Resorption by Bone Morphogenetic Protein (BMP)-2 and Expression of BMP Receptors in Mature Osteoclasts. *Bone* 27 (4), 479–486. doi:10.1016/s8756-3282(00)00358-6
- Kayabasi, G. K., Tigli Aydin, R. S., and Gümüşdereliolu, M. (2013). In Vitro chondrogenesis by BMP6 Gene Therapy. *J. Biomed. Mater. Res.* 101A (5), 1353–1361. doi:10.1002/jbm.a.34430
- Kempen, D. H. R., Lu, L., Heijink, A., Hefferan, T. E., Creemers, L. B., Maran, A., et al. (2009). Effect of Local Sequential VEGF and BMP-2 Delivery on Ectopic and Orthotopic Bone Regeneration. *Biomaterials* 30 (14), 2816–2825. doi:10.1016/j.biomaterials.2009.01.031
- Kim, S.-S., Sun Park, M., Jeon, O., Yong Choi, C., and Kim, B.-S. (2006). Poly(lactide-co-glycolide)/hydroxyapatite Composite Scaffolds for Bone Tissue Engineering. *Biomaterials* 27 (8), 1399–1409. doi:10.1016/j.biomaterials.2005.08.016
- Kim, Y., Kang, B.-J., Kim, W., Yun, H.-s., and Kweon, O.-k. (2018). Evaluation of Mesenchymal Stem Cell Sheets Overexpressing BMP-7 in Canine Critical-Sized Bone Defects. *Int. J. Mol. Sci.* 19 (7), 2073. doi:10.3390/ijms19072073
- Klosterhoff, B. S., Vantucci, C. E., Kaiser, J., Ong, K. G., Wood, L. B., Weiss, J. A., et al. (2022). Effects of Osteogenic Ambulatory Mechanical Stimulation on Early Stages of BMP-2 Mediated Bone Repair. *Connect. Tissue Res.* 63, 16–27. doi:10.1080/03008207.2021.1897582
- Ko, E., Yang, K., Shin, J., and Cho, S.-W. (2013). Polydopamine-Assisted Osteoinductive Peptide Immobilization of Polymer Scaffolds for Enhanced Bone Regeneration by Human Adipose-Derived Stem Cells. *Biomacromolecules* 14 (9), 3202–3213. doi:10.1021/bm4008343
- Koenig, B. B., Cook, J. S., Wolsing, D. H., Ting, J., Tiesman, J. P., Correa, P. E., et al. (1994). Characterization and Cloning of a Receptor for BMP-2 and BMP-4 from NIH 3T3 Cells. *Mol. Cell Biol.* 14 (9), 5961–5974. doi:10.1128/mcb.14.9.5961
- Kolambkar, Y. M., Dupont, K. M., Boerckel, J. D., Huebsch, N., Mooney, D. J., Huttmacher, D. W., et al. (2011). An Alginate-Based Hybrid System for Growth Factor Delivery in the Functional Repair of Large Bone Defects. *Biomaterials* 32 (1), 65–74. doi:10.1016/j.biomaterials.2010.08.074
- Kong, D., Shi, Y., Gao, Y., Fu, M., Kong, S., and Lin, G. (2020). Preparation of BMP-2 Loaded MPEG-PCL Microspheres and Evaluation of Their Bone Repair Properties. *Biomed. Pharmacother.* 130, 110516. doi:10.1016/j.biopha.2020.110516
- Koons, G. L., Kontoyiannis, P. D., Diba, M., Chim, L. K., Scott, D. W., and Mikos, A. G. (2021). Effect of 3D Printing Temperature on Bioactivity of Bone Morphogenetic Protein-2 Released from Polymeric Constructs. *Ann. Biomed. Eng.* 49 (9), 2114–2125. doi:10.1007/s10439-021-02736-9
- Kostenuik, P., and Mirza, F. M. (2017). Fracture Healing Physiology and the Quest for Therapies for Delayed Healing and Nonunion. *J. Orthop. Res.* 35 (2), 213–223. doi:10.1002/jor.23460
- Krishnan, V., Ma, Y. L., Moseley, J. M., Geiser, A. G., Friant, S., and Frolik, C. A. (2001). Bone Anabolic Effects of Sonic/Indian Hedgehog Are Mediated by BMP-2/4-dependent Pathways in the Neonatal Rat Metatarsal Model. *Endocrinology* 142 (2), 940–947. doi:10.1210/endo.142.2.7922
- Kusuyama, J., Seong, C., Nakamura, T., Ohnishi, T., Amir, M. S., Shima, K., et al. (2019). BMP9 Prevents Induction of Osteopontin in JNK-Inactivated Osteoblasts via Hey1-Id4 Interaction. *Int. J. Biochem. Cell Biol.* 116, 105614. doi:10.1016/j.biocel.2019.105614
- Lamplot, J. D., Angeline, M., Angeles, J., Beederman, M., Wagner, E., Rastegar, F., et al. (2014). Distinct Effects of Platelet-Rich Plasma and BMP13 on Rotator Cuff Tendon Injury Healing in a Rat Model. *Am. J. Sports Med.* 42 (12), 2877–2887. doi:10.1177/0363546514547171
- Larochette, N., El-Hafci, H., Potier, E., Setterblad, N., Bensidhoum, M., Petite, H., et al. (2020). Osteogenic-differentiated Mesenchymal Stem Cell-Secreted Extracellular Matrix as a Bone Morphogenetic Protein-2 Delivery System for Ectopic Bone Formation. *Acta Biomater.* 116, 186–200. doi:10.1016/j.actbio.2020.09.003
- Laurencin, C., Attawia, M. A., Lu, L. Q., Borden, M. D., Lu, H. H., Gorum, W. J., et al. (2001). Poly(lactide-co-glycolide)/hydroxyapatite Delivery of BMP-2-Producing Cells: a Regional Gene Therapy Approach to Bone Regeneration. *Biomaterials* 22 (11), 1271–1277. doi:10.1016/s0142-9612(00)00279-9
- Lavery, K., Swain, P., Falb, D., and Alaoui-Ismaili, M. H. (2008). BMP-2/4 and BMP-6/7 Differentially Utilize Cell Surface Receptors to Induce Osteoblastic Differentiation of Human Bone Marrow-Derived Mesenchymal Stem Cells. *J. Biol. Chem.* 283 (30), 20948–20958. doi:10.1074/jbc.M800850200
- Lee, D., Wufuer, M., Kim, I., Choi, T. H., Kim, B. J., Jung, H. G., et al. (2021). Sequential Dual-Drug Delivery of BMP-2 and Alendronate from Hydroxyapatite-Collagen Scaffolds for Enhanced Bone Regeneration. *Sci. Rep.* 11 (1), 746. doi:10.1038/s41598-020-80608-3
- Lee, E.-U., Lim, H.-C., Hong, J.-Y., Lee, J.-S., Jung, U.-W., and Choi, S.-H. (2016). Bone Regenerative Efficacy of Biphasic Calcium Phosphate Collagen Composite as a Carrier of rhBMP-2. *Clin. Oral Impl. Res.* 27 (11), e91–e99. doi:10.1111/clr.12568
- Lee, M.-H., Kwon, T.-G., Park, H.-S., Wozney, J. M., and Ryoo, H.-M. (2003). BMP-2-induced Osterix Expression Is Mediated by Dlx5 but Is Independent of Runx2. *Biochem. Biophysical Res. Commun.* 309 (3), 689–694. doi:10.1016/j.bbrc.2003.08.058
- Li, A., Li, J., Zhang, Z., Li, Z., Chi, H., Song, C., et al. (2021). Nanohydroxyapatite/polyamide 66 Crosslinked with QK and BMP-2-Derived Peptide Prevented Femur Nonunion in Rats. *J. Mater. Chem. B* 9 (9), 2249–2265. doi:10.1039/d0tb02554b

- Li, C., Vepari, C., Jin, H.-J., Kim, H. J., and Kaplan, D. L. (2006). Electrospun Silk-BMP-2 Scaffolds for Bone Tissue Engineering. *Biomaterials* 27 (16), 3115–3124. doi:10.1016/j.biomaterials.2006.01.022
- Li, L., Jiang, Y., Lin, H., Shen, H., Sohn, J., Alexander, P. G., et al. (2019). Muscle Injury Promotes Heterotopic Ossification by Stimulating Local Bone Morphogenetic Protein-7 Production. *J. Orthopaedic Translation* 18, 142–153. doi:10.1016/j.jot.2019.06.001
- Li, S., Li, X., Hou, W., Nune, K. C., Misra, R. D. K., Correa-Rodriguez, V. L., et al. (2018). Fabrication of Open-Cellular (Porous) Titanium alloy Implants: Osseointegration, Vascularization and Preliminary Human Trials. *Sci. China Mater.* 61 (4), 525–536. doi:10.1007/s40843-017-9063-6
- Li, Y., Liu, Y., Bai, H., Li, R., Shang, J., Zhu, Z., et al. (2021a). Sustained Release of VEGF to Promote Angiogenesis and Osteointegration of Three-Dimensional Printed Biomimetic Titanium Alloy Implants. *Front. Bioeng. Biotechnol.* 9, 757767. doi:10.3389/fbioe.2021.757767
- Li, Y., Liu, Y., and Guo, Q. (2021b). Silk Fibroin Hydrogel Scaffolds Incorporated with Chitosan Nanoparticles Repair Articular Cartilage Defects by Regulating TGF- β 1 and BMP-2. *Arthritis Res. Ther.* 23 (1), 50. doi:10.1186/s13075-020-02382-x
- Li, Y., Liu, Y., Li, R., Bai, H., Zhu, Z., Zhu, L., et al. (2021c). Collagen-based Biomaterials for Bone Tissue Engineering. *Mater. Des.* 210, 110049. doi:10.1016/j.matdes.2021.110049
- Lieberman, J. R., Le, L. Q., Wu, L., Finerman, G. A. M., Berk, A., Witte, O. N., et al. (1998). Regional Gene Therapy with a BMP-2-Producing Murine Stromal Cell Line Induces Heterotopic and Orthotopic Bone Formation in Rodents. *J. Orthop. Res.* 16 (3), 330–339. doi:10.1002/jor.1100160309
- Liu, F., Ventura, F., Doody, J., and Massagué, J. (1995). Human Type II Receptor for Bone Morphogenetic Proteins (BMPs): Extension of the Two-Kinase Receptor Model to the BMPs. *Mol. Cell Biol.* 15 (7), 3479–3486. doi:10.1128/mcb.15.7.3479
- Liu, K., Meng, C.-X., Lv, Z.-Y., Zhang, Y.-J., Li, J., Li, K.-Y., et al. (2020). Enhancement of BMP-2 and VEGF Carried by Mineralized Collagen for Mandibular Bone Regeneration. *Regenerative Biomater.* 7 (4), 435–440. doi:10.1093/rb/rbaa022
- Liu, Y., Degroot, K., and Hunziker, E. (2005). BMP-2 Liberated from Biomimetic Implant Coatings Induces and Sustains Direct Ossification in an Ectopic Rat Model. *Bone* 36 (5), 745–757. doi:10.1016/j.bone.2005.02.005
- Liu, Y., Enggist, L., Küffer, A. F., Buser, D., and Hunziker, E. B. (2007). The Influence of BMP-2 and its Mode of Delivery on the Osteoconductivity of Implant Surfaces during the Early Phase of Osseointegration. *Biomaterials* 28 (16), 2677–2686. doi:10.1016/j.biomaterials.2007.02.003
- Long, F., Shi, H., Li, P., Guo, S., Ma, Y., Wei, S., et al. (2021). A SMO2 Variant Inhibits BMP Signaling by Competitively Binding to BMPRII and Causes Growth Plate Defects. *Bone* 142, 115686. doi:10.1016/j.bone.2020.115686
- Luu, H. H., Song, W.-X., Luo, X., Manning, D., Luo, J., Deng, Z.-L., et al. (2007). Distinct Roles of Bone Morphogenetic Proteins in Osteogenic Differentiation of Mesenchymal Stem Cells. *J. Orthop. Res.* 25 (5), 665–677. doi:10.1002/jor.20359
- Meisel, H. J., Schnöring, M., Hohaus, C., Minkus, Y., Beier, A., Ganey, T., et al. (2008). Posterior Lumbar Interbody Fusion Using rhBMP-2. *Eur. Spine J.* 17 (12), 1735–1744. doi:10.1007/s00586-008-0799-2
- Meng, C., Su, W., Liu, M., Yao, S., Ding, Q., Yu, K., et al. (2021). Controlled Delivery of Bone Morphogenetic Protein-2-Related Peptide from Mineralised Extracellular Matrix-Based Scaffold Induces Bone Regeneration. *Mater. Sci. Eng. C* 126, 112182. doi:10.1016/j.msec.2021.112182
- Miyazawa, K., Shinozaki, M., Hara, T., Furuya, T., and Miyazono, K. (2002). Two Major Smad Pathways in TGF- β Superfamily Signalling. *Genes To Cells* 7 (12), 1191–1204. doi:10.1046/j.1365-2443.2002.00599.x
- Müller, S., Lindemann, S., and Gigout, A. (2019). Effects of Sprifermin, IGF1, IGF2, BMP7, or CNP on Bovine Chondrocytes in Monolayer and 3D Culture. *J. Orthop. Res.* 38, 653–662. doi:10.1002/jor.24491
- Nam, J. W., Khureltogtokh, S., Choi, H. M., Lee, A. R., Park, Y. B., and Kim, H. J. (2017). Randomised Controlled Clinical Trial of Augmentation of the Alveolar Ridge Using Recombinant Human Bone Morphogenetic Protein 2 with Hydroxyapatite and Bovine-Derived Xenografts: Comparison of Changes in Volume. *Br. J. Oral Maxillofac. Surg.* 55 (8), 822–829. doi:10.1016/j.bjoms.2017.07.017
- Nie, H., and Wang, C.-H. (2007). Fabrication and Characterization of PLGA/HAP Composite Scaffolds for Delivery of BMP-2 Plasmid DNA. *J. Controlled Release* 120 (1–2), 111–121. doi:10.1016/j.jconrel.2007.03.018
- Nishimura, R., Kato, Y., Chen, D., Harris, S. E., Mundy, G. R., and Yoneda, T. (1998). Smad5 and DPC4 Are Key Molecules in Mediating BMP-2-Induced Osteoblastic Differentiation of the Pluripotent Mesenchymal Precursor Cell Line C2C12. *J. Biol. Chem.* 273 (4), 1872–1879. doi:10.1074/jbc.273.4.1872
- Nosho, S., Tosa, I., Ono, M., Hara, E. S., Ishibashi, K., Mikai, A., et al. (2020). Distinct Osteogenic Potentials of BMP-2 and FGF-2 in Extramedullary and Medullary Microenvironments. *Int. J. Mol. Sci.* 21 (21), 7967. doi:10.3390/ijms21217967
- Park, J.-H., Kim, J.-W., and Kim, S.-J. (2017). Does the Addition of Bone Morphogenetic Protein 2 to Platelet-Rich Fibrin Improve Healing after Treatment for Medication-Related Osteonecrosis of the Jaw? *J. Oral Maxillofac. Surg.* 75 (6), 1176–1184. doi:10.1016/j.joms.2016.12.005
- Pelled, G., Sheyn, D., Tawackoli, W., Jun, D. S., Koh, Y., Su, S., et al. (2016). BMP6-Engineered MSCs Induce Vertebral Bone Repair in a Pig Model: A Pilot Study. *Stem Cell Int.* 2016, 1–8. doi:10.1155/2016/6530624
- Peng, H., Usas, A., Olshanski, A., Ho, A. M., Gearhart, B., Cooper, G. M., et al. (2005). VEGF Improves, whereas sFlt1 Inhibits, BMP2-Induced Bone Formation and Bone Healing through Modulation of Angiogenesis. *J. Bone Miner Res.* 20 (11), 2017–2027. doi:10.1359/jbmr.050708
- Peng, H., Wright, V., Usas, A., Gearhart, B., Shen, H.-C., Cummins, J., et al. (2002). Synergistic Enhancement of Bone Formation and Healing by Stem Cell-Expressed VEGF and Bone Morphogenetic Protein-4. *J. Clin. Invest.* 110 (6), 751–759. doi:10.1172/jci15153
- Pera, M. F., Andrade, J., Houssami, S., Reubini, B., Trounson, A., Stanley, E. G., et al. (2004). Regulation of Human Embryonic Stem Cell Differentiation by BMP-2 and its Antagonist Noggin. *J. Cell Sci.* 117 (7), 1269–1280. doi:10.1242/jcs.00970
- Percival, C. J., and Richtsmeier, J. T. (2013). Angiogenesis and Intramembranous Osteogenesis. *Dev. Dyn.* 242 (8), 909–922. doi:10.1002/dvdy.23992
- Pini, J., Giuliano, S., Matonti, J., Gannoun, L., Simkin, D., Rouleau, M., et al. (2018). Osteogenic and Chondrogenic Master Genes Expression Is Dependent on the Kir2.1 Potassium Channel through the Bone Morphogenetic Protein Pathway. *J. Bone Miner Res.* 33 (10), 1826–1841. doi:10.1002/jbmr.3474
- Poynton, A. R., and Lane, J. M. (2002). Safety Profile for the Clinical Use of Bone Morphogenetic Proteins in the Spine. *Spine* 27 (16), S40–S48. doi:10.1097/00007632-200208151-00010
- Quade, M., Vater, C., Schlootz, S., Bolte, J., Langanke, R., Bretschneider, H., et al. (2020). Strontium Enhances BMP-2 Mediated Bone Regeneration in a Femoral Murine Bone Defect Model. *J. Biomed. Mater. Res.* 108 (1), 174–182. doi:10.1002/jbm.b.34376
- Rajabnejad keleshteri, A., Moztarzadeh, F., Farokhi, M., Mehrizi, A. A., Basiri, H., and Mohseni, S. S. (2021). Preparation of Microfluidic-Based Pectin Microparticles Loaded Carbon Dots Conjugated with BMP-2 Embedded in Gelatin-Elastin-Hyaluronic Acid Hydrogel Scaffold for Bone Tissue Engineering Application. *Int. J. Biol. Macromolecules* 184, 29–41. doi:10.1016/j.ijbiomac.2021.05.148
- Rawadi, G., Vayssière, B., Dunn, F., Baron, R., and Roman-Roman, S. (2003). BMP-2 Controls Alkaline Phosphatase Expression and Osteoblast Mineralization by a Wnt Autocrine Loop. *J. Bone Miner Res.* 18 (10), 1842–1853. doi:10.1359/jbmr.2003.18.10.1842
- Ren, X., Weisgerber, D. W., Bischoff, D., Lewis, M. S., Reid, R. R., He, T.-C., et al. (2016). Nanoparticulate Mineralized Collagen Scaffolds and BMP-9 Induce a Long-Term Bone Cartilage Construct in Human Mesenchymal Stem Cells. *Adv. Healthc. Mater.* 5 (14), 1821–1830. doi:10.1002/adhm.201600187
- Rickard, D. J., Sullivan, T. A., Shenker, B. J., Leboy, P. S., and Kazhdan, I. (1994). Induction of Rapid Osteoblastic Differentiation in Rat Bone Marrow Stromal Cell Cultures by Dexamethasone and BMP-2. *Develop. Biol.* 161 (1), 218–228. doi:10.1006/dbio.1994.1022
- Rihn, J. A., Patel, R., Makda, J., Hong, J., Anderson, D. G., Vaccaro, A. R., et al. (2009). Complications Associated with Single-Level Transforaminal Lumbar Interbody Fusion. *Spine J.* 9 (8), 623–629. doi:10.1016/j.spinee.2009.04.004
- Ruvinov, E., Tavor Re'em, T., Witte, F., and Cohen, S. (2019). Articular Cartilage Regeneration Using Acellular Bioactive Affinity-Binding Alginate Hydrogel: A 6-month Study in a Mini-Pig Model of Osteochondral Defects. *J. Orthopaedic Translation* 16, 40–52. doi:10.1016/j.jot.2018.08.003

- Sang, Y., Zang, W., Yan, Y., Liu, Y., Fu, Q., Wang, K., et al. (2014). Study of Differential Effects of TGF- β 3/BMP2 on Chondrogenesis in MSC Cells by Gene Microarray Data Analysis. *Mol. Cel Biochem* 385 (1-2), 191–198. doi:10.1007/s11010-013-1827-z
- Sayama, C., Hadley, C., Monaco, G. N., Sen, A., Brayton, A., Briceño, V., et al. (2015). The Efficacy of Routine Use of Recombinant Human Bone Morphogenetic Protein-2 in Occipitocervical and Atlantoaxial Fusions of the Pediatric Spine: a Minimum of 12 Months' Follow-Up with Computed Tomography. *J. Neurosurg. Pediatr.* 16 (1), 14–20. doi:10.3171/2015.2.Peds14533
- Seo, B.-B., Koh, J.-T., and Song, S.-C. (2017). Tuning Physical Properties and BMP-2 Release Rates of Injectable Hydrogel Systems for an Optimal Bone Regeneration Effect. *Biomaterials* 122, 91–104. doi:10.1016/j.biomaterials.2017.01.016
- Seo, J.-p., Tsuzuki, N., Haneda, S., Yamada, K., Furuoka, H., Tabata, Y., et al. (2014). Osteoinductivity of Gelatin/ β -Tricalcium Phosphate Sponges Loaded with Different Concentrations of Mesenchymal Stem Cells and Bone Morphogenetic Protein-2 in an Equine Bone Defect Model. *Vet. Res. Commun.* 38 (1), 73–80. doi:10.1007/s11259-013-9587-5
- Shen, X., Zhang, Y., Gu, Y., Xu, Y., Liu, Y., Li, B., et al. (2016). Sequential and Sustained Release of SDF-1 and BMP-2 from Silk Fibroin-Nanohydroxyapatite Scaffold for the Enhancement of Bone Regeneration. *Biomaterials* 106, 205–216. doi:10.1016/j.biomaterials.2016.08.023
- Shu, B., Zhang, M., Xie, R., Wang, M., Jin, H., Hou, W., et al. (2011). BMP2, but Not BMP4, Is Crucial for Chondrocyte Proliferation and Maturation during Endochondral Bone Development. *J. Cel Sci.* 124 (20), 3428–3440. doi:10.1242/jcs.083659
- Shum, L., Wang, X., Kane, A. A., and Nuckolls, G. H. (2003). BMP4 Promotes Chondrocyte Proliferation and Hypertrophy in the Endochondral Cranial Base. *Int. J. Dev. Biol.* 47 (6), 423–431. <http://www.ijdb.edu.es/web/paper.php?doi=14598792>
- Singh, K., Nandiyala, S. V., Marquez-Lara, A., Cha, T. D., Khan, S. N., Fineberg, S. J., et al. (2013). Clinical Sequelae after rhBMP-2 Use in a Minimally Invasive Transforaminal Lumbar Interbody Fusion. *Spine J.* 13 (9), 1118–1125. doi:10.1016/j.spinee.2013.07.028
- Singh, R., Bleibleh, S., Kanakaris, N. K., and Giannoudis, P. V. (2016). Upper Limb Non-unions Treated with BMP-7: Efficacy and Clinical Results. *Injury* 47, S33–S39. doi:10.1016/s0020-1383(16)30837-3
- Snelling, S. J. B., Hulley, P. A., and Loughlin, J. (2010). BMP5 Activates Multiple Signaling Pathways and Promotes Chondrogenic Differentiation in the ATDC5 Growth Plate Model. *Growth Factors* 28 (4), 268–279. doi:10.3109/08977191003752296
- Sojo, K., Sawaki, Y., Hattori, H., Mizutani, H., and Ueda, M. (2005). Immunohistochemical Study of Vascular Endothelial Growth Factor (VEGF) and Bone Morphogenetic Protein-2, -4 (BMP-2, -4) on Lengthened Rat Femurs. *J. Craniomaxillofac. Surg.* 33 (4), 238–245. doi:10.1016/j.jcms.2005.02.004
- Song, Y., Ju, Y., Morita, Y., Xu, B., and Song, G. (2014). Surface Functionalization of Nanoporous Alumina with Bone Morphogenetic Protein 2 for Inducing Osteogenic Differentiation of Mesenchymal Stem Cells. *Mater. Sci. Eng. C* 37, 120–126. doi:10.1016/j.msec.2014.01.004
- Stiel, N., Stuecker, R., Kunkel, P., Ridderbusch, K., Hagemann, C., Breyer, S., et al. (2018). Treatment of Pediatric Spinal Deformity with Use of Recombinant Human Bone Morphogenetic Protein-2. *J. Mater. Sci. Mater. Med.* 29 (7), 6. doi:10.1007/s10856-018-6104-y
- Strong, A. L., Spreadborough, P. J., Dey, D., Yang, P., Li, S., Lee, A., et al. (2021). BMP Ligand Trap ALK3-Fc Attenuates Osteogenesis and Heterotopic Ossification in Blast-Related Lower Extremity Trauma. *Stem Cell Develop.* 30 (2), 91–105. doi:10.1089/scd.2020.0162
- Subbiah, R., Cheng, A., Ruehle, M. A., Hettiaratchi, M. H., Bertassoni, L. E., and Guldberg, R. E. (2020). Effects of Controlled Dual Growth Factor Delivery on Bone Regeneration Following Composite Bone-Muscle Injury. *Acta Biomater.* 114, 63–75. doi:10.1016/j.actbio.2020.07.026
- Sul, Y.-T., Johansson, C. B., Petronis, S., Krozer, A., Jeong, Y., Wennerberg, A., et al. (2002). Characteristics of the Surface Oxides on Turned and Electrochemically Oxidized Pure Titanium Implants up to Dielectric Breakdown. *Biomaterials* 23 (2), 491–501. doi:10.1016/s0142-9612(01)00131-4
- Suttapreyasri, S., Koontongkaew, S., Phongdara, A., and Leggat, U. (2006). Expression of Bone Morphogenetic Proteins in normal Human Intramembranous and Endochondral Bones. *Int. J. Oral Maxillofac. Surg.* 35 (5), 444–452. doi:10.1016/j.ijom.2006.01.021
- Taghavi, M., Parham, A., and Raji, A. (2020). The Combination of TGF-B3 and BMP-6 Synergistically Promotes the Chondrogenic Differentiation of Equine Bone Marrow-Derived Mesenchymal Stem Cells. *Int. J. Pept. Res. Ther.* 26 (2), 727–735. doi:10.1007/s10989-019-09880-w
- Tan, K. H., Chua, C. K., Leong, K. F., Cheah, C. M., Cheang, P., Abu Bakar, M. S., et al. (2003). Scaffold Development Using Selective Laser Sintering of Polyetheretherketone-Hydroxyapatite Biocomposite Blends. *Biomaterials* 24 (18), 3115–3123. doi:10.1016/s0142-9612(03)00131-5
- Taniguchi, N., Fujibayashi, S., Takemoto, M., Sasaki, K., Otsuki, B., Nakamura, T., et al. (2016). Effect of Pore Size on Bone Ingrowth into Porous Titanium Implants Fabricated by Additive Manufacturing: An *In Vivo* experiment. *Mater. Sci. Eng. C* 59, 690–701. doi:10.1016/j.msec.2015.10.069
- Tao, B., Deng, Y., Song, L., Ma, W., Qian, Y., Lin, C., et al. (2019). BMP2-loaded Titania Nanotubes Coating with pH-Responsive Multilayers for Bacterial Infections Inhibition and Osteogenic Activity Improvement. *Colloids Surf. B: Biointerfaces* 177, 242–252. doi:10.1016/j.colsurfb.2019.02.014
- Teng, F.-Y., Tai, I.-C., Ho, M.-L., Wang, J.-W., Weng, L. W., Wang, Y. J., et al. (2019). Controlled Release of BMP-2 from Titanium with Electrodeposition Modification Enhancing Critical Size Bone Formation. *Mater. Sci. Eng. C* 105, 109879. doi:10.1016/j.msec.2019.109879
- Teotia, A. K., Raina, D. B., Singh, C., Sinha, N., Isaksson, H., Tägil, M., et al. (2017). Nano-Hydroxyapatite Bone Substitute Functionalized with Bone Active Molecules for Enhanced Cranial Bone Regeneration. *ACS Appl. Mater. Inter.* 9 (8), 6816–6828. doi:10.1021/acsami.6b14782
- Toprak, Ö., Topuz, B., Monsef, Y. A., Oto, Ç., Orhan, K., and Karakeçili, A. (2021). BMP-6 Carrying Metal Organic Framework-Embedded in Bioresorbable Electrospun Fibers for Enhanced Bone Regeneration. *Mater. Sci. Eng. C* 120, 111738. doi:10.1016/j.msec.2020.111738
- Toth, J. M., Wang, M., Estes, B. T., Scifert, J. L., Seim, H. B., and Turner, A. S. (2006). Polyetheretherketone as a Biomaterial for Spinal Applications. *Biomaterials* 27 (3), 324–334. doi:10.1016/j.biomaterials.2005.07.011
- Tsuji, K., Bandyopadhyay, A., Harfe, B. D., Cox, K., Kakar, S., Gerstenfeld, L., et al. (2006). BMP2 Activity, Although Dispensable for Bone Formation, Is Required for the Initiation of Fracture Healing. *Nat. Genet.* 38 (12), 1424–1429. doi:10.1038/ng1916
- Urist, M. R. (1965). Bone: Formation by Autoinduction. *Science* 150 (3698), 893–899. doi:10.1126/science.150.3698.893
- Vaidya, R., Sethi, A., Bartol, S., Jacobson, M., Coe, C., and Craig, J. G. (2008). Complications in the Use of rhBMP-2 in PEEK Cages for Interbody Spinal Fusions. *J. Spinal Disord. Tech.* 21 (8), 557–562. doi:10.1097/BSD.0b013e31815ea897
- van Caam, A., Blaney Davidson, E., Garcia de Vinuesa, A., van Geffen, E., van den Berg, W., Goumans, M.-J., et al. (2015). The High Affinity ALK1-Ligand BMP9 Induces a Hypertrophy-like State in Chondrocytes that Is Antagonized by TGF β 1. *Osteoarthritis and Cartilage* 23 (6), 985–995. doi:10.1016/j.joca.2015.02.007
- Vantucci, C. E., Krishan, L., Cheng, A., Prather, A., Roy, K., and Guldberg, R. E. (2021). BMP-2 Delivery Strategy Modulates Local Bone Regeneration and Systemic Immune Responses to Complex Extremity Trauma. *Biomater. Sci.* 9 (5), 1668–1682. doi:10.1039/d0bm01728k
- von Rüden, C., Morgenstern, M., Hierholzer, C., Hackl, S., Gradinger, F. L., Woltmann, A., et al. (2016). The Missing Effect of Human Recombinant Bone Morphogenetic Proteins BMP-2 and BMP-7 in Surgical Treatment of Aseptic Forearm Nonunion. *Injury* 47 (4), 919–924. doi:10.1016/j.injury.2015.11.038
- von Wilmowsky, C., Vairaktaris, E., Pohle, D., Rechtenwald, T., Lutz, R., Münstedt, H., et al. (2008). Effects of Bioactive Glass and β -TCP Containing Three-Dimensional Laser Sintered Polyetheretherketone Composites on Osteoblasts *In Vitro*. *J. Biomed. Mater. Res.* 87A (4), 896–902. doi:10.1002/jbm.a.31822
- Wang, D., Jiang, X., Lu, A., Tu, M., Huang, W., and Huang, P. (2018). BMP14 Induces Tenogenic Differentiation of Bone Marrow Mesenchymal Stem Cells *In Vitro*. *Exp. Ther. Med.* 16 (2), 1165–1174. doi:10.3892/etm.2018.6293
- Wang, H., Hu, Y., He, F., Li, L., Li, P.-P., Deng, Y., et al. (2019). All-trans Retinoic Acid and COX-2 Cross-Talk to Regulate BMP9-Induced Osteogenic Differentiation via Wnt/ β -Catenin in Mesenchymal Stem Cells. *Biomed. Pharmacother.* 118, 109279. doi:10.1016/j.biopha.2019.109279

- Wang, J., Zhang, H., Zhang, W., Huang, E., Wang, N., Wu, N., et al. (2014). Bone Morphogenetic Protein-9 Effectively Induces Osteo/Odontoblastic Differentiation of the Reversibly Immortalized Stem Cells of Dental Apical Papilla. *Stem Cell Develop.* 23 (12), 1405–1416. doi:10.1089/scd.2013.0580
- Wang, L., Xu, W., Chen, Y., and Wang, J. (2019). Alveolar Bone Repair of Rhesus Monkeys by Using BMP-2 Gene and Mesenchymal Stem Cells Loaded Three-Dimensional Printed Bioglass Scaffold. *Sci. Rep.* 9 (1), 18175. doi:10.1038/s41598-019-54551-x
- Wang, N., Liu, W., Tan, T., Dong, C.-Q., Lin, D.-Y., Zhao, J., et al. (2017). Notch Signaling Negatively Regulates BMP9-Induced Osteogenic Differentiation of Mesenchymal Progenitor Cells by Inhibiting JunB Expression. *Oncotarget* 8 (65), 109661–109674. doi:10.18632/oncotarget.22763
- Wang, Q.-W., Chen, Z.-L., and Piao, Y.-J. (2005). Mesenchymal Stem Cells Differentiate into Tenocytes by Bone Morphogenetic Protein (BMP) 12 Gene Transfer. *J. Biosci. Bioeng.* 100 (4), 418–422. doi:10.1263/jbb.100.418
- Wang, T., Nimkingratana, P., Smith, C. A., Cheng, A., Hardingham, T. E., and Kimber, S. J. (2019). Enhanced Chondrogenesis from Human Embryonic Stem Cells. *Stem Cell Res.* 39, 101497. doi:10.1016/j.scr.2019.101497
- Wang, X., Huang, J., Huang, F., Zong, J.-C., Tang, X., Liu, Y., et al. (2017). Bone Morphogenetic Protein 9 Stimulates Callus Formation in Osteoporotic Rats during Fracture Healing. *Mol. Med. Rep.* 15 (5), 2537–2545. doi:10.3892/mmr.2017.6302
- Wu, J., Li, L., Fu, C., Yang, F., Jiao, Z., Shi, X., et al. (2018). Micro-porous Polyetheretherketone Implants Decorated with BMP-2 via Phosphorylated Gelatin Coating for Enhancing Cell Adhesion and Osteogenic Differentiation. *Colloids Surf. B: Biointerfaces* 169, 233–241. doi:10.1016/j.colsurfb.2018.05.027
- Wu, J., Liu, Y., Cao, Q., Yu, T., Zhang, J., Liu, Q., et al. (2020). Growth Factors Enhanced Angiogenesis and Osteogenesis on Polydopamine Coated Titanium Surface for Bone Regeneration. *Mater. Des.* 196, 109162. doi:10.1016/j.matdes.2020.109162
- Wu, M., Chen, G., and Li, Y.-P. (2016). TGF- β and BMP Signaling in Osteoblast, Skeletal Development, and Bone Formation, Homeostasis and Disease. *Bone Res.* 4, 16009. doi:10.1038/boneres.2016.9
- Wu, S., Xiao, Z., Song, J., Li, M., and Li, W. (2018). Evaluation of BMP-2 Enhances the Osteoblast Differentiation of Human Amnion Mesenchymal Stem Cells Seeded on Nano-Hydroxyapatite/Collagen/Poly(L-Lactide). *Int. J. Mol. Sci.* 19 (8), 2171. doi:10.3390/ijms19082171
- Wu, W., Geng, P., Li, G., Zhao, D., Zhang, H., and Zhao, J. (2015). Influence of Layer Thickness and Raster Angle on the Mechanical Properties of 3D-Printed PEEK and a Comparative Mechanical Study between PEEK and ABS. *Materials* 8 (9), 5834–5846. doi:10.3390/ma8095271
- Xu, K., Sun, Y., Kh Al-ani, M., Wang, C., Sha, Y., Sung, K. P., et al. (2018). Synergistic Promoting Effects of Bone Morphogenetic Protein 12/connective Tissue Growth Factor on Functional Differentiation of Tendon Derived Stem Cells and Patellar Tendon Window Defect Regeneration. *J. Biomech.* 66, 95–102. doi:10.1016/j.jbiomech.2017.11.004
- Xu, Y., Peng, J., Richards, G., Lu, S., and Eglin, D. (2019). Optimization of Electrospray Fabrication of Stem Cell-Embedded Alginate-Gelatin Microspheres and Their Assembly in 3D-Printed Poly(ϵ -Caprolactone) Scaffold for Cartilage Tissue Engineering. *J. Orthopaedic Translation* 18, 128–141. doi:10.1016/j.jot.2019.05.003
- Yamamoto, N., Akiyama, S., Katagiri, T., Namiki, M., Kurokawa, T., and Suda, T. (1997). Smad1 and Smad5 Act Downstream of Intracellular Signalings of BMP-2 that Inhibits Myogenic Differentiation and Induces Osteoblast Differentiation in C2C12 Myoblasts. *Biochem. biophysical Res. Commun.* 238 (2), 574–580. doi:10.1006/bbrc.1997.7325
- Yan, X., Zhou, Z., Guo, L., Zeng, Z., Guo, Z., Shao, Q., et al. (2018). BMP7-overexpressing Bone Marrow-derived Mesenchymal Stem Cells (BMSCs) Are More Effective Than Wild-type BMSCs in Healing Fractures. *Exp. Ther. Med.* 16 (2), 1381–1388. doi:10.3892/etm.2018.6339
- Yang, J., Kitami, M., Pan, H., Nakamura, M. T., Zhang, H., Liu, F., et al. (2021). Augmented BMP Signaling Commits Cranial Neural Crest Cells to a Chondrogenic Fate by Suppressing Autophagic β -catenin Degradation. *Sci. Signal.* 14 (665), 18. doi:10.1126/scisignal.aaz9368
- Ye, F., Xu, H., Yin, H., Zhao, X., Li, D., Zhu, Q., et al. (2019). The Role of BMP6 in the Proliferation and Differentiation of Chicken Cartilage Cells. *Plos One* 14 (7), e0204384. doi:10.1371/journal.pone.0204384
- Yokouchi, Y., Sakiyama, J., Kameda, T., Iba, H., Suzuki, A., Ueno, N., et al. (1996). BMP-2/-4 Mediate Programmed Cell Death in Chicken Limb Buds. *Development (Cambridge, England)* 122 (12), 3725–3734. doi:10.1242/dev.122.12.3725
- Yu, L., Dawson, L. A., Yan, M., Zimmel, K., Lin, Y.-L., Dolan, C. P., et al. (2019). BMP9 Stimulates Joint Regeneration at Digit Amputation Wounds in Mice. *Nat. Commun.* 10, 9. doi:10.1038/s41467-018-08278-4
- Yu, Y. Y., Lieu, S., Lu, C., and Colnot, C. (2010). Bone Morphogenetic Protein 2 Stimulates Endochondral Ossification by Regulating Periosteal Cell Fate during Bone Repair. *Bone* 47 (1), 65–73. doi:10.1016/j.bone.2010.03.012
- Zhang, L., Luo, Q., Shu, Y., Zeng, Z., Huang, B., Feng, Y., et al. (2019). Transcriptomic Landscape Regulated by the 14 Types of Bone Morphogenetic Proteins (BMPs) in Lineage Commitment and Differentiation of Mesenchymal Stem Cells (MSCs). *Genes Dis.* 6 (3), 258–275. doi:10.1016/j.gendis.2019.03.008
- Zhang, T., Wei, Q., Fan, D., Liu, X., Li, W., Song, C., et al. (2020). Improved Osseointegration with rhBMP-2 Intraoperatively Loaded in a Specifically Designed 3D-Printed Porous Ti6Al4V Vertebral Implant. *Biomater. Sci.* 8 (5), 1279–1289. doi:10.1039/c9bm01655d
- Zhang, W.-Z., Lan, T., Nie, C.-H., Guan, N.-N., and Gao, Z.-X. (2018). Characterization and Spatiotemporal Expression Analysis of Nine Bone Morphogenetic Protein Family Genes during Intermuscular Bone Development in blunt Snout Bream. *Gene* 642, 116–124. doi:10.1016/j.gene.2017.11.027
- Zhang, W., Yuan, Z., Meng, X., Zhang, J., Long, T., Yaochao, Z., et al. (2020). Preclinical Evaluation of a Mini-Arthroplasty Implant Based on Polyetheretherketone and Ti6Al4V for Treatment of a Focal Osteochondral Defect in the Femoral Head of the Hip. *Biomed. Mater.* 15 (5), 055027. doi:10.1088/1748-605X/ab998a
- Zhang, X., Lou, Q., Wang, L., Min, S., Zhao, M., and Quan, C. (2019). Immobilization of BMP-2-Derived Peptides on 3D-Printed Porous Scaffolds for Enhanced Osteogenesis. *Biomed. Mater.* 15 (1), 015002. doi:10.1088/1748-605X/ab4c78
- Zhao, C., Jiang, W., Zhou, N., Liao, J., Yang, M., Hu, N., et al. (2017). Sox9 Augments BMP2-Induced Chondrogenic Differentiation by Downregulating Smad7 in Mesenchymal Stem Cells (MSCs). *Genes Dis.* 4 (4), 229–239. doi:10.1016/j.gendis.2017.10.004
- Zhao, X., Han, Y., Li, J., Cai, B., Gao, H., Feng, W., et al. (2017). BMP-2 Immobilized PLGA/hydroxyapatite Fibrous Scaffold via Polydopamine Stimulates Osteoblast Growth. *Mater. Sci. Eng. C* 78, 658–666. doi:10.1016/j.msec.2017.03.186
- Zhong, J., Guo, B., Xie, J., Deng, S., Fu, N., Lin, S., et al. (2016). Crosstalk between Adipose-Derived Stem Cells and Chondrocytes: when Growth Factors Matter. *Bone Res.* 4, 10. doi:10.1038/boneres.2015.36
- Zhu, Z., Li, X., Li, Y., Zhu, L., Zhu, C., Che, Z., et al. (2021). Three-dimensionally Printed Porous Biomimetic Composite for Sustained Release of Recombinant Human Bone Morphogenetic Protein 9 to Promote Osteointegration. *Mater. Des.* 208, 109882. doi:10.1016/j.matdes.2021.109882

Conflict of Interest: The authors declare that the research was conducted in the absence of any commercial or financial relationships that could be construed as a potential conflict of interest.

Publisher's Note: All claims expressed in this article are solely those of the authors and do not necessarily represent those of their affiliated organizations, or those of the publisher, the editors and the reviewers. Any product that may be evaluated in this article, or claim that may be made by its manufacturer, is not guaranteed or endorsed by the publisher.

Copyright © 2022 Zhu, Liu, Wang, Zhu, Li, Zhu, Che, Liu, Liu and Huang. This is an open-access article distributed under the terms of the Creative Commons Attribution License (CC BY). The use, distribution or reproduction in other forums is permitted, provided the original author(s) and the copyright owner(s) are credited and that the original publication in this journal is cited, in accordance with accepted academic practice. No use, distribution or reproduction is permitted which does not comply with these terms.



Mineralizing Coating on 3D Printed Scaffolds for the Promotion of Osseointegration

Abshar Hasan^{1,2,3}, Romain Bagnol⁴, Robert Owen^{1,2}, Arsalan Latif⁵, Hassan M. Rostam⁵, Sherif Elsharkawy⁶, Felicity R. A. J. Rose^{1,2}, José Carlos Rodríguez-Cabello⁷, Amir M. Ghaemmaghami⁵, David Eglin^{4,8*} and Alvaro Mata^{1,2,3*}

¹School of Pharmacy, University of Nottingham, Nottingham, United Kingdom, ²Biodiscovery Institute, University of Nottingham, Nottingham, United Kingdom, ³Department of Chemical and Environmental Engineering, University of Nottingham, Nottingham, United Kingdom, ⁴Regenerative Orthopaedics, AO Research Institute, Davos, Switzerland, ⁵Immunology and Immuno-Bioengineering Group, School of Life Sciences, University of Nottingham, Nottingham, United Kingdom, ⁶Faculty of Dentistry, Oral & Craniofacial Sciences, King's College London, London, United Kingdom, ⁷BIOFORGE Group, University of Valladolid, CIBER-BBN, Valladolid, Spain, ⁸Ecole des Mines Saint-Etienne, Saint-Etienne, France

OPEN ACCESS

Edited by:

Barbara Zavan,
University of Padua, Italy

Reviewed by:

Giulia Brunello,
University Hospital of Düsseldorf,
Germany
Vinicius Rosa,
National University of Singapore,
Singapore

*Correspondence:

David Eglin
david.eglin@emse.fr
Alvaro Mata
a.mata@nottingham.ac.uk

Specialty section:

This article was submitted to
Tissue Engineering and Regenerative
Medicine,
a section of the journal
Frontiers in Bioengineering and
Biotechnology

Received: 15 December 2021

Accepted: 27 April 2022

Published: 27 June 2022

Citation:

Hasan A, Bagnol R, Owen R, Latif A,
Rostam HM, Elsharkawy S,
Rose FRAJ, Rodríguez-Cabello JC,
Ghaemmaghami AM, Eglin D and
Mata A (2022) Mineralizing Coating on
3D Printed Scaffolds for the Promotion
of Osseointegration.
Front. Bioeng. Biotechnol. 10:836386.
doi: 10.3389/fbioe.2022.836386

Design and fabrication of implants that can perform better than autologous bone grafts remain an unmet challenge for the hard tissue regeneration in craniomaxillofacial applications. Here, we report an integrated approach combining additive manufacturing with supramolecular chemistry to develop acellular mineralizing 3D printed scaffolds for hard tissue regeneration. Our approach relies on an elastin-like recombinamer (ELR) coating designed to trigger and guide the growth of ordered apatite on the surface of 3D printed nylon scaffolds. Three test samples including a) uncoated nylon scaffolds (referred to as “Uncoated”), b) ELR coated scaffolds (referred to as “ELR only”), and c) ELR coated and *in vitro* mineralized scaffolds (referred to as “Pre-mineralized”) were prepared and tested for *in vitro* and *in vivo* performance. All test samples supported normal human immortalized mesenchymal stem cell adhesion, growth, and differentiation with enhanced cell proliferation observed in the “Pre-mineralized” samples. Using a rabbit calvarial *in vivo* model, ‘Pre-mineralized’ scaffolds also exhibited higher bone ingrowth into scaffold pores and cavities with higher tissue-implant integration. However, the coated scaffolds (“ELR only” and “Pre-mineralized”) did not exhibit significantly more new bone formation compared to “Uncoated” scaffolds. Overall, the mineralizing coating offers an opportunity to enhance integration of 3D printed bone implants. However, there is a need to further decipher and tune their immunologic response to develop truly osteoinductive/conductive surfaces.

Keywords: biomineralization, elastin-like recombinamers, bone regeneration, 3D printing, nylon, tissueimplant integration

1 INTRODUCTION

The demand for engineered and functional bone grafts for hard tissue repair and regeneration in craniomaxillofacial (CMF) applications is increasing due to the need for more functional designs with enhanced osseointegration (Orciani et al., 2017). Autogenous grafts are deemed to be the “gold-standard” for bone materials due to their osteoinductive, osteoconductive, and osteogenic properties (Farré-Guasch et al., 2015). However, these grafts possess several disadvantages such as donor-site

morbidity, limited availability, post-operative pain, and blood loss (Aldaadaa et al., 2018). Additive manufacturing techniques offer opportunities to fabricate implants that serve as alternative grafts with advantages such as (i) complex and intricate geometrical structures, (ii) patient-specific anatomical architectures (Derby, 2012; Farré-Guasch et al., 2015), and (iii) reproducibility and cost effectiveness (Turnbull et al., 2018).

Rapid and effective osseointegration is a major goal of these types of manufactured implants. Osseointegration is an interfacial bonding phenomenon that relies on structural and functional interactions between living bone and the surface of implants during bone healing (Parithimarkalaignan and Padmanabhan, 2013). It primarily involves the growth of new bone from the native tissue towards the surface of the implant (Agarwal and García, 2015). Mechanical instability, mismatch of properties, and poor interactions at the bone-implant interface may result in non-adherent fibrous tissue formation, subsequently preventing osseointegration (Bahraminasab, 2020). In severe cases, this scenario can lead to aseptic loosening, implant failure, and adverse biological responses such as local chronic inflammation (Vallés et al., 2021). Three-dimensional (3D) printing offers the possibility of optimizing the porosity of bone implants with controlled parameters such as pore volume and diameter, pore density, and interconnectivity to promote osseointegration (Bahraminasab, 2020) by encouraging migration of bone cells and vascularization (Karageorgiou and Kaplan, 2005; Liu et al., 2020). However, 3D printed implants can suffer from a limited selection of printable materials, lack of specific chemical and physical signals to stimulate bone ingrowth and integration (Bahraminasab, 2020), poor bioactivity and control over surface roughness and texture (Tofail et al., 2018), and limited structural integrity (Ran et al., 2018).

3D printed bone constructs made from different materials to promote osseointegration have been heavily explored (Agarwal and García, 2015). CaP scaffolds have been reported to enhance osseointegration but they tend to be brittle, exhibit low compressive strengths, and display non-uniform internal structures (i.e., pore size and volume) (Wang et al., 2020). Such issues were overcome by using 3D printed metallic implants which exhibit high mechanical strength with tuneable internal structures and enhance osseointegration by increasing bone-implant interfacial strength (Petrie et al., 2009). However, they suffer from poor degradability of the implant material (Qu et al., 2019) and toxic effects caused by ions leaching from them (Prasad et al., 2017). Polymeric implants offer tunable degradability (Song et al., 2018), mechanical strength 5–10 folds better than human cancellous bone (Wang et al., 2020), and exhibit excellent biocompatibility to overcome issues related to metallic implants. However, most of the printable polymeric inks suffer from poor physio-chemical surface properties due to lack of efficient chemical functional moieties to promote cell growth and proliferation (Seyednejad et al., 2011). Thus, a variety of surface modification strategies have been investigated on polymeric scaffolds including attachment of mussel inspired polydopamine (Turnbull et al., 2018), osteogenic proteins (such as rhBMP2) (Lee et al., 2016) and mineralizing peptides (Zhang et al., 2019), and CaP coatings (Zhao et al., 2015) to

enhance cell adhesion, osteogenic differentiation, and osseointegration. However, these coatings exhibit disadvantages such as propensity for proteolytic degradation in the case of peptides (Brun et al., 2013), limited bioactivity (Malhotra and Habibovic, 2016) and poor stability (Cheng et al., 2005) in the case of CaP coatings.

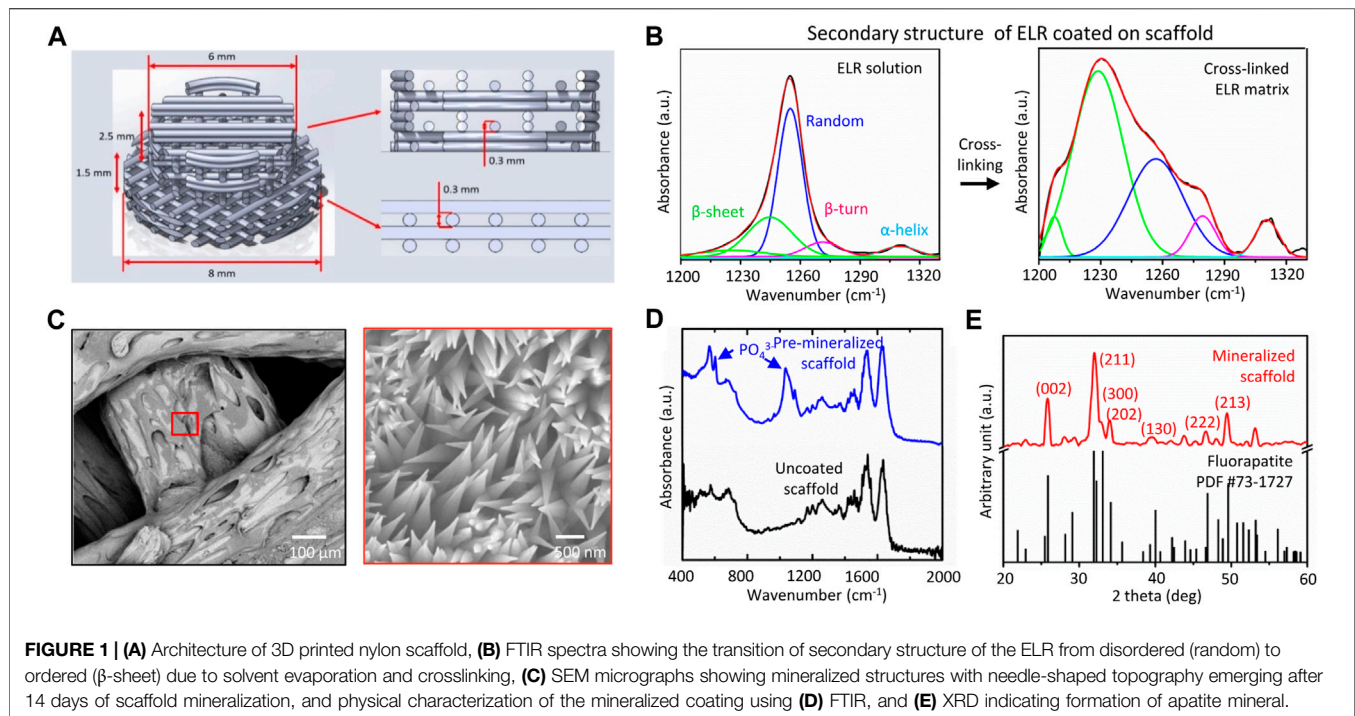
We have recently developed an elastin-like recombinamers (ELRs)-based mineralizing platform that can be easily coated over large and complex geometrical structures (Elsharkawy et al., 2018; Deng et al., 2021). The platform relies on the modulation of ELR order (e.g., β -sheet) and disorder (e.g., random coil) to form a supramolecular framework capable of nucleating and guiding the growth of hydroxyapatite (HAP) nanocrystals of ~50 nm in diameter that hierarchically organize into ~5 μ m thick bundles to form mineralized macrostructures of hundreds of microns in diameter. The ELR platform can be tailored to generate different levels of apatite organization (Elsharkawy et al., 2018), to match Young's modulus of trabecular tissue from the femoral neck (6.9 ± 4.3 GPa) to interstitial tissue from the diaphyseal cortex (25.0 ± 4.3 GPa) (Zysset et al., 1999). This capability suggests the possibility to generate mineralizing surfaces on bone implants that can be designed to match the properties of the surrounding tissue and at the same time grow apatite mineral from the implant towards the tissue, enhancing osseointegration. The mineralizing platform does not require major equipment and is simple to fabricate over large and geometrically complex structures.

In this study, we report on the integration of supramolecular chemistry, tunable organic-inorganic relationships, and additive manufacturing to engineer bone implants that can promote bone regeneration and osseointegration. We developed a simple process to uniformly coat 3D printed scaffolds while modulating ELR order-disorder ratios to trigger mineralization as a step towards osseointegration. The applicability of our coated ("ELR only" and "Pre-mineralized") materials was assessed both *in vitro* and *in vivo* in a rabbit calvarial model. We hypothesize that our coated scaffolds can: a) attract and facilitate cell growth, b) grow mineral towards the tissue, and c) enhance integration with the surrounding tissue. We anticipate that this approach can have important implications for the design of functional dental and orthopedic implants that can self-mineralize by drawing ions from the implant site (i.e., from body fluids) to enhance bone growth and osseointegration.

2 MATERIALS AND METHODS

2.1 Materials

ELR with statherin sequence (SN_A15) were purchased from Technical Proteins Nanobiotechnology, Valladolid, Spain. Anhydrous dimethylformamide (DMF), dimethyl sulfoxide (DMSO), hexamethylene diisocyanate (HDI), calcium chloride dihydrate (CaCl₂ · 2H₂O), sodium fluoride (NaF), and hydroxyapatite powder were procured from Sigma-Aldrich, United Kingdom. Rest of the chemicals were also procured from Sigma-Aldrich, United Kingdom unless specified.



2.2 3D Printed Nylon Scaffold Fabrication

Nylon scaffolds were printed using fused deposition modeling (FDM) technique with an Ultimaker three Printer (Ultimaker, Netherlands), with a 0.4 mm diameter nozzle (Ultimaker, Netherlands) using nylon polyamide (Ultimaker, Nylon Polyamide Transparent, print temperature 240–260°C) at room temperature and ambient humidity. The printing speed was 20 mm/s for the initial layer and ranged between 10 and 12 mm/s for all other layers. The scaffold geometry was a cork like structure composed of two superposed cylinders of respectively; 8 mm diameter and 1.5 mm height with a 0°/90° alternating pattern, with a 0.3 mm layer height, and 6 mm diameter and 2.5 mm height with a 0°/0°/90°/90° pattern with a 0.3 mm layer height. The scaffold pattern was optimized to achieve lateral and vertical outer porosity of 0.3 mm and perfect fit in the bone defect (**Figure 1A**). First, an STL model was created using SolidWorks 2020 (Dassault Systèmes, United States). Then, the software Ultimaker Cura 4.6 (Ultimaker, Netherlands) was used to create a G-code file, which was further tested and modified until the desired dimensions and porosity, assessed with a caliper and binocular, achieved, and reproduced.

2.3 ELR Coating Fabrication

ELR coating on nylon scaffolds were fabricated using the procedure described previously by our group (Elsharkawy et al., 2018). Briefly, lyophilized ELR powder was dissolved in solvent mixture of DMF/DMSO (at 9/1 ratio) to prepare 5% (w/v) ELR solution followed by addition of hexamethyl diisocyanate (HDI) crosslinker (cross-linker to lysine ratios of 12/1). Finally, 3D printed nylon scaffolds were dipped in the above ELR solution for 10–15 s and later left for drying overnight at room temperature (22°C) inside a glovebox (BELLE Technology,

United Kingdom) maintained at a humidity <20%. Dried and ELR coated scaffolds washed several times with de-ionized water to remove excess HDI and stored at 4°C until use and were termed as “ELR only” scaffold.

2.4 Mineralization Experiment

Mineralizing solution was prepared using previously reported methodology (Elsharkawy et al., 2018). Briefly, hydroxyapatite powder (2 mM) and sodium fluoride (2 mM) were dissolved in de-ionized water by dropwise adding nitric acid (69%, v/v) into the solution until it becomes clear. The pH of the above solution was adjusted to 6.0 using 30% (v/v) ammonium hydroxide solution. To create “Pre-mineralized” scaffolds, “ELR only” scaffolds were incubated in above solution (pH = 6) at 37°C for 2 weeks. Post mineralization, scaffolds were washed several times with deionized water (diH₂O), air dried, and stored at 37°C until use.

2.5 Characterization

2.5.1 Scanning Electron Microscopy

“Pre-mineralized” scaffold sample were mounted on aluminum stubs using double sided carbon tape followed by 10 nm thick Iridium coating (Model: 150T ES, Quorum, United Kingdom) to make the sample conductive. Surface topographies of mineralized scaffold samples were analyzed using JEOL 7100F scanning electron microscopy (JEOL, United Kingdom) operated at 15 kV. Scaffolds were handled gently using Teflon tweezers to prevent any damage to the coating.

2.5.2 Attenuated Total Reflection-Fourier-Transform Infrared Spectroscopy

ATR-FTIR spectroscopy analysis of “ELR only” and “Pre-mineralized” scaffolds before and after *in vitro* mineralization

was carried out using Cary 630 FTIR Spectrometer (Agilent, United Kingdom). Sixty four scans on average were recorded for each sample type at a resolution of 2 cm^{-1} in the range $4000\text{--}450\text{ cm}^{-1}$. The obtained spectra were analyzed by Origin 8.5 software to make the spectrum curve.

2.5.3 X-Ray Diffraction

XRD scans were recorded for phase Identification and quantification of the “Pre-mineralized” scaffold using D8 Advance with DaVinci X-ray diffractometer (Bruker, United Kingdom). Instrument was operated with flat plate θ/θ geometry and Ni-filtered Cu-K α radiation at 45 kV and 40 mA (K α 1 = 1.54059 \AA , K α 2 = 1.54442 \AA) (Elsharkawy et al., 2018). The values were recorded from 5° to 70° with a step size 0.02° , and data were obtained at step time of 1,600 s. PDF4 database (ICDD, USA, release 2014) was used for comparison.

2.6 In Vitro Studies

Human immortalized mesenchymal stem cells (hiMSCs) were generated in-house by lentiviral transfection of E6/E7 and hTERT genes as previously described (Mori et al., 2005; Balducci et al., 2014; Burroughs et al., 2021). Cells were cultured in basal media (BM) composed from Dulbecco’s modified Eagle’s medium (DMEM) supplemented with 10% (v/v) fetal bovine serum (FBS) and 1% (v/v) penicillin-streptomycin. Test samples were sterilized by submerging in 70% ethanol for 30 min then washing three times in sterile 1X phosphate buffer saline (PBS). They were then transferred to individual wells of a 96-well plate and exposed to UV for an hour to ensure complete sterilization. Test samples were then soaked in BM for 1 h to permit protein adsorption and promote cell attachment. To seed, hiMSCs were added at a density of 10,000 per cm^2 (2,800 per disc) at a concentration of 14,000 cells/mL (200 μL per disc) in BM. After 48 h, discs were transferred to a new 96-well plate to conserve only adhered cells. Later, 200 μL osteogenic induction media (OIM) consisting of BM supplemented with 100 nM dexamethanone, 50 $\mu\text{g}/\text{mL}$ ascorbic acid 2-phosphate and 5 mM β -glycerophosphate was added to each well and considered as day 1. Media was changed every 2–3 days and cells were maintained in a humidified incubator at 37°C and 5% CO_2 in air. Quadruplicate of each sample type was used for each of the *in vitro* experiment described below.

2.6.1 Metabolic Activity

To assess viability, metabolic activity was measured on days 1, 8 and 15 using PrestoBlue[®] (ThermoFisher Scientific, United Kingdom). Briefly, culture media was replaced with 200 μL of PrestoBlue[®] working solution (10% PrestoBlue[®] in BM) and incubated for 1 h. The solution was then transferred to a black 96-well plate and read at λ_{ex} : 560 nm, λ_{em} : 590 nm in a plate reader (Tecan Infinite 200, Switzerland), where fluorescence correlates with metabolic activity, and fresh OIM was added to the discs. Each group consisted of five samples ($n = 5$).

2.6.2 Alkaline Phosphatase Activity and Total DNA Quantification

To assess osteogenic differentiation, ALP activity and total DNA was quantified on days 8 and 15 using cell lysates as previously

described (Owen et al., 2020). Briefly, to digest, media was removed, and the discs were washed with PBS before transferring to a microcentrifuge tube containing 500 μL of cell digestion buffer (10 vol% cell assay buffer (1.5 M Tris-HCl, 1 mM ZnCl_2 , 1 mM MgCl_2 in diH_2O , 1% Triton-X100 in diH_2O). Samples ($n = 5$) were refrigerated for 1 h before freeze-thawing three times ($-80^\circ\text{C}/37^\circ\text{C}$, centrifuging (10,000 RCF) for 5 min and homogenizing the supernatant. ALP activity was determined using the Pierce[™] PNPP substrate kit (ThermoFisher Scientific, United Kingdom) according to the manufacturer’s instructions. Briefly, 20 μL of lysate was combined with 180 μL of substrate (p-nitrophenol phosphate, pNPP) in a 96-well plate. The change in absorbance was measured using a plate reader (Tecan infinite 200) at a wavelength of 405 nm every minute for 30 min. The ALP activity is expressed as nmol of p-nitrophenol per minute (nmol pNP/min), assuming that one absorbance value equals 25.2 nmol of product. This activity was normalized to the total DNA content per lysate. DNA was quantified using the Quant-it[™] high sensitivity dsDNA kit (ThermoFisher Scientific, United Kingdom), according to manufacturer’s instructions. Briefly, 20 μL of lysate was combined with 180 μL of substrate in a black 96-well plate. The plates were shaken to aid the DNA-substrate conjugation, left at room temperature for 10 min, then shaken again before measuring the fluorescence (λ_{ex} : 485nm, λ_{em} : 535nm). The shaking and fluorescence were performed and measured using a plate reader (Tecan infinite 200, Switzerland). The fluorescence was converted to ng of DNA using a standard curve and was scaled to the total lysate volume. Each group consisted of five samples ($n = 5$).

2.6.3 Fluorescence Imaging

Cell growth on the discs (sample size for each group, $n = 5$) was visualized on day 5 using fluorescence microscopy. Day 5 was chosen over day 8 as the adhered cells were too confluent after 8 days of culture to distinguish the effect of substrates on cell spreading and morphology. To fix, media was removed, and discs were washed twice with PBS before submerging in 3.7% formaldehyde for 20 min. To stain, fixed discs were washed twice in PBS then submerged in immunocytochemistry (ICC) buffer (1% BSA, 0.1% Triton-X100 in PBS) containing 1X Phalloidin-iFluor[™] 633 (Strattech, United Kingdom) for 1 h at room temperature. Discs were then washed in PBS before imaging. Images of hiMSCs on the disc surfaces (2048×2048 pixels) were obtained using a Leica TCS LSI (Leica Microsystems, United Kingdom) at λ_{ex} : 635 nm, λ_{em} : 650 nm.

2.7 In Vivo Studies

The osteogenesis inducing capacity of scaffolds was analyzed *in vivo* using 6 mm critical-size calvarial defect model in six female New Zealand white rabbits at AO research institute Davos, Switzerland. A total of four calvarial defects were created per animal and each animal had all three types of test groups (i.e., “Uncoated,” “ELR only,” and “Pre-mineralized” scaffolds) and positive control (Bio-Oss). Thus, sample size for each test groups and positive control groups was 6. The negative control group (empty defect) was retrieved from previous studies

performed at the AO research institute. Scaffolds were handled gently using Teflon tweezers to prevent any damage to the coating. Scaffolds were ethylene oxide sterilized prior to implantation. The animals were housed singly and received food and water *ad libitum*. All animals' research protocols were approved (Approval ref. No. 21) by the Animal Welfare & Ethical Review Body (AWERB) at the University of Nottingham and at the AO Research Institute Davos.

2.7.1 Surgical Intervention

The rabbits were sedated with a combination of medetomidine, midazolam, and fentanyl in the preparation area approximately 20 min before starting the aseptic preparation of the surgical field. A skin incision was made on midline of the caudal dorsal skull from the nasal bone to the occipital crest using a #10 scalpel blade. A bone cutting jig was placed on midline of the parietal bone, spanning the left and right parietal bones just caudal to the horizontal suture line. The locations of four evenly distributed defects were marked using blunt dissection of the periosteum through the jig using a #15 scalpel blade. Four 6 mm diameter cranial defects were created in the parietal bone with an Anspach® drill associated with a Codman perforator (DePuy Synthes, United States) using procedure described previously (Guillaume et al., 2019). Any remaining bone pieces were gently removed from the defects without damaging the dura mater. The hydrated scaffolds were fitted into the calvarial defects according to their respective study groups. A total of four calvarial defects were created per animal and each animal had all three types of test groups (i.e., “Uncoated,” “ELR only,” and “Pre-mineralized” scaffolds) and a positive control (Bio-Oss). The subcutaneous tissues were closed with 4–0 Monocryl in a simple interrupted pattern, and the skin is closed using 5-0 vicryl rapide in an intradermal pattern. The animals were postoperatively scanned in the Xtreme CT. Fluorochromes (Calcein green (1 ml/kg) and xylenol orange (1 ml/kg)) were administered at 2 and 4 weeks postoperatively for evaluation of new bone formation using histological analysis after euthanasia. The animals were euthanized after 6 weeks postoperatively by means of an intravenous overdose of barbiturate (Pentobarbital, Esconarkon®).

2.7.2 High-Resolution Micro-Computed Tomography Analysis

Micro-CT scans were recorded immediately after euthanasia *in situ* using high-resolution peripheral quantitative computed tomography (HR-pQCT) (Model: XTremeCT-II, Scanco Medical AG, Switzerland). The parameters of the scan were: voltage source 81 kV, current source 124 mA, image pixel size 9 mm, an aluminum filter of 0.5 mm, a tomographic rotation of 180°, and a sample rotation step of 0.8°. Later, the samples were fixed in 4% buffered formalin and examined under vivaCT (voltage source: 60 kV, current source: 900 µA, image pixel size: 82 µm, a tomographic rotation of 180°, and a sample rotation step of 0.4°) for the individual calvarial defects. A cylindrical volume of interest (VOI) was used to quantify the bone volume and bone mineral density corresponding with the size of the defect.

2.7.3 Histology Analysis

Histology analysis was performed using procedure reported previously by our group (Tejeda-Montes et al., 2014a). Briefly, the skull calvarias were extracted and fixed in 4% buffered formalin at pH = 7.2 for 2 days followed by bone decalcification using Surgipath Decalcifier II for 4 h. Later, they were embedded in paraffin and sectioned using microtome to prepare 3 mm thick sections and stained with hematoxylin and eosin (H&E) to observe under a microscope Zeiss AxioScope A (Carl Zeiss) with a Zeiss AxioCam MRc 5 camera (Carl Zeiss, Madrid, Spain) for qualitative and semiquantitative evaluation.

2.8 In Vitro Immunological Analysis

Monocytes were isolated and cultured using procedure developed previously (Awuah et al., 2019). Briefly, buffy coats were procured from healthy donors following approval (REC 260 - 1701) from ethics committee (Research Ethics Committee, Faculty of Medicine and Health Sciences, University of Nottingham). Monocytes were isolated from peripheral blood mononuclear cells. A MACS magnetic cell separation system (CD14 MicroBeads positive selection with LS columns, Miltenyi Biotec) was used for the isolation as previously described (Salazar et al., 2016). The obtained monocytes using this method exhibited ~95% purity as analyzed by CD14 expression. Monocytes (1×10^6 cells/mL) were prepared and cultured in RPMI-1640 medium at 37°C, 5% CO₂ in a humidified incubator and 250 µL of the cell suspensions were seeded on pre-sterilized test samples (sample size, $n = 6$) for 3 and 6 days. Post incubation, the level of IL-10 secreted into the media by macrophages was quantified by sandwich ELISA using DuoSet ELISA development kits (R&D Systems, United States) as per manufacturer's instructions.

2.9 Statistical Analysis

All the data are reported as mean \pm SD. Statistical analysis was performed using GraphPad Prism ver. 6 software between the means of different test groups using one-way and two-way analysis of variance (ANOVA) with the Tukey test. p values <0.05 were considered significant.

3 RESULTS AND DISCUSSIONS

3.1 Rationale of Design

Implant-tissue integration or osseointegration is critical for the success and function of implants. Osseointegration is defined as a formation of a direct interface between an orthopedic or dental implant and bone, without intervening soft tissue (Albrektsson and Albrektsson, 1987). 3D printed polymeric scaffolds can promote cell growth, differentiation, and biomineral formation, however, exhibit poor integration with the surrounding tissue (Jackson et al., 2018). Here, our study aims to integrate an ELR based self-mineralizing coating (by drawing Ca and P ions from the implant site) with 3D printed nylon scaffold for applications in bone repair and regeneration. Thus, the objectives of the study are: (a) fabrication and optimization of the 3D printed nylon scaffolds with high porosity, (b)

optimization of ELR coating on the scaffolds, (c) assessment of the applicability of our coated (“ELR only” and “Pre-mineralized”) materials both *in vitro* and *in vivo* in a rabbit calvarial model. We hypothesize that these scaffolds: a) can attract and facilitate cell growth, b) can grow mineral towards the tissue, and c) can enhance integration with the surrounding tissue. We developed a simple process to uniformly coat 3D printed scaffolds while modulating ELR order-disorder ratios to trigger mineralization as a step towards osseointegration. To investigate the role of the growing mineral on the surface of the scaffolds, experiments were conducted using ELR-coated scaffolds that were either fully mineralized (“Pre-mineralized”) or non-mineralized (“ELR only”). The ELRs comprised hydrophobic (VPGIG) and hydrophilic (VPGKG) moieties that enable modulation of secondary structure and optimization of order-disorder ratios to trigger mineralization as we previously demonstrated (Elsharkawy et al., 2018). Cells (hiMSCs) were used to assess the capacity of the mineralized surfaces to promote adhesion, proliferation, and differentiation *in vitro* while a rabbit calvarial model was used to assess bone regeneration and bone-implant integration *in vivo*. We also performed preliminary *in vitro* experiments using monocyte-derived macrophages to provide insights into the potential immunomodulatory effects of the mineralized coatings.

3.2 Coating Characterization and Mineralization

The pore size and porosity of implants are known to significantly influence bone formation and integration with the surrounding tissue. Thus, we designed our nylon scaffolds with pore diameters ranging between 300–600 μm , which is reported to be optimum for bone ingrowth (Mehrabanian and Nasr-Esfahani, 2011). 3D printed nylon scaffolds were coated with 5–10 μm thick ELR coating and were characterized for secondary structure composition using FTIR. In solution, the ELR exhibits a secondary structure consisting of a random (disordered) to β -sheet (ordered) ratio of 6.84 ± 0.71 (Figure 1B). Upon solvent evaporation, the resulting coating exhibit a secondary structure consisting of disordered to ordered ratio of 0.47 ± 0.04 . These values are aligned with those reported previously by our group on mineralizing membranes (Elsharkawy et al., 2018). ELR coated scaffolds were mineralized *in vitro* for 2 weeks and characterized for mineral growth. SEM micrographs of the mineralized scaffolds depicted well defined crystals with needle shape morphology nucleating and growing on the surface of the scaffolds (Figure 1C). Mineralization was confirmed by FTIR spectroscopy (Figure 1D) and XRD (Figure 1E) analysis displaying non-stoichiometric apatite spectral peaks that demonstrate a crystalline phase and structural parameters similar to fluorapatite, respectively, as previously reported (Elsharkawy et al., 2018; Deng et al., 2021).

3.3 In Vitro Studies

All test samples were first evaluated *via in vitro* cell-based assays and using hiMSCs.

3.3.1 Metabolic Activity Analysis

We performed metabolic activity analysis on different test samples using non-toxic PrestoBlue® at 1, 8, and 15 days after cell seeding. We observed that metabolic activity increased at a similar rate on all test samples, as indicated by the similar gradients. However, metabolic activity was significantly lower ($p < 0.05$) on “ELR only” at days 8 and 15 in comparison to “Uncoated” and “Pre-mineralized” (Figure 2A). We speculate that the observed lower metabolic activity on “ELR only” coated surfaces may result from the more hydrophobic nature of “ELR only” samples. Surface hydrophilicity plays a crucial role in controlling protein adsorption and conformation (Hasan et al., 2018) that in turns regulate cell adhesion and proliferation (Hasan et al., 2018; Hasan and Pandey, 2020). Hydrophobic surfaces are known to exhibit irreversible adsorption of ECM proteins (such as fibronectin, vitronectin, collagen) that leads to protein denaturation and consequently negative effects on cell adhesion (Cai et al., 2020). As the “ELR only” coating is markedly very hydrophobic (water contact angle = 115°) (Tejeda-Montes et al., 2012) than the ‘Pre-mineralized’ coating (water contact angle = $41^\circ \pm 9^\circ$), it is possible that this effect could lead to cells having lower metabolic activity and cell proliferation on “ELR only” coatings.

3.3.2 Cell Adhesion and Proliferation

Total DNA was quantified on days 8 and 15 as a measure of the number of hiMSCs on the samples and proliferation between the timepoints. Cells were harvested and DNA extracted then quantified using the Quant-iT™ high sensitivity dsDNA kit. While there was no difference between all samples on day 8, ‘Pre-mineralized’ samples exhibited significantly higher total DNA quantity ($p < 0.05$) by day 15 (Figure 2B). Higher values of DNA extracted from “Pre-mineralized” surfaces indicate enhanced cell proliferation as compared to the other samples. We attribute this enhanced level of total DNA to the bioactive nature of CaP mineral (Jeong et al., 2019) which has been reported to promote osseointegration (Zhu et al., 2021).

3.3.3 Alkaline Phosphatase Assay

ALP is an early osteogenic marker and is an enzyme associated with osteogenesis. It is expressed by MSCs as they undergo osteogenic differentiation and plays an essential role in matrix mineralization (Burroughs et al., 2021). Therefore, here, early osteoblast differentiation was characterized using an ALP assay normalized to DNA content. ALP activity increased after 8 and 15 days on all test samples. However, there was no statistical difference observed in total (Figure 2C) or normalized ALP (Figure 2D) between the samples, which indicates that cell exhibited similar differentiation response irrespective of the substrate type and suggests no negative effect on osteogenesis.

3.3.4 Cell Morphology

SEM and fluorescent imaging of adhered cells at day 5 revealed cell morphology with elongated shapes indicating good cellular attachment and spreading across all samples (Figures 2E,F,G). These results are consistent with the higher proliferation results

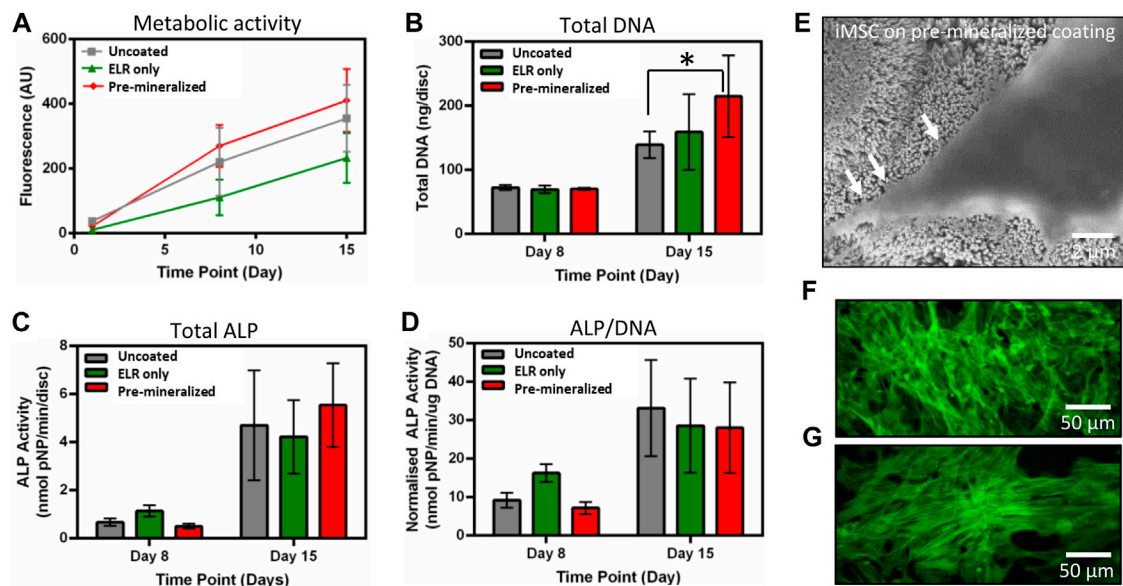


FIGURE 2 | *In vitro* characterization. (A) Metabolic activity, (B) total DNA, (C) total ALP, and (D) normalized ALP activity of hiMSCs on different test samples. (E) SEM micrographs of hiMSCs after 5 days of culture on “Pre-mineralized” samples depicting cell protrusions (as pointed by arrow heads) that indicate cell spreading and migration, and fluorescence microscopic images of hiMSCs cultured for 5 days on (F) “Pre-mineralized,” and (G) “ELR only” coated samples. Data presented at mean \pm SD ($n = 6$). In (B) * represents significant difference $p < 0.05$ between “Uncoated” and “Pre-mineralized” scaffold, estimated using one-way ANOVA in GraphPad Prism ver. 6 software.

(Figure 2B). Higher cell spreading with cellular extensions *in vitro* indicate cell migration which is crucial for bone tissue healing and regeneration (Fu et al., 2019).

Overall, these *in vitro* results indicate that all test samples are able to support normal hiMSCs performance with no negative effects observed on cell adhesion, growth, and differentiation. However, it is important to point the enhanced proliferation observed in the mineralized samples, suggesting the potential of the coating to promote cell growth *in vivo*.

3.4 In Vivo Studies

Given the observed *in vitro* mineralizing capacity and osteogenic differentiation of hiMSCs cells, the bone regeneration and infiltration capacity of the different test groups was investigated *in vivo* using an orthotopic 6 mm wide calvarial bone defect model in rabbits (Figure 3A). Calvarial bone defect model involves formation of bilateral round shaped defects in the parietal bone which can vary in size from 6–10 mm in diameter (Lee et al., 2010; Schmidlin et al., 2013; Bisht et al., 2021). Bone ossification was assessed by micro-CT and histology using Giemsa-Eosin staining after 6 weeks of implantation. The micro-CT analysis demonstrated that all tested samples exhibited new bone formation after 3 and 6 weeks of implantation. However, no significant difference in new bone volume within the defect among the test groups “Uncoated,” “ELR only,” and “Pre-mineralized” (Figures 3B,C) was quantified using micro-CT nor qualitatively observed *via* histology. The positive control Bio-Oss exhibited the lowest ossified tissue within the defect (Figure 3D). We speculate that this may result from a dense calcified material in large

amount in the defect, which do not significantly degrade within the 6 week period of the experiment (Bosetti et al., 2013) and may consequently require less time to reach full bone defect healing.

From the Giemsa-Eosin-stained histological sections (Figures 3E–H), all test groups exhibited bone regeneration along the rim region of the defects, with higher levels of ossified tissue at the center of defects treated with “Uncoated” and “ELR only” (Figures 3F,G). Nylon-based scaffolds have been shown to support pre-osteoblasts cells adhesion and proliferation (Abdal-hay et al., 2015) and we have previously showed that the ELR material, which contains the statherin-derived amino acid sequence DDDEEKFLRRIGRFG (SN_A15) known to promote HAP formation in the oral environment (Hay and Moreno, 2021), can stimulate osteoblastic differentiation *in vitro* (Tejeda-Montes et al., 2014b) and bone formation *in vivo* (Tejeda-Montes et al., 2014a). Furthermore, histology results revealed higher conformation of the new bone tissue to the scaffold’s geometry in “Pre-mineralized” scaffolds (Figure 4A) as compared to the other test groups. This was evident by the presence of undulations which indicate newly formed bone conforming tightly to and taking the shape of the architecture of the scaffold. This behavior of formation of bony undulations at the implant surface in response to the surface physio-chemical properties and implant’s geometry, referred as contact osteogenesis (Shah et al., 2019) indicates firm anchorage of the newly formed bone to the implant surface (Khosravi et al., 2018; Shah et al., 2019). When investigating bone ingrowth into small pores and cavities within the scaffolds, “Uncoated” and “Pre-mineralized” scaffolds exhibited more bone in-growth as

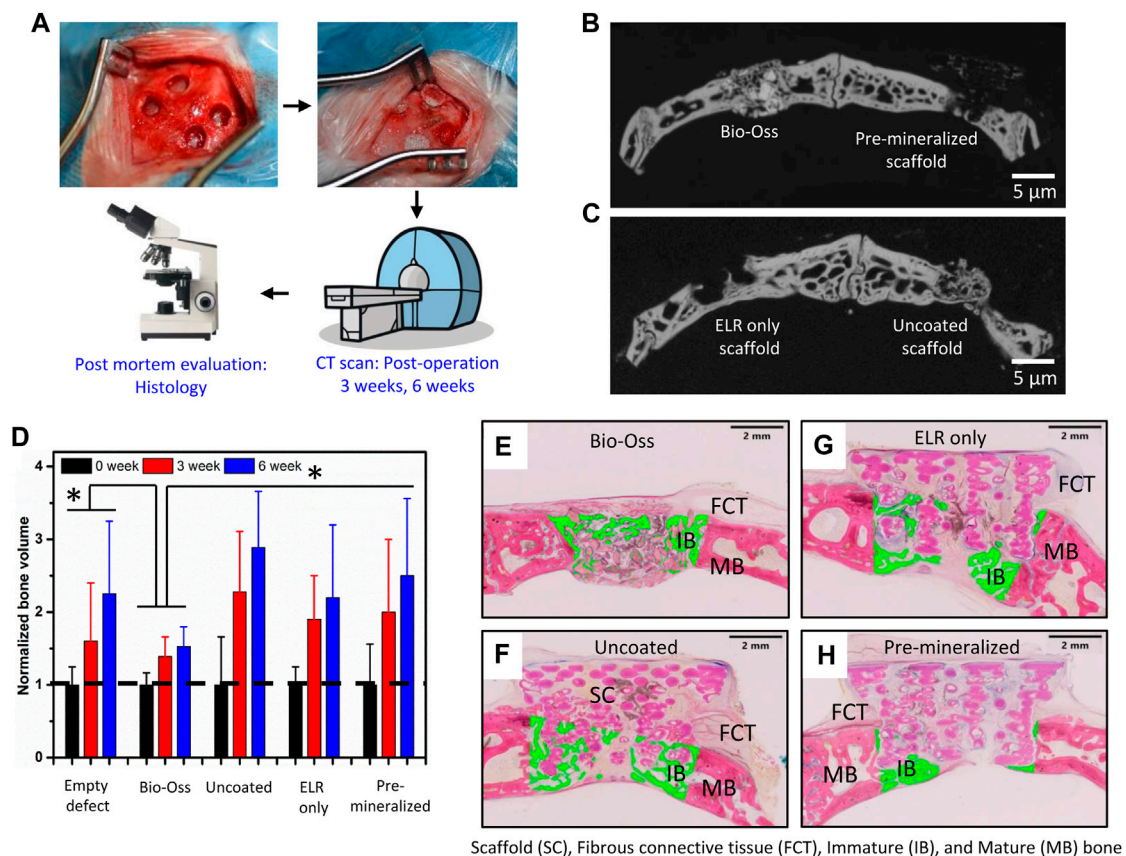


FIGURE 3 | *In vivo* characterization. **(A)** Schematic of the study plan and view of the rabbit calvarial bone defect before and after implantation. Micro CT images of new bone formation in **(B)**, left) the positive control (Bio-Oss) and **(B)**, right) “Pre-mineralized” scaffold and **(C)**, left) “ELR only” and **(C)**, right) “Uncoated” scaffolds. **(D)** Normalized volume of newly formed bone with different test samples after 0, 3, and 6 weeks of implantation. Histological sections stained with Giemsa-Eosin depicting new bone formation marked with green colour after 6 weeks of implantation including **(E)** positive control (Bio-Oss), **(F)** “Uncoated” nylon scaffold, **(G)** “ELR only” coated nylon scaffold, and **(H)** “Pre-mineralized” scaffold. Scaffold (SC), Fibrous connective tissue (FCT), Immature (IB) and Mature (MB) bone. In **(D)** * represents significant difference $p < 0.05$ in normalized bone volume between sample groups and at different time points, estimated using two-way ANOVA in GraphPad Prism ver. 6 software.

compared to “ELR only” (Figure 4B). Moreover, we did not observe any signs of fibrous tissue formation at the implant-tissue interface on all our scaffold types (i.e., “Uncoated,” “ELR only,” and “Pre-mineralized”) (Figures 4A,B). This is one of the characteristic of osseointegrated implants (Shah et al., 2019). Fibrous tissue formation is a surface responsive behavior. For instance, stiff surfaces can activate myofibroblasts (a scar-forming cell type) that leads to fibrous formation around the implant (Noskovicova et al., 2021b), thus, blocking implant-tissue integration (Noskovicova et al., 2021a). It is possible that a similar effect takes place at the surface of all our scaffold types (i.e., “Uncoated,” “ELR only,” and “Pre-mineralized”) avoiding activation of myofibroblasts and thus preventing fibrous tissue formation. However, more in-depth characterization such as (i) biomechanical analysis of implant-tissue interlocking (Brånemark et al., 1998) and (ii) high resolution electron tomography at implant-tissue interface to understand bone structure arrangement at nanoscale (Wang et al., 2017) would be required in further studies to gain more insights into osseointegration.

3.5 *In Vitro* Immunomodulatory Profile

Interestingly, we observed signs of inflammation with infiltrating lymphocytic cells (arrow heads) near the implant site of “ELR only” and more pronounced in “Pre-mineralized” scaffolds (Figure 4C). Presence of these inflammatory lymphocytic cells at the implant site (Figure 4C) indicates positive response to bone healing and osseointegration (Andrew et al., 1994; Trindade et al., 2016; Davies, 2019). Furthermore, lymphocyte cells are known to play crucial role in collagen deposition and organization during bone matrix formation in fracture healing (El Khassawna et al., 2017). HAP particles especially with needle-shape morphology (Lebre et al., 2017) and HAP coatings (Jiang et al., 2022) are known to exhibit excellent *in vivo* osteoimmunomodulatory properties. Inspired by these reported observations, we anticipated that the needle-shaped topographies generated by the mineralized material on the surface of our “Pre-mineralized” scaffolds may be playing an immunomodulatory role and thus motivated us to gain more insight into this potential effect. Therefore, we cultured human monocyte derived macrophages on different scaffolds and

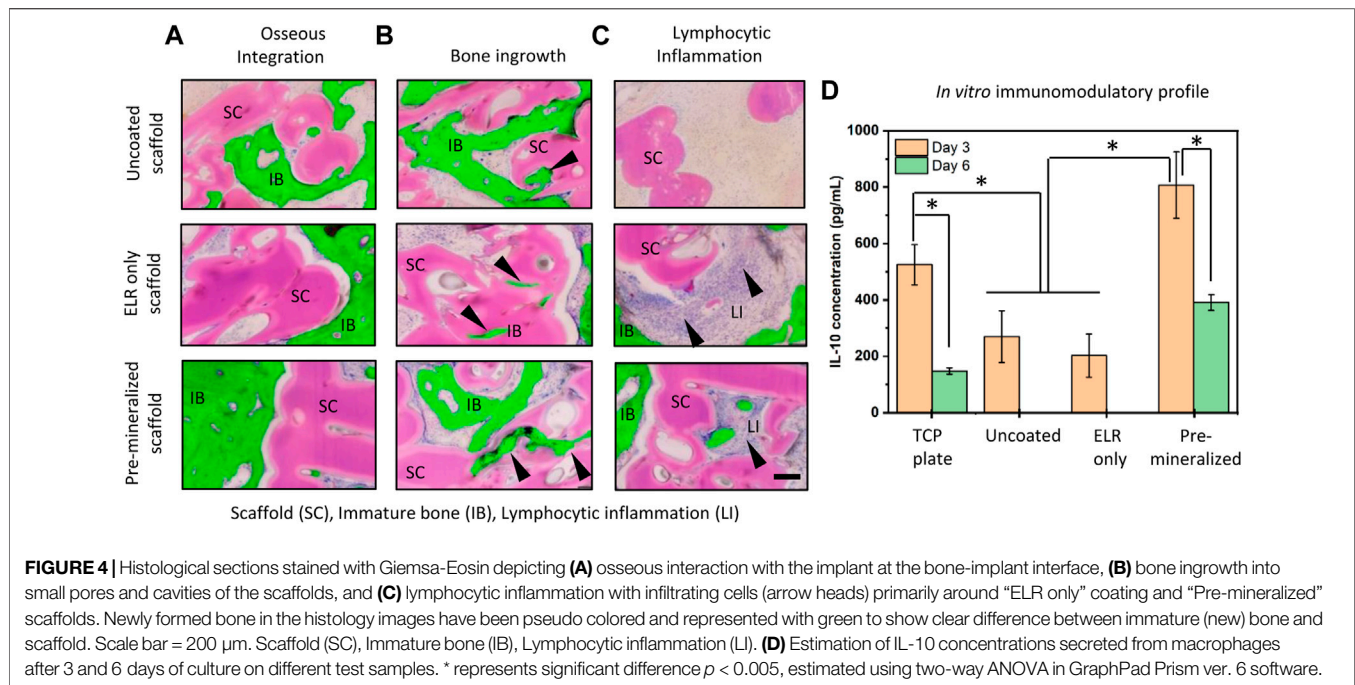


FIGURE 4 | Histological sections stained with Giemsa-Eosin depicting (A) osseous interaction with the implant at the bone-implant interface, (B) bone ingrowth into small pores and cavities of the scaffolds, and (C) lymphocytic inflammation with infiltrating cells (arrow heads) primarily around “ELR only” coating and “Pre-mineralized” scaffolds. Newly formed bone in the histology images have been pseudo colored and represented with green to show clear difference between immature (new) bone and scaffold. Scale bar = 200 μ m. Scaffold (SC), Immature bone (IB), Lymphocytic inflammation (LI). (D) Estimation of IL-10 concentrations secreted from macrophages after 3 and 6 days of culture on different test samples. * represents significant difference $p < 0.005$, estimated using two-way ANOVA in GraphPad Prism ver. 6 software.

quantified IL-10 secretion using sandwich ELISA (Figure 4D). IL-10 is a potent anti-inflammatory cytokine secreted by lymphocytes, macrophages, and dendritic cells, which is known to suppresses both immunoproliferative and inflammatory responses and plays a critical role in bone healing and remodeling (Jung et al., 2013) by inhibiting osteoclastic bone resorption and promoting osteoblastic bone formation (Zhang et al., 2014). Our results demonstrate that “Pre-mineralized” coatings exhibited significantly higher levels (807 ± 117 pg/ml) of IL-10 ($p < 0.005$) on day 3 which later dropped to lower levels (391 ± 28 pg/ml) after 6 days. Interestingly, we observed significantly lower concentrations of IL-10 on “Uncoated” (270 ± 92 pg/ml) and “ELR only” (202 ± 76 pg/ml) coatings as compared to “Pre-mineralized” coating at day 3 of culturing ($p < 0.005$) and IL-10 was undetectable at day 6 (Figure 4D). Overall, all test samples exhibited IL-10 concentrations which lie in the range which promotes bone healing, as reported previously (Chen et al., 2018). Previous studies in mice have shown that IL-10 deficiency can lead to poor bone formation and osteoblastogenesis, resulting in osteopenia and high bone fragility (Dresner-Pollak et al., 2004; Holgersen et al., 2015). However, it is crucial to note that the effect of IL-10 on osteogenesis is concentration dependent. For instance, low concentrations of IL-10 (10–1,000 pg/ml) promote osteogenesis via p38/MAPK signaling pathway, whereas higher concentrations (10,000–100,000 pg/ml) activate NF- κ B to downregulate p38/MAPK signaling, thus inhibiting osteogenesis (Chen et al., 2018). These results demonstrate that the mineralized coating is having a significant effect on IL-10 production and is likely leading to a different immunomodulatory response *in vivo* compared to the other groups tested. While a more in-depth analysis of this effect is important to understand these

immunomodulatory effects, this work is beyond the scope of the current study.

4 CONCLUSION

The present work reports on the possibility of integrating supramolecular chemistry and additive manufacturing to engineer and fabricate functional bone implants that can promote bone regeneration. 3D printed nylon scaffolds were coated with mineralizing ELR matrix and were assessed both *in vitro* and *in vivo* using a rabbit calvarial model for bone formation and osseointegration. Our results indicate that the mineral grown was apatite in nature and grew uniformly over large and uneven area of the scaffold. *In vitro*, all test samples (“Uncoated,” “ELR only,” and “Pre-mineralized”) supported hiMSCs adhesion, proliferation, and spreading of hiMSCs cells growing preferentially on “Pre-mineralized” samples. *In vivo*, all test samples exhibited higher levels of new bone formed within the defect compared to the control Bio-Oss. However, coated scaffolds (both “ELR only” and “Pre-mineralized”) did not lead to higher bone formation compared to “Uncoated” scaffolds.

In conclusion, our mineralizing coatings offer higher cell response *in vitro*, qualitatively higher conformation of the new bone tissue to the geometry of the scaffold, and no fibrous tissue formation at the implant-tissue interface. However, this study exhibit limitations that could be improved. For example, the coatings need to be optimized as they did not significantly enhance the volume of the newly formed bone. Furthermore, optimization of immunomodulation and in-depth integration analysis between tissue and scaffold need to be performed. Therefore, future studies should be aimed at (i) optimizing the coatings (ii) optimizing the architecture of the scaffold, (iii)

modulating the morphology of the HAP structures, (iv) assessing *in vivo* performance for longer periods of time to investigate mineral growth from the scaffold to the tissue, (v) characterizing implant-tissue inter-locking, and (vi) optimizing immunomodulation. It is important to mention that the supramolecular organization of the ELR molecules can be tailored during the coating process to modify and optimize the growth of the inorganic phase (Elsharkawy et al., 2018). In addition to this optimization to attempt to enhance osseointegration, degradability and absorbability of the material should also be characterized in future studies.

Overall, our results indicate the potential of the coatings to promote responses that can ultimately led to osseointegration. We envisage that this approach can have important implications for the design of smart biomaterials which can acellularly self-mineralize by drawing ions from the implant site and exhibit the capacity to enhance bone growth and osseointegration.

DATA AVAILABILITY STATEMENT

The original contributions presented in the study are included in the article/**Supplementary Material**, further inquiries can be directed to the corresponding authors.

ETHICS STATEMENT

The animal study was reviewed and approved by Animal Welfare and Ethical Review Body (AWERB), University of Nottingham, Nottingham, United Kingdom.

REFERENCE

- Abdal-hay, A., Hamdy, A. S., and Khalil, K. A. (2015). Fabrication of Durable High Performance Hybrid Nanofiber Scaffolds for Bone Tissue Regeneration Using a Novel, Simple *In Situ* Deposition Approach of Polyvinyl Alcohol on Electrospun Nylon 6 Nanofibers. *Mater. Lett.* 147, 25–28. doi:10.1016/j.matlet.2015.02.005
- Agarwal, R., and García, A. J. (2015). Biomaterial Strategies for Engineering Implants for Enhanced Osseointegration and Bone Repair. *Adv. drug Deliv. Rev.* 94, 53–62. doi:10.1016/j.addr.2015.03.013
- Albrektsson, T., and Albrektsson, B. (1987). Osseointegration of Bone Implants: A Review of an Alternative Mode of Fixation. *Acta Orthop. Scand.* 58, 567–577. doi:10.3109/17453678709146401
- Aldaadaa, A., Owji, N., and Knowles, J. (2018). Three-dimensional Printing in Maxillofacial Surgery: Hype versus Reality. *J. Tissue Eng.* 9, 2041731418770909. doi:10.1177/2041731418770909
- Andrew, J. G., Andrew, S., Freemont, A., and Marsh, D. (1994). Inflammatory Cells in Normal Human Fracture Healing. *Sort* 65, 462–466. doi:10.3109/17453679408995493
- Awuah, D., Alobaid, M., Latif, A., Salazar, F., Emes, R. D., and Ghaemmaghami, A. M. (2019). The Cross-Talk between miR-511-3p and C-type Lectin Receptors on Dendritic Cells Affects Dendritic Cell Function. *J. I.* 203, 148–157. doi:10.4049/jimmunol.1801108
- Bahraminasab, M. (2020). Challenges on Optimization of 3D-Printed Bone Scaffolds. *Biomed. Eng. Online* 19, 69. doi:10.1186/s12938-020-00810-2
- Balducci, L., Blasi, A., Saldarelli, M., Soleti, A., Pessina, A., Bonomi, A., et al. (2014). Immortalization of Human Adipose-Derived Stromal Cells: Production of Cell

AUTHOR CONTRIBUTIONS

AH, DE, SE, and AM conceptualized the work. AH and AM designed the experiments and performed the analysis. RB synthesized the scaffolds. RO performed the *in vitro* experiments and FRAJR performed the analysis. AL, HR, and AG performed immunology experiments. JR synthesised ELR molecules. AM and DE supervised AH and RB, respectively. AH and AM wrote the manuscript.

FUNDING

The work was financially supported by the AO foundation (AOCMF - 17–19M), ERC Starting Grant (STROFUNSCAFF), ERC Proof-of-concept Grant (MINGRAFT), the Engineering and Physical Sciences Research Council (EP/N006615/1), and the Medical Research Council (United Kingdom Regenerative Medicine Platform Hub Acellular Smart Materials 3D Architecture, MR/R015651/1). JR is grateful for the funding from the Spanish Government (PID2019 - 110709RB - 100, RED2018 - 102417 - T), Junta de Castilla y León (VA317P18, Infrared 2018 - UVA06), Interreg V España Portugal POCTEP (0624_2IQBIONEURO_6_E) and Centro en Red de Medicina Regenerativa y Terapia Celular de Castilla y León.”

SUPPLEMENTARY MATERIAL

The Supplementary Material for this article can be found online at: <https://www.frontiersin.org/articles/10.3389/fbioe.2022.836386/full#supplementary-material>

Lines with High Growth Rate, Mesenchymal Marker Expression and Capability to Secrete High Levels of Angiogenic Factors. *Stem Cell Res. Ther.* 5, 63. doi:10.1186/s13045-014-0145-2

- Bisht, B., Hope, A., Mukherjee, A., and Paul, M. K. (2021). Advances in the Fabrication of Scaffold and 3D Printing of Biomimetic Bone Graft. *Ann. Biomed. Eng.* 49 (4), 1128–1150. doi:10.1007/s10439-021-02752-9
- Bosetti, M., Bianchi, A. E., Zaffe, D., and Cannas, M. (2013). Comparative *In Vitro* Study of Four Commercial Biomaterials Used for Bone Grafting. *J. Appl. biomaterials Funct. Mater.* 11, 80–88. doi:10.5301/jabfm.5000149
- Brånemark, R., Öhrnell, L. O., Skalak, R., Carlsson, L., and Brånemark, P. I. (1998). Biomechanical Characterization of Osseointegration: An Experimental *In Vivo* Investigation in the Beagle Dog. *J. Orthop. Res.* 16, 61–69.
- Brun, P., Scorsetto, M., Vassanelli, S., Castagliuolo, I., Palù, G., Ghezzi, F., et al. (2013). Mechanisms Underlying the Attachment and Spreading of Human Osteoblasts: From Transient Interactions to Focal Adhesions on Vitronectin-Grafted Bioactive Surfaces. *Acta biomater.* 9, 6105–6115. doi:10.1016/j.actbio.2012.12.018
- Burroughs, L., Amer, M. H., Vassey, M., Koch, B., Figueredo, G. P., Mukonoweshuro, B., et al. (2021). Discovery of Synergistic Material-Topography Combinations to Achieve Immunomodulatory Osteoinductive Biomaterials Using a Novel *In Vitro* Screening Method: The ChemoTopoChip. *Biomaterials* 271, 120740. doi:10.1016/j.biomaterials.2021.120740
- Cai, S., Wu, C., Yang, W., Liang, W., Yu, H., and Liu, L. (2020). Recent Advance in Surface Modification for Regulating Cell Adhesion and Behaviors. *Nanotechnol. Rev.* 9, 971–989. doi:10.1515/ntrev-2020-0076
- Chen, E., Liu, G., Zhou, X., Zhang, W., Wang, C., Hu, D., et al. (2018). Concentration-dependent, Dual Roles of IL-10 in the Osteogenesis of

- Human BMSCsviaP38/MAPK and NF- κ B Signaling Pathways. *FASEB J.* 32, 4917–4929. doi:10.1096/fj.201701256rrr
- Cheng, K., Weng, W., Wang, H., and Zhang, S. (2005). *In Vitro* behavior of Osteoblast-like Cells on Fluoridated Hydroxyapatite Coatings. *Biomaterials* 26, 6288–6295. doi:10.1016/j.biomaterials.2005.03.041
- Davies, J. E. (2019). *Is Osseointegration a Foreign Body Reaction?* Hanover Park, Illinois, United States: Quintessence Publishing Co, Inc 4350 Chandler Drive.
- Deng, X., Hasan, A., Elsharkawy, S., Tejeda-Montes, E., Tarakina, N. V., Greco, G., et al. (2021). Topographically Guided Hierarchical Mineralization. *Mater. Today Bio* 11, 100119. doi:10.1016/j.mtbio.2021.100119
- Derby, B. (2012). Printing and Prototyping of Tissues and Scaffolds. *science* 338, 921–926. doi:10.1126/science.1226340
- Dresner-Pollak, R., Gelb, N., Rachmilewitz, D., Karmeli, F., and Weinreb, M. (2004). Interleukin 10-deficient Mice Develop Osteopenia, Decreased Bone Formation, and Mechanical Fragility of Long Bones. *Gastroenterology* 127, 792–801. doi:10.1053/j.gastro.2004.06.013
- El Khassawna, T., Serra, A., Bucher, C. H., Petersen, A., Schlundt, C., Könnecke, I., et al. (2017). T Lymphocytes Influence the Mineralization Process of Bone. *Front. Immunol.* 8, 562. doi:10.3389/fimmu.2017.00562
- Elsharkawy, S., Al-Jawad, M., Pantano, M. F., Tejeda-Montes, E., Mehta, K., Jamal, H., et al. (2018). Protein Disorder-Order Interplay to Guide the Growth of Hierarchical Mineralized Structures. *Nat. Commun.* 9, 2145. doi:10.1038/s41467-018-04319-0
- Farré-Guasch, E., Wolff, J., Helder, M. N., Schulten, E. A., Forouzanfar, T., and Klein-Nulend, J. (2015). Application of Additive Manufacturing in Oral and Maxillofacial Surgery. *J. Oral Maxillofac. Surg.* 73, 2408–2418. doi:10.1016/j.joms.2015.04.019
- Fu, X., Liu, G., Halim, A., Ju, Y., Luo, Q., and Song, G. (2019). Mesenchymal Stem Cell Migration and Tissue Repair. *Cells* 8, 784. doi:10.3390/cells8080784
- Guillaume, O., Schmid, T., Kluge, K., Weber, F. E., Richards, R. G., Eberli, U., et al. (2019). Introduction of the Anspach Drill as a Novel Surgical Driller for Creating Calvarial Defects in Animal Models. *J. Orthop. Res.* 37, 1183–1191. doi:10.1002/jor.24265
- Hasan, A., and Pandey, L. M. (2020). Surface Modification of Ti6Al4V by Forming Hybrid Self-Assembled Monolayers and its Effect on Collagen-I Adsorption, Osteoblast Adhesion and Integrin Expression. *Appl. Surf. Sci.* 505, 144611. doi:10.1016/j.apsusc.2019.144611
- Hasan, A., Waibhaw, G., and Pandey, L. M. (2018). Conformational and Organizational Insights into Serum Proteins during Competitive Adsorption on Self-Assembled Monolayers. *Langmuir* 34, 8178–8194. doi:10.1021/acs.langmuir.8b01110
- Hay, D. I., and Moreno, E. C. (2021). “Statherin and the Acidic Proline-Rich Proteins,” in *Human Saliva: Clinical Chemistry and Microbiology*. Editor J. O. Tenovou (Boca Raton, FL: CRC Press), 131–150. doi:10.1201/9781003210399-5
- Holgersen, K., Dobie, R., Farquharson, C., van't Hof, R., Ahmed, S. F., Hansen, A. K., et al. (2015). Piroxicam Treatment Augments Bone Abnormalities in Interleukin-10 Knockout Mice. *Inflamm. bowel Dis.* 21, 257–266. doi:10.1097/mib.0000000000000269
- Jackson, R. J., Patrick, P. S., Page, K., Powell, M. J., Lythgoe, M. F., Miodownik, M. A., et al. (2018). Chemically Treated 3D Printed Polymer Scaffolds for Biomaterial Formation. *ACS omega* 3, 4342–4351. doi:10.1021/acsomega.8b00219
- Jeong, J., Kim, J. H., Shim, J. H., Hwang, N. S., and Heo, C. Y. (2019). Bioactive Calcium Phosphate Materials and Applications in Bone Regeneration. *Biomater. Res.* 23, 4–11. doi:10.1186/s40824-018-0149-3
- Jiang, J., Liu, W., Xiong, Z., Hu, Y., and Xiao, J. (2022). Effects of Biomimetic Hydroxyapatite Coatings on Osteoimmunomodulation. *Biomater. Adv.* 134, 112640. doi:10.1016/j.msec.2021.112640
- Jung, Y.-K., Kim, G.-W., Park, H.-R., Lee, E.-J., Choi, J.-Y., Beier, F., et al. (2013). Role of Interleukin-10 in Endochondral Bone Formation in Mice: Anabolic Effect via the Bone Morphogenetic Protein/Smad Pathway. *Arthritis & Rheumatism* 65, 3153–3164. doi:10.1002/art.38181
- Karageorgiou, V., and Kaplan, D. (2005). Porosity of 3D Biomaterial Scaffolds and Osteogenesis. *Biomaterials* 26, 5474–5491. doi:10.1016/j.biomaterials.2005.02.002
- Khosravi, N., Maeda, A., Dacosta, R. S., and Davies, J. E. (2018). Nanosurfaces Modulate the Mechanism of Peri-Implant Endosseous Healing by Regulating Neovascular Morphogenesis. *Commun. Biol.* 1, 72–13. doi:10.1038/s42003-018-0074-y
- Lebre, F., Sridharan, R., Sawkins, M. J., Kelly, D. J., O'Brien, F. J., and Lavelle, E. C. (2017). The Shape and Size of Hydroxyapatite Particles Dictate Inflammatory Responses Following Implantation. *Sci. Rep.* 7, 2922. doi:10.1038/s41598-017-03086-0
- Lee, E.-H., Kim, J.-Y., Kweon, H. Y., Jo, Y.-Y., Min, S.-K., Park, Y.-W., et al. (2010). A Combination Graft of Low-Molecular-Weight Silk Fibroin with Choukroun Platelet-Rich Fibrin for Rabbit Calvarial Defect. *Oral Surg. Oral Med. Oral Pathology, Oral Radiology, Endodontology* 109, e33–e38. doi:10.1016/j.tripleo.2009.12.043
- Lee, S. J., Lee, D., Yoon, T. R., Kim, H. K., Jo, H. H., Park, J. S., et al. (2016). Surface Modification of 3D-Printed Porous Scaffolds via Mussel-Inspired Polydopamine and Effective Immobilization of rhBMP-2 to Promote Osteogenic Differentiation for Bone Tissue Engineering. *Acta biomater.* 40, 182–191. doi:10.1016/j.actbio.2016.02.006
- Liu, Y., Rath, B., Tingart, M., and Eschweiler, J. (2020). Role of Implants Surface Modification in Osseointegration: A Systematic Review. *J. Biomed. Mater. Res.* 108, 470–484. doi:10.1002/jbm.a.36829
- Malhotra, A., and Habibovic, P. (2016). Calcium Phosphates and Angiogenesis: Implications and Advances for Bone Regeneration. *Trends Biotechnol.* 34, 983–992. doi:10.1016/j.tibtech.2016.07.005
- Mehrabanian, M., and Nasr-Esfahani, M. (2011). HA/nylon 6,6 Porous Scaffolds Fabricated by Salt-Leaching/solvent Casting Technique: Effect of Nano-Sized Filler Content on Scaffold Properties. *Int. J. Nanomedicine* 6, 1651–1659. doi:10.2147/IJN.S21203
- Mori, T., Kiyono, T., Imabayashi, H., Takeda, Y., Tsuchiya, K., Miyoshi, S., et al. (2005). Combination of hTERT and Bmi-1, E6, or E7 Induces Prolongation of the Life Span of Bone Marrow Stromal Cells from an Elderly Donor without Affecting Their Neurogenic Potential. *Mol. Cell Biol.* 25, 5183–5195. doi:10.1128/mcb.25.12.5183-5195.2005
- Noskovicova, N., Schuster, R., Van Putten, S., Ezzo, M., Koehler, A., Boo, S., et al. (2021b). Suppression of the Fibrotic Encapsulation of Silicone Implants by Inhibiting the Mechanical Activation of Pro-fibrotic TGF- β . *Nat. Biomed. Eng.* 5, 1437–1456. doi:10.1038/s41551-021-00722-z
- Noskovicova, N., Hinz, B., and Pakshir, P. (2021a). Implant Fibrosis and the Underappreciated Role of Myofibroblasts in the Foreign Body Reaction. *Cells* 10, 1794. doi:10.3390/cells10071794
- Orciani, M., Fini, M., Di Primio, R., and Mattioli-Belmonte, M. (2017). Biofabrication and Bone Tissue Regeneration: Cell Source, Approaches, and Challenges. *Front. Bioeng. Biotechnol.* 5, 17. doi:10.3389/fbioe.2017.00017
- Owen, R., Bahmaee, H., Claeysens, F., and Reilly, G. C. (2020). Comparison of the Anabolic Effects of Reported Osteogenic Compounds on Human Mesenchymal Progenitor-Derived Osteoblasts. *Bioengineering* 7, 12. doi:10.3390/bioengineering7010012
- Parithimarkalaignan, S., and Padmanabhan, T. V. (2013). Osseointegration: An Update. *J. Indian Prosthodont Soc.* 13, 2–6. doi:10.1007/s13191-013-0252-z
- Petrie, T. A., Reyes, C. D., Burns, K. L., and García, A. J. (2009). Simple Application of Fibronection-Mimetic Coating Enhances Osseointegration of Titanium Implants. *J. Cell. Mol. Med.* 13, 2602–2612. doi:10.1111/j.1582-4934.2008.00476.x
- Prasad, K., Bazaka, O., Chua, M., Rochford, M., Fedrick, L., Spoor, J., et al. (2017). Metallic Biomaterials: Current Challenges and Opportunities. *Materials* 10, 884. doi:10.3390/ma10080884
- Qu, H., Fu, H., Han, Z., and Sun, Y. (2019). Biomaterials for Bone Tissue Engineering Scaffolds: A Review. *RSC Adv.* 9, 26252–26262. doi:10.1039/c9ra05214c
- Ran, Q., Yang, W., Hu, Y., Shen, X., Yu, Y., Xiang, Y., et al. (2018). Osteogenesis of 3D Printed Porous Ti6Al4V Implants with Different Pore Sizes. *J. Mech. Behav. Biomed. Mater.* 84, 1–11. doi:10.1016/j.jmbbm.2018.04.010
- Salazar, F., Hall, L., Negm, O. H., Awuah, D., Tighe, P. J., Shakib, F., et al. (2016). The Mannose Receptor Negatively Modulates the Toll-like Receptor 4-aryl Hydrocarbon Receptor-Indoleamine 2,3-dioxygenase axis in Dendritic Cells Affecting T Helper Cell Polarization. *J. Allergy Clin. Immunol.* 137, 1841–1851. e1842. doi:10.1016/j.jaci.2015.10.033

- Schmidlin, P. R., Nicholls, F., Kruse, A., Zwahlen, R. A., and Weber, F. E. (2013). Evaluation of Moldable, in Situ Hardening Calcium Phosphate Bone Graft Substitutes. *Clin. Oral Impl. Res.* 24, 149–157. doi:10.1111/j.1600-0501.2011.02315.x
- Seyednejad, H., Gawlińska, D., Dhert, W. J. A., Van Nostrum, C. F., Vermonden, T., and Hennink, W. E. (2011). Preparation and Characterization of a Three-Dimensional Printed Scaffold Based on a Functionalized Polyester for Bone Tissue Engineering Applications. *Acta biomater.* 7, 1999–2006. doi:10.1016/j.actbio.2011.01.018
- Shah, F. A., Thomsen, P., and Palmquist, A. (2019). Osseointegration and Current Interpretations of the Bone-Implant Interface. *Acta biomater.* 84, 1–15. doi:10.1016/j.actbio.2018.11.018
- Song, R., Murphy, M., Li, C., Ting, K., Soo, C., and Zheng, Z. (2018). Current Development of Biodegradable Polymeric Materials for Biomedical Applications. *DDT* Vol. 12, 3117–3145. doi:10.2147/dddt.s165440
- Tejeda-Montes, E., Klymov, A., Nejadnik, M. R., Alonso, M., Rodríguez-Cabello, J. C., Walboomers, X. F., et al. (2014a). Mineralization and Bone Regeneration Using a Bioactive Elastin-like Recombinamer Membrane. *Biomaterials* 35, 8339–8347. doi:10.1016/j.biomaterials.2014.05.095
- Tejeda-Montes, E., Smith, K. H., Poch, M., López-Bosque, M. J., Martín, L., Alonso, M., et al. (2012). Engineering Membrane Scaffolds with Both Physical and Biomolecular Signaling. *Acta biomater.* 8, 998–1009. doi:10.1016/j.actbio.2011.09.005
- Tejeda-Montes, E., Smith, K. H., Rebollo, E., Gómez, R., Alonso, M., Rodríguez-Cabello, J. C., et al. (2014b). Bioactive Membranes for Bone Regeneration Applications: Effect of Physical and Biomolecular Signals on Mesenchymal Stem Cell Behavior. *Acta biomater.* 10, 134–141. doi:10.1016/j.actbio.2013.09.001
- Tofail, S. A. M., Koumoulos, E. P., Bandyopadhyay, A., Bose, S., O'Donoghue, L., and Charitidis, C. (2018). Additive Manufacturing: Scientific and Technological Challenges, Market Uptake and Opportunities. *Mater. today* 21, 22–37. doi:10.1016/j.mattod.2017.07.001
- Trindade, R., Albrektsson, T., Tengvall, P., and Wennerberg, A. (2016). Foreign Body Reaction to Biomaterials: On Mechanisms for Buildup and Breakdown of Osseointegration. *Clin. implant Dent. Relat. Res.* 18, 192–203. doi:10.1111/cid.12274
- Turnbull, G., Clarke, J., Picard, F., Riches, P., Jia, L., Han, F., et al. (2018). 3D Bioactive Composite Scaffolds for Bone Tissue Engineering. *Bioact. Mater.* 3, 278–314. doi:10.1016/j.bioactmat.2017.10.001
- Vallés, G., García-Rey, E., Saldaña, L., García-Cimbrelo, E., and Vilaboa, N. (2021). Wear of Hip Prostheses Increases Serum IGFBP-1 Levels in Patients with Aseptic Loosening. *Sci. Rep.* 11, 576. doi:10.1038/s41598-020-79813-x
- Wang, C., Huang, W., Zhou, Y., He, L., He, Z., Chen, Z., et al. (2020). 3D Printing of Bone Tissue Engineering Scaffolds. *Bioact. Mater.* 5, 82–91. doi:10.1016/j.bioactmat.2020.01.004
- Wang, X., Shah, F. A., Palmquist, A., and Grandfield, K. (2017). 3D Characterization of Human Nano-Osseointegration by on-axis Electron Tomography without the Missing Wedge. *ACS Biomater. Sci. Eng.* 3, 49–55. doi:10.1021/acsbomaterials.6b00519
- Zhang, Q., Chen, B., Yan, F., Guo, J., Zhu, X., Ma, S., et al. (2014). Interleukin-10 Inhibits Bone Resorption: A Potential Therapeutic Strategy in Periodontitis and Other Bone Loss Diseases. *BioMed Res. Int.* 2014, 1–5. doi:10.1155/2014/284836
- Zhang, X., Lou, Q., Wang, L., Min, S., Zhao, M., and Quan, C. (2019). Immobilization of BMP-2-Derived Peptides on 3D-Printed Porous Scaffolds for Enhanced Osteogenesis. *Biomed. Mat.* 15, 015002. doi:10.1088/1748-605x/ab4c78
- Zhao, X., Lui, Y. S., Choo, C. K. C., Sow, W. T., Huang, C. L., Ng, K. W., et al. (2015). Calcium Phosphate Coated Keratin-PCL Scaffolds for Potential Bone Tissue Regeneration. *Mater. Sci. Eng. C* 49, 746–753. doi:10.1016/j.msec.2015.01.084
- Zhu, G., Wang, G., and Li, J. J. (2021). Advances in Implant Surface Modifications to Improve Osseointegration. *Mater. Adv.* 2 (21), 6901–6927. doi:10.1039/d1ma00675d
- Zysset, P. K., Guo, X. E., Hoffer, C. E., Moore, K. E., and Goldstein, S. A. (1999). Elastic Modulus and Hardness of Cortical and Trabecular Bone Lamellae Measured by Nanoindentation in the Human Femur. *J. biomechanics* 32, 1005–1012. doi:10.1016/s0021-9290(99)00111-6

Conflict of Interest: The authors declare that the research was conducted in the absence of any commercial or financial relationships that could be construed as a potential conflict of interest.

Publisher's Note: All claims expressed in this article are solely those of the authors and do not necessarily represent those of their affiliated organizations, or those of the publisher, the editors and the reviewers. Any product that may be evaluated in this article, or claim that may be made by its manufacturer, is not guaranteed or endorsed by the publisher.

Copyright © 2022 Hasan, Bagnol, Owen, Latif, Rostam, Elsharkawy, Rose, Rodríguez-Cabello, Ghaemmaghami, Eglin and Mata. This is an open-access article distributed under the terms of the Creative Commons Attribution License (CC BY). The use, distribution or reproduction in other forums is permitted, provided the original author(s) and the copyright owner(s) are credited and that the original publication in this journal is cited, in accordance with accepted academic practice. No use, distribution or reproduction is permitted which does not comply with these terms.

Advantages of publishing in Frontiers



OPEN ACCESS

Articles are free to read
for greatest visibility
and readership



FAST PUBLICATION

Around 90 days
from submission
to decision



HIGH QUALITY PEER-REVIEW

Rigorous, collaborative,
and constructive
peer-review



TRANSPARENT PEER-REVIEW

Editors and reviewers
acknowledged by name
on published articles

Frontiers

Avenue du Tribunal-Fédéral 34
1005 Lausanne | Switzerland

Visit us: www.frontiersin.org

Contact us: frontiersin.org/about/contact



REPRODUCIBILITY OF RESEARCH

Support open data
and methods to enhance
research reproducibility



DIGITAL PUBLISHING

Articles designed
for optimal readership
across devices



FOLLOW US

@frontiersin



IMPACT METRICS

Advanced article metrics
track visibility across
digital media



EXTENSIVE PROMOTION

Marketing
and promotion
of impactful research



LOOP RESEARCH NETWORK

Our network
increases your
article's readership